

## MOLECULAR REVIEW: *SESAMUM* EMERGING AS A DROUGHT TOLERANT OLDEST OIL CROP

Kalpna Kaloori<sup>1</sup>, Nirmala Babu Rao<sup>2</sup> and Balram Marathi<sup>3</sup>

<sup>1</sup>Department of Botany, University College of Science, Osmania University, Hyderabad, Telangana State, India

<sup>2</sup>Department of Botany, University College of Science, Osmania University, Hyderabad, Telangana State, India

<sup>3</sup>Department of Biotechnology, PJTSAU, Hyderabad, Telangana State, India

\*Author for Correspondence: [kaloorikalpana26@gmail.com](mailto:kaloorikalpana26@gmail.com)

### ABSTRACT

Sesamum is one of the oldest oil crop traditionally and medicinally used since ages and act as a substitute for cooking oil. Sesame is gaining popularity for its antioxidant derivatives, numerous health benefits and for economically very useful seed oil. Sesame oil with 85% unsaturated fatty acids, is highly stable with reducing effect on cholesterol levels and prevents coronary heart diseases among other several health benefits. Being short duration crop sesame grows in all seasons in a year, fits well into various cropping systems and emerging as an important drought tolerant oil crop. The objectives of the review were to emphasize on the work carried out mainly on molecular grounds in *Sesamum indicum*. Different molecular markers are used across Sesame accessions in wild and elite germplasm to study the genetic diversity across the world. Average to high polymorphism is detected with different molecular markers. Apart from genetic diversity studies, gene and association mapping work is also reviewed. High-density genetic linkage map and QTL(Quantitative Trait Loci) analysis for sesame provides a good foundation for further research on sesame genetics and for marker-assisted selection.

**Keywords:** *Sesamum indicum*, Genetic diversity, QTLs, Mapping

### INTRODUCTION

Sesame is an annual herb reaching an height of more than one meter (Mina Kazemian Ruhi *et al.*, 2014) and belongs to the family Pedaliaceae. *Sesamum indicum* L. syn *S. orientale* L. is cultivated species whereas *S. malabaricum* or *S. mulayanum* are wild species apart from *S. calycinum*, sp Baumii. Other species, *S. angustifolium*, and *S. radiatum* are also used as food (Elly Kafiriti and Omari Mponda, 2008). *Sesamum*, queen of oil seeds, originated in Africa (Ethiopia) spread through West Asia, China, Japan and thought to be first domesticated in Africa (Nayar and Mehra, 2008) and India (Bedigian, 2004). Around 60 to 65 countries all over the world produce sesame seed, distributed across Asia, Africa, Europe, Central and South America of tropical and temperate regions. Among them Asia and Africa are the major sesame producing countries. The world on an average produces close to 3 million tons of sesame seed every year. Major sesame producing countries are India, China, Myanmar, Sudan, Pakistan, Mexico, Ethiopia, Sri Lanka and Burma whereas Sudan and Nigeria are major exporting countries. According to NMOOP 2015-16 reports, India covers an area (lakh ha) of 18.93 under cultivation, followed by Myanmar (11.11), Nigeria (5.29), China (4.53), Ethiopia (3.20), Uganda (2.1) and other countries (34.1). China produces the highest yield of 1234 kg/ha seed and India an average yield of 413 kg/ha. In India, West Bengal produces maximum yield when compared to other sesame producing states for its many nutraceuticals, industrial and pharmaceutical uses (Bradley Morris, 2002). High amounts of both sesamin and sesamol compounds are present (Sirato-Yasumoto *et al.*, 2001) in sesame which increases the hepatic mitochondrial and peroxisomal fatty acid oxidation rate. It also contains antioxidant and health promoting activities (Kato *et al.*, 1998), apart from preventing cancer and heart diseases

### Review Article

(Cooney *et al.*, 2001). Keeping in view its increasing importance's an attempt has been made to review *Sesamum* Genetic Diversity, QTL analysis and Gene Mapping methods.

### GENETIC DIVERSITY WITH DIFFERENT MOLECULAR MARKERS

Plant genetic diversity can be conserved through modern analytical tools and techniques which are widely available for genetic manipulations. Genomic diversity studies plays important role in determining the evolution of traits. Different biological approaches were reviewed by Sharad Tiwari *et al.*, 2011 to overcome the slow pace of improvement in sesame crop through tissue culture, molecular marker-assisted breeding, functional genomics and genetic transformational studies. Similar study was also reviewed by Ekta Sharma *et al.*, in 2014 on genetic divergence in sesame emphasizing on different molecular markers usage. A over view of genetic diversity was assessed with molecular markers is given in Table:I. Komivi Dossa *et al.*, 2016 studied the genetic diversity of 96 sesame accessions collected from 22 countries distributed over six geographic regions of Africa and Asia were genotyped using 33 polymorphic SSR markers revealing large genetic variability within the germplasm. Similarly Rapheal *et al.*, 2018 identified more than fifty percent of SSR markers which are polymorphic in accessions collected in Northern Ghana region. A detail study was reviewed by Komivi Dossa *et al.*, 2017 regarding the genetic resources so far available.

Sovetgul *et al.*, 2018 studied 129 sesame landraces and cultivars using 70 simple sequence repeats (SSR) markers which resulted in 23 polymorphic markers which produced 157 alleles. The number of alleles arranged form 3-14. In a recent study in assessing the genetic diversity by Eveline de Sousa Araujo *et al.*, 2019 used ten SSR markers to assess 36 sesame germplasms which showed average polymorphism. Polymorphism was also obtained by Anandan *et al.*, 2017 when assessed among low diversified sesame accessions. Nweke Friday Nwalo, 2015 observed genetic diversity in Nigerian Sesame cultivars and its relationship with phytochemical composition using SSR markers and with spectrophotometric methods. High genetic variability was observed among the genotypes with significant variations in phytochemical composition. Similar study was also carried by Jong-Hyun Park *et al.*, 2013 in germplasm collected from different parts of the world with SSR markers. Vijaya Sudhakara Rao Kola *et al.*, 2012 used specific microsatellite markers, of which forty six markers found to be polymorphic with genetic similarity coefficient ranging from 79 to 92% suggesting that the cultivars developed are from diverse origin exhibiting good variability. Kiranmayi *et al.*, 2016 and Raphael Adu-Gyamfi *et al.*, 2019 concluded the same by working with SSR markers.

Whereas fairly low genetic diversity was observed in Turkish accessions when EST based SSRs were used (Ummu Seyitalioglu, 2010), whereas higher heterozygosity obtained when Daniel Endale Gebremichael and Heiko Parzies, 2010 used ten Simple Sequence Repeats (SSRs) markers to study genetic variation in Ethiopian accessions. In a study carried out by Anupam dixit *et al.*, 2005 fifty microsatellite sequences were isolated from an enriched library of sesame, out of which ten polymorphic microsatellites were used to determine the diversity. When Maini Bhattacharjee *et al.*, 2019 assessed 30 diverse genotypes for genetic diversity with SSRs, showed PIC 0.87. Whereas Labhya Rani Gogoi *et al.*, 2018 when assessed 33 indigenous genotypes of sesame with 27 polymorphic SSR markers resulted in an average of 2.87 allele per locus with polymorphism information content (PIC) value varied from 0.99 to 0.01. Aejaz Ahmad Dar *et al.*, 2017 studied germplasms collected from different agroclimatic zones of India and assessed with 22 RAPD and 18 SSR primers showing high genetic variability. Even in few germplasms assessed for genetic diversity showed polymorphism. Khames Mourad *et al.*, 2019 evaluated few germplasm assessed with only 5 SSR markers showed 53% polymorphism. Through employing selective hybridization strategy, 95 mining expressed sequence tags from the NCBI database used to characterize genetic diversity of 16 sesame germplasms by Jyothi Badri *et al.*, 2014. The number of alleles per microsatellite locus ranged from 2 to 5 with an average of 3.11 alleles.

Apart from SSRs, genetic diversity was also observed with other molecular markers such as ISSR (Admas Alemu *et al.*, 2013; Hitesh Kumar *et al.*, 2012), EST-SSR (Sarita Pandey *et al.*, 2015 and Arna

**Review Article**

Das *et al.*, 2013), RAPD (Fazal Akbar *et al.*, 2011) and AFLP (Hernan Laurentin *et al.*, 2008; Ghulam Ali, 2007). Dagmawi Teshome *et al.*, 2015 studied 82 sesame accessions from Ethiopia and 38 exotic germplasms with 6 ISSR primers which resulted in high polymorphism among the local germplasms. Similar work was also carried out by Mohammed Abate *et al.*, 2015 with 128 accessions with 7 ISSR primers gave 92.2% polymorphism. Admas Alemu *et al.*, 2013 studied the genetic diversity of sesame in major growing areas of Ethiopia. Six farmers cultivars and varieties of sesame from the north western Ethiopia each consisting of ten individual samples were analyzed using four inter simple sequence repeat (ISSR) markers. The four ISSR primers yielded 37 amplification products of which 36 bands exhibited polymorphism. ISSR markers were also used by Tapaswini Hota *et al.*, 2016 to study the genetic relationship and agro-morphological characters in sesame. Out of the tested 30 ISSR primers, 18 primers produced 114 detectable fragments of which 97(85.08%) were polymorphic.

Sesame accessions collected from Sudan were assessed for genetic diversity with RAPD markers showed high polymorphism (Abdellatef *et al.*, 2008). Twelve Cambodia and Vietnam sesame accessions were evaluated for genetic diversity with RAPD markers by Toan Duc Pham *et al.*, 2011 revealed relatively high genetic diversity. Similarly Satyendra Nath, 2014 studied with 200 RAPD markers to determine the genetic diversity among 60 Indian sesame genotypes. Germplasm collected from different geographical regions of the world were also analyzed for genetic diversity by Rajendra Pujar and Chandrashekar Patil, 2016. They studied 40 sesame germplasms screened RAPD markers and obtained 122 polymorphic fragments. High genetic diversity was also obtained by Soumen Saha *et al.*, 2019 when 15 sesame germplasm from West Bengal were analyzed for genetic diversity with RAPD markers. Patil *et al.*, 2016 also worked with RAPD markers to determine the polymorphism among the sesame accessions. Sarita Pandey *et al.*, 2015 confirmed that both genetic and phenotypic diversity in a combined way could efficiently evaluate the variations present by studying 60 genotypes with 36 microsatellite markers.

Ghulam Ali, 2007 assessed 96 sesame accessions collected from different parts for the world using AFLP technique. Twenty one primers generated a total of 445 bands and among them 157 were polymorphic. Florent Jean-Baptiste Quenum and Qichuan Yan, 2017 assessed genetic variation among a mini core germplasm of sesame using biochemical and RAPD markers. A SDS-PAGE of protein extracts of sesame seeds revealed 31 protein markers, out of which only 4 were polymorphic indicated that this technique is also suitable for studying genetic diversity. Mediterranean sesame accessions were analyzed for genetic diversity with 5292 high quality SNPs identified by double-digest restriction site associated DNA (dd RAD) sequencing by Merve Basak *et al.*, 2019. Results indicated a highly dense genetic resource among the collection and with a genetic distance between pairs of accessions 0.023 to 0.524.

Table I: Over view of the genetic diversity assessment with different molecular marker systems in *Sesamum indicum*

S.No.	Author	Collection	Accessions	Marker Type	Marker Number	Result
1	Anupam dixit <i>et al.</i> , 2005	Korean	16	SSR	50	PIC ranged from 0.34 to 0.80
2	Ghulam Ali 2007	Different parts of the world	96	AFLP	21	65% polymorphic
3	Abdellatef E <i>et al.</i> , 2008	Sudan	10	RAPD	25	Low level of similarity
4	Hernan Laurentin <i>et al.</i> , 2008	Different parts of the world	10	AFLP	8	Traits affected by chemical phenotype
5	Ummu Seyitalioglu 2010	Turkish	161	EST-SSR	318	Low Genetic Diversity
6	Daniel Endale Gebremichael and	Ethiopian	50	SSR	10	PIC ranged from 0.393 to 0.820

**Review Article**

	Heiko K Parzies 2010					
7	Fazal Akbar <i>et al.</i> , 2011	Pakistan	20	RAPD	10	75% polymorphic
8	Toan Duc Pham <i>et al.</i> , 2011	Cambodia and Vietnam	12	RAPD	10	Highly polymorphic
9	Sharad Tiwari <i>et al.</i> , 2011	Different parts of the world	96	AFLP	21	35% polymorphic
10	Vijaya Sudhakar Rao Kola 2012	India	9	SSR	207	Good Variability
11	Hitesh Kumar <i>et al.</i> , 2012	Punjab, India	94	ISSR	34	Overlapping diversity
12	Admas Alemu <i>et al.</i> , 2013	Ethiopia and North western region	6	ISSR	4	High genetic diversity
13	Arna Das <i>et al.</i> 2013	Indian genotypes	7	EST- SSR	4	Genetic diversity value above 0.5 between parents
14	Jong-Hyun Park <i>et al.</i> , 2014	Korea and China	70	SSR	14	PIC=0.23to 0.77
15	Satyendra Nath Sharma 2014	Indian genotypes	60	RAPD	10	High polymorphism
16	Nweke Friday Nwalo, 2015	Nigerian	30	SSR	10	High genetic variability
17	Sarita K Pandey <i>et al.</i> 2015	Different parts of the world	60	EST- SSR	36	High Diversity
18	Mohammed Abate <i>et al.</i> , 2015	Ethiopia	128	ISSR	7	92.2% polymorphic
19	Admas Alemu <i>et al.</i> , 2015	Farmer cultivars and north western Ethiopia	6	ISSR	4	High genetic diversity
20	Anne Frary <i>et al.</i> , 2015	Turkish	137	AFLP	140	Low Variability
21	Kiranmayi SL <i>et al.</i> , 2015	Andhra Pradesh, India	23	SSR	10	4 markers polymorphic
22	Komivi Dossa <i>et al.</i> , 2016	22 countries	96	SSR	33	Large genetic variability
23	Tapaswini Hota <i>et al.</i> , 2016	Different geographical regions of the India	33	ISSR	30	85.08% polymorphic
24	Kiranmayi <i>et al.</i> , 2016	Local area of Andhra Pradesh, India	23	SSR	10	4 % polymorphic
25	Rajendra B Pujar and Chandrashekar Patil G 2016	Dharwad, India	40	RAPD	28	High level of polymorphism

**Review Article**

26	Patil CG <i>et al.</i> , 2016	Dharwad, India	7	RAPD	28	Average Polymorphism
27	Anandan R <i>et al.</i> , 2017	Tamil Nadu, India	9	RAPD and SSR	10	Appropriate for evaluation of low diversified sesame varieties
28	Bazel H Ali Al somain <i>et al.</i> , 2017	Saudi and from different geographical environment	52	SRAP	17	High Degree of genetic polymorphism
29	Florent Jean-Baptiste Quenum and Qichuan Yan 2017	China	15 Mini core germplasm	RAPD	53	High Genetic Similarity
30	Sovetgul <i>et al.</i> , 2018	Korea	129	SSR	70	High variance individuals within populations
31	Labhya Rani Gogoi <i>et al.</i> , 2018	Jorhat, India	33 Indigenous genotypes	SSR	27	High diversity among local germplasm, PIC=0.43
32	Rapheal <i>et al.</i> , 2019	Northern Ghana	25 land races	SSR	38	Highly polymorphic
33	Eveline de Sousa Araujo <i>et al.</i> , 2019	Brazil	36	SSR	10	Significant genetic diversity
34	Souman Saha <i>et al.</i> , 2019	West Bengal, India	15	RAPD	25	High Genetic diversity
35	Maini Bhattacharjee <i>et al.</i> , 2019	Different parts of West Bengal, parts of India and USA and Bulgaria	30	SSR	32	PIC=0.87

**IDENTIFICATION OF QTLS AND LINKAGE MAPS**

Restriction Fragment Length Polymorphism is considered as the first DNA-based molecular marker system and it is used for the preparation of linkage maps and for mapping of several traits of interest in many crops. The greater abundance and other desirable features of RFLPs as compared to phenotype and protein markers, prompted the development of other relatively more convenient DNA marker systems like random amplified polymorphic DNA (RAPD), amplified fragment length polymorphism (AFLP), simple sequence repeat (SSR), etc. Single nucleotide polymorphism (SNP) has emerged as the most abundant molecular marker that is amenable to high-throughput genotyping. RAPD method detects high level of polymorphism in plants and used to construct high-density genetic maps in several crop species(Singh and Singh, 2015).

Haiyang Zhang *et al.*, 2013 were the first to study QTL with high density linkage map in Sesamum. Two accessions co11134(white seeded, P1) and R x BS (black seeded, P2) were taken for segregation, three replicates of the P<sub>1</sub>, P<sub>2</sub>, F<sub>1</sub>, BC1, BC2 and F<sub>2</sub> populations were grown. An F<sub>2</sub> population of 260 is taken to construct a genetic linkage map and locate QTLs. Estimated size of the sesame genome is 1380.938cM. A total of 653 marker loci were identified on 14 linkage groups. The dominant heritability for all QTLs

### Review Article

ranged from 1.28-7.18%. A significant negative correlation in oil content with that of protein content were found through association mapping among 369 world-wide sesame germplasm accessions under five environments using 112 polymorphic SSR markers when used by Chun Li *et al.*, 2014 (Table II)

Kun Wu *et al.*, 2014 identified a total of 3,769 SNPs from RAD-Seq using 89 polymorphic PCR markers including 44 Expressed Sequence Tag- simple sequence repeats (EST-SSRs), 10 genomic SSRs and 35 Insetion-Deletion Markers. The final map resulted in 1,230 markers distributed on 14 linkage groups. While Venkata Ramana Rao *et al.*, 2014 developed a molecular map for important agro-botanic traits in sesame. Two genotypes, Chandana and TAC-89-309 were studied for F<sub>2</sub> population, F<sub>1</sub> and Parents were evaluated under field conditions for nine agro-botanic traits. Based on parental polymorphism (23.07%), a mapping population of 120 F<sub>2</sub> individual with 60 RAPD markers were selected to map nine linkage groups, and about 60% of the genome with length ranging between 58.8 to 423.8cM resulted in identification of nineteen QTL and two genomic regions. Out of the 19 QTLs identified, one QTL for corolla colour, number of nodes were detected.

Yanxin Zhang *et al.*, 2013 constructed a high density genetic map containing 201,488,285 pair-end reads. Total of 71,793 high quality SLAFs were detected of which 3,673 SLAFs were polymorphic and 1,272 of the polymorphic markers met the requirement of use in the construction of a genetic map. Lin Bin *et al.*, 2009 used three types of PCR-based markers to construct a map for F<sub>2</sub> segregating population of an intraspecific cross between two cultivars of sesame. Ten EST-SSR markers, 80 AFLP markers and 244 RSAMPL markers were screened to obtain 284 polymorphic loci. A total of 220 molecular markers were mapped in 30 linkage groups with a genetic length of 936.72cM. Haiyang Zhang *et al.*, 2013 studied sesame cp(chloroplast) genome which is a circular molecule containing a total of 153,338 base pairs and a total of 114 unique genes. Similar study was carried out by Dong-Keun Yi and Ki-Joong Kim (2012) on complete chloroplast (cp) genome of *S. indicum*. The length is almost similar with slight variation of 153,324bp and has a pair of inverted repeat (IR) regions that comprise 25,141bp each. The two IR regions divide the genome into a large single copy (LSC) region and a small single copy (SSC) region. The LSC region is 85,170bp, whereas the SSC region is 17,872bp. The complete cp sequence of *S.indicum* is 153,324bp in length of which 58% is coding regions and 42% is non-coding regions.

In recent studies, genome-wide SNP makers were used for assessing genetic diversity structure and linkage disequilibrium by Chengqi Cui *et al.*, 2017. Genotyping of 366 sesame germplasm accessions by using 89,924 high quality SNPs. All these SNPs covered all 13 linkage groups. Largest number of SNPs were found on LG5 followed by LG3 and least number occurred on LG4 with lowest marker density on LG6. Further studies by Haiyang Zhang *et al.* 2016 in determining the growth habit indicated that sesame recessive gene controls the determinate trait dt1 and a second determinate line, dt2. Later, Hua Du *et al.* 2019 constructed a genetic map which compromised of 2159 SNP markers distributed on 13 linkage groups and was 2128.51cM in length with an average distance of 0.99 cM between adjacent markers.

Linhai Wang *et al.*, 2017 through his study, developed 7,357 SSR markers from sesame genome and transcriptomes and a genetic map was constructed by generating 424 novel polymorphic markers using cross pollination with 548 recombinant inbred lines. The genetic map developed with 13 linkage groups, ranged in size of 113.6 to 179.9cM and 14 QTL for sesame Charcoal rot disease resistance. Similar approach was carried out by Ayse Ozgur Uncu *et al.*, 2016 studied through sequencing analysis resulted in a total of 15,521 SNPs. Ramya and Bhat, 2018 developed 60 SSR markers used in genomic hybridization assay, of which 12 were found to be polymorphic. The linkage map constructed contained 26 markers in three linkage groups covering a distance of 298.6cM, 694.4cM and 86.4cM. Similar study was also carried out by Xin Wei *et al.*, 2014 in genetic linkage map construction and marker assisted selective breeding in sesame to identify a total of 218 SSR markers through whole genome survey.

Genes for morphological as well as biological traits were also studied to construct high resolution genetic maps. Hongxian Mei, 2017 constructed a genetic map with 9,378 SLAF markers with 13 linkage groups. The map spanned a total genome of 1,974.23 cM and the mean LG length of 151.86 cM. Genes for basal branching habit and flowers per leaf axils were mapped to LG5 and LG11 respectively. Haiyang Zhang;

**Review Article**

Hongmei Miao *et al.*, 2013 analyzed genetic segregation and quantitative trait loci(QTL) for sesame seed coat in 6 generations. Results showed that two major genes with additive-dominant epistatic effects and polygene with additive-dominant epistatic effects were responsible for controlling seed coat color trait. Rong Zhou *et al.*, 2018 studied genome-wide association of 39 sesame seed yield related traits. They observed a total of 646 loci were significantly associated with the 39 traits and resolved to 547 quantitative trait loci(QTLs). Genome wide association study was carried out by Komivi Dossa *et al.*, 2019 for traits related to drought tolerance using 400 diverse sesame accessions, including landraces and modern cultivars revealed ten stable QTLs explaining more than 40% of the phenotypic variation and four linkage groups were significantly associated with drought tolerance related traits.

Table II: Genetic and Association mapping studies in *Sesamum indicum*

S.No.	Author	Trait/genome assembly	Marker Type/method	Population studied	Result
1	Lin-Bin <i>et al.</i> , 2009	Linkage map	EST-SSR, AFLP, RSAMPL	F2 segregation	Genome length 1,232.53 cM
2	Dong-Keun Yi and Ki-Joong Kim 2012	Chloroplast genome	Cp DNA sequence analysis	-----	Chloroplast genome size 153,324 bp in length
3	Yanxin Zhang <i>et al.</i> , 2013	High density genetic map	SLAF-seq	F2 population	Final map length 1,474.87cM
4	Haiyang Zhang, <i>et al.</i> , 2013	Seed coat colour	AFLP and RSAMPL	P1, P2, F1, BC1, BC2, and F2	Two major genes for seed coat colour
5	Haiyang Zhang <i>et al.</i> , 2013	Chloroplast genome	Illumina technology	-----	Chloroplast genome size 153,338 bp in length
6	Chun <i>et al.</i> , 2014	Seed oil and protein content	SSR	369 germplasm accessions	A negative correlation to oil content to protein content
7	Venkata Ramana Rao <i>et al.</i> , 2014	Agro-botanic traits	60 RAPD	120 F2	19 QTLs identified
8	Kun Wu <i>et al.</i> , 2014	Grain traits	RAD-seq	RIL	13 QTL identified
9	Ayse Qzgur Uncu <i>et al.</i> , 2016	-----	Genotyping by Sequencing approach	RIL population	15,521 SNPs identified
10	Haiyang Zhang 2016	Growth habit	Re-sequencing	Parents and F2 population	Same recessive gene controls the dt1 and dt2
11	Linhai Wang <i>et al.</i> , 2016	Plant height and seed coat colour	Genome assembly	430 recombinant inbred lines	41 QTLs for plant height and 9 for seed coat colour
12	Chengqui Cui <i>et al.</i> , 2017	Growth habit	Genome wide SNP	366 sesame accessions	LG5, LG3 largest SNPs identified
13	Linhai Wang <i>et al.</i> , 2017	Charcoal rot resistance	SSR	548 recombinant inbred lines	14 QTL for charcoal rot disease resistance

**Review Article**

14	Hongxian Mei <i>et al.</i> , 2017	Basal branching & flower per leaf axil	SLAF-seq	300 population of BC1	Genetic distance 1,974.23cM
15	Ramya P an Bhat KV 2018	Yield traits	SSR	Hybridization Assay	Three linkage groups
16	Rong Zhou <i>et al.</i> , 2018	39 seed yield related	Genome wide association studies	705 diverse lines	82 QTLs and candidate genes, SiLPT3 and SiACS8
17	Hua Du <i>et al.</i> , 2019	Seed related	SLAF-seq	F2 population	Genetic map 2128.51 cM in length
18	Komivi Dossa <i>et al.</i> , 2019	Drought tolerance	Genome wide association studies	400 diverse accessions	Ten stable QTLs identified

**CONCLUSION**

Due to increasing demand for edible oils with the growing population, there is substantial need to increase cultivation of oil crops. Among the different oil crops cultivated, *Sesamum indicum* cultivation is increasing on a larger scale, and there is a need for extensive research in obtaining better varieties which are high in yield traits. So far minimum molecular studies were carried out. Still there is a need for further studies and its confirmation. And more important, there is a need to stabilize the results obtained and further carry out extensive studies which improves the yielding aspects by balancing abiotic and biotic factors through molecular techniques in *Sesamum indicum*

**REFERENCES**

**Abdellatif E, Sirelkhaten R, Mohamed Ahmed MM, Radwan KH and Khalafalle MM (2008).** Study of genetic diversity in Sudanese sesame (*Sesamum indicum* L.) germplasm using random amplified polymorphic DNA(RAPD) markers. *African Journal of Biotechnology*, **7**(24) 4423-4427.

**Admas Alemu, Yohannes Petros and Kassahun Tesfaye (2013).** Genetic Distance of Sesame (*Sesamum indicum* L.) Cultivars and Varieties from North Western Ethiopia using Inter Simple Sequence Repeat Markers. *East African Journal of Sciences*, **7**(1) 31-40.

**Anupam Dixit, Ming-Hua Jin, Jong-Wook Chung, Jae-Woong Yu, Hun-Ki Chung, Kyung-Ho Ma, Yong-Jin Park and Eun-GI Cho (2005).** Development of Polymorphic microsatellite markers in sesame (*Sesamum indicum* L.). *Molecular Ecology Notes*, **5** 736-738.

**Aejaz Ahmad Dar, Sushma Mudigunda, Pramod Kumar Mittal, Neelkantan Arumugam (2017).** Comparative assessment of genetic diversity in *Sesamum indicum* L. using RAPD and SSR markers. *3 Biotech*, **7** 10.

**Anandan R, Deenathayalan T, Prakash M, Sunilkumar B and Narayanan (GS 2017).** Assessment of genetic diversity among sesame (*Sesamum indicum* L.) germplasm as revealed by RAPD and SSR markers. *Indian Journal of Biochemistry and Biophysics*, **55** 143-150.

**Arna Das, Sarita Pandey, Tapash Dasgupta (2013).** Association of Heterosis with Combining Ability And Genetic Divergence in Sesame (*Sesamum indicum* L.). *International Journal of Scientific and Technology Research*, **2**(12) 307-314.

**Ayse Ozgur Uncu, Anne Frary, Petr Karlovsky, Sami Donganlar (2016).** High through put single nucleotide polymorphism(SNP) identification and mapping in the sesame (*Sesamum indicum* L.) genome with genotyping by Sequencing (GBS) analysis. *Molecular Breeding*, **36** 173.

**Bedigian D (2004).** History and Lore of Sesame in Southwest Asia. *Economic Botany*, **58**(3) 329-353.



**Review Article**

**Bradley Morris J (2002).** Food, Industrial, Nutraceutical, and Pharmaceutical Uses of Sesame Genetic Resources. *Trends in new crops and new uses*. ASHS Press, Alexandria, VA.

**Chengqi Cui, Hongxian Mei, Yanyang Liu, Haiyang Zhang and Yongzhan Zheng (2017).** Genetic Diversity Population structure and Linkage Disequilibrium of an Association-Mapping Panel Revealed by Genome-wide SNP markers in Sesame. *Frontiers in Plant Science*, **8** 1189.

**Cooney RV, Custer LJ, Okinaka L and Franke AA (2001).** Effects of dietary sesame seeds on plasma tocopherol levels. *Nutrition and Cancer*, **39**(1) 66-71.

**Chun Li, Hongmei Miao, Libin Wei, Tide Zhang, Xiuhua Han, Haiyang Zhang (2014).** Association Mapping of Seed oil and Protein content in *Sesamum indicum* L. using SSR markers. *PLOS ONE* **9**(8). E105757.

**Daniel Endale Gebremichael and Heiko Parzies K (2010).** Genetic Variability Among landraces of Sesame in Ethiopia. *African Crop Science Journal*, **19**(1) 1-13.

**Dong-Keun Yi, and Ki-Joong Kim (2012).** Complete Chloroplast Genome Sequence of Important Oilseed Crop *Sesamum indicum* L. *PLOS ONE*, **7**(5) e35872.

**Dagmawi Teshome Woldeesenbet, Assahun Tesfaye and Endashaw Bekale (2015).** Genetic diversity of Sesame germplasm collection(*Sesamum indicum* L.) Implication for conservation, improvement and use. *International Journal for Biotechnology and Molecular Biology Research*, **6**(2) 7-18.

**Ekta Sharma, Tajamul Islam Shah and Fatima Khan (2014).** A review enlightening genetic divergence in *Sesamum indicum* based on morphological and molecular studies. *International Journal of Agriculture and Crop Sciences*, **7**(1) 1-9.

**Elly Kafiriti and Omari Mponda (2008).** Soils, Plant Growth And Crop Production – Growth and Production of Sesame. *Encyclopedia of Life Support Systems (EOLSS)*.

**Eveline de Sousa Araujo, Nair Helena Castro Arriel, Roseane Cavalcanti dos Santos, Liziane Maria de Lima (2019).** Assessment of Genetic Diversity variability in sesame accessions using SSR markers and morpho agronomic traits. *Australian Journal of Crop Science*, **13**(01) 45-54.

**Fazal Akbar, Ahiq Rabbani M, Shahid Masood M and Zabta Shinwari K (2011).** Genetic Diversity of Sesame (*Sesamum indicum* L.) Germplasm From Pakistan using RAPD markers. *Pakistan Journal of Botany*, **43**(4) 2153-2160.

**Florent Jean-Baptiste Quenum and Qichuan Yan (2017).** Assessing Genetic Variation and relationships among a mini core Germplasm of Sesame (*Sesamum indicum* L.) using Biochemical and RAPD markers. *American Journal of Plant Sciences*, **8** 311-327.

**Ghulam Ali M, Sirato Yasumoto, Masumi Seki-Katsuta (2007).** Assessment of genetic diversity in sesame(*Sesamum indicum* L.) detected by Amplified Fragment Length Polymorphism(AFLP) markers. *Electronic Journal of Biotechnology*, **10**(1). ISSN 0717-3458.

**Haiyang Zhang, Chun Li, Hongmei Miao, Songjin Xiong (2013).** Insights from the Complete Chloroplast Genome into the Evolution of *Sesamum indicum* L. *PLOS ONE*, **8**(11) e80508.

**Haiyang Zhang, Hongmei Miao, Lei Wang, Lingbo Qu, Hongyan Liu, Qiang Wang and Meiwang Yue (2013).** Genome sequencing of the important oilseed crop *Sesamum indicum* L. *Genome Biology* **14** 401.

**Haiyang Zhang, Hongmei Miao, Libin Wei, Chun Li, Ruihong Zhao and Cuiying Wang (2013).** Genetic Analysis and QTL Mapping of Seed coat colour in sesame (*Sesamum indicum* L.). *PLOS ONE* **8**(5) e63898.

**Haiyang Zhang, Hongmei Miao, Chun Li, Libin Wei, Yinghui Duan, Qin Ma, Jingjing Kong, Fangfang xu and Shuxian Chang (2016).** Ultra-dense SNP genetic map construction and identification of SiDt gene controlling the determinate growth habit in *Sesamum indicum* L. *Scientific Reports*. **6** 31556.

**Hua Du, Haiyang Zhang, Libin Wei, Chun Li, Yinghui Duan and Huili Wang (2019).** A high-density genetic map constructed using specific length amplified fragment(SLAF) sequencing and QTL mapping of seed related traits in Sesame (*Sesamum indicum* L.) *BMC Plant Biology*, **19** 588.

**Review Article**

**Hongxian Mei, Yanyang Liu, Zhenwei Du, Ke Wu, Chengqi Cui, Xiaolin Jiang, Haiyang Zhang and Yongzhan Zheng (2017).** High-Density Genetic Map Construction and Gene Mapping of Basal Branching Habit and Flowers per Leaf Axil in Sesame. *Frontiers in Plant Sciences*, **8** 636.

**Hernan Laurentin, Astrid Ratzinger and Petr Karlovsky (2008).** Relationship between metabolic and genomic diversity in sesame (*Sesamum indicum* L.). *BMC Genomics*, **9** 250.

**Hitesh Kumar, Gurpreet Kaur and Shashi Banga (2012).** Molecular Characterization and Assessment of Genetic diversity in sesame (*Sesamum indicum* L.) germplasm collection using ISSR markers. *Journal of Crop Improvement*, **26** 540-557.

**Jong-Hyun Park, Sudan Suresh, Gyu-Taek Cho, Nag-Gor Choi, Hyung-Jin Baek, Chul-Won Lee and Jong-Wook Chung (2013).** Assessment of molecular genetic diversity and population structure of sesame (*Sesamum indicum* L.) core collection accessions using simple sequence repeat markers. *Plant Genetic Resources*, **12**(1) 112-119.

**Jyothi Badri, Vijay Yepuri, Anuradha Ghanta, Sivaramakrishnan Siva, Ebrahimali Abubacker Siddiq (2014).** Development of microsatellite markers in sesame(*Sesamum indicum*L.). *Turkish Journal of Agriculture and Forestry*, **38** 603-614.

**Kato MJ, Chu A, Davin LB, Lewis NG (1998).** Biosynthesis of antioxidant lignans in *Sesamum indicum* seeds. *Phytochemistry*, **47** 583-591.

**Khames A Mourad, Rasha YS Abd El-Khalek and Nemat A Naguib (2019).** Determination of Genetic Diversity in Sesame. *Zagazig Journal Agriculture Research* **46**(2) 279-293.

**Kiranmayi SL, Roja V, Padmalatha K, Sivaraj N and Sivaramakrishnan S (2016).** Genetic Diversity Analysis in sesame(*Sesamum indicum*) using morphological, Biochemical and Molecular techniques. *International Journal of Applied Biology and Pharmaceutical Technology*, **7**(1) ISSN 0976-4550.

**Komivi Dossa, Xin Wei, Yanxin Zhang, Daniel Fonceka, Wenjuan Yang, Diaga Diouf, Boshou Liao, Ndiaga Cisse and Xiurong Zhang (2016).** Analysis of Genetic Diversity and population Structure of Sesame Accessions from Africa as Major Centres of its Cultivation. *Genes*, **7** 14.

**Komivi Dossa, Donghua Li, Rong Zhou, Jingyin Yu, Linhai Wang, Yanxin Zhang, Jun You, Ali Liu, Marie A Mmadi, Daniel Fonceka, Diaga Diouf, Ndiaga Cisse, Xin Wei and Xiurong Zhang (2019).** The genetic basis of drought tolerance in the high oil crop *Sesamum indicum*. *Plant Biotechnology Journal*, 1-16.

**Komivi Dossa, Diaga Diouf, Linhai Wang, Xin Wei, Yanxin Zhang, Mareme Niamg, Daniel Fonceka, Jingyin Yu, Marie A Mmadi, Louis W Yehouessi, Boshou Liao, xiurong Zhang, Ndiaga Cisse (2017).** Review: The Emerging Oilseed Crop *Sesamum indicum*. Enters the “Omics” Era. *Front Plant Science*, **8** 1154.

**Kun Wu, Hongyan Liu, Minmin Yang, Ye Tao, Huihui Ma, Wenxiong Wu, Yang Zuo and Yingzhong Zhao (2014).** High density genetic map construction and QTLs analysis of grain yield related traits in Sesame(*Sesamum indicum* L.) based on RAD-Seq technology. *BMC Plant Biology*, **14** 274.

**Labhya Rani Gogoi, Sushil Kumar Singh and Sarma RN (2018).** Assessment of Genetic diversity in Indigenous Sesamum genotypes. *International Journal of Current Microbiology and Applied Sciences*, **7**(6) 1509-1520.

**Lin-Bin Wei, Hai-Yang Zhang, Yong-zhan Zhang, Hong-Mei Miao, Tian-Zhen Zhang and Wang-Zhen Guo (2009).** A Genetic Linkage Map Construction for Sesame (*Sesamum indicum* L.). *Genes & Genomics*, **31**(2) 199-208.

**Linhai Wang, Yanxin Zhang, Xiaodong Zhu, Xiaofeng Zhu, Donghua Li, Xianmei Zhang, Yuan Gao, Guobin, Xin Wei and Xiurong Zhang (2017).** Development of an SSR-based genetic map in sesame and identification of quantitative trait loci associated with charcoal rot resistance. *Scientific Reports*, **7** 8349.

**Maini Bhattacharjee, Adil Iqbal, Sanjana Singha, Disharee Nath, Sh Prakash and Tapash Dasgupta (2019).** Genetic diversity in *Sesamum indicum*. *Bangladesh Journal of Botany*, **48**(3) 497-506.

**Review Article**

- Merve Basak, Bulent Uzun and Engin Yol (2019).** Genetic Diversity and population structure of the Mediterranean sesame core collection with use of genome-wide SNPs developed by double digest RAD-Seq. *PLOS ONE*, **4**(10) e0223757.
- Mina Kazemian Ruhi, Ahmad Majd and Parisa Jonoubi (2014).** Study of Anatomical Structure of Vegetative Organs, Floral Meristem and Pollen Development in sesame. *International Journal of Plant, Animal and Environmental Sciences*, **5**(1) ISSN 2231-4490.
- Mohammed Abate, Firew Mekbib, Amsalu Ayana and Mandefro Nigusie (2015).** Assessment of Genetic Diversity in Ethiopian Sesame (*Sesamum indicum* L.) Germplasm using ISSR markers. *British Biotechnology Journal*, **8**(4) 1-13.
- Nayar NM and Mehra K (2008).** Sesame: Its users, botany, cytogenetics and origins. *Economic Botany*, **24**(1) 20-31.
- Nweke, Friday Nwalo (2015).** Genetic diversity of Nigerian Sesame cultivars (*Sesamum indicum* L.) based on simple sequence repeat (SSR) markers and its relationship with phytochemicals. *International Journal of Current Microbiology and Applied Sciences*, **4**(1) 898-908.
- Patil CG Rujar RB and Patil BR (2016).** Molecular Polymorphism in cultivate *Sesame indicum* L. and its wild species using PCR based Molecular Markers. *International Journal of Pure and Applied Sciences*, **4**(2) 287-295.
- Ramya P and Bhat KV (2018).** Genetic Analysis of yield contributing traits and mapping of QTLs In a recombinant inbred line (RIL) population of sesame (*Sesamum indicum* L.) *Electronic Journal of Plant Breeding* **9**(1) 264-274.
- Rajendrnra Pujar B and Chandrashekar Patil G (2016).** Analysis of genetic diversity in sesame (*Sesamum indicum* L.) germplasm using RAPD markers and disease resistance screening through RGA markers. *Asian Journal of Biological and Life Sciences*, **5**(3).
- Raphael Adu-Gyamfi, Ruth Prempeh and Issahaku Zakaria (2019).** Diversity Assessment of some sesame (*Sesamum indicum* L.) genotypes cultivated in Northern Ghana using Morphological and Simple Sequence Repeat(SSR) markers. *Advance in Agriculture*.
- Rong Zhou, Komivi Dossa, Donghua Li, Jingyin Yu, Jun You, xin Wei and Xiurong Zhang (2018).** Genome-wide Association studies of 39 seed yield-related traits in sesame (*Sesamum indicum* L.). *International Journal of Molecular Sciences*, **19** 2794.
- Sarita K Pandey, Arna Das, Pooja Rai and Tapash Dasgupta (2015).** Morphological and Genetic diversity Assessment of Sesame (*Sesamum indicum* L.) accessions differing in origin. *Physiology .Molecular Biology of Plants*, **21**(4) 519-529.
- Satyendra Nath Sharma, Vinod Kumar, Chitra Sharma, Nidhi Shukla , Archana Gupta, Anjay Tripathi and SEema Paroatha (2014).** Characterization and analysis of genetic diversity in Indian Sesame (*Sesamum indicum* L.) genotypes. *Indian Journal of Genetics*, **74**(3) 344-352.
- Sharad Tiwari, Sunil Kumar and Itli Gontia (2011).** Mini Review: Biotechnological approaches for sesame (*Sesamum indicum* L.) and Niger (*Guizotia abyssinica* L.f.Cass.) *Asia-Pacific Journal of Molecular Biology*, **19**(1) 2-9.
- Sirato-Yasumoto S, Katsuta M, Okuyama Y, Takahashi Y and Ide T (2001).** Effect of Sesame seeds rich in sesamin and sesamol on fatty acid oxidation in rat liver. *Journal of Agricultural and Food Chemistry*, **49**(5) 2647-2651.
- Singh BD and Singh AK (2015).** Book: Marker-Assisted Plant Breeding Principles and Practices.1 *India Springer ISBN 978-81-322-2316-0*.
- Soumen Saha, Tarak Nath dhar, Parthadeb Ghosh, Tulsı Dey (2019).** Molecular Characterization of Sesame germplasms of West Bengal, India using RAPD markers. *Acta Biologica Szegediensis*, **63**(1) 15-24.
- Sovetgul Asekova, Krishnanand Kulkarni P, Ki Won Oh, Myung-Hee Lee, Eunyoung Oh, Jung-In Kim, Un-Sang Yeo, Suk-Bok Pae, Tae Joung Ha, Sung Up Kim (2018).** Analysis of Molecular

**Review Article**

Variance and Population Structure of Sesame(*Sesamum indicum* L.) Genotyping using simple Sequence Repeat Markers. *Plant Breeding Biotech*, **6**(4) 321-336.

**Tapaswini Hota, Chinmaya Pradhan, Gyana Ranjan rout (2016)**. Agromorphological and Molecular Characterization of *Sesamum indicum* L. –An Oil Seed Crop. *American Journal of Plant Sciences*, **7** 2399-2411.

**Ummu Seyitalioglu (2010)**. Msc.Thesis: Molecular Genetic Analysis in Sesame(*Sesamum indicum* L.): *Graduate School of Engineering and Sciences of Izmir Institute of Technology*.

**Ventaka Ramana Rao, Prasuna K, Anuradha G, Srividya Lakshminarayana Vemireddy R, Gourishankar V, Sridhar S, Jayaprada M, Raja Reddy K, Eswara Reddy NP and Siddiq EA (2014)**. Molecular mapping of important agro-botanic traits in sesame. *Electronic Journal of Plant Breeding*, **5**(3) 475-488.

**Vijaya Sudhakara Rao Kola, Vijay Yepuri, Malathi Surapaneni, Jyothi Badri, Vemireddy LR, Anuradha Ghanta and Ebrahimali Abudaker Siddiq (2012)**. Genetic Diversity and DNA Fingerprinting in Sesame (*Sesamum indicum* L.) Cultivars of ANGRAU. *The Asian and Australasian Journal of Plant Science and Biotechnology*, **6**(1) 98-101.

**Xin Wei, Linhai Wang, Yanxin Zhang, Xiaoqiong Qi, Xiaoling Wang, Xia Ding, Jing Zhang and Xiurong Zhang (2014)**. Development of Simple Sequence Repeat(SSR) Markers of Sesame (*Sesamum indicum*) from a Genome Survey. *Molecules*, **19** 5150-5162.

**Yanxin Zhang, Linhaia Wang, Huaigen Xin, Donghua Li, Chouxian Ma, Xia Ding, Weiguo Hong and Xiurong Zhang (2013)**. Construction of a high-density genetic map for sesame based on large amplified fragment (SLAF) Sequencing. *BMC Plant Biology*, **13** 141.

Research Article

**An Empirical Study of Association between Working Capital Management (WCM) and Profitability: Evidence from Bombay Stock Exchange (BSE) Listed FMCG Companies**

D. Sujatha<sup>a</sup>, Dr. Ch Shankar<sup>b</sup>

<sup>a</sup>Research Scholar, KLHBS, KLEF, Hyderabad

<sup>b</sup>Associate Professor of Finance, Koneru Lakshmaia Education Foundation (Deemed to be) University, Hyderabad

**Abstract**

WCM is also known as short-term financial management and is focused mainly with CA and CL activities. Due to its high impacts on profitability and liquidity, WCM is important to the success of enterprises. The study's primary objective was to examine at the impact of WCM on Profitability with reference to the BSE Listed FMCG Companies. Panel Data has been collected for Analysis, 71 FMCG listed Companies, 5 years balance sheets data used for analysis. The analysis tracked down a solid negative connection between the proportions of WC management including AR, AP, CCC, FATA, SL and DR with profitability. The findings of an investigation of the association between WCM and profitability on the Bombay Stock Exchange clearly found that the number of days AR, INV, and profitability are mostly negative. As an outcome, we say that managers can increase revenue by reducing the number of days AR and INV.

**Keywords:** Working Capital, WCM, Profitability, FMCG

**I. Introduction**

WCM is also known as short-term financial management and is focused mainly with CA and CL activities. WCM is also known as short-term financial management and is focused mainly with CA and CL activities (Richard Kofi Akoto, et, al. 2013). The way WC is managed has a significant impact on a company's profitability. This result shows that there is a specific amount of WC requirements that may optimise returns.(Deloof, 2003) defines WCM entails planning and regulating CA and CL in a way that, on the one hand, decreases the risk of incompetence in meeting required short-term needs and, on the other hand, prevents wasteful investment in these assets. (Bis.org and Eljelly, 2004). WCM is described as an accounting strategy that focuses on maintaining correct CA and CL levels. WCM gives a corporation with adequate liquidity to fulfil its short-term obligations (Raheman & Nasr, 2007). WCM is very important in terms of profitability growth. This is because the firm's activities are difficult to manage without a good WCM. WCM has been a big concern, particularly in developed nations, and as a result, research has been performed in many areas of the world, particularly in developed nations, to explain the link between WCM and profitability (Ntui Ponsian, et.al 2014).

**II. Literature Review:**

## An Empirical Study of Association Between Working Capital Management (WCM) and Profitability: Evidence from Bombay Stock Exchange (BSE) Listed FMCG Companies

**Deloof, 2003** the Study on WCM and Profitability with 1009 Belgium NFF firms for the Duration of 1992-1996. Managers may boost profitability by lowering the amount of days on the job, according to the research. AR and INV are active. A Smaller number of profitable firms stand by longer to cover their bills.

**Ioannis Lazaridis & Dimitrios Tryfonidis, 2006** investigate Study between the relationship of Profitability and WCM, with 131 From 2001 to 2004, firms were listed in the ASE. The findings of our investigation revealed that there is a real relationship between profitability, as evaluated by GPR, and the CCC. Furthermore, managers may earn revenues for their business by properly controlling the CCC and maintaining each part (AR, AP, INV) best level.

**Huynh et. al, 2010** investigate study between From 2006 to 2008, the link between profitability, CCC, and its components for listed enterprises in VSK. According to the findings, there is a considerable negative association between profitability as evaluated by GPR and the CCC. This implies that CCC raises, it lead to decreasing the profitabilit.

**Richard Kofi Akoto, et, al.,2013** Research reveals a significant unfavourable link between profitability and AR days, studied by WCM and the profitability of 13 companies in Ghana from 2005 to 2009. However, the business' CCC, CA ratio, size, and CA turnover all have a significant impact on profitability. According to the study, managers may produce value for their investors by generating incentives for their AR to be reduced to 30 days In order to enhance demand for local goods in the short and long term, community policies that safeguard indigenous firms and hinder distributor migration should be established in Ghana.

**Jakpar S1 et,al, 2017** With a sample of 164 enterprises included in MBBM from 2007 to 2011, the influence of WCM on the profitability of companies was evaluated. Exact evidence has established that the exogenous variable, ACP, INV and company size, and their endogenous variable - which is company profitability - have a positive link. The findings also demonstrate that the debt ratio (liverages) and the profitability of the company are somewhat reversed, but the company has the capacity to quickly convert WC into cash, since the proxy for the CCC log does not affect profitability.

**Kofi Amponsah-Kwatiah & Michael Asiamah, 2020** The impact examines between WCM on profitability in Ghana with From 2015 to 2019, 20 manufacturing enterprises were listed on the NYSE. According to the findings, INV management, AR, AP, CCC, CA, CR, and firm size all have a beneficial impact on ROA and ROE, however leverage has a negative impact.

### Research Methodology:

#### 1. Objectives & Hypothesis:

The study focuses on identifying the impact of WCM on Profitability (Dr. Ch Shankar, 2020).

H<sub>1</sub>: Considerable relation in between AR & GPR.

H<sub>2</sub>: Considerable relation in between AP & GPR.

H<sub>3</sub>: Considerable relation in between IN & GPR.

H<sub>4</sub>: Considerable relation in between SL & GPR.

H<sub>5</sub>: Considerable relation in between DR & GPR.

H<sub>6</sub>: Considerable relation in between FATA & GPR.

#### 2. Data Collection:

Panel Data has been collected for Analysis, 71 FMCG listed Companies, 5 years balance sheets data used for analysis.

#### 3. Variables:

The variables extracted from previous studies and existing literature. the following variables considered for this study:

- a. Gross Operating Profitability (GPR): GPR may be computed by gross revenues and gross expenses. The total assets minus financial contributions can be divided by Total Assets minus Financial Asses (Adam Hayes, 2021).

$$GPR = (\text{Sales} - \text{Cost of Goods Sold}) / (\text{Total Assets} - \text{Financial Assets})$$

- b. Account Receivables (AR): The formula to calculate AR Turnover is to add the beginning and ending AR to get the average AR for the period and then divide it into the net credit sales for the year.

$$AR = \text{Average of accounts receivable} / \text{Sales} * 365$$

- c. Account Payables (AP): AP turnover is calculated by dividing the total purchases made on credit by the average AP balance for any given period.

$$AP = \text{Average of accounts payable} / \text{Cost of goods sold} * 365$$

- d. INV (IN): Cost of beginning INV to cost of purchases during the period. This is the CoGavailable for sale. Multiply the gross profit % by sales to find the estimated CoGsold. Subtract the CoGavailable for sold from the CoGsold to get the ending INV.

$$INV = \text{Average of inventory} / \text{Cost of goods sold} * 365$$

- e. Sales (SL): Ln is the natural logarithm of the pre-emergency book value of the millions of dollars in assets. Ln(sales) is a natural record of company sales in millions a year before the offer. (Institut numerique, 2012).

- f. Debt Ratio (DR): The debt ratio is often referred to as the debt-to-asset ratio or the debt-to-total-assets ratio. Therefore, the debt ratio formulation is: total debt divided by total assets. The debt ratio is the percentage of total asset quantities due to creditors (as recorded on the balance sheet) (Harold Averkamp, 2020).

$$DR = \text{Total debt} / \text{Total assets}$$

- g. Fixed Assets to Total Assets: The fixed-to-net value ratio is a tool of financial analytics that indicates in% the part of the total FA-binding assets of your organisation. It demonstrates the extent to which firm funds, such as property, plant, and equipment, are frozen in the form of FA. (Chron Contributor, 2020).

$$FATA = \text{Fixed financial assets} / \text{Total assets}$$

### III. Data Analysis:

#### 1. Descriptive Analysis:

**Table 1: Descriptive Statistics**

	N	Minimum	Maximum	Mean	Std. Deviation	Variance	Skewness		Kurtosis	
	Statistic	Statistic	Statistic	Statistic	Statistic	Statistic	Statistic	Std. Error	Statistic	Std. Error
GPR	71	-.2884	1.0999	.210244	.2170051	.047	1.367	.285	4.188	.563

**An Empirical Study of Association Between Working Capital Management (WCM) and Profitability:  
Evidence from Bombay Stock Exchange (BSE) Listed FMCG Companies**

AR	71	.0574	165.2523	38.855764	33.0799850	1094.285	1.528	.285	2.907	.563
AP	71	2.8222	218.0730	46.401898	36.9049052	1361.972	2.233	.285	7.143	.563
IN	71	-148.8648	156.4138	80.164265	49.3727639	2437.670	-1.506	.285	5.510	.563
CCC	71	-130.5986	219.3115	72.618130	68.9425962	4753.082	-.308	.285	.342	.563
DR	71	.1611	2.6828	.725341	.4785038	.229	1.734	.285	4.257	.563
FATA	71	.0000	.5168	.031445	.0811119	.007	4.014	.285	19.138	.563
SL	71	6.766422	12.246105	8.98122479	1.206611904	1.456	.232	.285	.015	.563
Valid N (listwise)	71									

Intpretation:

The total observations sums N = 71 Companies 5 years data. The GPR average is 0.210 and variance is 0.47. AR mean 38.85 and the variance shows 1094.285 where as AP mean is 46.40 and the SD is 36.90. The average INV is 80.16 where as variance is 2437.67. the debt ratio is 0.725 and the variance is 0.229.

**2. Correlations:**

**Table 2: Correlations**

	GPR	AR	AP	IN	CCC	DR	FATA	SL
GPR Pearson Correlation	1	-.353**	-.036	-.055	-.189	-.144	.129	.313**
Sig. (2-tailed)		.003	.769	.651	.114	.230	.283	.008
N	71	71	71	71	71	71	71	71
AR Pearson Correlation	-.353**	1	.108	-.313**	.198	.160	.051	-.352**
Sig. (2-tailed)	.003		.372	.008	.097	.183	.675	.003
N	71	71	71	71	71	71	71	71
AP Pearson Correlation	-.036	.108	1	-.314**	-.708**	.577**	.013	.140
Sig. (2-tailed)	.769	.372		.008	.000	.000	.913	.243
N	71	71	71	71	71	71	71	71
IN Pearson Correlation	-.055	-.313**	-.314**	1	.734**	.012	.031	.215
Sig. (2-tailed)	.651	.008	.008		.000	.919	.800	.072



N		71	71	71	71	71	71	71	71
CCC	Pearson Correlation	-.189	.198	-.708**	.734**	1	-.223	.039	-.090
	Sig. (2-tailed)	.114	.097	.000	.000		.061	.746	.454
	N	71	71	71	71	71	71	71	71
DR	Pearson Correlation	-.144	.160	.577**	.012	-.223	1	.023	.219
	Sig. (2-tailed)	.230	.183	.000	.919	.061		.850	.067
	N	71	71	71	71	71	71	71	71
FATA	Pearson Correlation	.129	.051	.013	.031	.039	.023	1	.121
	Sig. (2-tailed)	.283	.675	.913	.800	.746	.850		.316
	N	71	71	71	71	71	71	71	71
SL	Pearson Correlation	.313**	-.352**	.140	.215	-.090	.219	.121	1
	Sig. (2-tailed)	.008	.003	.243	.072	.454	.067	.316	
	N	71	71	71	71	71	71	71	71

\*\* .2-tailed Correlation significant at 0.01 level.

Intpretation:

GPR shows a negative relationship with AR, AP,IN, CCC and DR, and it has a positive correlationship with FATA and SL. AR shows a positive relationships with AP, IN, CCC and FATA. AP shows a high correlationship with CCC. IN shows a high positive correlationship with CCC. FATA shows a less positive corelation with other variables.

**3. Regression:**

**Variables Entered/Removed<sup>a</sup>**

Model	Variables Entered	Variables Removed	Method
1	SL, CCC, FATA, DR, AR, AP <sup>b</sup>	.	Enter

a. Dependent Variable: GPR

b. Tolerance = .000 limit reached.

**Model Summary<sup>b</sup>**

Model	R	R Square	Adjusted R Square	Std. Error of the Estimate	Change Statistics					Durbin-Watson
					R Square Change	F Change	df1	df2	Sig. Change	

An Empirical Study of Association Between Working Capital Management (WCM) and Profitability:  
Evidence from Bombay Stock Exchange (BSE) Listed FMCG Companies

1	.492 <sup>a</sup>	.242	.171	.1975520	.242	3.411	6	64	.006	2.172
---	-------------------	------	------	----------	------	-------	---	----	------	-------

a. Predictors: (Constant), SL, CCC, FATA, DR, AR, AP

b. Dependent Variable: GPR

**ANOVA<sup>a</sup>**

Model		Sum of Squares	df	Mean Square	F	Sig.
1	Regression	.799	6	.133	3.411	.006 <sup>b</sup>
	Residual	2.498	64	.039		
	Total	3.296	70			

a. Dependent Variable: GPR

b. Predictors: (Constant), SL, CCC, FATA, DR, AR, AP

**Collinearity Diagnostics<sup>a</sup>**

Model	Dimension	Eigenvalue	Condition Index	Variance Proportions						
				(Constant)	AR	AP	CCC	DR	FATA	SL
1	1	4.811	1.000	.00	.01	.00	.00	.01	.01	.00
	2	.850	2.379	.00	.00	.02	.02	.01	.74	.00
	3	.778	2.487	.00	.01	.03	.11	.01	.23	.00
	4	.336	3.781	.00	.67	.00	.01	.01	.00	.00
	5	.162	5.448	.01	.01	.02	.05	.70	.00	.01
	6	.056	9.271	.02	.12	.93	.80	.23	.00	.02
	7	.007	26.723	.97	.18	.00	.00	.04	.02	.96

a. Dependent Variable: GPR

**Coefficients<sup>a</sup>**

Model		Unstandardized Coefficients		Standardized Coefficients	t	Sig.	Collinearity Statistics	
		B	Std. Error	Beta			Tolerance	VIF
1	(Constant)	-.029	.208		-.140	.889		
	AR	-.001	.001	-.159	-1.210	.231	.687	1.456
	AP	-.001	.001	-.200	-.977	.332	.283	3.538

CCC	-.001	.001	-.310	-1.750	.085	.377	2.649
DR	-.061	.065	-.135	-.942	.350	.576	1.736
FATA	.327	.295	.122	1.108	.272	.973	1.027
SL	.049	.022	.272	2.191	.032	.768	1.302

a. Dependent Variable: GPR

#### Intepretation:

The CCC is used popular to determine effectiveness of WCM. From the aftereffect of the regression, running shows that there is a negative correlation among's CCC and GPR. This implies increase or decrease in CCC fundamentally influences the profitability of the firm. R2 change is 17.1%.The coefficient of the F measurement is 3.411. The coefficient is - 0.310 by p-value 0.085.

“The regression model verified for multicollinearity. VIF or explanatory tolerances are used to determine if predictors are closely associated with the remainder of the predictors. If your forecaster is correlated VIF examines the variance of the projected retrogression rate rise (Dimitrios 2006). Lazaridis, Ioannis & Tryfonidis. Muticollinearity is typically used as the biggest VIF incorporating all predictors. All of the foretellers have an inflation factor of 1-3.5, which fully shows that the predictors in the regression models do not have multicollinearity (D.C. Montgomery and E.A. Peck (1982).

#### IV. Findings, Conclusions and Suggestions:

This paper support for existing literatures such as Deloof(2003), Ioannis Lazaridis & Dimitrios Tryfonidis (2006), Huynh Phuong Dong & Jyh-tay Su (2010) , Richard Kofi Akoto, et, al. (2013) and who tracked down a solid negative connection between the proportions of WCM including AR, AP, CCC, FATA, SL and DR with profitability.

The negative correlation between AR-measured profitability and CCC-measured WCM efficiency demonstrates that when CCC is longer, profitability is smaller. This study indicates that managers can increase shareholder value by lowering the CCC to a tolerable level.

The results of a research of the relationship between WCM and profitability on the BSE also show that there is a negative relationship between the number of days AR, the number of days INV, and profitability. As a result, we contend that managers increase profitability by reducing the number of days AR and INV.

Furthermore, our analysis suggests that profitable enterprises are waiting for retentive to pay their expenses. However, compared to other earlier research on the association between WCM and profitability, the duration of the present study is brief. The sample does not reflect the population profoundly, thus. Furthermore, the research only refers to internal elements but does not examine outside influences the degree of economic activity as a stupid industry. For future studies these constraints might be overcome by a gander.

#### REFERENCE

- [1] Adam Hayes (2021), “Corporate Finance & Accounting”, Retrieved from <https://www.investopedia.com/terms/g/grossprofit.asp>
- [2] Amponsah-Kwatiah, K. and Asiamah, M. (2020), "WCMand profitability of listed manufacturing firms in Ghana", International Journal of Productivity and Performance Management, Vol. ahead-of-print No. ahead-of-print. <https://doi.org/10.1108/IJPPM-02-2020-0043>
- [3] Chron Contributor (2020) “How to Interpret Assets-to-Net-Worth Ratios”, Retrieved from <https://smallbusiness.chron.com/interpret-assetstonetworth-ratios-57281.html>
- [4] D.C. Montgomery and E.A. Peck (1982). Introduction to Linear Regression Analysis. John Wiley & Sons.

An Empirical Study of Association Between Working Capital Management (WCM) and Profitability:  
Evidence from Bombay Stock Exchange (BSE) Listed FMCG Companies

- [5] Deloof M. (2003), “Does WCM Affect Profitability of Belgian Firms?”, ‘Journal of Business Finance & Accounting’, 30 (3) & (4), p. 585
- [6] Eljelly, A. M. (2004). “Liquidity-profitability tradeoff: An Empirical Investigation in an Emerging Market”. *International Journal of Commerce and Management*, 14(2), 48-61.
- [7] Dr. Ch Shankar (2020), “Decision Behavior of Farmers’ on Adoption of Price Risk Management: Structure Equation Modeling Approach”, *PSYCHOLOGY AND EDUCATION* (2020) 57(9): 1718-1725, ISSN: 00333077
- [8] Harold Averkamp (2020), “Accounting Couch”, Retrieved from <http://www.accountingcoach.com/blog/debt-ratio>
- [9] Huynh Phuong Dong & Jyh-tay Su (2010) “The Relationship between WCM and Profitability: A Vietnam Case”. *International Research Journal of Finance and Economics*, ISSN 1450-2887 Issue 49 (2010)
- [10] Institut numerique (2012), II-Data Description, Retrieved from <https://www.institut-numerique.org/ii-data-description-4ffd9c5e60102>
- [11] Jakpar S1, Tinggi, Siang, Johari, Myint & Sadique (2017), “WCM and Profitability: Evidence from Manufacturing Sector in Malaysia”, ‘Journal of Business & Financial Affairs’ ISSN: 2167-0234, Volume 6 • Issue 2 • 1000255.
- [12] Lazaridis, Ioannis & Tryfonidis, Dimitrios (2006) “Relationship between WCM and Profitability of Listed Companies in the Athens Stock Exchange”. ‘Journal of Financial Management and Analysis’, Vol. 19, No. 1, January-June 2006.
- [13] Ntui Ponsian, Kiemi Chrispina, Gwatako Tago, Halim Mkiibi. (2014), “The effect of WCM on profitability”, *International Journal of Economics, Finance and Management Sciences*, ISSN: 2326-9553 (Print); ISSN: 2326-9561 (Online), December 19, 2014
- [14] Richard Kofi Akoto, Dadson Awunyo-Vitor & Peter Lawer Angmor (2013). ‘WCM and profitability: Evidence from Ghanaian listed manufacturing firms’. *Journal of Economics and International Finance*, ISSN: 2006-9812, Vol.5(9), pp. 373-379

## **Importance of Consumer Behavior – A Case Study of Maggi Noodle, Nestle India**

**Dr. Ennala Deepa**

Assistant Professor, KLH Business School,  
Koneru Lakshmaiah Education Foundation (Deemed to be University), Off Campus,  
Hyderabad, Telangana, India

**J. Saujanya**

Research Scholar, KLH Business School,  
Koneru Lakshmaiah Education Foundation (Deemed to be University), Off Campus,  
Hyderabad, Telangana, India

**Dr. Venkateswararao Podile,**

Professor, KL Business School,  
Koneru Lakshmaiah Education Foundation (Deemed to be University), Vaddeswaram, AP, India.

### **Abstract**

Consumer buyer behavior is considered to be an inseparable part of marketing and Kotler and Keller (2011) state that consumer buying behavior is the study of the ways of buying and disposing of goods, services, ideas or experiences by the individuals, groups and organizations in order to satisfy their needs and wants. In today's world, consumers' product and service preferences are constantly changing. Marketing managers must understand these desires in order to create a proper marketing mix for a well-defined market. Understanding the customer behavior is very essential to design marketing strategies which influences the customer buying behavior. This paper focuses on the various factors to consider in order understanding the customer behavior. The importance of having loyal customers and building the same is shown by taking Maggi as a case study. Based on the case study conclusion has been made of what are the points to be considered.

**Key Words:** Customer Connect, Customer Loyalty, Marketing Mix, Monopoly.

### **Objective**

Marketing is identifying the customer needs, wants and meeting them. But in today's marketing world Customer behavior plays an important role in defining the marketing strategies. Hence this paper talks in-depth about the importance of customer behavior analysis for running a successful business by taking case study of Maggi. Maggi has been in India for 38 years, and it has revolutionized the way people eat breakfast. From evening snacks at 5 p.m. to morning breakfast,

Maggi has replaced all types of breakfast from south to north, from Dosa to Paratha to Dhokla. The taste, as well as how simple and fast it could be made, played a role; in this article, we'll look at how the product survived after the ban based on customer.

## **Introduction**

It all began in May 2015, Food Safety Regulators from Barabanki, a district of Uttar Pradesh, India reported that samples of 'Maggi Two Minute Noodles' had unexpectedly high levels of monosodium glutamate, as well as up to seventeen times the permissible limit of lead. A repeat test at the Central Food Laboratory in Kolkata, a referral lab, was also conducted. The Gorakhpur lab tested for monosodium glutamate (MSG) to check Nestle's claim that Maggi had none. Both tests found MSG; in addition, the Kolkata lab found very high quantities of lead, 17.2 parts per million, according to Uttar Pradesh authorities. On 3rd June 2015, the New Delhi Government banned the sale of Maggi in New Delhi stores for 15 days due to these findings. On 4th June 2015, the Gujarat FDA banned the noodles for 30 days after 27 out of 39 samples were detected with objectionable levels of metallic lead, among other things. Assam had banned sale, distribution and storage of Maggi's "extra delicious chicken noodles" variety for 30 days since 4th June 2015 after tests carried out at the state public health laboratory concluded the particular variety to contain added MSG and excessively high lead content. Some of India's biggest retailers like Future Group which includes Big Bazaar, Easyday and Nilgiris also imposed a nationwide ban on Maggi. Thereafter multiple state authorities in India found an unacceptable amount of lead and it has been banned in more than 5 other states in India.

Present marketing strategies are built around the words customer connect, customer loyalty, changing trends, society responsibilities etc., customer behavior towards products and services are changing, this change is due to various reasons break of social barriers, awareness of other competitor products, no compromise and intolerance attitude, this era is of "new trends" marketers have to continuously cope up with the changes. Hence now customer's habits and attitude matter more. In the paper we will be discussing how impulse buyer has to be treated or strategy should be different, as reference of impulse buyers have been taken from the papers; 'Longitudinal analysis versus cross-sectional analysis in assessing the factors influencing shoppers impulse purchase behavior'. Also, information on Marketing strategies have been taken from 'Marketing Strategies of Micro Finance Institutions in India'.

## **Methodology**

In the present paper will be focusing on customer behavior which plays the crucial role in designing marketing strategies. We will understand the factors that influence the customer behavior. In-depth analysis of the same will be done by taking into consideration of live example. With the help of

the example, we can understand customer behavior on introduction of the product and customer behavior of different level of product cycle.

## **Literature Review**

Maggi was new product for the Indian market, new product or we can say an alien product to be accepted in traditional Indian market is a task, in the paper Success of New Product Launch by New Process Flow, Deepa, talks about the importance of the same.

Customer perception of the product plays a major role in consumer buying behavior, the paper Digital Marketing A Catalyst In Creating Brand Image Through Customer, Ennala Deepa , talks about how perception creates customer and then there loyalty.

Impact of service environment for effective customer behavior in Retail Industry with reference to Heritage super market, Mr. L Komagan and Dr. Kiran Kumar Thoti Turkish Journal of Computer And Mathematics Education, retail business has boomed post FDI in India, hence marketing and de-marketing products In retail business plays a major role.

Brand Loyalty, plays a Vital role and how it works for Brand loyal customers is a task, reference of brand loyalty has been taken from the Factors Determining the Role of Brand in Purchase Decision Of Sportswear, Kunal Gaurav

As per the article “The return of Maggi: A Case Study” by Syed Kazim and Ajai Thomas Abraham, talks about the history of the product Maggi, post exposure of lead content, the decline of sales, competition of the product. The information was very much relevant to build the article introduction.

Article “the relationship between customer loyalty and customer satisfaction”, John T Bowen, and Shiang-Lin Chen, talks about how customer loyalty is linked with satisfaction and measurement if customer loyalty

A Customer Loyalty Model For E-Service Context, Hsin-Hui Lin and Pin Luarn This research is a response to the call for customer loyalty research in the e-service context. Utilizing the proposed loyalty model as a theoretical framework, the direct and indirect influences of customer satisfaction, trust, perceived value, and attitudinal commitment on behavioral (purchase) loyalty were observed. The contributions of this study to customer loyalty research are twofold. First, it has successfully applied the traditional conceptualization of customer loyalty in a new e-service context that is different from the marketplace examined in prior studies. Second, customer satisfaction, trust, perceived value, and attitudinal commitment were found to be important determinants of purchase loyalty. It was also suggested in this study that commitment plays a

crucial intervening role in the relationship of customer satisfaction and perceived value to loyalty. The findings of this study have implications for e-service managers to develop their customer loyalty. Considering the millions of dollars that have been invested in e-services worldwide, it is of paramount importance to ensure that customers will have repeat Web purchase behaviors and show loyalty to a specific e-service brand

A study on Maggi ban and simultaneously launch of Patanjali Atta noodle, Ayushi Jain - TMIMT International Journal "Special Issue- 2016", ISSN 2348-988X, this paper talks about how customers are considering the product which is good for the health. Nestle India Ltd.'s Maggi-2-minute noodles row has led to a sort of chaos in the whole country. Parents, children, workers, investors, suppliers, etc. just do not know how to deal with the situation. This is the India's worst food scare in a decade after that of presence of pesticides in soft drinks. The scare over Maggi instant noodles, India's one of the most popular snacks, has gripped increasingly various sections of the society. So, the research is imperative to assess that upto what extent this Maggi row has impacted India so that future plans for remedy can be prepared accordingly

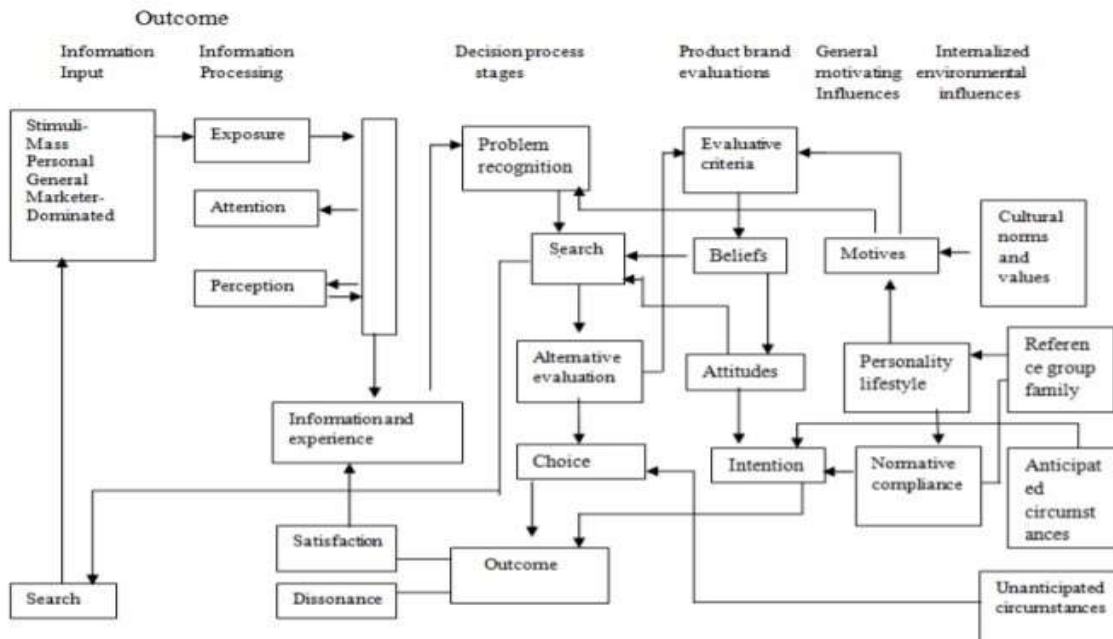
Customer Preference For Selecting The Dairy Products In Covid-19, Circumstances with references to Andhra Pradesh, Dr. Orguganti Surya Soma Sankar, Dr. Kiran Kumar Thoti, information of the paper can be taken to understand the customer preference and due to milk adulterity going on , the paper information can be used for demarketing such product for social benefits.

Impact of service environment for effective customer behavior in Retail Industry with reference to Heritage super market, Mr. L Komagan and Dr. Kiran Kumar Thoti Turkish Journal of Computer And Mathematics Education, retail business has boomed post FDI in India, hence marketing and de-marketing products In retail business plays a major role.

Mr. Rahul .M.Mhabde , Mrs. Rajeshri Son2 Analytical study on Consumer behavior towards "Maggi Instant noodle" in Mumbai –A post ban, Vol-3 Issue-1 2017 IJARIII- ISSN(O)-2395-4396, data has been studied the article survey shows, of the 50 respondent majority of respondent preferred to eat noodle i.e. 74% of the total population. Following the graphical representation of the same. majority of population buy Maggi instant noodle over any other brand which shoes the popularity of Maggi in the market. following is the graphical representation of the same, it is observed that majority of respondent are not aware about presence of unhealthy lead and the same number of respondents i.e.. 36% are not sure about the same, it has been observed that majority of population still buy Maggi which conclude that respondent decision making is not much affected due to ban. comparative analysis shows that frequency to consume has reduced after its relaunch. Before ban majority population were consummating Maggi thrice a week. i.e. 30% of the total population were of this category however data shows that it has gone down to 4% after its relaunch. It means ban has affected consumption frequency of Maggi. it shows that Maggi is still choice of the consumer as maximum consumer consumed Maggi after it is back in market. majority of population are under the belief said that Maggi test is same as before. they believe t at ban has not change the test and confidence of consumer



## Analysis

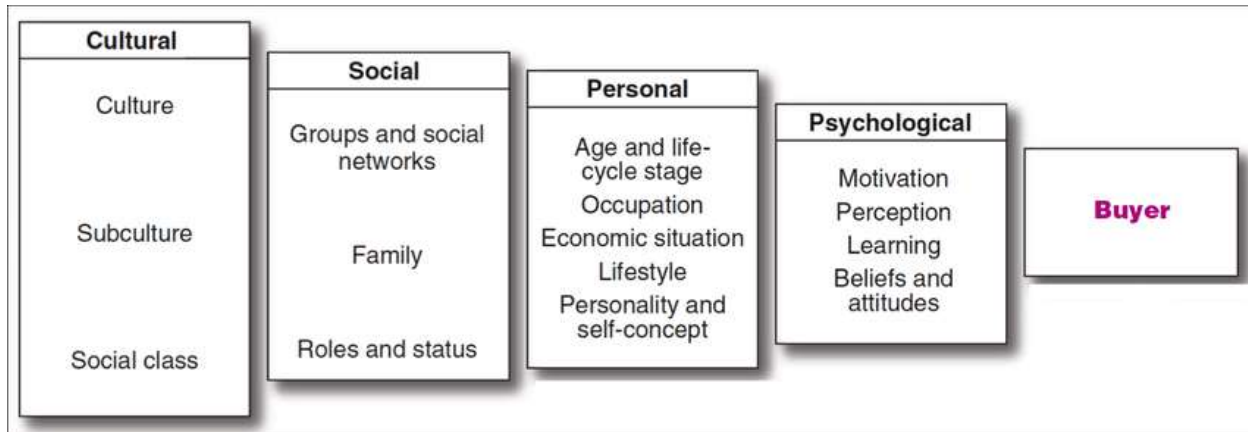


Reference: Engel-Kollat-Blackwell Model

The reference of Engel-Kollat-Blackwell Model, can be taken to understand the perception and attention the customer is exposed to which plays a vital role in the customer buying behaviour. Which is very relevant to the case we are studying.

Firstly, let's understand what factors influence the behavior of the customer. Culture factors exert a broad and deep influence. Culture is the most basic cause of person's wants and behavior. A person's likes, dislikes, wants, desires etc., are built on his/her family. Next the social class Upper, Middle, Working and Lower class. Social class is not determined by a single factor, such as income, but is measured as combination of occupation, income, education, wealth and other variables. Social Factors, word of mouth influence, the impact of the personal words and recommendations of trusted friends, associates and other consumers on buying behavior. Marketers of brands subjected to strong influence must figure out how to reach opinion leaders. Personal factors age, occupation, Economic situation, Lifestyle etc., a person buying choice can

be further influenced by Psychological factors motivation, perception, learning and beliefs and attitudes.



Customer behavior enables companies to take appropriate marketing decision on Marketing Mix the 6P's Product, Price, Promotion, Packing, Positioning and Place of Distribution.

Maggi instant noodles. Maggi 2minutes an instant food product, was introduced in 1982. Maggi noodle's is the leading brand of instant noodles in India enjoying market share of 79.3%. In this product the marketers have created a want. In that time the Indian customers were very conservative and did not expose themselves to any changes. Hence to get there product accepted as a major challenge. The main marketing point was "instant noodles" this is first kind of food category introduced in India. Based on its USP the working women were targeted but the approach failed. To understand the cause of the failure Maggi conducted a study which revealed that the Maggi taste was liked by children. Hence the targeted customers were children through mothers.

Maggi was a Monopoly and later had competitors but to create the brand it followed the STPD analysis. Segmentation: Maggi brand have segmented the market on the basis of lifestyle and habits of Urban Families. Target: they targeted the kids, office going, and working woman. Positioning: Maggi has positioned itself in the SNACKS category since Indians did not consider noodles as proper food the Maggi have developed itself in instant food product with positioning statements such as "2 minutes noodles" and "Easy to cook" " good to eat". POD: post of differentiations, the brand differentiated they brand from its competitors in terms of taste flavors and packing.

By introducing product like Maggi the need was created not identified. Smart companies like Maggi try to understand the customer behavior decision process. "The Buyer Decision Process"



## Importance of Consumer Behavior – A Case Study of Maggi Noodle, Nestle India

Let's understand the customer behavior. When evaluating the potential alternatives, consumer used two types of information the first is the list of brands from which they plan to make their selection and the second criteria from which they plan to make their decision. Beliefs and attitude are acquired by experience and learning, Maggi has always provided its consumers with something new time to time which has developed a good belief has helped them to choose them from their alternatives. Customer behavior depends on experience with the product, if performance falls short of expectation the consumer is disappointed and if it meets the expectation of the consumer is satisfied.

Following is the purchase based on age category:

	1990	1995	2000	2005	2010	2015
Children 2-9yrs	169999	181521	187940	189211	184457	184376
Teenagers 10-14yrs	89781	100560	109302	114583	117137	114226
Teenagers 13-19yrs	120293	127645	142432	153781	160728	162495
Studying Age 18-22	80812	85918	92074	103179	110642	115126
Young Adult 15-29	230839	249149	270576	294103	319267	336193
Middle Age 30-59	243295	277343	316065	358164	398405	440655
Baby Boomers 40-59	134212	151646	174986	202754	232801	261349
Pensioners 60+	57029	65643	75712	86585	99728	117168

### Findings

By understanding the Maggi noodle, we can say they have following strengths:

- ✓ Family based advertising, high advertising share
- ✓ Emotional relationship with the consumer
- ✓ A strong distribution channel

The main point to focus on “Emotional relationship with the consumer” Customers are so used to the product that it is identified by the following:

- ✓ Yellow Packing
- ✓ Tasty Snack
- ✓ Sunday Breakfast
- ✓ Fun in having

They created a Family Brand by providing taste and preference of consumers, they closely watched consumers preferences they introduced Chicken Maggi, wheat flour Maggi. They exceeded the expectation.

July 2015 Maggi was banned By (FSSAI) Food Safety and Standards Authority of India calling it unsafe and hazardous for consumption. On June 8 post 3days after the ban the Maggi share price went down to 5,539.8 lowest during that year

<b>Consumption Before Ban</b>							
Age	Everyday	Thrice a week	Twice a week	Once a week	Once a month	Never	Total
15-25	1	5	8	6	4	1	25
25-35	0	4	5	4	4	0	17
35-45	0	2	2	3	1	0	8
<b>Total</b>	<b>1</b>	<b>11</b>	<b>15</b>	<b>13</b>	<b>9</b>	<b>1</b>	<b>50</b>

<b>Consumption After Ban</b>						
Age	Everyday	Twice a week	Once a week	Once a month	Never	Total
15-25	1	2	5	14	3	25
25-35	0	1	3	10	3	17
35-45	1	1	3	1	2	8
<b>Total</b>	<b>2</b>	<b>4</b>	<b>11</b>	<b>25</b>	<b>8</b>	<b>50</b>

Maggi has maintained trust and confidence even after post ban period. A product's success/failure is the evaluation of consumer response to a particular marketing strategy. It also indicates if the organization has been successful in fulfilling their wants and needs and their impact on the society. To sum up all the arguments stated above, it is clear that better understanding the consumer buying behavior through studying and identifying their needs leads to huge long-term benefits to the businesses.

## **Conclusion**

The points to be considered by marketers while designing the marketing strategies are the psychology of how customer thinks and feels the brand product. What are his /her thought process, behavior while purchase of the product in the market. Customer knowledge on the product. Product importance for the consumer or ranking. How consumers are influenced by their environment, culture, media. Limitations in consumer knowledge or information processing abilities influence decisions and marketing outcome.

### References

- Beeton, S. and Benfield, R., 2002. Demand Control. *Journal of Sustainable Tourism*, Volume no 10(issue no 6), pp.497-513.
- Grinstein, A. and Nisan, U., 2021. Ethnic Variation in Environmental Belief and Behavior. *Environment and Behavior*, 36(2), pp.157–85.
- Deepa, E., 2021. Digital Marketing A Catalyst In Creating Brand Image Through Customer. *Turkish Journal Of Computer and Mathematics Education*, 12(4), pp.1308-1315.
- Deepa, E., 2020. Success of New Product Launch by New Process Flow. *European Journal of Molecular and Clinical Medicine*, 7(7), pp.2515-8260.
- Surya Soma Sankar, O. and Kumar, K., 2020. Customer reference for selecting the diary products in Covid-19 circumstance with reference to Andhra Pradesh. *Journal of critic view*, 7(5), pp.2394 – 5125.
- Komagan, L. and Thoti, K., 2021. Impact of service environment for effective customer behavior in Retail Industry with reference to Heritage super market. *Turkish Journal of Computer and Mathematics Education*, 12(3), pp.4537-4364.
- Gaurav, K., Suraj Ray, A. and Kishore Sahu, N., 2020. Factors Determining the Role of Brand in Purchase Decision Of Sportswear, PalArch's. *Journal Of Archaeology of Egypt/Egyptology*, 17(7).
- S Geeta and E Deepa *International Journal of Management (IJM)*, 2020. Marketing Strategies of Micro Finance Institutions in India. 11(9), pp.1667-1674.
- Marketing Strategies of Micro Finance Institutions in India, Dr. Geeta and Dr. Deepa, *International Journal of Management (IJM) Volume, 11, Issue 9, September 2020, pp 1667-1674, Article ID: IJM\_11\_09\_159*
- Mr Rahul .M.Mhabde , Mrs Rajeshri Son2 Analytical study on Consumer behavior towards “Maggi Instant noodle” in Mumbai –A post ban, Vol-3 Issue-1 2017 *IJARIE-ISSN(O)-2395-4396*
- <https://www.slideshare.net/UtkarshVerma12/brand-loyalty-and-consumer-buying-behavior-towards-Maggi>
- <https://www.slideshare.net/PraneshSharma/43379925-Magginoodlesmarketingplan>

# Purification and characterization of bioactive compounds extracted from *Suaeda maritima* leaf and its impact on pathogenicity of *Pseudomonas aeruginosa* in *Catla catla* fingerlings

G Beulah <sup>1</sup>, D Divya <sup>1</sup>, N S Sampath Kumar <sup>2</sup>, M V N Sravya <sup>1</sup>, K Govinda Rao <sup>1</sup>, Anjani Devi Chintagunta <sup>2</sup>, G Divya <sup>2</sup>, S Hari Chandana <sup>2</sup>, B D Blessy <sup>2</sup>, G Simhachalam <sup>3</sup>

Affiliations — collapse

## Affiliations

- <sup>1</sup> Department of Zoology and Aquaculture, Acharya Nagarjuna University, Guntur, Andhra Pradesh, India, 522510.
- <sup>2</sup> Department of Biotechnology, Vignan's Foundation for Science, Technology and Research, Vadlamudi, Andhra Pradesh, India, 522213.
- <sup>3</sup> Department of Zoology and Aquaculture, Acharya Nagarjuna University, Guntur, Andhra Pradesh, India, 522510. [chalamgp99@gmail.com](mailto:chalamgp99@gmail.com).

PMID: 34623537 PMCID: [PMC8501176](#) DOI: [10.1186/s13568-021-01295-5](#)

# Security And Energy In A Wireless Body Area Network: A Protocol Evaluation

P. Madhuri Paul<sup>1</sup>, Dr Prasadu Peddi<sup>2</sup>

<sup>1</sup>Research Scholar, dept of computer science, Shri Jagdishprasad Jhabarmal Tibrewala University, Rajasthan.

<sup>2</sup>Assistant Professor, dept of computer science and Engineering, Shri Jagdishprasad Jhabarmal Tibrewala University

---

## ABSTRACT

Wireless sensor networks, often known as "WSNs," are networks that collect data from sensors that are embedded in the surrounding environment and put it to specific uses. The base station (BS) in the sensor network is responsible for the collection of data and the subsequent wireless transmission of that data to the sensors. Each sensor has a central processing unit (CPU) that has memory, a source of electricity, and actuators. The proliferation of wireless sensor networks (WSN) in recent years has been nothing short of spectacular. Applications for wireless sensor networks (WSN) that use body area networks (BAN) are varied and appealing. Through the use of wireless body area networks, medical professionals are able to keep track of their patients' fitness levels, chronic conditions, and overall health. Sensor devices and diagnostic software or hardware are the two components that make up the Internet of Things. Over the course of the last 10 years, much research has been conducted on this topic. There have been a number of procedures, guidelines, and suggestions developed. In hospitals and other medical facilities, a system known as the Wireless Body Area Network (WBAN) uses coordinating devices like smart phones or personal digital assistants to collect and wirelessly transfer the data that is collected from other sensor nodes. Apps designed for medical use may now continually monitor key signal data and capture biological signs at the receiver end. The collection, analysis, and transmission of data are all capabilities offered by these applications. Last but not least, they will provide the user with feedback. The surge in popularity of wireless body area networks may be attributed to the fact that they are simple to use.

**Keywords:** Wireless SensorNetwork, Medical Server, Wireless Wearable Body Area Network (WBAN), Energy Consumption, applications, research trends.

## 1. INTRODUCTION

Several aspects of medical treatment, such as diagnosis, therapy, and patient monitoring, have been demonstrated to have benefited significantly by advances in biomedical technology. The biomedical system is more effective than other ways for preserving human lives. As time passes, these systems get smaller, more dependable, and more patient-friendly. Utilizing these methods will increase productivity. In the biomedical field, wireless technology is currently gaining popularity. It enables patients and staff members to convey information, resulting in more autonomy. Body Area Networks that operate over the air (WBAN).

There has been an increase in the number of persons utilising wireless communication networks. This opens the door to a vast array of opportunities in the medical and healthcare fields. Body area network particularly developed for wireless usage. A sensor network that permits the placement of a variety of sensors either within or outside the body. These sensors are implanted into the patient's body and may simultaneously communicate with one another and the physician. Wireless body area networks enable the development of solutions that are both adaptable and economical. WBAN is used because of the benefits provided by sensor nodes, including the patient's enhanced mobility. Because of this, people are able to carry out their daily tasks without any limitations, including mobility. In addition, WBAN offers a location-independent monitoring system that allows the physician to monitor the health of the patient remotely. The sensor captures and communicates samples to the attending medical personnel after being applied to the patient. Internet connectivity is required for WBAN in order for sensor nodes to send data remotely and maintain data.

A wireless body network is a technology used to monitor people's health and find early warning signs of possible danger. There is interaction between medical personnel and caregivers. This system is capable of segmentation based on the operating configurations. The implanted area network is used inside the body, whereas the wearable area network is utilized outside.

## **2. Wireless Body Area Networks (WBAN)**

Wireless Body Area Networks are a new technology that allows for real-time health monitoring and diagnosis of life-threatening diseases. WBAN supports many medical and nonmedical applications and operates in close proximity to, inside, or on the human body. IEEE 802 has formed a TaskGroup known as IEEE 802.15.6 to standardize WBAN. This task force is charged with creating a standard for communication which is low-power, and can be used in many applications, both medical and non-medical.

IEEE 802.15 Task Group 6 BAN is currently working on a protocol for communication that is optimized for devices that use low power. IEEE 802.15 TG6 is a group formed on November 7, 2007 when it has since begun operations in Taipei as TG6. The group had received 34 suggestions. They were then combined into one candidate. A draft of the standard was created at the beginning of March in 2009. The draft has gone through thorough editing. It was later followed with five Letter Ballots. The Letter Ballot #79 was approved on July 13, 2011. It was authorized on July



22nd to begin the Sponsor Ballot. It is expected to be finalized in November 2011 during the TG6 conference in Atlanta, USA.

WBAN technology allows individuals to instantly exchange digital business cards or profiles through social networking by simply shaking their hands. WBAN architectures are used in medical applications. Fig.1.

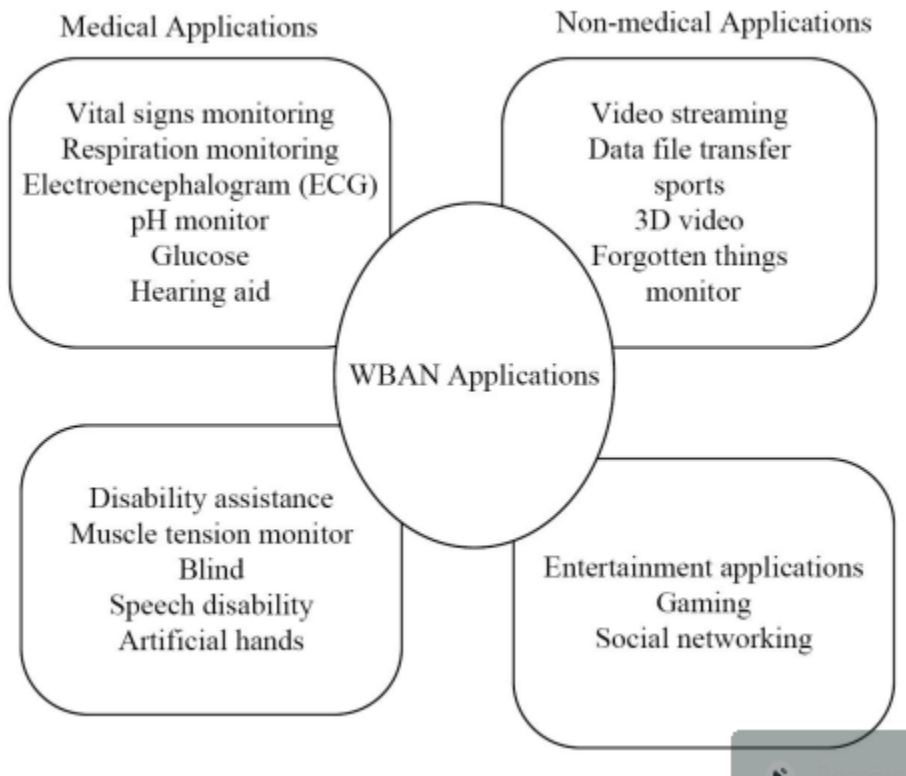


Fig 1: WBAN Applications targeted by IEEE 802.15.6

### 3 WBAN Security Issues and Requirements

WBAN presents a number of research issues that must be considered when designing radio frequency (RF), wireless systems. These include frequency band selection model of the channel, design and antenna, and designing PHY-related protocols. QoS reliability, QoS privacy and security are all significant concerns. These concerns, particularly security concerns [10] were carefully studied and are now being addressed by a variety of emerging technologies.

**Data Confidentiality** - Data confidentiality is a key issue in WBANs. Data confidentiality is essential to prevent data disclosure. WBANs are not allowed to divulge crucial information to external or neighbouring networks. WBANs should utilize encryption with symmetric keys because public-key cryptography is costly for sensors with limited energy.

**Data Integrity.** Although data confidentiality is important, it does not guarantee that the data will be protected from outside modifications. An adversary will always be able to alter the data. He/she can add fragments to The data can be altered or changed to alter the information contained in the

packet. The packet is then transmitted to the coordinator. Data integrity issues can often be dangerous, especially for life-critical events or in cases where emergency data has been modified. Bad communication environment may also result in data loss.

Data authentication is the verification of the origin node's identity. In addition to manipulating Data packets that the adversary could also alter packet streams by adding fake messages. The coordinator must be able to confirm the source of the data. Data authentication may be accomplished using an Authentication Message Code. This is done to differentiate the two (from Medium Access Control) and is displayed with bold letters. It is typically determined with an encryption code that is shared with the user.

Data Freshness. To make the coordinator think twice In order to confuse the coordinator, an adversary may collect data while it is in transit , and then play them back in the future using an old key. Freshness of data refers to the fact that the information is not old and one is able to read through old messages. There are two kinds of freshness of data. The weak type ensures partial ordering of data frames, but it doesn't guarantee delays. The strong type assures that data frames are ordered without delay.

Secure Localization. A majority of WBAN applications require accurate localization. The absence of intelligent tracking techniques allows attackers to make false reports regarding the location of a patient via false signal strength reporting or replaying signals.

Availability: A physician's information must be available at all times. An adversary may attempt to disable or capture a node in WBAN, which could lead to loss of lives. A good way to avoid losing control of a network node that is being attacked is to change it to a different node.

Secure Management: The coordinator must ensure key distribution to all nodes in order to decryption and encryption operation. The coordinator secures the addition or removal of nodes during association and disassociation.

#### **4. ADOPTING PROTOCOLS FOR WBAN**

With new technology in healthcare, WBANs are now available. Wearable sensors collect vital information from patients and send it to the sink with the sink using short-range wireless communication methods (9the sink by using short-range wireless communication methods [9. WBANs are classified into three categories three levels: master nodes; power sensor nodes, as well as the Internet or local. The sensor nodes with low batteries have to function for prolonged periods without charging [10]. They can be implanted, or placed in the body. Second-level nodes, sometimes referred to coordinator or gateway nodes, can be used to control all sensors. They also consume less power because of their use. This last level, the Internet or local level, is used to monitor. These three levels require energy, and energy consumption remains a challenge for WBANs. There are many routing protocols that can be used to route data. This has an impact on the energy consumption of WBANs [11]. The life span of sensor nodes is limited and it consumes energy.

1. Each path is designed for data routing. They should be aware of their energy and not generate a lot of heat as nodes are located in the human body.
  2. Complex algorithms are the main obstacle to energy efficient routing.
- Although many routing protocols are designed to be efficient, there are still some flaws. Some do not address delay tolerance and postural information. [10].

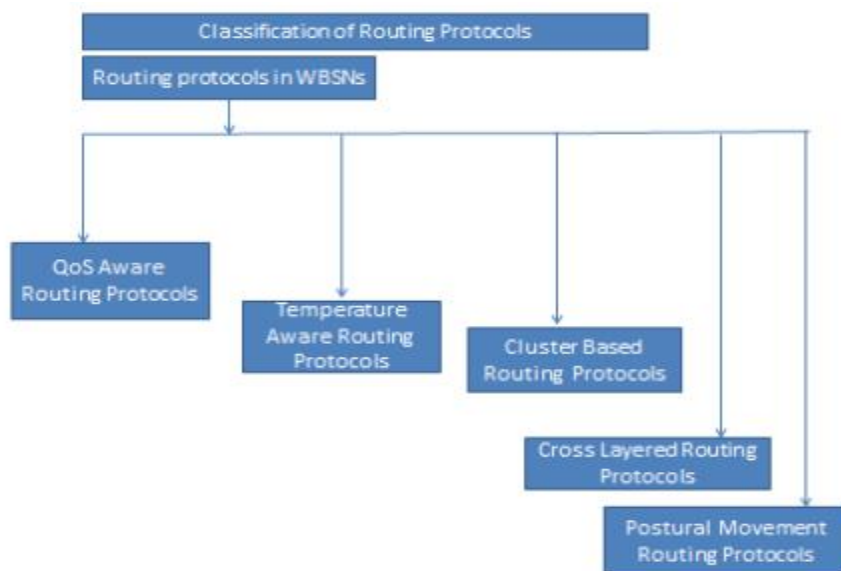


Fig 2 : Classification of WBANs Routing Protocols

Many protocols are not concerned with temperature rise. There has been a lot of research into routing protocols. Liang and other [11] proposed the idea of a Prediction that is based on Secure and Reliable(PSR) routing system that is safe and secure routing.

Khan, et . al. [12] An Energy Aware Wearing Routing Protocol, (EPR), has been suggested to reduce the load on energy and traffic. The proposed model is an energy-conscious and QoS aware routing protocol for communications devices within health care. But, these protocols aren't without their flaws.

Nadeem and others Nadeem, et. al. stable and can increase throughput. It is able to improve the efficiency of links in WBANs. To minimize heat generated by sensors, thermally aware routing protocols have been proposed. Cluster-based routing has been suggested to cut down on the amount of power and delay required in addition to enhancing longevity of the network and link quality. [14].

Postural-Movement-based routing protocols were proposed for handling the link disconnection that occurs due to the body movement. The cross-layered routing protocol has been suggested to solve the issues of the network as well as MAC Layer [15]. Following a brief overview of the protocols, we'll go over the protocols in the section on routing.

## 5. Design Issues Of Routing Protocols

WBANs need to be linked to control, monitoring and remote systems. Thus, the systems need to offer high reliability and low latency. Network-specific requirements make it difficult to create an appropriate routing protocol effective for WBANs. In the next article, we will be discussing the routing issues that are related to WBANs.

a) **Dynamic Nature of Network** WBANs network is dynamic because of the dynamic topologies and mobility of nodes. The dynamic nature and duration of the network reduces its lifespan [16]. Link quality is also affected by body postural and bodily movement. So routing protocols need to be adaptive in order to deal with topological changes within the network.

b) **Heterogeneous Environment** Different types of heterogeneous environments can be used to analyze various parameters with WBANs. These NODES that are heterogeneous are utilized to calculate, store data, as well as power consumption. WBANs are often challenged by the heterogeneity and complexity of the environment.

c) **Topological Partitioning** WBANs have another problem: topological partitioning. This is because of body movement and the limited distance of communication devices. It is crucial to use a reliable routing protocol in place to handle this challenge. The protocol can be one-hop, multihop or cluster-based depending on how large the network is.

d) **Energy Efficiency** WBANs face major challenges when it comes to energy utilization. Patients are often uncomfortable and find replacing batteries difficult. Sensor batteries' life spans depend on the applications and batteries used. Overheating can cause tissue damage and death. WBANs are very concerned about energy consumption and network life expectancy. These networks still have to deal with energy consumption problems due to limited energy resources.

e) **Interference and Temperature** Another issue when designing routing protocols in WBANs is temperature rise. Temperature rise can be attributed to two factors: energy consumption by nodes and antenna radiation absorption. It is therefore important to develop and design energy-efficient routing protocols that use minimal energy and have less interference.

f) **Limited Resources** WBANs need limited resources. They have a narrow bandwidth of communication, a limited amount of storage and energy, as well as limited bandwidth. These constraints must be taken into account when routing protocols are designed.

g) **Security and Privacy** WBANs are also concerned about privacy and security. All tires should have security and devices must be able to authenticate and remain intact. Security must be maintained at both the data and system levels [11]. Security must be at both the data and system levels [11]. There are numerous security measures that you can employ to safeguard your personal data. Privacy is, however is the term used to describe patients' rights to restrict the collection of personal data as well as their usage. WBANs must meet all security requirements in order to protect patient data.

h) **Quality of Services (QoSs)** For data transmissions within WBANs that are different from those described above, QoSs may be required. The [18] author describes The patient's data can be classified into three categories three types: sensitive, critical and normal. EEG, heartbeat as well

as other important information is collected by sensors. Sensors for sensitive data collect data using images processing, video streaming vital signals, as well as monitoring the rate of respiration. The data on body temperature is the foundation of regular data. It is crucial for routing protocols to be developed to meet all QoS requirements. QoSs need to have high speed of packet delivery, minimal transmission delay, and no collisions. QoSs may also be assessed at lower levels of protocols.

Protocols	Goal	Delay	Temperature Rise	Address Scheme	PDR	Discarding Mechanism
TARA	Reduce possibility of over heating	Very high	Very high	Global	Very low	No
LTR	Reduce energy consumption and temperature rise	High	High	Global	Low	Yes
ALTR	Reduce end to end delay	Medium	Low	Global	High	No
LTRT	Find route with minimum temperature	Low	Very low	Global	Very high	Yes
HPR	Prevent formation of hotspot, and reduce end to end delay	Low	Very low	Global	High	Yes
RAIN	Reduce temperature rise and average delay	Low	Very low	Local	High	Yes
TSHR	Medium	Very low	Low	Very High	No	No
M-ATTEMPT	Low	Low	Very low	High	Yes	No

Fig 3 : Comparison of Protocols

## 6. CONCLUSION

Wireless body area networks, more often referred to as WBANs, are a rapidly developing field that provide a diverse variety of advantages. It is difficult to send the information that the sensors pick up back to the drain because of the movements of the human body as well as other restrictions. WBANs categories the routing protocol into the following five primary groups: methods for routing that are based on QoS, which include temperature-based, cluster-based (cross-layer), postural movements, and base QoS. In this study, we will focus on and critically examine several temperature-aware routing techniques for wireless body area networks (WBANs). Temperature-aware protocols do not consider other aspects of routing, such as energy consumption or utilization delay, packet delivery, or energy use. This review will help researchers design an efficient temperature-sensitive WBAN routing method, which is one of the benefits of reading it. The next step is to do research on the primary requirements and challenges related to environmentally conscientious routing systems (WBANs).

## References:

- [1] E Nigussie, T Xu, M Potkonjak. Securing wireless body sensor networks using bijective functionbased hardware primitive. Intelligent Sensors, Sensor Networks and Information Processing (ISSNIP), 2015 IEEE Tenth International Conference on, 2015: 1-6.

- [2] A Milenković, C Otto, E Jovanov. Wireless sensor networks for personal health monitoring: Issues and an implementation. *Computer communications*. 2006; 29: 2521-2533.
- [3] KN Qureshi, AH Abdullah, RW Anwar. The Evolution in Health Care with Information and communication Technologies. *ELSEVIER, 2nd International Conference of Applied Information and Communications Technology*. Oman. 2014.
- [4] Y Hao, R Foster. Wireless body sensor networks for health-monitoring applications. *Physiological measurement*. 2008; 29: R27.
- [5] MM Monowar, M Mehedi Hassan, F Bajaber, MA Hamid, A Alamri. Thermal-aware multiconstrained intrabody QoS routing for wireless body area networks. *International Journal of Distributed Sensor Networks*. 2014.
- [6] A Rahim, N Javaid, M Aslam, U Qasim, Z Khan. Adaptive-reliable medium access control protocol for wireless body area networks. *Sensor, Mesh and Ad Hoc Communications and Networks (SECON), 2012 9th Annual IEEE Communications Society Conference on*, 2012: 56-58.
- [7] S Movassaghilani, M Abolhasan, J Lipman. *A Review of Routing Protocols in Wireless Body Area Networks*. 2013.
- [8] KN Qureshi, AH Abdullah. Adaptation of wireless sensor network in industries and their architecture, standards and applications. *World Applied Sciences Journal*. 2014; 30: 1218-1223.
- [9] S Pathania, N Bilandi. *Security Issues In Wireless Body Area Network*. 2014.
- [10] M Quwaider, S Biswas. DTN routing in body sensor networks with dynamic postural partitioning. *Ad Hoc Networks*. 2010; 8: 824-841.
- [11] X Liang, X Li, Q Shen, R Lu, X Lin, X Shen, et al. Exploiting prediction to enable secure and reliable routing in wireless body area networks. *INFOCOM, Proceedings IEEE*. 2012: 388-396.
- [12] ZA Khan, S Sivakumar, W Phillips, N Aslam. A new patient monitoring framework and Energy-aware Peering Routing Protocol (EPR) for Body Area Network communication. *Journal of Ambient Intelligence and Humanized Computing*. 2014; 5: 409-423.
- [13] Q Nadeem, N Javaid, S Mohammad, M Khan, S Sarfraz, M Gull. Simple: Stable increased-throughput multi-hop protocol for link efficiency in wireless body area networks. *Broadband and Wireless Computing, Communication and Applications (BWCCA). Eighth International Conference on*. 2013: 221-226.
- [14] M Aslam, M Rasheed, T Shah, A Rahim, Z Khan, U Qasim, et al. Energy optimization and Performance Analysis of Cluster Based Routing Protocols Extended from LEACH for WSNs. *arXiv preprint arXiv:1309.4373*. 2013.
- [15] Prasadu Peddi (2020), MINING POSTS AND COMMENTS FROM ONLINE SOCIAL NETWORKS, *Turkish Journal of Computer and Mathematics Education*, Vol 11, No 3, pp: 1018-1030.
- [16] H Ng, M Sim, C Tan. Security issues of wireless sensor networks in healthcare applications. *BT Technology Journal*. 2006; 24: 138-144.

[17] M Ameen, A Nessa, KS Kwak. QoS issues with focus on wireless body area networks. Convergence and Hybrid Information Technology. ICCIT'08. Third International Conference on. 2008; 801-807.

[18] A Rahim, N Javaid, M Aslam, Z Rahman, U Qasim, ZA Khan. A comprehensive survey of MAC protocols for wireless body area networks. Broadband, Wireless Computing, Communication and Applications (BWCCA), 2012 Seventh International Conference on. 2012: 434-439.

[19] CHW Oey, S Moh. A survey on temperature-aware routing protocols in wireless body sensor networks. Sensors. 2013; 13: 9860-9877.

[20] Yogesh Hole et al 2019 J. Phys.: Conf. Ser. 1362 012121

#### **Author Bibliography:**

**Mrs. P. Madhuri Paul** is working as Assistant Professor, Department of MCA at St. Ann's College for Women, Hyderabad. She has completed MCA from Osmania University and M.Tech (CSE) from JNTU Hyderabad. She is a Research Scholar at Department of Computer Science, Shri Jagdishprasad Jhabarmal Tibrewala University, Jhunjhunu, Rajasthan, India. She has authored and published book on Information Technology fundamentals.. She has about 13 years of teaching experience handling many challenging subjects all through her career. She has published more than 8 papers in various National, International Journals and in the proceedings of International conferences. Her research interests include wireless sensor networks and data communications. She is recognized for his amicable and affable nature coupled with excellent networking skills and is known for her passion to mingle with people and work with quality standards.

**OPEN ACCESS**

## Review—Miniaturized and Microfluidic Devices for Automated Nanoparticle Synthesis

To cite this article: Khairunnisa Amreen and Sanket Goel 2021 *ECS J. Solid State Sci. Technol.* **10** 017002

View the [article online](#) for updates and enhancements.

### You may also like

- [Microfluidic viscometers for biochemical and biomedical applications: A review](#)  
S B Puneeth, Madhusudan B Kulkarni and Sanket Goel
- [Biomaterials for microfluidic technology](#)  
Zehao Chen, Zhendong Lv, Zhen Zhang et al.
- [Advances in continuous-flow based microfluidic PCR devices—a review](#)  
Madhusudan B Kulkarni and Sanket Goel



 **Connect with decision-makers at ECS**

Accelerate sales with ECS exhibits, sponsorships, and advertising!

▶ Learn more and engage at the 244th ECS Meeting!





# Review—Miniaturized and Microfluidic Devices for Automated Nanoparticle Synthesis

Khairunnisa Amreen and Sanket Goel<sup>z</sup> 

*MEMS, Microfluidics and Nanoelectronics Lab, Department of Electrical and Electronics Engineering, Birla Institute of Technology and Science, Hyderabad 500078, India*

Recently, the usage of automated microfluidic integrated platforms in chemical synthesis has emerged as an extremely useful tool for nano/micro structures fabrication. Owing to their cost-effectiveness, portability and low sample consumption, these devices has gained substantial attention especially towards industrial outlook. The physical, chemical, mechanical and magnetic properties of the nanomaterials are greatly influenced by their morphological aspects. The broad spectrum applications of nanostructures in versatile fields like biomedical, energy storage/harvest, biosensing, catalysis, imaging, electronics and engineering, hugely depend on their morphology. Therefore, an automated, robust but customizable synthesis is the key to attain uniformity and reproducibility of morphology. Therefore, microfluidic devices offer features like control fluid flow, faster mixing of reagents, precise heat transfer mechanism and well-regulated pressure, giving a homogenous quality of nanocrystalline material for multiplexed applications. The studies have reported that the micro-devices assisted synthesized nanoparticles have less particle size distribution curve than those prepared traditionally. During the last decade, nano-and-micro sized crystals, colloids, particles, clusters have been synthesized so far using micro-controlled devices. This review summarizes the recent advances and the future scope of various miniaturized and microfluidic automated devices to realize nano crystalline materials.

© 2021 The Author(s). Published on behalf of The Electrochemical Society by IOP Publishing Limited. This is an open access article distributed under the terms of the Creative Commons Attribution 4.0 License (CC BY, <http://creativecommons.org/licenses/by/4.0/>), which permits unrestricted reuse of the work in any medium, provided the original work is properly cited. [DOI: 10.1149/2162-8777/abdb19]



Manuscript submitted October 9, 2020; revised manuscript received January 2, 2021. Published January 22, 2021. *This paper is part of the JSS Focus Issue on Solid State Reviews.*

The realization of the unique properties of nanocrystalline materials and their broad way applications has increased the demand for their synthesis on a large scale. The need for fabrication of these materials with outstanding physical/chemical properties has grown extensive.<sup>1</sup> As versatile applications of nanoparticles are emerging day by day, the nonmanufacturing methods for these materials via cost effective, fast and highly reproducible approaches rendering negligible impact on the environment is the need of the hour.<sup>2</sup> The physico-chemical properties of the nanocrystals are dependent on their structural morphology. Hence, the shape, size and crystallinity of the engineered materials has to be monitored throughout the production. The bigger challenge is to attain the precise reproducibility in each batch. In this context, the emergence of microfluidic as a forerunner technology in chemical synthesis with more precision has acquired substantial attention, especially in the industrial sector.<sup>3</sup>

Microfluidic devices offer manufacturing of nanocrystals with controlled size distribution and crystal phase. The microfluidic based synthetic routes provide added advantages like improved accuracy, portability, cost efficiency due to lesser raw material consumption, safer storage and handling. Other advantages include controlled flow of reagents leading to size uniformity, maintaining identical reaction conditions ensuring reproducibility, automation, thus, lesser prone to manual errors and most importantly eco-friendly as these routes utilizes fewer reagents and chemicals,<sup>4</sup> over conventional chemical ones. In addition, they offer varied range of applications from biomedical to industrial. These devices are strategically designed to control the flow of reagents in the microchannels so that the resultant nanoparticles are uniform even with low reagent consumption. Also, efficient mixing of the reagents in the channels, offer rapid rate of chemical reaction with equivalent heat and mass transfer. Therefore, the obtained nanoparticles show case great degree of evenness.<sup>5</sup>

Traditionally, the synthesis of nanoparticles is accomplished by two basic approaches namely (a) Top-down approach (b) Bottom-up approach.<sup>6</sup> Figure 1 shows the general schematic representation of the two approaches.

## Top-Down Approach

Herein, nanomaterials, <100 nm sized particles are prepared through breaking down of bulk material. Usually, lithographic techniques like optical, (photon based) method, wherein an image is projected on to a photo sensitive emulsion coated substrate like silicon wafer. It is most commonly used in lithography especially in the industrial front, electron beam, X-ray, etching and advanced micro-machining which involve mechanical, thermal and electro-chemical are employed to cut, mill and shape the particles.<sup>7</sup> It is basically done by either milling or attrition. However, though they are useful in small scale production of nanoparticles and shows appreciable reproducibility, yet these approaches are quite difficult to deploy for the synthesis on grand scale. In such cases, the bottom-up method is adopted.

## Bottom-Up Approach

In this chemical synthesis method, the nanoparticles are grown chemically through formation of molecules and clusters via atom-by-atom arrangement till the ideal particle morphology is obtained.<sup>1</sup> Owing to the ease of practical application of this method in industrial level production, bottom-up approach has gained significant attention and is widely adapted. Several chemical methods wherein, super saturated reagent solutions are used for producing spontaneous nanoparticles with consistent shape and size are reported.<sup>8</sup> Although advantageous over the top-down approach, this method has its own drawbacks. Reagent consumption and handling becomes challenging. To overcome this, microfluidic devices has proven to be a boon. They notably reduce the reagent volume and produce high quality nanocrystals with desired properties.

Microfluidic devices utilize bottom-up approach, i.e.; chemical synthesis route of nanomaterial fabrication. Bottom-up route has two stages (a) Nucleation phase (b) Growth phase. In the nucleation phase, the precursor particles (starting material) form precipitation in the reaction solution followed by growth phase, wherein, solutes get deposited and forms the desired particle size under the influence of pyro lytic, temperature, heat, pressure etc.<sup>9</sup> The chemical reaction takes place spontaneously to a point where reaction mixture becomes supersaturated. Finally, the solute particles aggregate to form the desired particles. As this phenomenon is highly dependent on

<sup>z</sup>E-mail: [sgoel@hyderabad.bits-pilani.ac.in](mailto:sgoel@hyderabad.bits-pilani.ac.in)

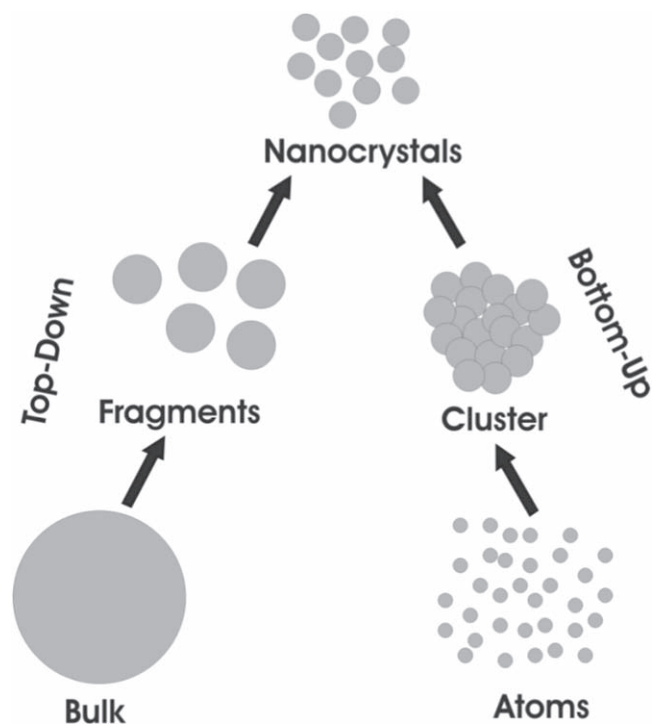


**Figure 1.** Schematic representation of the two approaches (a) Top-down (b) Bottom-Up for nanocrystals synthesis.

external factors like concentration of reagent, temperature and pressure. In this regard, microfluidic devices ensure uniform and rapid mixing of reagents to allow equivalent concentration, at the same time, these devices are designed strategically to maintain heat, mass, temperature, pressure all through the chemical reaction mixture.<sup>10</sup>

**Mixing in microfluidic chemical reactors.**—Crucial function of these mini reactors is the appropriate mixing of starting reagents. Thus, the microfluidic devices focus on enhancing the mixing strategies in short length microchannels, henceforth, reducing the overall device size. Likewise, thorough mixing of the reagents helps in improving the throughput of these systems for development of efficient lab-on-chip technology. Mixing in microfluidic reactors is quite essential for various chemical, biological reactions to take place, for dilution of sample and homogenizing the reagent for complete reaction to take place. Owing to the problem of laminar flow in the microchannels, mixing becomes challenging. The laminar flow arises due to low Reynolds number. This can be theoretically explained like, the hydraulic diameter of channel is used as length given by  $4A/P_w$ .  $A$  represents the cross-sectional area, and  $P_w$  wetted perimeter of the channel. Due to high surface-volume ratio and low length, greater heat and mass transfer occur within devices. The low hydraulic diameter, back pressure from the kinetic velocity of the sample and small flow velocities leads to laminar flows giving low Reynolds number. Hence, turbulent mixing of reagent that usually takes place in bulk reactors is not possible in these devices.<sup>11–13</sup>

In recent years, several literature reports have shown different microfluidic mixing techniques. Broadly, they are categorized as active and passive mixing. Active mixing involves an external force like magnetic, electro kinetic, acoustic, ultrasonic etc. are required for inducing the appropriate mixing.<sup>12</sup> Whereas, the passive mixing does not require any such additional force. Commonly, diffusive mixing, i.e.; a type of passive mixing is widely used in microfluidics. The basic pattern has “T” shaped microchannel wherein, flow of the two different reagents into “T” shaped inlets takes place which further flows into the common outlet. While in the outlet, the diffusion of the particles takes place due to concentration gradient.

Figure 2a shows a typical “T” shaped microfluidic channel. A slightly improved version is a “Y” shaped microchannel (Fig. 2b) wherein, two inlets allow the fluids to come in contact and diffuse. A single outlet permits the mixed solution out. In order to improve the mixing further, several modifications in the channel shapes are being done based on the requirement. For instance, a simple “Y” shaped microchannel can be further modified as a serpentine microchannel to enhance the mixing. Figure 2c shows the schematic representation of this basic design. Similarly, over the years, a variety of designs have been developed. There are microchannels fabricated for more than one inlets and so on. Figure 2d, shows a design of microfluidic channel with multiple inlets for three different reagents to enter and diffuse in a single channel and exit through single outlet. As can be seen in Fig. 2d, reagent C enters into the channel only after reagent A and B are thoroughly mixed. Figure 2e is a sample design wherein, three inlets allow three different reagents to enter the channel at different times. The flow of the reagents is monitored. To further improve the mixing, ridges, grooves and slanted wells are incorporated within the channels.<sup>12</sup> Therefore, mixing in microfluidic reactors are easily tailored based on the conditions and parameters required.

**Flow monitoring.**—In order to complete the chemical synthesis in the microfluidic reactors, efficient usage of flow controller plays a key role in monitoring the reagent flow. There are primarily three flow monitoring systems based on the source of pressure controller used. (a) Compressed air (b) Mechanical energy based and (c) Non-mechanical energy based.

**Compressed air.**—This Pressure controller utilizes compressed air source to pressurize the reservoir containing reagent which is in turn is connected to the microfluidic channel through tubes. The reagent moves into the channel due to pressure difference.

**Mechanical energy based.**—Utilizes mechanical pumps like most commonly, peristaltic and the syringe pumps to displace the desired volume reagent into the channels. Syringe pumps, containing an electrical stepper motor pushing the syringe filled with reagent liquid at a fixed rate, being user friendly and precise are used more predominantly. By modulating the syringe size and motor speed, flow rate can be monitored. On the other hand, the peristaltic pump has a mechanical rotor that gives compressions and relaxations which draws the reagent and gives the flow.

**Non-mechanical energy based.**—Also known as passive technique, utilizes non-mechanical energy or chemical energy processes like capillary action, hydrostatic force, electro-osmosis etc. to flow the reagent into the channels.<sup>14</sup>

In order to monitor the flow rate via any of the above technique, flow sensors like thermal, mass and mechanical are employed. Thus, flow of reagents and mixing of them for the chemical reaction to take place are carefully monitored.

**Temperature controller.**—Thermal management in a microfluidic platform is imperative and plays an essential role in nanomaterial synthesis. For the same, micro-controller based portable thermal management devices perform this task. Recently, Madhusudan et al., reported an IoT Enabled Portable Thermal Management System for synthesizing Manganese oxide nanoparticles. Herein, an automated device is fabricated that has a microcontroller, DC-DC converter, cartridge heaters, and feedback thermocouple sensors. These help in control of specified temperature via Proportional-Derivative-Integral (PID) based technique. Thus, it gives accuracy and precision. Figure 3 shows the image of a microfluidic reactor over the heating block.<sup>15</sup> An arduino based heating platform enabled an integrated PID controller feature, thus, easy of use and faster response was achieved.

To synthesize the MnO<sub>2</sub> particles, the authors designed a Poly (methyl methacrylate)(PMMA) (also known as an acrylic polymer)

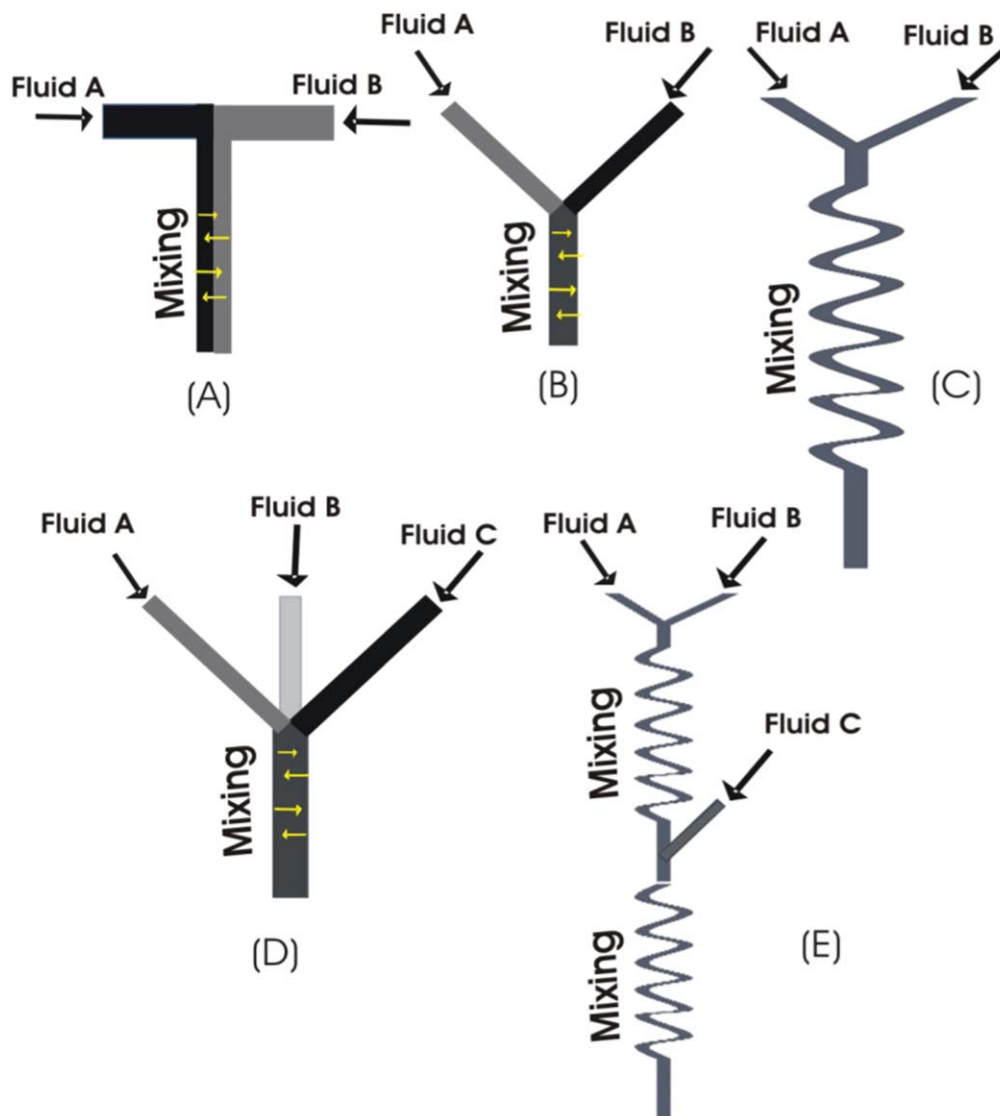


**Figure 2.** Schematic representation of a “T”, “Y”, “Y”-serpentine shaped microfluidic channel.

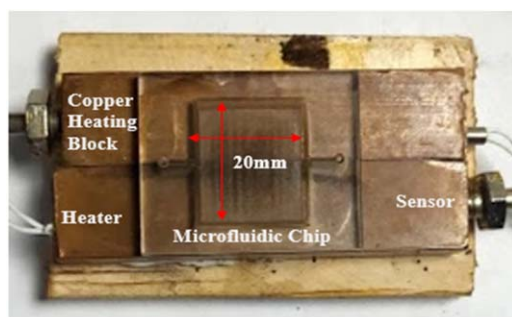


**Figure 3.** Micro-channel placed over the thermal management device (Copyright@2020).

microfluidic device. This device offered appropriate reaction parameters, faster mass and heat transfer, and high reproducibility. The starting materials were manganese sulphate ( $\text{MnSO}_4 \cdot \text{H}_2\text{O}$ ) and Potassium permanganate ( $\text{KMnO}_4$ ) in 1:2 ratio dissolved in 10 ml of DI water. The solution was magnetically stirred and 1 ml of it was transferred into the microfluidic device kept over the fabricated heating block. The reaction mixture in the microfluidic device was heated to  $90^\circ\text{C}$  continuously for 12 h. The resulted product was a

brownish black color powder. It was filtered and washed with DI water and dried at  $65^\circ\text{C}$  for 3 h before use.<sup>15</sup> The authors have further compared the advantages conventional hydrothermal method with the proposed portable microfluidic method. Table I summarizes the overall advantages of synthesis of nanoparticles in a micro-miniaturized devices over conventional bulk synthesis methods.

#### Fabrication of Microfluidic/Miniaturized Reactors

The most common technique adopted for fabricating microfluidic device is soft lithography. No matter how efficient this method is, it battles a huge drawback of clean room requirement. Hence, the clean room establishment is costly and fabrication in clean room is labor intensive, requires skilled technicians.<sup>16</sup> To overcome this, certain methods like laser jet printers,<sup>17</sup> photolithography,<sup>16,18</sup> 3D-printing,<sup>16,17</sup> laminates,<sup>16</sup> Moulding,<sup>16</sup> Embossing,<sup>16</sup> are being explored recently for the fabrication.

**Molding.**—This technique involves formation of a master mould using photolithography with materials like silicon. Liquid polymer is poured over this mould, cured and solidified. There are broadly three types of molding methods: (1) Replica molding (Soft lithography) (2) Inject molding (3) Hot embossing. These techniques involve the use of high temperatures, heat and pressure over liquid polymers

**Table I. Comparative table of conventional and portable microfluidic device based synthesis of MnO<sub>2</sub> particles.<sup>15</sup>**

Parameters	Traditional Bulk Hydrothermal Process	Synthesis in Micro/Miniaturized Devices
Thermal Features	Requires high pressure and temperatures for the reaction	Generally, reaction occurs at low temperatures
Processing time	Takes more time for complete synthesis	Less reaction time for nanoparticle synthesis
Space Occupancy	Bulky Instrumentation, requires thermal oven or furnace	Portable device, miniaturized device. Easy to handle
Volume	Higher volume of reagents	Lesser volume of reagents
Reaction chamber	Requires autoclave/oven in most of the cases	Microchannel reservoir with $\mu\text{l}$ to a few ml of sample

poured on master molds followed by solidifying the elastomers to form microdevices.<sup>16</sup>

**Soft lithography.**—Since 1998,<sup>16</sup> huge domination of soft lithographic techniques using polymer materials like polydimethylsiloxane (PDMS)<sup>19</sup> for making these devices have been observed. Soft lithography is method of self-assembling and replica moulding; a non-photolithographic technique. Xia et al. in 1998, reported a detailed study on soft-lithographic fabrication.<sup>18</sup> They reported that an elastomeric block consisting of designed structures on its surface plays a key role in fabrication. The process involves conversion of liquid materials like polyimides, PDMS, polyurethanes, etc. into solid elastomers. Cast moulding is used for making these PDMS or other elastomeric stamps. Herein, a master mould is prepared via micromachining, the liquid polymer mixed a commercially available curing agent (mixture of platinum complex and copolymers) is poured over this master which has desired pattern on its surface. Further, heating to high temperatures will solidify the material.<sup>18</sup> Figure 4 is a basic schematic representation of the process.

**Photo lithography.**—This technique basically uses optical means for drawing desired patterns on the substrate. Otherwise known as optical lithography, it is used to draw channels, patterns on thin film or bulkier substrates. Conventional projection photolithographic techniques are capable of designing patterns on small substrates  $\sim 250$  nm. However, modern photo lithographic techniques utilizes soft X-ray, e-beam, focused ion beam, Ultra-violet beam and can make patterns upto 100 nm size.<sup>18</sup>

**Laminates.**—This technique involves stacking and bonding of independently cut layers. Basically it has three layers; bottom layer, intermediate layer wherein channels are cut, and top layer. These layers are bonded to form a firm device. However, the number of layers can vary as per the requirement of the device. There are three important steps in these. (1) Selection of material (2) cutting the desired channels on the layer (3) bonding the stacked layers. Glass slides, polymer layers like PMMA, polycarbonate, PLA etc., adhesive transfer tapes are the preferred materials used. Knife plotter or laser cutting (commonly CO<sub>2</sub> laser) is often used for cutting the desired micro channels and patterns. Although laser cutting offers much precise dimensions, it is expensive and skill oriented handling is needed. In comparison, knife plotter is cost-effective. Nevertheless, the choice of the cutting method is influenced by the material used. The use of adhesives, like double sided tapes, and thermal bonding are the common methods of bonding the stacked layers. In thermal bonding, the temperature of each layer is increased to near the glass transition temperature ( $T_g$ -temperature at which 30–50 carbon chains starts to move in an amorphous material. They undergo transition from a solid rigid state to more flexible state) followed by applying force which bonds the stacked layers into functional device.<sup>16</sup>

**3D printing.**—Also known as additive manufacturing is a layer-by-layer material deposition technique wherein, new layer of a specified material gets deposited over its previous layers. Conductive filaments like Ploy Lactic acid (PLA), Acrylonitrile Butadiene Styrene (ABS), Wood Fiber (Cellulose + PLA), Polyethylene Terephthalate (PET), Poly Vinyl Alcohol used in 3D printed devices. The general

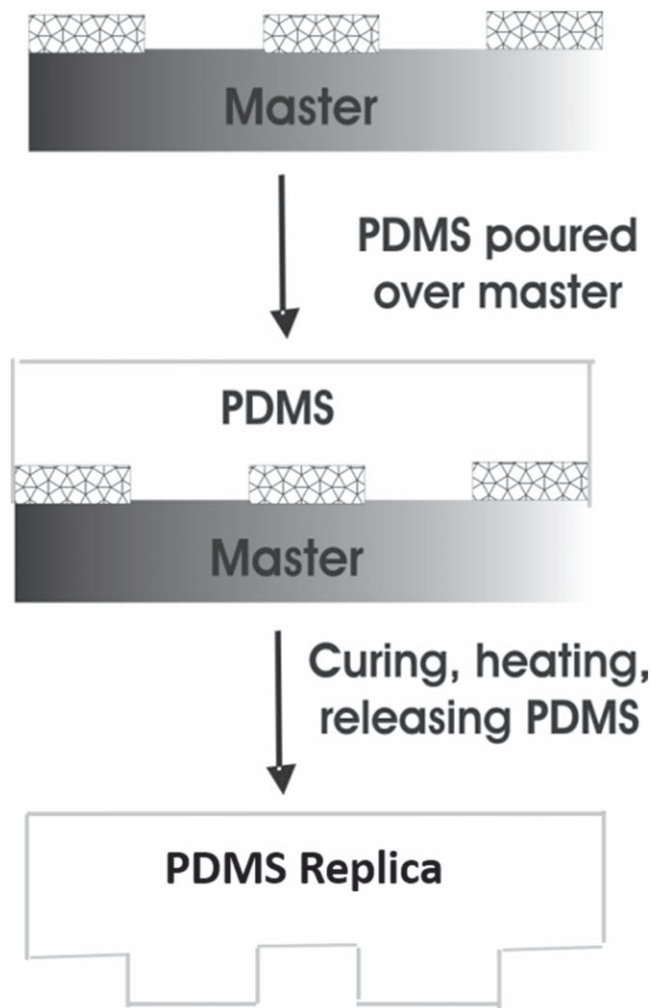


**Figure 4.** Schematic representation of PDMS replica fabrication.

method of fabrication involves a designing a 3D microfluidic device using a Computer Aided Design (CAD) software. Further, this designed model is converted to a Standard Triangle Language (STL) file which is compatible with the 3D printer software. This software forms 3D image into a sequential 2D layer giving a G-code file which then the 3D printer can fabricate the device via layer by layer material deposition. Figure 5 gives an over view of various 3D printing methods.<sup>16</sup>

Any of the above mentioned techniques are suitable for fabrication of microfluidic chemical reactors. Selection of the technique and the material depends upon the parameters of the reaction condition like, temperature, pressure, heat generation, starting material etc.

### Types of Microfluidic Reactors for Nanomaterial Synthesis

**Classification of microfluidic reactor based on flow condition.**—The broad classification of the microfluidic reactors based

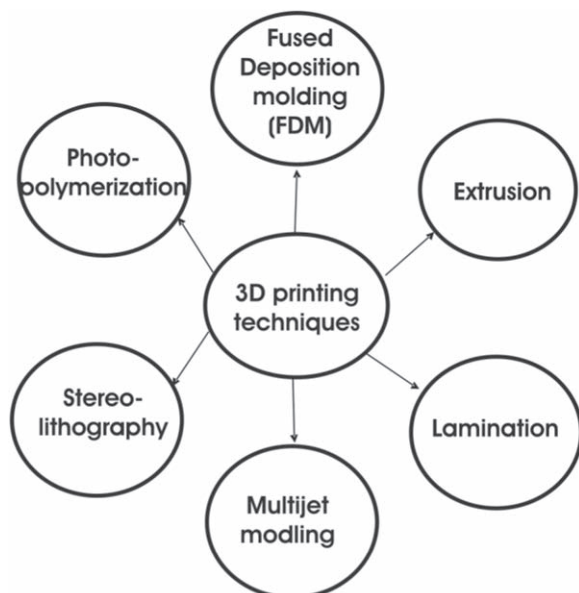


Figure 5. Over view of various 3D printing techniques.

on flow condition is typically of three categories. (1) Continuous flow microreactor (2) Microdroplet segmented flow microreactor (3) Capillary tube microreactor.

**Continuous flow synthesis.**—In the continuous flow reactor, diffusion dependent laminar flow allows a steady mix and reaction of the starting material. Continuous flow synthesis allows the reaction between the reagents in micro channels. The optimal particle dimensions are obtained by efficient reagent concentration, mixing, controlled temperature, reaction time etc.<sup>4</sup> Significant amount of reports are documented in the literature for continuous flow based nanoparticle synthesis in the microfluidic devices. For example, in 2002, Edel et al., reported a procedure for synthesis of Cadmium Sulfide (CdS) nano particles. Herein, they used a simple two inlet based microreactor through which the aqueous solutions of sodium sulfide and cadmium nitrate were made to flow in the reactor. Syringe pump was deployed to deliver these starting material into the microchannels. The channels of the reactor were structured in such a way that it mixes the two reagents via splitting into multiple streams before contact. Post mixing, channels were combined to a single outlet. The total volume required was not more than 600 nL. The flow rate was optimized between 10–300 ml min<sup>-1</sup>. They also found that, as the flow rate was increased, the uniformity of the particles was also improved. The particles were obtained just by mixing of the reagents and analyzed by absorption spectra.<sup>20</sup>

Likewise, Wang et al., fabricated titania nanoparticles in their designed interface microchannel reactor. Figure 6 shows the typical diagram of their micro reactor.<sup>21</sup>

Hexanol/Titanium Tetraisopropoxide and Formamide were delivered through two syringe pumps in the micro reactor as reagents. The microchannels allowed mixing of the reagents resulting in formation of titania particle which were collected through outlets in the bottle.<sup>21</sup> In another work, Chan et al., in 2003 reported Cadmium Selenide nanoparticles by changing flow rate, concentration of reagent, reaction time and temperature. Se/Cd(CH<sub>3</sub>)<sub>2</sub>/tributylphosphine was the starting reagent mixed with surfactant was delivered to the reactor via syringe pump. The reactor temperature was set at 180 °C for optimal time 300 s. The reaction occurred to yield CdSe nanoparticles.<sup>22</sup> Lin et al., stated a methodology for synthesizing mono dispersed silver nanoparticles. Herein, they used a thermal reduction process. Silver Pentaffluoropropionate and Trioctylamine taken in isoamyl ether were used as the starting reagents. The reactor channel was a stainless steel 20 cm lengthy tubular coil. Syringe pump was used to

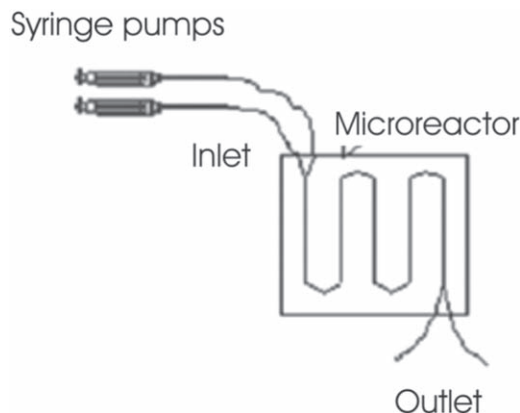


Figure 6. Schematic representation of the microfluidic reactor fabricated by Wang et al.

introduce the reagents in the microchannel. The micro tubular channel was immersed in an oil bath to maintain a temperature range of 100 °C to 140 °C. The formed particles were collected through the outlet in glass tubes. They investigated and compared the size of the formed Ag nano particles varying flow rate, temperature and reaction time.<sup>23</sup> In 2007, Shalom et al. reported synthesis of thiol functionalized gold nanoparticles in a continuous flow micro reactor. A photolithographic method was used for the device fabrication in which precursor reagents, pre-prepared gold thiolate polymer and aq. Sodium borohydride were used. The reaction happened at a room temperature with a reaction time of 4–40 s. The effect of reaction time and temperature was also studied.<sup>24</sup> Xu et al., in 2015, reported Nickel nano particle synthesis via aqueous reduction process. Nickel sulfate was used as the starting material and Hydrazine as a reducing agent. A “T” shaped continuous flow reactor channel of 1.58 mm was used. Separate pumps were used to deliver the reagents. The reaction temperature was maintained 80 °C, however, effect of temperature and reaction time was also investigated.<sup>25</sup> Recently, Heshmatnezhad et al., in 2020, came up with method of synthesizing polycaprolactone nanoparticles in a continuous flow microfluidic chip device. The device was prepared by a standard wet-chemical etching process and thermal bonding. Syringe pump was used for flow monitoring. They have also investigated five different designs of microfluidic devices for efficient synthesis of the polycaprolactone nanoparticles.<sup>26</sup>

**Microdroplet (emulsion) segmented flow.**—In a two-phase segmented flow synthesis, nanoparticles are formed due to the chemical reactions taking place within the microdroplets. This type of synthesis wherein emulsion droplets are used as reactors is not new.<sup>27</sup> Usually, organic or fluorocarbon oils are used for generation of these droplets.<sup>28</sup> Figure 7a depicts a typical diagram explaining how the microdroplets formed in the micro channels acts as micro chemical reactors (modified print copyright permission@2020).<sup>29</sup> The aqueous droplets carry starting materials along with the buffer. The reaction parameters like temperature and concentrations must be optimized by different permutation and combination. The reactions are carried out in two categories (1) Liquid plugs encapsulated in an immiscible liquid. (2) Aqueous slugs separated with other immiscible phase. Figure 7b gives the schematic representation of these two types of microdroplet reactors (modified print copyright permission@2020).<sup>29</sup>

### Microdroplet Generation Process

Microdroplets get generated through various techniques. Ikram et al. summarized some of the commonly used droplet generation devices. Figure 8 gives the pictorial representation of various processes.<sup>30</sup>

The generation of these microdroplets can be obtained through different approaches. Some of the common methods are discussed below.

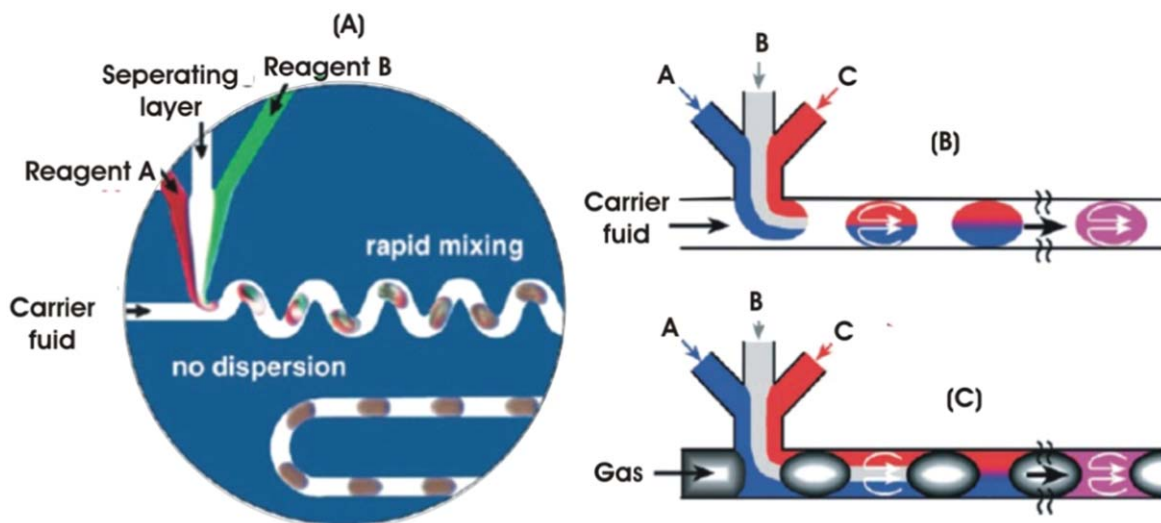


**Figure 7.** (a): Schematic representation of a basic micro droplet based reactor. (b) Schematic of two types of micro droplet reactor (Copyright permission@2020).

(i) Piezoelectric Ejector:

In 2001, Jones et al., developed a method for generating tiny droplets of picolitre volume through piezoelectric ejector. The device developed by them could deposit droplets of approximately 7 nl on polyimide surface. Since, the droplet generated is exposed to the atmospheric ambience, the use of this approach in chemical synthesis is a disadvantage as the reagent could evaporate even before the reaction occurs. Also, controlling the multiple droplets using this technique is a herculean task.<sup>31</sup> Thus, attempts to improve this technique are being done. Bransky et al., reported an improved piezoelectric actuator based droplet generator that can translate electric voltage to mechanical translation to determine the fluid segment volume.<sup>32</sup>

electric field is employed. Droplets get generated when aqueous medium is introduced into an immiscible liquid (oil). Generally, “T”-junction and flow focusing technique is used. In a “T”-junction method, aqueous phase is introduced into a continuous oil phase perpendicularly. Owing to the force between two distinct phases, droplet generation occurs.<sup>33</sup> In a typical flow focusing technique, liquid (aqueous) flows into the central channel and an immiscible liquid (oil) flow through the two outer side channels. These two phases are forced to flow downstream of the three channels via orifice. The outer fluid applies pressure on the inner fluid into narrow stand that forms droplets.<sup>34</sup> This techniques give reduced size droplets hence advantageous.<sup>35</sup>

(ii) Microfluidic channels:

In order to achieve high-throughput generation of microdroplets from microfluidic channels, the use of needles, micro-injectors and

(iii) Electric field based generator:

He et al., in 2005 described electro-generation of aqueous micro droplets ranging from femtoliter to picoliter volume. Likewise, Link et al., in 2006 reported electronic control of microdroplets generation based on the combination of electrostatic charge on the droplets and

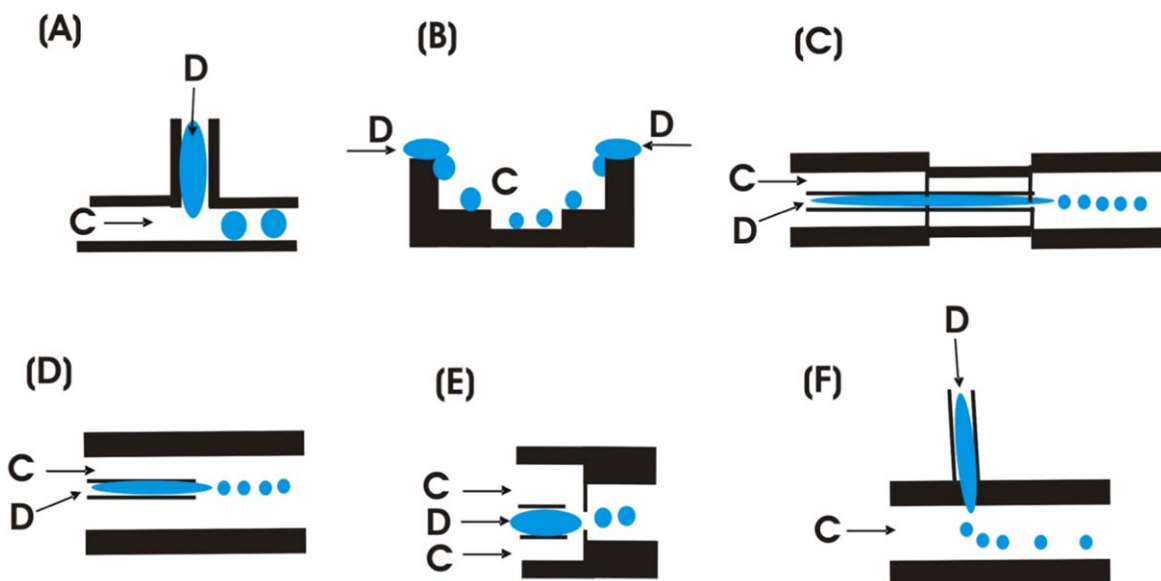


**Figure 8.** Schematic representation of common microdroplet generation methods. D-dispersed phase, C-Continuous phase. (a) Flow focusing (b) T-junction (c) Cross flow (d) Cross-flow device (e) Capillary based (f) Flow focus.

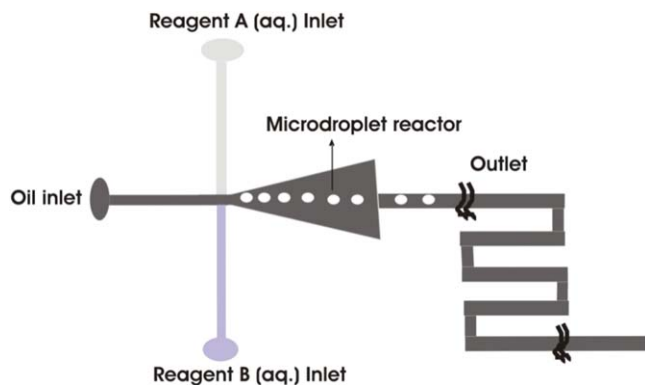


**Figure 9.** Schematic diagram of the droplet microfluidic reactor designed by Hung et al. (modified and redrawn).

the high electric fields employed on the micro device. The device was fabricated with soft lithography using PDMS as base material. Electric field was generated by ITO electrodes patterned along the microchannels. Flow focusing technique is deployed for drop formation. High electric field pulse is applied to the two liquid phase interfaces (oil-water). This leads to generation of electrostatic force between the interfaces leading to droplet formation. A minimum of 1 kV of electric field is needed for this. This method has a key advantage that it does not require any complex flow controls and gives high throughput manipulation of droplets.<sup>36,37</sup>

#### (iv) Mechanical valve:

Lee et al., in 2009, developed a new strategy wherein they used mechanical valve to generate microdroplets. Mechanical cutting technique was used to generate droplet at “T” shaped microchannel. Soft lithography was used to make PDMS micro device with T shaped channel. A main flow channel forms T junction in accordance with other side flow two channels. The main channel has a continuous phase flow and the dispensed phase enters into the main channel through the side channels. A mechanical valve was attached to the side channels hence, dispensed phase flow into the main channel was controlled. Droplets were generated when the side channels carrying the dispensed phase was closed completely with the valve. The opening time of the mechanical valve was regulated to get the uniformity in size of the droplets generated.<sup>38</sup>

However, the generation of microdroplet is not limited to the discussed methods only. Other techniques like light actuation (UV-light),<sup>39</sup> elastomeric sponges,<sup>40</sup> pneumatic actuation,<sup>41</sup> surfactant based,<sup>42</sup> centrifuge based,<sup>43</sup> temperature controlled,<sup>44</sup> microinjection<sup>45</sup> etc. Wei et al., in 2019, gave a detailed overview of various advances in the microdroplet generation approaches.<sup>46</sup>

### Types of Microdroplet Reactors

These microdroplet reactors can be emulsions, capsules of polyelectrolyte, micelles, vesicles etc. The major advantage of this microreactor based preparation is that the particles will not aggregate.

**Emulsions.**—These microreactors are water droplets in oil. Each droplet carries the reagent.<sup>47</sup> Herein, either both the starting materials are dissolved separately in a dispersion medium or one can of it can be dissolved in a surfactant. Another technique called micellar exchange process can be used wherein, different microdroplets carrying separate reagents can aggregate together to form single droplet comprising of all the reacting chemicals and allow the chemical reaction.<sup>48</sup> Literature reports preparation of several metal oxides like ZnO<sub>2</sub>, SiO<sub>2</sub>, TiO<sub>2</sub>, FeO<sub>3</sub> via micellar exchange approach wherein, corresponding metal salts are dissolved in aqueous media

and base to the oil. Owing to the advantages like ease of handling, single-step preparation and less time consumption, these methods are used. Nevertheless, certain drawbacks like pH control, ionic concentration strength control limits this method for fabricating fewer types of nanomaterials only.

**Micellar.**—Micellar are water droplets encapsulated by surfactants stabilized via their hydrophilic heads. The hydrophobic tails has continuous solvent contact. Reagents are dissolved within the water center of the micelle where reaction occurs.<sup>48</sup> This method has been reported in the literature for synthesis of semiconductors (Q-Size), of ZnS, PbS, CdS, ZnSe, CdSe, CdTe etc.<sup>48</sup> The use of anionic surfactant has also gained much attention. Herein, metal salt is entrapped in the micellar center and then anion is added in the solvent phase. Preparation of metal particles like Au, Ag, Pd, Fe, Co, Cu have been reported through this method. Metal salts are embedded in the micelle core and reduced by strong reducing agent like H<sub>2</sub>gas, Sodium Boro Hydride, Hydrazine etc.

**Capsules.**—Polyelectrolyte capsules were introduced by Donath et al. in 1998. Capsules were prepared using polymers like polystyrene sulfonate, polyvinyl sulfate, polyallylamine. Colloidal particles when immersed in these ionic polyelectrolytes alternating the charge, gives self-assembled multilayered adsorbed over the surface. These deposition leads to formation of hollow cores forming capsule like structures. The polyelectrolytes are highly permeable, thus, reagents can enter these capsules and acts as microreactor.<sup>48</sup> These capsules offers features like tunable pH, concentration variation and highly selective permeability, henceforth, advantageous to fabricate magnetic, fluorescent and optical nanoparticles. Although efficient, it has limitations related to controlling the permeability especially if the ions are smaller. In addition, the preparation of the capsules is skill based and time-consuming. Therefore, not many types of nanoparticles can be synthesized in these.<sup>48</sup>

Significant literature is available using this method of synthesis. For instance, in 2004, Millman et al., reported a novel method for synthesizing anisotropic particles. Herein, they used microchips controlled by electric field. The process involved perfluorinated oil droplets that carried starting reagents/polymer solutions. Self-assembled anisotropic particles were obtained.<sup>28</sup> Likewise, Shestopalov et al., developed a multi-stepped synthesis CdS and CdSe nano particles in a PDMS microfluidic device in milliseconds.<sup>49</sup> Hung et al. reported in 2006, an interesting approach of Cadmium sulfide nanoparticle synthesis. They fabricated a double-T junction microfluidic device with three inlets and a switch-back outlet. Molding technique via PDMS stamp was used for fabricating the device. Reagents; Cadmium Nitrate and Sodium sulfide were delivered to the channels with syringe pump and silicon oil was used for droplet generation. Each droplet acted as a microreactor for formation of CdS particles which were collected through outlet.

Figure 9 represents the schematic picture of the device created by Hung et al.<sup>50</sup> Similarly, Wacker et al. in 2012, developed fluorescent silica nanoparticles in PDMS based microfluidic device using soft lithography. By manipulating the reaction time and the concentration of the reagents, the size of the particles obtained were varied. A comparative investigation of the nanoparticles synthesized in microdroplet reactor and bulk revealed that the size of the nanoparticles obtained in microdroplet could be controlled widely as the growth of speed is more. They further functionalized the nanoparticles with fluorescent dye.<sup>51</sup>

It was later in the year 2017, when Abalde-Cela et al., came up with synthesis of branched gold nano particles in two different approaches. This was the first time when on-chip synthesis of branched gold nanoparticles was achieved. They attempted surfactant free and PVP (surfactant) based methods and compared the morphological aspects of the nanoparticles obtained in them. Photolithography technique was used to design the PDMS based microfluidic devices.

Figure 10 represents the designs of the two devices by Abalde-Cela et al. For surfactant free synthesis, Hydrochloric acid,

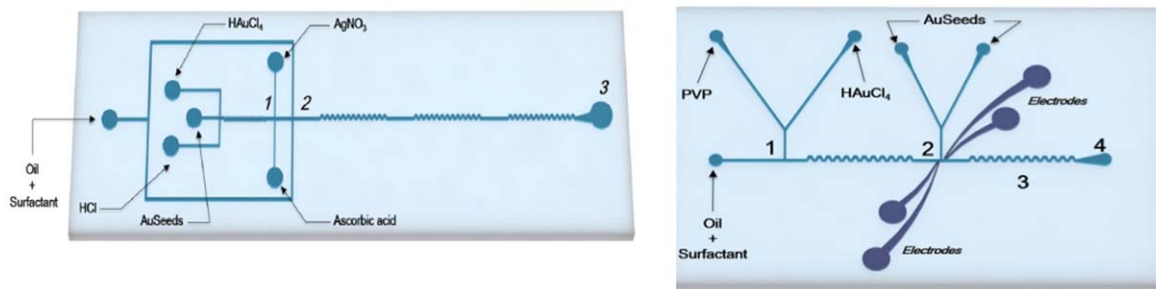


**Figure 10.** Images of the (a) Surfactant free (b) surfactant based microfluidic synthesis chip design for branched gold nano particle synthesis; reprint from Abalde-Cela et al. 2018 (Copyright permission@2020).

Chlorauric acid, ascorbic acid, Silver nitrate and gold seeds were delivered to the channels along with surfactant. The reaction took place in the microdroplets and resultant nanoparticles were collected. Whereas for the surfactant based, PVP in DMF, Chlorauric acid were used as reagents, Au-nanoparticles were reduced in the droplets generated due to the chemical reaction of the reagents. Thus, synthesis was obtained on chip.<sup>52</sup>

Apart from the traditional chemical synthesis approach, the microdroplet reactors are also being utilized in biosynthetic route of fabricating metal nanoparticles. Figure 11 gives a detail description of the biosynthetic route used (reprint from Lee et al. 2012). Lee et al., reported artificial cellular bioreactors using hydrogel polymer, *E. coli* cell and microdroplet. The device used was fabricated with photolithography using a silicon mold of PDMS. Plasma bonding was used. Microdroplets of cell extract and N-isopropylacrylamide (NIPAM) monomer were generated with a flow focusing technique. Upon polymerization, NIPAM acts as an artificial membrane. Thus, forming cellular bioreactor. The size of these reactors were controlled between 26 to 53  $\mu\text{m}$  in dimension. Precursor solutions: i.e.; metal salts are introduced in the artificial cellular membranes through absorption. The cellular extract reduces the salts into nanoparticles. Gold, Selenium, Cadmium, and Iron were precursors used. Using this bioreactor, metallic nanoparticles, quantum dots, magnetic nanoparticles and nanocrystals were fabricated successfully. TEM characterization and UV-vis was used to study the morphological features of these different nanomaterials synthesized in these biomimetic reactors.<sup>53</sup>

Green synthesis of metallic nanoparticles in micro reactors were also attempted. For example; Fernandes et al., in 2013 reported green synthesized silver nanoparticles in a microreactor. The reagents used were betanin (phytochemical from beetroot), silver nitrate (metal salt) and sodium hydroxide for pH balance. They utilized a commercially available microreactor with capability of four pumps. Aqueous solutions of betanin and silver nitrate were introduced in the micromixer through syringe pumps. Post thorough mixing, aqueous solution of sodium hydroxide was introduced into the pre mixed reactant and kept at 80 °C. The effect of reaction time and concentration of reagents was investigated with reference to the particle morphology.<sup>54</sup>

**Capillary tube microreactor.**—Herein, normal tube reactors are scaled down to micro dimension capillary tube. It comprises of a flow cross-sectional area. These tubes are generally made up of stainless steel, glass, silica and polymer. Due to the micro size of tubes, temperature control is uniform giving size controlled nanoparticles. In order to achieve multiple step synthesis, many tubes can be connected in series. Nanoparticles like ZnS, CdSe are prepared using this method.<sup>55</sup> He et al., reported preparation of silver nanoparticles in a capillary tube reactor. Polytetrafluoroethylene capillary tube was used as microreactor. Silver acetate, oleylamine and 1,2-dichlorobenzene were the starting materials used. The reagents were introduced into coiled capillary tube kept in oil bath at 170 °C. Different size of colloidal silver nanoparticles were synthesized by manipulating the flow rate and reagent concentration. Reaction time was dependent on the flow rate.<sup>56</sup>

### Types of Nanoparticles Synthesized in Various Microfluidic/Miniaturized Devices

Nanoparticles ranging from metallic/inorganic, semiconductors, polymer, biomaterial, magnetic, quantum dots, ternary particles, colloidal etc. have been synthesized using microfluidic devices. Literature reports various methods for the same.

**Metal/Inorganic nanoparticles.**—Metal nanoparticles are usually synthesized in these reactors using metal salts as precursor materials. Various metal nanoparticles like, gold, silver, palladium, zinc, nickel, cobalt, copper, iron, titanium etc. have been prepared. In 2004, Wagner et al., reported preparation of Au nanoparticles utilizing Au seeds prepared from chlorauric acid and trisodium citrate and ascorbic acid as reducing agent. The microfluidic device had three inlets, one outlet, two mixing areas, engraved via wet etching on Pyrex glass and silicon. Syringe pumps were used to introduce these reagents into microfluidic device channel of 2.3  $\mu\text{l}$  volume. Figure 12a shows schematic of the device.<sup>57</sup> Similarly, Shalom et al., reported thiol functionalized Au nanoparticles,<sup>24</sup> with two reagent inlets and one outlet on a chrome glass substrate. They employed standard photolithographic and chemical etching approach to engrave the microchannels. Lazarus et al. reported protocol for fabricating mono dispersed Au nanoparticles using ionic liquids. They designed a PDMS based device using photolithography with four inlets and one outlet of size 3\*5 cm, volume capacity of 7.6  $\mu\text{l}$ . The central middle inlet was used to generate oil droplets at the junction while other three supplied reagents. A serpentine channel was used for mixing/reaction zone. Figure 12b is the schematic representation of the device.<sup>2</sup> Weng et al. in 2008, synthesized hexagonal gold nanoparticles in microfluidic reactor. Reagents used were chlorauric acid and sodium citrate. The device fabricated had micro-pumps, micro-valve for flow control, micro-mixer to mix the reagents and a micro temperature controller. Figure 12c gives the schematic over view of the device.<sup>58</sup> Yang et al. in 2010 reported PDMS based microfluidic device with micropump, valve and vortex micro mixer. The automated system enables reagents to transfer, mix and react. The chip is placed on a commercial temperature controller at a fixed temperature of 100 °C, chlorauric acid and sodium citrate are the starting materials introduced in the mixer and reaction is allowed. Sodium citrate acts as reducing agent forming Au-nanoparticles at 100 °C.<sup>59</sup> Ftouni et al., reported Au-nanoparticles of 1.8 nm diameter by citrate reduction.<sup>60</sup> Monodispersed Au nanoparticles were synthesized in a simple glass microfluidic device with Y shaped channel. Tetrachlorauric acid was used as metal salt, and a combination of sodium citrate and tannic acid as reducing agent. These solutions were injected into chip through syringe filters and reaction lead to formation of uniform Au-nanoparticles which were collected through the outlet. Reaction zone on the chip was about 131.5 mm. Figure 12d shows the schematic diagram of their microfluidic device.<sup>61</sup> A glass capillary microfluidic device was fabricated for synthesis of polyvinylpyrrolidone capped Au-nanoparticles. Ascorbic acid and tetrachloraurate trihydrate ( $\text{HAuCl}_4 \cdot 3\text{H}_2\text{O}$ ) were used as source of metal salt and reducing agent. Two glass capillary tubes: one round tube with 1 mm outer and 0.58 mm inner diameter, square tube with 1.05 mm inner diameter were used.<sup>62</sup>



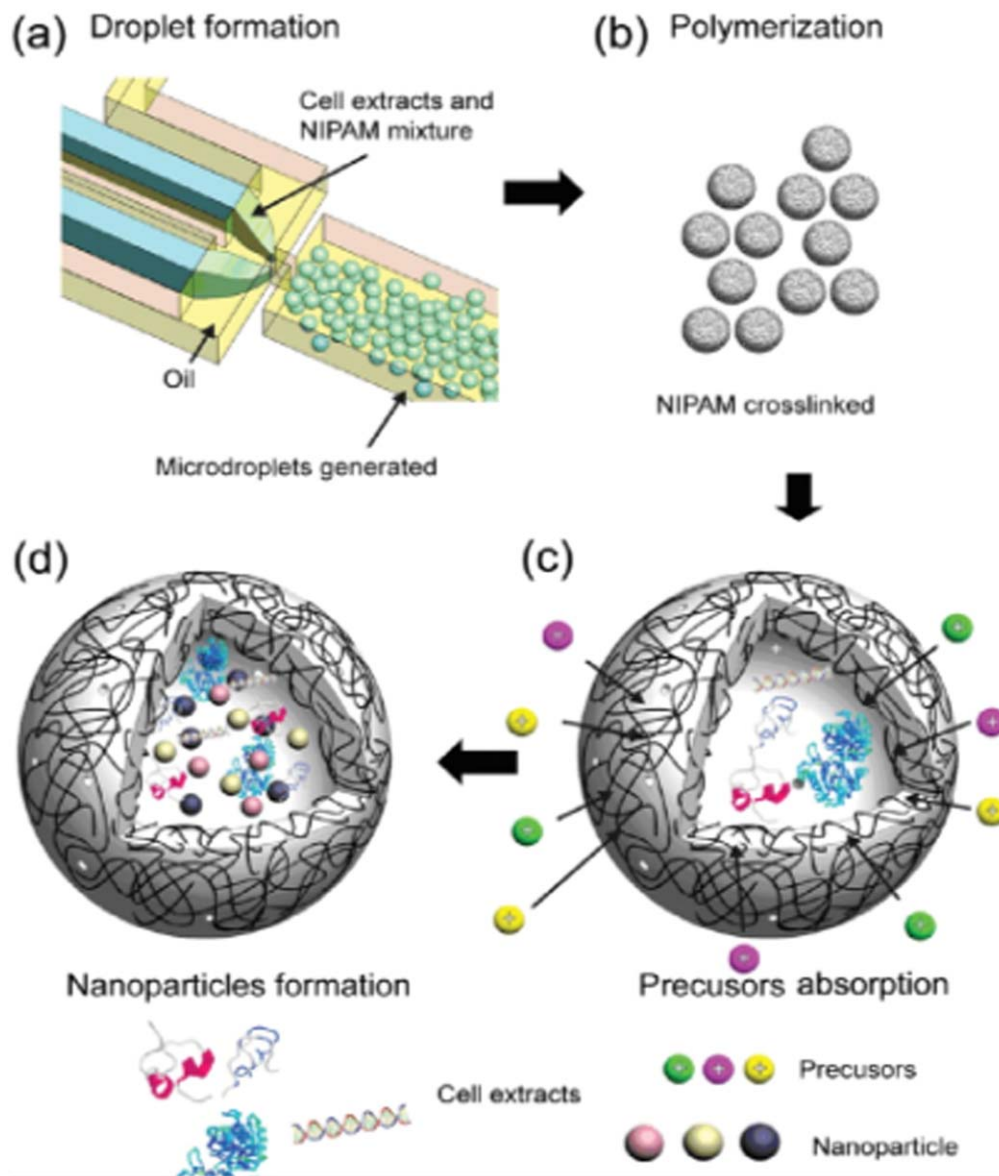


**Figure 11.** Schematic representation of metal nanoparticles formed from biosynthesis using *E. coli* (reprint from Lee et al. 2012 copyright@2020).

Silver metallic salts upon treating with reducing agents under controlled temperature and reaction conditions gives silver nanoparticles. Microfluidic reactors can be used for this. Patil et al., fabricated Ag nanoparticles in a typical Y channel microfluidic reactor. Figure 12e is schematic drawing of their device. Silver nitrate solution with added surfactant; sodium dodecyl sulfate was introduced into the channel through one inlet using syringe pump and sodium borohydride with surfactant from the other inlet. Effect of flow rate, reaction time and temperature was investigated. The resultant Ag nanoparticles were collected through the outlet.<sup>63</sup> Ionic liquids were also used for Ag nanoparticle synthesis.<sup>2</sup> Baber et al. in 2016, fabricated Ag nanoparticles in an impinging jet reactor. Syringe pump was used to let the reagents (Silver nitrate with trisodium citrate through inlet one and sodium borohydride through inlet two) into the jet reactor. Flow rate was monitored to obtain desired jet speed. Once the jets of reagents collided, reaction takes place giving nanoparticles. Figure 12f shows schematic representation of impinging jet reactor.<sup>64</sup> Lei et al. developed a microfluidic device with PDMS using soft lithography. A simple three inlet based device, of micro-channel width (200  $\mu\text{m}$ ) and height (50  $\mu\text{m}$ ) with T junction, one outlet was used. Herein, segmented microdroplet method was adapted.

Mineral oil containing surfactant was the continuous phase in which the two aqueous reagent solutions, silver nitrate and sodium borohydride, flows into the co-flowing oil phase forming microdroplet reactor. The reaction occurred at room temperature and syringe pumps were used for monitoring the flow. Figure 12g is the schematic diagram of the device.<sup>65</sup> Kwak et al., customized the microfluidic reactor for synthesis of Ag nanoparticles. The microreactor had two "T" junctions, three inlets and single outlet. Aqueous solution of reagents silver nitrate and polyethyleneimine were introduced to inlets through microsyringe. First T junction was used for introducing reagents in static mixer and second for generation of droplets. Reaction was carried out at 60 °C for 60 min and resultant particles were collected in isopropyl alcohol followed by centrifugation. Figure 13a is the schematic representation of the device.<sup>66</sup> Composites of silver nanoparticles-chitosan were also attempted in microfluidic chip devices. PMMA sheet engraved with microfluidic channels with CO<sub>2</sub> laser was used. It comprised of three inlets, one outlet, orifice and one cross junction channel. Middle inlet was introduced with dispersed phase i.e.; silver nitrate with chitosan, the other two were for continuous oil phase. Droplets were generated at T junction and further droplets were collected through outlet in sodium

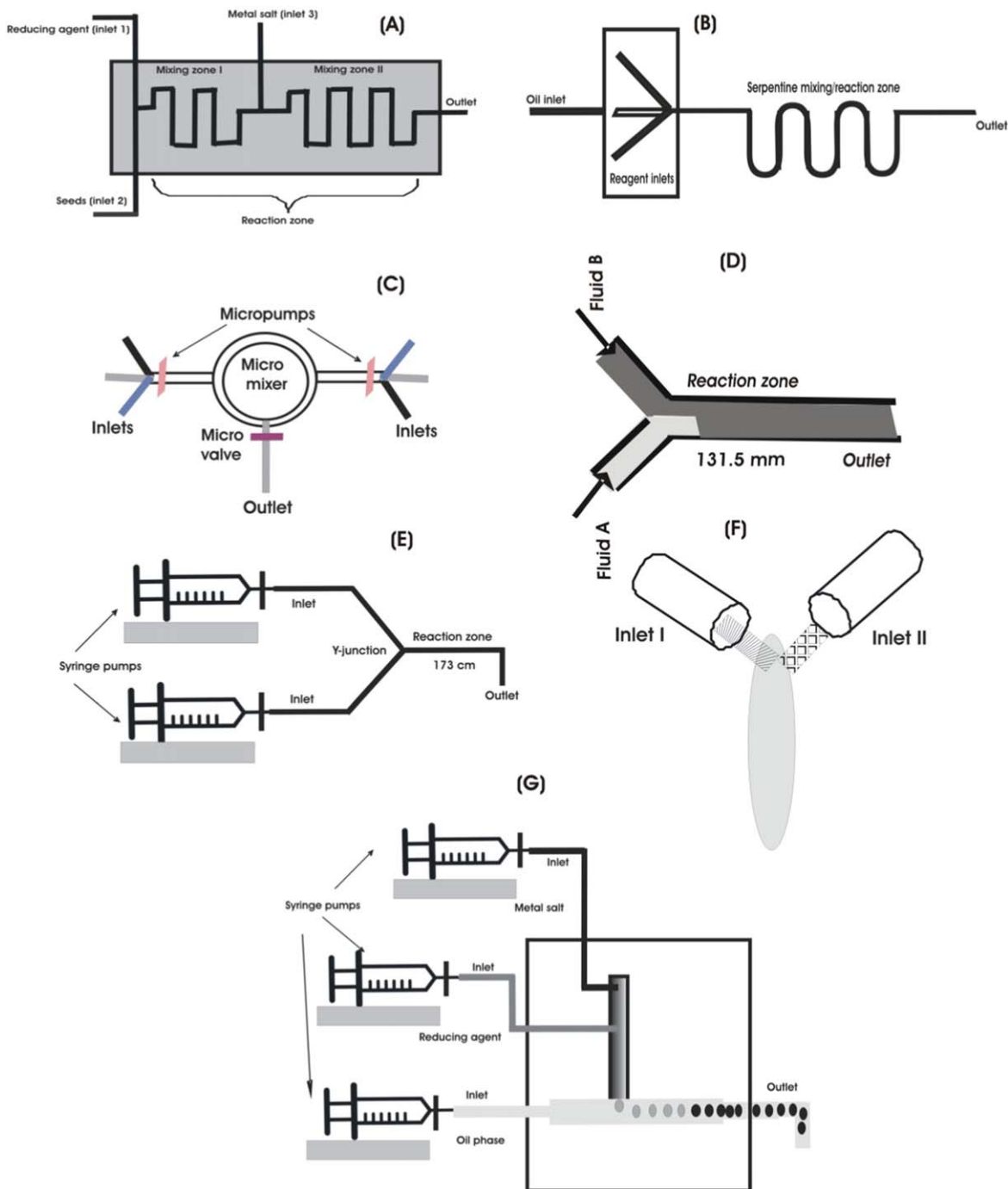


**Figure 12.** Schematic representations of the various microfluidic devices reported.

hydroxide solution which acted as a reducing agent forming silver nano-chitosan composites. Figure 13b gives the schematic diagram.<sup>67</sup>

Song et al. fabricated a microfluidic device using polyetheretherketone for fabrication of palladium nanoparticles. Herein, Palladium chloride and lithium hydrotriethyl borate in THF were used as reagents. The device had five inlet parallel channels to increase the production and yield. Metal salt was added through four inlets and reducing agent through one into the mixer where reaction took place. Figure 13c depicts the schematic representation of the device along with the reprint of microfluidic chip.<sup>68</sup> Karim et al., reported a unique microreactor for synthesis of palladium nanoparticles of size as small as 1 nm. Palladium acetate and oleylamine and trioctylphosphine were used as reagents. Microfluidic device had a

serpentine channel of  $270\ \mu\text{m}$  in depth,  $700\ \mu\text{m}$  in width, 80 cm in length and  $150\ \mu\text{l}$  of the total volume requirement. Reaction time was 95 min. The inlet and outlet ports were kept cooler using additional serpentine channel with flowing RT water. The reaction zone serpentine channel was heated to  $60\ ^\circ\text{C}$  and  $100\ ^\circ\text{C}$  to obtain palladium nanoparticles. Figure 13d is the reprint of the device from karim et al.<sup>69</sup> Palladium nanorods were synthesized by Sebastian et al. The microfluidic device consisted of three inlets, one outlet divided into two zones; mixing and reaction zone. Laminar segmented flow, wherein,  $\text{Na}_2\text{PdCl}_4$  as metal salt, in mixtures of water, ethylene glycol, polyvinyl pyrrolidone, and KBr were used. Pd nanorods were formed by usage of air as segmentation, temperatures were modulated from  $160\ ^\circ\text{C}$  to  $190\ ^\circ\text{C}$ . Reaction time was 2 min. The obtained nanorods

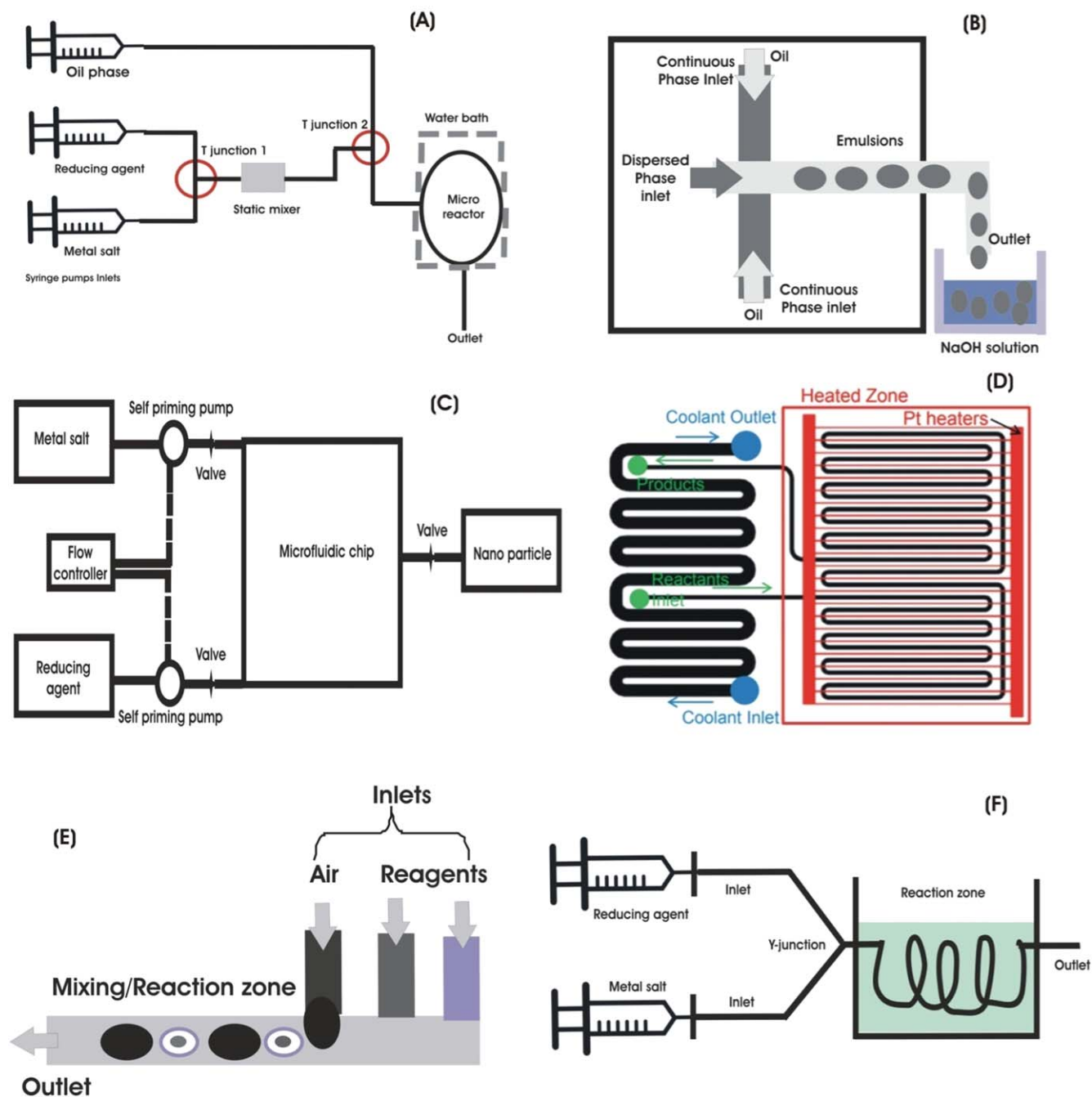


**Figure 13.** Schematic representations of various types of microfluidic devices. (D) reprint from Karim et al. (Copyright permission@2020).

were upto 4 nm in size. Figure 13e is the schematic representation of the microfluidic device designed by them.<sup>70</sup> Sharada et al. designed a simple continuous flow microreactor with two inlets. Syringe pumps were used to introduce palladium chloride and sodium borohydride in a Y shaped channel. The Y shaped junction lead to coiled capillary tube which not only allowed mixing of reagents but also led to reaction between reagents. The tube was kept in a water bath wherein temperature was controlled upto constant 25 °C. Pd nanoparticles formed were collected through single outlet. Figure 13f depicts the experimental set up of the microfluidic device.<sup>71</sup> Very recently, Gioria et al. in 2020, reported green synthesis route. Herein, a mixture of palladium chloride, starch and glucose were used as reagent one and introduced to one inlet through syringe pump. Sodium hydroxide was introduced through second inlet. T shaped junction let the reagents to a micro mixer which leads into coiled Tygon tube of 1.3 mm diameter

(reaction zone). The tube was kept in a water bath at 60 °C. The formed particles were then collected through single outlet. Figure 14a shows the typical schematic diagram of the microfluidic device.<sup>72</sup>

Inorganic metal oxide nanoparticles are also prepared in these microreactors. For example, ZnO nanoparticles were synthesized by Kang et al. Microchannels were created using silicon substrate. The device had T shaped junction with two inlets, channel and single outlet. Syringe pump was used to inject starting material aqueous zinc acetate dehydrate through one inlet and sodium hydroxide through other inlet. The channel allowed reaction and mixing of reagents and was kept at 60 °C. The formed ZnO was collected through single outlet. Figure 14b is the schematic representation of the microfluidic channel.<sup>73</sup> Wang et al., prepared ZnO nanoparticles using microemulsions in a microchannel reactors. The microemulsions has smaller reaction zone therefore, limiting the size to nano.

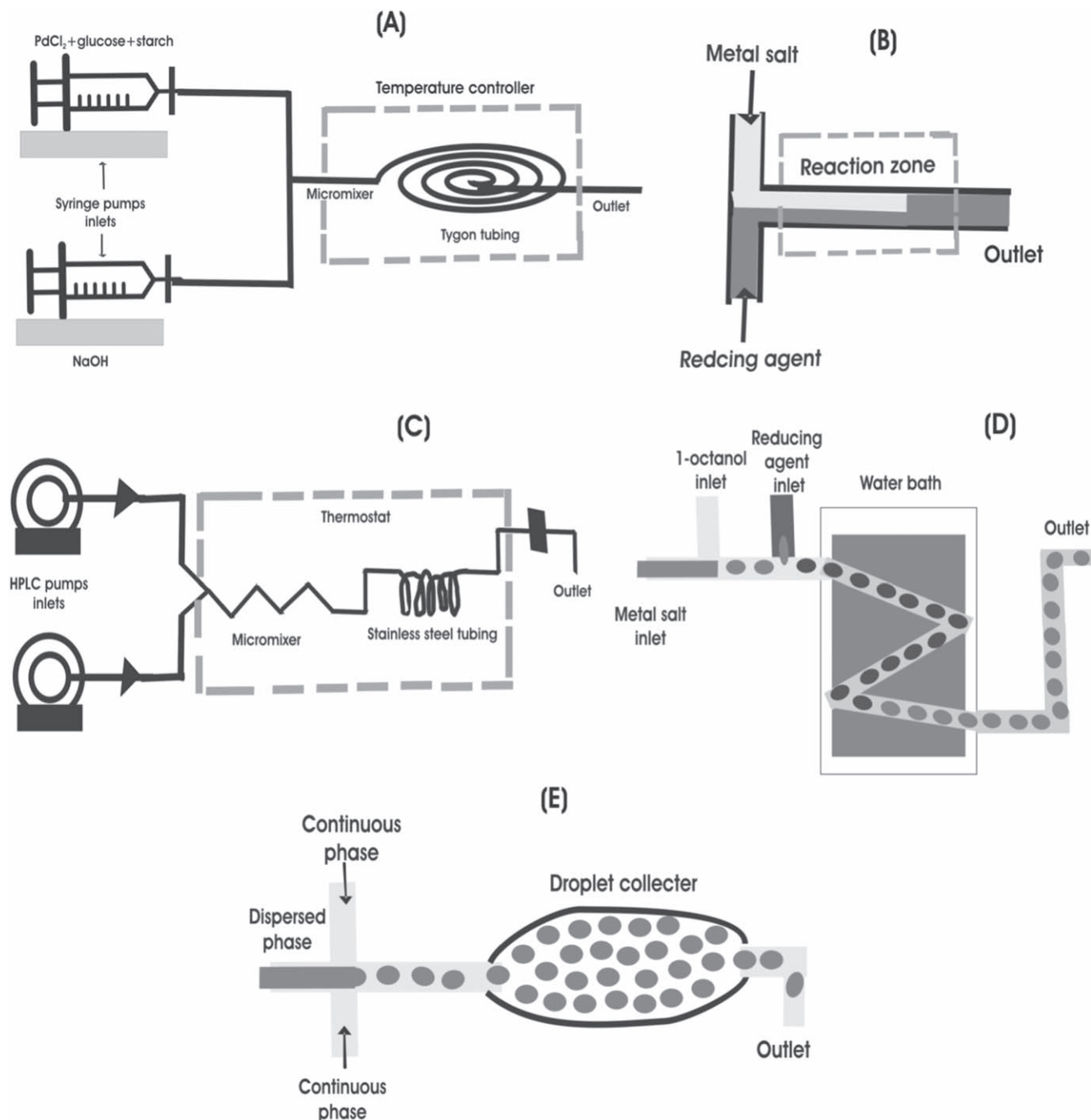


**Figure 14.** Pictorial representation of various microfluidic devices used as microreactors.

Three different types of zinc salts, zinc nitrate, zinc sulfate and zinc chloride were investigated as starting reagent. Sodium hydroxide was the reducing reagent. Concentration of metal salt, temperature and flow rate was investigated. The particles obtained were of 16 nm. The microreactor had two inlets for injected reagents through HPLC pumps into a micromixer. Micromixer was  $300 \times 300 \mu\text{M}$ , connected to a stainless steel tube reactor (Spiral) of  $6.35 \text{ mm} \times 1 \text{ m}$ . The reactor was kept on temperature controller. The formed product is collected through outlet. Figure 14c shows the schematic of the microfluidic reactor.<sup>74</sup> Zukas et al., reported ZnO synthesis in a PDMS based microfluidic device with three inlets and single outlet. One inlet was fed with aqueous zinc acetate, another inlet with 1-octanol, whose droplets were generated. Second inlet was fed with sodium hydroxide in 1-octanol, at a T junction. The droplets with reagents was let into tubular channel kept in water bath at

temperature varying from  $25 \text{ }^\circ\text{C}$ – $80 \text{ }^\circ\text{C}$ . Post completing the reaction, ZnO particles were collected through single outlet. Figure 14d is the pictorial representation.<sup>75</sup> Ghifari et al. reported, ZnO synthesis via flow focusing method. Microdevice using softlithography, PDMS was prepared with channels of width and depth as  $60 \mu\text{M} \times 60 \mu\text{M}$ . Syringe pump was used to inject the continuous oil phase and dispersed phase at T junction. Figure 14e shows the schematic diagram of the microdevice.<sup>76</sup>

Iron oxide particles being magnetic in nature have great potential in various applications. Literature reports several approaches wherein Iron oxide nanoparticles are synthesized in microfluidic reactors. For example, Hassan et al., fabricated a coaxial flow based device using laminar flow. Capillary tube channels with PDMS substrate is used to fabricate the device. Acidic Ferric chloride solution is used as metal salt and tetramethylammonium hydroxide as reducing agent.

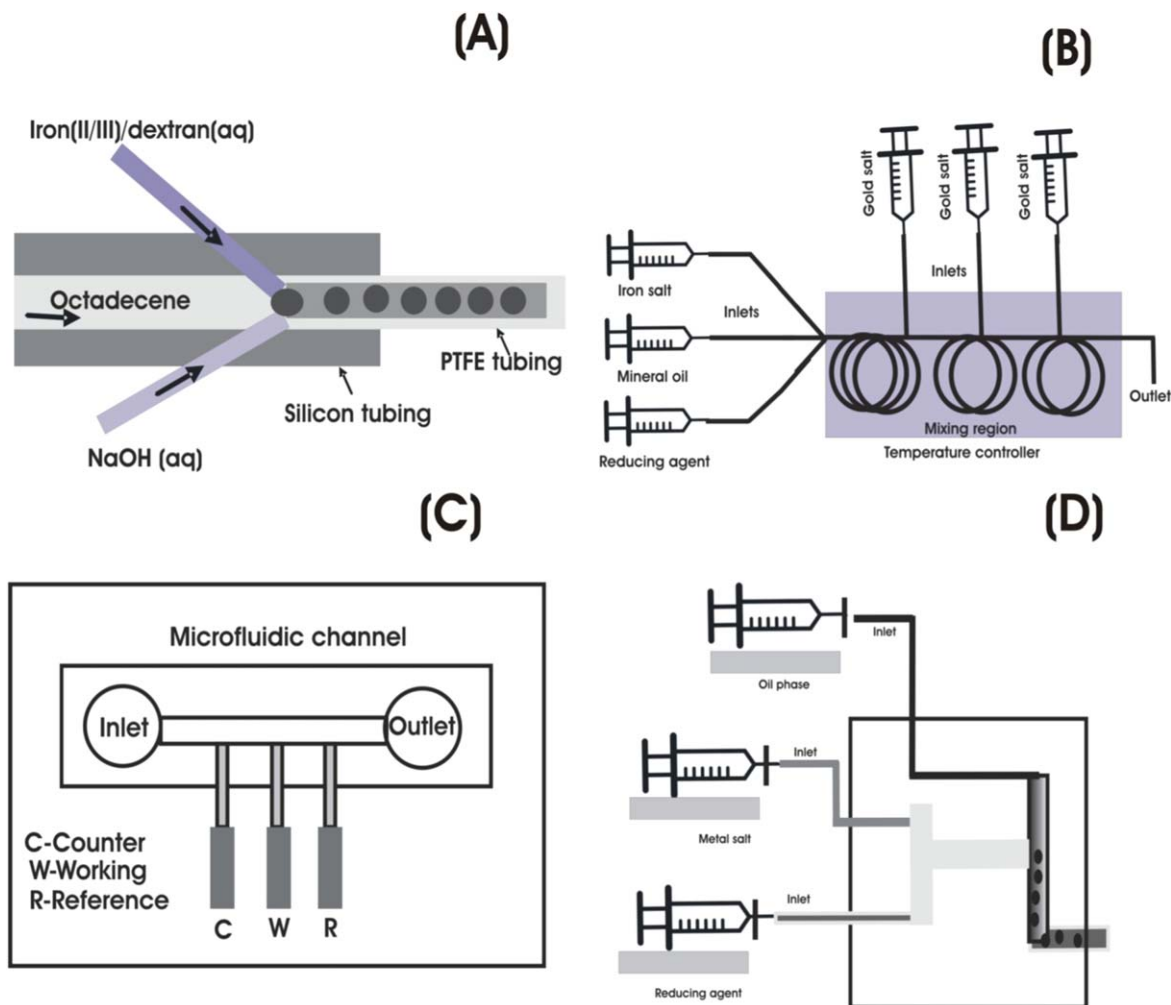


**Figure 15.** Schematic representation of various microfluidic devices used for nanoparticle synthesis.

Flow rate was manipulated in such a way that magnetic iron oxide particles of size  $< 7$  nm were obtained. Microdevice had capillary tubes with two inlets and one outlet. One inlet had continuous flow of the reducing agent. The other inlet supplied Iron(II/III) salt solutions into the flowing reducing agent stream. The product was collected from outlet.<sup>77</sup> Frenz et al. designed microdevice with two hydro dynamically separated nozzles. The starting reagents were Ferrous/Ferric chloride in hydrochloric acid as metal salt and ammonium hydroxide as reducing agent. The particles obtained were of 4 nm and magnetic in nature.<sup>78</sup> Lee et al., in 2009 designed PDMS and glass substrate based microfluidic device with micropumps, micro valve and micro mixer. Electromagnetic valve were used for controlling the flow. Iron oxide was synthesized at room temperature with co-precipitation method. The device had a central micro loop mixer. On the either side of the mixer were five inlets. Two on one side and three on other. Bottom of the micro loop mixer was the single outlet channel. Through inlet 1, HCl was injected followed by Ferric and Ferrous chloride through 2 and 3 inlet which was fed into the micro mixer. Through inlet 4 and 5, NaOH was injected to the micro mixer. Reaction took place at ambient temperature for 12 min. Post which Iron oxide particles were formed as dark brown precipitate in the micromixer. The valve was used to collect them through the outlet.<sup>79</sup>

In 2012, Kumar et al. developed dextran coated super paramagnetic Iron oxide nanoparticles using glass capillary microdroplet reactor device. Capillary glass tubes were used as inlets to feed the reagents aqueous Ferrous and Ferric chloride as metal salt, ammonium hydroxide as reducing agent, with precursor dextran.

Octadecene was used as carrier fluid. The reagents were fed into the channels through separate syringe pumps. The size of tubes was 2 mm. Figure 15a gives the schematic representation of the microdevice.<sup>80</sup> Synthesis of super paramagnetic Iron oxide nanoparticles at elevated temperature ( $280\text{ }^{\circ}\text{C}$ ) was reported by Uson et al. The fabricated device had two stages with different temperatures. Iron(III) acetylacetonate was the metal salt used as precursor along with triethylene glycol and Hydrochloric acid. The inlets fed the reagents to spiral micro mixer then to the first stage. First stage was kept at  $180\text{ }^{\circ}\text{C}$  which caused nucleation followed by second stage at  $280\text{ }^{\circ}\text{C}$  where growth takes place.<sup>81</sup> Recently, Ahrberg et al. in 2020 developed a sophisticated microdroplet reactor for preparing Iron oxide and gold core-shell hybrid nanoparticles. Capillary tubing based reactor was used for the same. The reactor had a three side inlet: central Tygon tubing inlet carrying mineral oil (for droplet generation) connected at a junction with two capillary tubes above and below carrying the Ferric chloride and Sodium hydroxide. The generated droplets (carrying reagents) were fed into spiral mixing tubing. The mixing zone was connected with three more inlets from which gold salt solution was fed as a precursor. The gold solution encapsulated the microdroplet carrying Iron oxide formed giving gold/Iron oxide hybrids which were collected through single outlet. Figure 15b gives schematic representation of their microdevice.<sup>82</sup>

Copper nanoparticle synthesis in microfluidic system has also gained much attention due to their increasing applications. A simple method is to use copper salt and a reducing agent. Many research groups have designed various microreactors for the same. For

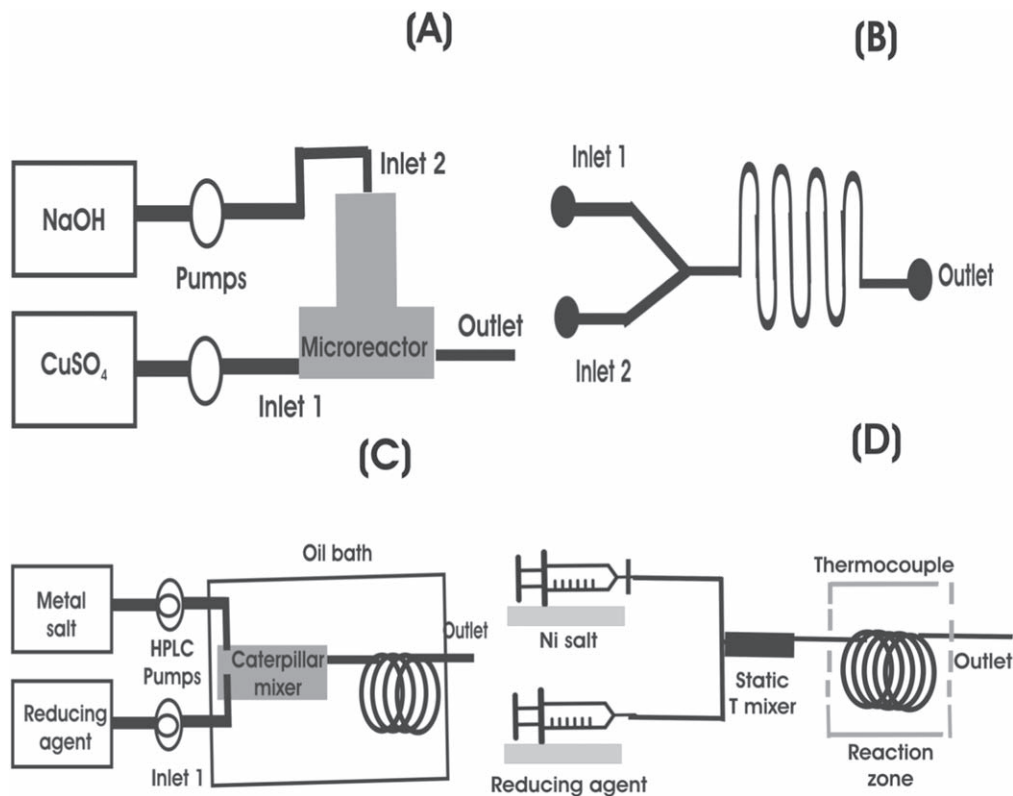


**Figure 16.** Schematic representations of various micro devices used for synthesis of nano particles.

example, Zhang et al. developed a simple two and three inlet, one outlet based Y shaped channel. Syringe pumps were used to introduced pre-prepared  $[\text{Cu}(\text{NH}_3)_4](\text{OH})_2$  as precursor and dilute  $\text{N}_2\text{H}_4$ (Hydrazine) as reducing agent. A curved channel enabled mixing and reaction to give Cu nanoparticles of 3.4 nm diameter in 28 seconds.<sup>83</sup> 3D-Cu/Carbon core sheath nanostructures were prepared via in situ electrodeposition by Parisi et al. The fabricated microdevice was through softlithography, PDMS based integrated with three-electrodes on silicon base. Copper acetate hydrate was the Cu precursor used. On applying potential, the nanostructures were electrodeposited in the microchannel. Figure 15c is the schematic representation of their experimental set up of microfluidic device.<sup>84</sup> Xu et al. developed Cu nanoparticle in a T shaped microfluidic device. It had three inlets, with oil as continuous phase in one. The other two had aqueous reagents, copper sulfate and sodium borohydride as reducing agent fed into the T junction through syringe pumps. The reaction took place at RT and the formed particles were collected through single outlet. Figure 15d is the diagrammatic representation of their microdevice.<sup>85</sup>

A nanocomposite of  $\text{Cu}@\text{Cu}_2\text{O}$  was prepared using solution phase approach in microfluidic system at room temperature. Copper sulfate and sodium borohydride were used at pH 10–12. PVP was used as dispersant. Microdevice used was stainless steel inter digital micromixer of  $40 \mu\text{m}$  width. Reaction was carried out at RT and flow rate was maintained as  $15 \text{ ml min}^{-1}$ .<sup>25</sup> Xu et al. in 2015 developed an easy approach of preparing copper nano colloids in a continuous flow micro system. Starting material; copper sulfate and reducing agent sodium borohydride was continuously supplied from a reservoir through pumps into a commercially available T shaped, stainless steel microreactor of diameter 1/16 inches. The microreactor had two inlets and one outlet. The reaction took place at room temperature. Figure 16a gives the schematic representation of the microdevice.<sup>86</sup> Likewise, Liang et al. designed a glass microfluidic device of  $260 \mu\text{m}$  wide and  $70 \mu\text{m}$  deep for Cu nanoparticle synthesis. Y shaped channel with 2 inlets lead into a serpentine

channel reaction zone followed by 1 outlet. Copper (II) chloride dehydrate and L-Ascorbic acid in ethylene glycol were introduced through inlet 1 and 2 using syringe pumps. The device was kept at a constant temperature  $160^\circ\text{C}$  using a thermostat. The synthesized particles were collected through the outlet. Figure 16b gives the schematic representation of the microdevice.<sup>87</sup>

Several methods have been reported in the literature in recent decade for synthesis of Cobalt nanoparticles in microfluidic devices. Song et al. developed a has controlled microdevice. The device was a polymeric microreactor which had two inlets that injected Cobalt chloride and lithium hydro triethylborate through pumps into a serpentine channel. The temperature was monitored throughout the reaction. The obtained particles were collected through the outlet.<sup>68</sup> Nano crystals of Co nanoparticles were fabricated in a microfluidic reactor by Song et al. The synthesis was carried at low temperatures not more than  $50^\circ\text{C}$ .<sup>88</sup> Hassan et al., synthesized hybrid nanoparticles of cobalt ferrite ( $\text{CoFe}_2\text{O}_4$ ). The reaction occurred in two simultaneous microreactors coupled together. In the first microreactor, mixing of reagents at room temperature took place to form hydroxides of Iron and cobalt. The second reactor's temperature was elevated to  $98^\circ\text{C}$ , wherein, the hydroxides converted to crystalline  $\text{CoFe}_2\text{O}_4$ .<sup>89</sup>

Unlike Cobalt, literature reports significant approaches about Nickel nanoparticles synthesis in micro reactors. For example, Goyal et al., developed multiplexed microreactor with PDMS for preparing nanoparticles of various metals like Nickel, Iron and Palladium using the metal salts and reducing agent. Herein, thermal decomposition played the key role in synthesis.<sup>90</sup> Similarly, Zheng et al., developed Ni nanoparticles in continuous flow system. Nickel chloride in ethanol and hydrazine hydrate in sodium hydroxide were used as reagents injected into caterpillar micromixer through HPLC pumps. The reaction was carried out in a fluorinated-ethylene-propylene tube 1 mm diameter. The tube was kept in an oil bath to maintain temperature. Effect of temperature, surfactant, and reaction time was studied. The particles obtained were as small

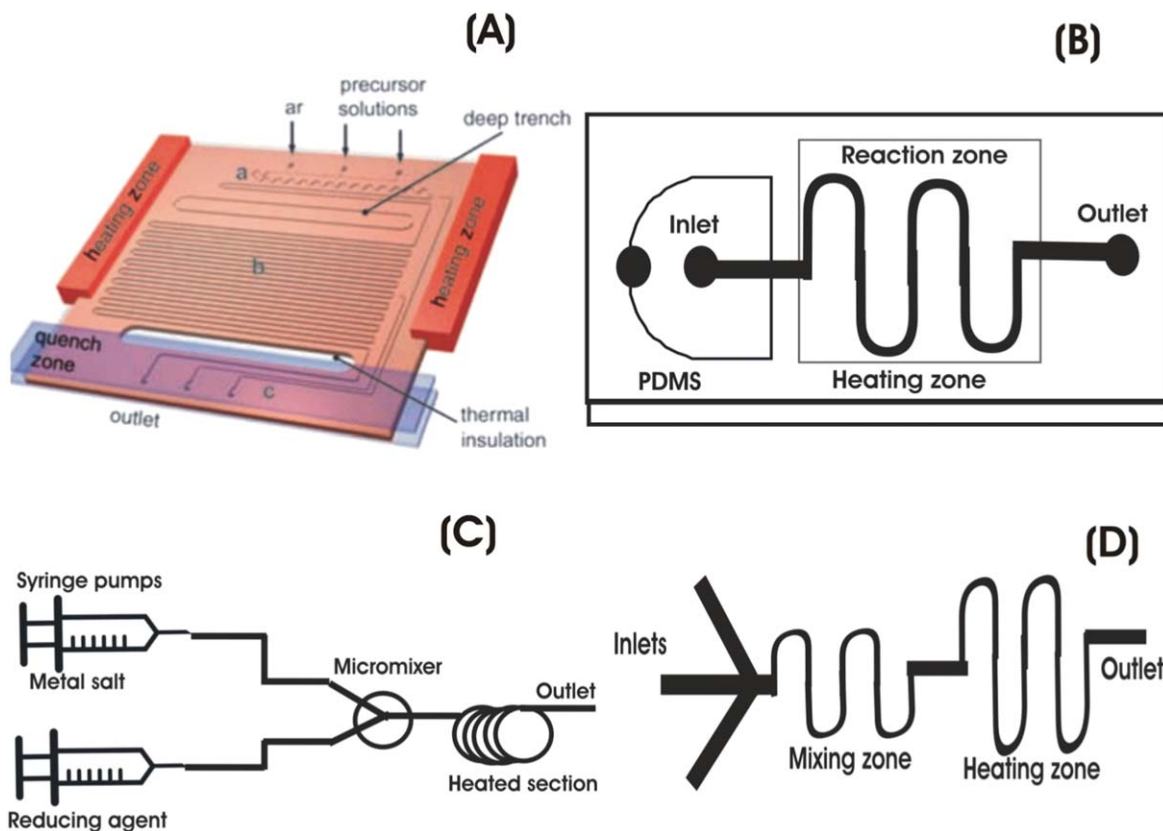


**Figure 17.** Reprints (Copyright permission@2020) and schematic representation of microfluidic devices for nanoparticles.

as 68 nm. Figure 16c gives the schematic representation of the microfluidic reactor set up.<sup>91</sup> Eluri et al. developed an uncomplicated method for Ni nanoparticle synthesis using continuous flow. Nickel chloride in ethylene glycol and hydrazine hydrate in sodium hydroxide were fed into T shaped micro channel mixer through two inlets via syringe pumps. T mixer was connected to a stainless steel tubular coiled reactor. To maintain the temperature, tubular reactor was kept in a glycol bath. The formed particles were collected through the single outlet. Figure 16d gives the schematic picture of the microfluidic reactor set up.<sup>92</sup> Similar approach wherein, nickel sulfate and hydrazine were employed for Ni nanoparticle synthesis microreactor was attempted. The device had T shaped micro mixer followed by a tubular reactor maintained in water bath at 80 °C. The formed particles were collected through outlet.<sup>25</sup>

Titanium oxide synthesis in microfluidic reactor is of much significance. Cottom et al., developed a simplified Y junction serpentine channel based micro reactor for TiO<sub>2</sub>nanorods synthesis. The channel was 100 μM wide and 100 cm long. The microreactor was kept in an oven at 90 °C to accelerate the reaction.<sup>93</sup> Eun et al. described a single step synthesis of titania hollow spheres with nanoparticles. In micro capillary reactor.<sup>94</sup> Lan et al. described a process of synthesizing Titania-silica core-shell microspheres using titanium alkoxide as starting reagent. Coaxial flow channels let silica sol droplet formation dispersed in oil phase. Titanium alkoxide was hydrolyzed to form titanium hydroxide surrounded by gel shell.<sup>95</sup> However, synthesis of titania is not limited to the above discussed methods. In addition, other metal nanoparticles like Manganese, Magnesium, Calcium etc. are also reported.

**Quantum dots.**—Quantum dots (QDs) are nanocrystals capable of transporting electrons. Microfluidic reactors have been successfully used for efficient synthesis of QDs. Owing to the ease of synthesis, high conductivity, and light stability, CdSe quantum dots are most commonly prepared.<sup>96</sup> As discussed earlier, Shestopalov

et al., developed CdSe QDs in a continuous micro fluidic system.<sup>49</sup> Hung et al. developed microdroplet based CdS particles.<sup>50</sup> CdSe nanocrystals in high temperature were synthesized by Chan et al.<sup>22</sup> The microfluidic device was made up of glass wafer that had inlets leading into serpentine channel of 65 cm in length, 150 μM width and 47 μM depth. In 2005, Yen et al., developed protocol for synthesizing CdSe QDs. They used gas-liquid based segmented flow technique for mixing and reaction of the reagents. Cadmium 2,4-pentanedionate and octylphosphine selenide were used as starting reagents for Cd and Se. The reaction occurred at elevated temperatures in the microreactor made up of silicon. The microreactor has two zones, heating zone where reaction takes place and a cooling region near outlet. The reaction channel is a serpentine channel with 1 m length and 380 μM diameter Fig. 17a is a reprint of the microdevice used by them.<sup>97</sup> Zhang et al. used microfluidic spinning technology for solvent less green synthesis of CdSe QDs. Cadmium acetate dehydrate and selenium powder were used as precursors.<sup>98</sup> Tian et al. slightly modified the procedure of CdSe QDs preparation by preheating the precursor. They investigated the QDs prepared by non-preheated and preheated precursors. They pre-heating lead to formation of high quality QDs. The microfluidic device was simple two inlet and one outlet based. Reagents were injected through syringe pumps and Y shaped mixer led into tubular coiled reactor kept in oil bath. The reaction time was 40 s at 270 °C. The particles were collected through outlet.<sup>99</sup> They also reported CdSe nanocrystal QDs by preparing the precursor cadmium oxide and selenium with fatty amines ligands. Two inlet Y junction microfluidic chip of PMMA was designed for the same. Syringe pumps were used for introducing reagent into serpentine micromixer followed reaction zone kept in oil bath for 45 s. Reaction temperature was optimized and resultant particles were collected through the outlet. Wag et al. demonstrated a shape controlled synthesis of CdSe nanocrystals. The microchannel was made up of polytetrafluoroethylene and steel. The total length of the channel was 208 cm, comprising 15 cm of polytetrafluoroethylene tube and 153 cm of stainless steel tube

followed by 40 cm PTFE tube. The inside diameter of the microchannel was 0.75 mm. Precursor solution was fed through syringe pumps. Reaction was carried out in different temperatures 150 °C to 300 °C.<sup>100</sup> Similarly, Kwak et al. developed strategy for size controlled growth of CdSe QDs in continuous flow. CdSe precursor were fed through syringe pumps, and N<sub>2</sub> gas was also let into the reactor. The capillary tube reactor was kept in oil bath at temperature 250 °C for different time duration.<sup>66</sup> Liu et al. synthesized CdSe in microfluidic and bulk methods and did a comparative study. Cadmium oxide and selenium were the reagents used as precursors. The microfluidic device had three inlets, preheating chamber, tubular spiral reactor and outlet. Syringe pumps were used to deliver reagents to the preheating chamber followed by mixing and reaction in spiral tubular reactor kept in hot bath to maintain temperature. The prepared QDs were collected through single outlet.<sup>101</sup>

Apart from CdSe QDs, other metals based QDs are also fabricated. Like, Shu et al., in 2015, reported first time the Ag<sub>2</sub>S QDs using microdroplet reactor. These QDs were water soluble. PDMS based micro device was prepared with flow focusing technique. The starting reagent used were 3-mercaptopropionic acid in soybean oil as continuous phase while glycol containing silver nitrate acted as the dispersed phase. A serpentine channel with 60 μM width kept over temperature controller acted as reaction zone. Figure 17b gives the schematic representation of the microdevice.<sup>102</sup> Size controlled ZnO QDs were fabricated by Schejn et al. Anhydrous zinc acetate and tetramethylammonium hydroxide were the precursor solutions used. Two syringe pumps were used to inject the precursors into Y junction micromixer. This led into a circular tubing which was heated at temperatures varying from 20 °C–90 °C. Formed ZnO QDs were collected through outlet. Figure 17c is the diagrammatic representation of the microdevice.<sup>103</sup> Kwon et al. firstly reported in situ preparation of ZnSe/ZnS core-shell QDs. Zinc acetate and Selenium powder pre prepared precursor solutions were injected into micro reactor. The device had three inlets and one outlet. It had a mixing zone and heating zone made up of serpentine channel. The reaction took place at a heating temperature of 220 °C. Figure 17d is the schematic representation of the microdevice.<sup>104</sup> Lignos et al., in 2015 prepared PbS QDs in microdroplet reactor.<sup>105</sup>

Carbon QDs preparation is also being explored. A simple organic carbon source is used as a precursor. Usually, these precursors are exposed to elevated temperatures leading to their decomposition and eventually forming desired QDs. A few of the simplistic carbon QDs prepared are: Lu et al. in 2014, prepared carbon QDs from glucose starting reagent. Syringe pump introduced glucose to Teflon capillary tube. The capillary was heated at 180 °C in oil bath for 2 min. The product resulted was collected from outlet.<sup>106</sup> Using ascorbic acid as source of carbon dissolved in DMSO solvent, Pedro et al. fabricated carbon QDs in microfluidic reactor. The microreactor was examined at various temperatures 180 °C–240 °C. The size of the particle obtained were 3.3 nm.<sup>107</sup> Rao et al., in 2017, developed carbon QDs using anhydrous citric acid and ethylenediamine as precursors. Syringe pumps were used for injecting the precursors into the microreactor. The microreactor had a serpentine channel and the reactor was heated between 80 °C–160 °C using a temperature controller.<sup>108</sup> Tang et al. prepared nitrogen doped carbon dots in micro reactor. Foamy copper with varying porosities was used. Microreactor temperature was varied from 150 °C–280 °C for less than 8 mins.<sup>109</sup>

**Semiconductor nanoparticles.**—Owing to their properties and wide spread applications in optical, electrical, mechanical, chemical and energy harvesting applications, semiconductor nanoparticles are high in demand. Numerous bulk synthesis of variety of semiconductor nanoparticles with metals like Au, Ag, Pd, Pt, Cu, Cd etc. are reported. However, CdS, CdSe, CdSe/ZnS are most commonly prepared semiconductor nanoparticles in the microreactors due to their uncomplicated procedure and extensive application in optical, electrical devices and as fluorescence tags.<sup>55</sup> Some of the common

ways of preparation of CdS and CdSe in microfluidic devices has been discussed above.<sup>20,22,49,50,53,66,97,100,101</sup> It is also reported that capping the CdSe nanocrystals with ZnS or CdS improves their fluorescence behavior.<sup>55</sup> Hence, Talapin et. al in 2001, Wang et al. in 2005, Luan et al. in 2008, Toyota et al. in 2010 developed various techniques of capping.<sup>55</sup> In last decade extensive research has been done for developing various capping procedures.<sup>110–113</sup>

**Polymer nanoparticles/biomaterials.**—Biocompatible polymer materials like hydrogels, alginate, polyethylene glycol, poly(lactic acid) poly (glycolic acid) etc. are common biomaterials used in drug delivery and other biomedical applications. Therefore, preparation of these polymer based nanoparticles and biomaterials in microfluidic system is of great importance.<sup>4</sup> Synthesis of organic nanoparticles in microfluidic system is challenging due to the occurrence of uncontrolled polymerization, particle size distribution. Karnik et al. reported that an appropriate mixing can resolve this. They developed poly(lactic-co-glycolic acid)-b-poly(ethylene glycol) nanoparticle. They optimized flow rate, polymer concentration and composition for size control and uniformity. A “T” junction microfluidic channel was used with polymer in acetonitrile solvent and water, with a flow focusing technique and nanoprecipitation. Figure 18a shows the schematic representation of the microdevice used by them.<sup>114</sup> Dendukuri et al. prepared polymer micro particles with “T” junction microchannels made up of PDMS. Water with surfactant was used as continuous phase and polymer as dispersed phase. The inner diameter of the channel was 40 μM, however, the polymer particles were collected at 200 μM channel outlet.<sup>115</sup> A PDMS based device for preparing nylon-6,6 coated aqueous droplets was developed. Flow focusing technique was used wherein two inlets were for continuous phase and one for dispersed phase. Microdroplets coated with nylon-6,6 were obtained through the outlet.<sup>116</sup> Lim et al. reported preparation of poly(lactide-co-glycolide)-b-polyethyleneglycol (PLGA-PEG) nanoparticles of 13–150 nm. Three dimensional, hydrodynamic flow focus methods in a microfluidic device. Figure 18b is the reprint of microdevice.<sup>117</sup> Kohler et al. prepared Polyacrylamid-Silver composite particles. Silver seeds were prepared by reducing silver nitrate with sodium borohydride. These seeds were pre mixed with polymer and fed into the microreactor made up of PDMS.<sup>118</sup> Puigmartí-Luis et al., developed polymer nanofibers with metal ions in microfluidic reactor. The reactor had simple Y shaped junctions with four inlets and single outlet. Laminar flow was employed to introduce the reagents into channels.<sup>119</sup> A hybrid of Lipid and poly-(lactic-co-glycolic) acid (PLGA) in acetonitrile composite nanoparticles were prepared. The morphology was manipulated by varying viscosities. T junction microfluidic channel with three inlets and one outlet of width 50 μM, height 60 μM and length 2.5 μM was used for this. PLGA in acetonitrile and Lip-PEG was used as reagents.<sup>120</sup> Randeau et al. described a unique microfluidic device to prepare alginate nanoparticles. Flow focus technique was used to form biopolymer nanoparticles of size 10–300 nm. Polymer concentration and kinetics cross linking reaction.<sup>121</sup> Ding et al. gave an elaborative overview of microfluidic preparation of nanoparticles with polymeric drug nanoparticles.<sup>122</sup> Very recently, Zhang et al., prepared polymer protein nanoparticles via electro kinetics, rapid mixing based microfluidics. They were able to obtain a better size distribution by controlling the mass ratio of protein and the polymer starting reagent. Figure 18c is the reprint of their microfluidic device.<sup>123</sup>

Synthesis of biocompatible materials in microfluidic devices has also been investigated. Zhang et al. made hydrogel biopolymer microcapsules. An organic phase was used to emulsify biopolymer into droplets. The concentration of cross linking agent and residence time of droplet in the microfluidic device was optimized to get uniform structure. This method was used for preparing capsules of alginate, carrageenan and carboxymethyl cellulose.<sup>124</sup> Sugiura et al., developed calcium alginate beads encapsulating living cells. The beads of 50–200 μm. Live cells were trapped in 162 μm beads.<sup>47</sup> Calcium alginate microparticles in microfluidic device were fabricated by Liu



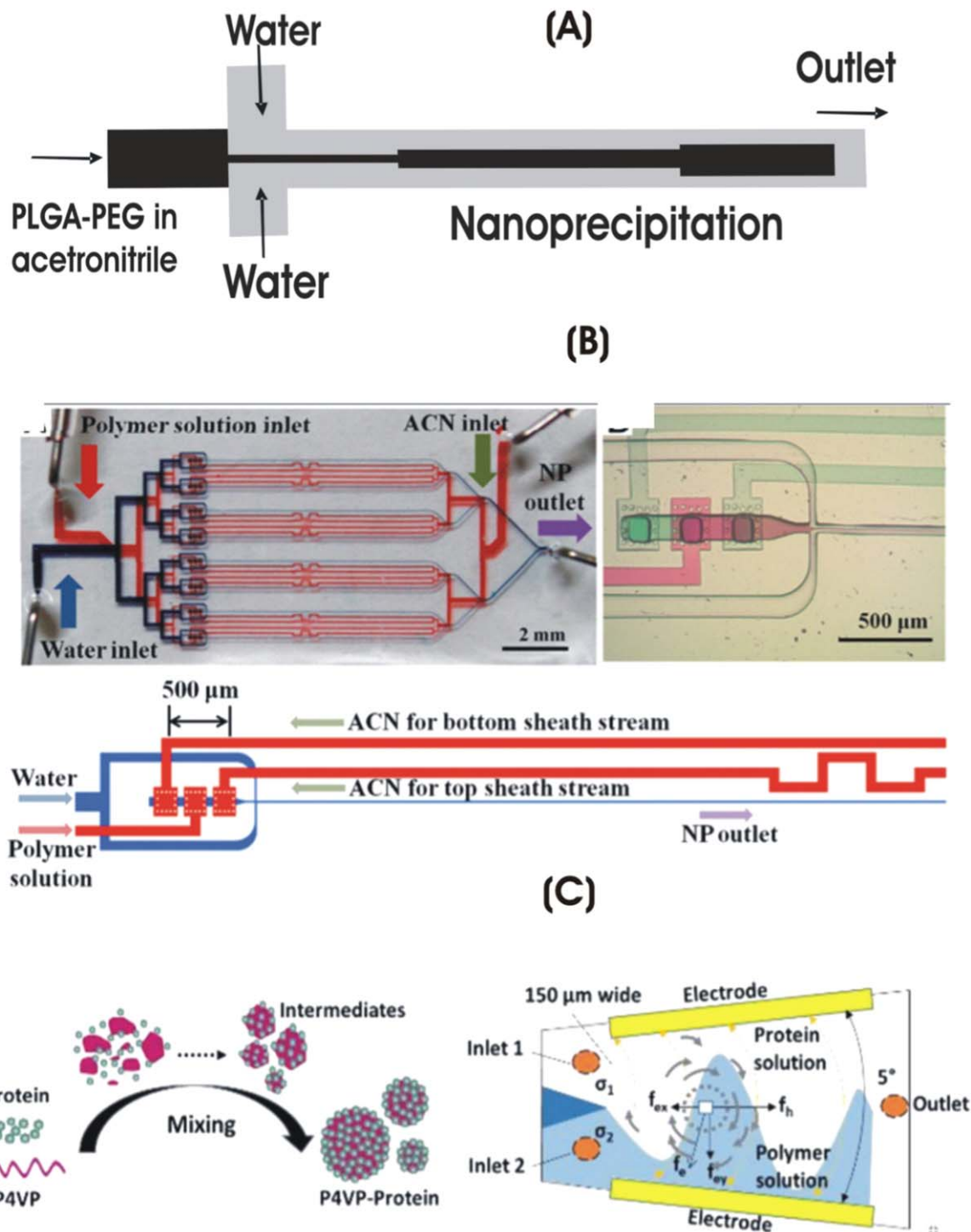
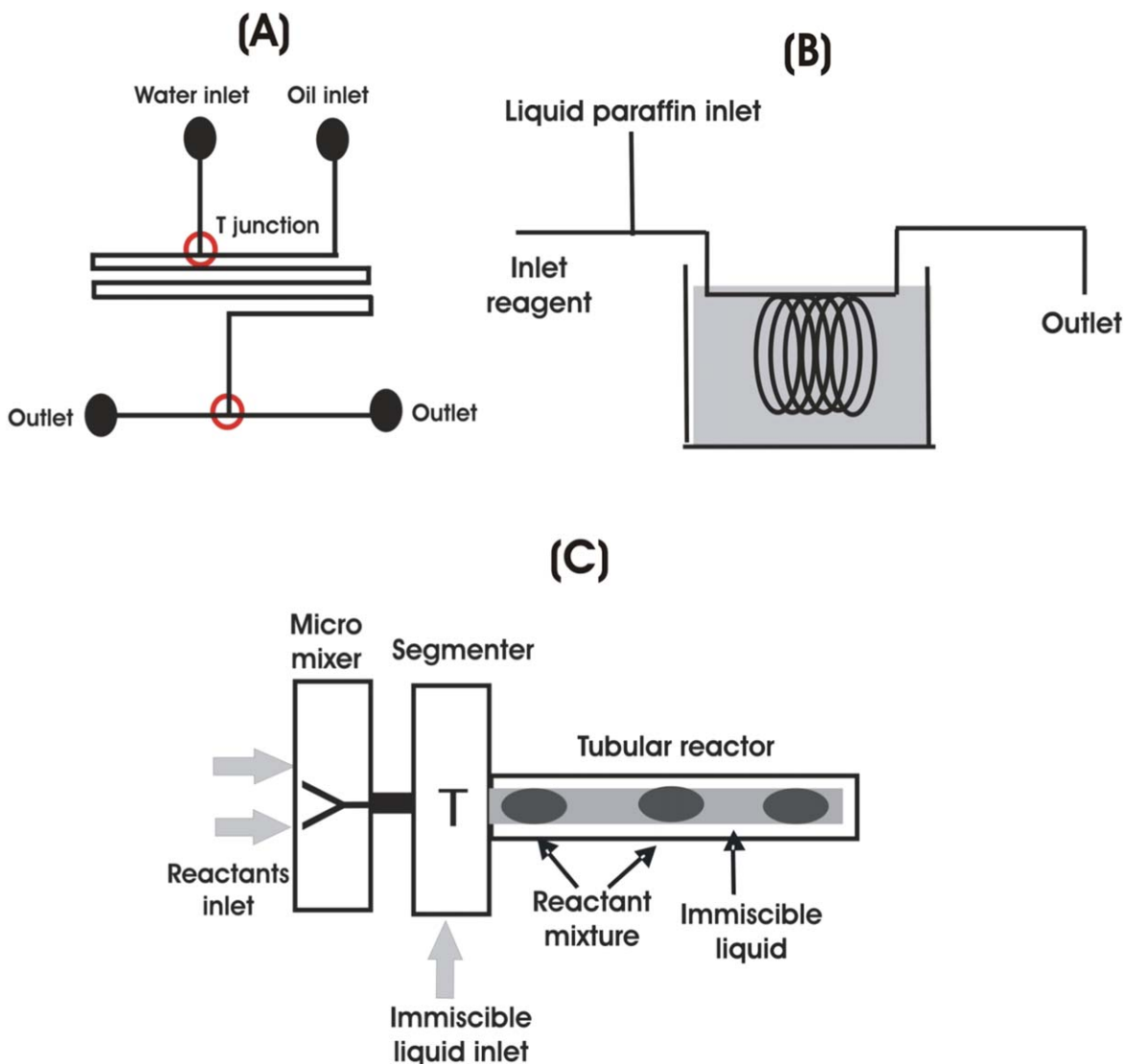


Figure 18. Microdevices designed for synthesis of nanoparticles. Reprints with copyright permission@2020.

et al. A continuous microfluidic reactor was used. Size was controlled by adjusting flow rates. Sodium alginate and calcium chloride are the starting material. Flow focusing technique was used. The microdevice had a T shaped channel with wherein, central inlet channels are 200 μm wide and tapers to 50 μm at junction. It has a orifice of 200 μm long with width as 50 μm which increases to 100 μm.<sup>125</sup> DeGeest et al. fabricated microgels using dextranhydroxyethyl methacrylate and oil. 10 μm size biodegradable hydrogel particles were formed in the PDMS microfluidic device with two inlets and one outlet. These particles were highly useful in protein delivery.<sup>126</sup> Polymeric microparticles using hydrogel and oil were prepared by

photopolymerization in microfluidic device made up of PDMS. Glass micropipette capillary was used to generate microparticles.<sup>127</sup> A detailed review about magnetic composite polymers applied to microfluidic devices has been discussed by Gray.<sup>128</sup>

**Others.**—Core-shell particles, colloidal particles, composites like zeolites, ternary particles (particles with two or more physical or chemically different surface) etc. have also been prepared using microfluidic devices. Nei et al. in 2006, reported a method for fabricating ternary polymer particles of 40–100 μm. Thermodynamic and hydrodynamic forces and UV irradiation were used for instant



**Figure 19.** Schematic representations of the various microfluidic devices used.

polymerization. The device used was made from polyurethane and had flow-focusing technique. Monomers were injected into middle channels whereas surfactant into side channels. The channel length was  $200\ \mu\text{M}$ . Towards the exit from middle channel, monomers were sent through orifice giving droplets.<sup>129</sup> Zhao et al. fabricated ternary calcium alginate particles. It had two hemispheres, one magnetic and another for cell trapping. The magnetic portion can be altered through magnetic field whereas the other half was biocompatible for carrying cells. A PDMS and glass microchip device was fabricated with Ni array of dimensions  $80 \times 80 \times 20\ \mu\text{M}$  with a spacing of  $120\ \mu\text{M}$ .<sup>130</sup> Yi et al. in 2003 designed a microfluidic device with softlithography for fabricating uniform colloidal particles. The device had two inlets, one for aqueous and one for oil phase, two outlets. The channels are connected with T junctions to create droplets and serpentine channel to mix and react the reagents. The resulted particles are collected from the two outlets. Figure 19a gives the schematic representation of the microdevice.<sup>131</sup> Khan et al. demonstrated strategy for synthesis of colloidal silica particles in laminar flow and segmented flow reactors. Owing to improved mixing, segmented flow technique gave appropriate mixing, hence, uniform particles were gained. They have designed three different types of microdevices. One with two liquid inlets, and one outlet, with  $400\ \mu\text{M}$  length and  $0.975\ \text{m}$  long. The other had two liquid, one gas inlets and one outlet with

$400\ \mu\text{M}$  width  $150\ \mu\text{M}$  depth and  $0.975\ \text{m}$  length channels. Another device had four liquid inlets, one gas inlet and one outlet  $300\ \mu\text{M}$  width,  $2.3\ \text{m}$  length and  $200\ \mu\text{M}$  depth.<sup>132</sup> Pan et al., in 2009 prepared Zeolite crystals via two-phase segmented microfluidic device. Various particle sizes zeolite was prepared. Sodium aluminate, sodium silicate and sodium hydroxide were the starting reagents used. Coaxial dual tubes were used in microreactor for enhanced fabrication. Figure 19b shows the schematic of the microfluidic set up.<sup>133</sup> Gong et al., in 2009, fabricated core-shell particles with aspirin in center surrounded by chitosan. Magnetic nanoparticles were embedded inside the core-shell. Flow focusing micro reactor was used for this.<sup>134</sup> Wang et al. in 2009 synthesized barium sulfate nanoparticles in a high throughput tube in tube microfluidic reactor. The microreactor had two tubes, inner and outer. Dispersed phase goes through inner tube, continuous phase passes through outer tube. The gap between these tubes was  $750\ \mu\text{M}$  which also acted as mixing zone. The pore size of tubes were varied and studied. The size of the particle was controlled between  $30\text{--}150\ \text{nm}$ . Particle size was reduced by increasing the flow rate and reactant concentration.<sup>135</sup> Various nanocomposites like calcite, nickel-manganese mixed oxalate, barium titanate was fabricated by Jongen et al. A continuous segmented flow reactor was used. The powders obtained were of better quality than commercial. The reactor had a micro mixer, segmenter and reaction took place in tubular reactor.

Figure 19c is the schematic of the microreactor.<sup>136</sup> All these varied nanostructures and materials prepared by microdevices can be used for multiplexed sensing applications.<sup>137</sup>

### Future Outlook

The vast information available in the literature clearly predicts that off lately, there has been a tremendous advancement in synthesizing approaches of various types of nanoparticles under controlled microfluidic environment. In comparison to the conventional bulk synthesis, these micro-device based methodologies have given several advantages like portability, automation, better control of morphology, reproducibility, cost affectivity due to lesser reagent use etc. This review focusses on recent emerging trends in the micro-based devices, with various designs, throughputs, materials and reaction mechanisms for nanomaterial synthesis. Several types of nanoparticles, such as metallic, non-metallic, composites, polymers, quantum dots etc., have been prepared with significantly innovative attributes. Therefore, it is clearly foreseen that there is ample amount of future scope in design and development of novel microfluidic techniques for fabrication of nanoparticles with specified functionalities and desired properties. This could give a cutting edge leverage to various industrial sectors like biomedical, genetics, electronic and electrical, mechanical etc. The design of the microfluidic reactors plays a key role in the quality output. Broadly there are four types of designs used, microchips, micro capillaries, micro-tubular coils, and segmented flow. The design is chosen based upon the ease of operation considering the scalability aspect.

The choice of material used for making device also is of great importance. Depending upon the reaction parameters, like thermal system, hydrothermal, pH, reagents, photosensitivity, the material is chosen. Commonly used materials involve but not limited to glass, silicon, PDMS, polymers etc. However, with modern soft-lithography strategy, other organic, inorganic polymers and composites are also being used based on the requirement. Hence, noteworthy upgradation is expected in future. Nonetheless, despite aforementioned advantages, the wet chemical synthesis of nanoparticles in micro-devices possess certain limitations and challenges as well. For instance, controlling of critical morphological features like shape, size and crystal structure of the nanomaterial is still challenging. In order to overcome this, novel designs for laminar flow control and segmented flow reactors are being adapted. Secondly, improving the yield obtained is a herculean task. Owing to the fact that, these devices have lesser reagent consumption, the yield obtained is also affected. Attempts are being made to overcome this through manipulation of flow rate and retention time. Specifying the shape of nanomaterials is another challenge that has to be addressed in future. Mostly it is observed that spherical nanomaterials are formed using these microreactors. However, near future with approaches like changes in microchannel design and dimensions, anisotropic, cubical and fibrous nanoparticles can also be prepared. Blockage and leakage of microchannels is also one of the challenges to be overcome. Usually due to the agglomeration of formed nanoparticles or reagents, there are blockages developed in the microchannels effecting the performance of the device. At times, leakages due to improper bonding in the midway of the reaction may also occur. These issues can be resolved by optimizing the reaction conditions like pH, temperature, flow pumps, use of surfactants, detergents and stabilizers to remove blockage, appropriate bonding adhesives and methods. It is also predicted that fabrication of new flexible materials for manufacturing of these devices could also help in resolving this issue.

Prediction of reaction mechanism of the nanoparticle formation is another challenge in the microfluidic conditions as the intermediate reactant products cannot be accessed in this case. However, in case of bulk wet-chemical process, the intermediate products can be obtained and characterized and reaction can also be arrested mid-way to predict the mechanism. However, this still remains challenging in microfluidic environment. It is anticipated

that in near future, the design manipulation and reaction condition of devices could solve this problem. Lastly, the scaling up of this approach to meet the industrial demand is highly challenging. Substantial amount of research is still under progress to resolve this issue. The major setback is from the fabrication of micro-devices with suitable materials in large quantity pertaining cost-efficiency. Owing to the ongoing development it is expected that notable development is expected in future resolving these above-mentioned challenges.<sup>138</sup>

### Conclusions

The present paper summarizes a brief overview of miniaturized/microfluidic devices for automated synthesis of nanoparticles. Wide applications of nanostructures in industry and academia for mechanical, electrical, optical, biomedical etc. has increased their demand for fabrication. Their unique properties are dependent on their morphology. Thus, various methods to obtain uniform shape and size nanoparticles are essential. The key factor is to get reproducibility in each batch synthesized. In this regard, miniaturized microfluidic devices offers great control over shape, size and reproducibility. Owing to the fact that microfluidic devices require less reagents as starting precursor materials and are easily tunable for manipulating temperature and pressure, they not only are eco-friendly but also produces uniform particles in each batch. This paper also describes bottom up approach of nanoparticle synthesis in micro devices. Various methods of fabricating micro devices are also discussed. Typical microchannel designs, microdroplet formations and reagent mixing techniques are also reviewed. Some of the reported literatures wherein in nanostructures of inorganic/metal, polymer, composite, semiconductor, quantum dots etc. are briefly stated. With a rapid growth in application of microfluidic devices for nanomaterial synthesis, there is great future scope and demand of these methods.

### Acknowledgments

Khairunnisa Amreen would like to acknowledge SERB NPDF Scheme (PDF/2018/003658) for the financial assistance.

### ORCID

Sanket Goel  <https://orcid.org/0000-0002-9739-4178>

### References

1. S. Krishnadasan, A. Yashina, A. J. DeMello, and J. C. DeMello, *Advances in Chemical Engineering*, **38**, 195 (2010).
2. L. L. Lazarus, A. S. J. Yang, S. Chu, R. L. Brutchey, and N. Malmstadt, *Lab Chip*, **10**, 3377 (2010).
3. K. S. Elvira, X. C. I. Solvas, R. C. R. Wootton, and A. J. Demello, *Nat. Chem.*, **5**, 905 (2013).
4. L. H. Hung and A. P. Lee, *J. Med. Biol. Eng.*, **27**, 1 (2007).
5. M. Maeki, T. Saito, Y. Sato, T. Yasui, N. Kaji, A. Ishida, H. Tani, Y. Baba, H. Harashima, and M. Tokeshi, *RSC Adv.*, **5**, 46181 (2015).
6. Y. Wang and Y. Xia, *Nano Lett.*, **4**, 1 (2004).
7. D. Xia, D. Li, Z. Ku, Y. Luo, and S. R. J. Brueck, *Langmuir*, **23**, 5377 (2007).
8. J. Park, K. An, Y. Hwang, J. E. G. Park, H. J. Noh, J. Y. Kim, J. H. Park, N. M. Hwang, and T. Hyeon, *Nat. Mater.*, **3**, 891 (2004).
9. V. M. Arole and S. V. Munde, *JAAS Material Sci. (Special Issue)*, **1**, 2 (2014).
10. A. J. DeMello, *Nature*, **442**, 394 (2006).
11. C. Y. Lee, C. L. Chang, Y. N. Wang, and L. M. Fu, *Int. J. Mol. Sci.*, **12**, 3263 (2011).
12. K. Ward and Z. H. Fan, *J. Micromech. Microeng.*, **25**, 094001 (2015).
13. M. L. Braunger, I. Fier, V. Rodrigues, P. E. Arratia, and Antonio R. Jr., *Chemosensors*, **8**, 13 (2020).
14. X. Li, D. R. Ballerini, and W. Shen, *Biomicrofluidics*, **6**, 011301 (2012).
15. M. Kulkarni, Yashas, P. K. Enaganti, K. Amreen, and S. Goel, *Nanotechnology*, **31**, 425504 (2020).
16. B. K. Gale, A. R. Jafek, C. J. Lambert, B. L. Goenner, H. Moghimifam, U. C. Nze, and S. K. Kamarapu, *Inventions*, **3**, 360 (2018).
17. V. I. Vullev, J. Wan, V. Heinrich, P. Landsman, P. E. Bower, B. Xia, B. Millare, and G. Jones, *J. Am. Chem. Soc.*, **128**, 16062 (2006).
18. Y. Xia and G. M. Whitesides, *Angew. Chemie—Int. Ed.*, **37**, 550 (1998).
19. A. Plecis and Y. Chen, *Microelectron. Eng.*, **84**, 1265 (2007).
20. J. B. Edel, R. Fortt, J. C. DeMello, and A. J. DeMello, *Chem. Commun.*, **2**, 1136 (2002).
21. H. Wang, H. Nakamura, M. Uehara, M. Miyazaki, and H. Maeda, *Chem. Commun.*, **2**, 1462 (2002).

22. E. M. Chan, R. A. Mathies, and A. P. Alivisatos, *Nano Lett.*, **3**, 199 (2003).
23. X. Z. Lin, A. D. Terepka, and H. Yang, *Nano Lett.*, **4**, 2227 (2004).
24. D. Shalom, R. C. R. Wootton, R. F. Winkle, B. F. Cottam, R. Vilar, A. J. DeMello, and C. P. Wilde, *Mater. Lett.*, **61**, 1146 (2007).
25. L. Xu, C. Srinivasakannan, J. Peng, D. Zhang, and G. Chen, *Chem. Eng. Process. Process Intensif.*, **93**, 44 (2015).
26. F. Heshmatnezhad and A. R. Solaimany Nazar, *J. Flow Chem.*, **10**, 12 (2020).
27. O. D. K. Furusawa and K. Nagayama, *Langmuir*, **12**, 2385 (1996).
28. J. R. Millman, K. H. Bhatt, B. G. Prevo, and O. D. Velev, *Nat. Mater.*, **4**, 98 (2005).
29. H. Song, D. L. Chen, and R. F. Ismagilov, *Angew. Chemie—Int. Ed.*, **45**, 7336 (2006).
30. I. U. Khan, C. A. Serra, N. Anton, and T. F. Vandamme, *Expert Opin. Drug Deliv.*, **12**, 547 (2015).
31. T. B. Jones, M. Gunji, M. Washizu, and M. J. Feldman, *J. Appl. Phys.*, **89**, 1441 (2001).
32. A. Bransky, N. Korin, M. Khoury, and S. Levenberg, *Lab Chip*, **9**, 516 (2009).
33. P. Garstecki, M. J. Fuerstman, H. A. Stone, and G. M. Whitesides, *Lab Chip*, **6**, 437 (2006).
34. S. L. Anna, N. Bontoux, and H. A. Stone, *Appl. Phys. Lett.*, **82**, 364 (2003).
35. A. Huebner, S. Sharma, M. Srisa-Art, F. Hollfelder, J. B. Edel, and A. J. DeMello, *Lab Chip*, **8**, 1244 (2008).
36. D. R. Link, E. Grasland-Mongrain, A. Duri, F. Sarrazin, Z. Cheng, G. Cristobal, M. Marquez, and D. A. Weitz, *Angew. Chemie—Int. Ed.*, **45**, 2556 (2006).
37. M. He, J. S. Kuo, and D. T. Chiu, *Appl. Phys. Lett.*, **87**, 14 (2005).
38. W. S. Lee, S. Jambovane, D. Kim, and J. W. Hong, *Microfluid. Nanofluidics*, **7**, 431 (2009).
39. A. Diguat, H. Li, N. Queyriaux, Y. Chen, and D. Baigl, *Lab Chip*, **11**, 2666 (2011).
40. P. Thurgood, S. Baratchi, C. Szydzik, J. Y. Zhu, S. Nahavandi, A. Mitchell, and K. Khoshmanesh, *Sensor. Actuat. B Chem.*, **274**, 645 (2018).
41. N. Lass, L. Riegger, R. Zengerle, and P. Koltay, *Micromachines*, **4**, 49 (2013).
42. Y. Li, K. Wang, and G. Luo, *Ind. Eng. Chem. Res.*, **56**, 12131 (2017).
43. H. Yamashita, M. Morita, H. Sugiura, K. Fujiwara, H. Onoe, and M. J. Takinoue, *Biosci. Bioeng.*, **119**, 492 (2015).
44. K. Wang, L. Xie, Y. Lu, and G. Luo, *Lab Chip*, **13**, 73 (2013).
45. S. Li, D. Zheng, N. Li, X. Wang, Y. Liu, M. Sun, and X. Zhao, *Micromachines*, **8**, 88 (2017).
46. Y. Y. Wei, Z. Q. Sun, H. H. Ren, and L. Li, *Chinese J. Anal. Chem.*, **47**, 795 (2019).
47. S. Katsura, A. Yamaguchi, N. Harada, K. Hirano, and A. Mizuno, *Conference Record of the 1999 IEEE Industry Applications Conference. Thirty-Forth IAS Annual Meeting (Cat. No.99CH36370)*, Phoenix, AZ, USA, **2**, 1124 (1999), (<https://doi.org/10.1109/IAS.1999.801645>).
48. D. G. Shchukin and G. B. Sukhorukov, *Adv. Mater.*, **16**, 671 (2004).
49. I. Shestopalov, J. D. Tice, and R. F. Ismagilov, *Lab Chip*, **4**, 316 (2004).
50. L. H. Hung, K. M. Choi, W. Tseng, Y. Tan, J. Shea, and A. Phillip, 174 (2006), <http://arxiv.org/abs/10.1039/b513908b>.
51. J. B. Wacker, I. Lignos, V. K. Parashar, and M. A. M. Gijs, *Lab Chip*, **12**, 3111 (2012).
52. S. Abalde-Cela, P. Taladriz-Blanco, M. G. De Oliveira, and C. Abell, *Sci. Rep.*, **8**, 1 (2018).
53. K. G. Lee, J. Hong, K. W. Wang, N. S. Heo, D. H. Kim, S. Y. Lee, S. J. Lee, and T. J. Park, *ACS Nano*, **6**, 6998 (2012).
54. D. L. A. Fernandes, C. Paun, M. V. Pavliuk, A. B. Fernandes, E. L. Bastos, and J. Sá, *RSC Adv.*, **6**, 95693 (2016).
55. C. X. Zhao, L. He, S. Z. Qiao, and A. P. J. Middelberg, *Chem. Eng. Sci.*, **66**, 1463 (2011).
56. S. T. He, Y. L. Liu, and H. Maeda, *J. Nanoparticle Res.*, **10**, 209 (2008).
57. J. Wagner, T. Kirmer, G. Mayer, J. Albert, and J. M. Köhler, *Chem. Eng. J.*, **101**, 251 (2004).
58. C. H. Weng, C. C. Huang, C. S. Yeh, H. Y. Lei, and G. Bin Lee, *J. Micromech. Microeng.*, **18**, 035019 (2008).
59. S. Y. Yang, F. Y. Cheng, C. S. Yeh, and G. Bin Lee, *Microfluid. Nanofluidics*, **8**, 303 (2010).
60. J. Ftouni, M. Penhoat, A. Addad, E. Payen, C. Rolando, and J. S. Girardon, *Nanoscale*, **4**, 4450 (2012).
61. H. Yagyu, Y. Tanabe, S. Takano, and M. Hamamoto, *Micro Nano Lett.*, **12**, 536 (2017).
62. M. V. Bandulasena, G. T. Vladislavljević, O. G. Odumbaku, and B. Benyahia, *Chem. Eng. Sci.*, **171**, 233 (2017).
63. G. A. Patil, M. L. Bari, B. A. Bhanvase, V. Ganvir, S. Mishra, and S. H. Sonawane, *Chem. Eng. Process. Process Intensif.*, **62**, 69 (2012).
64. R. Baber, L. Mazzei, N. T. K. Thanh, and A. Gavriilidis, *J. Flow Chem.*, **6**, 268 (2016).
65. L. Xu, J. Peng, M. Yan, D. Zhang, and A. Q. Shen, *Chem. Eng. Process. Process Intensif.*, **102**, 186 (2016).
66. C. H. Kwak, S. M. Kang, E. Jung, Y. Haldorai, Y. K. Han, W. S. Kim, T. Yu, and Y. S. Huh, *J. Ind. Eng. Chem.*, **63**, 405 (2018).
67. C. H. Yang, L. S. Wang, S. Y. Chen, M. C. Huang, Y. H. Li, Y. C. Lin, P. F. Chen, J. F. Shaw, and K. S. Huang, *Int. J. Pharm.*, **510**, 493 (2016).
68. Y. Song, C. S. S. R. Kumar, and J. Hormes, *J. Nanosci. Nanotechnol.*, **4**, 788 (2004).
69. A. M. Karim et al., *J. Phys. Chem. C*, **119**, 13257 (2015).
70. Z. Qiao, Z. Wang, C. Zhang, S. Yuan, Y. Zhu, and J. Wang, *AIChE J.*, **59**, 215 (2012).
71. S. Sharada, P. L. Suryawanshi, P. Rajesh Kumar, S. P. Gumfekar, T. B. Narsaiah, and S. H. Sonawane, *Colloids Surfaces A Physicochem. Eng. Asp.*, **498**, 297 (2016).
72. E. Gioria, C. Signorini, F. Wisniewski, and L. Gutierrez, *J. Environ. Chem. Eng.*, **8**, 104096 (2020).
73. H. J. Lee, G. Lee, N. R. Jang, J. H. Yun, J. Y. Song, and B. S. Kim, *Tech. Proc. 2011 NSTI Nanotechnol. Conf. Expo, NSTI-Nanotech 2011*, **1**, 371 (2011).
74. Y. Wang, X. Zhang, A. Wang, X. Li, G. Wang, and L. Zhao, *Chem. Eng. J.*, **235**, 191 (2014).
75. B. G. Zukas and N. R. Gupta, *Ind. Eng. Chem. Res.*, **56**, 7184 (2017).
76. N. Ghifari, A. Chahboun, and A. El Abed, *Int. Conf. Transparent Opt. Networks, 2019-July 1* (2019), (<https://doi.org/10.1109/ICTON.2019.8840433>).
77. A. Abou Hassan, O. Sandre, V. Cabuil, and P. Tabeling, *Chem. Commun.*, **2008**, 1783 (2008).
78. L. Frenz, A. El Harrak, M. Pauly, S. Bégin-Colin, A. D. Griffiths, and J. C. Baret, *Angew. Chemie—Int. Ed.*, **47**, 6817 (2008).
79. W. B. Lee, C. H. Weng, F. Y. Cheng, C. S. Yeh, H. Y. Lei, and G. B. Lee, *Biomed. Microdevices*, **11**, 161 (2009).
80. K. Kumar, A. M. Nightingale, S. H. Krishnadasan, N. Kamaly, M. Wylenzinska-Arridge, K. Zeissler, W. R. Branford, E. Ware, A. J. Demello, and J. C. Demello, *J. Mater. Chem.*, **22**, 4704 (2012).
81. L. Uson, M. Arruebo, V. Sebastian, and J. Santamaria, *Chem. Eng. J.*, **340**, 66 (2018).
82. C. D. Ahrberg, J. Wook Choi, and B. Geun Chung, *Sci. Rep.*, **10**, 1737 (2020).
83. Y. Zhang, W. Jiang, and L. Wang, *Microfluid. Nanofluidics*, **9**, 727 (2010).
84. J. Parisi, Y. Liu, L. Su, and Y. Lei, *RSC Adv.*, **3**, 1388 (2013).
85. L. Xu, J. Peng, C. Srinivasakannan, L. Zhang, D. Zhang, C. Liu, S. Wang, and A. Q. Shen, *RSC Adv.*, **4**, 25155 (2014).
86. L. Xu, C. Srinivasakannan, J. Peng, M. Yan, D. Zhang, and L. Zhang, *Appl. Surf. Sci.*, **331**, 449 (2015).
87. Y. Liang, Y. Shinozaki, and H. Yagyu, *Proceedings*, **2**, 1110 (2018).
88. Y. Song, T. Zhang, W. Yang, S. Albin, and L. L. Henry, *Cryst. Growth Des.*, **8**, 3766 (2008).
89. A. Abou-Hassan, S. Neveu, V. Dupuis, and V. Cabuil, *RSC Adv.*, **2**, 11263 (2012).
90. A. Goyal, M. Mohl, A. Kumar, R. Puskas, A. Kukovec, Z. Konya, I. Kiricsi, and P. M. Ajayan, *Compos. Sci. Technol.*, **71**, 129 (2011).
91. C. Zeng, C. Wang, F. Wang, Y. Zhang, and L. Zhang, *Chem. Eng. J.*, **204–205**, 48 (2012).
92. R. Eluri and B. Paul, *J. Nanoparticle Res.*, **14**, 1 (2012).
93. B. F. Cottam, S. Krishnadasan, A. J. DeMello, J. C. DeMello, and M. S. P. Shaffer, *Lab Chip*, **7**, 167 (2007).
94. T. H. Eun, S. H. Kim, W. J. Jeong, S. J. Jeon, S. H. Kim, and S. M. Yang, *Chem. Mater.*, **21**, 201 (2009).
95. W. Lan, S. Li, J. Xu, and G. Luo, *Langmuir*, **27**, 13242 (2011).
96. A. M. Nightingale and J. C. De Mello, *J. Mater. Chem.*, **20**, 8454 (2010).
97. B. K. H. Yen, A. Günther, M. A. Schmidt, K. F. Jensen, and M. G. Bawendi, *Angew. Chemie*, **117**, 5583 (2005).
98. W. Liu, Y. Zhang, C. F. Wang, and S. Chen, *RSC Adv.*, **5**, 107804 (2015).
99. Z. H. Tian, J. H. Xu, Y. J. Wang, and G. S. Luo, *Chem. Eng. J.*, **285**, 20 (2016).
100. J. Wang, H. Zhao, Y. Zhu, and Y. Song, *J. Phys. Chem. C*, **121**, 3567 (2017).
101. J. Liu, Y. Gu, Q. Wu, X. Wang, L. Zhao, A. Demello, W. Wen, R. Tong, and X. Gong, *Crystals*, **9**, 1 (2019).
102. Y. Shu, P. Jiang, D. W. Pang, and Z. L. Zhang, *Nanotechnology*, **26**, 275701 (2015).
103. A. Schej, M. Frégnaux, J. M. Commenge, L. Balan, L. Falk, and R. Schneider, *Nanotechnology*, **25**, 145606 (2014).
104. B. H. Kwon, K. G. Lee, T. J. Park, H. Kim, T. J. Lee, S. J. Lee, and D. Y. Jeon, *Small*, **8**, 3257 (2012).
105. I. Lignos, S. Stavrakis, A. Kilaj, and A. J. deMello, *Small*, **11**, 4009 (2015).
106. Y. Lu, L. Zhang, and H. Lin, *Chem.—A Eur. J.*, **20**, 4246 (2014).
107. S. G. De-Pedro, A. S. Castillo, M. Ariza-Avidad, A. Lapresta-Fernández, C. Sánchez-González, C. S. Martínez-Cisneros, M. Puyol, L. F. Capitan-Vallvey, and J. Alonso-Chamarro, *Nanoscale*, **6**, 6018 (2014).
108. L. Rao, Y. Tang, Z. Li, X. Ding, G. Liang, H. Lu, C. Yan, K. Tang, and B. Yu, *Mater. Sci. Eng. C*, **81**, 213 (2017).
109. Y. Tang, Z. Li, X. Ding, G. Liang, H. Lu, C. Yan, K. Tang, and B. Yu, *Sensors Actuators, B Chem.*, **258**, 637 (2018).
110. B. Swain, M. H. Hong, L. Kang, B. S. Kim, N. H. Kim, and C. G. Lee, *Chem. Eng. J.*, **308**, 311 (2017).
111. S. Li, J. C. Hsiao, P. D. Howes, and A. J. deMello, *Nanotechnol. Microfluid.* (Wiley-VCH Verlag GmbH & Co. KGaA) chap. 4, 109 (2020), (<https://doi.org/10.1002/9783527818341.ch4>).
112. J. Nette, P. D. Howes, and A. J. deMello, *Adv. Mater. Technol.*, **5**, 2000060 (2020).
113. M. Alizadeh-Ghods, M. Pourhassan-Moghaddam, A. Zavari-Nematabad, B. Walker, N. Annabi, and A. Akbarzadeh, *Part. Part. Syst. Character.*, **36**, 1 (2019).
114. R. Karnik, F. Gu, P. Basto, C. Cannizzaro, L. Dean, W. Kyei-manu, R. Langer, and O. C. Farokhzad, *Nano Lett.*, **8**, 2906 (2008).
115. D. Dendukuri, K. Tsoi, T. A. Hattton, and P. S. Doyle, *Langmuir*, **21**, 2113 (2005).
116. S. Takeuchi, P. Garstecki, D. B. Weibel, and G. M. Whitesides, *Adv. Mater.*, **17**, 1067 (2005).
117. J. M. Lim, N. Bertrand, P. M. Valencia, M. Rhee, R. Langer, S. Jon, O. C. Farokhzad, and R. Karnik, *Nanomedicine Nanotechnology, Biol. Med.*, **10**, 401 (2014).
118. J. M. Köhler, A. März, J. Popp, A. Knauer, I. Kraus, J. Faerber, and C. Serra, *Anal. Chem.*, **85**, 313 (2013).

119. J. Puigmartí-Luis, M. Rubio-Martínez, U. Hartfelder, I. Imaz, D. MasPOCH, and P. S. Dittrich, *J. Am. Chem. Soc.*, **133**, 4216 (2011).
120. P. M. Valencia, P. A. Basto, L. Zhang, M. Rhee, R. Langer, O. C. Farokhzad, and R. Karnik, *ACS Nano*, **4**, 1671 (2010).
121. E. Rondeau and J. J. Cooper-White, *Langmuir*, **24**, 6937 (2008).
122. S. Ding, N. Anton, T. F. Vandamme, and C. A. Serra, *Expert Opin. Drug Deliv.*, **13**, 1447 (2016).
123. L. Zhang, A. Beatty, L. Lu, A. Abdalrahman, T. M. Makris, G. Wang, and Q. Wang, *Mater. Sci. Eng. C*, **111**, 110768 (2020).
124. H. Zhang, E. Tumarkin, R. Peerani, Z. Nie, R. M. A. Sullan, G. C. Walker, and E. Kumacheva, *J. Am. Chem. Soc.*, **128**, 12205 (2006).
125. K. Liu, H. J. Ding, J. Liu, Y. Chen, and X. Z. Zhao, *Langmuir*, **22**, 9453 (2006).
126. B. G. De Geest, J. P. Urbanski, T. Thorsen, J. Demeester, and S. C. De Smedt, *Langmuir*, **21**, 10275 (2005).
127. W. J. Jeong, J. Y. Kim, J. Choo, E. K. Lee, C. S. Han, D. J. Beebe, G. H. Seong, and S. H. Lee, *Langmuir*, **21**, 3738 (2005).
128. B. L. Gray, *J. Electrochem. Soc.*, **161**, B3173 (2014).
129. Z. Nie, W. Li, M. Seo, S. Xu, and E. Kumacheva, *J. Am. Chem. Soc.*, **128**, 9408 (2006).
130. L. B. Zhao, L. Pan, K. Zhang, S. S. Guo, W. Liu, Y. Wang, Y. Chen, X. Z. Zhao, and H. L. W. Chan, *Lab Chip*, **9**, 2981 (2009).
131. G. R. Yi, T. Thorsen, V. N. Manoharan, M. J. Hwang, S. J. Jeon, D. J. Pine, S. R. Quake, and S. M. Yang, *Adv. Mater.*, **15**, 1300 (2003).
132. S. A. Khan, A. Günther, M. A. Schmidt, and K. F. Jensen, *Langmuir*, **20**, 8604 (2004).
133. Y. Pan, J. Yao, L. Zhang, and N. Xu, *Ind. Eng. Chem. Res.*, **48**, 8471 (2009).
134. X. Gong, S. Peng, W. Wen, P. Sheng, and W. Li, *Adv. Funct. Mater.*, **19**, 292 (2009).
135. Q. A. Wang, X. Zhang, A. Wang, X. Li, G. Wang, and L. Zhao, *Chem. Eng. J.*, **149**, 473 (2009).
136. N. Jongen et al., *Chem. Eng. Technol.*, **26**, 304 (2003).
137. A. A. Karim, Y. Reda, and A. A. Fattah, *J. Electrochem. Soc.*, **167**, 037554 (2020).
138. Y. Song, J. Hormes, and C. S. S. R. Kumar, *Small*, **4**, 698 (2008).

# Effects of heat and mass transfer on MHD nonlinear free convection non-Newtonian fluids flow embedded in a thermally stratified porous medium

Gladys Tharapatla  | Pamula RajKumari |  
Gurrampati V. Ramana Reddy

Department of Mathematics, Koneru Lakshmaiah Education Foundation, Vaddeswaram, India

## Correspondence

Gladys Tharapatla, Department of Mathematics, Koneru Lakshmaiah Education Foundation, Vaddeswaram 500028, Andhra Pradesh, India.  
Email: [gladysharshitha@gmail.com](mailto:gladysharshitha@gmail.com)

## Abstract

This communication examines heat alongside mass transport in a nonlinear free convection magnetohydrodynamics (MHD) non-Newtonian fluid flow with thermal radiation and heat generation deep-rooted in a thermally stratified penetrable medium. The Casson and Williamson fluid considered in this communication flows simultaneously across the boundary layer and are mixed together. The model of heat alongside mass transport is set up with chemical reaction and thermal radiation alongside heat generation to form a system of partial differential equations (PDEs). Appropriate similarity variables are used to simplify the PDEs to obtain systems of coupled ordinary differential equations. An efficiently developed numerical approach called the spectral homotopy analysis method was used in providing solutions to the transformed equations. A large value of Casson term is observed to degenerate the velocity plot while the Williamson parameter enhances the velocity profile. The parameter of thermal stratification is found to enhance the rate of heat transport within the boundary layer. An incremental value of the magnetic parameter declines the velocity of the fluid and the entire boundary layer thickness.

The present result was compared with previous studies and was seen to be in good agreement.

#### KEYWORDS

Casson and Williamson fluids, heat and mass transport, Lorentz force, MHD, nonlinear convection flow, spectral homotopy analysis method, thermally stratified medium

## 1 | INTRODUCTION

The viscous flow of heat alongside mass transport of non-Newtonian fluids past an accelerating permeable surface has attracted the interest of researchers in applied science because of the various applications in the pipe industry, production of food, petroleum reservoir, extraction of metal, and so on. All physical properties along with the shear stress of non-Newtonian fluids vary and are hereby classified into the Ellis model, Carreau model, Casson fluid model, Williamson model, and so on. Among all these models, the Casson and Williamson fluid has unique properties. The Casson is a yield exhibiting type of fluid while the Williamson is known for having low viscosity at  $\mu_0$  and high viscosity at  $\mu_\infty$ , respectively. The study of Idowu and Falodun<sup>1</sup> explored under the impact of Soret-Dufour, effects of varying thermal conductivity alongside viscosity on non-Newtonian liquids flow in a vertical penetrable plate. In 2018, Fagbade et al.<sup>2</sup> elucidated the natural magnetohydrodynamic (MHD) convection motion of a viscoelastic liquid. Rehman et al.<sup>3</sup> examined double-stratification in Casson liquid motion. Their model was solved with numerical techniques and they finalized that as the Casson parameters approach infinity, their model turned to Newtonian. Tamoor et al.<sup>4</sup> presented the MHD motion of Casson liquid. They found in their study that, the velocity declines with a large value of the Casson parameter. Rehman et al.<sup>5</sup> conducted a numerical simulation of MHD Casson Navier's slip nanofluid flow. They finalized that a higher value of the Casson term diminishes the velocity profile. Seth et al.<sup>6</sup> examined double diffusion of MHD Casson liquid flow with Newton heating and thermo-diffusion influence. Hayat et al.<sup>7</sup> elucidated the boundary layer flow of Williamson liquids. They employed analytical solutions to their flow equations and found out that an increase in the Williamson parameter produces an increase to the velocity profile. Tesfaye et al.<sup>8</sup> recently examined heat along with mass transport in the unsteady flow of a Williamson nanofluid. They found out in their study that the rate of heat transport increases with the unsteadiness parameter. Lund et al.<sup>9</sup> elucidate the flow of Williamson fluids along with MHD and slippage. They concluded in their exploration that the magnetic parameter declines the thickness of the hydrodynamic layer of the liquid. Megahed<sup>10</sup> examined Williamson fluids flow because of a nonlinearly stretching sheet. The recent study of Idowu and Falodun<sup>11</sup> elucidates the flow of Casson liquid over an Inclined plate. They employed the spectral homotopy analysis method (SHAM) to solve their model equations and noticed a large Casson term degenerates the velocity.

Heat and mass transport (double-diffusive) motion of a fluid situated in a stratified thermal and penetrable medium is gaining attention in the recent time. In a working liquid, the stratified thermal medium finds importance when the fluid environment is at a higher temperature. Hence, the importance of thermal radiation in such boundary layer flows. The importance of this area lies in heat exchanger devices, thermal explosion, and the nuclear

literature. Mukhopadhyay<sup>12</sup> examined heat transport past an exponentially stretching sheet situated in a stratified thermal medium. Raju et al.<sup>13</sup> examined heat along with mass movement in the MHD motion of a Casson liquid. They concluded in their study that the Casson fluid model shows a good heat transport analysis compared to the Newtonian model. Wahab et al.<sup>14</sup> elucidate the impact of viscosity, which depends on temperature, on non-Newtonian fluid flow together with double stratification. Their flow equations were solved numerically and a decrease in velocity profile is observed with large stratification parameter. Ali et al.<sup>15</sup> examined heat alongside mass transport on MHD motion of free convection. A large Prandtl number is noticed to elevate the Nusselt number in their study. Koriko et al.<sup>16</sup> elucidate MHD motion of a Micropolar fluid in a thermally stratified medium. In their study, an analytical solution was obtained and the results show that a large stratification parameter degenerates the velocity plot. Stratified thermal motion of Jeffrey liquid with the heat flux non-Fourier model has been examined by Ijaz and Ayub.<sup>17</sup> They concluded in their study that a large stratification number degenerates the temperature plot. Hayat et al.<sup>18</sup> elucidate the temperature as well as concentration stratification impact on the motion of Oldroyd-B fluid. The influence of coupled stratification on heat alongside mass transport in MHD motion of a nanoliquid has been investigated by Mutuku and Makinde.<sup>19</sup> In 2019, Falodun and Omowaye<sup>20</sup> elucidated double-diffusive motion of heat alongside mass transport embedded in a stratified thermal channel.

MHD in convective motion through a penetrable medium has gained much attention in recent times because of its engineering applications. Most fluids that are electrically conducting have an MHD nature. It is applicable in power engineering, MHD accelerators, metallurgy, and so on. Hayat et al.<sup>21</sup> elucidate Marangoni flow with Joule heating alongside nonlinear radiation. They concluded in their study that large radiation leads to a thick thermal layer. Ramana Reddy et al.<sup>22</sup> elucidate MHD non-Newtonian liquids flow. They concluded that Casson fluid influences the fluid velocity more than the Maxwell fluid. Upreti et al.<sup>23</sup> determined the solution to the MHD flow of an Ag–water nanofluid. Their results show that the MHD nature of the fluid declines the velocity profile. Hayat et al.<sup>24</sup> discussed MHD Jeffrey liquid motion owing to a nonlinear radially stretching sheet. The MHD nature of the flow has a decreasing effect on the velocity profile. Rashidi et al.<sup>25</sup> elucidate heat alongside mass transport in MHD motion of a viscoelastic liquid. Idowu and Falodun<sup>26</sup> explained the impact of magnetism alongside radiation on the motion of free convection in a penetrable medium. The impact of Soret alongside Dufour on the motion of natural convection in a penetrable medium with viscosity diversity has been investigated by Moorthy and Senthilvadivu.<sup>27</sup> Kumari and Sreedevi<sup>28</sup> elucidate heat plus mass transport motion of a viscous conducting electrically liquid. Alao et al.<sup>29</sup> elucidate Soret alongside Dufour's impact on heat alongside mass transport of chemically reacting motion of a liquid. Jhansi et al.<sup>30</sup> studied heat together with mass transport behavior on MHD motion past a slanted plate situated in a penetrable medium. Kumari et al.<sup>31</sup> investigated the mathematical analysis of the convective warmth moreover accumulations transmit pour of micro-polar liquid through an absorbent standard in a rectangular enclosure with heat sources. Ayegbusi et al.<sup>32</sup> explored MHD heat alongside mass transport convective motion with thermal radiation. Research on the mechanism of heat alongside mass transport motion has been elucidated by Ahmed et al.<sup>33</sup> Reddy and Ferdow<sup>34</sup> recently examined species and thermal radiation on micropolar hydromagnetic dusty liquid flow across a paraboloid revolution. In another study of Reddy et al.,<sup>35</sup> zero-mass flux and Cattaneo-Christov heat flux through a Prandtl non-Newtonian nanofluid in Darcy-Forchheimer porous space was examined. Reddy et al.<sup>36</sup> explored temperature-dependent viscosity and second-order slip flow on a MHD Casson radiative nanofluid over a stretching sheet. Sandeep and Reddy<sup>37</sup> studied MHD Oldroyd-B fluid



flow across a melting surface with cross-diffusion and double stratification. Machireddy and Sandeep<sup>38</sup> considered heat and mass transfer in a radiative MHD Carreau fluid with cross-diffusion.

Our survey of the literature indicates that studies on heat alongside mass transport in MHD nonlinear convection motion of non-Newtonian liquids in a thermally stratified medium is minimal. Few studies on thermally stratified medium have considered the Newtonian model while studies on non-Newtonian fluids in thermally stratified medium do not consider nonlinear free convection flow. We are therefore motivated by the literature discussed in this study to elucidate heat alongside mass transport in an MHD nonlinear free convection non-Newtonian fluid flow situated in a stratified thermal penetrable medium. To our understanding, studies of this type have not been done before in the literature. The present study is unique because it elucidates the simultaneous motion of Casson and Williamson fluids together in a penetrable stratified thermal medium.

## 2 | EQUATIONS OF MOTION

We considered the motion of double non-Newtonian liquids in a stratified thermal penetrable medium with linear and nonlinear convection flow. The fluid motion direction is vertically upward in the  $x$ -direction. A magnetism of uniform potency ( $B_0$ ) is enforced on the liquid motion. At the wall, we have the temperature to be  $T_w(x)$ , concentration to be  $C_w(x)$  and velocity to be  $U_w(x)$  while the free stream temperature alongside concentration  $T_\infty$  and  $C_\infty$  are considered to exist outside the thermally stratified porous medium as shown

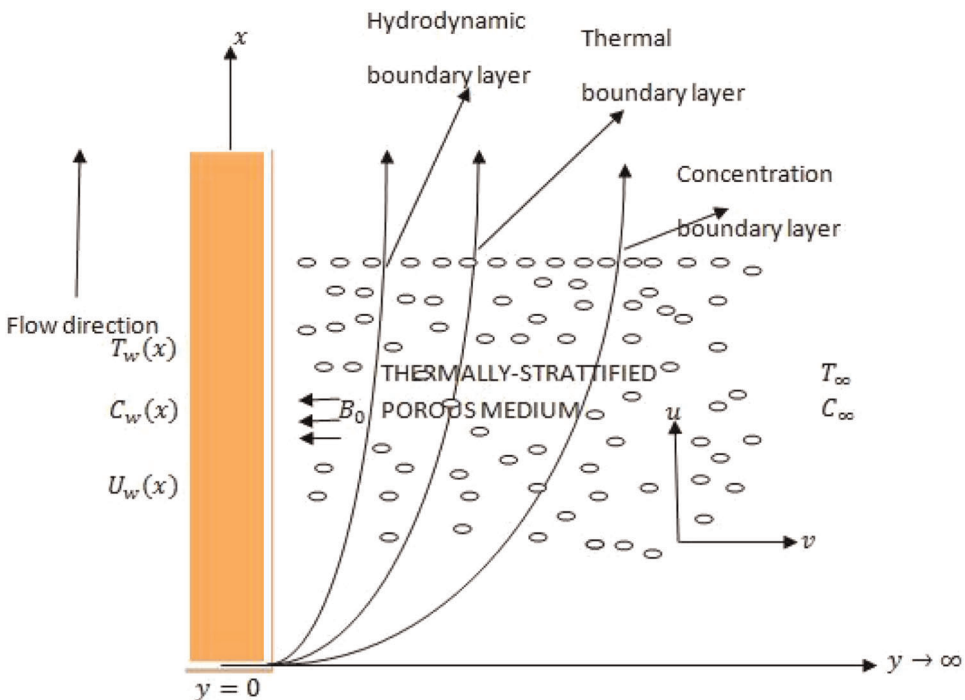


FIGURE 1 Physical geometry [Color figure can be viewed at [wileyonlinelibrary.com](http://wileyonlinelibrary.com)]

in Figure 1. The difference between the wall temperature and concentration are given as  $(T_w - T_\infty)$  and  $(C_w - C_\infty)$ , respectively. The Casson fluid flows together with Williamson fluid within the thermally stratified porous medium and is mixed together. The thermally stratified porous medium is assumed to be homogeneous. We assumed the level of species concentration to be large, thus the effect of Soret-Dufour is significant. The fluid particles flow from a hot to a cold region, thus the thermophoresis term is considered to be significant. All fluid attributes are considered to be unchanged. The Boussinesq and boundary layer approximation is valid. The rheological equation of a Casson fluid base on Idowu and Falodun<sup>1</sup> can be written as:

$$\tau_{ij} = \left( \mu_b(T) + \frac{P_y}{\sqrt{2\pi}} \right) 2e_{ij} \quad \text{when } \pi > \pi_c \quad \tau_{ij} = \left( \mu_b(T) + \frac{P_y}{\sqrt{2\pi_c}} \right) 2e_{ij} \quad \text{when } \pi < \pi_c, \quad (1)$$

where  $P_y$  indicate fluid yield stress given as

$$P_y = \frac{\mu_b(T) \sqrt{(2\pi)}}{\beta}, \quad (2)$$

$\mu_b$  = plastic dynamic viscosity,  $\pi = e_{ij}e_{ij}$  = deformation rate multiplying itself and  $e_{ij}$  = rate of deformation and  $\pi_c$  is the critical value regarding the Casson model. With the motion of Casson fluid, where  $\pi > \pi_c$ , we can have the expression

$$\mu_0 = \mu_b(T) + \frac{P_y}{\sqrt{2\pi}}. \quad (3)$$

Invoking Equation (2) into (3), the kinematic viscosity is valid on plastic dynamic viscosity  $\mu_b$ , the density  $\rho$  and the Casson term  $\beta$  leads to

$$\mu_0 = \frac{\mu_b(T)}{\rho} \left( 1 + \frac{1}{\beta} \right). \quad (4)$$

The liquid is set into motion because of the stretching sheet. The Williamson fluid constitutive equation gives:

$$S = -pI + \tau, \quad (5)$$

$$\tau = \left[ \mu_\infty + \frac{(\mu_0 - \mu_\infty)}{1 - \Gamma(\dot{\gamma})} \right] A_1. \quad (6)$$

From which the pressure is  $p$ ,  $I$  denotes Identity,  $\tau$  is stress tensor,  $\mu_0$  is zero along with the infinite rate of shear and  $\mu_\infty$ ,  $\Gamma > 0$  denotes constant time,  $A_1$  denotes tensor of Rivlin-Erickson and  $\dot{\gamma}$  is given as

$$\dot{\gamma} = \sqrt{\frac{1}{2}\pi}, \quad \text{where } \pi = \text{trace}(A_1^2), \quad (7)$$

$$\dot{\gamma} - \left[ \left( \frac{\partial u}{\partial c} \right)^2 + \frac{1}{2} \left( \frac{\partial u}{\partial x} + \frac{\partial v}{\partial x} \right)^2 + \left( \frac{\partial v}{\partial y} \right)^2 \right]^{\frac{1}{2}} = 0, \quad (8)$$

where  $\pi$  = second invariant strain tensor. It should be noted in this study that the case when  $\mu_\infty = 0$  and  $\Gamma\dot{\gamma} < 1$  is explored in the present study. Hence, Equation (6) is the extra stress tensor which takes the form:

$$\tau - \left[ \frac{\mu_0}{1 - \Gamma\dot{\gamma}} \right] A_1 = 0. \quad (9)$$

Therefore, the components of the extra stress tensor shown in Equation (9) are:

$$\begin{aligned} \tau_{xx} - 2\mu_0[1 + \Gamma\dot{\gamma}] \frac{\partial u}{\partial x} &= 0, \tau_{xy} = \tau_{yx} = \mu_0[1 + \Gamma\dot{\gamma}] \left( \frac{\partial u}{\partial y} + \frac{\partial v}{\partial x} \right), \\ \tau_{yy} &= 2\mu_0[1 + \Gamma\dot{\gamma}] \frac{\partial v}{\partial y}, \tau_{xz} = \tau_{yz} = \tau_{zx} = \tau_{zy} = \tau_{zz} = 0. \end{aligned} \quad (10)$$

The heat flux on the fluid motion is based on the utilization of Rosseland approximation as explored in Alao et al.<sup>28</sup> and Fagbade et al.<sup>2</sup> and

$$q_r = - \frac{4\sigma_s}{3k_e} \frac{\partial T^4}{\partial y}, \quad (11)$$

where Stefan-Boltzman constant =  $\sigma_s$ , mean absorption coefficient =  $k_e$ . It is summarized that the differences between temperature in the fluid motion are small and  $T^4$  could be written in a linear function by simplifying  $T^4$  about  $T_\infty$  by employing the Taylor series and the previous terms of higher-order to give

$$T^4 \cong 4T_\infty^3 T - 3T_\infty^4 \quad (12)$$

substituting (12) into (11), the energy equation becomes

$$- \frac{\partial q_r}{\partial y} = \frac{16\sigma_s T_\infty^3}{3k_e} \frac{\partial^2 T}{\partial y^2}. \quad (13)$$

Based on the exploration of Idowu and Falodun,<sup>26</sup>  $V_T$  in Equation (4) is given as

$$V_T = -k\nu \frac{\nabla T}{T_{ref}} = - \frac{k\nu}{T_{ref}} \frac{\partial T}{\partial y}, \quad (14)$$

where  $k$  denoted the thermophoretic coefficient given as

$$k = \frac{2C_s \left( \frac{\lambda_g}{\lambda_p} + C_t K_n \right) \left[ 1 + K_n \left( C_1 + C_2 e^{-\frac{C_3}{K_n}} \right) \right]}{(1 + 3C_m K_n) \left( 1 + 2 \frac{\lambda_g}{\lambda_p} + 2C_t K_n \right)}. \quad (15)$$

$C_1, C_2, C_3, C_m, C_s$ , and  $C_t$  are constants,  $\lambda_g$  and  $\lambda_p$  denote fluid thermal conductivities and diffused particles,  $K_n$  denote the Knudsen number.

Based on all the assumptions above, the equations that govern the present model are:

$$\frac{\partial u}{\partial x} + \frac{\partial v}{\partial y} = 0, \quad (16)$$

$$\rho \left( u \frac{\partial u}{\partial x} + v \frac{\partial u}{\partial y} \right) = \mu \left( 1 + \frac{1}{\beta} \right) \frac{\partial^2 u}{\partial y^2} + \sqrt{2} \nu \Gamma \frac{\partial u}{\partial y} \frac{\partial^2 u}{\partial y^2} + g\rho [\beta_1(T - T_\infty) + \beta_2(T - T_\infty)^2] \\ + g\rho [\beta_3(C - C_\infty) + \beta_4(C - C_\infty)^2] - \left( \sigma B_0^2(x) + \frac{\mu}{K_p} \left( 1 + \frac{1}{\beta} \right) \right) u, \quad (17)$$

$$u \frac{\partial T}{\partial x} + v \frac{\partial T}{\partial y} = \alpha_1 \frac{\partial^2 T}{\partial y^2} + \frac{Dk_T}{c_s c_p} \frac{\partial^2 C}{\partial y^2} + \frac{\mu}{\rho c_p} \left( 1 + \frac{1}{\beta} \right) \left( \frac{\partial u}{\partial y} \right)^2 - \frac{1}{\rho c_p} \frac{\partial q_r}{\partial y} + \frac{Q}{\rho c_p} (T - T_\infty), \quad (18)$$

$$u \frac{\partial C}{\partial x} + v \frac{\partial C}{\partial y} = D \frac{\partial^2 C}{\partial y^2} + \frac{Dk_T}{T_m} \frac{\partial^2 T}{\partial y^2} - K'(C - C_\infty) - \frac{\partial(V_T C)}{\partial y}. \quad (19)$$

Subject to:

$$u = U_w(x) = Bx, v = -v(x), T = T_w, C = C_w, \text{ at } y = 0 \quad (20)$$

$$u \rightarrow 0, T \rightarrow T_\infty, C \rightarrow C_\infty, \text{ as } y \rightarrow \infty, \quad (21)$$

$u$  and  $v$  represents the relations  $u = \frac{\partial \psi}{\partial y}$  and  $v = -\frac{\partial \psi}{\partial x}$ . With this definition of  $u$  and  $v$ , the free stream is  $\psi(x, y)$ . It automatically satisfies the continuity equation. The following variables are utilized on the model

$$\eta = \left( \frac{B}{\nu} \right)^{\frac{1}{2}} y, \psi = (\nu B)^{\frac{1}{2}} x f(\eta), \theta(\eta) = (T - T_\infty)(T_w - T_\infty)^{-1}, \phi(\eta) = (C - C_\infty)(C_w - C_\infty)^{-1}. \quad (22)$$

The wall temperature ( $T_w$ ) and concentration ( $C_w$ ) and ambient temperature  $T_\infty$  and concentration  $C_\infty$  as defined in Falodun and Omowaye<sup>20</sup> is given as:

$$T_w = T_0 + m_1 x, C_w = C_0 + m_3 x, T_\infty = T_0 + m_2 x, C_\infty = C_0 + m_4 x \quad (23)$$

Employing the above similarity variables on the equations of motion (17)–(19) subject to (20) and (21) obtains the following coupled ordinary differential equation (ODE):

$$\left( 1 + \frac{1}{\beta} \right) f''' + ff'' - (f')^2 + A_T \theta^2 + Ac\phi^2 + Gr\theta + Gc\phi - \left( M + \frac{1}{P_o} \right) f' + \alpha f'' f''' = 0, \quad (24)$$

$$\left( 1 + \frac{4}{3}R \right) \theta'' + Prf\theta' + Do\phi'' + Ec \left( 1 + \frac{1}{\beta} \right) (f'')^2 + He\theta = 0, \quad (25)$$

$$\phi'' + Scf\phi' - ScCr\phi + ScSo\theta'' + \tau[\phi\theta'' + \theta'\phi'] = 0, \quad (26)$$

subject to:

$$f'(\eta) = 1, f(\eta) = S_w, \theta(\eta) = (-St + 1), \phi(\eta) = (-St + 1), \text{ at } \eta = 0, \quad (27)$$

$$\theta(\eta) \rightarrow 0, f'(\eta) \rightarrow 0, \phi(\eta) \rightarrow 0, \text{ as } \eta \rightarrow \infty \quad (28)$$

where  $A_T = \frac{g\beta_T(T_w - T_\infty)^2}{B^2x}$  is the nonlinear convective parameter for temperature,  $Ac = \frac{g\beta_c(C_w - C_\infty)^2}{B^2x}$  is the nonlinear convective parameter for concentration,  $Gr = \frac{g\beta_T(T_w - T_\infty)}{B^2x}$  is the linear convective

parameter for temperature,  $Gc = \frac{g\beta_c(C_w - C_\infty)}{B^2x}$  is the linear convective parameter for concentration,  $M = \frac{\sigma B_0^2(x)}{\nu}$  signifies the magnetic term,  $Po = \frac{K_p B}{\mu}$  signifies the permeability term,  $\alpha = \Gamma U_w(x) \left(\frac{2B}{\nu}\right)^{\frac{1}{2}}$  is the non-Newtonian Williamson term,  $Pr = \frac{\nu}{\alpha}$  signifies the Prandtl number,  $R = \frac{4\sigma_s T_\infty^2}{Ke}$  signifies the radiation term,  $Do = \frac{Dk_T(C_w - C_\infty)}{\nu c_p (T_w - T_\infty)}$  is the Dufour number,  $Ec = \frac{(Bx)^2}{c_p(T_w - T_\infty)}$  signifies the Eckert number,  $He = \frac{Q}{\rho c_p B}$  signifies heat generation term,  $Sc = \frac{\nu}{D}$  signifies the Schmidt number,  $Cr = \frac{K_1}{B}$  signifies the chemical reaction term,  $So = \frac{Dk_T(T_w - T_\infty)}{\nu \Gamma_m(C_w - C_\infty)}$  signifies the Soret number, and  $\tau = \frac{K}{T_{ref}}$  is the thermophoresis parameter.

The practical curiosity for engineering are the local skin friction coefficient ( $C_f$ ), Sherwood number ( $Sh$ ), and Nusselt number ( $Nu$ ). They are given in this study as follows:

$$C_f = \frac{\tau_w}{\rho \nu u^2} \text{ where } \tau_w = \left[ \left( \mu_B + \frac{P_y}{\sqrt{2\pi}} \right) + \sqrt{2} \nu \Gamma \frac{\partial^2 u}{\partial y^2} \right] \frac{\partial u}{\partial y} \Big|_{y=0},$$

$$Nu = \frac{q_w}{\frac{\alpha_1}{\nu}(T_w - T_\infty)} = \theta'(0) \text{ where } q_w = K \left( \frac{\partial T}{\partial y} \right)_{y=0} = \frac{\alpha_1}{\nu} (T_w - T_\infty) \theta'(0),$$

$$Sh = \frac{m_w}{\frac{D}{\nu}(C_w - C_\infty)} = \phi'(0) \text{ where } m_w = D \left( \frac{\partial C}{\partial y} \right)_{y=0} = \frac{D}{\nu} (C_w - C_\infty) \phi'(0).$$

### 3 | METHOD OF SOLVING THE EQUATIONS OF MOTION

The dimensionless Equations (24)–(26) subject to (27) and (28) has been solved by employing SHAM. SHAM is a numerical approach that combines the concept of the spectral method with the homotopy analysis method. To apply SHAM, we use the Chebyshev spectral collocation approach to decompose the equations into linear and nonlinear forms. Furthermore, the Chebyshev differentiation matrix is applied to the linear terms to form a systematic matrix form of the equation. To proceed with the application of SHAM, first all regions of the problem are changed from  $[0, \infty)$  to  $[-1, 1]$  by employing the domain truncation technique.<sup>39</sup> Therefore, the solution would be obtained within the interval  $[0, \eta_\infty]$  and not  $[0, \infty)$  again. The above description of SHAM leads to the following algebraic mapping

$$\xi = \frac{2\eta}{L} - 1, \xi \in [-1, 1]. \tag{29}$$

The algebraic equation below is applied on the system of Equations (24)–(26):

$$f(\eta) = f(\xi) + f_0(\eta), \theta(\eta) = \theta(\xi) + \theta_0(\eta), \phi(\eta) = \phi(\xi) + \phi_0(\eta) \tag{30}$$

substituting Equation (30) into (24)–(26) to obtain

$$\begin{aligned} & \left( 1 + \frac{1}{\beta} \right) f''' + ff'' + a_1 f + a_2 f'' - f'f' + a_3 f' + A_T \theta^2 + Ac\phi^2 + a_4 \theta + Gr\theta + Gc\phi + a_5 \phi \\ & - \left( M + \frac{1}{Po} \right) f' + \alpha f''f''' + a_6 f' + a_7 f''' = H_1(\eta) \end{aligned} \tag{31}$$

$$\left(1 + \frac{4}{3}R\right)\theta'' + Prf\theta' + b_1f + b_2\theta' + Do\phi'' + He\theta + Ec\left(1 + \frac{1}{\beta}\right)f''f'' + b_3f'' = H_2(\eta) \quad (32)$$

$$\phi'' + Scf\phi' + c_1f + c_2\phi' - ScCr\phi + ScSo\theta'' + \tau\phi\theta'' + c_3\phi + c_4\theta'' + \tau\theta'\phi' + c_5\theta' + c_6\phi' = H_3(\eta) \quad (33)$$

where the coefficient parameters are defined as follows:

$$\begin{aligned} a_1 &= f_0'', a_2 = f_0', a_3 = 2f_0', a_4 = 2A_T\theta_0, a_5 = 2Ac\phi_0, a_6 = \alpha f_0''', a_7 = \alpha f_0'', b_1 = Pr\theta_0', b_2 \\ &= Prf_0', b_3 = 2Ec\left(1 + \frac{1}{\beta}\right)f_0'' c_1 = Sc\phi_0', c_2 = Scf_0', c_3 = \tau\theta_0'', c_4 = \tau\phi_0, c_5 = \tau\phi_0', c_6 = \tau\theta_0'H_1(\eta) \\ &= \left(1 + \frac{1}{\beta}\right)f_0''' - f_0f_0'' - (f_0')^2 - A_T(\theta_0)^2 - Ac(\phi_0)^2 + \left(M + \frac{1}{Po}\right)f_0' - (f_0'')^2 - Gr\theta_0 \\ &\quad - Gc\phi_0H_2(\eta) = -\left(1 + \frac{4}{3}R\right)\theta_0'' - Prf_0'\theta_0' - Do\phi_0'' - He\theta_0 - Ec\left(1 + \frac{1}{\beta}\right)(f_0'')^2H_3(\eta) \\ &= -\phi_0'' - Scf_0'\phi_0' + ScCr\phi_0 - ScSo\theta_0'' - \tau\phi_0\theta_0'' - \tau\theta_0'\phi_0', \end{aligned}$$

subject to:

$$f_l(-1) = f_l'(-1) = f_l'(1) = 0, \theta(-1) = \theta_l(1) = 0, \phi_l(-1) = \phi_l(1) = 0. \quad (34)$$

The boundary constraints (34) is chosen to be zero subject to the domain  $[-1, 1]$  so as to utilize the linear part to resolve the SHAM outcomes. The CPM is used on (31)–(33). The functions  $f_l(\xi)$ ,  $\theta_l(\xi)$ , and  $\phi_l$  in (31)–(33) are evaluated as a Chebyshev series of polynomials presented by Idowu and Falodun<sup>26</sup> as:

$$f_l(\xi) = f_l^N(\xi_j) + \sum_{k=0}^N \bar{f}_k T_{1k}(\xi_j), j = 0, \dots, N \quad (35)$$

$$\theta_l(\xi) = \theta_l^N(\xi_j) + \sum_{k=0}^N \bar{\theta}_k T_{2k}(\xi_j), j = 0, \dots, N \quad (36)$$

$$\phi_l(\xi) = \phi_l^N(\xi_j) + \sum_{k=0}^N \bar{\phi}_k T_{3k}(\xi_j), j = 0, \dots, N \quad (37)$$

where  $T_{1k}$ ,  $T_{2k}$  and  $T_{3k}$  are the  $k$ th Chebyshev polynomial and  $\xi_0, \xi_1, \dots, \xi_N$  are collocation points of Gauss-Lobatto. The simplified domain nodes  $[-1, 1]$  are described by collocation points of Gauss-Lobatto explained by Idowu and Falodun<sup>26</sup>

$$\xi_j = \cos\left(\frac{\pi j}{N}\right) \quad (38)$$

provided  $j = 0, 1, \dots, N$  and  $N + 1$  signify the collocation points total number.<sup>40</sup> The unknown functions  $f_l(\xi)$ ,  $\theta_l(\xi)$ , and  $\phi_l(\xi)$  are evaluated by utilizing the Lagrange type of interpolation. It is employed to estimate the value of functions  $f_l(\xi)$ ,  $\theta_l(\xi)$ , and  $\phi_l(\xi)$  at the points of Gauss-Lobatto points as depicted in (38).

### 4 | RESULTS AND DISCUSSIONS

The dimensionless Equations (24)–(26) subject to (27) and (28) has been solved using SHAM. To explain the physics of the problem, we obtained results for all encountered parameters such as the Casson term ( $\beta$ ), magnetic term ( $M$ ), linear and nonlinear convection parameter, permeability parameter ( $Po$ ), heat generation parameter ( $He$ ) plotted in Figures 2 to 15.

Figure 2 illustrates the impact of Williamson term ( $\alpha$ ) on the velocity and temperature profile. A large value of  $\alpha$  is noticed in Figure 2 to increase both the velocity along with the temperature profile, respectively. The Williamson model is a type of non-Newtonian fluid with low viscosity. However, with low viscosity possessed by the Williamson fluid, there are no physical parameters is able to drag the fluid particles with the thermally-stratified medium.

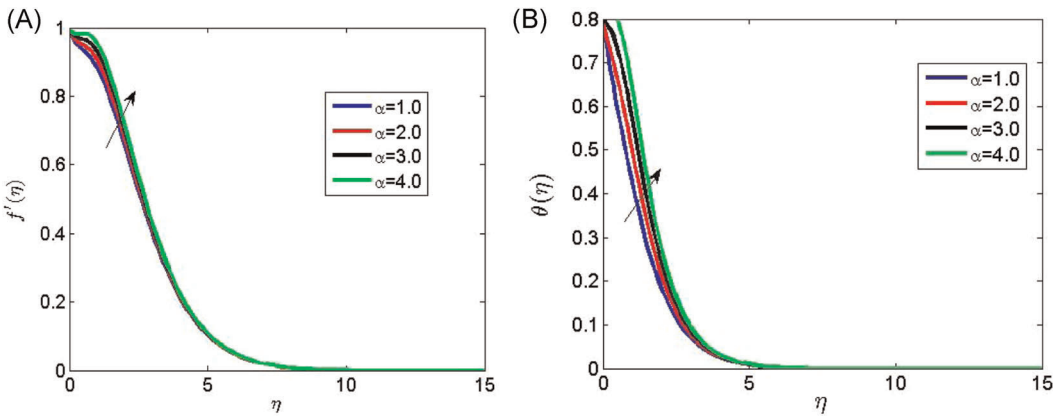


FIGURE 2 Effect of Williamson parameter on the (A) velocity as well as (B) temperature plot when  $A_r = A_c = R = \tau = 0.5, Gr = He = St = 0.2, Gc = 0.3, M = Sw = 1.0, Po = 0.6, \alpha = 2.0, Pr = 0.71, Do = So = \beta = 3.0, Ec = 0.1, Sc = 0.61, Cr = 0.3$  [Color figure can be viewed at [wileyonlinelibrary.com](http://wileyonlinelibrary.com)]

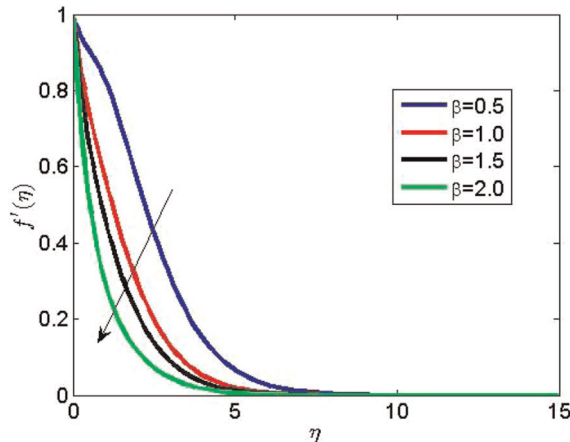


FIGURE 3 Effect of Casson term on the velocity plot when  $A_r = A_c = R = \tau = 0.5, Gr = He = St = 0.2, Gc = 0.3, M = Sw = 1.0, Po = 0.6, \alpha = 2.0, Pr = 0.71, Do = So = \beta = 3.0, Ec = 0.1, Sc = 0.61, Cr = 0.3$  [Color figure can be viewed at [wileyonlinelibrary.com](http://wileyonlinelibrary.com)]

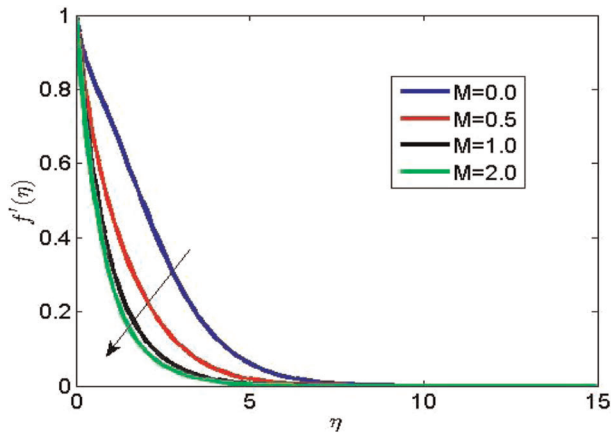


FIGURE 4 On the velocity plot, magnetic parameter is effected when  $A_T = A_c = R = \tau = 0.5$ ,  $Gr = He = St = 0.2$ ,  $Gc = 0.3$ ,  $M = Sw = 1.0$ ,  $Po = 0.6$ ,  $\alpha = 2.0$ ,  $Pr = 0.71$ ,  $Do = So = \beta = 3.0$ ,  $Ec = 0.1$ ,  $Sc = 0.61$ ,  $Cr = 0.3$  [Color figure can be viewed at [wileyonlinelibrary.com](http://wileyonlinelibrary.com)]

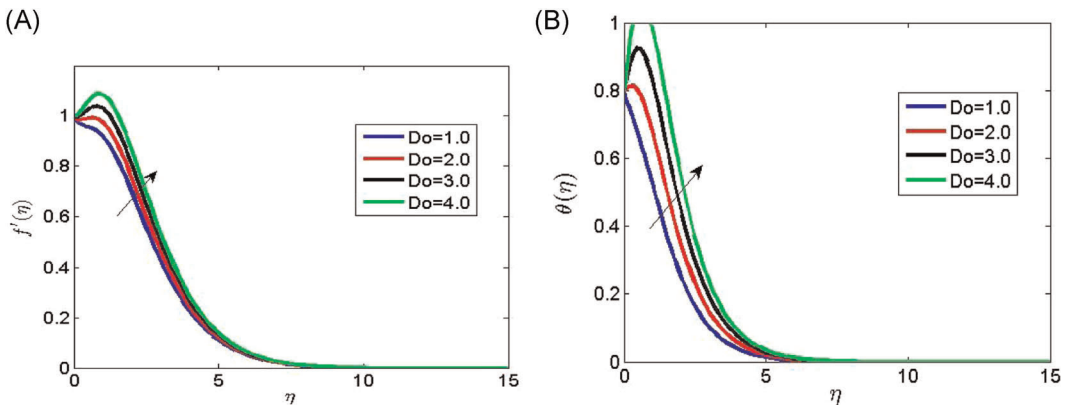


FIGURE 5 Dufour parameter's on the (A) velocity as well as (B) temperature plot when  $A_T = A_c = R = \tau = 0.5$ ,  $Gr = He = St = 0.2$ ,  $Gc = 0.3$ ,  $M = Sw = 1.0$ ,  $Po = 0.6$ ,  $\alpha = 2.0$ ,  $Pr = 0.71$ ,  $Do = So = \beta = 3.0$ ,  $Ec = 0.1$ ,  $Sc = 0.61$ ,  $Cr = 0.3$  [Color figure can be viewed at [wileyonlinelibrary.com](http://wileyonlinelibrary.com)]

Physically, the Williamson liquid possess viscosity, which is responsible for the resistance of fluid motion within the boundary layer. Our experiment shows that increase in the Williamson term enhances the hydrodynamic and thermal layer thickness.

Figure 3 depicts the effect of the Casson term ( $\beta$ ) on the velocity plot. The Casson is a yield exhibition non-Newtonian liquid that possesses a plastic dynamic viscosity. This plastic dynamic viscosity with the magnetic term in the flow degenerates the liquid velocity and the entire momentum layer by decreasing the velocity plot. On the velocity plot, the behavior of the imposed magnetic field is shown in Figure 4. On the mixed motion of Williamson and Casson liquids, the magnetism led to an opposing force called the Lorentz force. By reducing the velocity plot, this force dragged out the fluid motion of a conducting fluid electrically. Now, a large value of  $M$  increased the strength of Lorentz force and brings about drastic degeneration to velocity as well as the thickness of the layer as depicted in Figure 4. The plastic dynamic viscosity of the Casson liquid causes resistance to the velocity of the fluid and its entire



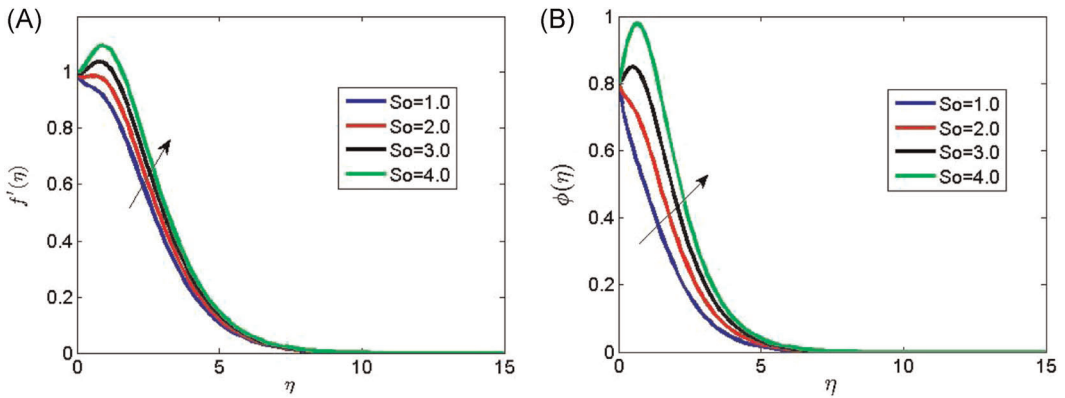


FIGURE 6 Impact of Soret parameter on the (A) velocity as well as (B) concentration profile when  $A_r = A_c = R = \tau = 0.5$ ,  $Gr = He = St = 0.2$ ,  $Gc = 0.3$ ,  $M = Sw = 1.0$ ,  $Po = 0.6$ ,  $\alpha = 2.0$ ,  $Pr = 0.71$ ,  $Do = So = \beta = 3.0$ ,  $Ec = 0.1$ ,  $Sc = 0.61$ ,  $Cr = 0.3$  [Color figure can be viewed at [wileyonlinelibrary.com](http://wileyonlinelibrary.com)]

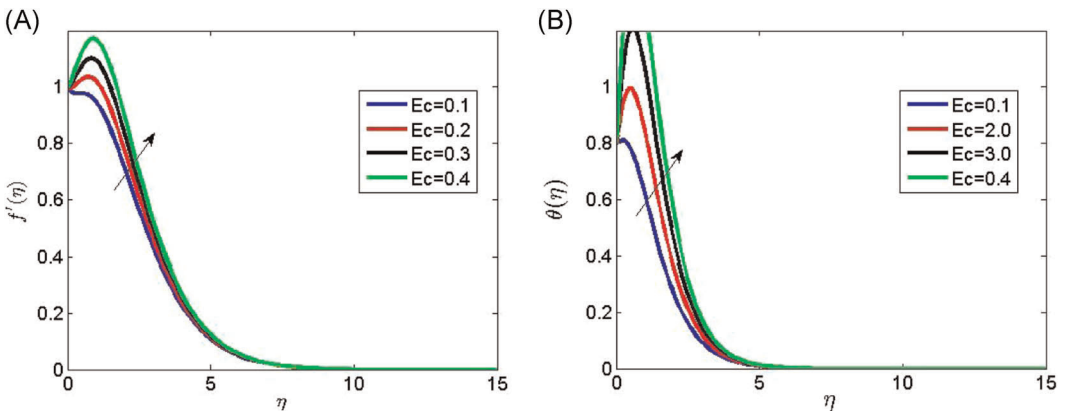


FIGURE 7 Eckert number's on the (A) velocity as well as (B) temperature plot when  $A_r = A_c = R = \tau = 0.5$ ,  $Gr = He = St = 0.2$ ,  $Gc = 0.3$ ,  $M = Sw = 1.0$ ,  $Po = 0.6$ ,  $\alpha = 2.0$ ,  $Pr = 0.71$ ,  $Do = So = \beta = 3.0$ ,  $Ec = 0.1$ ,  $Sc = 0.61$ ,  $Cr = 0.3$  [Color figure can be viewed at [wileyonlinelibrary.com](http://wileyonlinelibrary.com)]

hydrodynamic layer thickness. This degeneration experienced by the fluid was experienced within the thermally-stratified porous medium.

On the profiles of temperature and velocity, the impacts of Dufour parameter ( $Do$ ) are portrayed in Figure 5. The increment in the velocity alongside temperature plots is noticed simultaneously with the incremental values of  $Do$ . Physically, the fluid particles of Casson and Williamson transport uniformly within the thermally-stratified medium. Hence, our experiments shows that as the fluids flows together, a hike in the temperature along with a thick hydrodynamic and thermal layer is observed for large  $Do$ . Figure 6 shows the Soret number ( $So$ ) behavior on velocity as well as concentration plots. Increase in  $So$  is detected to elevate the velocity as well concentration plots. This means that thermal-diffusion of the fluid within the thermally stratified medium adds to the concentration of the liquid. In Figure 7, an incremental value of Eckert term ( $Ec$ ) is detected to hike the velocity along with temperature profile.  $Ec$  portrays the kinetic energy of the flow and its associated enthalpy. The viscous dissipation term

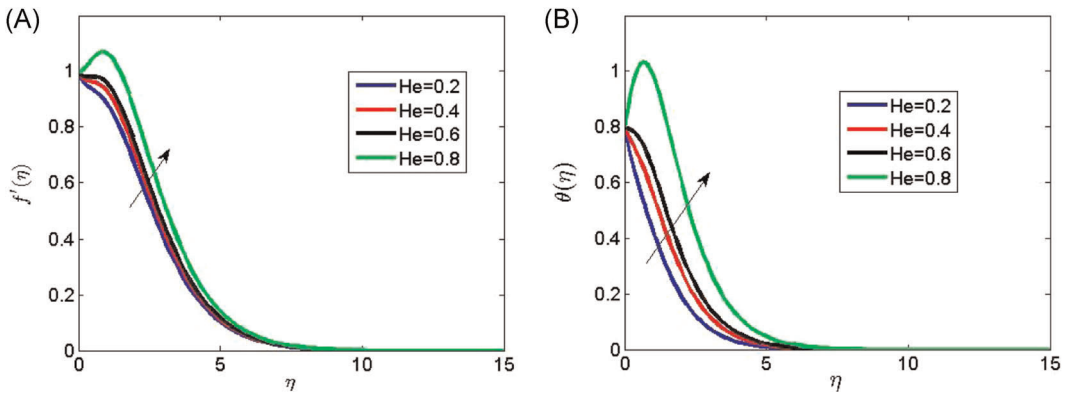


FIGURE 8 Impact of heat generation term on the (A) velocity as well as (B) temperature plot when  $A_T = A_c = R = \tau = 0.5$ ,  $Gr = He = St = 0.2$ ,  $Gc = 0.3$ ,  $M = Sw = 1.0$ ,  $Po = 0.6$ ,  $\alpha = 2.0$ ,  $Pr = 0.71$ ,  $Do = So = \beta = 3.0$ ,  $Ec = 0.1$ ,  $Sc = 0.61$ ,  $Cr = 0.3$  [Color figure can be viewed at [wileyonlinelibrary.com](http://wileyonlinelibrary.com)]

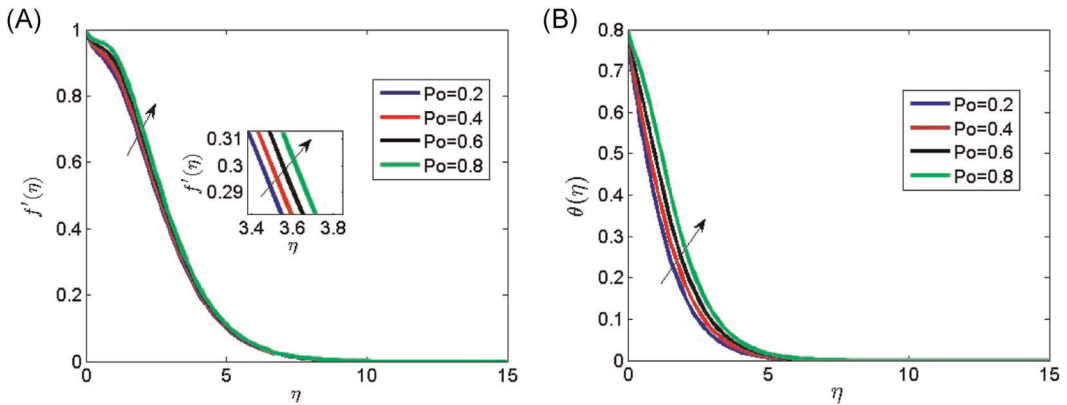
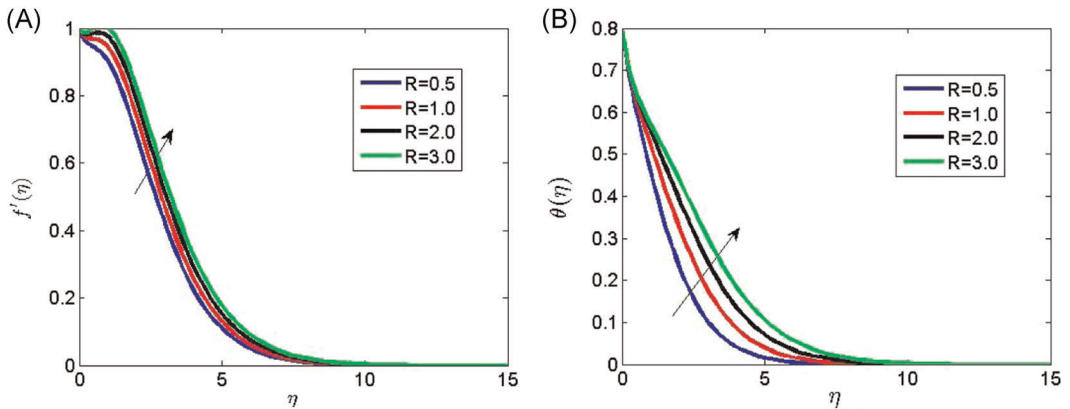


FIGURE 9 Permeability term effect on the (A) velocity as well as (B) temperature plot when  $A_T = A_c = R = \tau = 0.5$ ,  $Gr = He = St = 0.2$ ,  $Gc = 0.3$ ,  $M = Sw = 1.0$ ,  $Po = 0.6$ ,  $\alpha = 2.0$ ,  $Pr = 0.71$ ,  $Do = So = \beta = 3.0$ ,  $Ec = 0.1$ ,  $Sc = 0.61$ ,  $Cr = 0.3$  [Color figure can be viewed at [wileyonlinelibrary.com](http://wileyonlinelibrary.com)]

(Eckert number) added more heat energy to the fluid environment. Physically, the Eckert number and thermal radiation in a fluid flow increase the rate of heat transfer. Now, considering the Eckert number, thermal radiation with a thermally stratified medium assist to boost the heat transport rate by elevating the thickness of thermal boundary layer. Hence, a large value of  $Ec$  as shown in Figure 7 increases the plots of velocity as well as temperature. Physically, the viscous dissipation term is a function of momentum added to the energy equation. After the application of suitable similarity variables, the viscous dissipation term gives us the dimensionless Eckert number ( $Ec$ ).

The impacts of the parameter of heat generation ( $He$ ) on the velocity and temperature plots are depicted in Figure 8. It is detected that the elevation of the liquid's temperature and the velocity is more than that of the free stream by a large value of  $He$ . Hence, the thickness of the layer is increased with the increasing  $He$ . Our experiments indicate that a large value of  $He$  brings about a spontaneous increase in the thermal layer. Figure 9 shows the effects of the



**FIGURE 10** Radiation term effect on the (A) velocity as well as (B) temperature plot when  $A_T = A_c = R = \tau = 0.5$ ,  $Gr = He = St = 0.2$ ,  $Gc = 0.3$ ,  $M = Sw = 1.0$ ,  $Po = 0.6$ ,  $\alpha = 2.0$ ,  $Pr = 0.71$ ,  $Do = So = \beta = 3.0$ ,  $Ec = 0.1$ ,  $Sc = 0.61$ ,  $Cr = 0.3$  [Color figure can be viewed at [wileyonlinelibrary.com](http://wileyonlinelibrary.com)]

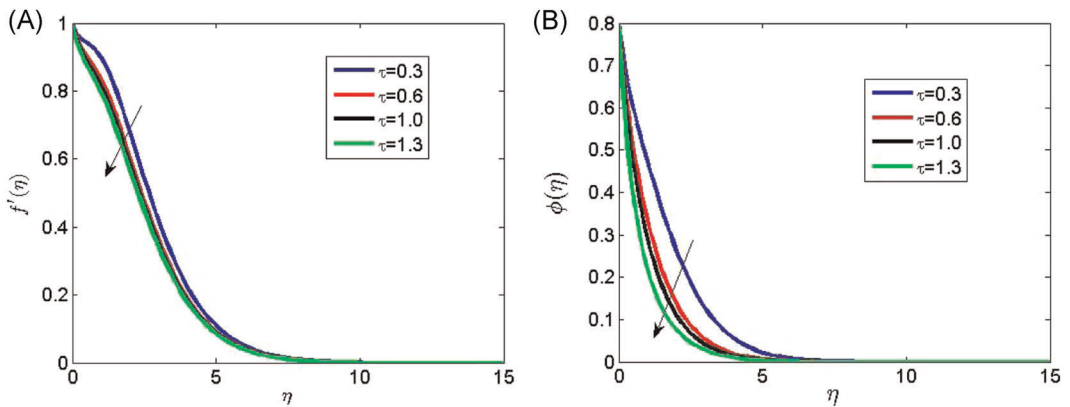


**FIGURE 11** Impact of thermophoretic parameter on the (A) velocity as well as (B) concentration profile when  $A_T = A_c = R = \tau = 0.5$ ,  $Gr = He = St = 0.2$ ,  $Gc = 0.3$ ,  $M = Sw = 1.0$ ,  $Po = 0.6$ ,  $\alpha = 2.0$ ,  $Pr = 0.71$ ,  $Do = So = \beta = 3.0$ ,  $Ec = 0.1$ ,  $Sc = 0.61$ ,  $Cr = 0.3$  [Color figure can be viewed at [wileyonlinelibrary.com](http://wileyonlinelibrary.com)]

permeability term ( $Po$ ) on velocity and temperature profiles. The porosity within the thermally stratified medium allows more transport of liquid particles. Physically, a large value of  $Po$  expands the hole and the fluid particles move faster within the boundary layer. Due to this fact, they gather more momentum and enhance their temperature profile. In Figure 10, the thermal radiation ( $R$ ) effects on profiles of temperature and velocity are depicted. Thermal radiation enhances convective flow with the increasing of the fluid environment's temperature. Hence,  $R$  is very important if the fluid particles' temperature is very high. A large value of  $R$  in Figure 10 is detected to elevate the velocity and temperature profile respectively. Physically, increasing  $R$  boosts the fluid environment's thermal condition. Hence, an increase in  $R$  shown in Figure 10 elevates the hydrodynamic and thermal layer thickness.

Figure 11 shows the effects of the thermophoresis term ( $\tau$ ) on velocity as well as concentration profile. Thermophoresis is migration of fluid particles from a cold region to a hot region. During fluid flow, a force called the thermophoretic force drags the fluid flow by

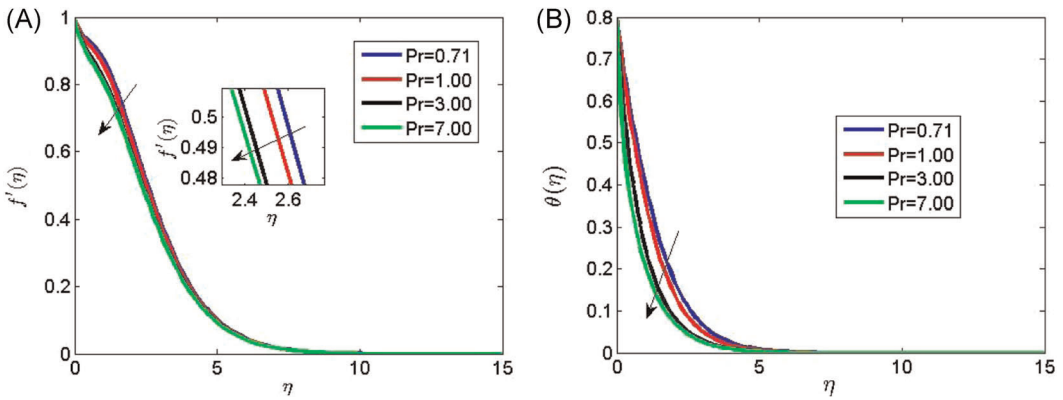


FIGURE 12 Impact of Prandtl number on the (A) velocity as well as (B) temperature profile when  $A_r = A_c = R = \tau = 0.5$ ,  $Gr = He = St = 0.2$ ,  $Gc = 0.3$ ,  $M = Sw = 1.0$ ,  $Po = 0.6$ ,  $\alpha = 2.0$ ,  $Pr = 0.71$ ,  $Do = So = \beta = 3.0$ ,  $Ec = 0.1$ ,  $Sc = 0.61$ ,  $Cr = 0.3$  [Color figure can be viewed at [wileyonlinelibrary.com](http://wileyonlinelibrary.com)]

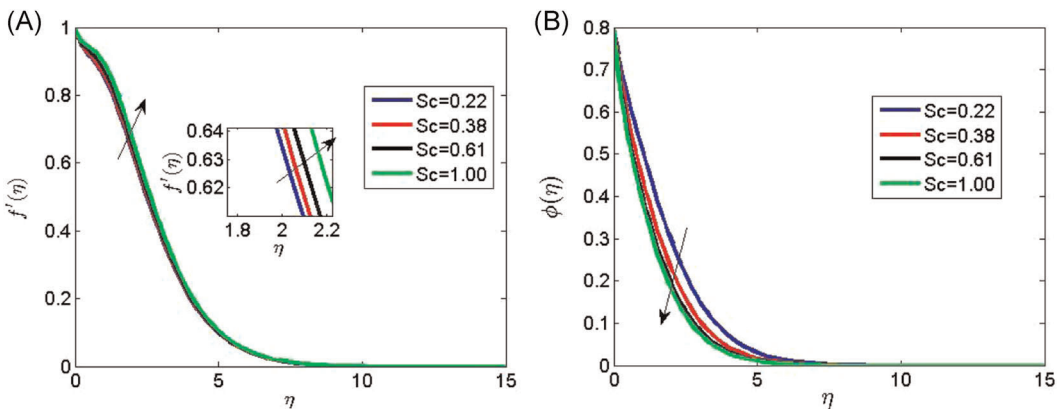


FIGURE 13 Effect of Schmidt number on the (A) velocity and (B) concentration profile when  $A_r = A_c = R = \tau = 0.5$ ,  $Gr = He = St = 0.2$ ,  $Gc = 0.3$ ,  $M = Sw = 1.0$ ,  $Po = 0.6$ ,  $\alpha = 2.0$ ,  $Pr = 0.71$ ,  $Do = So = \beta = 3.0$ ,  $Ec = 0.1$ ,  $Sc = 0.61$ ,  $Cr = 0.3$  [Color figure can be viewed at [wileyonlinelibrary.com](http://wileyonlinelibrary.com)]

decreasing the fluid velocity and concentration profile. Also, the particles of Casson and Williamson fluid considered in this study possess an MHD nature, that is, they are electrically conducting. The profiles of concentration and velocity are generated owing to the increment of thermophoresis by the MHD nature. Physically, the thermophoresis parameter is a function of temperature and concentration, and it is responsible for the diffusion of fluid particles from a region of high temperature to a lower region.

Figure 12 represents the Prandtl number ( $Pr$ ) effect on velocity as well as temperature profiles. The profile of temperature and velocity is reduced by a large value of  $Pr$ . The momentum diffusivity divided by thermal diffusivity is portrayed by  $Pr$ . Practically, any fluid with small  $Pr$  or possess much thermal conductivity with a thick thermal layer. Hence, the transport of liquid particles from the layer is very fast for large  $Pr$ . Figure 13 describes the Schmidt number ( $Sc$ ) effect on velocity and concentration plots. The velocity plot is increased with an

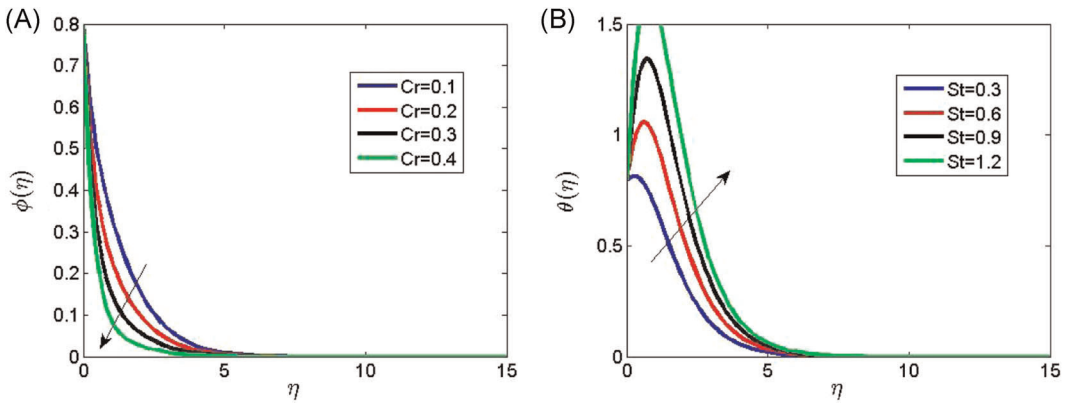


FIGURE 14 Influence of (A) chemical reaction term on the concentration plot and (B) thermal stratification parameter on temperature profile when  $A_T = A_c = R = \tau = 0.5$ ,  $Gr = He = St = 0.2$ ,  $Gc = 0.3$ ,  $M = Sw = 1.0$ ,  $Po = 0.6$ ,  $\alpha = 2.0$ ,  $Pr = 0.71$ ,  $Do = So = \beta = 3.0$ ,  $Ec = 0.1$ ,  $Sc = 0.61$ ,  $Cr = 0.3$  [Color figure can be viewed at [wileyonlinelibrary.com](http://wileyonlinelibrary.com)]

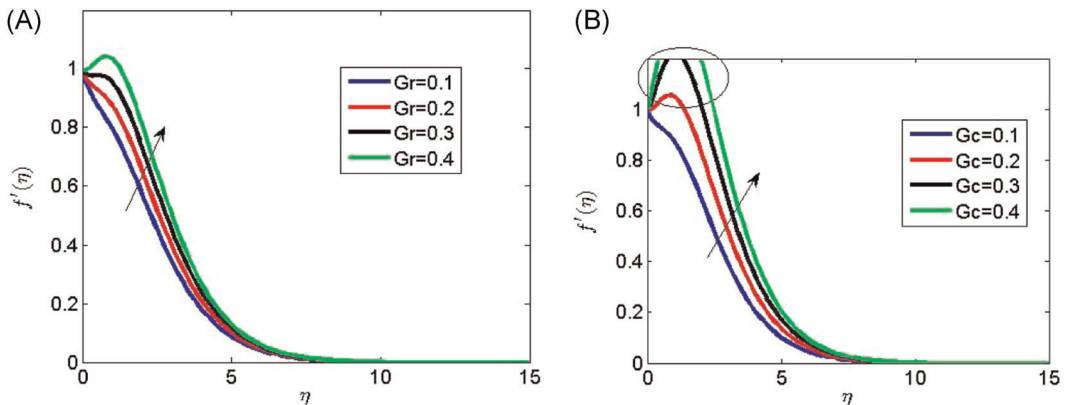


FIGURE 15 Impact of (A) thermal Grashof number on the velocity plot and (B) mass Grashof number on the velocity plot when  $A_T = A_c = R = \tau = 0.5$ ,  $Gr = He = St = 0.2$ ,  $Gc = 0.3$ ,  $M = Sw = 1.0$ ,  $Po = 0.6$ ,  $\alpha = 2.0$ ,  $Pr = 0.71$ ,  $Do = So = \beta = 3.0$ ,  $Ec = 0.1$ ,  $Sc = 0.61$ ,  $Cr = 0.3$  [Color figure can be viewed at [wileyonlinelibrary.com](http://wileyonlinelibrary.com)]

increasing value of  $Sc$  but the concentration profile is reduced. Physically,  $Sc$  portrays the quotient of momentum diffusivity to mass diffusivity. It worth noting that a large value of  $Sc$  results in an increase in mass diffusivity. Hence, the thickness of the concentration layer degenerates. Figure 14 depicts the chemical reaction term ( $Cr$ ) effect on concentration plot and the thermal stratification ( $St$ ) on temperature. An increase in  $Cr$  is noticed to reduce the concentration profile. This shows a destructive chemical reaction. Hence, the effects of this type of chemical reaction produces a degeneration in the concentration profile. It is obvious in Figure 14 that increases in  $St$  lead to enhancement in rate of heat transport. With a higher  $St$ , the surface of the layer gets more heated than the free stream. Figure 15 illustrates the effect of thermal ( $Gr$ ) and mass ( $Gc$ ) Grashof number on the velocity plot. An incremental value of  $Gr$  and  $Gc$  is detected in Figure 15 to elevate the velocity profile. This is evident because of the force of buoyancy in the flow.

Table 1 shows the numerical computations for local skin friction coefficient ( $C_f$ ), local Nusselt number ( $Nu$ ), and local Sherwood number ( $Sh$ ) for the flow parameters, nonlinear convection parameter for temperature ( $A_T$ ), and nonlinear convection parameter for concentration ( $Ac$ ),  $\beta$ ,  $Gr$ ,  $Gc$ ,  $M$ ,  $Po$ , and  $\alpha$ . From Table 1, a large  $A_T$  is noticed to hike  $C_f$  and  $Nu$  respectively. This implies that a large value of  $A_T$  enhances the hydrodynamic and thermal layer thickness, Hence, a large  $A_T$  enhances the rate of heat of heat transport in this study. Also, an increase in  $Ac$  is observed to increase  $C_f$  and  $Sh$ , respectively. This shows that increases in  $Ac$  enhances the rate of mass transport in this study. From Table 1, an increase in  $\beta$  is noticed

TABLE 1 Numerical computations for  $C_f$ ,  $Nu$ , and  $Sh$  for different values of flow parameters  $A_T$ ,  $Ac$ ,  $\beta$ ,  $Gr$ ,  $Gc$ ,  $M$ ,  $Po$ , and  $\alpha$

$A_T$	$Ac$	$\beta$	$Gr$	$Gc$	$M$	$Po$	$\alpha$	$C_f$	$Nh$	$Sh$
0.1								0.997529	0.063182	0.625763
0.2								1.019148	0.163385	0.625763
0.3								1.040766	1.062385	0.625763
	0.2							0.999670	0.588247	0.605663
	0.4							1.019148	0.588247	0.625763
	0.4							1.038626	0.588247	1.058104
		0.5						1.063925	0.590317	0.625763
		1.0						1.355618	0.591869	0.625763
		1.5						1.686619	0.582387	0.625763
			0.1					0.887121	0.077130	0.615660
			0.2					0.897330	0.077130	0.615660
			0.3					0.997521	0.077130	0.615660
				0.1				0.999912	1.022385	0.615660
				0.2				1.029224	1.022385	0.615660
				0.3				1.045661	1.022385	0.615660
					0.1			1.114850	0.588247	0.625763
					0.5			1.070989	0.588247	0.625763
					1.0			1.034028	0.588247	0.625763
						0.2		1.019148	0.477351	0.977524
						0.4		0.992600	0.477351	0.977524
						0.6		0.982698	0.477351	0.977524
							1.0	1.037554	1.062885	1.531118
							2.0	1.052165	1.062885	1.531118
							3.0	1.058890	1.062885	1.531118

to increase  $C_f$  and  $Nu$ . The effect of  $Gr$  and  $Gc$  is noticeable on skin friction. This means that a large  $Gr$  boosts the thickness of the hydrodynamic layer. The degeneration of skin friction is observed by increasing  $M$  from the table. This is true because the magnetic parameter leads to the Lorentz force, which drags the flow of an electrically conducting liquid's flow. An increase in  $Po$  in Table 1 is noticed to increase the local skin friction and is negligible on  $Nu$  and  $Sh$ . Also, an increase in  $\alpha$  increases  $C_f$  and has no effect on  $Nu$  and  $Sh$ , respectively. In Table 2, an increment in  $R$  is seen to degenerate  $C_f$  but increases  $Nu$ . This shows that the largeness in

TABLE 2 Numerical computations for  $C_f$ ,  $Nu$ , and  $Sh$  for flow parameters  $R, Pr, Do, Ec, He, Sc, Cr, So$ , and  $\tau$

$R$	$Pr$	$Do$	$Ec$	$He$	$Sc$	$Cr$	$So$	$\tau$	$C_f$	$Nh$	$Sh$
0.5									0.985071	0.465525	0.625763
1.0									0.968914	0.492748	0.625763
2.0									0.959660	0.523025	0.625763
	0.71								1.019148	0.588247	0.625763
	1.00								1.024477	0.670345	0.625763
	3.00								1.038152	1.152344	0.625763
		1.0							1.004423	1.180334	0.811584
		2.0							0.986017	0.293545	0.811584
		3.0							0.967611	0.074830	0.811584
			0.1						1.016721	0.443207	0.325862
			0.2						1.014024	0.527696	0.325862
			0.3						1.011328	0.460418	0.325862
				0.2					1.009534	0.393140	0.250406
				0.4					1.016199	0.405005	0.250406
				0.6					1.021876	0.532687	0.250406
					0.22				1.025529	0.639059	0.725244
					0.38				1.022911	0.588247	0.684431
					0.61				1.019148	0.588247	0.625863
						0.1			1.010650	0.588247	0.506558
						0.2			1.012942	0.588247	0.538986
						0.3			1.015117	0.588247	0.569580
							1.0		1.009167	0.463419	0.470165
							2.0		0.989205	0.463419	0.158970
							3.0		0.969244	0.463419	0.152224
								0.3	1.016518	0.522645	0.625763
								0.6	1.007754	0.303973	0.615661
								1.0	0.998990	0.085308	0.600710

$R$  boosts the heat transport rate and the thermal layer thickness. Also, an increment in the value of  $Pr$  is detected in Table 2 to hike  $C_f$  and increase the local Nusselt number ( $Nu$ ). The effect of  $Do$  is noticeable on  $Nu$ , while that of  $So$  is noticeable on  $Sh$ . In Table 2, an increase in the value of  $Ec$  and  $He$  is seen to enhance the local Nusselt number. This implies that increases in  $Ec$  and  $He$  accelerate the rate of heat transport. A large value of  $Sc$  and  $Cr$  boosted the concentration layer thickness.

## 5 | CONCLUSION

An exploration of the effect of heat alongside mass transport in nonlinear convection MHD movement of non-Newtonian liquids located in a thermally stratified channel with pores, radiation, and heat generation alongside chemical reaction was performed. A suitable function was used to transform the governing partial differential equations into total differential equations. SHAM was used to determine the numerical solution for these set of equations. The graphical presentation of numerical results was done along with the profiles of flow fields and rate of heat as well as mass transport rate. It was discovered that a large magnetic tem degenerates the velocity along with the local skin friction coefficient, respectively. Increases in the heat generation parameter resulted in an increase in the heat transport rate. It was detected that the increasing of the temperature profile is caused by an increment in radiation parameter, while the increment in the heat transport rate and skin friction caused an increment in the Prandtl number. Also, it was discovered that a large value of Schmidt number caused degeneration to the skin-friction coefficient.

The results in this study can be found useful in food processing, drilling operations, and bioengineering. The practical applications are basically in oil-pipeline friction reduction, and surfactant applications to large-scale heating and cooling systems. It is also applicable in the use of high-polymer additives to enhance flow in petroleum pipe-lines which is very useful for commercial purposes. The Soret and Dufour effects on the fluid flow are significant. Hence, these find application in field of engineering such as isotope separation. The present analysis can play a predominant role by application to science and technology.

## ORCID

Gladys Tharapatla  <https://orcid.org/0000-0003-4532-9654>

## REFERENCES

1. Idowu AS, Falodun BO. Variable thermal conductivity and viscosity effects on non-Newtonian fluids flow through a vertical porous plate under Soret-Dufour influence. *Math Comput Simul.* 2020;177:358-384.
2. Fagbade AI, Falodun BO, Omowaye AJ. MHD natural convection flow of viscoelastic fluid over an accelerating permeable surface with thermal radiation and heat source or sink: Spectral homotopy analysis approach. *Ain Shams Eng J.* 2018;9:1029-1041.
3. Ur RK, Ashfaq Malik A, Malik MY, Sandeep N, Saba NUI. Numerical study of double stratification in Casson fluid flow in the presence of mixed convection and chemical reaction. *Results Phys.* 2017;7: 2997-3006.
4. Tamoor M, Waqas M, Ijaz Khan M, Alsaedi A, Hayat T. Magneto hydrodynamic flow of Casson fluid over a stretching cylinder. *Results Phys.* 2017;7:498-502.
5. Ur RK, Malik MY, Zahri M, Tahir M. Numerical analysis of MHD Casson Navier's slip nanofluid flow yield by rigid rotating disk. *Results Phys.* 2018;8:744-751.



6. Shanker SG, Kumar R, Tripathi R, Bhattacharyya A. Double diffusive MHD Casson fluid flow in a non-Darcy porous medium with Newtonian heating and thermo-diffusion effects. *Int J Heat Technol.* 2018; 36(4):1517-1527.
7. Hayat T, Shafiq A, Alsaedi A. Hydromagnetic boundary layer flow of Williamson fluid in the presence of thermal radiation and Ohmic dissipation. *Alex Eng J.* 2016;55:2229-2240.
8. Kebede T, Haile E, Awgichew G, Walelign T. Heat and mass transfer in unsteady boundary layer flow of williamson nanofluids. *J Appl Math.* 2020;2020:1-13. <https://doi.org/10.1155/2020/1890972>
9. Lund LA, Omar Z, Analysis IK. of dual solution for MHD flow of Williamson fluid with slippage. *Heliyon.* 2019;5:e01345. <https://doi.org/10.1016/j.heliyon.2019.e01345>
10. Megahed Ahmed M. Williamson fluid flow due to a nonlinearly stretching sheet with viscous dissipation and thermal radiation. *J Egyptian Math Soc.* 2019;27:1-12. <https://doi.org/10.1186/s42787-019-0016-y>
11. Idowu AS, Falodun BO. Effects of thermophoresis, Soret-Dufour on heat and mass transfer flow of magnetohydrodynamics non-Newtonian nanofluid over an inclined plate. *Arab J Basic Appl Sci.* 2020;27(1): 149-165. <https://doi.org/10.1080/25765299.2020.1746017>
12. Swati M. MHD boundary layer flow and heat transfer over an exponentially stretching sheet embedded in a thermally stratified medium. *Alex Eng J.* 2013;52:259-265.
13. Raju CSK, Sandeep N, Sugunamma V, Jayachandra Babu M, Ramana Reddy JV. Heat and mass transfer in magnetohydrodynamic Casson fluid over an exponentially permeable stretching surface. *Eng Sci Technol Int J.* 2016;19:45-52.
14. Abdul W, Zeb H, Bhatti S, Gulistan M, Kadry S, Nam Y. Numerical study for the effects of temperature dependent viscosity flow of non-Newtonian fluid with double stratification. *Appl Sci.* 2020;10:708. <https://doi.org/10.3390/app10020708>
15. Farhad A, Khan I, Samiulhaq, et al. Conjugate effects of heat and mass transfer on MHD free convection flow over an inclined plate embedded in a porous medium. *PLOS One.* 2013;8(6):1-11.
16. Kolade K, Oreyeni T, Omowaye A, Animasaun IL. Homotopy analysis of MHD free convective micropolar fluid flow along a vertical surface embedded in non-Darcian thermally-stratified medium. *Open J Fluid Dynam.* 2016;6:198-221. <http://www.scirp.org/journal/ojfd>
17. Ijaz M, Ayub M. Thermally stratified flow of Jeffrey fluid with homogeneous-heterogeneous reactions and non-Fourier heat flux model. *Heliyon.* 2019;5:e02303.
18. Hayat T, Muhammad T, Shehzad SA, Alsaedi A. Temperature and concentration stratification effects in mixed convection flow of an oldroyd-b fluid with thermal radiation and chemical reaction. *PLOS One.* 2015; 10(6):e0127646. <https://doi.org/10.1371/journal.pone.0127646>
19. Nduku MW, Daniel MO. Double stratification effects on heat and mass transfer in unsteady MHD nanofluid flow over a flat surface. *Asia Pacific J Computat Eng.* 2017;4:2. <https://doi.org/10.1186/s40540-017-0021-2>
20. Falodun BO, Omowaye AJ. Double-diffusive MHD convective flow of heat and mass transfer over a stretching sheet embedded in a thermally-stratified porous medium. *World J Eng.* 2019;16/6:712-724. <https://doi.org/10.1108/WJE-09-2018-0306>
21. Tasawar H, Shaheen U, Shafiq A, Alsaedi A, Asghar S. Marangoni mixed convection flow with Joule heating and nonlinear radiation. *AIP Adv.* 2015;5:077140.
22. Ramana Reddy JV, Anantha Kumar K, Sugunamma V, Sandeep N. Effect of cross diffusion on MHD non-Newtonian fluids flow past a stretching sheet with non-uniform heat source/sink: a comparative study. *Alex Eng J.* 2018;57:1829-1838.
23. Himanshu U, Pandey AK, Kumar M. MHD flow of Ag-water nanofluid over a flat porous plate with viscous-Ohmic dissipation, suction/injection and heat generation/absorption. *Alex Eng J.* 2018;57: 1839-1847.
24. Hayat T, Bashir G, Waqas M, Alsaedi A. MHD flow of Jeffrey liquid due to a nonlinear radially stretched sheet in presence of Newtonian heating. *Results Phys.* 2016;6:817-823.
25. Mehdi RM, Ali M, Rostami B, Rostami P, Xie G-N. Heat and mass transfer for MHD viscoelastic fluid flow over a vertical stretching sheet with considering soret and Dufour effects. *Math Prob Eng.* 2015;2015:1-12.
26. Idowu AS, Falodun BO. Influence of magnetic field and thermal radiation on steady free convective flow in a porous medium. *Nigerian J Technol Dev.* 2019;15(3):84-97.

27. Moorthy MBK, Senthilvadivu K. Soret and Dufour effects on natural convection flow past a vertical surface in a porous medium with variable viscosity. *J Appl Math.* 2012;2012:1-15. <https://doi.org/10.1155/2012/634806>
28. Kumari PR, Sree Devi D. Effect of radiation and radiation absorption on convective heat and mass transfer flow of a viscous electrically conducting fluid in a non-uniformly heated vertical channel. *Int J Mech Prod Eng Res Dev.* 2018;8(7):2249-6890.
29. Alao FI, Fagbade AI, Falodun BO. Effects of thermal radiation, Soret and Dufour on an unsteady heat and mass transfer flow of a chemically reacting fluid past a semi-infinite vertical plate with viscous dissipation. *J Nigerian Math Soc.* 2016;35:142-158.
30. Jhansi Rani K, Ramana Reddy GV, Ramana Murthy CV, Ramana, Murthy MV. Heat and mass transfer effects on MHD free convection flow over an inclined plate embedded in a porous medium. *Int J Chem Sci.* 2015;13(4):1998-2016.
31. Kumari P. A mathematical analysis of convective heat and mass transfer pour of a non-Newtonian fluid through porous medium in a rectangular duct with heat sources. *J Adv Res Dynam Control Syst.* 2017;2017: 84-91.
32. Ayegbusi FD, Onwubuoya C, Falodun BO. Unsteady problem of magnetohydrodynamic heat plus mass transfer convective flow over a moveable plate with effects of thermophoresis and thermal radiation. *Heat Transfer.* 2020;49:1-20. <https://doi.org/10.1002/htj.21790>
33. Ahmed LO, Falodun BO, Abdulwaheed J. Mechanism of Soret-Dufour, magnetohydrodynamics, heat and mass transfer flow with buoyancy force, and viscous dissipation effects. *Heat Transfer.* 2020;49:2831-2848. <https://doi.org/10.1002/htj.21748>
34. Gnaneswara Reddy M, Ferdows M. Species and thermal radiation on micropolar hydromagnetic dusty fluid flow across a paraboloid revolution. *J Therm Anal Calorim.* 2020. <https://doi.org/10.1007/s10973-020-09254-1>
35. Reddy MG, Vijayakumari P, Kumar KG, Shehzad SA. Zero-mass flux and Cattaneo-Christov heat flux through a Prandtl non-Newtonian nanofluid in Darcy-Forchheimer porous space. 2020. <https://doi.org/10.1002/htj.21872>
36. Gnaneswara RM, Subba GR. Temperature-dependent viscosity and second order slip flow on MHD Casson radiative nanofluid over stretching sheet. *J Nanofluids.* 2017;6(5):830-839. <https://doi.org/10.1166/jon.2017.1387>
37. Sandeep N, Gnaneswara Reddy M. MHD Oldroyd-B fluid flow across a melting surface with cross diffusion and double stratification. *Eur Phys J Plus.* 2017;132:147. <https://doi.org/10.1140/epjp/i2017-11417-9>
38. Gnaneswara MR, Naramgar S. Heat and mass transfer in radiative MHD Carreau fluid with cross diffusion. *Ain Shams Eng J.* 2018;9:1189-1204.
39. Sibanda P, Motsa SS, Makukula ZG. A spectral-homotopy analysis method for heat transfer flow of a third grade fluid between parallel plates. *Int J Numer Methods Heat Fluid Flow.* 2012;22:4-23.
40. Trefethen LN. *Spectral methods in MATLAB.* Philadelphia, PA: Society for Industrial and Applied Mathematics; 2000.

**How to cite this article:** Tharapatla G, RajKumari P, Ramana Reddy G. Effects of heat and mass transfer on MHD nonlinear free convection non-Newtonian fluids flow embedded in a thermally stratified porous medium. *Heat Transfer.* 2021;50:3480-3500. <https://doi.org/10.1002/htj.22037>



# Smartphone enabled miniaturized temperature controller platform to synthesize NiO/CuO nanoparticles for electrochemical sensing and nanomicelles for ocular drug delivery applications

Madhusudan B Kulkarni<sup>1</sup> · K Velmurugan<sup>2</sup> · Enaganti Prasanth<sup>1</sup> · Khairunnisa Amreen<sup>1</sup> · Jayabalan Nirmal<sup>2</sup> · Sanket Goel<sup>1</sup>

Accepted: 31 May 2021

© The Author(s), under exclusive licence to Springer Science+Business Media, LLC, part of Springer Nature 2021

## Abstract

Undoubtedly, various kinds of nanomaterials are of great significance due to their enormous applications in diverse areas. The structure and productivity of nanomaterials are heavily dependent on the process used for their synthesis. The synthesizing process plays a vital role in shaping nanomaterials effectively for better productivity. The conventional method requires expensive and massive thermal instruments, a huge volume of reagents. This paper aims to develop an Automatic Miniaturized Temperature Controller (AMTC) device for the synthesis of nickel oxide (NiO), copper oxide (CuO) nanoparticles, and nanomicelles. The device features a low-cost, miniaturized, easy-to-operate with plug-and-play power source, precise temperature control, and geotagged real-time data logging facility for the producing nanoparticles. With a temperature accuracy of  $\pm 2$  °C, NiO and CuO nanoparticles, and nanomicelles are synthesized on AMTC device, and are subjected to different characterizations to analyze their morphological structure. The obtained mean size of NiO and CuO is 27.14 nm and 85.13 nm respectively. As a proof-of-principle, the synthesized NiO and CuO nanomaterials are validated for electrochemical sensing of dopamine, hydrazine, and uric acid. Furthermore, the study is conducted, wherein, Dexamethasone (Dex) loaded nanomicelles are developed using AMTC device and compared to the conventional thin-film hydration method. Subsequently, as a proof-of-application, the developed nanomicelles are evaluated for transcorneal penetration using ex vivo goat cornea model. Ultimately, the proposed device can be utilized for performing a variety of controlled thermal reactions on a minuscule platform with an integrated and miniaturized approach for various applications.

**Keywords** Electrochemical sensing · Automatic temperature controller (AMTC) · Nanoparticles (NPs) · Nickel oxide (NiO) · Copper oxide (CuO) · Dex loaded nanomicelles · Trans corneal diffusion · Ocular drug delivery

## 1 Introduction

Recently, nano-sized materials such as nanotubes, nanowires, nanoparticles, and nanomicelles manifest novel properties that are considerably distinct from those of discrete

molecules and atoms, or bulk materials (Jamkhande et al. 2019; Ndolomingo et al. 2020). Due to these reasons, many researchers are working persistently to develop several competent techniques to produce superior quality nanoparticles leading to numerous applications in various fields like biomedical, industrial, environmental, and food agriculture (Ealias and Saravanakumar 2017; Mohan et al. 2020). The curiosity in the synthesis of nanomaterials has grown drastically due to their precise chemical, structural, and physical properties (Kulkarni and Goel 2020a), leading to the production of nanomaterials with definite size and structure (Powar and Patel 2019) and dimension (Silva et al. 2019). Such nanomaterials can be used extensively in various research areas such as imaging, catalysis, data storage, sensing, drug delivery, and bacterial analysis (Wang et al. 2017; Puneeth et al. 2021). The conventional method for the synthesis of

✉ Sanket Goel  
sgoel@hyderabad.bits-pilani.ac.in

<sup>1</sup> MEMS, Microfluidics and NanoElectronics (MMNE) Lab, Department of Electrical and Electronics Engineering, Birla Institute of Technology and Science (BITS) Pilani, Hyderabad Campus, Hyderabad 500078, Telangana, India

<sup>2</sup> Translational Pharmaceutics Research Laboratory (TPRL), Department of Pharmacy, Birla Institute of Technology and Science (BITS) Pilani, Hyderabad Campus, Hyderabad 500078, Hyderabad, Telangana, India

nanomaterials suffers from the slow response and the need for autoclaves and heavy thermal instruments. Moreover, such methods hamper from being expensive, arduous, and time-consuming, which leads to rendering the process unprofitable for smaller quantities (Yang and Park 2019).

Nickel oxide (NiO) nanomaterials showcase a significant evolution of metal oxide with a spherical lattice structure (Ni et al. 2012). It has increased the attention due to their potential use in a diversity of applications like batteries (Feng et al. 2014), supercapacitors (Li et al. 2018), catalysis (U.S. J., Goel, S. 2020), fuel cell (Dector et al. 2021), and gas sensors (Thota and Kumar 2007). It exhibits excellent durability and electrochemical stability (Saravanan et al. 2013). With a broad-band gap of 3.6–4 eV, a NiO semiconductor has become an important candidate for various applications like solar cells (Meneses et al. 2007). The NiO nanomaterials are typically produced by the co-precipitation technique using divergent precursors (Ekeroth et al. 2019; Chopra et al. 2010). Similarly, copper oxide (CuO) nanomaterials have increased considerable attention due to their excellent magnetic, electrical, physical, optical properties, and have an extensive range of applications in biological, biomedical, and industrial fields (Phiwdang et al. 2013; Pandey et al. 2012). Evidently, these properties can be further enhanced by selecting an appropriate synthesizing method, as it can regulate the size, shape, and morphology of the nanomaterials. Various nanostructures of CuO have been produced in the form of the nanorod, nanowire, nanoneedle, nanomicelles, nanoflakes, nano-flower, and nanospheres, and nanobullets (Maqbool et al. 2017). Numerous approaches have been projected to synthesize CuO nanoparticles with distinct methods like sonochemical (Kesavan and Chen 2020), quick precipitation (Batool and Valiyaveettil 2020), and thermal oxidation (Kulkarni et al. 2020). The hydrothermal method is common and mostly used for synthesizing nanoparticles as a traditional approach. Mainly the traditional nanomaterial synthesis suffers due to uncontrolled time for mixing with a delayed response (Dobrucka et al. 2021). Besides, traditional processing needs the groundwork of particles in mass production leading to the huge prerequisite of valuable and expensive materials and distinct types of equipment (Li et al. 2020). Hence, there is a need to automate and integrate a method to synthesize the nanoparticles with low thermal power and energy, inexpensive and fast response time for small-scale production, and good yield (Qu et al. 2020; Shi and Chopra 2011).

Micelles, with an exceptional drug-entrapment capacity, have a smaller size and easy formulation. Nanomicelles are commonly utilized for the formulation of pure aqueous solutions to load poorly water-soluble drugs, which are created using amphiphilic molecules (Vadlapudi and Mitra 2013). Moreover, nanomicellar formulations can also improve drug availability in ocular tissues, representing better therapeutic

outcomes (Patel et al. 2015). Several researchers are focusing on the development of nanomicellar formulations for ocular use and studies have been carried out to examine the potentials of the ocular nanomicelle application to treat various ocular diseases (Vadlapudi et al. 2014; Patel 2013). Nanomicelles are proven to be a good method for the ocular delivery of especially hydrophobic drugs (Omerovi and Vrani 2020). They offer numerous advantages, like corneal penetration, ocular biocompatibility, ease of sterilization. Further, the nanomicelles improve the bioavailability of the hydrophobic drugs due to the nano-size of drug particles, precorneal retention time, stability, and utilization of various polymers and surfactants (Alami-Milani et al. 2019).

Ocular structures possess various barriers to prevent xenobiotics including therapeutic drugs to reach various tissues of the eye, thus reduce the ocular bioavailability of various drugs (Gote et al. 2019). The barriers comprise of both static (corneal epithelium, corneal stroma, corneal endothelium) and dynamic barriers (tear dilution, conjunctival, blood-aqueous barrier, and retinal-blood barriers) (Chrai et al. 1974). These barriers provide challenges for the topically administered drugs to achieve optimum therapeutic concentrations at the targeted therapeutic site in the anterior and posterior segment (Nirmal et al. 2013a, 2013b).

To synthesize various nanomaterials, such as NiO and ZnO nanomaterials, and nanomicelles, a miniaturized arduino pro-mini microcontroller-based temperature controller platform, with precise temperature controlling capability, can lead to distinguished and notable results, and find application in numerous areas. These include diagnostics of various diseases, screening of drugs, electrochemical, drug delivery, tissue engineering, biomedical imaging, bacterial process, and droplet-based approach for biosensing (Chaipan et al. 2017; Kulkarni and Goel 2020b). A smaller volume of the sample permits a precise solution transferal on the microchannel reservoir and this technology has newly grown as an important milestone to synthesize nanoparticles (Islam et al. 2018). The role of reaction temperature has influenced greatly on particle size and shape, with lower temperatures resulting in more and thinner particles with a greater surface area than those produced at higher temperatures (Jiang et al. 2011). High temperatures can induce the formation of different crystalline phases with different characteristics. The size of the particle is also greatly dependent on various factors such as pH, reagents, the process of operation, reaction temperature and time, and further, the inclusion of purification steps like sonication and centrifugation all these play a role in determining the physical characteristics and stability of nanoparticle formation (Liu et al. 2020; Sigwadi et al. 2017).

These days, a temperature controller platform has become very indispensable and plays a crucial role in many fields of study. Its emergent applications can be seen in many household appliances for cooling and heating applications,

biomedical, biochemical, industrial automation, process control stations, food industries, and pharmaceuticals (Kamaly et al. 2012). PID (proportional integral derivative) based temperature controller is widely used due to its accuracy and constancy, whereby PID can be implemented using the open-source library function available in off-the-shelf microcontroller like Arduino IDE (Hamid et al. 2009). It is extremely effective and efficient in upholding the required temperature despite swift changes in ambient thermal conditions, offering more exactness and reliability than classical on/off controllers (Asraf et al. 2017). Therefore, a cost-effective, low-powered, portable Automatic Miniaturized Temperature Controller (AMTC) is realized using fewer electronic modules such as a microcontroller, customized switching circuitry with BJT and MOSFET, and Bluetooth/IoT for real-time data analysis for regulating, manipulating, and monitoring the temperature data. Conventional temperature controller devices such as hot air oven, boiler, and muffle furnace are widely used for traditional nanoparticle synthesis. These benchtop devices are bulky, require human intervention, dissipates more thermal loss, and are quite expensive (Park et al. 2020). Table. 1 summarize the difference between existing conventional-based temperature controller devices used for nanoparticle synthesis and various AMTC systems for synthesizing the nanomaterials and nanomicelles in a micro-scale platform.

The present work describes the development of an economical, integrated, and miniaturized AMTC platform which can be easily used for the synthesis of several nanoparticles and nanomicelles. Here, as a proof-of-principle, the synthesis of nickel oxide (NiO), copper oxide (CuO) nanoparticles, and Dex loaded nanomicelles were carried out on an AMTC device. An Arduino pro-mini microcontroller was realized which acted as the main chip by controlling and monitoring the heaters and sensors which are integrated on the printed circuit board. The FESEM and EDX characterization for synthesized NiO and CuO nanoparticles were executed to study and investigate the morphology and elemental composition. Further, nanomicelles

characterization and its application for ocular-based drug delivery were carried out using this proposed system. The FESEM and EDX characterization revealed the formation of the nanostructures for both NiO and CuO. Further, the produced NiO nanoparticles were used for electrocatalyst sensing of uric acid and hydrazine, and CuO nanomaterials were used for electrocatalyst sensing of uric acid and dopamine respectively. Furthermore, as a proof-of-application, the developed nanomicelles were evaluated for transcorneal penetration using exvivo goat cornea model.

## 2 Experimental

### 2.1 Automatic temperature controller (AMTC) module

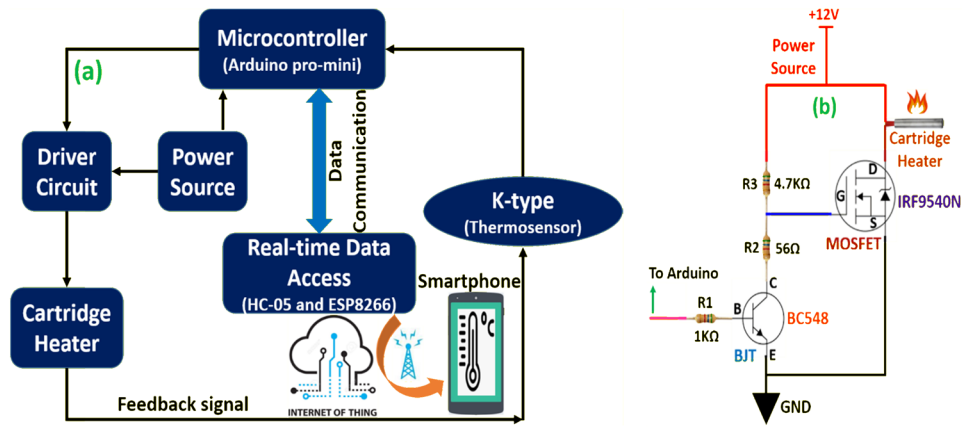
The AMTC system plays an indispensable role in nanoparticle synthesis, where it is crucial to provide a quick and precise temperature. Figure 1a shows a block diagram that includes a microcontroller, driving and switching circuit, cartridge heater, and thermocouple sensor (k-type). In this device, a smaller microcontroller in the family of arduino, Arduino pro-mini 328 (18 × 33mm<sup>2</sup>), has been incorporated. The low-cost and miniaturized arduino pro-mini supports auto-reset, 14 digital input/output pins, and 6 analog input pins. Pro-mini works on 5 V/16 MHz and maximum output current of has an in-built library for proportional-derivative-integral (PID) controller making it a more precise temperature controller module. In this work, an Arduino IDE ([www.arduino.cc](http://www.arduino.cc)) with open-source software was used for coding the instructions. Arduino pro mini is accountable for regulating, coordinating, manipulating, and monitoring the device.

The DC-DC buck convertor (LM2596) breakout module can be set to the desired voltage at the output (load) by step down voltage from its applied input voltage. From an adapter (12 V/3.75A), it can be directly connected to the buck converter where 5 V DC is achieved and fed to power the arduino pro mini. Figure 1b shows a schematic diagram

**Table. 1** Comparison between a conventional controller and microfluidic AMTC system

Approach	Conventional based temperature controller			Microfluidic based temperature controller		
	Hot air oven (Wang et al. 2013)	Muffle furnace (Lu et al. 2011)	Boiler (Yan et al. 2015)	Hot plate (Lee et al. 2009)	Oil Bath (Nightingale and Mello 2009)	Cartridge heater (Nakayama et al. 2006)
Temperature range	800 °C	1600 °C	550 °C	350 °C	200 °C	250 °C
Accuracy	± 1 °C	± 2 °C	± 5 °C	± 2 °C	± 3 °C	± 2 °C
Heat dissipation	More	More	Medium	Medium	Low	Low
Power consumption	1200 W	1520 W	1000 W	800 W	500 W	38 W
Cost	Expensive	Costly	Average	Costlier	Average	Cheaper
Size	Bulky	Heavy	Hefty	Small	Medium	Miniature

**Fig. 1** (a) A simple block diagram of the AMTC system (b) Schematic of self-developed switching circuitry



of self-developed switching circuitry that was designed and developed for executing the regular switching operation to have control over current flow in a driver circuit, without the need for manual cutting or splice of the power source wires. Hereby, the switching circuit was designed with a basic bipolar transistor (BC548), power MOS-field effect transistor (IRF9540N), and limiting resistors (Kulkarni et al. 2021). This takes care of the current flowing across the heater and switches accordingly following the arduino instructions. The microcontroller triggers the signal in boolean logic (0 and 1) through pulse width modulation (PWM) which is associated with the base pin of the bipolar transistor (BJT). Gate terminal of field-effect transistor (FET) was connected to 12 V DC via limiting resistors. The drain terminal was connected to one end of the heater and another end of the heater is connected to 12 V DC. Thus, the overall switching was operated by these aforementioned transistors. A circular

tube-shaped cartridge heater ( $25 \times 3\text{mm}^2$ ), coated with stainless steel material of higher grade, was used for the heating process. The cartridge heater is a voltage-controlled device with a power rating of 38 W, wherein the amount of current required to drive is very minimal, and a good ramping rate was calibrated with temperature and time.

Figure 2 shows a schematic representation of the arduino pro-mini-based AMTC system. A k-type thermocouple sensor was used for manipulating and recording the desired temperature across the heater connected to arduino pro-mini and acts as a feedback signal. It has many advantages like a wide temperature measuring range, reliability, stability, precision, and smaller size. The MAX6675 is a breakout module that was used with the thermocouple responsible to reduce the error, fluctuation, and noise of the sensing signal. It operates at a 5 V power source and has full-duplex Serial Peripheral Interface (SPI) standards allowing the master

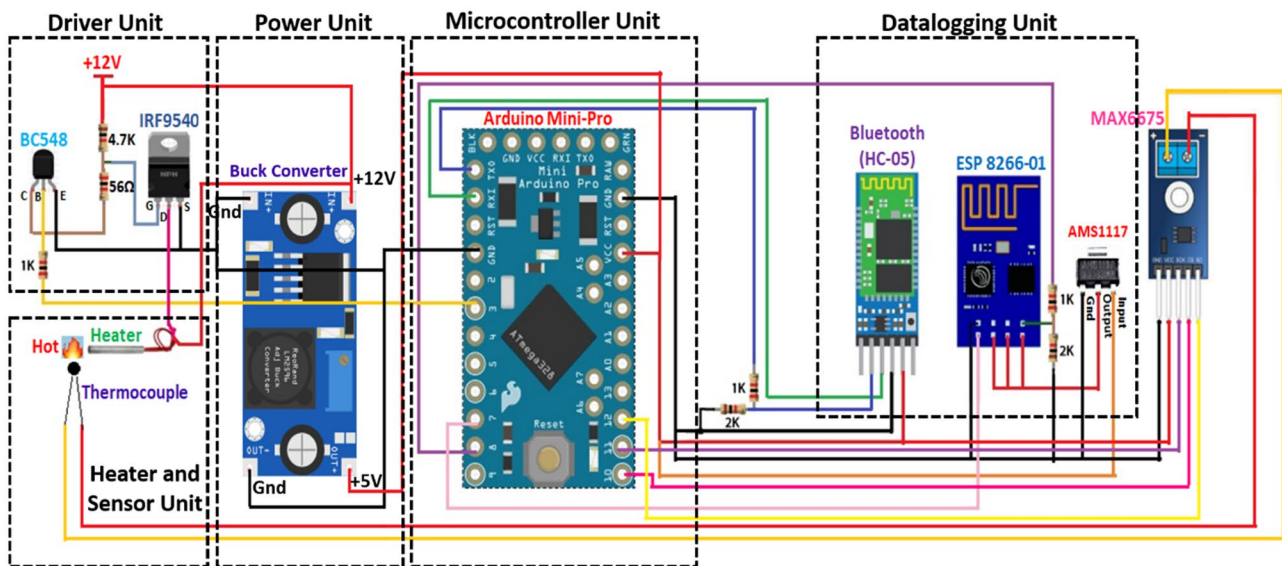


**Fig. 2** Schematic diagram for Arduino pro-mini based AMTC system

and slave to send the data simultaneously. Here, arduino provides a simple method of tuning all PID terms (Proportional ( $K_p$ ), Integral ( $K_I$ ), and Derivative ( $K_D$ )). The PID controller has feedback control that delivers a good output performance stability perceived by considering optimized values such as  $K_p = 160$ ,  $K_I = 1$ , and  $K_D = 80$  as per the prerequisite with very low tolerance. Herein, the PID controller controls the temperature, executes the upper and lower limits within  $\pm 2$  °C. The device consists of Bluetooth and geotagging-based data logging features making it easier for data acquisition and data storage. The real-time data can be directly analyzed and stored on a smartphone through the open-source app and ThingSpeak permits users to collective, analyze, and visualize live data streaming facilities.

## 2.2 Chemicals and apparatus

The chemical used for the experimentation, uric acid, hydrazine, dopamine, Multi-walled carbon nanotube (MWCNT), Nickel nitrate, copper chloride, ascorbic acid, and urea, were purchased from Sigma Aldrich. Dexamethasone, Tocopherol Poly (ethylene glycol) 1000 Succinate (TPGS) and poloxamer P407, Acetonitrile. OrigaLsys Electrochem (OrigaFlex 500) instrument was used for the electrochemical sensing of uric acid, hydrazine, and dopamine. Dynamic light scattering (DLS) technique (Nano ZS 90, Malvern Instruments Ltd., UK), High-Pressure Liquid Chromatography (HPLC), Sonicator (GT Sonic ultra-sonic cleaner (China), Franz diffusion cell apparatus (PermeGear Inc., USA).

## 2.3 Synthesis of NiO, CuO Nanoparticles, and Nanomicelles

### 2.3.1 Preparation of NiO nanoparticles

The precursor's nickel nitrate ( $\text{Ni}(\text{NO}_3)_2$ ) and urea ( $\text{CH}_4\text{N}_2\text{O}$ ) were prepared in the ratio of 1:2 concentrations. The precursor was dissolved in DI water of volume 2 ml. The solution was well stirred using a magnetic stirrer for 15 min and then 2 ml of the reaction was poured onto 5 ml of a small borosil beaker, subsequently placed on the heating block. Further, it was heated from atmospheric thermal conditions to 180 °C for 60 min. The obtained green-colored powder was washed with DI water several times using the filtration method and kept in the oven for drying the powder at 65 °C for 3 h.

### 2.3.2 Preparation of CuO nanoparticles

The preparation of copper oxide was carried out by a conventional chemical precipitation process. Copper chloride and ascorbic acid precursors were taken in the ratio of 4:1 concentration and added in 4 ml DI water and sonicated for 30 min. The 3 ml of the reaction was transferred to a small

petri dish ( $D = 50$  mm) which was positioned on the heater and the pH value was measured and maintained neutral. The solution was kept at 75 °C for 3 h, thereby obtaining a light-brownish-colored product.

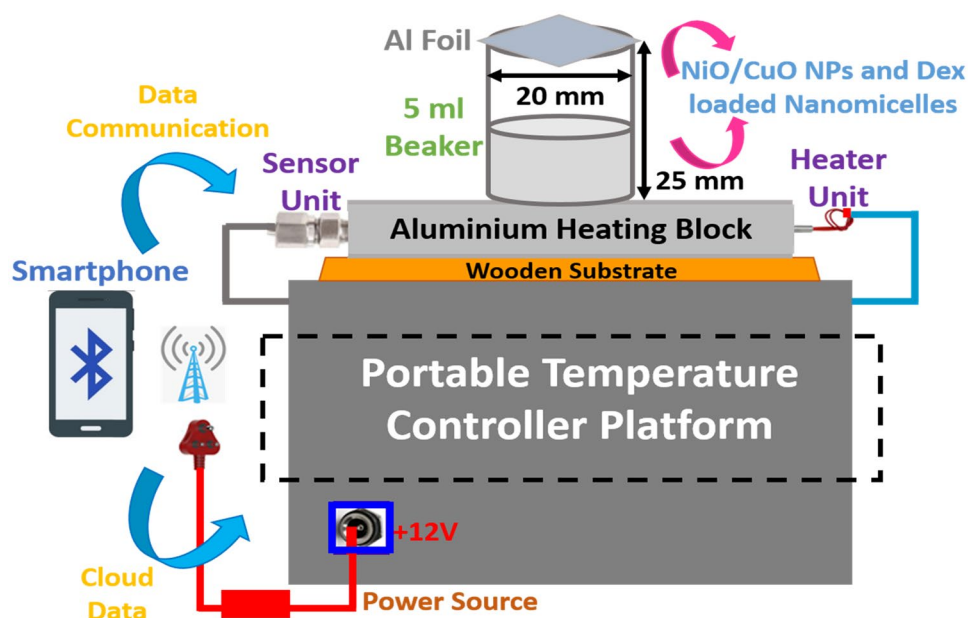
### 2.3.3 Preparation of nano-micelles

The Nanomicelle formulation of Dex was prepared by thin-film hydration method using: (i) Formulation preparation and solvent evaporation (ii) Rehydration. Further, Dexamethasone (0.1%) was accurately weighed and dissolved in Acetonitrile. Then, Tocopheryl Polyethylene Glycol Succinate (TPGS) (3%) and Poloxamer 407 (0.1%) were weighed and dissolved separately in Acetonitrile. These two solutions were then mixed and vortexed for few minutes to get a homogeneous solution. Here, 3 ml of Acetonitrile was used to dissolve the drug completely. 3 ml of Phosphate-buffered solution was taken for final formulation. As a routine practice, this can be evident from various literature (Cholkar et al. 2014; Mandal et al. 2017; Velpandian et al. 2021), that specifies only to quantify the drugs and not the excipients.

The transcorneal penetration studies were performed using goat cornea using the franz diffusion apparatus. HPLC is used to analyze the concentration of the drug in the sample. The goat eyes were purchased from a butcher shop and the cornea was isolated from the whole eye. The removed cornea was washed with PBS buffer pH 7.4 and mounted between the donor and acceptor chamber of the diffusion cell. The acceptor compartment was filled with PBS buffer pH 7.4 and the temperature was maintained at 37 °C with stirring using a magnetic stirrer at 100 rpm throughout the study. The donor compartment was filled with Dex formulation. The samples were collected from the sample port of the franz diffusion apparatus using a syringe at time points 5, 15, 30, 60, 120, and 240 min respectively, and replaced with the same amount of PBS buffer pH 7.4. The collected samples were stored at -20 °C until analysis using HPLC. The circle-shaped cornea was dissected from the goat eye and the thickness of the cornea was measured using a digital micrometer before every experiment to maintain the average thickness of the cornea for various diffusion cells for transcorneal penetration studies and the average thickness was around 0.724 mm. The diameter of the goat cornea was around 17 mm. Goat cornea, pH 7.4 buffer, digital micrometer, and hamilton syringe were used for the exvivo study. In spite of exvivo studies remains as an efficient tool to understand the transcorneal penetration of drugs and formulations, the model cannot imitate the factors like tear drainage and blinking latency which is found in the human eye.

Further, the resultant reaction mixture was kept on the self-designed AMTC system to execute the proposed method, and also, conventional rotatory evaporator method was carried out, to evaporate the solvent completely, later the

**Fig. 3** Overview of a smart-phone-enabled synthesis of nanoparticle on a portable heating device



obtained dry thin film was rehydrated with Phosphate Buffer Solution (PBS) pH 7.4 and sonicated for 5 min. Meanwhile, the process was carried out for the preparation of placebo nanomicelles without Dex.

## 2.4 Experimentation

Figure 3 shows an overview of smartphone-enabled nanoparticle synthesis on a portable heating device. The portable temperature controller module includes a microcontroller, DC buck converter, a switching circuit, cartridge heater, and sensor. The experimentation setup also shows the aluminium heating block ( $50 \times 15 \times 10 \text{ mm}^3$ ) used for heating. Both heater and sensor were inserted into the opposite ends of the block. The complete device was powered up by the 12 V/3A

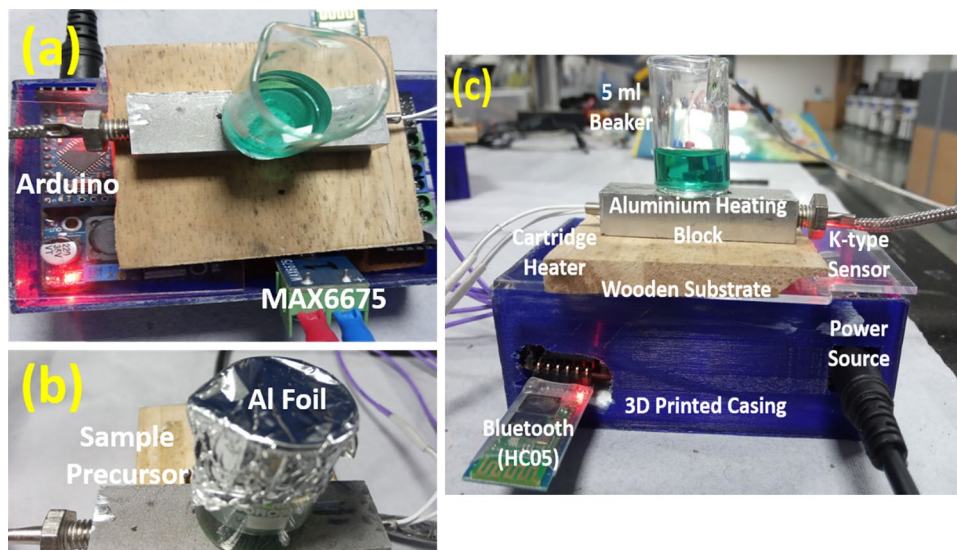
adapter. The 5 ml small beaker was kept on the heating block covered with the thin aluminium foil of thickness  $11 \mu\text{m}$ . The real-time temperature data was made available directly on the smartphone through Bluetooth module (HC-05) and IoT (ESP 8266–01) breakout module using an open-source app. Hence, continuous data analysis and data storage can be observed and maintained easily.

## 3 Results and discussion

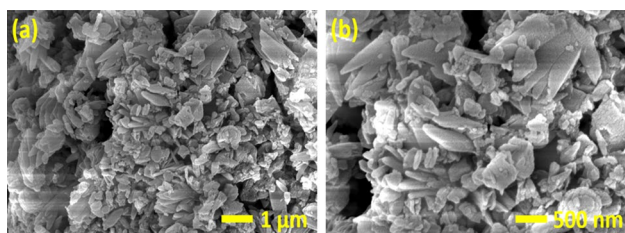
### 3.1 Heating process for synthesis of nanoparticle

Figure 4a shows the top-view of the temperature controller device. The heater output was controlled by the microcontroller and the thermocouple was used as a feedback

**Fig. 4** (a) Top-view of temperature controller device (b) A 5 ml beaker with solution placed on a heating block covered with Al Foil (c) Complete 3D printed casing of heating module







**Fig. 5** SEM images of synthesized Nickel oxide (NiO) nanoparticles appears to be spherical shape nanostructures at a magnification rate (a) 60,000x (b) 300,000x

sensor for monitoring the temperature. The thermocouple sensor has a 12-bit resolution and can provide temperature measurements from 0 °C to 1024 °C with a precision of 0.25 °C. The sensor acted as a feedback response connected to arduino pro-mini by sending the continuous sensor data for temperature monitoring. The accuracy of the temperature controller was around ± 2 °C. The data logging is very simpler with continuous analysis and accessing of the temperature values on the smartphone. All the electronic modules were integrated and soldered on to single 3.93'(L) by 2.36'(W) of a printed circuit board (99.8 × 59.9mm<sup>2</sup>). Figure 4b shows a 5 ml beaker with solution placed on a heating block covered with Al Foil. The dimensions of the complete device with 3D printed casing were 100 (L) × 60 (W) × 32 mm<sup>3</sup> (H) respectively. The smartphone-enabled data accessing and data recording is easier-to-use, faster, and simple. Figure 5c shows the complete 3D printed casing of the heating module.

### 3.2 Characterization of the NiO and CuO nanoparticle

#### 3.2.1 NiO nanoparticle

The synthesized NiO nanoparticles were studied to understand the surface morphological features by the field emission scanning electron microscope (FESEM). The obtained images specify the presence of synthesized NiO nanomaterials, which appeared to be spherical with magnification up to 300 nm as shown in Fig. 5a. Further, it can be observed that the nanoparticles are greatly agglomerated and appear to be a cluster of NiO nanoparticles. The prepared NiO nanomaterials have an average diameter of 27.14 nm as shown in Fig. 5b. The NiO nanoparticles were synthesized at 450°

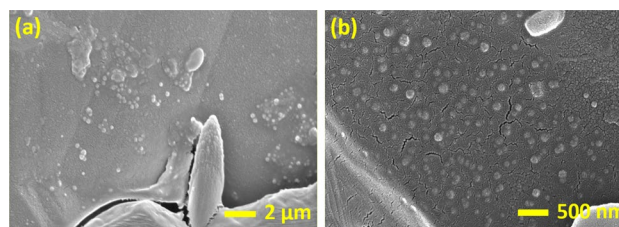


**Fig. 6** SEM images of synthesized Copper oxide (CuO) nanoparticles appears to be spherical shaped nanostructures at a magnification rate (a) 25,000x (b) 120,000x

calcination temperature and the obtained results were studied to recognize the potential of the projected method. The results were benchmarked with the literature which shows comparable results with an average diameter of 32.9 nm produced through the sol–gel method (Wardani et al. 2019).

#### 3.2.2 CuO nanoparticle

The SEM images of the synthesized CuO nanoparticles were observed with agglomerated nanospheres structures with an average diameter of 85.13 nm. Figure 6a, b shows the SEM images which describe the structural and surface morphologies of the formed CuO. The characterization outcome illustrates the substantial presence of major elements of nanoparticles and further, these were compared with the traditional methods (Singh 2016).

To analyze the elemental composition existing in produced NiO and CuO nanomaterials, Energy-dispersive X-ray spectroscopy (EDX) was studied. Table 2 shows the EDX analysis, the statistical results show the percentage of content of major elements of NiO and CuO respectively. Energy-dispersive X-ray spectroscopy (EDX) is an analytical method utilized for the chemical composition or elemental analysis of a reaction mixture. It depends on the examination of an interaction of some basis of X-ray excitation and a reaction n mixture.

Further, Fig. 7a, b show the EDX spectrum for key elements of Ni, O for NiO nanoparticles, and Cu, O, and C elements for CuO nanoparticles.

Figure 8a, b show the size distribution curve of NiO and CuO nanomaterials respectively. Further, the sizes of NiO and CuO nanoparticles were examined naturally with ImageJ software ([www.imagej.net](http://www.imagej.net)), an open-source platform, for the examining of nanomaterials used to identify

**Table 2** EDX Analysis of Key Elements of NiO and CuO

Elements	Weight(%)	Atomic(%)	Elements	Weight(%)	Atomic(%)
Oxygen	34.99	66.38	Oxygen	51.12	52.86
Nickel	65.01	33.62	Carbon	30.80	42.43
			Copper	18.08	4.71

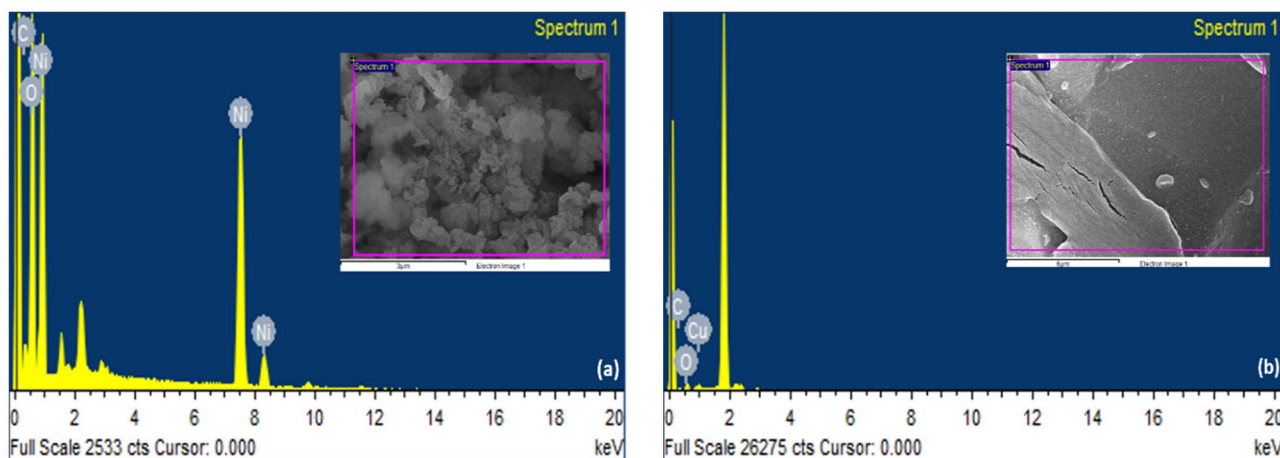


**Fig. 7** (a) Processing of the EDX spectrum for Ni, O elements (b) Processing of the EDX spectrum for Cu, O, and C elements

the size distribution curve. Based on the obtained results from FESEM, the mean nanoparticle size ( $w_c$ ) and standard deviation ( $\sigma$ ) were calculated.

### 3.2.3 Dex loaded nanomicelles for ocular drug delivery application

Dex-loaded nanomicelles were prepared by utilizing both conventional methods based on standard thin-film rehydration and the proposed AMTC system. Herein, the obtained parameters, such as particle size and zeta potential of Dex-loaded nanomicelles (0.1%), were determined by the Dynamic Light Scattering (DLS) technique, after filtering with 0.45  $\mu\text{m}$  sterile nylon membrane filter (Nexflo syringe filter, sterile, 0.45  $\mu\text{m}$ ). TPGS and poloxamer P407 were used as a polymer and stabilizer respectively. Further, the same process was carried out for the preparation of Placebo nanomicelles without Dex. The obtained results from the AMTC system were quite promising with

good reproducibility features having similar particle size and standard deviation when compared to the conventional method (Yu et al. 2015; Wang et al. 2016).

### 3.3 Electro-catalytic oxidation of uric acid and dopamine for NiO nanoparticles

Electro-catalytic-based detection of uric acid and dopamine with multi-walled carbon nanotube (MWCNT)–Nickel oxide nanostructures (MWCNT@NiO) were carried out in a 3-electrode system at neutral pH. Herein, 2B pencil graphite (PG) lead modified with MWCNT@NiO compound was used as a working electrode, Silver/silver chloride (Ag/AgCl) as a reference electrode, and platinum as a counter electrode. The working electrode was prepared by drop-casting 5  $\mu\text{l}$  of MWCNT-ethanol suspension on PG, followed by air drying for 3 min. A 4 mg of NiO nanoparticle was added in 500  $\mu\text{l}$  of ethanol and was sonicated for 6 min. 2  $\mu\text{l}$  of the prepared NiO-ethanol suspension was coated on top of the

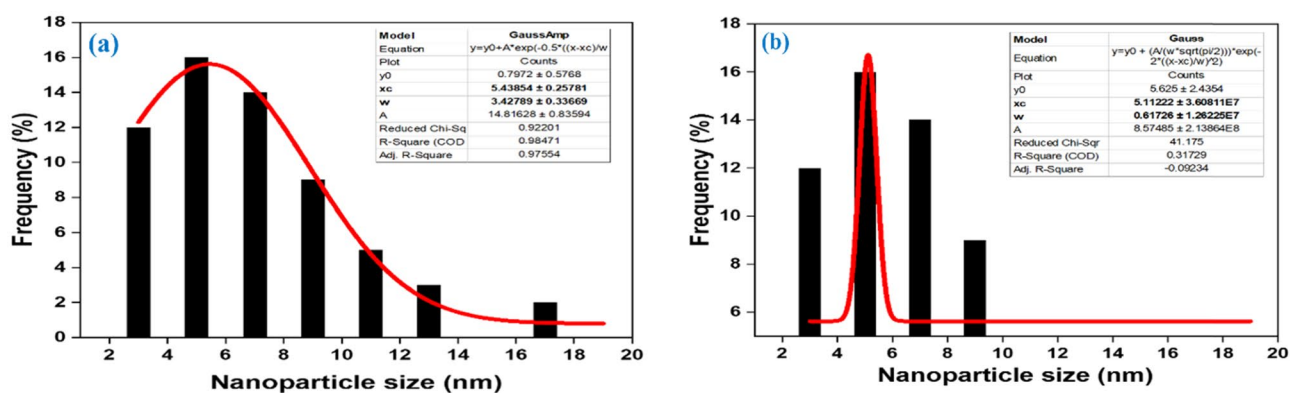


**Fig. 8** (a) NiO nanoparticle size distribution curve (b) CuO nanoparticle size distribution curve

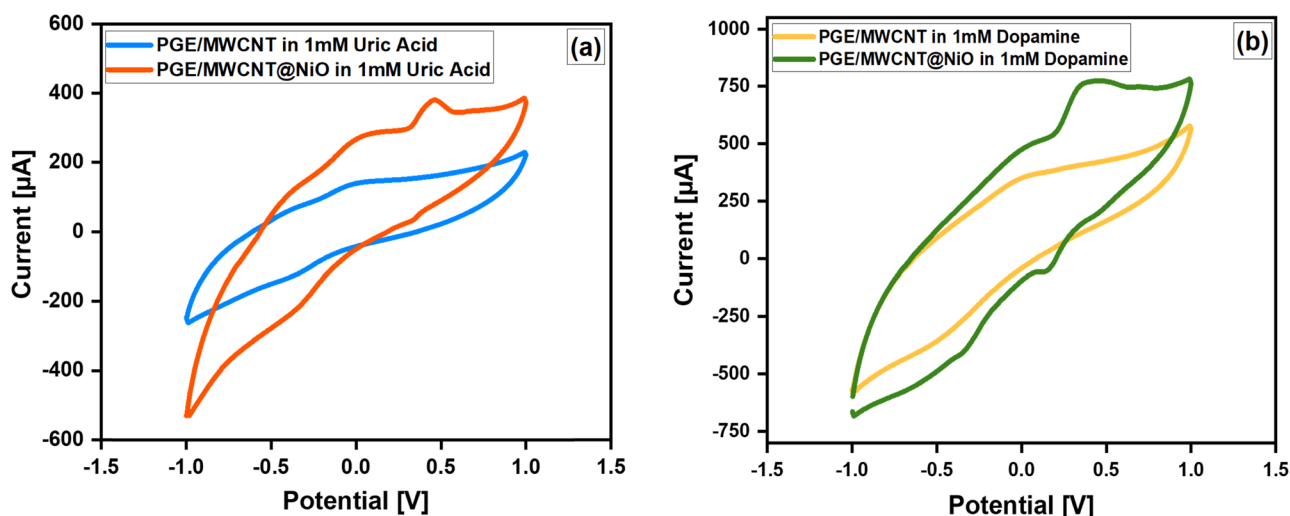


**Fig. 9** (a) CV response of PGE/MWCNT and PGE/MWCNT@NiO in 1 mM Uric acid solution at  $50 \text{ mV s}^{-1}$  (b) CV response of PGE/MWCNT and PGE/MWCNT@NiO in 1 mM Dopamine (DA) solution at  $50 \text{ mV s}^{-1}$

PGE/MWCNT to form PGE/MWCNT@NiO. The working electrode was kept for drying at  $60^\circ \text{C}$  for 2 min in a hot air oven. The cyclic voltammetry technique was utilized at a scan rate of  $50 \text{ mVs}^{-1}$  in 1 mM of Uric acid and 1 mM dopamine. Figure 9a depicts that the blank electrode (PGE/MWCNT) alone gave no oxidation peak of uric acid whereas, PGE/MWCNT@NiO gave clear oxidation at  $E' = 0.43 \text{ V}$  vs Ag/AgCl conforming to the oxidation of uric acid. Successively, it was identified that the produced NiO nanoparticles are electrochemically energetic and play a major role in the detection of uric acid.

Similarly, Fig. 9b shows the blank electrode (PGE/MWCNT) wherein, there was no oxidation peak was noticed. On the other hand, PGE/MWCNT@NiO provides a distinct

oxidation peak at  $E' = 0.33 \text{ V}$  vs Ag/AgCl electrode which is consistent with the oxidation peak indicating the detection of dopamine (DA).

### 3.4 Electro-catalytic oxidation of hydrazine and uric acid for CuO nanoparticles

The Electro-catalytic based detection of hydrazine with copper oxide nanostructures (PGE@CuO) was carried out in a 3-electrode system at neutral pH. Herein, 2B pencil graphite (PG) lead modified with CuO nanoparticles was used as a working electrode, Ag/AgCl as a reference, and platinum as a counter electrode. The working electrode was prepared by drop-casting  $5 \mu\text{l}$  of CuO on PG and was kept for drying at

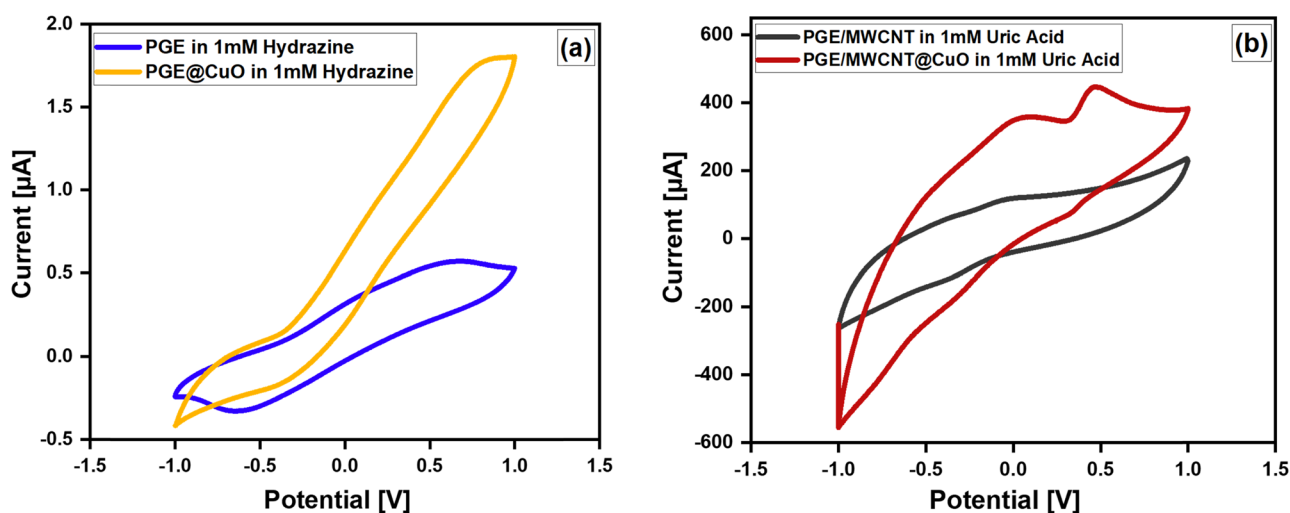


**Fig. 10** (a) CV response of PGE and PGE@CuO in 1 mM hydrazine solution at  $50 \text{ mV s}^{-1}$  (b) CV response of PGE and PGE@CuO in 1 mM uric acid solution at  $50 \text{ mV s}^{-1}$

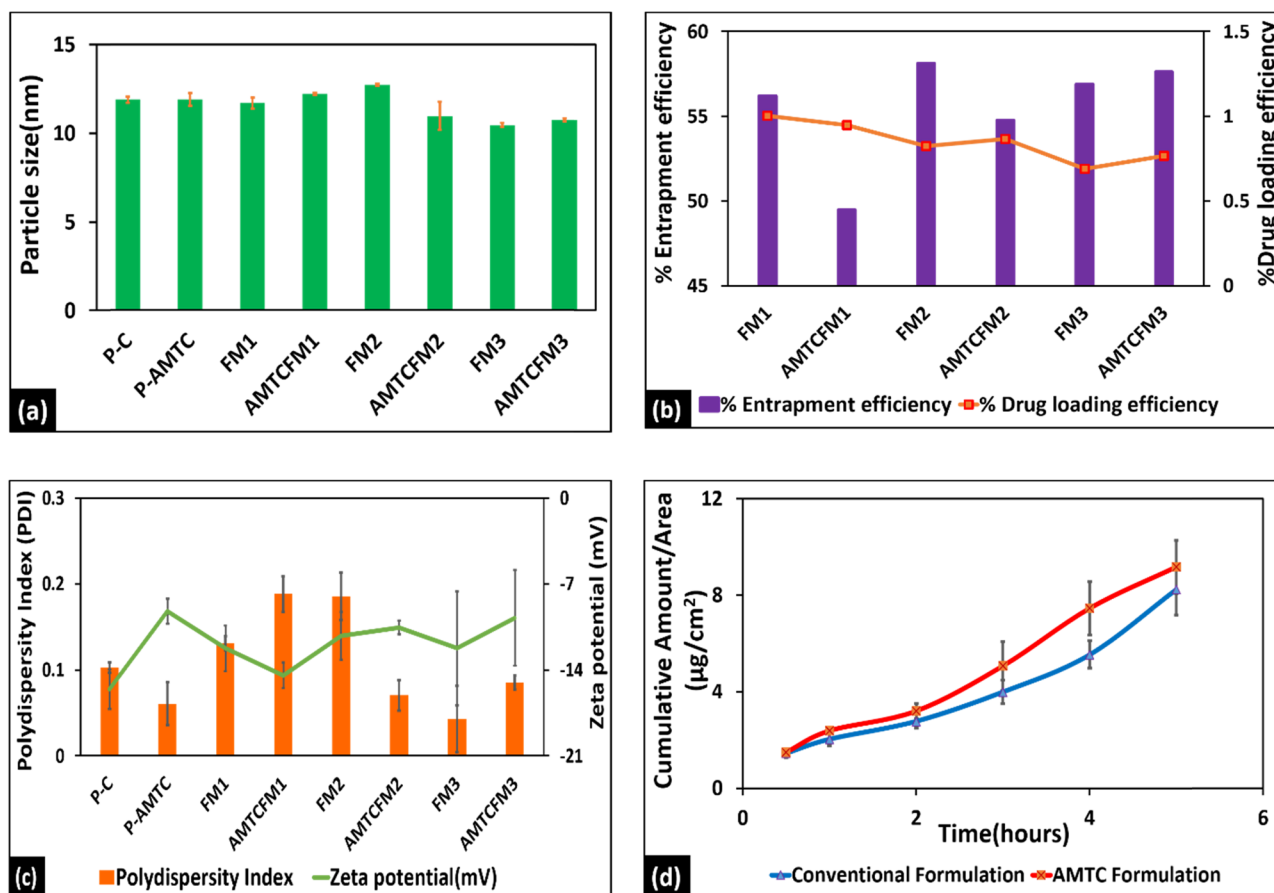


**Fig. 11** Comparison of various evaluation parameters of 0.1% Dex-loaded Nanomicelles using Conventional and AMTC method. (a) Particle size distribution. (b) Entrapment efficiency and Drug loading efficiency. (c) Polydispersity index and Zeta potential. (d)

Transcorneal penetration study. Note: P-C-Placebo Conventional; P-AMTC-Placebo Automated Temperature Control; FM-Formulation; AMTCFM- Automated Temperature Control Formulation

60 °C for 2 min in a hot air oven. The cyclic voltammetry technique was again harnessed at a scan rate of 50 mVs<sup>-1</sup> in 1 mM of Uric acid and hydrazine. Figure 10a depicts that the blank electrode (PGE) alone gave no oxidation peak whereas, PG@CuO gave clear oxidation at  $E' = -0.35$  V vs Ag/AgCl agreeing with the oxidation peak of hydrazine. Subsequently, it was known that CuO synthesized nanoparticles are electrochemically active and play an important role in hydrazine detection.

Likewise, Fig. 10b shows the blank electrode (PG) wherein, there was no oxidation peak observed in 1 mM solution of uric acid, while the PG@CuO provides a distinct oxidation peak at  $E' = 0.46$  V vs Ag/AgCl electrode which is consistent with the electrocatalytic oxidation of uric acid. By further alteration, it can be used to fabricate an electrochemical sensor for uric acid and dopamine in real samples employing the microfluidic platform.

### 3.5 Evaluation of particle size, polydispersity index (PDI), zeta potential, and transcorneal penetration of 0.1% dex-loaded nanomicelles

The developed Dex-loaded nanomicelles were characterized for particle size, zeta potential, entrapment efficacy, drug loading, and transcorneal penetration studies. The entrapment efficacy and loading efficiency were determined by High-Pressure Liquid Chromatography (HPLC). Transcorneal studies were performed on the diffusion apparatus using goat cornea. Dex nanomicelles were optimized with a composition of Dex: TPGS (1:60 ratio). The mean diameter by conventional and AMTC based nanomicelles was found to be  $10.45 \pm 0.08$  nm and  $10.74 \pm 0.08$  nm, with a polydispersity index (PDI) of 0.043 and 0.085, respectively. Apparent permeability of 0.1% Dex-loaded nanomicelles using conventional and AMTC methods were 0.17217 and

0.18686 mm<sup>2</sup>/hr respectively. Clear nanomicelles were obtained using both conventional and AMTC nanomicelles. The particle size distribution, polydispersity index, zeta potential, entrapment efficiency, drug loading efficiency, and transcorneal penetration of 0.1% Dex-loaded nanomicelles using conventional and AMTC methods were shown in Fig. 11a–d. The present study reveals that the Dex-loaded nanomicelles developed using the AMTC method were comparable to the conventional thin-film hydration method. The characterization parameters showed nanomicelles prepared using both methods showed promising results. The AMTC method is more cost-effective, consumes less power, standalone device, and requires less reaction time and drug sample as compared to the conventional thin-film hydration method.

## 4 Conclusion

The present work intends to synthesize the nanoparticles in a minuscule volume of samples which can be used for numerous biological, environmental, cosmetics and energy applications. Herein, the main focus was to design and develop a miniaturized, low-cost, easy-to-carry, simple temperature controller device using the arduino pro-mini platform which uses a proportional-derivative-integral (PID) concept for controlling the temperature. The minuscular device was completely integrated and automated on a PCB positioned in a 3D-printed housing. The thermal system showcased a temperature sensitivity of  $\pm 2$  °C. The real-time geotagged temperature data was made accessible through a smartphone with Bluetooth and IoT modules by installing an open-source app and stored for data analysis for a later stage. The complete portable device dimension comes with 100 (L)  $\times$  60 (W)  $\times$  32 mm<sup>3</sup> (H) respectively. The synthesis of nanoparticles in a miniaturized platform has its variety of sublime features such as precise temperature control, efficient mass and heat transfer, ambient ease, faster loading of samples, and overall safety. Herein, the nickel oxide and copper oxide nanoparticles and Dex loaded nanomicelles were synthesized on this proposed miniaturized device. In both the reaction samples, NiO was heated at 180 °C for 60 min and CuO was heated at 75 °C for 3 h respectively. Stringent characteristics, like FESEM and EDX, have been accomplished and analyzed which shows the formation of NiO and CuO nanoparticles. The obtained mean size of NiO and CuO nanostructures was 27.14 nm and 85.13 nm. In further, nanoparticles were employed for the electrocatalyst sensing of hydrazine, dopamine, and uric acid using the cyclic voltammetry technique. Furthermore, the study was conducted by loading Dex nanomicelles which were developed using an AMTC and compared to the conventional thin-film hydration method. The results showed a promising platform for the proposed

method. The characterization parameters showed nanomicelles prepared using both methods are almost similar. Further, as a proof-of-concept, the developed nanomicelles were evaluated for transcorneal penetration using ex vivo goat cornea model. The salient features of the proposed AMTC system are standalone, automated, low-cost, compact, miniaturized, low-power consumption, less reaction time and volume as compared to the conventional thin-film hydration method. In the future scope, this proposed method has the potential to accelerate the synthesis of nanoparticles and Dex loaded nanomicelles in a microfluidic platform.

**Acknowledgements** The authors would like to thank BITS-Pilani, Hyderabad campus for the infrastructural facility, the Central Analytical Laboratory (CAL) BITS-Pilani, Hyderabad Campus for the help provided in characterization techniques. Madhusudan B Kulkarni would like to thank Tata Consultancy Services (TCS) for providing a scholarship under TCS Research Scholar Program Cycle-15. Khairunnisa Amreen would like to acknowledge the NPDF scheme (PDF/2018/003658) for financial support. We would like to thank the Parenteral Drug Association, Indian Chapter for providing grant support to Nirmal J.

## REFERENCES

- P.G. Jamkhande, N.W. Ghule, A.H. Bamer, M.G. Kalaskar, Metal Nanoparticles Synthesis: An Overview on Methods of Preparation, Advantages and Disadvantages, and Applications. *J. Drug Deliv. Sci. Technol.* **53**, 101174 (2019). <https://doi.org/10.1016/j.jddst.2019.101174>
- M.J. Ndolomingo, N. Bingwa, R. Meijboom, Review of Supported Metal Nanoparticles: Synthesis Methodologies, Advantages and Application as Catalysts. *J. Mater. Sci.* **55**(15), 6195–6241 (2020). <https://doi.org/10.1007/s10853-020-04415-x>
- Ealias, A.M. Saravanakumar, M. P. A Review on the Classification, Characterisation, Synthesis of Nanoparticles and Their Application. *IOP Conf. Ser. Mater. Sci. Eng.* **263**(3) (2017). <https://doi.org/10.1088/1757-899X/263/3/032019>
- J.M. Mohan, K. Amreen, A. Javed, S.K. Dubey, S. Goel, Miniaturized Electrochemical Platform with Ink-Jetted Electrodes for Multiplexed and Interference Mitigated Biochemical Sensing. *Appl. Nanosci.* **10**(10), 3745–3755 (2020). <https://doi.org/10.1007/s13204-020-01480-1>
- M.B. Kulkarni, S. Goel, Microfluidic Devices for Synthesizing Nanomaterials — a Review. *Nano Express* **1**(1), 1–30 (2020a)
- N.S. Powar, V. Patel, Cu Nanoparticle: Synthesis, Characterization and Application Review Article Cu Nanoparticle: Synthesis, Characterization and Application. *Chem. Methodol.* **3**, 457–480 (2019). <https://doi.org/10.22034/chemm.2019.154075.1112>
- S.J.R. Da. Silva, K. Pardee, L. Pena, Loop-Mediated Isothermal Amplification (LAMP) for the Diagnosis of Zika Virus: A Review. *Viruses* **12**(1), 1–20 (2019). <https://doi.org/10.3390/v12010019>
- X. Wang, C. Hughes, S. Park, X. Ma, H.J. Cho, ZnO Nanoparticle-Based Optical Sensors Fabricated by High Current Density Electrodeposition and Flame Oxidation. *Proc. IEEE Sensors* **1**, 5–7 (2017). <https://doi.org/10.1109/ICSENS.2016.7808843>
- S.B. Puneeth, M.B. Kulkarni, S. Goel, Microfluidic Viscometers for Biochemical and Biomedical Applications : A Review. *Eng. Res. Express* **3**, 1–29 (2021)
- G. Yang, S.J. Park, Conventional and Microwave Hydrothermal Synthesis and Application of Functional Materials: A Review.

- Materials (basel) **12**(21), 12–13 (2019). <https://doi.org/10.3390/ma12213640>
- S. Ni, T. Li, X. Yang, Fabrication of NiO Nanoflakes and Its Application in Lithium Ion Battery. *Mater. Chem. Phys.* **132**(2–3), 1108–1111 (2012). <https://doi.org/10.1016/j.matchemphys.2011.12.082>
- Li. Feng, L. Xuan, Z. Zhao, H. Bai, Y. Guo, J. Su, C. wei, X. Chen, MnO<sub>2</sub> Prepared by Hydrothermal Method and Electrochemical Performance as Anode for Lithium-Ion Battery. *Nanoscale Res. Lett.* **9**(1), 1–8 (2014). <https://doi.org/10.1186/1556-276X-9-290>
- M. Li, W. Lei, Y. Yu, W. Yang, J. Li, D. Chen, S. Xu, M. Feng, H. Li, High-Performance Asymmetric Supercapacitors Based on Monodisperse MnO Nanocrystals with High Energy Densities. *Nanoscale* **10**(34), 15926–15931 (2018). <https://doi.org/10.1039/c8nr04541k>
- U.S.J.S. Goel, Surface Modified 3D Printed Carbon Bioelectrodes for Glucose/O<sub>2</sub> Enzymatic Biofuel Cell: Comparison and Optimization. *Sustain. Energy Technol. Assessments.* **42**, 100811 (2020). <https://doi.org/10.1016/j.seta.2020.100811>
- D. Dector, D. Ortega-Díaz, J.M. Olivares-Ramírez, A. Dector, J.J. Pérez-Bueno, D. Fernández, D.M. Amaya-Cruz, A. Reyes-Rojas, Harvesting Energy from Real Human Urine in a Photo-Microfluidic Fuel Cell Using TiO<sub>2</sub>-Ni Anode Electrode. *Int. J. Hydrogen Energy.* xxxx, 1–11 (2021). <https://doi.org/10.1016/j.ijhydene.2021.02.148>
- S. Thota, J. Kumar, Sol-Gel Synthesis and Anomalous Magnetic Behaviour of NiO Nanoparticles. *J. Phys. Chem. Solids* **68**(10), 1951–1964 (2007). <https://doi.org/10.1016/j.jpcs.2007.06.010>
- R. Saravanan, N. Karthikeyan, V.K. Gupta, E. Thirumal, P. Thangadurai, V. Narayanan, A. Stephen, ZnO/Ag Nanocomposite: An Efficient Catalyst for Degradation Studies of Textile Effluents under Visible Light. *Mater. Sci. Eng. C* **33**(4), 2235–2244 (2013). <https://doi.org/10.1016/j.msec.2013.01.046>
- C.T. Meneses, W.H. Flores, F. Garcia, J.M. Sasaki, A Simple Route to the Synthesis of High-Quality NiO Nanoparticles. *J. Nanoparticle Res.* **9**(3), 501–505 (2007). <https://doi.org/10.1007/s11051-006-9109-2>
- S. Ekeröth, S. Ikeda, R.D. Boyd, T. Shimizu, U. Helmersson, Growth of Semi-Coherent Ni and NiO Dual-Phase Nanoparticles Using Hollow Cathode Sputtering. *J. Nanoparticle Res.* **21**(2), 1–8 (2019). <https://doi.org/10.1007/s11051-019-4479-4>
- N. Chopra, L. Claypoole, L.G. Bachas, Morphological Control of Ni/NiO Core/Shell Nanoparticles and Production of Hollow NiO Nanostructures. *J. Nanoparticle Res.* **12**(8), 2883–2893 (2010). <https://doi.org/10.1007/s11051-010-9879-4>
- K. Phiwadang, S. Suphankij, W. Mekprasart, W. Pecharapa, Synthesis of CuO Nanoparticles by Precipitation Method Using Different Precursors. *Energy Procedia* **34**, 740–745 (2013). <https://doi.org/10.1016/j.egypro.2013.06.808>
- P. Pandey, S. Merwyn, G.S. Agarwal, B. K. Tripathi, S.C. Pant, Electrochemical Synthesis of Multi-Armed CuO Nanoparticles and Their Remarkable Bactericidal Potential against Waterborne Bacteria. *J. Nanoparticle Res.* **14**(1) (2012). <https://doi.org/10.1007/s11051-011-0709-0>
- Q. Maqbool, S. Iftikhar, M. Nazar, F. Abbas, A. Saleem, T. Hussain, R. Kausar, S. Anwaar, N. Jabeen, Green Fabricated CuO Nanobullets via Olea Europaea Leaf Extract Shows Auspicious Antimicrobial Potential. *IET Nanobiotechnol.* **11**(4), 463–468 (2017). <https://doi.org/10.1049/iet-nbt.2016.0125>
- G. Kesavan, S.M. Chen, Sonochemically Exfoliated Graphitic-Carbon Nitride for the Electrochemical Detection of Flutamide in Environmental Samples. *Diam. Relat. Mater.* **108**, 107975 (2020). <https://doi.org/10.1016/j.diamond.2020.107975>
- A. Batool, S. Valiyaveetil, Co-Precipitation - An Efficient Method for Removal of Polymer Nanoparticles from Water. *ACS Sustain. Chem. Eng.* (2020). <https://doi.org/10.1021/acssuschemeng.0c04511>
- M.B. Kulkarni, P.K. Yashas Enaganti, K. Amreen, S. Goel, Internet of Things Enabled Portable Thermal Management System with Microfluidic Platform to Synthesize MnO<sub>2</sub> Nanoparticles for Electrochemical Sensing. *Nanotechnology*, **2020**, *31* (42), 1–8. <https://doi.org/10.1088/1361-6528/ab9ed8>
- R. Dobrucka, A. Romaniuk, D. Mariusz, Facile Synthesis of Au / ZnO / Ag Nanoparticles Using Glechoma Hederacea L. Extract , and Their Activity against Leukemia. *Biomed. Microdevices*, **2021**, 1–15. <https://doi.org/10.1007/s10544-021-00557-0>
- M. Li, L. Gu, T. Li, S. Hao, F. Tan, D. Chen, D. Zhu, Y. Xu, C. Sun, Z. Yang, Tio<sub>2</sub>-Seeded Hydrothermal Growth of Spherical Batio<sub>3</sub> Nanocrystals for Capacitor Energy-Storage Application. *Curr. Comput.-Aided Drug Des.* **10**(3), 1–15 (2020). <https://doi.org/10.3390/cryst10030202>
- Z. Qu, K. Wang, G. Alfranca, J.M. de la Fuente, D.A. Cui, Plasmonic Thermal Sensing Based Portable Device for Lateral Flow Assay Detection and Quantification. *Nanoscale Res. Lett.* **15**(1) (2020). <https://doi.org/10.1186/s11671-019-3240-3>
- W. Shi, N. Chopra, Surfactant-Free Synthesis of Novel Copper Oxide (CuO) Nanowire - Cobalt Oxide (Co<sub>3</sub>O<sub>4</sub>) Nanoparticle Heterostructures and Their Morphological Control. *J. Nanoparticle Res.* **13**(2), 851–868 (2011). <https://doi.org/10.1007/s11051-010-0086-0>
- A.D. Vadlapudi, A.K. Mitra, Nanomicelles: An Emerging Platform for Drug Delivery to the Eye. *Ther. Deliv.* **4**(1), 1–3 (2013). <https://doi.org/10.4155/tde.12.122>
- S. Patel, C. Garapati, P. Chowdhury, H. Gupta, J. Nesamony, S. Nauli, S.H.S. Boddu, Development and Evaluation of Dexamethasone Nanomicelles with Potential for Treating Posterior Uveitis after Topical Application. *J. Ocul. Pharmacol. Ther.* **31**(4), 215–227 (2015). <https://doi.org/10.1089/jop.2014.0152>
- A.D. Vadlapudi, K. Cholkar, R.K. Vadlapatla, A.K. Mitra, Aqueous Nanomicellar Formulation for Topical Delivery of Biotinylated Lipid Prodrug of Acyclovir: Formulation Development and Ocular Biocompatibility. *J. Ocul. Pharmacol. Ther.* **30**(1), 49–58 (2014). <https://doi.org/10.1089/jop.2013.0157>
- A. Patel, Ocular Drug Delivery Systems: An Overview. *World J. Pharmacol.* **2**(2), 47 (2013). <https://doi.org/10.5497/wjp.v2.i2.47>
- N. Omerovi, E. Vrani, Application of Nanoparticles in Ocular Drug Delivery Systems. 61–78 (2020)
- M. Alami-Milani, P. Zakeri-Milani, H. Valizadeh, S. Sattari, S. Salatin, M. Jelvehgari, Evaluation of Anti-Inflammatory Impact of Dexamethasone-Loaded PCL-PEG-PCL Micelles on Endotoxin-Induced Uveitis in Rabbits. *Pharm. Dev. Technol.* **24**(6), 680–688 (2019). <https://doi.org/10.1080/10837450.2019.1578370>
- V. Gote, S. Sikder, J. Sicotte, D. Pal, Ocular Drug Delivery: Present Innovations and Future Challenges. *J. Pharmacol. Exp. Ther.* **370**(3), 602–624 (2019). <https://doi.org/10.1124/jpet.119.256933>
- S.S. Chrai, M.C. Makoid, S.P. Eriksen, J.R. Robinson, Drop Size and Initial Dosing Frequency Problems of Topically Applied Ophthalmic Drugs. *J. Pharm. Sci.* **63**(3), 333–338 (1974). <https://doi.org/10.1002/jps.2600630304>
- J. Nirmal, S.B. Singh, N.R. Biswas, V. Thavaraj, R.V. Azad, T. Velpandian, Potential Pharmacokinetic Role of Organic Cation Transporters in Modulating the Transcorneal Penetration of Its Substrates Administered Topically. *Eye* **27**(10), 1196–1203 (2013a). <https://doi.org/10.1038/eye.2013.146>
- J. Nirmal, A. Sirohiwal, S.B. Singh, N.R. Biswas, V. Thavaraj, R.V. Azad, T. Velpandian, Role of Organic Cation Transporters in the Ocular Disposition of Its Intravenously Injected Substrate in Rabbits: Implications for Ocular Drug Therapy. *Exp. Eye Res.* **116**, 27–35 (2013b). <https://doi.org/10.1016/j.exer.2013.07.004>
- C. Chaipan, A. Pryszyk, H. Dean, P. Pognard, V. Benes, A.D. Griffiths, C.A. Merten, Single-Virus Droplet Microfluidics for High-Throughput

- Screening of Neutralizing Epitopes on HIV Particles. *Cell Chem. Biol.* **24**(6), 751–757.e3 (2017). <https://doi.org/10.1016/j.chembiol.2017.05.009>
- M.B. Kulkarni, S. Goel, Advances in Continuous-Flow Based Microfluidic PCR Devices – A Review. *Eng. Res. Express.* **2**(4), 0–21 (2020). <https://doi.org/10.1088/2631-8695/abd287>
- M.M. Islam, A. Loewen, P.B. Allen, Simple, Low-Cost Fabrication of Acrylic Based Droplet Microfluidics and Its Use to Generate DNA-Coated Particles. *Sci. Rep.* **8**(1), 1–11 (2018). <https://doi.org/10.1038/s41598-018-27037-5>
- X.C. Jiang, W.M. Chen, C.Y. Chen, S.X. Xiong, A.B. Yu, Role of Temperature in the Growth of Silver Nanoparticles Through a Synergetic Reduction Approach. *Nanoscale Res. Lett.* **6**(1), 1–9 (2011). <https://doi.org/10.1007/s11671-010-9780-1>
- H. Liu, H. Zhang, J. Wang, J. Wei, Effect of Temperature on the Size of Biosynthesized Silver Nanoparticle: Deep Insight into Microscopic Kinetics Analysis. *Arab. J. Chem.* **13**(1), 1011–1019 (2020). <https://doi.org/10.1016/j.arabjc.2017.09.004>
- R. Sigwadi, S. Dhlamini, T. Mokrani, P. Nonjola, Effect of Synthesis Temperature on Particles Size and Morphology of Zirconium Oxide Nanoparticle. *J. Nano Res.* **50**, 18–31 (2017)
- N. Kamaly, Z. Xiao, P.M. Valencia, A.F. Radovic-Moreno, O.C. Farokhzad, Targeted Polymeric Therapeutic Nanoparticles: Design, Development and Clinical Translation. *Chem. Soc. Rev.* **41**(7), 2971–3010 (2012). <https://doi.org/10.1039/c2cs15344k>
- N.H.A. Hamid, M.M. Kamal, F.H. Yahaya, Application of PID Controller in Controlling Refrigerator Temperature. *Proc. 5th Int. Colloq. Signal Process. Its Appl. CSPA 2009*(2009), 378–384 (2009). <https://doi.org/10.1109/CSPA.2009.5069255>
- H.M. Asraf, K.A. Nur Dalila, A.W. Muhammad Hakim, R.H. Muhammad Faizzuan Hon, Development of Experimental Simulator via Arduino-Based PID Temperature Control System Using LabVIEW. *J. Telecommun. Electron. Comput. Eng.* **9**(1–5), 53–57 (2017)
- J. Park, R.A. Martin, J.D. Kelly, J.D. Hedengren, Benchmark Temperature Microcontroller for Process Dynamics and Control. *Comput. Chem. Eng.* **135**, 106736 (2020). <https://doi.org/10.1016/j.compchemeng.2020.106736>
- J.L. Wang, Y.Q. Li, Y.J. Byon, S.G. Mei, G.L. Zhang, Synthesis and Characterization of NiTiO<sub>3</sub> Yellow Nano Pigment with High Solar Radiation Reflection Efficiency. *Powder Technol.* **235**, 303–306 (2013). <https://doi.org/10.1016/j.powtec.2012.10.044>
- H.F. Lu, R.Y. Hong, H.Z. Li, Influence of Surfactants on Co-Precipitation Synthesis of Strontium Ferrite. *J. Alloys Compd.* **509**(41), 10127–10131 (2011). <https://doi.org/10.1016/j.jallcom.2011.08.058>
- Q. Yan, Y. Lu, F. To, Y. Li, F. Yu, Synthesis of Tungsten Carbide Nanoparticles in Biochar Matrix as a Catalyst for Dry Reforming of Methane to Syngas. *Catal. Sci. Technol.* **5**(6), 3270–3280 (2015). <https://doi.org/10.1039/c5cy00029g>
- W. Lee, C.H. Bin Weng, F.Y. Cheng, C.S. Yeh, H.Y. Lei, G. Lee Bin, Biomedical Microdevices Synthesis of Iron Oxide Nanoparticles Using a Microfluidic System. *Biomed. Microdevices.* **11**(1), 161–171 (2009). <https://doi.org/10.1007/s10544-008-9221-4>
- A.M. Nightingale, J.C. De Mello, Controlled Synthesis of III-V Quantum Dots in Microfluidic Reactors. *ChemPhysChem* **10**(15), 2612–2614 (2009). <https://doi.org/10.1002/cphc.200900462>
- T. Nakayama, Y. Kurosawa, S. Furui, K. Kerman, M. Kobayashi, S.R. Rao, Y. Yonezawa, K. Nakano, A. Hino, S. Yamamura et al., Circumventing Air Bubbles in Microfluidic Systems and Quantitative Continuous-Flow PCR Applications. *Anal. Bioanal. Chem.* **386**(5), 1327–1333 (2006). <https://doi.org/10.1007/s00216-006-0688-7>
- M.B. Kulkarni, P.K. Enaganti, K. Amreen, S. Goel, Integrated Temperature Controlling Platform to Synthesize ZnO Nanoparticles and Its Deposition on Al-Foil For. *IEEE Sens. J.* **21**(7), 9538–9545 (2021). <https://doi.org/10.1109/JSEN.2021.3053642>
- K. Cholkar, S. Hariharan, S. Gunda, A.K. Mitra, Optimization of Dexamethasone Mixed Nanomicellar Formulation. *Ageing Int.* **15**(6), 1454–1467 (2014). <https://doi.org/10.1208/s12249-014-0159-y>
- A. Mandal, K. Cholkar, V. Khurana, A. Shah, V. Agrahari, R. Bisht, D. Pal, A.K. Mitra, Topical Formulation of Self-Assembled Antiviral Prodrug Nanomicelles for Targeted Retinal Delivery. *Mol. Pharm.* **14**(6), 2056–2069 (2017). <https://doi.org/10.1021/acs.molpharmaceut.7b00128>
- T. Velpandian, J. Nirmal, H.P. Sharma, S. Sharma, N. Sharma, N. Halder, Novel Water Soluble Sterile Natamycin Formulation (Natasol) for Fungal Keratitis. *Eur. J. Pharm. Sci.* **163**, 635–105857 (2021). <https://doi.org/10.1016/j.ejps.2021.105857>
- M. Wardani, Y. Yulizar, I. Abdullah, D.O. Bagus Apriandanu, Synthesis of NiO Nanoparticles via Green Route Using Ageratum Conyzoides L. Leaf Extract and Their Catalytic Activity. *IOP Conf. Ser. Mater. Sci. Eng.* **509**(1) (2019). <https://doi.org/10.1088/1757-899X/509/1/012077>
- J. A. Singh, Brief Review on Synthesis and Characterization of Copper Oxide Nanoparticles and Its Applications. *J. Bioelectron. Nanotechnol.* **2016**, *1* (1), 1–9. <https://doi.org/10.13188/2475-224x.1000003>.
- J. Yu, Y. Zhou, W. Chen, J. Ren, L. Zhang, L. Lu, G. Luo, H. Huang, Preparation, Characterization and Evaluation of  $\alpha$ -Tocopherol Succinate-Modified Dextran Micelles as Potential Drug Carriers. *Materials (basel)* **8**(10), 6685–6696 (2015). <https://doi.org/10.3390/ma8105332>
- Q. Wang, J. Jiang, W. Chen, H. Jiang, Z. Zhang, X. Sun, Targeted Delivery of Low-Dose Dexamethasone Using PCL-PEG Micelles for Effective Treatment of Rheumatoid Arthritis. *J. Control. Release* **230**, 64–72 (2016). <https://doi.org/10.1016/j.jconrel.2016.03.035>

**Publisher's Note** Springer Nature remains neutral with regard to jurisdictional claims in published maps and institutional affiliations.

# Highly Sensitive and Interference-Free Electrochemical Nitrite Detection in a 3D Printed Miniaturized Device

Abhishesh Pal, Khairunnisa Amreen<sup>ID</sup>, Satish Kumar Dubey<sup>ID</sup>, and Sanket Goel<sup>ID</sup>, *Senior Member, IEEE*

**Abstract**—3D printing has a significant impact on various applications as it facilitates greater control over the designed shapes, leads to rapid prototyping and mass production with transferable designs at a lower cost. These attributes provide great versatility and thus make the devices industry-friendly. Herein, we demonstrate a simple and disposable 3D printed device, fabricated in single-step, as an electrochemical nitrite sensor using commercially available carbon loaded polylactic acid (PLA) filament. Nitrite, usually ingested through water and food, can be harmful when taken in excess. Thus, its efficient and accurate on-site detection becomes imperative. The device showed appreciable sensitivity and good selectivity towards nitrite having a limit-of-detection (LOD) of  $1.96 \mu\text{M}$ . Furthermore, the device has been shown to monitor nitrite in real soil and water samples with appreciable recovery values. Eventually, the device is capable to be multiplexed with varying soil parameters.

**Index Terms**—3D printed device, electrochemical sensing, nitrite detection, miniaturized device.

## I. INTRODUCTION

**T**O fulfill the food and agriculture requirements around the world, most of the countries have switched to agricultural methods harnessing inorganic fertilizers to improve soil productivity. These fertilizers often contain nitrite as an essential element which, if consumed in a disproportionate amount, may affect the oxygen-carrying capacity of the blood by converting hemoglobin to methemoglobin, which is an

irreversible process [1]. Superfluous consumption of nitrite can cause infant methemoglobinemia also known as blue baby syndrome, unwanted abortion, and defects in the central nervous system [2]. In general, human beings consume 60–80 % of nitrite through food and 15–20 % through water. The World Health Organization (WHO) suggests that the upper tolerable limit of nitrite in water for human consumption is 3 mg/L or 3 ppm [3].

There are numerous methods of nitrite detection such as electrochemical, electrochemiluminescent, chromatographic, spectrophotometric, chemiluminescent, capillary electrophoresis, and spectrofluorimetric with each having its own set of advantages and disadvantages [4]. Spectrophotometric methods are widely used for nitrite detection and have detection limit ranging from  $0.02 - 2 \mu\text{M}$  employing Griess assay, while with conventional electrochemical detection methods furnished detection limits in the range spanning from  $10^{-5}$  to  $10^{-2}$  M. Chromatography yielded a detection limit in a range of  $0.9 - 4.4$  nM whereas with capillary electrophoresis the nitrite could be sensed upto  $0.1 \mu\text{M}$  [34]. Electrochemical methods when employed on the same device become unstable due to fouling of the electrode when exposed to real samples over time and hinder their potential use for automated on-site detection [35]. However, methods can be performed, as it consumed few or no reagents and does not need complex or time-consuming pretreatment, besides this, the detection can be easily designed and is inexpensive [36]. Optical methods can usually reach a very low detection limit with good precision, and when combined with separation methods the detection limits can further be reduced [37]. Optical methods often come with drawbacks such as optical interference and electrical integration. In this regard, electrochemical sensors can be used [5]. Compared to the other techniques, electrochemical methods are simple, highly sensitive, and cost-efficient [2]. Several literature reports on electrochemical detection methods for nitrate have been studied [2], [4], [6], [7].

Electrochemical methods for nitrite detection mostly use a conventional three-electrode system. Further, to enhance the sensitivity and selectivity, nanomaterials are used to modify the electrodes, such as copper nano-dendrites and reduced graphene oxide which increase the surface-to-volume ratio to achieve superior responses [8]. These nanoparticles are functionalized and deposited on the electrode surface to modify surface properties to evoke Griess reaction [9]. In some cases,

Manuscript received July 27, 2020; revised February 5, 2021; accepted February 15, 2021. Date of publication March 4, 2021; date of current version April 1, 2021. This work was supported by the Department of Science and Technology through the Department of Science and Technology (DST)-Agro-Tech Program under Grant DST/TDT/ AGRO-13/20190. (Corresponding author: Sanket Goel.)

Abhishesh Pal is with the Department of Mechanical Engineering, and MEMS, Microfluidics and Nanoelectronics (MMNE) Laboratory, Department of Electrical and Electronics Engineering, Birla Institute of Technology and Science (BITS) Pilani, Hyderabad Campus, Hyderabad 500078, India (e-mail: p20190462@hyderabad.bits-pilani.ac.in).

Khairunnisa Amreen and Sanket Goel are with MEMS, Microfluidics and Nanoelectronics (MMNE) Laboratory, Department of Electrical and Electronics Engineering, Birla Institute of Technology and Science (BITS) Pilani, Hyderabad Campus, Hyderabad 500078, India (e-mail: khairunnisa.amreen@hyderabad.bits-pilani.ac.in; sgoel@hyderabad.bits-pilani.ac.in).

Satish Kumar Dubey is with the Department of Mechanical Engineering, Birla Institute of Technology and Science (BITS) Pilani, Hyderabad Campus, Hyderabad 500078, India (e-mail: satishdubey@hyderabad.bits-pilani.ac.in).

Digital Object Identifier 10.1109/TNB.2021.3063730



**TABLE I**  
COMPARISON WITH PREVIOUS REPORTED WORKS FOR ELECTROCHEMICAL SENSING OF NITRITE

Electrode	Linear range of Detection	LOD	Application	Remarks	Ref.
SPCE modified with graphite/ $\beta$ -cyclodextrin composite	0.7 $\mu$ M to 2.15 mM	0.26 $\pm$ 0.01 $\mu$ M	Tap water and drinking water	Enhanced electrocatalytic activity	[12]
electrochemically activated graphite modified SPCE	0.1 mM – 16.4 mM	38 nM	—	Simple and low cost disposable device	[13]
PEDOT/MWCNTs modified SPCE	0.05 mM - 1 mM	0.96 $\mu$ M	Tap water	Lower operating potential makes it viable	[14]
3D printed graphene/PLA	25 – 1300 $\mu$ M L <sup>-1</sup>	0.03 $\mu$ M L <sup>-1</sup>	Sensing nitrite in biological fluids	—	[17]
Hb immobilized, colloidal gold nanoparticle modified (Hb-Au-SPCE)	3x10 <sup>-7</sup> to 7x10 <sup>-4</sup> mol dm <sup>-3</sup>	1x10 <sup>-7</sup> mol dm <sup>-3</sup>	—	Disposable device that retains bioactivity	[18]
SPE with Mn3O4 and thin graphene oxide sheet	0.1 $\mu$ M – 1300 $\mu$ M	20 nM	Beef and water	Excellent electrocatalytic ability toward nitrite oxidation	[19]
Orthorhombic CaFe2O4 (CFO) clusters modified SPE	0.016 – 1921 $\mu$ M	6.6 nM	Meat, tap water and drinking water	Substantial increment in anodic peak current densities	[20]
Paper electrodes modified with graphene nanosheets and gold nanoparticles	0.3–720 $\mu$ M	0.1 $\mu$ M	Lake and river water, industrial sewage	Inexpensive and disposable device	[21]
Pd nanostructures deposited SWCNT thin films	2 $\mu$ M – 238 $\mu$ M and 283 $\mu$ M – 1230 $\mu$ M	0.25 $\mu$ M	—	Metal nanoparticles along with MWCNT to achieve appreciable selectivity and stability	[22]
Nitrite detection on 3D printed platform	25-1500 $\mu$ M	1.96 $\mu$ M	Tap water and soil samples	3D printed micro device with appreciable sensitivity and selectivity	This work

a mediator has been used along with the carbon nanotubes (CNT) on a glassy carbon electrode (GCE) to help electrocatalytic reduction of nitrite by enhancing electron transfer [10].

The nitrite detection using carbon and its composites is a very well-established method. Screen-printed carbon electrodes (SPCEs) along with modifications have been utilized to realize a miniaturized device. Here, screen-printing, with modified carbon ink, was successfully utilized for nitrite detection in drinking and groundwater [11]. In a different work, for nitrite detection, SPCEs were modified with graphite and  $\beta$ -cyclodextrin [12], electrochemically modified graphite [13], poly(3,4-ethylene dioxothiophene) and multi-wall carbon nanotubes (MWCNT) [14], etc. However, most of the reported works enumerate bulk systems hindering the device portability and therefore ease-of-use.

Miniaturization has significantly changed and has been an add-on in several fields. With the huge advancement in technology, it is now easier to fabricate complex smaller products with added functionality. Miniaturized devices help reduce the amount of liquid handled, eventually results in a faster analysis at lesser operational cost.

3D printing is one of the essential tools to achieve miniaturization and it can further offer flexibility and replicability of the products fabricated. It has been transforming various fields such as manufacturing, industry, medical, etc. Tailor-made intricate designs can be made with fused deposition modeling (FDM). 3D printing substantiates this by extrusion of the thermoplastic polymer [15]. The application of 3D printing technology can be extended to electrochemical sensing as well [16]. This method is simple, low-cost, and facilitates multi-material structures with high versatility. 3D printed electrochemical sensors offer rapid prototyping, enhanced manufacturing speed, and deliver sensors with intricate electrode

geometries [38]. However, the 3D printed electrodes are affected by the intrinsic kinetic barrier for the electron transfer which affects the electrochemical property of the electrode [39]. Literature reveals that the FDM 3D printed devices cost lesser due to the low-cost of 3D printers and thermoplastic filaments. Commercially available conductive filaments containing carbon black which is a byproduct of the petroleum product which makes such filaments cheaper. FDM-based 3D-printing system costs approximately <US\$200 with high precision [42]. Overall, the 3D printing approach involves extremely low-capital, operational, and material costs. Typically, the total fabrication time of the device is 11 minutes with per-device cost of approximately \$0.08 [43]. Other methods like spectrophotometry, chemiluminescence, or chromatography require pretreatment and calibration of the device which is not cost-effective [44]. Table I provides a comparison of the previously reported work with the present system.

Herein, a 3D printed device is demonstrated to detect nitrite electrochemically. So far, based on our best knowledge, there is no study on leveraging 3D printed devices made from carbon black based PLA for the detection of nitrite. Specificity, repeatability, and electrodes have been studied in-depth in this work.

However, 3D-printed steel electrodes have been reported to determine heavy elements Pb(II) and Cd(II) [23]. Plastic 3D printed devices using fused deposition modeling (FDM) were reported to determine Pb(II), Hg(II), Cu(II), and Zn(II) [24]–[28]. In the present work, a 3D printed miniaturized device with 3 electrode system was harnessed to detect nitrite with cyclic voltammetry (CV) and square wave voltammetry (SWV). This device was fabricated using a dual-extruder FDM 3D printer in a single-step using commercially available plastic filaments. The device had a cell

made up of non-conductive polylactic acid (PLA). The three electrodes were printed on a 3D printer using a conductive carbon loaded PLA filament. The fabricated device gave interference mitigated response towards nitrite with LOD as  $1.96 \mu\text{M}$ . Furthermore, the real soil sample and real water sample analysis were carried out with appreciable recovery values.

## II. EXPERIMENT SECTION

### A. Materials and Reagents

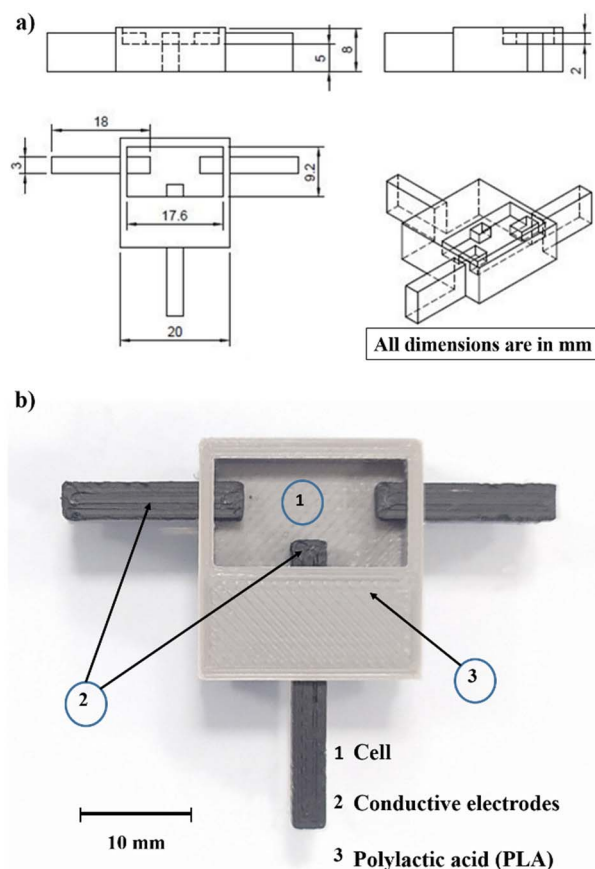
Sodium Nitrite and Ammonium persulfate were obtained from Sigma-Aldrich. Potassium nitrate from Avra, Sodium carbonate from TCI, Sodium chloride extrapure AR, and Potassium Ferricyanide procured from SRL. MilliQ water (Millipore)  $18.2 \text{ M}\Omega\cdot\text{cm}$  was used in all the experiments. Phosphate buffer solution (PBS) of 0.1 M concentration at pH 7 was utilized for all electrochemical tests. The PBS was prepared using sodium phosphate monobasic dihydrate and sodium phosphate dibasic dehydrate extrapure, both purchased from SRL. The Ag/AgCl ink was procured from ALS Co. Ltd., Tokyo Japan. Whatman filter paper #1 and #113 were purchased from Whatman. The electrochemical analysis was done using Galvanostat / Potentiostat (SP-150, Bio-Logic, France) of V11.02 version along with EC-Lab software. The non-conductive filament (glass blue) of diameter  $1.75 \pm 0.03 \text{ mm}$  was obtained from Rever Industries. The carbon-loaded PLA conductive filament (both diameter 1.75 mm) was obtained from Proto-pasta and Amolen. The micrographs were taken using Apreo scanning electron microscope (SEM) from Thermo Fisher Scientific.

### B. Design and Fabrication of the Miniaturized 3d Printed Device

The device was designed with CATIA software (Scheme 1) and the file was saved in .stl format and opened in Flashprint software to set the printing parameters. The platform temperature was  $50 \text{ }^\circ\text{C}$ , the temperature of the head dispenser for non-conductive PLA was  $200 \text{ }^\circ\text{C}$  and the temperature of the head dispenser for conductive carbon-loaded PLA was  $220 \text{ }^\circ\text{C}$ , and printing speed and head travel speed were  $50 \text{ mm/s}$  and  $70 \text{ mm/s}$  respectively. After setting these printing parameters, the file was saved in .x3g format and subsequently saved on the SD card. Eventually, the SD card was inserted in the slot of flash forge creator pro (Flash forge, USA) 3D printer to begin printing.

### C. Electrochemical Measurements

The electrochemical evaluation was conducted with potentiostat/galvanostat (Biologic SP-150). The measurements were carried out with the fabricated device ( $600 \mu\text{L}$ ) having conventional 3 electrodes, with bare conductive electrodes as both counter and working electrodes while the Ag/AgCl coated electrode was the reference electrode. Cyclic voltammetric tests (scan rate of  $50 \text{ mV/s}$ ) and square wave voltammetry tests, with optimized parameters (pulse height of  $80 \text{ mV}$ , a pulse width of  $120 \text{ ms}$ , and step height of  $5 \text{ mV}$ ) were



SCHEME 1. a) Design of the 3D printed device designed using CATIA software b) Prototype of the device.

conducted in the potential window of  $0.5 - 1.1 \text{ V}$  with different concentrations of nitrite in the cell. The concentration was varied from  $25 - 1500 \mu\text{M}$  in 0.1 M PBS at pH 7.

## III. RESULTS AND DISCUSSION

### A. Filament Screening and Electroactivity

A screening of two conductive, carbon black based materials was done to check their suitability as an electrode in the 3D printed device. The materials chosen were namely Proto-pasta conductive PLA and Amolen conductive black PLA in the form of filament of diameter 1.75 mm. CV was performed on both devices to test Nitrite ( $1 \text{ mM}$ ) wherein the device with Proto-pasta electrode gave better peaks and evoked much more current for the nitrite oxidation in comparison with Amolen conductive PLA as shown in Fig. 1a). Besides, nitrite was also tested with Proto-pasta electrodes with and without Dimethylformamide (DMF) surface treatment. It is evident in Fig. 1b that DMF treatment of all three electrodes and Ag/AgCl modification to the reference electrode gives a well-defined peak as compared to the untreated electrode. Consequently, DMF treated proto-pasta device with one electrode modified to Ag/AgCl (reference electrode) was used for all evaluations further.

The electrochemical responses to  $5 \text{ mM}$  potassium ferricyanide were evaluated on both DMF treated and non-treated

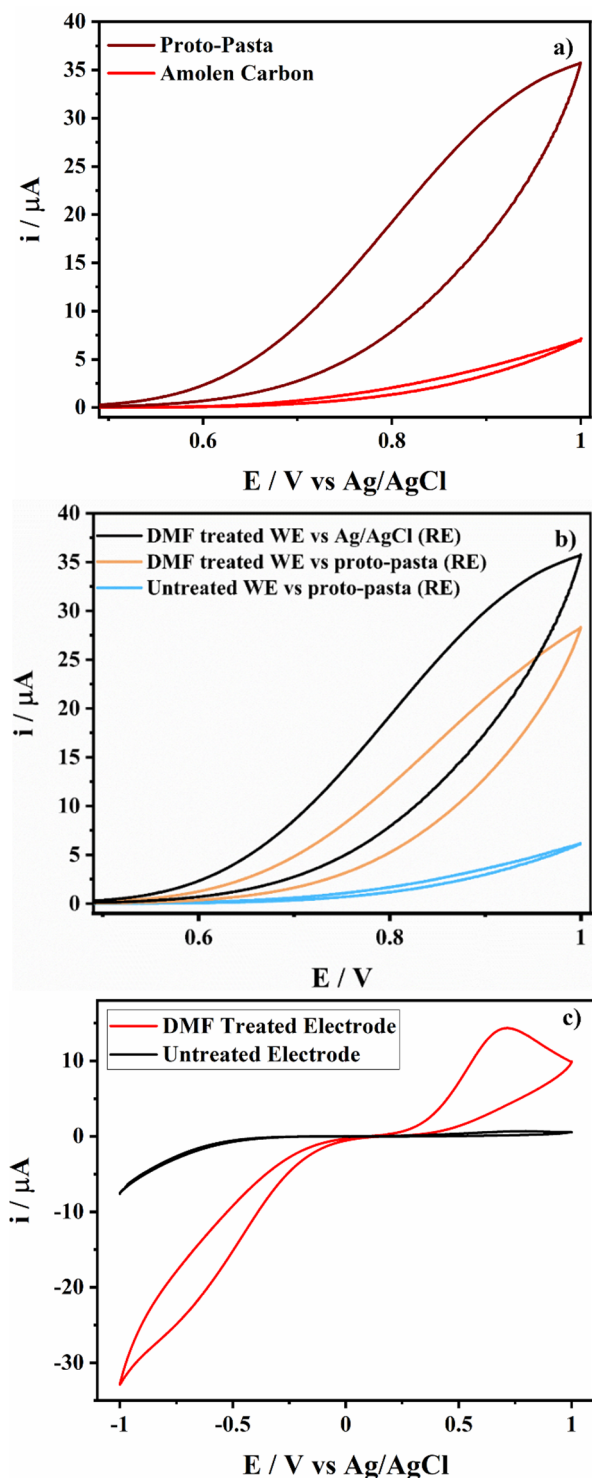


Fig. 1. Comparative CV response of (a) two conductive filaments: Proto-Pasta and Amolen carbon (b) DMF treated and untreated Proto-Pasta working electrode in 1 mM Nitrite at pH 7 in PB solution at  $\nu = 50$  mV/s in a potential window of 0 – 1 V vs Ag/AgCl. (c) Comparative CV response of DMF treated and untreated proto-pasta electrode in 5 mM Ferricyanide at a scan rate of 50 mV/s.

proto-pasta devices. Cyclic Voltammetry (CV) was performed by taking 600  $\mu L$  of potassium ferricyanide in the cell within the potential window of  $-1$  to  $+1$  V (scan rate = 50mV/s). It was observed that the electrodes treated with DMF for 10 minutes provided higher current values and better signals

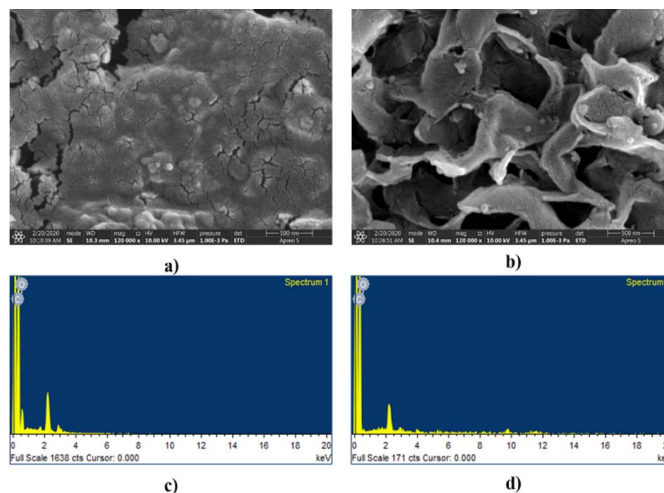


Fig. 2. SEM images of Proto-pasta filament (a) before DMF treatment (b) after DMF treatment, EDX results (c) before DMT treatment (d) after DMF treatment.

TABLE II

EDX DATA SHOWING AN INCREASE IN CARBON WEIGHT % AND ATOMIC % ON THE ELECTRODE SURFACE AFTER TREATMENT WITH DMF

	Unmodified surface		DMF treated surface	
Elements	Weight %	Atomic %	Weight %	Atomic %
1 Carbon	78.95	83.32	92.28	94.09
2 Oxygen	21.05	16.68	7.72	5.91

compared to the unmodified proto pasta electrode owing to the surface modifications (Fig. 1c).

### B. Characterization of the Electrode

Unmodified and DMF-treated carbon-loaded electrodes were characterized using scanning electron microscopy (SEM) and energy dispersive X-ray (EDX) spectroscopy. The PLA-based conductive filament was treated with dimethylformaldehyde (DMF) by keeping the conductive electrodes immersed in the DMF for an optimized time of 10 minutes to get the best results. Treatment increases the surface area which is supposed to enhance the electron transfer and hence enhanced sensitivity of the 3D printed device [40]. SEM images showed that DMF treated surface has a flakes-like surface which provided more surface area compared to an untreated surface (Fig. 2a and 2b). Besides, the EDX data indicated an increase in both weight and atomic percentage of carbon on the surface treated with DMF (Fig. 2c and 2d).

Thus, this could be the plausible reason for better signal obtained with higher peak current in the DMF treated electrode surface. Table II represents the elemental analysis of the treated and untreated electrodes. As can be seen, post-treatment with DMF, the percentage of carbon increased significantly.

### C. Electrocatalytic Nitrite Detection

The applicability of the device for the detection of nitrite was checked using CV. The CV of 1 mM nitrite was taken in

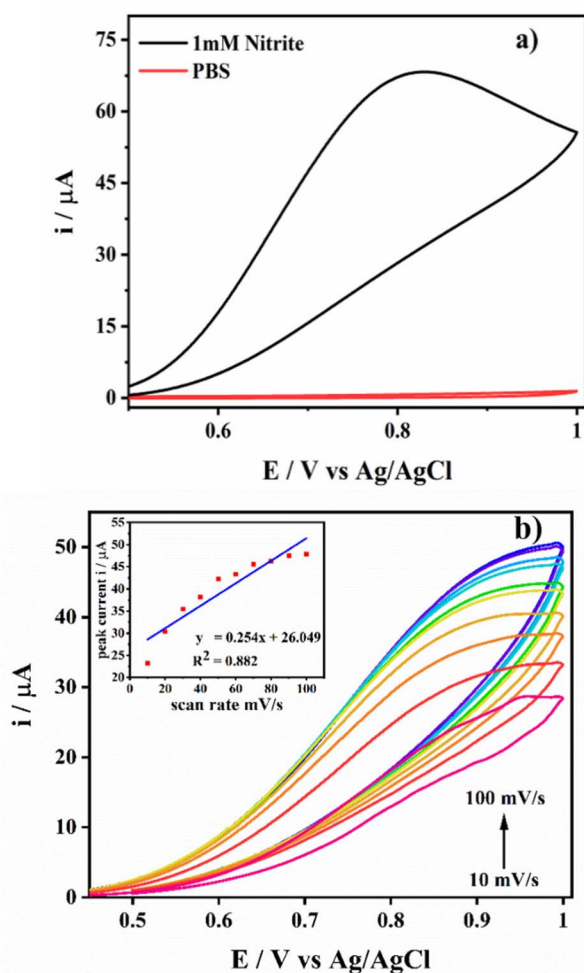


Fig. 3. a) Comparative CV response for 1 mM nitrite in PBS (pH 7) and PBS alone with the modified electrode b) CV of scan rate effect obtained for nitrite (1 mM) at various scan rates (10–100 mV/s) in PBS (pH 7) along with calibration plot for peak current vs scan rate.

the potential window 0.5–1 V (scan rate = 50 mV/s). A clear oxidation peak of nitrite was obtained at 0.82 V (Fig. 3a) which is consistent with the literature wherein the peak potentials of nitrite varied between 0.73–1.18 V [3], [29]–[32]. Whereas, the control experiment, with PBS alone, failed to give any such response (Fig. 3a).

#### D. Scan Rate Effect

CV signals of the device were analyzed at variable scan rates (10–100 mV/s) for 1 mM nitrite solution in PBS. The oxidation peaks current increased linearly as the scan rate was gradually increased with a correlation coefficient,  $R^2 = 0.88$  (Fig. 3b). Typically, it follows the Randles-Sevcik equation. This linearity can be attributed to the diffusion-controlled electrocatalytic process typically, it follows the Randles-Sevcik equation [33]

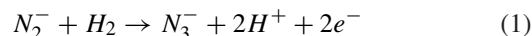
$$i_p = (2.69 \times 10^5) n^{3/2} A c D^{1/2} v^{1/2}$$

$n$  = total no of electrons ( $n = 1$ ),  $v$  = scan rate (V/s),  $n$  = no of electrons involved in rate determining step,  $\alpha$  = transfer

coefficient  $A$  = electrode surface area,  $c$  = concentration of the reactant,  $D$  = diffusion coefficient ( $7.6 \times 10^{-6} \text{ cm}^2 \text{ s}^{-1}$ ).

#### E. Effect of Nitrite Concentration

The fabricated device was tested for the effect of variable nitrite concentration with square wave voltammetry (SWV). The voltammogram shows oxidation peak potential for  $\text{NO}_2^-$  at around 0.82 (Fig. 3a). The probable oxidation mechanism of  $\text{NO}_2^-$  to  $\text{NO}_3^-$  is as follows [12], [13].



Clear oxidation peaks for nitrite were observed in the wide concentration range of 25–1500  $\mu\text{M}$  (Fig. 4a). The peak current values obtained varied linearly with corresponding concentrations ( $R^2 = 0.994$ ). LOD was calculated using the equation,  $\text{LOD} = 3\text{SD}/S$ , where SD is the standard deviation of the curve at the least concentration measured and  $S$  is the slope of the calibration curve [41], to be 1.96  $\mu\text{M}$  which corresponds to 0.135 ppm or 0.135 mg/L that is lower than WHO's recommended 3 ppm safety limit.

#### F. Reproducibility and Stability Analysis

The device was tested for its reproducibility with SWV in a 1 mM nitrite solution in PBS (pH 7). Three different devices were tested and the change in the peak current was observed to be less than 7% (Fig. 4b). To investigate the stability of the device, SWV was done repeatedly on the same device with the same concentration ( $n = 35$ ). Wherein, the device showed appreciable stability and the decrease in the peak current was only 7% (Fig. 4c).

#### G. Effect of Interference

Using SWV, an interference study was also accomplished for the probable interfering agents such as potassium Nitrite, Sodium Chloride, Sodium Carbonate, and Ammonium Persulfate to check the specificity of nitrite detection in presence of co-existing analytes. 1 mM nitrite solution was flushed in the 3D printed cell followed by subsequent addition of the interfering agents one by one of equivalent concentration. During the addition, it was ensured that the pH of the solution remained 7 at room temperature. The change in the peak current was < 8% (Fig. 5a). Also, no new peaks were witnessed in the interference study. Thus, it can be concluded that the device had good specificity towards nitrite. Individual testing of interfering analytes was carried out using SWV with nitrite and all other interferents (1 mM) separately in a potential window 0.5–1.1 V. Besides nitrite, no other peaks were observed (Fig. 5b). This result points out the specificity of the device to nitrite detection over other ions like  $\text{K}^+$ ,  $\text{NO}_3^-$ ,  $\text{Na}^+$ ,  $\text{Cl}^-$ ,  $\text{HCO}_3^-$ ,  $\text{SO}_4^-$  and  $\text{HO}^-$ .

#### H. Real Soil and Water Sample Test

The test was carried out on the real soil samples for nitrite detection. Since the major source of nitrite is soil, the soil sample was collected from the roots of the plant where nitrite could be found more likely. Fine particles were sieved out

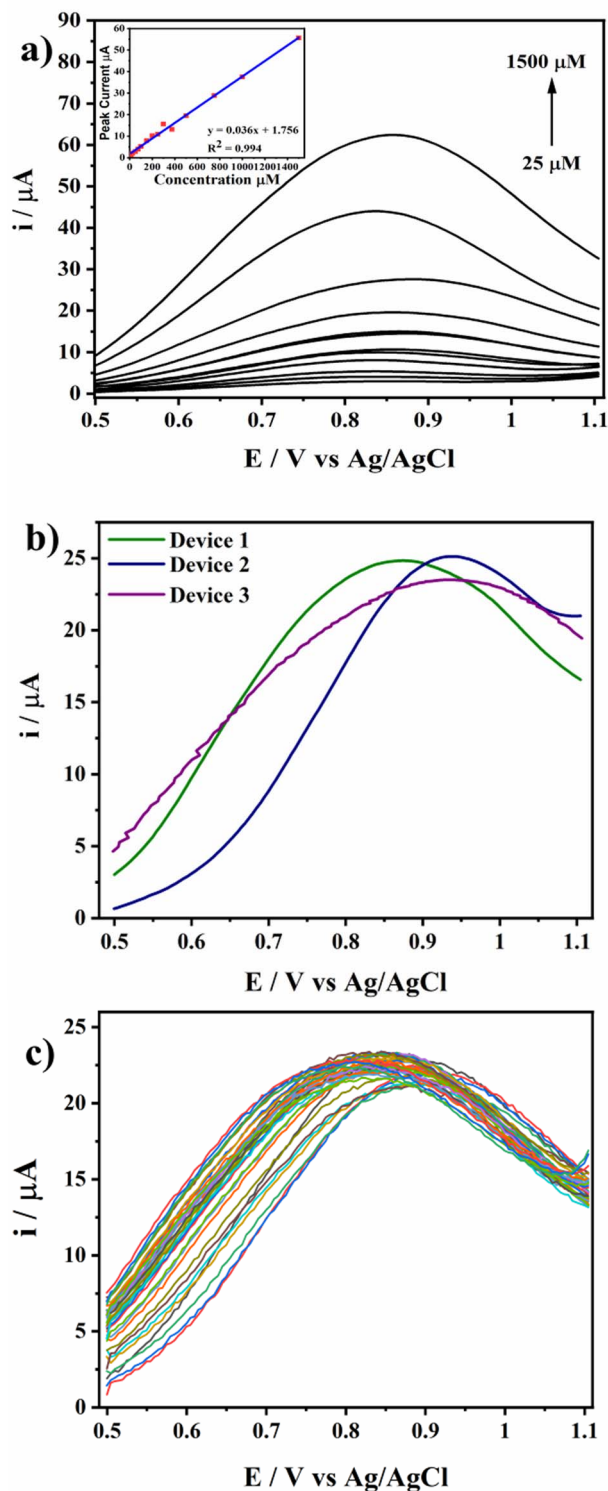


Fig. 4. a) Square Wave Voltammetry signals for detection of Nitrite in the concentration range 25 – 1500 $\mu$ M and corresponding baseline-corrected calibration plot. b) SWV of 1mM nitrite in PBS on three devices c) SWV of 1 mM nitrite on a single device repeated ( $n = 35$ ).

and collected from the sample soil. 5 mg of fine soil was sonicated in 10 ml of ultra-pure MilliQ water for 30 minutes. Undissolved particles were removed by double filtration using Whatman filter paper #1 and #113.

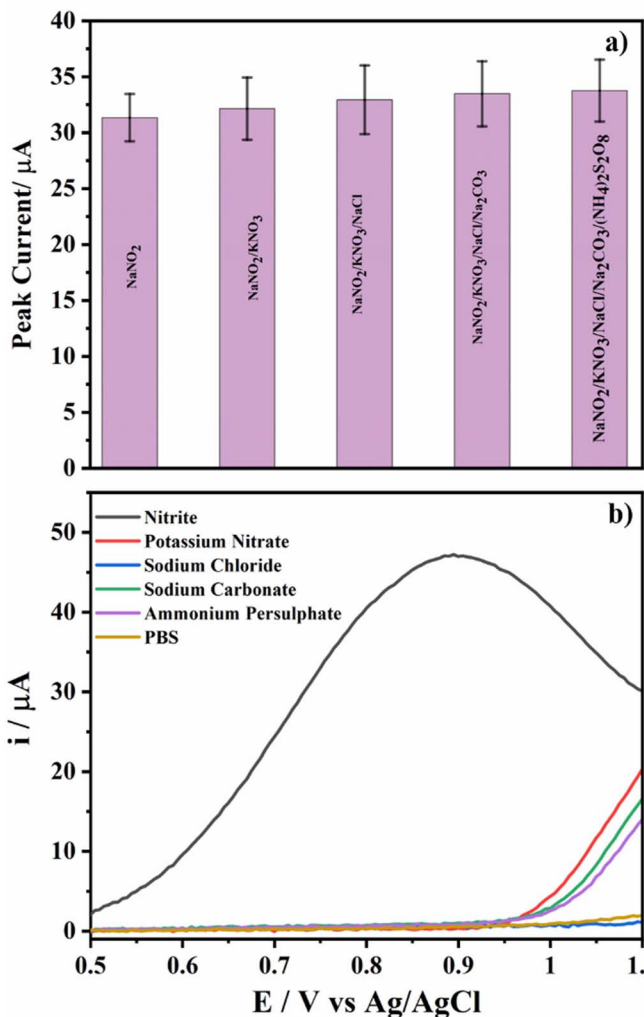


Fig. 5. a) A comparative bar chart showing the change in peak current values obtained by square wave voltammetry (SWV) in the 1 mM nitrite solution and all interferences b) SWV obtained for 1 Mm individual analyte, nitrite, potassium nitrite, sodium chloride, sodium carbonate in PBS along with PBS pH 7.

TABLE III  
RECOVERY VALUES FOR REAL SOIL AND TAP WATER SAMPLES

Sample	Nitrite added ( $\mu$ M)	Nitrite recovered ( $\mu$ M)	Recovery (%)
Soil Sample	25	37.33	149
	50	60.11	120
	75	84.28	112
Water sample	25	27.22	108
	50	52.19	104
	75	73.12	97

Subsequently, 5 ml of the filtrate was added with pH 7 PBS. This solution was analyzed using the developed device and SWV was performed. Following this, the standard solution was spiked with 25  $\mu$ M of nitrite, and SWV was again performed. This step was repeated three times in the linear region to observe an increase in the peak current values with an increase in the nitrite concentration (Fig. 6b). Results showed good

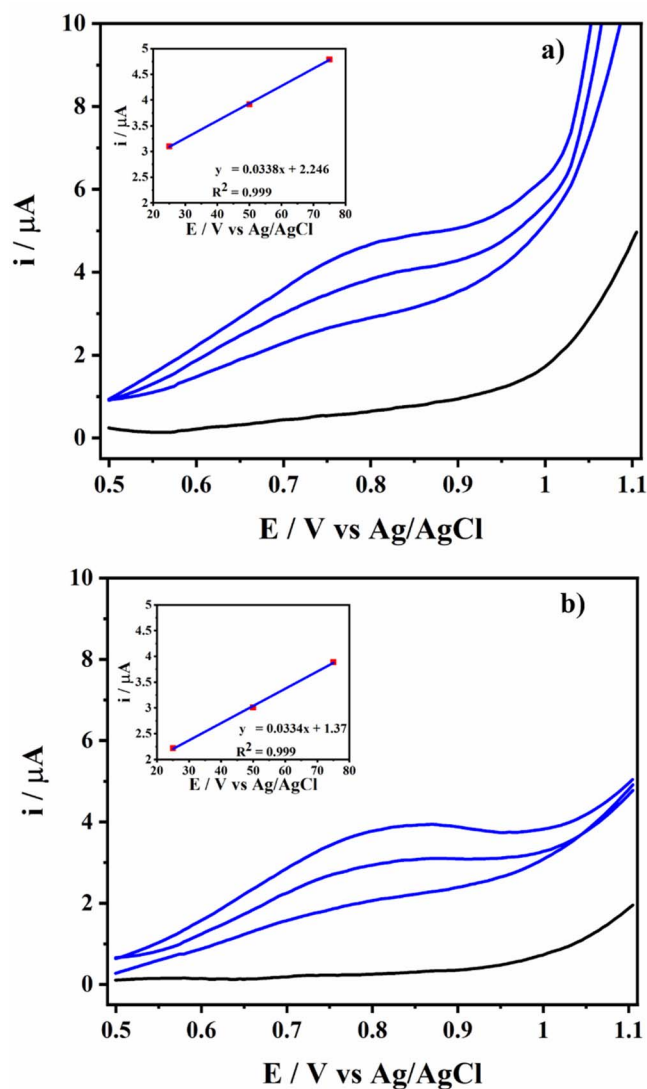


Fig. 6. a) Real soil sample test for nitrite detection with 25  $\mu\text{M}$  step increase in concentration and the corresponding variation of peak current vs concentration in the real sample analysis b) Real water sample test for nitrite detection with 25  $\mu\text{M}$  step increase in concentration and corresponding variation of peak current vs concentration in the real sample analysis.

linearity with  $R^2$  value equal to 0.999 (Fig. 6a). Similarly, the real sample test for the tap water was carried out. Linear growth in the peak current was witnessed with concentrations of 25, 50, and 75  $\mu\text{M}$  nitrite. In this case, as well the  $R^2$  value was 0.999 (Fig. 6b). The progressive spiking of the real sample from 25 – 75  $\mu\text{M}$  for both water and soil samples was performed 3 times to ensure more reliable results. Appreciable recovery values were obtained for both soil and water samples at 25, 50, and 75  $\mu\text{M}$  concentrations as shown in Table III.

#### IV. CONCLUSION

In this work, a micro-device, fabricated using a dual extruder 3D printer in a single-step, has been used to determine and detect nitrite. The device displayed its specificity towards nitrite with LOD being 1.96  $\mu\text{M}$ . This is the first such report to the best of our knowledge wherein a completely 3D printed

polymeric platform has been utilized for nitrite detection. 3D printing offers numerous advantages over the conventional manufacturing process. Owing to its simplicity, cost-effectiveness, size, reproducibility, and sensitivity, it can be effective for on-site estimation of nitrite content. When tested for real soil and water samples, the device was able to sense nitrite. The device demonstrated appreciable reproducibility and repeatability. However, the sensitivity of the device can be further increased by modifying the working electrode with materials like gold.

#### REFERENCES

- [1] D. H. K. Lee, "Nitrates, nitrites, and methemoglobinemia," *Environ. Res.*, vol. 3, nos. 5–6, pp. 484–511, Dec. 1970.
- [2] Y. Mao, Y. Bao, D.-X. Han, and B. Zhao, "Research progress on nitrite electrochemical sensor," *Chin. J. Anal. Chem.*, vol. 46, no. 2, pp. 147–155, Feb. 2018.
- [3] S. Radhakrishnan, K. Krishnamoorthy, C. Sekar, J. Wilson, and S. J. Kim, "A highly sensitive electrochemical sensor for nitrite detection based on  $\text{Fe}_2\text{O}_3$  nanoparticles decorated reduced graphene oxide nanosheets," *Appl. Catal. B, Environ.*, vols. 148–149, pp. 22–28, Apr. 2014.
- [4] Q. H. Wang *et al.*, "Methods for the detection and determination of nitrite and nitrate: A review," *Talanta*, vol. 165, pp. 709–720, Apr. 2017.
- [5] U. Barman, G. Mukhopadhyay, N. Goswami, S. S. Ghosh, and R. P. Paily, "Detection of glutathione by glutathione-S-transferase-nanoconjugate ensemble electrochemical device," *IEEE Trans. Nanobiosci.*, vol. 16, no. 4, pp. 271–279, Jun. 2017.
- [6] Z. Yilong, Z. Dean, and L. Daoliang, "Electrochemical and other methods for detection and determination of dissolved nitrite: A review," *Int. J. Electrochem. Sci.*, vol. 10, no. 2, pp. 1144–1168, 2015.
- [7] M. J. Moorcroft, J. Davis, and R. G. Compton, "Detection and determination of nitrate and nitrite: A review," *Talanta*, vol. 54, pp. 785–803, Jun. 2001.
- [8] D. Zhang *et al.*, "Direct electrodeposition of reduced graphene oxide and dendritic copper nanoclusters on glassy carbon electrode for electrochemical detection of nitrite," *Electrochimica Acta*, vol. 107, pp. 656–663, Sep. 2013.
- [9] P. Miao, M. Shen, L. Ning, G. Chen, and Y. Yin, "Functionalization of platinum nanoparticles for electrochemical detection of nitrite," *Anal. Bioanal. Chem.*, vol. 399, no. 7, pp. 2407–2411, Mar. 2011.
- [10] C. Deng, J. Chen, Z. Nie, M. Yang, and S. Si, "Electrochemical detection of nitrite based on the polythionine/carbon nanotube modified electrode," *Thin Solid Films*, vol. 520, no. 23, pp. 7026–7029, Sep. 2012.
- [11] C. G. Neuhold, J. Wang, X. Cai, and K. Kalcher, "Screen-printed electrodes for nitrite based on anion-exchanger-doped carbon inks," *Analyst*, vol. 120, no. 9, pp. 2377–2380, 1995.
- [12] S. Palanisamy, B. Thirumalraj, and S.-M. Chen, "A novel amperometric nitrite sensor based on screen printed carbon electrode modified with graphite/ $\beta$ -cyclodextrin composite," *J. Electroanal. Chem.*, vol. 760, pp. 97–104, Jan. 2016.
- [13] S. Palanisamy, C. Karuppiah, S.-M. Chen, and P. Periakaruppan, "Highly sensitive and selective amperometric nitrite sensor based on electrochemically activated graphite modified screen printed carbon electrode," *J. Electroanal. Chem.*, vol. 727, pp. 34–38, Aug. 2014.
- [14] C.-Y. Lin, V. S. Vasantha, and K.-C. Ho, "Detection of nitrite using poly (3,4-ethylenedioxythiophene) modified SPCEs," *Sens. Actuators B, Chem.*, vol. 140, no. 1, pp. 51–57, Jun. 2009.
- [15] P. Rewatkar and S. Goel, "3D printed bioelectrodes for enzymatic biofuel cell: Simple, rapid, optimized and enhanced approach," *IEEE Trans. Nanobiosci.*, vol. 19, no. 1, pp. 4–10, Jan. 2020.
- [16] A. Ambrosi and M. Pumera, "3D-printing technologies for electrochemical applications," *Chem. Soc. Rev.*, vol. 45, no. 10, pp. 2740–2755, 2016.
- [17] C. L. M. Palenzuela, F. Novotný, P. Krupicka, Z. Sofer, and M. Pumera, "3D-printed graphene/polylactic acid electrodes promise high sensitivity in electroanalysis," *Anal. Chem.*, vol. 90, no. 9, pp. 5753–5757, May 2018.
- [18] X. Xu, S. Liu, B. Li, and H. Ju, "Disposable nitrite sensor based on hemoglobin-colloidal gold nanoparticle modified screen-printed electrode," *Anal. Lett.*, vol. 36, no. 11, pp. 2427–2442, Jan. 2003.

- [19] A. Muthumariappan, M. Govindasamy, S.-M. Chen, K. Sakthivel, and V. Mani, "Screen-printed electrode modified with a composite prepared from graphene oxide nanosheets and  $Mn_3O_4$  microcubes for ultrasensitive determination of nitrite," *Microchimica Acta*, vol. 184, no. 9, pp. 3625–3634, Sep. 2017.
- [20] P. Balasubramanian, R. Settu, S. M. Chen, T. W. Chen, and G. Sharmila, "A new electrochemical sensor for highly sensitive and selective detection of nitrite in food samples based on sonochemical synthesized calcium ferrite ( $CaFe_2O_4$ ) clusters modified screen printed carbon electrode," *J. Colloid Interface Sci.*, vol. 524, pp. 417–426, Aug. 2018.
- [21] P. Wang, M. Wang, F. Zhou, G. Yang, L. Qu, and X. Miao, "Development of a paper-based, inexpensive, and disposable electrochemical sensing platform for nitrite detection," *Electrochem. Commun.*, vol. 81, pp. 74–78, Aug. 2017.
- [22] X.-H. Pham *et al.*, "Electrochemical detection of nitrite using urchin-like palladium nanostructures on carbon nanotube thin film electrodes," *Sens. Actuators B, Chem.*, vol. 193, pp. 815–822, Mar. 2014.
- [23] K. Y. Lee, A. Ambrosi, and M. Pumera, "3D-printed metal electrodes for heavy metals detection by anodic stripping voltammetry," *Electroanalysis*, vol. 29, no. 11, pp. 2444–2453, 2017.
- [24] V. Katseli, N. Thomaidis, A. Economou, and C. Kokkinos, "Miniature 3D-printed integrated electrochemical cell for trace voltammetric Hg (II) determination," *Sens. Actuators B, Chem.*, vol. 308, Apr. 2020, Art. no. 127715.
- [25] V. Katseli, A. Economou, and C. Kokkinos, "Single-step fabrication of an integrated 3D-printed device for electrochemical sensing applications," *Electrochem. commun.*, vol. 103, pp. 100–103, Jun. 2019.
- [26] Z. Rymansaib *et al.*, "All-polystyrene 3D-printed electrochemical device with embedded carbon nanofiber-graphite-polystyrene composite conductor," *Electroanalysis*, vol. 28, no. 7, pp. 1517–1523, 2016.
- [27] C. Y. Foo, H. N. Lim, M. A. Mahdi, M. H. Wahid, and N. M. Huang, "Three-dimensional printed electrode and its novel applications in electronic devices," *Sci. Rep.*, vol. 8, no. 1, pp. 1–11, 2018.
- [28] K. C. Honeychurch, Z. Rymansaib, and P. Irvani, "Anodic stripping voltammetric determination of zinc at a 3-D printed carbon nanofiber-graphite-polystyrene electrode using a carbon pseudo-reference electrode," *Sens. Actuators B, Chem.*, vol. 267, pp. 476–482, Aug. 2018.
- [29] X. Huang, Y. Li, Y. Chen, and L. Wang, "Electrochemical determination of nitrite and iodate by use of gold nanoparticles/poly(3-methylthiophene) composites coated glassy carbon electrode," *Sens. Actuators B, Chem.*, vol. 134, no. 2, pp. 780–786, 2008.
- [30] B. R. Kozub, N. V. Rees, and R. G. Compton, "Electrochemical determination of nitrite at a bare glassy carbon electrode; why chemically modify electrodes?" *Sens. Actuators B, Chem.*, vol. 143, no. 2, pp. 539–546, Jan. 2010.
- [31] T.-S. Liu, T.-F. Kang, L.-P. Lu, Y. Zhang, and S.-Y. Cheng, "Au-Fe(III) nanoparticle modified glassy carbon electrode for electrochemical nitrite sensor," *J. Electroanal. Chem.*, vol. 632, nos. 1–2, pp. 197–200, Jul. 2009.
- [32] J. Zhang, Y. Zhang, J. Zhou, and L. Wang, "Construction of a highly sensitive non-enzymatic nitrite sensor using electrochemically reduced holey graphene," *Analytica Chim. Acta*, vol. 1043, pp. 28–34, Dec. 2018.
- [33] C. Liu, H. Zhang, Y. Tang, and S. Luo, "Controllable growth of graphene/Cu composite and its nanoarchitecture-dependent electrocatalytic activity to hydrazine oxidation," *J. Mater. Chem. A*, vol. 2, no. 13, pp. 4580–4587, 2014.

# An Analysis Of Edge-Cloud Computing Networks For Computation Offloading

Naga Lakshmi Somu<sup>1</sup>, Dr Prasadu Peddi<sup>2</sup>

<sup>1</sup>Research Scholar, Department of Computer Science, Shri Jagdishprasad Jhabarmal Tibrewala University, Rajasthan.

<sup>2</sup>Assistant Professor, of Computer Science, Shri Jagdishprasad Jhabarmal Tibrewala University, Rajasthan.

---

## ABSTRACT

The proliferation of large amounts of data brought about by the Internet of Things in the commercial and academic spheres has resulted in a significant rise in the number of cloud data centers that provide data analytics services. As a result of the persistent and pervasive requirement to analyze data in close proximity to its original source, edge computing has become more common in recent years. This is one of the reasons why edge computing has become so popular. As a result of edge computing, the processing load on the network's periphery as well as the data centre may be reduced. In addition to this, it is more private and may better accommodate the requirements of the service providers. Edge computing offloads processing by dynamically distributing workloads between a cloud data centre, edge servers, and an edge device. This helps edge computing improve the transmission of network traffic and increases the responsiveness of the system. In this study, we undertake a thorough literature analysis in order to demonstrate how far we have come in the field of computational offloading to edge computing. Specifically, we want to illustrate how far we have progressed in the area of edge computing. Analyses are conducted on a number of elements of offloading computation, including its influence on energy usage, service quality, and customer happiness. Methods for allocating resources are covered, such as gaming, along with methods for balancing system performance and overheads while offloading computations.

**Keywords:** Task partitioning, Offloading, Edge computing, computation offloading, Optimization, edge-cloud collaboration.

## 1 INTRODUCTION

A cloud-based computing system is system to provide services, which gives clients access to distributed and scalable computing capabilities, which include storage, networking and computing within cloud-based data centers. Cloud Service Providers (CSPs) offer flexibility and efficiency for their customers through offering services like software as a service (SaaS) or platform as a



service (PaaS) and infrastructure as a service (IaaS). For instance, they can expand or reduce the amount of their services depending on their clients requirements, develop customized applications and access cloud services from any place connected to the internet. Cloud-based solutions are perfect for companies with increasing or changing demands for internet bandwidth. Furthermore, by using cloud computing, enterprises can launch their applications faster, without having to worry about the cost of infrastructure maintaining, recovery and automated software updates. To maximize the advantages that cloud computing offers, different deployment models , such as the private cloud as well as public cloud and hybrid cloud are essential to ensure the reliability of systems and their capacity to meet the business requirements. Since its beginning cloud computing has transformed the business model across all verticals as well as the human everyday life in a dramatic way. In addition, the corporate IT investments in cloud-based services will be more rapid than that of traditional (non-cloud) IT offerings, this move to software-only solutions makes cloud computing among the most disruptive elements within IT markets. It is therefore expected that cloud computing will end up increasing in popularity and will be a common feature within every commercial or personal market, which is in line with the increasing use of the Internet in the present.

Computational offloading was thought of as a means to overcome the limitation in resource that mobile phones have. Computational offloading can be described as the method of sending a task as well as the associated data to distant high-end resources such as clouds servers and edge servers for processing according to the requirements [2]. Many factors impact the decision to offload, including local device resources like storage, CPU and battery usage, along with the amount of time needed for processing through the network, as well as the volume of transferred data [3].

The concept of edge computing that was first proposed that brings the storage and computation closer to the users Environments UEs that was that was proposed in 2009 is the cloudlet. The concept behind cloudlet is to put computers with high computing power at strategically placed spots to provide computational resources as well as storage for UEs within the vicinity. The cloudlet concept of cloudlet concept of computing "hotspots" is similar to WiFi hotspots but instead of Internet connectivity, cloudlets provide cloud-based services to mobile users. Cloudlets are expected to be accessible to mobile UEs by WiFi connectivity is viewed as a sign of

TABLE I: High level comparison of Edge computing concepts

<b>Technical aspect</b>	<b>Edge Computing</b>	<b>Cloud Computing</b>
<b>Deployment</b>	Centralized	Distributed
<b>Distance to the UE</b>	High	Low
<b>Latency</b>	High	Low

<b>Jitter</b>	High	Low
<b>Computational power</b>	Ample	Low
<b>Storage capacity</b>	Ample	Low

Varghese and Buyya [1] Examine the evolution and development of cloud computing. We begin with cloudlets, ad-hoc clouds multicloud, heterogeneous clouds and multicloud. Micro-clouds are presented, as well as four different cloud computing models including fog computing and mobile edge computing, as well as the use of volunteer computing in addition to software-defined computing and serverless computing. They also discuss the possible consequences that cloud computing can be bringing to IoT (Internet of Things) and big data-driven autonomous learning systems. They also analyze the challenges involved in designing a cloud computing technology that is suited to the improvement of reliability and security in a long-lasting cloud system, as well as efficient methods for managing resources.

## 2 COMPUTATION OFFLOADING

Computation offloading allows you to run applications that are extremely demanding remotely to gain advantages from the the power of cloud (or the edge) servers that are able to outlast CPU and battery limitations on the mobile side.

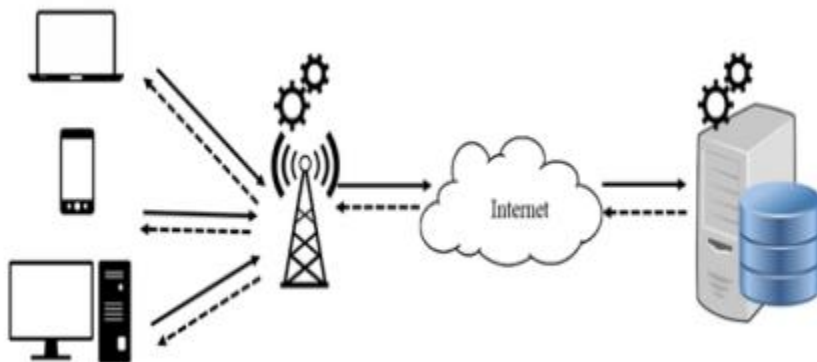


Fig 1: Offloading architecture

Offloading of computation can be either dynamic or static. The static offloading process first evaluates the performance of offloading with offline profiling or models for performance estimation. The load-offloading dynamic process starts by conducting a static examination of the source code and other resources. When the application is running, it is examined dynamically, which allows it to split applications into two main components.

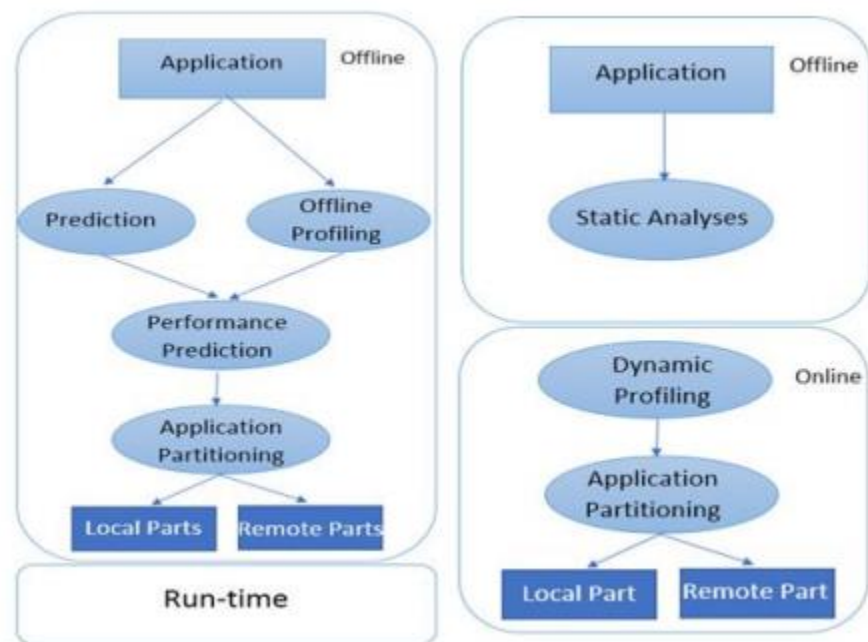


Fig 2: Static and dynamic offloading - (a) Static offloading (b) Dynamic offloading

Computation offloading is considered to be an efficient method to ensure high-quality service to the user by delegating the tasks that require a lot of computation or are latency sensitive to edge devices or adjacent edge servers [12]. The main reason behind the offloading of computations is that it helps reduce the time it takes to react to the service, and to improve the quality of service. Additionally, if the edge node isn't equipped with the capacity to complete this task it could be moved into a cloud or edge data centre to boost the performance of the whole system. When deciding to offload computations, a variety of factors must be taken into consideration such as efficiency improvement and energy efficiency reduction. There are many problems to be considered prior to the offloading of computations:

- (1) Does the task be delegated? The task scheduler needs to determine whether the task is able to be delegated, i.e., what is the best method to offload it, a partial or full offload?
- (2) What is the best time to delegate the task? The task scheduler has to determine the appropriate time for offloading in accordance with various limitations.
- (3) Which location should you offload? The answer is what is the ideal location for the offloading of workloads in accordance with the available resources.
- (4) Which policy for offloading will be implemented? What is the principal goal of offloading of workloads and single performance metric maximization or joint optimization or tradeoffs between multiple goals? For example, massive edge devices differ in terms of their architectural performance indicators, performance and power supply modes which result in different energy efficiency distributions between devices. In addition, dynamic changes to the bandwidth and latency of networks between clouds data centers and edge equipment can result in changes in

energy consumption for data transmission. So, a diverse policies for offloading computations result in different energy consumption. So, a sound algorithm for offloading computations must determine the most effective balance between total time delay for computation, the data transmission, as well as the related performance indicators.

Within this segment, we'll look at the research that is currently being done on computation offloading. We will also discuss some issues and possible research direction.

### **3 WHAT TO OFFLOAD THE SELECTION OF THE OFFLOADED WORKLOAD**

Edge computing's promise to cut the latency of applications and consumption of bandwidth will not be realized until the cloud data centers are transferred to the edge device or servers. In the case of an cloud-edge co-existing system the primary tasks being executed by cloud data centers need to be split, and some tasks should be relegated to run on edge devices, as and edge servers. In certain instances like IoT the local processor can be utilized dispersed across a large variety of devices and local computing resources aren't sufficient to handle the demands of complicated applications. Therefore, a careful allocation of workloads offloaded to devices at the edge will aid in achieving lower latency as well as better system performance.

Locally caching content is the most popular method of speedier delivery of content across a broad range of applications. Similar to cache data coming from cloud data centers, transferring it to nearby edge devices as well as near edge server may provide less latency for the delivery of content. For instance, modern web servers have lots of dynamically-generated pages , and dynamic websites dominate web traffic, especially ones that have dynamic content such as streaming music or streaming videos.

To improve the quality of the user satisfaction (QoE) by making data available to users, and offloading the processes to proxy servers or by caching portions of dynamic pages , as well as creating pages with compositions upon access to the page are all effective techniques. Yuan et al. [13] suggested not to transfer the central information to the clients and also offloading or caching on the edge server in order to decrease the speed of application. In addition, filtering the majority of server requests into web proxy servers can significantly decrease the server's load. Chen et al. [14] introduced the idea of using network caching to make use of the storage capacity of multiple networks in order to reduce traffic on networks.

#### **3.1 WHEN TO OFFLOAD: THE PRECISE TIMING**

As conditions on the network are constantly changing as applications run, the any decision regarding workload offloading has to determine the time when the load should be delegated. Also the task scheduler needs to precisely determine the best time to offload with regard to the system's state and conditions. For instance data caching when networks are congested can enhance the performance of the system as well as transferring large amounts of transfer of data to cloud data center is feasible in the event that the connection to the cloud data centers is adequate to allow data

communications. In the last section we have discussed the subject of selecting an offloaded task like data caching, the storage of data and offloading processing and analysis. In this article, we will look at the method of addressing the question of when it is appropriate to offload. The question as to when to take offload can be transformed into a question of when exactly at what times the offloading of workloads will yield the greatest productivity gains while reducing costs, like the consumption of energy and bandwidth. When the offloading of computation is selected the task and the data are divided into smaller chunks. Due to the dynamics of the connections to networks and the accessibility of edge devices the precise timing of workload offloading is crucial for more system performance and reduce use of resources. Furthermore, the order in which execution is performed by the partitioned workload may have an consequences on system performance. Monitoring system performance and the characterization of workloads such as task arrival rates and deadlines could help in making an informed decision about offloading.

### **3.2 WHERE TO OFFLOAD: THE SCHEDULING OF OFFLOADED WORKLOADS**

The offloading of the work can be accomplished by assigning of partitioned tasks to specific edge server and devices. The selection of the appropriate edges servers and edge equipment demands multi-objective optimization, which includes the consumption of energy and the performance of bandwidths, bandwidths for networks and a data privacy security method. In this case an inherent scheduling rule uses energy. Tasks are transferred to cloud servers to save energy. Meanwhile, the tasks that require data are moved to edge servers so that they can provide lower latency and less use on the network. In particular offloaded task scheduling needs to be based on the overall system state including the status of the network, task requirements and device information, for example. If, for instance, the bandwidth of the network is adequate cloud servers could be selected for the execution of workloads and edge servers, as well as local machines are the best locations for the execution of workloads. Additionally, if the work needs low latency, edge servers are the best place to allow task execution. MpOS [8] is among offloading frameworks which complete all tasks that are related to the decision to offload on mobile devices using a the decision tree. The MpOS framework has the potential to reduce power consumption for mobile phones by using the adaptive monitoring method and can lower energy consumption by as much as 55 percent.

### **3.3 ENERGY AND QOS TRADEOFF BETWEEN COMPUTATION AS WELL AS DATA TRANSMISSION**

Today increasing numbers of applications run on smart mobile devices. The quality of the user's experience is the most important method to determine the efficiency of apps and devices. However, mobile phones situated in the middle of networks typically aren't equipped with sufficient resources, such as capacity for storage and computing and battery capacity, making it challenging to satisfy the increasing demands that mobile customers have. To provide better standard services, these resources need to be assigned and scheduled in accordance with the requirements of users and service levels agreements (SLAs). Thus, applications that are sensitive to delays should be

prioritised, and those that require computation should have sufficient computing resources. To attain this, "quality of service" (QoS) is an individual's perception of quality of service as well as the performance of the devices, systems or networks as well as software. The transfer of calculations to servers at the edge and returning the outcome of the computation back to mobile devices could drastically reduce the requirement for the resources available to the mobile phone. In order to offload computations, you must to comply with QoS requirements and QoE. It is also necessary to create an appropriate schedule for offloading tasks and determine the time of offloading of each project.

#### **4 COMPUTATIONAL OFFLOADING CHALLENGES AND ISSUES**

This section will focus on the main issues that arise in MEC environments through the concept that offloads computation.

**Resource allocation:** One of the toughest issues to solve. It is determining the amount of resources needed to complete an operation. If the resources aren't sufficient then the offload procedure is the one that will be most preferred. If the available resources are greater than the amount that needed for service then the system won't be used [15].

**Scalability:** Real-time applications typically run by multiple users at once which are controlled by different algorithms responsible for the multitude of demands of users. In order to allow the app to expand without harm, it is essential that the method of offloading needs to be improved in order to ensure that the process of offloading is improved [16].

**Security:** In the process of offloading, tasks as well as user's information are transferred through the network, increasing the possibility of theft and misuse of data. To minimize the risk, it is essential to work with a reputable company once the decision to sell off is made [15].

A tradeoff in energy usage Offloading itself is an energy-intensive procedure that requires energy and bandwidth, therefore the decision to decommission should be made in line with the trade-offs [16].

**Making decisions:** It can be an issue to decide when to let a job go due to a myriad of variables like delays, energy consumption or even payment costs [8].

**Accessibility** Mobile devices have to be connected to the cloud/edge constantly and this is often difficult due to the insufficient coverage of networks, network congestion, the deficiency of bandwidth, and many other issues with networks. [16].

**Mobility:** This is a an issue for connecting the device to its edge[19].

**Load balancing:** Edge nodes and datacentres can get overwhelmed any moment. This can result in delays, and in some circumstances, result not accurate. To prevent this from happening load-balancing is employed to divide tasks between other edge nodes which are underloaded [15]. The load-balancer is a tool that helps to share tasks with other edge no.

**Utilization of resources:** The number of resources available at the edge is limited when compared with cloud-based infrastructure. Therefore, a management of resource utilization is essential to reap the maximum benefits from limited resources while avoiding excessive system burden [20].

## **5 MAIN COMPUTATIONAL OFFLOADING FRAMEWORKS**

This section focuses on the major computational offloading systems that are being developed by researchers to improve various parameters like time and energy, scalability, and so on. Some are examined in relation to edge while others are explored with respect to computing.

Zhang et al. [2] A theoretical framework was proposed to cut down on the energy use based upon wireless conditions parameters that can be used for applications that make decisions to offload. They employed a threshold policy that was based on the wireless transmission model, as well as the energy coefficients ratio of computations in both cloud and mobile environment.

Orisini et al. [5] suggested the CloudAware framework to offload tasks to devices that can perform edge computing. They suggested that their CloudAware framework could allow for real-time and ad-hoc communication and would integrate computation offloading and contextual adaptation based on the experience of the developers and the component scheme to take the decision to offload. However, they presented their design without implementing or testing.

Habak et al. [7] The Femtocloud system was invented by The Femtocloud technology, that made use of the capabilities of mobile devices to establish a cooperative computation cluster in solid environments, such as coffee shops , classrooms, and other places where people frequently meet. The framework showed the advantages of being more flexible as compared to the cloudlet. Furthermore it was built on unfixed, cooperative services in the edge layer that make up the networks. The analysis conducted by the creators of their method was conducted on tests and simulations , and proved that the system worked with regard to energy consumption and computation. It also reduced the time to complete computation.

Huang et al. [9] looked into wireless-powered MEC networks. They have developed a deep learning online offloading algorithm called DROO which divides an optimization problem into two distinct problems including how to allocate resources as well as the decision about offloading. The results of their evaluation showed that the algorithm was able to perform as expected. proposed algorithm.

### **5.1 Overview of Optimization Techniques**

Optimization is the ability of an act, which may be a formula, or model, in order in order to create something such as an arrangement or decision as flawless as it is feasible. It could also be described as "a mathematical discipline that concerns the finding of the extreme (minima and maxima) of numbers, functions, or systems" [13]. This refers to the minimization as well as maximization. The techniques of optimization can be employed to solve an optimization problem that could be single or multi-objective. Single-objective optimization is a method to tackle a single purpose to offer the best solution for each problem. Multi-objective Optimization helps accomplish multiple objectives at the same time and gives a range of possibilities instead of an all-encompassing solution [12]. The methods of optimization may be classified in linear as well as Nonlinear Programming Optimization. Programming optimization for linear programs is an objective

function in linear form which seeks to increase or minimize the impact of linear constraints. However nonlinear programming seeks to maximize or reduce objectives that are nonlinear [13]. In addition, nonlinear programming may be classified as deterministic or stochastic. Deterministic optimization approaches employ mathematical models that are strict using identical inputs, they can produce the same result each time. In this instance the best solution is typically local and is not able to be global. Therefore, deterministic optimization techniques are more appropriate for single-objective issues as opposed to multi-objective ones.

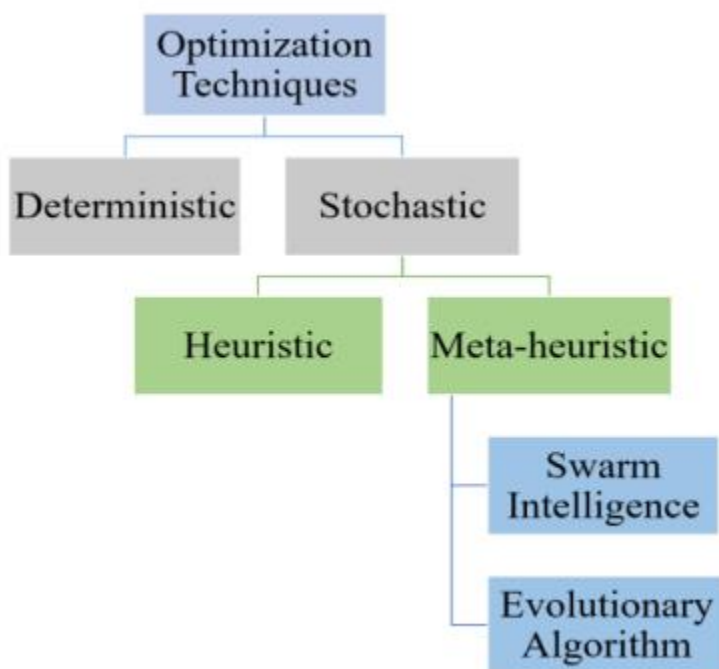


Fig. 3. Optimization techniques

## 5.2 Comparing Existing Solutions

The above solutions are summarized in Table 2, which shows that certain of the optimization strategies suggested to optimize offloading were predictable in nature, while others were based. AI-based systems typically depend on the software in the SI algorithm to optimize offloading. In actuality, SI supports heterogeneous, global and distributed environments, such as MEC. Additionally, SI is produced by automatic, self-organization and adaptive methods. In this regard, we examine the solutions more thoroughly in order to determine the best one to use in the study. In order to achieve this, the most appropriate requirements were determined as follows:

- 1.) Algorithm: SI algorithm is employed to maximize offloading.
- 2.) Distribution: Determines whether the architecture is centralized in cloud, or distributed on an edge layer.



3.) Optimization parameter: Parameters to be considered during the optimization.

(1) Time: The total execution time and transmission time for every task.

(2) Energy Consumption of energy for each job (execution as well as transmission).

(3) Cost the cost of the application's execution.

(4) Scalability The capacity of the application to expand without causing harm.

(5) Utilization of resources Utilizing scarce resources without creating an increase in the overhead of the system.

(6) Balance of load A capability to share work by collaborating with edge nodes which are under-loaded.

(7) Queue congestion is the avoidance of queue congestion in situations where the arrival rate of tasks exceeds the rate of service which results in system overhead.

(8) No. of repetitions: It is correlated to the duration of the work. In accordance with the requirements, there is a comparison of models based on SI.

## **6 DISCUSSION, OPEN ISSUES, AND FUTURE DIRECTIONS**

It was demonstrated by this research that over the last few times, optimization methods are being developed to optimize offloading decision-making, especially Swarm Intelligence (SI) models because they provide a perfect match to the fluid and distributed component in edge computing. In reality, SI produces a better solution in the shortest time and is able to meet the requirements of real-time applications.

One of the major research areas is the integration of the SI-based offloading theories and edge computing to improve central solutions and make them more adaptable to the shared schema and while taking into account different objectives. As was mentioned previously, Cuckoo Search seems to be an ideal algorithm to tackle multi-objective offloading optimization since it delivers excellent performance in this domain when compared with others AI algorithm, which is shown in. In the end, applying Cuckoo into an edge-based system will enhance offloading and enable more secure solutions to assist mobile devices that run demanding applications. Furthermore, the offloading of computational computation to the edge could be enhanced by using CSA along with the parallel processing between edges that can boost the capacity of computation and reduces time..

## **7. CONCLUSION**

The number of individuals using mobile devices to access the internet is rising. In fact, during the last several years, the number of individuals utilizing mobile devices has exploded. Mobile devices should be able to run real-time applications like gaming, e-commerce, healthcare, and many more. Additionally, users of mobile devices anticipate that the quality of service (QoS) they get will be of a high standard comparable to that of desktop-based programmers. On the other side, real-time applications need more resources, including the capacity to store data, power from the battery, computing power, and storage. Offloading involves delivering all or a portion of a mobile task to

a high-end source, such as edge servers or cloud servers, where it is processed before being sent back to the mobile device. Making the most of a Smartphone's resources is made easier by doing this. Making the most of a Smartphone's resources involves offloading. On the other hand, offloading computation requires effort and time, both of which are crucial for real-time applications to operate at their best.

## REFERENCES

- [1] Alok Tripathi; Abhinav Mishra, "Cloud computing security considerations", IEEE 2011
- [2] Yongmin Zhang; Xiaolong Lan; Ju Ren; Lin Cai, "Efficient Computing Resource Sharing for Mobile Edge-Cloud Computing Networks", IEEE, 2020
- [3] Prasadu Peddi (2017) "Design of Simulators for Job Group Resource Allocation Scheduling In Grid and Cloud Computing Environments", ISSN: 2319- 8753 volume 6 issue 8 pp: 17805-17811.
- [4] TAO Jing; JIN shen; TANG Jia; JI Yutong; ZHANG Ning, "Application of Cloud Edge Collaboration Architecture in Power IoT", IEEE 2020
- [5] Tianchu Zhao; Sheng Zhou; Linqi Song; Zhiyuan Jiang; Xueying Guo; Zhisheng Niu "Energy-optimal and delay-bounded computation offloading in mobile edge computing with heterogeneous clouds", IEEE 2020
- [6] Lih-Jen Kau; Cheng-Chang Chung; Ming-Sian Chen "A cloud computing-based image codec system for lossless compression of images on a Cortex-A8 platform", 28-30 Nov. 2012, IEEE
- [7] Nandiwardhana Waranugraha; Muhammad Suryanegara, "The Development of IoT-Smart Basket: Performance Comparison between Edge Computing and Cloud Computing System", IEEE, 2020
- [8] Michael Fagan; Mohammad Maifi Hasan Khan; Bing Wang, "Leveraging Cloud Infrastructure for Troubleshooting Edge Computing Systems", 17-19 Dec. 2012, IEEE
- [9] Per Skarin "Cloud-Assisted Model Predictive Control", IEEE, 2019
- [10] Erdinc Korpeoglu; Cetin Sahin; Divyakant Agrawal; Amr El Abbadi; Takeo Hosomi; Yoshiki Seo, "Dragonfly: Cloud Assisted Peer-to-Peer Architecture for Multipoint Media Streaming Applications" , IEEE, 2013
- [11] Prasadu Peddi (2020), MINING POSTS AND COMMENTS FROM ONLINE SOCIAL NETWORKS, Turkish Journal of Computer and Mathematics Education, Vol 11, No 3, pp: 1018-1030
- [12] A. Akinbi; E. Pereira; C. Beaumont, "Evaluating security mechanisms implemented on public Platform-as-a-Service cloud environments case study: Windows Azure", IEEE, 2013
- [13] Utsav Drolia; Rolando Martins; Jiaqi Tan; Ankit Chheda; Monil Sanghavi; Rajeev Gandhi; Priya Narasimhan "The Case for Mobile Edge-Clouds", IEEE, 2013
- [14] Eyal De Lara; Carolina S. Gomes; Steve Langridge; S. Hossein Mortazavi; Meysam Roodi, "Poster Abstract: Hierarchical Serverless Computing for the Mobile Edge", IEEE 2016
- [15] Prasadu Peddi (2016), Comparative study on cloud optimized resource and prediction using machine learning algorithm, ISSN: 2455-6300, volume 1, issue 3, pp: 88-94.

[16] Hongxing Li; Guochu Shou; Yihong Hu; Zhigang Guo "Mobile Edge Computing: Progress and Challenges", 2016, IEEE

[17] Yogesh Hole et al 2019 J. Phys.: Conf. Ser. 1362 012121

**Author Bibliography:**

**Naga Lakshmi Somu** is working as Assistant Professor in St. Ann's College for Women Hyderabad, Telangana, India. She is Research Scholar at Department of Computer Science & Engineering, Shri Jagdishprasad Jhabarmal Tibrewala University, Jhunjhunu, Rajasthan, India. She has obtained her MCA St. Ann's College for Women, Hyderabad, Telangana, India. Her research interests are Internet Cloud Computing.

**Email:** [lakshmi.msccs@gmail.com](mailto:lakshmi.msccs@gmail.com)

# Survey Of Iot Threats And Countermeasures: Identifying Solutions And Addressing Future Challenges

Pushpa Latha Thumma<sup>1</sup>, Dr Prasadu Peddi<sup>2</sup>

<sup>1</sup>Research Scholar, Dept of Computer Science, Shri Jagdishprasad Jhabarmal Tibrewala University, Rajasthan.

<sup>2</sup>Assistant Professor, dept of computer science and Engineering, Shri Jagdishprasad Jhabarmal Tibrewala University.

---

## ABSTRACT

The Internet of Things (IOT) may be described in a variety of ways. It encompasses many parts of your life, from linked homes and communities to connected automobiles and streets, roadways, and gadgets that monitor your activities. It is expected that one trillion Internet-connected devices will be accessible by 2020 as the eyes and ears of all apps linking these linked objects. The Internet of Things enables billions of people to communicate internationally over a public and private internet protocol network. Around 12.5 billion gadgets and ordinary things were linked to the Internet in 2010. The core concept of the Internet of Things (IoT) has been around for about two decades. Many companies and scholars are fascinated by its enormous effect on society and everyday life. IoT vulnerabilities are becoming increasingly common as the number of IoT devices on the market grows. According to analyses and findings, the enormous adoption of IoT has exposed it to new security dangers. This paper discusses IoT security concerns as well as other unresolved topics. The article also provides a foundation for future research. It also includes a list of security protocols that may be used to support a broad range of IoT applications.

**Keywords:** IoT, IoT applications, IoT Security, Edge Computing, Distributed Systems, Machine Learning.

## 1. INTRODUCTION

IoT-connected devices will reach 75 billion in 2025, according to 1 These devices can improve people's lives as well as the efficiency of businesses. However, they increase vulnerability to cybercriminals and hackers. IoT-enabled components and devices are increasingly interdependently integrating into every sector of work. The operations of interdependent components will be severely affected if one of these components is damaged. Experts and policy-

makers are becoming more concerned about protecting IT infrastructure and information from such attacks. Cyber-sabotage attacks are most likely to target people, technology and enterprise constituents. All industries have made industrial security a top priority. Many industrial control systems (ICSs) are legacy systems that have connectivity issues and are vulnerable to attacks. These systems were not intended for such connectivity and security design upgrades are required. The Internet of Things is gaining popularity, connecting every piece of equipment to it to make it easier to manage and communicate with them. This has led to an increase in the number and severity of cyberattack vectors as more industrial control systems become interconnected. The key to successful IoT application to industry is the ability to monitor the network infrastructure in real time and the associated service operations. This will allow for the automation of data delivery, which can lead to secure and high-quality services.

The Internet of Things' future is anticipated to be endless [4]. You can speed up the growth in the field of Industrial Internet through speeding up the development and that of integrating artificial intelligence mass use, automation, regulation of their usage and increasing the speed of its use. Massive amounts of actionable information will be available to you, which can also lead to automation of business processes. The IT market will see a significant shift. The Internet of things trend isn't just for the commercial and industrial sectors. It also surrounds us at our home as it controls various appliances and hospitals. We must ensure that these technologies are safe. There are many benefits, but also dangers. Insecurity can make us vulnerable to security threats and vulnerabilities. There is a possibility for cybercriminals to take advantage of security weaknesses to gain access to data and other information. They may misuse and alter it in order to use it for their own benefit. You could be at risk to various types of attacks, such as flooding, interference, denial-of-service (DOS) black holes, wormholes and black holes as well as Sybil and sinkhole types. Each layer is able to fulfill the security requirements of another layer the security requirements vary from one layer to the next [5].

## **2. What is IoT?**

Kevin Ashton created the term "Internet of Things" (IoT). It was used primarily for basic things. "A basic creation" by "adding radio frequency ID and restart operation to everyday items." We chose the term "things" over the word "devices" simply because this technology encompasses everything that can be connected to the Internet. Although the term may seem somewhat new to us, it actually existed in real life since the seventies, in particular 1974. This was the year that automated teller machines were introduced, and they are now considered to be one of the IoT devices. However, 87% of IoT users did not understand the meaning of the term in 2015. These paradoxes are quite bizarre, as in 2008 Cisco reported that there were more devices connected to the Internet than people. All over the globe. In 2018, this number was almost five billion.



most secure and practical solutions. The manufacturer should make sure the devices are only authorized to contact services. It is imperative that you verify the authenticity of all communications before sending and receiving data. Fig. 2 shows the attack on the various layers of the Internet of Things.

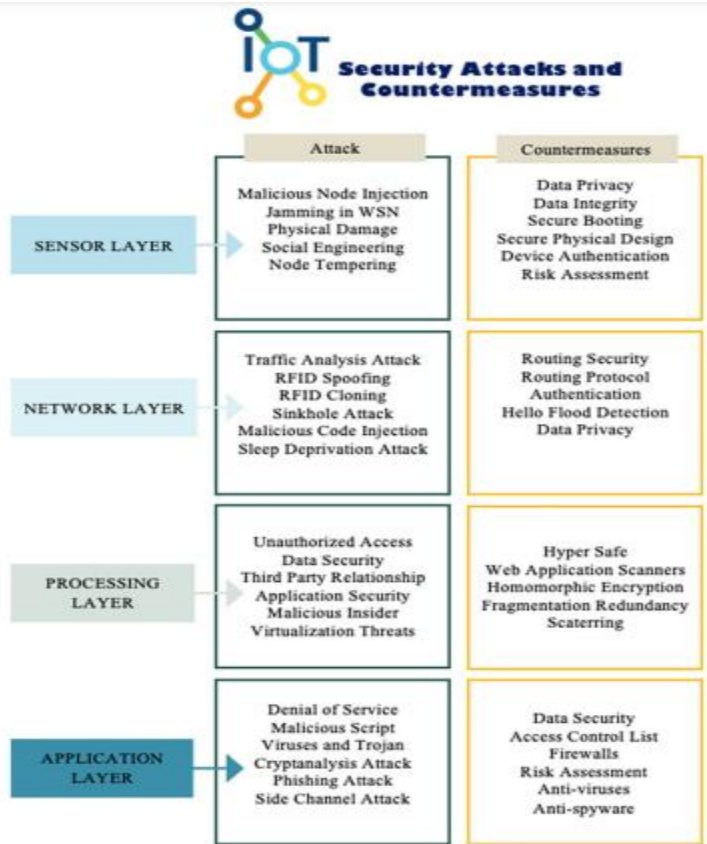


Fig 2: IOT Attack and Countermeasures.

### 5. Security analytics

The analysis process includes gathering data, running analyses on it, assessing its effectiveness, and finally submitting reports. If any errors or illegal activity is found here, we will take care of it. Additionally, it offered fresh models that can anticipate and detect suspicious activity using artificial intelligence, big data, and other tools. The demand for a wider range of security analysis techniques is being driven by the urgent need to detect security lapses and assaults.

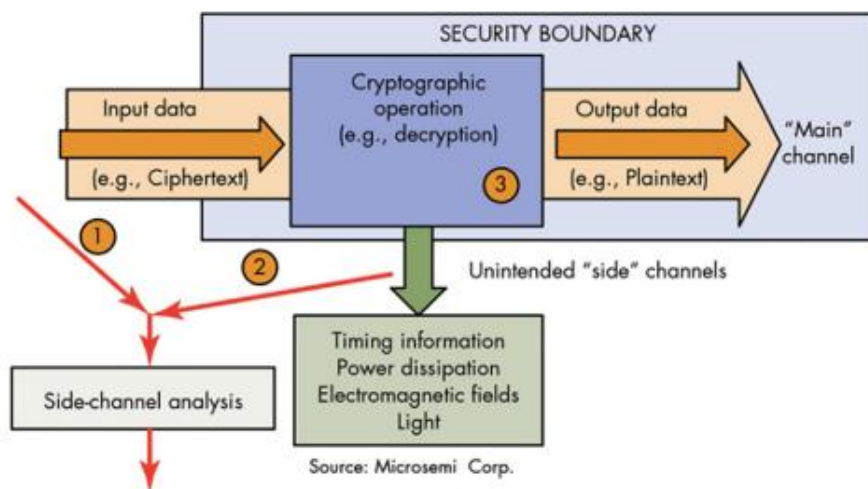


Fig. 3. Security-side-channel attacks .

## 6. CONCLUSION

This article examines the difficulties brought by privacy and security concerns in IoT devices. In addition, it examines the most major applications, such as "smart city," "smart housing," and "smart house," along with the associated dangers and hazards. In addition, we walked over each method and reviewed its implementation. In addition, we reviewed the potential dangers presented by each Internet of Things layer as well as the necessary steps to take against them. In addition, we discussed the most important techniques and tools for developing such a system, which will contribute to enhancing the security of the Internet of Things.

## References

- [1] H.A. Salam, A. Ahmed, A. Muhammad, The Internet of smart things in the field of health care, *J. Acad. Res.* (2019).
- [2] M. Humayun, M. Niazi, N.Z. Jhanjhi, M. Alshayeb, S. Mahmood, Cybersecurity threats and vulnerabilities: A systematic mapping study, *Arab. J. Sci. Eng.* 45 (4) (2020) 3171–3189.
- [3] M.A. AlZain, B. Soh, E. Pardede, A survey on data security issues in cloud computing: From single to multi-clouds, *J. Softw.* 8 (5) (2013) 1068–1078.
- [4] H. Alshambri et al., Cybersecurity attacks on wireless sensor networks in smart cities: an exposition, *Int. J. Sci. Technol. Res.* 8 (1) (2020).
- [5] M. Aazam, et al. PRE-Fog: IoT trace based probabilistic resource estimation at Fog. 2016 13th IEEE Annual Consumer Communications and Networking Conference. CCNC. 2016.
- [6] S. Sicari, A. Rizzardi, L.A. Grieco, A. Coen-Porisini, Security, privacy and trust in internet of things: The road ahead, *Computer Netw.* 76 (2015) 146–164.
- [7] D.K. Alferidah, N.Z. Jhanjhi, A Review on Security and Privacy Issues and Challenges in Internet of Things, *Int. J. Computer Sci. Netw. Sec. IJCSNS* 20 (4) (2020) 263–286.
- [8] B. Atoum. History of Internet of things. 2020; Available from: <https://e3arabi.com/>.



- [9] B. Chu, W. Burnett, J.W. Chung, Z. Bao, Bring on the bodyNET, *Nat. News* 549 (7672) (2017) 328–330.
- [10] P. Sethi, S.R. Sarangi. *Internet of Things: Architectures, Protocols, and Applications*. 2017.
- [11] D.K. Alferidah, N. Jhanjhi. *Cybersecurity Impact over Bigdata and IoT Growth*. 2020 International Conference on Computational Intelligence (ICCI). Bandar Seri Iskandar, Malaysia. 2020. 103–108. doi: 10.1109/ICCI51257.2020.9247722..
- [12] P. Sethi, S.R. Sarangi, *Internet of Things: Architectures, Protocols, and Applications*, J. Electric. Computer Eng. 2017 (2017) 1–25.
- [13] J. Vasseur, et al. The ip routing protocol designed for low power and lossy networks. *Internet Protocol for Smart Objects (IPSO) Alliance*. 2011.
- [14] Prasadu Peddi (2018), “A Study For Big Data Using Disseminated Fuzzy Decision Trees”, ISSN: 2366- 1313, Vol 3, issue 2, pp:46-57.
- [15] K. Uppalapati, *How IoT protocols and standards support secure data exchange in the IoT, Ecosystem? (2019)*.
- [16] M.A. Alzain, E. Pardede. Using multi shares for ensuring privacy in database-as-a-service. In: 2011 44th Hawaii International Conference on System Sciences. 2011. IEEE.
- [17] B.O. Al-Amri, M.A. AlZain, J. Al-Amri, M. Baz, M. Masud, A comprehensive study of privacy preserving techniques in cloud computing environment, *Advanc. Sci. Technol. Eng. Sys. J.* 5 (2) (2020) 419–424.
- [18] O.S. Faragallah, A. Afifi, W. El-Shafai, H.S. El-Sayed, E.A. Naeem, M.A. Alzain, J.F. Al-Amri, B. Soh, F.E.A. El-Samie, Investigation of chaotic image encryption in spatial and frft domains for cybersecurity applications, *IEEE Access* 8 (2020) 42491–42503.
- [19] O.S. Faragallah, A. Afifi, W. El-Shafai, H.S. El-Sayed, M.A. Alzain, J.F. Al-Amri, F.E. A. El-Samie, Efficiently encrypting color images with few details based on rc6 and different operation modes for cybersecurity applications, *IEEE Access* 8 (2020) 103200–103218.
- [20] M.A. AlZain, et al. Managing Multi-Cloud Data Dependability Faults, in *Knowledge-Intensive Economies and Opportunities for Social, Organizational, and Technological Growth*. 2019. IGI Global. 207–221.
- [21] Yogesh Hole et al 2019 *J. Phys.: Conf. Ser.* 1362 012121

### **Author Bibliography:**

**Pushpa Latha Thumma** is working as an assistant professor at St. Ann's College for Women in Hyderabad, Telangana, India. Presently, she is a research scholar at Shri JYT University, Rajasthan. She obtained her MCA from St. Ann's College for Women, Hyderabad, Telangana. She has written books on cyber security and information technology fundamentals. Her research interests are the Internet of Things, artificial intelligence, and cyber security.

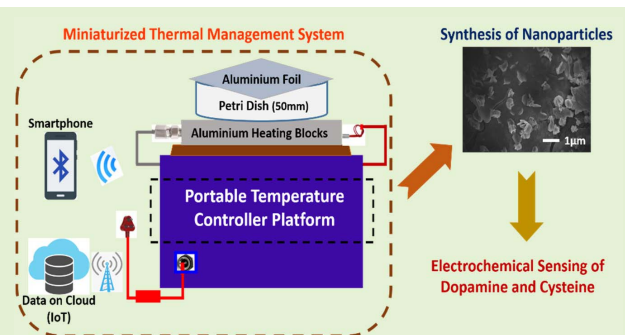
[pushpareddy28@gmail.com](mailto:pushpareddy28@gmail.com)

# Integrated Temperature Controlling Platform to Synthesize ZnO Nanoparticles and Its Deposition on Al-Foil for Biosensing

Madhusudan B. Kulkarni, *Student Member, IEEE*, Prasanth K. Enaganti<sup>1</sup>,  
Khairunnisa Amreen<sup>1</sup>, and Sanket Goel<sup>1</sup>, *Senior Member, IEEE*

**Abstract**—Nanoparticles are considered important in numerous applications, therefore it is very imperative to have an easy, effective, and efficient nanoparticle synthesis technique. This work is aimed at the design and development of a portable thermal management device with features such as low-cost, accurate, easy-to-use, and miniaturized for nanoparticle synthesis and application. The main function of the proposed device is to control, manipulate, and monitor the cartridge heater and sensor respectively. The device is incorporated with a NodeMCU integrated with a PID temperature controller with a precision of  $\pm 2^\circ\text{C}$ . A customized cartridge heater was used for heating purpose and a resistive temperature sensor acts as a feedback loop. A small petri dish of 50 mm (D), as a reservoir for the synthesis of ZnO nanoparticles, was kept at  $70^\circ\text{C}$  for 3 h. The obtained results were subjected to FESEM and XRF characterization techniques to analyze surface morphology of nanoparticle samples which were obtained as flower-like shape and nanobars structure of 830nm in width. The synthesized ZnO nanoparticles were verified for electrocatalytic sensing of Dopamine. As a proof-of-principle, to check the Chemical Vapor Deposition of the synthesized ZnO nanomaterial on the bare aluminum foil of  $18\ \mu\text{m}$  at a small scale, without any complex measures or need of a controlled environment, is also provided. Further, this aluminum foil was used as a working electrode where cysteine was successfully sensed electrochemically. This portable thermal device can be used for carrying out several thermal-based reactions and analysis.

**Index Terms**—NodeMCU, nanoparticles (NPs), electrochemical, zinc oxide (ZnO), film deposition, field emission scanning electron microscope (FESEM), X-ray fluorescence (XRF).



## I. INTRODUCTION

IN RECENT decades, physically and chemically synthesized nanoparticles and nanocomposites have drastically drawn attention which is considered to be critical elements in various applications like photoelectric [1], electrochemical [2], sensing [3], [4], synaptic learning [5], photoluminescent [6], photovoltaic [7], spectroscopic [8] properties, and other fundamental researches [9]. Nanoparticles exhibit a wide range

Manuscript received December 30, 2020; accepted January 17, 2021. Date of publication January 22, 2021; date of current version March 5, 2021. This work was supported by the Center for Human Disease Research (CHDR), BITS-Pilani, Hyderabad Campus. The work of Khairunnisa Amreen was supported by the Science and Engineering Research Board-National Post Doctoral Fellow (SERB-NPDF) Scheme under Grant PDF/2018/003658. The associate editor coordinating the review of this article and approving it for publication was Dr. Chirasree Roychaudhuri. (*Corresponding author: Sanket Goel.*)

The authors are with the MEMS, Microfluidics and Nanoelectronics Laboratory, Department of Electrical and Electronics Engineering, Birla Institute of Technology and Science (BITS) Pilani, Hyderabad Campus, Hyderabad 500078, India (e-mail: sgoel@hyderabad.bits-pilani.ac.in; sanketgoel@gmail.com).

Digital Object Identifier 10.1109/JSEN.2021.3053642

of applications in the domain of biomedical, energy, drug delivery, optical materials, and so on [10]–[13]. Therefore, it is very essential to design and develop a portable device with a small scale platform for synthesizing nanoparticles and nanomaterials. Nanoparticles and nanocomposites can be well synthesized with a portable platform, with monodispersed volume. Hence, there is much needed handy device for the same [14], [15].

Zinc oxide particles, due to their appealing physicochemical properties hold significant promise in multiple applications [7], [16], [17]. ZnO, a powerful metal-oxide-semiconductor with a large-direct band gap (3.37 eV), is a potential photocatalyst because of its electrochemical efficiency [18]. The ZnO-based micro-/nanostructures are highly necessary for fundamental research and commercial needs and are highly desirable and are used as optical sensors [19], [20]. One of the efficient ways for the synthesis of nanoparticles is the deposition of nanoparticles as thin films using various chemical vapor deposition (CVD) techniques [21]. Various nanoparticles are synthesized using a different technique for numerous appli-

TABLE I

COMPARISON OF CONVENTIONAL WITH MICROFLUIDIC TECHNIQUES

Sl.No	Parameters	Traditional Technique	Microfluidic Technique
1	Size	Bulky Instrument, Laborious process [26]	Miniaturized tool
2	Cost	Expensive oven/muffle furnace [43]	Low-cost microdevice
3	Temperature facets	High pressure, Reaction temperature [44]	Low-temperature operation
4	Equipment and Containers	Autoclave; Batch reactors [45]	Microfluidic channel
5	Output Processing	Large output processing [46]	Microscale approach, Minuscule operation
6	Power Requirement	High power consumption [47]	Low power consumption

cations, one such method was notified, the green synthesized nanoparticle [22]. Here, a conventional approach was incorporated for preparing iron and gold-based nanoparticles that are used for biomedical and environmental applications [23]. In another method, barium titanate nanoparticle synthesis was carried on sol-gel electrospray for bio-medicinal applications [24].

The conventional methods need sample preparation in the macro-scale, with a high-pressure thermal management system, for heating purposes which makes them more expensive [25]. Different conventional techniques that have been developed to produce ZnO micro/nanostructures like liquid-phase process [26], hydrothermal [27], coprecipitation [28], sol-gel [29], optical [30], sputter deposition [31], ion-beam assisted deposition [32], direct nitridation [33], further, an unusual epitaxial technique is used to grow ZnO nanocrystals [34], but most of these methods often suffer from the longer period, bulky batch reactors and are more costly [35], [36]. The real challenge of these conventional methods is precise nucleation control [37]. Due to the relatively low reproducibility and poor control over conventional batch reaction processes, there is still considerable demand to improve the delicate and complex methods to meet the practical needs of various fields [38].

The temperature controller module is one of the essential and most widely used devices in research fields such as home appliances, biomedical, healthcare, industrial automation, heating, and cooling applications and there is the need of time now-a-days because of its rising applications [39]. An Arduino based portable temperature controller device was designed, developed, and simulated with a PID controller [40] method where it showed good output stability and accuracy of  $\pm 2^\circ\text{C}$ . This temperature controller comes with versatile benefits like stability, accuracy, reliability, and good ramping rate [41], [42]. The general comparison of proposed and conventional methods is given in Table I.

The proposed method for nanoparticle synthesis plays a vital role in establishing a microfluidic environment as the developed microdevice can be used for synthesizing nanomaterials on a microscale using a microfluidic channel in the future prospects. Further, microfluidic enables various features in a minuscule atmosphere with a reduced sample volume, execution time, low-temperature process [48], [49], and also

TABLE II

SUMMARY OF MICROFLUIDIC APPROACH WITH PROPOSED APPROACH

Sl.No	Specifications	Microfluidic Approach	Proposed Approach
1	Microchannel Design	Tubular Microreactor	Chamber-based
2	Temperature range	100-140°C	70°C
3	Temperature sensitivity	$\pm 1^\circ\text{C}$	$\pm 2^\circ\text{C}$
4	Heating element	Commercial hot plate	Customized Cartridge heater
5	Sensing source	Thermocouple	Pt100 RTD
6	Handling Process	Manual	Automated
7	Synthesized nanomaterials	Ag NPs	ZnO NPs and Al Foil based deposition technique
8	Particle size distribution	250-400nm	7.9nm
11	Power Usage	100-240V	12V
12	Real-time Data Logging Facility	Only Onboard	IoT enabled module

provides automated, integrated, and miniaturized operation on a single platform. Herein, we have compared the microfluidic approach with the proposed approach through various specifications. For instance, Lin *et al.* [50] demonstrated a continuous flow-based tubular microreactor for the synthesis of silver nanoparticles in a microfluidic platform. A comparison of the continuous flow-based microreactor approach [50] with the proposed approach is provided in Table II. Further, with these specifications, the proposed method can be easily used for various micro/nanoscale based biosensing applications.

The present work describes the development of a low-cost, automated, reliable, portable thermal management device for the synthesis of nanoparticle and clean room free chemical vapor deposition. The device has a NodeMCU microcontroller which is the main chip for instructing and controlling the heater and sensor. The driver circuit acts as a switching profile for the heater, and, hence, it takes care of high and low signals. The electronic components were mounted and integrated onto a single printed circuit board covered by a 3D printed casing. The device has a real-time data logging facility that is directly connected to a server cloud through IoT (ThingSpeak) by creating the channel Ids for data accessing and storage. This proposed device eliminates the need for a bulky conventional hot air oven or muffle furnace for the synthesis of nanoparticles. Even more, it eliminates the necessity of autoclave for the nanoparticle synthesis by hydrothermal reaction. A simple petri dish is used in the process, and the entire procedure can be carried out in a short time. A minimal volume ( $\mu\text{l}$  to a few ml) is sufficient for the synthesis of nanoparticles. Here, the ZnO nanoparticles were successfully synthesized and used for electrochemical sensing of dopamine. In further, ZnO particles were deposited as a thin film on a clean aluminium foil sheet which was further used for electrochemical sensing cysteine.

## II. EXPERIMENTAL

### A. Integrated Portable Thermal Management System

For the synthesis of nanoparticles, the thermal management system plays a vital role and it is essential to provide the desired temperature for the said amount of time accurately

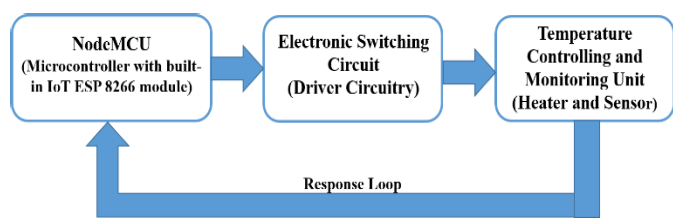


Fig. 1. Block diagram representation of Temperature controlling and monitoring unit.

and consistently [51]. Here, a low-cost, easy-to-use automated and integrated device is being designed and developed for universal biochemical applications. It includes a 32-bit microcontroller chipset [52] with 4 MB of memory and operates in the 3 – 3.6 V range, which is responsible for controlling and coordinating the inputs and outputs connected to it. The advantage of this kind of microchip is that it has an on-board ESP 8266 (IEEE 802.11 b/g/n) Wi-Fi module which enables IoT features like geotagging of data and cloud computing [53]. A simple block diagram of the temperature controlling and monitoring unit is shown in Fig. 1.

The most common and widely used semiconductor devices such as Bipolar Junction Transistor (BJT) and Metal Oxide Semiconductor Field Effect Transistor (MOSFET) have several advantages that can be used as an amplifier, oscillator, and switching circuit. Here, both the devices were used for designing the driver circuit to control the current flow switching across heaters, functions as a logic ‘0’ and ‘1’, respectively. Cartridge heaters ([www.ragatiyaheaters.in](http://www.ragatiyaheaters.in)) were used as a heating medium as these are voltage controlled and consumes less power with fewer amperes of current for driving to maximum temperature in less time. These customized cartridge heaters were made up of stainless steel (SS) of higher grades. The schematic diagram of the temperature controller system is given in Fig. 2. The power rating is 38W and the customized heater dimensions are 3 mm (D) × 25 mm (L). Pt100, a resistance temperature detector (RTD), was used for monitoring the temperature connected to the microchip as a feedback loop, across the specimen. The Pt100 temperature sensor was used due to its high accuracy, wide temperature range, good stability, and repeatability [54].

IRFZ44N (MOSFET) is used for electronic circuit switching and amplifying along with a limiting resistor to drive the heaters. The pulse width modulation (PWM) signal gets triggered by an embedded controller. Herein, an open-source software ([www.arduino.cc](http://www.arduino.cc)) was used to manipulate the input instruction to control the current towards the cartridge heater. PID is one of the methods available on-board module of microcontroller used for controlling the desired temperature with a precision of  $\pm 2^{\circ}\text{C}$ . The proposed device can also be used for microfluidic nucleic acid amplification and rheological applications [55].

### B. Cost Estimation Analysis

The cost estimation analysis of the proposed device is presented in Table III. The cost calculation for all the components is analyzed in terms of USD (\$). Also, we have compared

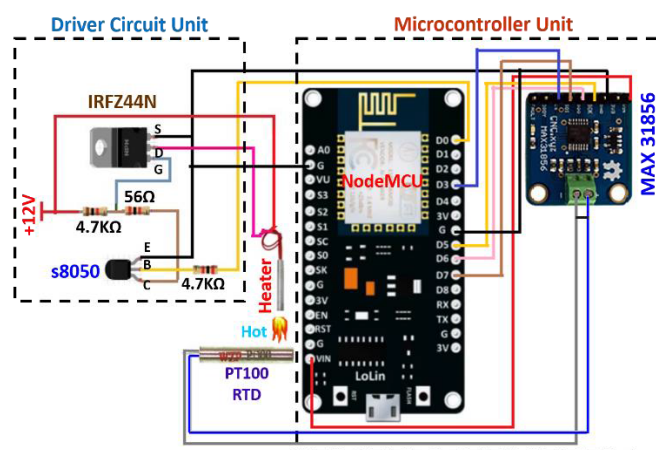


Fig. 2. NodeMCU based temperature controller module.

TABLE III  
COST ESTIMATION OF PROPOSED DEVICE

Sl.No	Components	Cost/Price (\$)
1	NodeMCU	3.40
2	MAX31856	7.89
3	Pt100 Sensor	1.56
4	s8050	0.14
5	IRFZ44N	0.88
6	Cartridge Heater	4.76
7	Resistors and Connectors	0.14
<b>TOTAL ESTIMATION</b>		<b>18.77</b>

the proposed system with the existing commercial hot plate device with parameters like cost, size, accuracy and portability, and power consumption. In all the aforementioned aspects, the proposed thermal management system is preferable and it has additional features with included PID controller and IoT for real-time data logging facility. Further, the proposed new device was used as a heating source with the desired temperature for electrochemical sensing applications.

### C. Materials

1) *Chemicals and Reagents*: Dopamine (98%), Cysteine (97%), graphitized mesoporous carbon (>99.95%), Zinc nitrate (98%), Ascorbic acid ( $\geq 99\%$ ), Sodium hydrogen phosphate dibasic, and monobasic ( $\geq 99.99\%$ ) with high purity rate, were purchased from Sigma Aldrich.

2) *Apparatus*: Electrochemical sensing of dopamine and cysteine was carried out using Cyclic Voltammetry (CV) (OrigaFlex from OrigaLsys, France).

### D. Synthesis of ZnO Nanoparticle

The mixture of zinc nitrate ( $\text{Zn}(\text{NO}_3)_2$ ) and ascorbic acid ( $\text{C}_6\text{H}_8\text{O}_6$ ) were prepared in the ratio of 4:1. In 4 ml of DI water, the precursors were added and kept for sonication for 30 min. 4 ml of the reaction mixture was transferred onto the petri dish (diameter = 50 mm) which was placed on an aluminium heating block of the thermal system for heating purposes. Herein, ascorbic acid acted as a reducing agent to

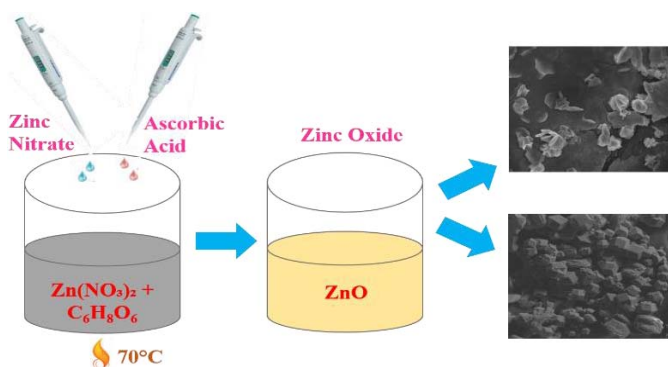
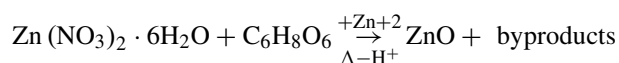


Fig. 3. Schematic process of ZnO nanoparticle synthesis.

form ZnO by the reaction [56].



A neutral pH was maintained with 1 mM of NaOH. The reaction mixture was kept for heating at a set temperature of 70°C for 3 h. After the process, the obtained yellowish-colored precipitated liquid was tested by FESEM and EDX characterization to analyze the formed ZnO. The preparation method for the synthesis of ZnO nanoparticles is given in Fig. 3. At an initial stage, synthesis of ZnO nanoparticles was carried out for 4 mL of fluid, but even lower volume can be used.

### E. Electrochemical Sensing

The cyclic voltammetry (CV) measurements were carried out using a 2B grade HB pencil graphite chemically modified with Graphitized Mesoporous Carbon (GMC)- Zinc Oxide (ZnO) composite and further it was used as working electrode (WE). Besides, the aluminium foil deposited with ZnO thin film was also investigated as working electrodes, and a platinum wire was used as the counter while Ag/AgCl was used as a reference electrode in neutral phosphate buffer solution (PBS) at 10 mV s<sup>-1</sup>.

## III. RESULTS AND DISCUSSIONS

### A. Heating Unit for the Synthesis of NPs

The 3D printed integrated heating unit was developed and all the electronic components were mounted on a printed circuit board (PCB). NodeMCU is the heart of the complete device which gives the instructions and commands to sensors and driver circuit. Pt100 temperature sensor was incorporated with the MAX31856 breakout module for reducing the fluctuation and limits the error and noise. The feedback loop acts as an intermediate between the temperature sensor and controller sending the response of the heater continuously, and, thus, the desired temperature was maintained for a constant time. The temperature controller calibration was done and the accuracy of ±2°C was achieved. The real-time temperature values were directed to the ThingSpeak cloud through the IoT module for data accessing and data storage. The device was made as plug-and-play for power sourcing to the complete PCB board. The real-time temperature data logging was an

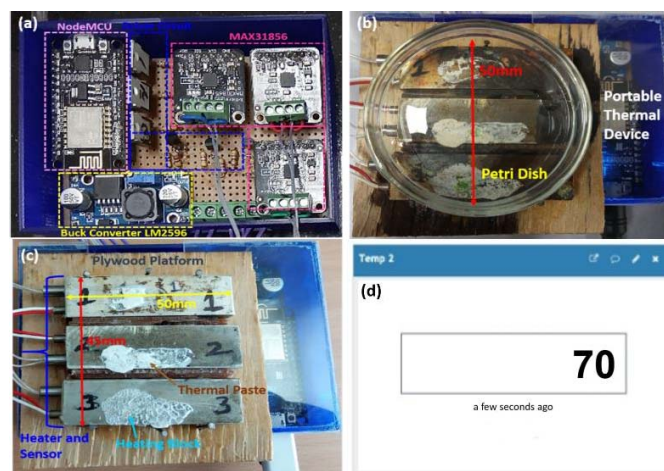


Fig. 4. (a) Complete Automated Electronic Device, (b) Petri dish placed on the device, (c) Heating Block Stage. (d) IoT ThingSpeak data logging platform.

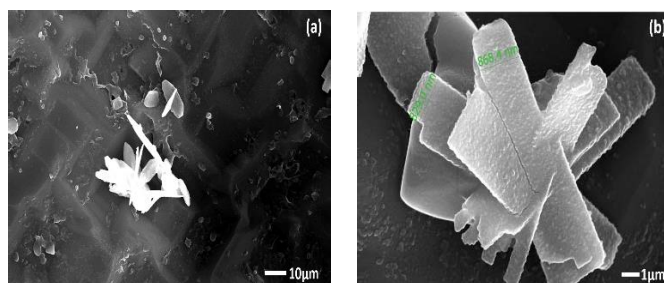


Fig. 5. FESEM images for the different wavelength of ZnO flower-shaped and nanobars at a magnification of (a) 8,000 x (b) 60,000 x.

additional advantage for continuous monitoring and storage of the data on the cloud through the controller board. The overall dimensions of the device were 10.4 × 7 × 3.8 cm<sup>3</sup>.

The complete portable heating control thermal device integrated and automated with plug-and-play for powering up the device is presented in Fig. 4. In Fig 4(c), the small petri dish is shown, as used for the synthesis and placed on the heating blocks. The image of the IoT ThingSpeak platform, which is an open-source cloud for real-time data accessing and storage of temperature values, is displayed in Fig 4(d). Additionally, an infrared image was captured from the fluke thermal image camera (PTi120) to know the exact thermal response on top of the petri dish which was set for 70°C. The added feature with ThingSpeak was real-time data logging, allowing an easy path for data storage and analysis. The concept of the design and development of the thermal management system was extended with three heaters and sensors respectively with three aluminium heating blocks for creating the heating stage for the petri dish which is as shown in Fig. 4(a) and 4(b).

### B. Characterization of the ZnO Nanoparticle

#### 1) Field Emission Scanning Electron Microscope (FESEM):

The FESEM images of flower-shaped ZnO nanocrystals are shown in Fig 5(a). The obtained results were analyzed to understand the potentiality of the proposed technique, and the results were compared with existing literature which shows

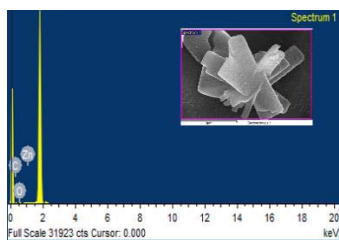


Fig. 6. Processing of the EDX spectrum for Zn, O, C elements.

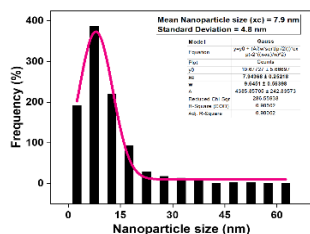


Fig. 7. ZnO nanoparticle size distribution curve.

TABLE IV  
EDX ANALYSIS OF MAJOR ELEMENTS OF ZnO

Elements	Weight (%)	Atomic (%)
Carbon (K)	28.45	40.95
Oxygen (O)	49.16	53.12
Zinc (Zn)	22.39	5.92

similar results [57], [58]. The phase of nanoplates was in a liquid state. The unique bar structures (asymmetrical clusters) of ZnO nanoparticles were successfully synthesized by a proposed portable thermal device, further, these structures were compared with the literature [59], [60]. Fig 5(b) shows the nanobars structured ZnO, wherein the FESEM images give an average bar width of 830 nm.

To characterize the chemical composition of the nanobars, the Energy-dispersive X-ray spectroscopy (EDX) was utilized. As seen in Fig. 6, the EDX spectrum verifies the presence of Zn, C, and O in ZnO nanoparticles.

ImageJ software ([www.imagej.net](http://www.imagej.net)), an open-source platform, was used for the analysis of nanoparticles to determine the size distribution curve. Based on the obtained results from FESEM images, the mean nanoparticle size ( $\mu c$ ) and standard deviation ( $\sigma$ ) were calculated. The size distribution of ZnO nanoparticles with a maximum at around 7.9 nm is shown in Fig. 7. Further, ZnO nanoparticle size was analyzed automatically with ImageJ software using the plugins in the menu Image > Adjust > Threshold. After setting the thresholding to analyze the particles in a segmented image, the plugin used in the menu command was Analyze > Analyze particles.

The EDX results are listed in Table IV. In Table IV, the EDX analysis shows less Zinc (Zn) atomic percentage, and, hence, to confirm the formation of ZnO nanoparticles, the X-ray fluorescence characterization was carried out. This is a prototype study to realize the synthesis of nanoparticles in the non-conventional, miniaturized system, avoiding the complex hydrothermal process which includes a muffle furnace.

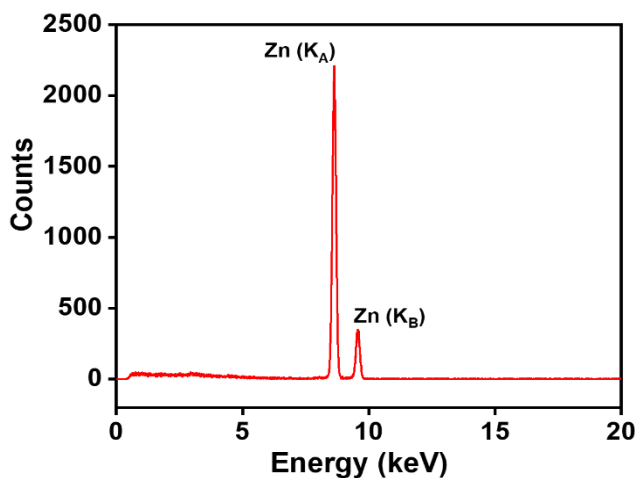


Fig. 8. XRF spectrum of ZnO nanoparticles.

Herein, an integrated, portable thermal management system was employed as a heating source. In addition, a less reagent consuming minuscule petri dish was used to eliminate the complications of the traditional bulk volume synthesis.

2) *X-Ray Fluorescence (XRF)*: X-ray fluorescence analysis was used for determining elementary material composition. The XRF spectrum recorded for the ZnO nanoparticles is shown in Fig. 8. The spectrum contains the characteristic peaks of Zn(KA) at 8.2 keV, Zn(KB) at 9.4 keV. The XRF analysis shows the possible confirmation of the formation of the ZnO and the concentration percentage of Zn was 79.35%. The obtained XRF spectrum of ZnO was compared with the literature which shows similar results. Wherein, the characteristic peaks of Zn(K $\alpha$ ) and Zn(K $\beta$ ) were 8.6 keV and 9.6keV respectively, also the concentration percentage of Zn was described at 95.25% [61].

### C. Electro-Catalytic Oxidation of Dopamine

In electro-catalytic detection of Dopamine, a neurotransmitter with graphitized mesoporous carbon (GMC)-Zinc oxide (ZnO) nanostructures (GMC@ZnO) was attempted in a three-electrode bulk system at neutral pH. Here, the 2B pencil graphite lead modified with GMC-ZnO composite, was used as a working electrode (WE), Ag/AgCl as a reference electrode (RE), and platinum as the counter electrode (CE). The working electrode was prepared by drop-casting 2  $\mu$ L of GMC-ethanol suspension on PGE, followed by air drying for 2 min. 2  $\mu$ L of prepared ZnO nanostructures were top coated on PGE/GMC to form PGE/GMC@ZnO. WE was dried at 60°C for 2 min.

The CV response was recorded at a scan rate of 10 mVs<sup>-1</sup> in 1 mM of Dopamine. As seen in Fig. 9, it was established that the blank electrode (PGE/GMC) alone gave no oxidation peak, whereas PGE/GMC@ZnO gave oxidation at  $E' = 0.47$  V vs Ag/AgCl corresponding to the oxidation of dopamine. Consequently, it was discovered that the synthesized ZnO is electrochemically active and plays a key role in dopamine detection. With further modification, it might be further used for the fabrication of electrochemical sensors for dopamine in real samples using a microfluidic platform. Further, it can be used for different sensing applications in a microfluidic envi-

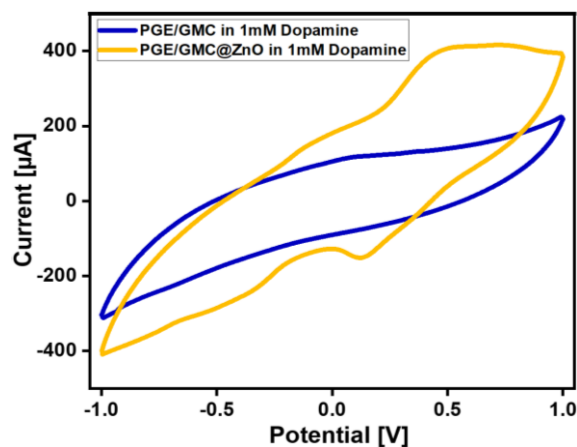


Fig. 9. CV response of 2B Pencil Graphite/GMC and 2B pencil/GMC@ZnO in 1 mM Dopamine (DA) solution at  $10 \text{ mV s}^{-1}$ .

ronment for controlled sample transfer on minuscule volume operations.

#### D. Portable Chemical Vapor Deposition (CVD) Technique

The fabricated device was further tested to check the chemical vapor deposition of nanomaterial thin films on a small scale without any complex procedures involving a cleanroom [62]. Herein, the reaction mixture of 4 mM zinc nitrate with 1 mM of ascorbic acid (reducing reagent), sonicated for 30 min was taken in a small circular petri dish covered with a clean Al foil of thickness  $18 \mu\text{m}$  and kept at  $70^\circ\text{C}$  for 3 h. To clean the Al foil for the deposition process, it was electrochemically pre-treated with PBS solution ( $-0.2\text{V}$  to  $+1\text{V}$ ) for 20 cycles @  $50\text{mV s}^{-1}$ . Here, the triplicated experiments using the deposited Al foil gave a response with an error margin of  $<3\%$ . Further, the deposited foil was showing reproducibility for sensing, and the film of nanoparticle synthesis remained intact and gave an identical response each time. However, after rigorous washing with acetone, the film can be scraped off and no electrochemical response was obtained after that. In comparison to the proposed method, the synthesis of nanomaterial of carbon using catalytic based chemical vapor deposition was incorporated [63], [64].

Fig. 10(a) shows the portable thermal management device, where the petri dish is placed on top of the heating blocks for chemical vapor deposition and Fig. 10(b) illustrates ZnO nanoparticle deposition on foil which is of 18 microns, the dimension of the foil was 50mm. Further, the synthesized ZnO nanoparticles were deposited through the CVD method as a thin film over an Al foil substrate. The deposited foil was further applied for an electro-analytical biochemical sensing application. To authenticate the deposition of ZnO film over the foil, the bare foil and ZnO film deposited foil was subjected to electrochemical studies. The ZnO deposited foil gave a distinct oxidation peak with cysteine that was relatable with the peak obtained using a standard glassy carbon electrode (GCE) coated with ZnO. Whereas, the bare foil and bare GCE both failed to give any characteristic response towards the cysteine electrocatalytic oxidation. Hence, it was confirmed

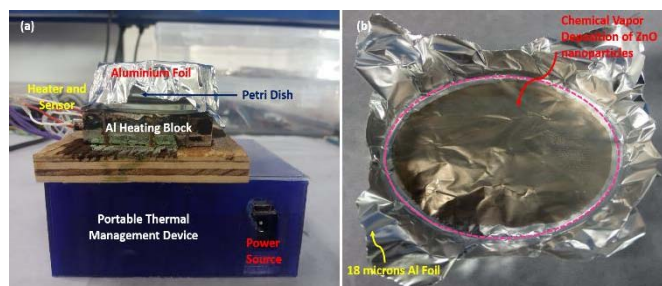


Fig. 10. (a) Portable thermal device for Chemical vapor deposition technique (b) ZnO nanoparticle deposited Aluminium (Al) Foil.

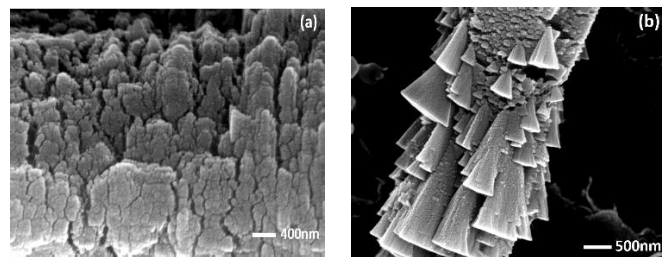


Fig. 11. FESEM images of (a) bare aluminium (Al) Foil (b) aluminium foil deposited with ZnO.

that the foil was successfully chemically modified with ZnO film.

The FESEM images in Fig. 11(a and b) show the comparison between the morphologies of bare Aluminium foil and ZnO nanoparticles deposited on Aluminium foil. The conical-shaped ZnO nanoparticles deposited onto the Aluminium foil can be observed in Fig. 11 (b). Whereas, the bare (plain) Al foil in Fig. 11 (a) has no such structures identifying the chemical vapor deposition of a thin film on the foil surface. Further, this ZnO deposited Al foil was used for the electrochemical sensing of cysteine.

#### E. Electrochemical Sensing Application of Foil@ZnO

To check the analytical application of the chemical vapor deposited ZnO thin film on Al foil, the deposited foil was cut into a dimension of  $4 \times 10 \text{ mm}^2$  pieces and used as a working electrode, Ag/AgCl as a reference, and platinum wire as counter electrodes for analytical sensing application. The non-deposited Al foil side was covered with parafilm to avoid unintended interactions. The CV experiments were performed in a pH 7 PBS solution with and without 1 mM cysteine.

The comparative CV responses are represented in Fig. 12, where it was found that Foil@ZnO gave distinct electro-catalytic oxidation of cysteine at  $0.51 \text{ V}$  vs. Ag/AgCl with a 1 mM cysteine solution. Whereas, plain Al foil (Foil-cysteine) failed to give a response. A control experiment with Foil@ZnO in blank pH 7 PBS was also performed which did not give any characteristic peak. Therefore, it was established that the ZnO deposited over Al foil played a key role in electrochemical sensing of cysteine and has the potential to be further used as an alternative to the conventional electrodes. Also, the foil being flexible, this type of foil-based electrode modification process can be used in miniaturized and microfluidic electrochemical sensing platform development.

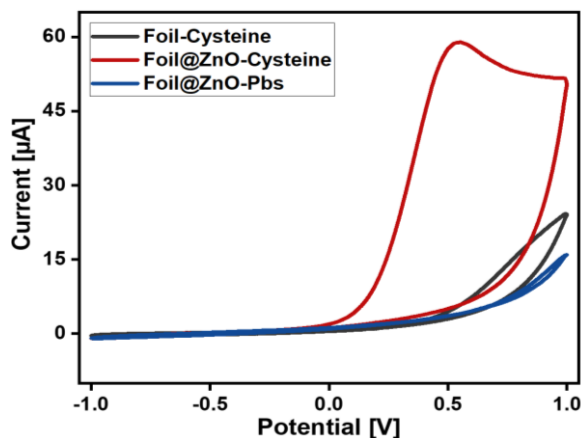


Fig. 12. CV responses of Foil@ZnO in blank PBS pH 7, 1mM Cysteine and Plain Al Foil with 1mM Cysteine at  $10 \text{ mV s}^{-1}$ .

#### IV. CONCLUSION

The present work was aimed to design and develop an inexpensive, accurate, portable, easy-to-use, and miniaturized temperature controller module using NodeMCU microcontroller with built-in ESP 8266 IoT chipset which enables unification and automation of the device. A customized cartridge heater made of 316-grade stainless steel of 25 mm x 3 mm dimensions was incorporated for heating the aluminium blocks. The 3D printed casing functionality invokes integration with the PID based temperature control system with good output stability and accuracy of  $\pm 2^\circ\text{C}$  which has advantages like fast ramping speed, precise, simple set-point temperature control with additional features of ESP 8266 such as real-time data access and cloud server storage making the device fully automated and integrated for point-of-source applications. The maximum attainable temperature of the proposed thermal management system is around  $300^\circ\text{C} - 320^\circ\text{C}$ . A small petri dish of 50 mm in diameter was used for the precursor transfer and it was placed on the heating blocks, where a microliter of solution fluid was used for the synthesis of ZnO nanoparticles. The proposed thermal management device is suitable and can be used to synthesize any nanoparticles. Herein, ZnO nanoparticles were synthesized with the help of a developed portable heating unit in microscale. The microscale synthesis of nanoparticles has its diversity of exquisite features such as accurate temperature handling, precise monitoring of reaction conditions, rapid mass and heat transfer, safe operation, environmental comfort, quick loading, and easy set-up of highly reproducible reagents and samples. To fabricate ZnO nanoparticles, the experimental setup was kept at  $70^\circ\text{C}$  for 3 h. The FESEM and XRF characterizations were implemented for the ZnO nanoparticle samples. The FESEM images show an average bar width of 830 nm. The nanoparticle size distribution curve was obtained from ImageJ software, where a mean nanoparticle size of 7.9 nm and a standard deviation of 4.8 nm was calculated. The ZnO nanoparticles were utilized for electrochemical sensing of dopamine. As a proof-of-concept, these nanoparticles were tested further to provide a portable chemical vapor deposition method (CVD) for the nanomaterial thin film preparation on plain Al foil 18  $\mu\text{m}$  in thickness at a small scale without any complex procedures such as cleanroom use. The ZnO deposited foil was

used as a working electrode in the electrochemical sensing of cysteine. In future scope, this technique has the potential to be used for the deposition of thin films and thermal synthesis of nano-particles.

#### ACKNOWLEDGMENT

The authors are grateful to Central Analytical Laboratory (CAL), BITS-Pilani, Hyderabad Campus for the help provided in characterization techniques. Madhusudan B. Kulkarni would like to thank Tata Consultancy Services (TCS) for providing a scholarship under TCS Research Scholar Program Cycle-15 during this project work.

#### REFERENCES

- [1] Z. Yang *et al.*, "Nanoparticle intercalation-modulated stretchable conductive graphene fibers with combined photoelectric properties," *Carbon*, vol. 141, pp. 218–225, Jan. 2019.
- [2] S. S. Rathnakumar *et al.*, "Stalling behaviour of chloride ions: A non-enzymatic electrochemical detection of  $\alpha$ -endosulfan using CuO interface," *Sens. Actuators B, Chem.*, vol. 293, pp. 100–106, Aug. 2019.
- [3] K. Kaviyarasu *et al.*, "ZnO doped single wall carbon nanotube as an active medium for gas sensor and solar absorber," *J. Mater. Sci., Mater. Electron.*, vol. 30, no. 1, pp. 147–158, Jan. 2019.
- [4] F. Fang, J. Futter, A. Markwitz, and J. Kennedy, "UV and humidity sensing properties of ZnO nanorods prepared by the arc discharge method," *Nanotechnology*, vol. 20, no. 24, Jun. 2009, Art. no. 245502.
- [5] M. Das, A. Kumar, R. Singh, M. T. Htay, and S. Mukherjee, "Realization of synaptic learning and memory functions in  $\text{Y}_2\text{O}_3$  based memristive device fabricated by dual ion beam sputtering," *Nanotechnology*, vol. 29, no. 5, Feb. 2018, Art. no. 055203.
- [6] L. Ma *et al.*, "Engineering oxygen vacancies towards self-activated  $\text{BaLuAl}_x\text{Zn}_{4-x}\text{O}_{7-(1-x)/2}$  photoluminescent materials: An experimental and theoretical analysis," *Phys. Chem. Chem. Phys.*, vol. 17, no. 46, pp. 31188–31194, 2015.
- [7] B. S. Sengar *et al.*, "Band alignment of Cd-free (Zn, Mg)O layer with  $\text{Cu}_2\text{ZnSn}(\text{S,Se})_4$  and its effect on the photovoltaic properties," *Opt. Mater.*, vol. 84, pp. 748–756, Oct. 2018.
- [8] C. S. Lim *et al.*, "Microwave-employed sol-gel synthesis of scheelite-type microcrystalline  $\text{AgGd}(\text{MoO}_4)_2:\text{Yb}^{3+}/\text{Ho}^{3+}$  upconversion yellow phosphors and their spectroscopic properties," *Crystals*, vol. 10, p. 1000, Nov. 2020.
- [9] P. M. Valencia, O. C. Farokhzad, R. Karnik, and R. Langer, "Microfluidic technologies for accelerating the clinical translation of nanoparticles," *Nature Nanotechnol.*, vol. 7, no. 10, pp. 623–629, Oct. 2012.
- [10] K. Ratajczak and M. Stobiecka, "High-performance modified cellulose paper-based biosensors for medical diagnostics and early cancer screening: A concise review," *Carbohydr. Polym.*, vol. 229, Feb. 2020, Art. no. 115463.
- [11] S. Aula, S. Lakkireddy, K. Jamil, A. Kapley, A. V. N. Swamy, and H. R. Lakkireddy, "Biophysical, biopharmaceutical and toxicological significance of biomedical nanoparticles," *RSC Adv.*, vol. 5, no. 59, pp. 47830–47859, 2015.
- [12] B. Nasser, N. Soleimani, N. Rabiee, A. Kalbasi, M. Karimi, and M. R. Hamblin, "Point-of-care microfluidic devices for pathogen detection," *Biosensors Bioelectron.*, vol. 117, pp. 112–128, Oct. 2018.
- [13] F. B. Myers, R. H. Henrikson, J. Bone, and L. P. Lee, "A handheld point-of-care genomic diagnostic system," *PLoS ONE*, vol. 8, no. 8, Aug. 2013, Art. no. e70266.
- [14] M. J. Ndolomingo, N. Bingwa, and R. Meijboom, "Review of supported metal nanoparticles: Synthesis methodologies, advantages and application as catalysts," *J. Mater. Sci.*, vol. 55, no. 15, pp. 6195–6241, May 2020.
- [15] P. G. Jamkhande, N. W. Ghule, A. H. Bamer, and M. G. Kalaskar, "Metal nanoparticles synthesis: An overview on methods of preparation, advantages and disadvantages, and applications," *J. Drug Del. Sci. Technol.*, vol. 53, Oct. 2019, Art. no. 101174.
- [16] V. Garg *et al.*, "Investigation of dual-ion beam sputter-instigated plasmon generation in TCOs: A case study of GZO," *ACS Appl. Mater. Interface*, vol. 10, no. 6, pp. 5464–5474, Feb. 2018.
- [17] L. Dyshlyuk *et al.*, "Antimicrobial potential of ZnO,  $\text{TiO}_2$  and  $\text{SiO}_2$  nanoparticles in protecting building materials from biodegradation," *Int. Biodeterioration Biodegradation*, vol. 146, Jan. 2020, Art. no. 104821.
- [18] P.-C. Chou *et al.*, "Nitrogen oxide ( $\text{NO}_2$ ) gas sensing performance of ZnO nanoparticles (NPs)/sapphire-based sensors," *IEEE Sensors J.*, vol. 15, no. 7, pp. 3759–3763, Jul. 2015.



- [19] N. Hao, M. Zhang, and J. X. J. Zhang, "Microfluidics for ZnO micro-nanomaterials development: Rational design, controllable synthesis, and on-chip bioapplications," *Biomater. Sci.*, vol. 8, no. 7, pp. 1783–1801, Mar. 2020, doi: [10.1039/C9BM01787A](https://doi.org/10.1039/C9BM01787A).
- [20] S. B. Khan, M. Faisal, M. M. Rahman, and A. Jamal, "Low-temperature growth of ZnO nanoparticles: Photocatalyst and acetone sensor," *Talanta*, vol. 85, no. 2, pp. 943–949, Aug. 2011.
- [21] C. B. Ong, L. Y. Ng, and A. W. Mohammad, "A review of ZnO nanoparticles as solar photocatalysts: Synthesis, mechanisms and applications," *Renew. Sustain. Energy Rev.*, vol. 81, pp. 536–551, Jan. 2018.
- [22] M. B. Kulkarni and S. Goel, "Microfluidic devices for synthesizing nanomaterials—A review," *Nano Exp.*, vol. 1, no. 1, pp. 1–30, 2020.
- [23] X. Wang, C. Hughes, S. Park, X. Ma, and H. J. Cho, "ZnO nanoparticle-based optical sensors fabricated by high current density electrodeposition and flame oxidation," in *Proc. IEEE Sensors*, vol. 1, Oct./Nov. 2017, pp. 5–7.
- [24] A. M. Uhl and J. S. Andrew, "Sol-gel-based electrospray synthesis of barium titanate nanoparticles," *IEEE Trans. Nanobiosci.*, vol. 19, no. 2, pp. 162–166, Apr. 2020.
- [25] Y. Liang, N. Guo, L. Li, R. Li, G. Ji, and S. Gan, "Fabrication of porous 3D flower-like Ag/ZnO heterostructure composites with enhanced photocatalytic performance," *Appl. Surf. Sci.*, vol. 332, pp. 32–39, Mar. 2015.
- [26] G. Yang and S.-J. Park, "Conventional and microwave hydrothermal synthesis and application of functional materials: A review," *Materials*, vol. 12, no. 7, p. 1177, Apr. 2019.
- [27] Y. Chen *et al.*, "Synthesis, crystal structure, and optical gap of two-dimensional halide solid solutions CsPb<sub>2</sub>(Cl<sub>1-x</sub>Br<sub>x</sub>)<sub>5</sub>," *Inorg. Chem.*, vol. 57, no. 15, pp. 9531–9537, 2018.
- [28] A. Batool and S. Valiyaveetil, "Co-precipitation—An efficient method for removal of polymer nanoparticles from water," *ACS Sustain. Chem. Eng.*, vol. 8, pp. 13481–13487, Aug. 2020.
- [29] V. K. Gupta, R. Sadeghi, and F. Karimi, "A novel electrochemical sensor based on ZnO nanoparticle and ionic liquid binder for square wave voltammetric determination of dioxidopa in pharmaceutical and urine samples," *Sens. Actuators B, Chem.*, vol. 186, pp. 603–609, Sep. 2013.
- [30] C. V. Ramana, V. H. Mudavakkat, K. K. Bharathi, V. V. Atuchin, L. D. Pokrovsky, and V. N. Kruchinin, "Enhanced optical constants of nanocrystalline yttrium oxide thin films," *Appl. Phys. Lett.*, vol. 98, no. 3, pp. 98–101, 2011.
- [31] C. V. Ramana *et al.*, "Growth and surface characterization of sputter-deposited molybdenum oxide thin films," *Appl. Surf. Sci.*, vol. 253, no. 12, pp. 5368–5374, Apr. 2007.
- [32] C. V. Ramana *et al.*, "Spectroscopic ellipsometry characterization of the optical properties and thermal stability of ZrO<sub>2</sub> films made by ion-beam assisted deposition," *Appl. Phys. Lett.*, vol. 92, no. 1, pp. 1–4, 2008.
- [33] P. M. Sylenko, A. M. Shlapak, S. S. Petrovska, O. Y. Khyzhun, Y. M. Solonin, and V. V. Atuchin, "Direct nitridation synthesis and characterization of Si<sub>3</sub>N<sub>4</sub> nanofibers," *Res. Chem. Intermediates*, vol. 41, no. 12, pp. 10037–10048, Dec. 2015.
- [34] V. V. Atuchin, E. N. Galashov, A. S. Kozhukhov, L. D. Pokrovsky, and V. N. Shlegel, "Epitaxial growth of ZnO nanocrystals at ZnWO<sub>4</sub>(010) cleaved surface," *J. Cryst. Growth*, vol. 318, no. 1, pp. 1147–1150, Mar. 2011.
- [35] M. Sajid and J. Páotka-Wasyłka, "Nanoparticles: Synthesis, characteristics, and applications in analytical and other sciences," *Microchem. J.*, vol. 154, May 2020, Art. no. 104623.
- [36] E. M. Modan, "Advantages and disadvantages of chemical methods in the elaboration of nanomaterials," *Metall. Mater. Sci.*, vol. 43, no. 1, pp. 53–60, Mar. 2020.
- [37] M. B. Gumpu, N. Nesakumar, B. L. Ramachandra, and J. B. B. Rayappan, "Zinc oxide nanoparticles-based electrochemical sensor for the detection of nitrate ions in water with a low detection limit—A chemometric approach," *J. Anal. Chem.*, vol. 72, no. 3, pp. 316–326, Mar. 2017.
- [38] X. Li, C. Zhao, and X. Liu, "A paper-based microfluidic biosensor integrating zinc oxide nanowires for electrochemical glucose detection," *Microsyst. Nanoeng.*, vol. 1, no. 1, pp. 1–7, Dec. 2015.
- [39] J. Park, R. A. Martin, J. D. Kelly, and J. D. Hedengren, "Benchmark temperature microcontroller for process dynamics and control," *Comput. Chem. Eng.*, vol. 135, Apr. 2020, Art. no. 106736.
- [40] M. B. Kulkarni, P. K. Enaganti, K. Amreen, and S. Goel, "Internet of Things enabled portable thermal management system with microfluidic platform to synthesize MnO<sub>2</sub> nanoparticles for electrochemical sensing," *Nanotechnology*, vol. 31, no. 42, pp. 1–8, 2020.
- [41] H. M. Asraf, K. A. N. Dalila, A. W. M. Hakim, and R. H. Hon, "Development of experimental simulator via Arduino-based PID temperature control system using LabVIEW," *J. Telecommun. Electron. Comput. Eng.*, vol. 9, nos. 1–5, pp. 53–57, 2017.
- [42] R. O. Moreno, R. A. Armindo, and R. L. Moreno, "Development of a low-cost automated calorimeter for determining soil specific heat," *Comput. Electron. Agricult.*, vol. 162, pp. 348–356, Jul. 2019.
- [43] R. Ma, Y. Bando, L. Zhang, and T. Sasaki, "Layered MnO<sub>2</sub> nanobelts: Hydrothermal synthesis and electrochemical measurements," *Adv. Mater.*, vol. 16, no. 11, pp. 918–922, Jun. 2004.
- [44] S. Zhu, H. Zhou, M. Hibino, I. Honma, and M. Ichihara, "Synthesis of MnO<sub>2</sub> nanoparticles confined in ordered mesoporous carbon using a sonochemical method," *Adv. Funct. Mater.*, vol. 15, no. 3, pp. 381–386, Mar. 2005.
- [45] D. Ghosh, S. Bhandari, and D. Khashtgir, "Synthesis of MnO<sub>2</sub> nanoparticles and their effective utilization as UV protectors for outdoor high voltage polymeric insulators used in power transmission lines," *Phys. Chem. Chem. Phys.*, vol. 18, no. 48, pp. 32876–32890, 2016.
- [46] J. Liu, F. An, C. Zhu, and D. Zhou, "Efficient transformation of DDT with peroxymonosulfate activation by different crystallographic MnO<sub>2</sub>," *Sci. Total Environ.*, vol. 759, Mar. 2021, Art. no. 142864.
- [47] P. Tayraukham, N. Jantarit, N. Osakoo, and J. Wittayakun, "Synthesis of pure phase NaP<sub>2</sub> zeolite from the gel of nay by conventional and microwave-assisted hydrothermal methods," *Crystals*, vol. 10, no. 10, pp. 1–11, 2020.
- [48] P. Rewatkar and S. Goel, "Next-generation 3D printed microfluidic membraneless enzymatic biofuel cell: Cost-effective and rapid approach," *IEEE Trans. Electron Devices*, vol. 66, no. 8, pp. 3628–3635, Aug. 2019.
- [49] P. Rewatkar and S. Goel, "3D printed bioelectrodes for enzymatic biofuel cell: Simple, rapid, optimized and enhanced approach," *IEEE Trans. Nanobiosci.*, vol. 19, no. 1, pp. 4–10, Jan. 2020.
- [50] X. Z. Lin, A. D. Terepka, and H. Yang, "Synthesis of silver nanoparticles in a continuous flow tubular microreactor," *Nano Lett.*, vol. 4, no. 11, pp. 2227–2232, Nov. 2004.
- [51] R. J. Hargreaves *et al.*, "An accurate, extensive, and practical line list of methane for the HITEMP database," *Astrophys. J. Suppl. Ser.*, vol. 247, no. 2, p. 55, Apr. 2020.
- [52] P. R. Nagarajan, B. George, V. J. Kumar, and S. Member, "Improved single-element resistive sensor-to-microcontroller interface," *IEEE Trans. Instrum. Meas.*, vol. 66, no. 10, pp. 2736–2744, Oct. 2017.
- [53] M. Sharma, S. Raghavendra, and S. Agrawal, "Development of an open-source tool for UAV photogrammetric data processing," *J. Indian Soc. Remote Sens.*, vol. 3, pp. 1–6, Nov. 2020.
- [54] J. Liu, Y. Li, and H. Zhao, "A temperature measurement system based on PT100," in *Proc. Int. Conf. Electr. Control Eng.*, Jun. 2010, pp. 296–298.
- [55] M. B. Kulkarni and S. Goel, "Advances in continuous-flow based microfluidic PCR devices—A review," *Eng. Res. Exp.*, vol. 2, no. 4, p. 21, 2020.
- [56] N. Matinise, X. G. Fuku, K. Kaviyarasu, N. Mayedwa, and M. Maaza, "ZnO nanoparticles via Moringa oleifera green synthesis: Physical properties & mechanism of formation," *Appl. Surf. Sci.*, vol. 406, pp. 339–347, 2017.
- [57] S. Nguyen Xuan, "Facial synthesis and characterization of polypyrrole/zinc oxide(ZnO) nanorode and flower-like shape composites," *VNU J. Sci., Math.*, vol. 34, no. 1, pp. 40–45, Mar. 2018.
- [58] J. Qiu *et al.*, "Synthesis and characterization of flower-like bundles of ZnO nanosheets by a surfactant-free hydrothermal process," *J. Nanomater.*, vol. 2014, Dec. 2014, Art. no. 281461.
- [59] C. Chen *et al.*, "Synthesis of a flower-like SnO/ZnO nanostructure with high catalytic activity and stability under natural sunlight," *J. Alloys Compounds*, vol. 826, Jun. 2020, Art. no. 154122.
- [60] P. Basnet and S. Chatterjee, "Structure-directing property and growth mechanism induced by capping agents in nanostructured ZnO during hydrothermal synthesis—A systematic review," *Nano-Struct. Nano-Objects*, vol. 22, Apr. 2020, Art. no. 100426.
- [61] T.-H. Chang, Y.-C. Lu, M.-J. Yang, J.-W. Huang, P.-F. Linda Chang, and H.-Y. Hsueh, "Multibranched flower-like ZnO particles from eco-friendly hydrothermal synthesis as green antimicrobials in agriculture," *J. Cleaner Prod.*, vol. 262, Jul. 2020, Art. no. 121342.
- [62] T. L. Valerio, G. A. R. Maia, L. F. Gonçalves, A. Viomar, E. D. P. Banczek, and P. R. P. Rodrigues, "Study of the Nb<sub>2</sub>O<sub>5</sub> insertion in ZnO to dye-sensitized solar cells," *Mater. Res.*, vol. 22, no. 1, pp. 1–5, 2019.
- [63] H. Sutanto, S. Wibowo, I. Nurhasanah, E. Hidayanto, and H. Hadiyanto, "Ag doped ZnO thin films synthesized by spray coating technique for methylene blue photodegradation under UV irradiation," *Int. J. Chem. Eng.*, vol. 2016, Feb. 2016, Art. no. 6195326.
- [64] D.-N. Phan, H. Y. Choi, S.-G. Oh, M. Kim, and H. Lee, "Fabrication of ZnO nanoparticle-decorated nanofiber mat with high uniformity protected by constructing tri-layer structure," *Polymers*, vol. 12, no. 9, p. 1859, Aug. 2020.

## REGULAR ARTICLE

## Highlights

# Association of reduced maternal sHLA-G5 isoform levels and elevated TNF- $\alpha$ /IL-4 cytokine ratio with Recurrent Pregnancy Loss: A study on South Indian women

Dhatri Madduru<sup>1</sup> | Kethora Dirsipam<sup>2</sup> | Mahalakshmi Goli<sup>3</sup> | Venkata Ramana Devi<sup>1</sup> | Parveen Jahan<sup>4</sup> 

<sup>1</sup>Department of Biochemistry, Osmania University, Hyderabad, Telangana, India

<sup>2</sup>Institute of Genetics and Hospital for Genetic Diseases, Osmania University, Hyderabad, Telangana, India

<sup>3</sup>Department of Obstetrics and Gynaecology, Gandhi Medical College and Hospital, Secunderabad, Telangana, India

<sup>4</sup>School of Sciences, Maulana Azad National Urdu University, Hyderabad, Telangana, India

**Correspondence**

Dr. Parveen Jahan, Professor, School of Sciences, Maulana Azad National Urdu University, Gachibowli, Hyderabad-500032, India.

Email: drparveenjahan2020@gmail.com

Dr. Venkata Ramana Devi, Professor, Department of Biochemistry, University College of Science, Osmania University, Tarnaka, Hyderabad-500007, India.

Email: vrd.biochem111@gmail.com

**Abstract**

Inflammation is of critical importance in successful implantation during pregnancy. However, the establishment of maternal immune tolerance towards semi-allograft foetus is more exigent and is achieved predominantly by human leukocyte antigen-G (HLA-G) isoforms with a special emphasis on soluble HLA-G5 (sHLA-G5). Constant inflammation and lack of resolution by anti-inflammatory milieu, due to aberrant expression of critical immunoregulatory molecules such as sHLA-G5 and dysfunctional T helper cells 1 and 2 (Th1-Th2) cytokine shift, can lead to adverse pregnancy outcomes including recurrent pregnancy loss (RPL). Serum samples of 270 pregnant women (135 healthy parous and 135 with a history of RPL) were evaluated for the concentrations of sHLA-G5, interleukin-4 (IL-4) and tumour necrosis factor-alpha (TNF- $\alpha$ ) using sandwich enzyme-linked immunosorbent assay (ELISA) and found elevated levels of sHLA-G5 and IL-4 in controls and higher TNF- $\alpha$  levels and TNF- $\alpha$ :IL-4 ratio in patients ( $P < .05$ ). Stratified data analysis based on the time of sample collection, that is the first and second trimesters exhibited higher sHLA-G5 and IL-4 in both first and second trimesters in controls than patients, while they displayed lower levels concerning TNF- $\alpha$  and TNF- $\alpha$ :IL-4 ratio ( $P < .05$ ). However, within patients and controls in the first or second trimesters, there was a significant variation concerning sHLA-G5 alone. Further, the outcome of pregnancies studied in the present investigation revealed a significant elevation in sHLA-G5 levels among women with successful pregnancies compared with women who experienced pregnancy loss, therefore, concluding the potential application of sHLA-G5 isoform as a marker in assisting improved pregnancy outcomes.

## 1 | INTRODUCTION

Inflammation is critical for the embryo implantation process in a pregnancy, but immune tolerance is of much more significance to facilitate the growth of a semi-allograft foetus, possessing antigens from two histo-incompatible parents.<sup>1</sup> The unique feature of a normal pregnancy is the dual

function of the maternal immune system where, it is tolerant towards haploidentical foetus bearing paternal antigens, and at the same time, displays the ability to protect mother and foetus from infections.<sup>2</sup> The dynamic modulation of the immune system is accomplished principally by human leukocyte antigen-G (HLA-G), a non-classical HLA-class Ib molecule expressed on extravillous cytotrophoblast (EVT)

cells present in the maternofetal interface during pregnancy. The alternative splicing of HLA-G mRNA generates seven isoforms (membrane-bound: HLA-G1, -G2, -G3, -G4 and soluble proteins: HLA-G5, -G6 and -G7) of which HLA-G5 is structurally analogous to the full-length membrane-bound HLA-G1 except for the absence of transmembrane and intracytoplasmic domains.<sup>3,4</sup> Soluble HLA-G (sHLA-G) isoforms have been detected in maternal-foetal circulation, blood plasma or serum, cord blood, amniotic fluid, trophoblasts, human oocytes, human embryonic stem cells and pre-implantation embryos.<sup>3,5,6</sup> During pregnancy, sHLA-G was reported to protect the foetus by inducing apoptosis of activated cluster of differentiation 8+ (CD8+) T cells through activation of Fas/FasL pathway and by promoting regulatory T-cell (Treg cells) generation. Furthermore, interaction with killer cell immunoglobulin-like receptor-2 Ig domains and long cytoplasmic tail 4 (KIR2DL4) receptor on natural killer (NK) cells induces the secretion of pro-inflammatory and pro-angiogenic factors for vascular growth and remodelling in the uterus during early stages although inhibiting cytotoxicity of NK cells.<sup>7-10</sup>

In general, pregnancy is partitioned into three distinctive immunological stages regulated by diverse sets of cytokines that control the growth of the foetus and placental development.<sup>11</sup> Pre-implanted embryo produces cytokines whose production is stringently regulated to recruit macrophages and uterine natural killer (uNK) cells of mother to promote inflammatory microenvironment, decidualization and vascular remodelling of spiral arteries to nourish and supply oxygen to the growing foetus. The second phase of pregnancy is an anti-inflammatory state where a symbiotic relationship between mother and foetus is established. This dynamic cytokine shift from pro-inflammatory Th1 cytokines to anti-inflammatory Th2 cytokines (IL-3, IL-4, IL-10 etc.) is mediated by NK cell and lymphokine-activated cell regulation. The third and final stage of pregnancy is associated with the completion of foetal development and preparation for parturition through the onset of the inflammatory phase by coordinated production of prostaglandins, pro-inflammatory cytokines and matrix metalloproteases.<sup>1,2,11</sup>

The aforementioned information suggests that dynamic Th1-Th2 cytokine shift regulates the pregnancy outcome by creating and resolving the pro- and anti-inflammatory phases throughout the pregnancy. Aberrant/constant inflammation and lack of resolution by anti-inflammatory milieu due to disturbed expression of critical immunoregulatory molecules such as sHLA-G can lead to adverse pregnancy outcomes including recurrent pregnancy loss (RPL). In the present study, to investigate the above contention serum concentrations of sHLA-G5, IL-4 and TNF- $\alpha$  were measured in healthy parous women and RPL patients during the first or second trimesters of pregnancy from south India.

## 2 | MATERIALS AND METHODS

### 2.1 | Ethics statement

The present study was approved by the Institutional Ethical Committee of Osmania University, Hyderabad, India, and Gandhi Medical College, Secunderabad, India. All the samples from the participated subjects in the study were obtained with written informed consent following the Declaration of Helsinki (2000) guidelines.

### 2.2 | Subjects

In the present study, a total of 270 pregnant women belonging to first and second trimesters were recruited which includes 135 patients with a history of RPL and 135 age-matched healthy controls from Gandhi Medical College and Hospital, Secunderabad, India. The required sample size with 3% of disease prevalence and 3% precision was obtained to be 124.<sup>12</sup> Women with at least 2 spontaneous miscarriages before 20 weeks of gestation with a maximum age limit of 40 years were recruited under the RPL group, whereas women with at least 2 live births and with no history of miscarriage/abortion were considered in the healthy controls group. Both patients and controls were recruited based on their medical history of pregnancy complications, and diagnostic investigations were performed for factors associated with pregnancy loss, that is T3 (Triiodothyronine), T4 (Thyroxine), TSH (Thyroid Stimulating Hormone), prolactin, progesterone, oestrogen, blood sugar, HbA1C (Haemoglobin A1C) (diabetes), antibodies profiles (antiphospholipid antibodies, anti-cardiolipin antibodies, antithyroid antibodies etc), polycystic ovarian syndrome (PCOS) (Ultrasound, oligo-ovulation or an-ovulation and biochemical/clinical hyperandrogenism), oligomenorrhoea, cervical incompetence, parental chromosomal abnormalities, TORCH profile (Toxoplasma gondii, rubella, cytomegalovirus and herpes simplex virus) as well as clinical pregnancies documented using ultrasound or histopathology by the Department of Obstetrics and Gynaecology of Gandhi Medical College and Hospital, Secunderabad, India. In addition, the complete information about clinical, demographical and family history such as body mass index (BMI), haemoglobin (Hb), age at menarche, age at the first conception, number and nature of abortions, consanguinity, gynaecological problems and complex diseases of each subject recruited was documented using a prestructured questionnaire.

Based on the above data women with a history of only one spontaneous abortion, induced abortions and abortions with known reasons such as anatomical problems and hormonal imbalances were excluded from the study. A blood sample of five millilitres was collected in ethylenediaminetetraacetic

acid (EDTA) (BD Vacutainer, Ref No. 367873) and clot activator (BD Vacutainer, Ref No. 367837) vacutainer tubes by venipuncture from both RPL patients and controls belonging to the first or second trimesters of pregnancy. The blood sample was collected only once from each subject enrolled in the study, and based on the gestational age at the time of sample collection, the subjects were stratified into first- (68 healthy controls and 74 RPL patients) and second-trimester (67 healthy controls and 61 RPL patients) groups. Blood samples were centrifuged at 600 g for 15 min at 4°C to separate the serum and stored at -80°C until the time of assay. The outcome of the pregnancy of all the subjects was followed up, and data were collected.

### 2.3 | Estimation of full-length soluble HLA-G5 (sHLA-G5) protein, IL-4 and TNF- $\alpha$ levels using sandwich ELISA

All the 270 serum samples were subjected to sandwich enzyme-linked immunosorbent assay (ELISA) kit following the manufacturer's protocol to estimate the sHLA-G5 (KINESISDx, Los Angeles, USA, Catalog No. K12-0441), IL-4 (Diacclone, France, Catalog No. 950.020.096) and TNF- $\alpha$  (Boster immunoleader PicoKine™, Fremont, CA, USA, Catalog No. EK0525) concentrations.

### 2.4 | Statistical analysis

The statistical analyses concerning the measurement of sHLA-G5, IL-4 and TNF- $\alpha$  concentrations in the serum and TNF- $\alpha$ :IL-4 ratio of patients, controls and subgroups (first and second trimesters) such as descriptive statistics, mean values, standard deviation and independent Student's *t* test was performed using IBM SPSS software version 27 (Chicago, IL). The data were then analysed using one-way analysis of variance (ANOVA) (GraphPad Prism 6.0 version, San Diego, CA, USA) to find the variation between patients, controls, first- and second-trimester groups as well as for the follow-up data. A two-tailed *P*-value was taken, and <.05 was considered statistically significant. To further reduce the risk of Type I errors, Bonferroni correction was used to adjust the *P*-values. Adjusted *P*-values <.05 were considered significant, which corresponds to an expected false discovery rate of 5%. Multivariate analysis of variance (MANOVA)—Wilk's test was performed in controls and patients to determine the differences in means between clinical variables such as age, age at menarche, the number of abortions and nature of abortions and their effect on sHLA-G5 as well as selected cytokine levels using XLSTAT software (Data Analysis and Statistical Solution for Microsoft Excel, Addinsoft, Paris, France 2017).

## 3 | RESULTS

A total of 135 healthy parous women and 135 RPL patients from south India were enrolled in the present study. The demographic and clinical details of the study group are given in Tables 1 and 2. The estimated serum concentrations of sHLA-G5, IL-4, TNF- $\alpha$  and TNF- $\alpha$ : IL-4 ratio of both patients and controls are represented in Figure 1. Furthermore, the stratified data on the serum levels of sHLA-G5, IL-4, TNF- $\alpha$  and TNF- $\alpha$ : IL-4 ratio of first- or second-trimester samples is shown in Figure 2. The comparison between first- and second-trimester samples within controls and patients is represented in Figure 3.

### 3.1 | sHLA-G5 serum concentrations

The serum concentrations of soluble HLA-G5 isoform were found to be elevated in controls when compared to patients ( $147.81 \pm 21.23$  pg/mL versus  $58.93 \pm 28.25$  pg/mL; *P*-value = .0001) in overall as well as in both first- and second-trimester groups (ANOVA, *P* <.0001 after Bonferroni's correction). In addition, the levels of sHLA-G5 were high in the first-trimester group in both controls (*P* <.0001) and RPL patients (*P* =.0078) compared with the second-trimester group.

### 3.2 | IL-4 serum concentrations

The anti-inflammatory (Th2) cytokine IL-4 levels were significantly higher among controls than patients ( $22.72 \pm 15.34$  pg/mL versus  $8.76 \pm 2.60$  pg/mL; *P* =.0001). Stratified data analysis of first- and second-trimester groups showed significantly increased levels of IL-4 in controls compared with RPL patients (*P* <.0001 after Bonferroni's correction). Relatively, IL-4 levels were high in the second trimester both in controls and patients compared with the first trimester; however, it was not statistically significant.

### 3.3 | TNF- $\alpha$ serum concentrations

TNF- $\alpha$  levels were elevated in patients compared with controls ( $335.13 \pm 110.72$  pg/mL versus  $146.47 \pm 139.48$  pg/mL). Both the first- and second-trimester groups of patients exhibited higher levels of TNF- $\alpha$  compared with their counterparts in controls (ANOVA, *P* <.0001 after Bonferroni's correction). Elevated levels of TNF- $\alpha$  were observed in the first trimester than in the second trimester in controls; however, it was in reverse trend in patients (*P* >.05).

**TABLE 1** Demographic, clinical and family data of the subjects enrolled in the present study (Data are *n* (%))

Category	Patients ( <i>n</i> = 135)	Controls ( <i>n</i> = 135)
<b>Hb levels (g/dL)</b>		
<12	129 (95.5%)	124 (91.8%)
≥12	6 (4.5%)	11 (8.2%)
<b>Maternal age (in years)</b>		
≤9	2 (1.5%)	1 (0.7%)
20–34	127 (94.1%)	129 (95.6%)
≥35	6 (4.4%)	5 (3.7%)
<b>Age at the first conception (in years)</b>		
<18 (13–17)	25 (18.5%)	44 (32.6%)
18–30	107 (79.3%)	91 (67.4%)
>30	3 (2.2%)	0 (0%)
<b>Menstrual status</b>		
Irregular	9 (6.6%)	2 (1.5%)
Regular	126 (93.4%)	133 (98.5%)
<b>Consanguinity</b>		
Yes	36 (26.7%)	35 (25.9%)
No	99 (73.3%)	100 (74.1%)
<b>Type of abortion</b>		
Primary aborters	104 (77%)	0 (0%)
Secondary aborters	31 (23%)	0 (0%)
<b>Number of abortions</b>		
>3	16 (11.8%)	0 (0%)
≤3	119 (88.2%)	0 (0%)
<b>Addictions (Gutka, Alcohol etc)</b>		
Yes	13 (9.6%)	32 (23.7%)
No	122 (90.4%)	103 (76.3%)
<b>BMI (kg/m<sup>2</sup>)</b>		
<18.5 (low)	28 (20.7%)	31 (23%)
18.5–24.9 (normal)	78 (57.8%)	104 (77%)
>24.9 (high)	29 (21.5%)	0 (0%)
<b>Age at menarche (in years)</b>		
≤11 (low)	23 (17%)	16 (11.85%)
12–14 (normal)	95 (70.4%)	104 (77%)
≥15 (high)	17 (12.6%)	15 (11.15%)

Abbreviation: *n*, number of subjects.

Primary aborters are those who have lost all previous pregnancies, and secondary aborters are those who have had at least one successful pregnancy.

Consanguinity can be defined as descendants of the same ancestry, in the present study consanguineous marriage was documented which can be defined as marriage between two closely related individuals.

### 3.4 | TNF-α:IL-4 ratio

The ratio of TNF-α to IL-4 was evaluated and observed to be significantly elevated in patients when compared to controls

(44.20 ± 26.50 vs 13.39 ± 25.51) and also in both the first and second trimesters (ANOVA, *P* < .0001 after Bonferroni's correction). The ratio was high in the first trimester than the second trimester in controls, whereas it was in reverse trend in patients, but they were not statistically significant.

### 3.5 | Multivariate analysis of variance

There was a statistically significant effect of clinical parameters age, age at menarche and number of abortions on sHLA-G5, IL-4, TNF-α levels and TNF-α:IL-4 ratio in RPL patients, and however, the significance with only age was found in controls (Table 3).

### 3.6 | Analysis of follow-up data

All the 270 pregnant women enrolled in the present study were followed up for the outcome of their pregnancy. All the women enrolled in the controls group of the present study had successful pregnancies; however, out of 135 RPL patients, 98, that is 73% of women experienced another pregnancy loss while 37, that is 27% of women had successful live births. The levels of sHLA-G5 were significantly higher in women with successful pregnancies than those who had a foetal loss (89.99 ± 5.54 vs 47.20 vs 24.17) (ANOVA, *P* < .0001), but TNF-α showed significantly reduced levels in women experiencing pregnancy loss compared with those who had successful live births (319.2 ± 104.71 vs 377.33 ± 116.46) (ANOVA, *P* = .036). However, IL-4 levels and TNF-α:IL-4 ratios did not significantly differ among the two groups. It is essential to note that irrespective of the outcome, all the samples from RPL patients exhibited lower concentrations of sHLA-G5, IL-4 and higher concentrations of TNF-α and TNF-α:IL-4 ratio compared with healthy controls. Interestingly, all the women who had pregnancy loss displayed a concentration of sHLA-G5 below 79 pg/mL (Table 4).

## 4 | DISCUSSION

Successful pregnancy depends on maternal immune tolerance towards semi-allograft foetus as well as the balance between pro- and anti-inflammatory cytokines.<sup>2,13</sup> During the induction of immune tolerance by immunomodulatory molecules such as HLA-G, a reduction in Th1 cytokines and upregulation of Th2 cytokines was reported.<sup>2</sup> To further elucidate the role of sHLA-G5 isoform and pro- and anti-inflammatory cytokines in healthy pregnancy and RPL, in this study, the systemic circulating levels of sHLA-G5, IL-4, TNF-α and TNF-α:IL-4 ratio in serum samples were estimated among healthy parous women and RPL patients of south India. A

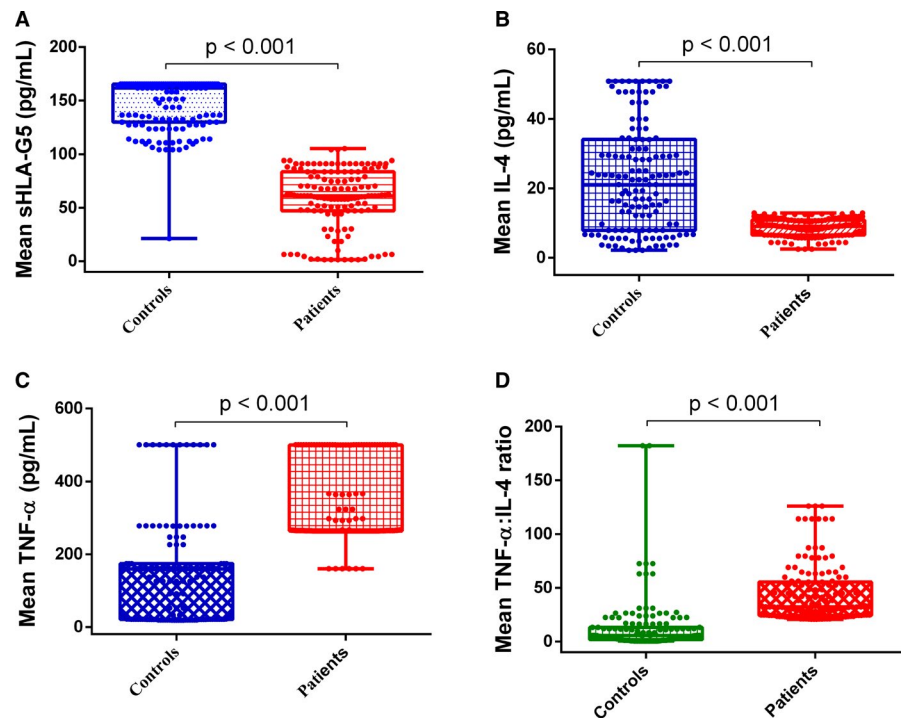
**TABLE 2** Clinical characteristics of the subjects enrolled in the present study (Data are Mean  $\pm$  SD)

Features	Controls ( <i>n</i> = 135)	Patients ( <i>n</i> = 135)	<i>P</i> -value
BMI (kg/m <sup>2</sup> )	<b>19.67 <math>\pm</math> 2.05</b>	<b>22.06 <math>\pm</math> 4.16</b>	<b>.0001</b>
Hb (g/dL)	9.66 $\pm$ 1.60	9.90 $\pm$ 1.26	.172
Maternal Age (years)	24.87 $\pm$ 4.50	24.93 $\pm$ 4.20	.911
Age at the first conception (years)	<b>18.33 <math>\pm</math> 2.74</b>	<b>20.34 <math>\pm</math> 3.75</b>	<b>.0001</b>
Age at menarche (years)	12.75 $\pm$ 1.38	12.84 $\pm$ 1.47	.580
Mean gestational age during sample collection (in months)	4.52 $\pm$ 2.23	4.31 $\pm$ 2.28	.44
Mean gestational age of the first-trimester samples during sample collection (in months)	<i>n</i> = 68 (50.4%) 24.88 $\pm$ 4.51	<i>n</i> = 74 (54.8%) 24.87 $\pm$ 4.2	.989
Mean gestational age of the second-trimester samples during sample collection (in months)	<i>n</i> = 67 (49.6%) 24.93 $\pm$ 4.6	<i>n</i> = 61 (45.2%) 25 $\pm$ 4.24	.929

Bold indicates statistically significant values (*P* .05).

Abbreviations: *n*, number of subjects; SD, standard deviation.

**FIGURE 1** Serum concentration of (A) sHLA-G5 (pg/mL) (B) IL-4 (pg/mL) (C) TNF- $\alpha$  (pg/mL) (D) TNF- $\alpha$ :IL-4 ratio measured and analysed using one-way ANOVA in controls and RPL patients. The data presented as mean  $\pm$  SD of concentrations with adjusted *P*-values  $\leq$  .05 considered significant after using the Bonferroni correction



substantially increased level of sHLA-G5, IL-4 and a decrease in TNF- $\alpha$  and TNF- $\alpha$ : IL-4 ratio was observed in healthy parous women. Furthermore, concerning sHLA-G5 concentrations, there was a noteworthy elevation in the first-trimester samples compared with second-trimester both in patients and controls however, no considerable difference with regard to cytokines and their ratio was observed.

During pregnancy, sHLA-G functions locally at the maternofoetal interface apart from entering into the systemic circulation to modulate maternal immune responses. It induces apoptosis of activated CD8<sup>+</sup> T cells through CD95/CD95L interaction, modulates CD4<sup>+</sup> T-cell proliferation and inhibits NK cell-mediated cytotoxicity.<sup>14</sup> It also serves as activating molecule to promote the secretion of pro-inflammatory

cytokines and the interaction between early trophoblast cells and endothelial cells of spiral arteries allowing trophoblast invasion and vascular remodelling.<sup>15</sup>

In support of our observation, the literature suggests a correlation between low or undetectable sHLA-G5 levels in systemic circulation among spontaneous abortion threatened women with first-trimester foetal loss of unknown aetiology and pre-eclampsia compared with the healthy controls.<sup>6,16-21</sup> Researchers have reported that a threshold value of 59.73 IU/mL and above of sHLA-G5 increase the chances of a successful pregnancy by twofold in normal parous women<sup>6</sup> suggesting its potential as a prognostic factor for improved chances of pregnancy. Previous studies reported an elevation of sHLA-G levels during the first gestational trimester, which

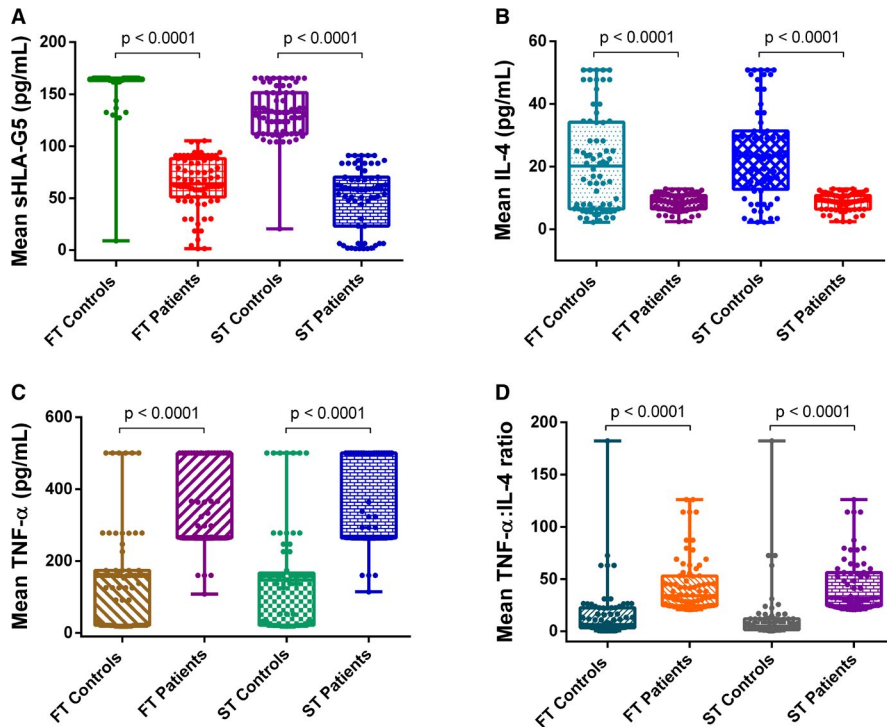


**FIGURE 2** Serum concentration of (A) sHLA-G5 (pg/mL) (B) IL-4 (pg/mL) (C) TNF- $\alpha$  (pg/mL) (D) TNF- $\alpha$ :IL-4 ratio measured and analysed using one-way ANOVA in controls and RPL patients of the first trimester (FT) and second trimester (ST). The data presented as mean  $\pm$  SD of concentrations between RPL patients and controls with adjusted  $P$ -values  $\leq .05$  considered significant after using the Bonferroni correction

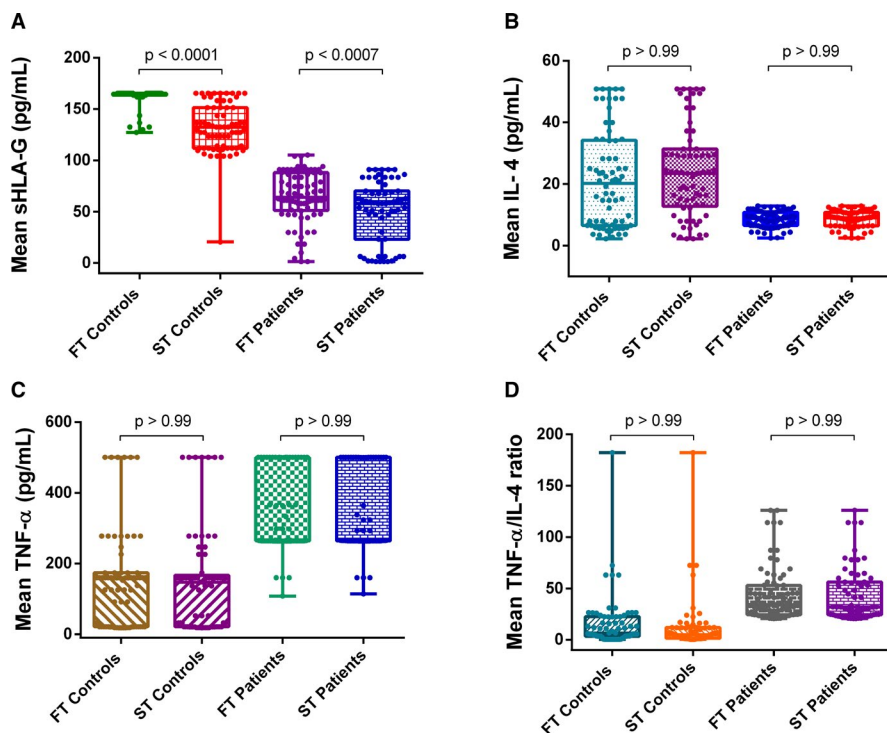


**FIGURE 3** Serum concentration of (A) sHLA-G5 (pg/mL) (B) IL-4 (pg/mL) (C) TNF- $\alpha$  (pg/mL) (D) TNF- $\alpha$ :IL-4 ratio measured and analysed using one-way ANOVA in controls and RPL patients of the first trimester (FT) and second trimester (ST). The data presented as mean  $\pm$  SD of concentrations between FT and ST of controls and FT and ST of patients with adjusted  $P$ -values  $\leq .05$  considered significant after using the Bonferroni correction

reaches the highest peak at month three of gestation<sup>22,23</sup> and starts to decline during the third trimester.<sup>24</sup> Our results were in accordance with these previous reports suggesting a dynamic modulation of sHLA-G5 levels in maternal peripheral blood at different gestational periods during a healthy pregnancy. Furthermore, the follow-up data of enrolled patients and controls showed elevated levels of sHLA-G5 with a minimum concentration of 79 pg/mL among patients who

had successful pregnancy compared with those who experienced another pregnancy loss indicating the mandatory role of sHLA-G5 in favourable pregnancy.

The second observation of the present study is higher concentrations of TNF- $\alpha$  in RPL patients than in healthy parous women. TNF- $\alpha$ , a pleiotropic cytokine, involved in pro-inflammatory responses and development of endocrine, autoimmune and neoplastic diseases.<sup>25</sup> It influences placental

**TABLE 3** The effect of differences in means between clinical parameters on sHLA-G5, IL-4, TNF- $\alpha$  and TNF- $\alpha$ :IL-4 ratio in RPL patients and controls

Effect	F-value	Wilk's Lambda value	P-value
<b>Patients</b>			
Age	<b>3.398</b>	<b>0.151</b>	<b>&lt;.0001</b>
Age at menarche	<b>4.533</b>	<b>0.338</b>	<b>&lt;.0001</b>
Number of abortions	<b>5.478</b>	<b>0.389</b>	<b>&lt;.0001</b>
Nature of abortions	1.645	0.938	.169
<b>Controls</b>			
Age	<b>1.467</b>	<b>0.455</b>	<b>.015</b>
Age at menarche	0.967	0.758	.521

Note: Bold indicates statistically significant values ( $P < .05$ ).

The MANOVA-Wilk's test data presented with  $P$ -values  $\leq .05$  considered significant.

architecture and differentiation, hormone synthesis, follicle and embryonic development, uterine cyclicity, steroidogenesis and parturition. In addition to the implantation during early trimesters of pregnancy, the timely development and establishment of the uterine pro-inflammatory milieu by elevated Th1 cytokines and chemokines in the myometrium (uterine muscle) helps in the induction of labour by recruiting immune cells during later stages of gestation suggesting the essential role of the regulated delicate expression of TNF- $\alpha$  in the placenta for the survival of the pregnancy, although its persisted expression may be detrimental at later stages of gestation.<sup>26-29</sup> The role of TNF- $\alpha$  in causing miscarriage may be attributed to its potential to induce apoptosis, enhanced production of prostaglandins subsequently leading to uterine contractions. In addition, it exerts adverse effects by decreasing blood flow to the embryo resulting in blood vessel thrombosis (vascular autoamputation), interfering with the invasion of spiral arteries, endothelial dysfunction with damage to decidual vasculature, membrane matrices degradation predisposing to foetal membrane rupture.<sup>30-34</sup>

In concordance with our results, an aberrant expression of TNF- $\alpha$  was shown to be associated with adverse placental development and function subsequently resulting in pregnancy complications.<sup>35</sup> In vitro studies concluded that TNF- $\alpha$  derived from maternal T cells stimulates apoptosis of cytotrophoblasts and syncytiotrophoblast (ST) cells in combination with interferon-gamma (IFN- $\gamma$ ) by inducing monocyte adhesion to ST cells to disrupt trophoblast monolayers. To protect against this damage, villous ST cells produce progesterone to promote Th2 cytokine (IL-4) production and dampen Th1 cytokine (TNF- $\alpha$ ) production. Therefore, when placental protective mechanisms fail or expression of TNF- $\alpha$  persists, trophoblast damage may occur.<sup>36</sup> Another study found that Th1 cytokines (TNF- $\alpha$ , IFN- $\gamma$ ) in vitro induce trophoblast apoptosis mediated by Fas-Fas L activation.<sup>37</sup> Several reports

showed that significantly increased levels of TNF- $\alpha$  in the serum of women with RPL compared with healthy women.<sup>35,38-40</sup> Therefore, the timing, location and network of cytokine signals are critical for the maintenance of healthy pregnancy.<sup>41</sup>

The third finding of our study is an overall increase in IL-4 levels in healthy parous women than in patients. IL-4 is a pleiotropic anti-inflammatory cytokine that functions by suppressing the pro-inflammatory milieu. IL-4 facilitates the polarization of antigen-stimulated naïve Th cells into Th2 effector cells and propagates Th2 responses by binding to the receptor IL-4R $\alpha$  and by activating signal transducer and activator of transcription (STAT) 6 signalling pathway. It is also implicated that IL-4 has a role in Treg cell development and maintenance through STAT6 signalling. This leads to a successful pregnancy where, not only the placenta but also maternal decidua, amniochorionic membranes, cytotrophoblasts, foetal and maternal endothelial cells produces IL-4. Studies in animal models reported that abortion prone CBA/J females exhibit reduced levels of circulating and placental IL-4.<sup>42,43</sup>

Our results were on par with previous studies where low levels of IL-4 and IL-4 producing cells were reported by researchers in women with spontaneous abortions.<sup>2</sup> Literature also suggests that T-cell clones from decidua of women with normal pregnancy produce higher concentrations of IL-4 than from recurrent aborters.<sup>44,45</sup> This can be concerned with dynamic changes in cytokine levels associated with the pregnancy.<sup>46</sup> The above results can be attributed to the fact that at the commencement of pregnancy, a predominantly Th1 immune response (cell-mediated) driven by pro-inflammatory cytokines such as TNF- $\alpha$  exists while it later shifts to Th2 response (humoral) with the production of anti-inflammatory cytokines such as IL-4. This dynamic shift helps in the implantation of an embryo, trophoblast development and angiogenesis and subsequently establishes maternal immune tolerance in healthy pregnancy which may be failing in the RPL cases.<sup>47</sup>

Successful pregnancy is dependent on phase- and time-specific shifting of Th1-Th2 balance with Th2 cytokine profile associated with immune tolerance and persistent Th1 response is often linked with gravidity complications such as recurrent spontaneous abortions (RSA) and pre-eclampsia.<sup>11,29,48</sup> It is not the individual cytokine but the relative concentrations of pro- and anti-inflammatory cytokines that may resolve the overall milieu in pregnancy. Therefore, the TNF- $\alpha$ :IL-4 ratio was investigated between the first and second trimesters among healthy controls and patients in the present study and found higher in the first trimester than the second trimester in controls, but no change was observed between trimesters in patients. Our results indicate a shift in Th1 to Th2 cytokine profile during the second trimester necessitates the maintenance and development of the placenta and foetus.



**TABLE 4** Follow-up data of present study representing serum concentrations of sHLA-G5, IL-4, TNF- $\alpha$  and TNF- $\alpha$ :IL-4 ratio in controls and RPL patients with successful and loss of pregnancies

Category	Controls Mean $\pm$ SD (n = 135)	RPL patients with pregnancy loss Mean $\pm$ SD (n = 98) (72.6%)	RPL patients with successful pregnancy Mean $\pm$ SD (n = 37) (27.4%)	Adj. P*-value	Adj. P**,-value	Adj. P***-value
sHLA-G5	147.81 $\pm$ 21.23	47.2 $\pm$ 24.17	89.99 $\pm$ 5.54	<.0001	<.0001	<.0001
IL-4	22.72 $\pm$ 15.34	8.74 $\pm$ 2.67	8.81 $\pm$ 2.42	<.0001	<.0001	>.99
TNF- $\alpha$	146.47 $\pm$ 139.48	319.2 $\pm$ 104.71	377.33 $\pm$ 116.46	<.0001	<.0001	.036
TNF- $\alpha$ :IL-4 ratio	13.39 $\pm$ 25.51	42.54 $\pm$ 26.19	48.6 $\pm$ 27.18	<.0001	<.0001	.78

Note: Bold indicates statistically significant values (P .05).

The one-way ANOVA data presented with adjusted P-values  $\leq$  .05 considered significant after using the Bonferroni correction.

Abbreviations: n, number of subjects; SD, standard deviation.

P\*—Between controls and patients with pregnancy loss.

P\*\*—Between controls and patients with successful pregnancy.

P\*\*\*—Between patients with pregnancy loss and patients with successful pregnancy.

Kim et al observed increased TNF- $\alpha$  +/IL-4 + and TNF- $\alpha$  +/IL-10+ T-cell ratios and Th1-guided polarization in women with multiple unsuccessful in vitro fertilization (IVF) cycles.<sup>38,49</sup> Similarly, Clark et al, in mouse models, observed the release of TNF- $\alpha$  by decidua and found a correlation between Th1/Th2 cytokine ratio at maternofetal interface and susceptibility to abortions.<sup>50</sup> On the contrary low levels of Th1 cytokine/IL-4 ratios were reported in women with spontaneous abortions by Chatterjee et al.<sup>2</sup> Nevertheless, systematic studies are warranted with respect to multiple pro- and anti-inflammatory cytokine signatures to understand the delicate balance of cytokine signalling in pregnancy maintenance, which may help in evolving better management strategies for RPL cases.

sHLA-G molecules were shown to contribute to maternal cytokine profile modulation especially the upregulation of anti-inflammatory cytokines such as IL-3, IL-4 and IL-10.<sup>51</sup> Lombardelli et al provided substantial evidence that HLA-G5 can interact with inhibitory leukocyte immunoglobulin-like receptor-2 (ILT2) receptor on decidual CD4+ T cells to induce them to produce IL-4 which appears to be one of the critical anti-inflammatory cytokines for successful pregnancy outcome.<sup>4</sup> Rebmann et al<sup>52</sup> reported that the cells expressing HLA-G can modulate decidual mononuclear cells or peripheral blood mononuclear cells to produce and release cytokines which shift Th1/Th2 balance towards relatively Th2 dominance. Our data exploration showed no significant correlation between sHLA-G5 levels and IL-4 or TNF- $\alpha$ . This suggests that further studies are required to understand the interplay of master immunoregulatory molecules and cytokines.

## 5 | CONCLUSION

In conclusion, from our observations, it appears that the sHLA-G5 isoform can serve as a potential marker to predict the capability of the mother to establish tolerance towards semi-allograft foetus and can contribute to improving pregnancy outcome. However, one needs to recognize the role of different isoforms of HLA-G as an immunomodulatory molecule that regulate the cytokine profile apart from sHLA-G5. Nevertheless, the evaluation of embryonic sHLA-G5 levels can provide a better understanding of predicting pregnancy outcome. Systematic prospective studies by assessing the sHLA-G5 levels and cytokine signature in narrow intervals of gestational period along with correlating the biomarkers with pregnancy outcome will yield valuable information to develop a predictive diagnostic marker, further to improve preventive and management strategies for RPL. In addition, comprehensive knowledge of shifts in the maternal cytokine and immune cell profile during early pregnancy could provide a better understanding of immune response,

to distinguish successful pregnancy from adverse pregnancy complications.

## ACKNOWLEDGMENT

We acknowledge the cooperation extended by the blood donors. This study is funded by University Grants Commission (UGC), Government of India, New Delhi for providing Basic Scientific Research (BSR) fellowship (JRF and SRF) (Award letter no: 370/VRD/HOD/BIOCHEM/OU/2015) to DM and Indian Council for Medical Research (ICMR) (ID 2019-1022), Government of India.

## CONFLICT OF INTEREST

The authors declare no conflict of interest regarding the publication of this paper.

## AUTHORS CONTRIBUTION

Dhatri Madduru (DM) performed experimental work, data collection, data analysis and interpretation, drafting the article. Kethora Dirsipam (KD) involved in data analysis and contributed to analysis tools. Goli Mahalakshmi (GM) involved in sampling. Venkata Ramana Devi (VRD) involved in supervision and critical inputs for the article. Parveen Jahan (PJ) involved in conceptualization and study design, formal analysis, proofreading and critical revision of the manuscript. All authors read and approved the manuscript before the final submission.

## DATA AVAILABILITY STATEMENT

The data that support the findings of this study are available from the corresponding author upon reasonable request.

## ORCID

Parveen Jahan  <https://orcid.org/0000-0003-3203-1816>

## REFERENCES

- Dutta S, Sengupta P. Defining pregnancy phases with cytokine shift. *J Pregnancy Reprod.* 2017;1(4):1-3. doi:<https://doi.org/10.15761/JPR.1000124>
- Chatterjee P, Chiasson VL, Bounds KR, Mitchell BM. Regulation of the anti-inflammatory cytokines interleukin-4 and interleukin-10 during pregnancy. *Front Immunol.* 2014;5:1-6. doi:<https://doi.org/10.3389/fimmu.2014.00253>
- Fuzzi B, Rizzo R, Criscuoli L, et al. HLA-G expression in early embryos is a fundamental prerequisite for the obtainment of pregnancy. *Eur J Immunol.* 2002;32(2):311-315. doi:[https://doi.org/10.1002/1521-4141\(200202\)32:2<311:AID-IMMU311>3.0.CO;2-8](https://doi.org/10.1002/1521-4141(200202)32:2<311:AID-IMMU311>3.0.CO;2-8)
- Lombardelli L, Aguerre-Girr M, Logiodice F, et al. HLA-G5 induces IL-4 secretion critical for successful pregnancy through differential expression of ILT2 receptor on decidual CD4+ T cells and macrophages. *J Immunol.* 2013;191(7):3651-3662. doi:<https://doi.org/10.4049/jimmunol.1300567>
- Dahl M, Hviid TVF. Human leucocyte antigen class Ib molecules in pregnancy success and early pregnancy loss. *Hum Reprod Update.* 2012;18(1):92-109. doi:<https://doi.org/10.1093/humupd/dmr043>
- Nowak I, Wilczyrska K, Radwan P, et al. Association of soluble HLA-G plasma level and HLA-G genetic polymorphism with pregnancy outcome of patients undergoing in vitro fertilization embryo transfer. *Front Immunol.* 2020;10:1-20. doi:<https://doi.org/10.3389/fimmu.2019.02982>
- Hunt JS, Petroff MG, McIntire RH, Ober C. HLA-G and immune tolerance in pregnancy. *FASEB J.* 2005;19(7):681-693. doi:<https://doi.org/10.1096/fj.04-2078rev>
- Meer A, Lukassen HGM, van Cranenbroek B, et al. Soluble HLA-G promotes Th1-type cytokine production by cytokine-activated uterine and peripheral natural killer cells. *Mol Hum Reprod.* 2007;13(2):123-133. doi:<https://doi.org/10.1093/molehr/gall100>
- Le Bouteiller P. HLA-G in human early pregnancy: control of uterine immune cell activation and likely vascular remodeling. *Biomed J.* 2015;38(1):32-38. doi:<https://doi.org/10.4103/2319-4170.131376>
- Vianna P, Mondadori AG, Bauer ME, Dornfeld D, Chies JAB. HLA-G and CD8+ regulatory T cells in the inflammatory environment of pre-eclampsia. *Reproduction.* 2016;152(6):741-751. doi:<https://doi.org/10.1530/REP-15-0608>
- Wegmann TG, Lin H, Guilbert L, Mosmann TR. Bidirectional cytokine interactions in the maternal-fetal relationship: is successful pregnancy a TH2 phenomenon? *Immunol Today.* 1993;14(7):353-356. doi:[https://doi.org/10.1016/0167-5699\(93\)90235-D](https://doi.org/10.1016/0167-5699(93)90235-D)
- Daniel WW, Cross CL. *Biostatistics: A Foundation for Analysis in the Health Sciences*, 7th ed. John Wiley & Sons; 1999.
- Sykes L, MacIntyre DA, Yap XJ, Tiong GT, Bennett PR. The Th1:Th2 dichotomy of pregnancy and preterm labour. *Mediators Inflamm.* 2012;2012:1-12.
- Solier C, Aguerre-Girr M, Lenfant F, et al. Secretion of proapoptotic intron 4-retaining soluble HLA-G1 by human villous trophoblast. *Eur J Immunol.* 2002;32(12):3576-3586. doi:[https://doi.org/10.1002/1521-4141\(200212\)32:12<3576:AID-IMMU3576>3.0.CO;2-M](https://doi.org/10.1002/1521-4141(200212)32:12<3576:AID-IMMU3576>3.0.CO;2-M)
- Dahl M, Djuricic S, Hviid TVF. The many faces of human leukocyte antigen-G: relevance to the fate of pregnancy. *J Immunol Res.* 2014;2014:1-11. doi:<https://doi.org/10.1155/2014/591489>
- Athanassakis I, Paflis M, Ranella A, Vassiliadis S. Detection of soluble HLA-G levels in maternal serum can be predictive for a successful pregnancy. *Transplant Proc.* 1999;31(4):1834-1837. doi:[https://doi.org/10.1016/s0041-1345\(99\)00181-5](https://doi.org/10.1016/s0041-1345(99)00181-5)
- Abediankenari S, Farzad F, Rahmani Z, Hashemi-Soteh MB. HLA-G and G7 isoforms in pregnant women. *Iran J Allergy Asthma Immunol.* 2015; 14(2): 217-221.
- Pfeiffer KA, Fimmers R, Engels G, van der Ven H, van der Ven K. The HLA-G genotype is potentially associated with idiopathic recurrent spontaneous abortion. *Mol Hum Reprod.* 2001;7(4):373-378. doi:<https://doi.org/10.1093/molehr/7.4.373>
- Rebmann V, Van der Ven K, Pässler M, Pfeiffer K, Krebs D, Grosse-Wilde H. Association of soluble HLA-G plasma levels with HLA-G alleles. *Tissue Antigens.* 2001;57(1):15-21. doi:<https://doi.org/10.1034/j.1399-0039.2001.057001015.x>
- Rizzo R, Andersen AS, Lassen MR, et al. Soluble human leukocyte antigen-G isoforms in maternal plasma in early and late pregnancy. *Am J Reprod Immunol.* 2009;62(5):320-338. doi:<https://doi.org/10.1111/j.1600-0897.2009.00742.x>

21. Zhu X, Han T, Yin G, Wang X, Yao Y. Expression of human leukocyte antigen-G during normal placentation and in preeclamptic pregnancies. *Hypertens Pregnancy*. 2012;31(2):252-260. doi:<https://doi.org/10.3109/10641955.2011.638955>
22. Hunt JS, Jadhav L, Chu W, Geraghty DE, Ober C. Soluble HLA-G circulates in maternal blood during pregnancy. *Am J Obstet Gynecol*. 2000;183(3):682-688. doi:<https://doi.org/10.1067/mob.2000.106762>
23. Alegre E, Diaz-Lagares A, LeMaoult J, Lopez-Moratalla N, Carosella ED, Gonzalez A. Maternal antigen presenting cells are a source of plasmatic HLA-G during pregnancy: longitudinal study during pregnancy. *Hum Immunol*. 2007;68(8):661-667. doi:<https://doi.org/10.1016/j.humimm.2007.04.007>
24. Hackmon R, Hallak M, Krup M, et al. HLA-G antigen and parturition: maternal serum, fetal serum, and amniotic fluid levels during pregnancy. *Fetal Diagn Ther*. 2004;19(5):404-409. doi:<https://doi.org/10.1159/000078992>
25. Hehlhans T, Pfeffer K. The intriguing biology of the tumour necrosis factor/tumour necrosis factor receptor superfamily: players, rules and the games. *Immunology*. 2005;115(1):1-20. doi:<https://doi.org/10.1111/j.1365-2567.2005.02143.x>
26. Haider S, Knofler M. Human tumour necrosis factor: physiological and pathological roles in placenta and endometrium. *Placenta*. 2009;30(2):111-123. doi:<https://doi.org/10.1016/j.placenta.2008.10.012>
27. Shynlova O, Lee Y-H, Srikhajon K, Lye SJ. Physiologic uterine inflammation and labor onset: integration of endocrine and mechanical signals. *Reprod Sci*. 2013;20(2):154-167. doi:<https://doi.org/10.1177/1933719112446084>
28. Li H-H, Xing-Hua X, Tong J, Zhang K-Y, Zhang C, Chen Z-J. Association of TNF- $\alpha$  genetic polymorphisms with recurrent pregnancy loss risk: a systematic review and meta-analysis. *Reprod Biol Endocrinol*. 2016;14(6):1-10. doi:<https://doi.org/10.1186/s12958-016-0140-6>
29. Wang W, Sung N, Gilman-Sachs A, Kwak-Kim J. T helper (Th) cell profiles in pregnancy and recurrent pregnancy losses: Th1/Th2/Th9/Th17/Th22/Tfh Cells. *Front Immunol*. 2020;11:2025. doi:<https://doi.org/10.3389/fimmu.2020.02025>
30. Clark DA, Chaouat G, Arck PC, Mittrucker HW, Levy GA. Cytokine-dependent abortion in CBA  $\times$  DBA/2 mice is mediated by the procoagulant fgl2 prothrombinase [correction of prothombinase]. *J Immunol*. 1998;160:545-549.
31. Laird SM, Tuckerman EM, Cork BA, Linjawi S, Blakemore AIF, Li TC. A review of immune cells and molecules in women with recurrent miscarriage. *Hum Reprod Update*. 2003;9(2):163-174. doi:<https://doi.org/10.1093/humupd/dmg013>
32. Abdullah GA, Mahdi NK. The role of cytokines among women with spontaneous miscarriage. *Med J Islamic World Acad Sci*. 2013;21(3):119-124.
33. Azizieh FY, Raghupathy RG. Tumour necrosis factor- $\alpha$  and pregnancy complications: a prospective study. *Med Princ Pract*. 2015;24(2):165-170. doi:<https://doi.org/10.1159/000369363>
34. AlJameil N, Tabassu H, AlMayouf H, et al. Identification of serum cytokines as markers in women with recurrent pregnancy loss or miscarriage using MILLIPLEX analysis. *Biomed Res*. 2018;29(18):3512-3517. doi:<https://doi.org/10.4066/biomedicalresearch.29-18-1030>
35. Knöfler M, Mösl B, Bauer S, Griesinger G, Husslein P. TNF- $\alpha$ /TNFRI in primary and immortalized first trimester cytotrophoblasts. *Placenta*. 2000;21(5-6):525-535. doi:<https://doi.org/10.1053/plac.1999.0501>
36. Garcia-Lloret MI, Winkler-Lowen B, Guilbert LJ. Monocytes adhering by LFA-1 to placental syncytiotrophoblasts induce local apoptosis via release of TNF- $\alpha$ . A model for hematogenous initiation of placental inflammations. *J Leukoc Biol*. 2000;68(6):903-908. doi:<https://doi.org/10.1189/jlb.68.6.903>
37. Aschkenazi S, Straszewski S, Verwer KM, Foellmer H, Rutherford T, Mor G. Differential regulation, and function of the Fas/Fas ligand system in human trophoblast cells. *Biol Reprod*. 2002;66(6):1853-1861. doi:<https://doi.org/10.1095/biolreprod66.6.1853>
38. Rezaei A, Dabbagh A. T-Helper (1) cytokines increase during early pregnancy in women with a history of recurrent spontaneous abortion. *Med Sci Monit*. 2002;8(8):607-610.
39. Al-Hilli NM. Maternal serum tumor necrosis factor- $\alpha$  in patients with missed and recurrent miscarriage. *Med J Babylon*. 2009;6(3-4):521-526.
40. Hua F, Li CH, Wang H, Xu HG. Relationship between expression of COX-2, TNF- $\alpha$ , IL-6 and autoimmune-type recurrent miscarriage. *Asian Pac J Trop Med*. 2013;6(12):990-994. doi:[https://doi.org/10.1016/S1995-7645\(13\)60178-9](https://doi.org/10.1016/S1995-7645(13)60178-9)
41. Guilbert LJ. There is a bias against type 1 (inflammatory) cytokine expression and function in pregnancy. *J Reprod Immunol*. 1996;32(2):105-110. doi:[https://doi.org/10.1016/s0165-0378\(96\)00996-5](https://doi.org/10.1016/s0165-0378(96)00996-5)
42. Chaouat G, Assal Meliani A, Martal J, et al. IL-10 prevents naturally occurring fetal loss in the CBA  $\times$  DBA/2 mating combination, and local defect in IL-10 production in this abortion-prone combination is corrected by in vivo injection of IFN- $\tau$ . *J Immunol*. 1995;154(9):4261-4268.
43. Jin LP, Zhou YH, Zhu XY, Wang MY, Li DJ. Adoptive transfer of paternal antigen-hyporesponsive T cells facilitates a Th2 bias in peripheral lymphocytes and at materno-fetal interface in murine abortion-prone matings. *Am J Reprod Immunol*. 2006;56(4):258-266. doi:<https://doi.org/10.1111/j.1600-0897.2006.00425.x>
44. Makhseed M, Raghupathy R, Azizieh F, Omu A, Al-Shamali E, Ashkanani L. Th1 and Th2 cytokine profiles in recurrent aborters with successful pregnancy and with subsequent abortions. *Hum Reprod*. 2001;16(10):2219-2226. doi:<https://doi.org/10.1093/humrep/16.10.2219>
45. Kwak-Kim JYH, Gilman-Sachs A, Kim CE. T Helper 1 and 2 immune responses in relationship to pregnancy, nonpregnancy, recurrent spontaneous abortions and infertility of repeated implantation failures. Markert UR (ed): *Immunology of Gametes and Embryo Implantation*. Chem Immunol Allergy. Basel, Karger. 2005; 88:64-79. <https://doi.org/https://doi.org/10.1159/000087821>
46. Moreau P, Flajollet S, Carosella ED. Non-classical transcriptional regulation of HLA-G: an update. *J Cell Mol Med*. 2009;13(9B):2973-2989. doi:<https://doi.org/10.1111/j.1582-4934.2009.00800.x>
47. Durmanova V, Homolova M, Drobny J, Shawkatova I, Buc M. Role of HLA-G and other immune mechanisms in pregnancy. *Cent Eur J Biol*. 2013;8(3):226-239. doi:<https://doi.org/10.2478/s11535-013-0130-4>
48. Hviid TVF. HLA-G in human reproduction: aspects of genetics, function, and pregnancy complications. *Hum Reprod Update*. 2006;12(3):209-232. doi:<https://doi.org/10.1093/humupd/dmi048>
49. Kwak-Kim JY, Chung-Bang HS, Ng SC, et al. Increased Thelper1 cytokine responses by circulating T cells are present in women with recurrent pregnancy losses and in infertile women with multiple

- implantation failures after IVF. *Hum Reprod.* 2003;18(4):767-773. doi:<https://doi.org/10.1093/humrep/deg156>
50. Clark DA, Croitoru K. TH1/TH2, imbalance due to cytokine-producing NK, gammadelta T and NK-gammadelta T cells in murine pregnancy decidua in success or failure of pregnancy. *Am J Reprod Immunol.* 2001;45(5):257-265. doi:<https://doi.org/10.1111/j.8755-8920.2001.450501.x>
51. Kusanovic JP, Romero R, Jodicke C, et al. Amniotic fluid soluble human leukocyte antigen-G in term and preterm parturition, and intra-amniotic infection/inflammation. *J Matern Fetal Neonatal Med.* 2009;22(12):1151-1166. doi:<https://doi.org/10.3109/14767050903019684>
52. Rebmann V, da Silva F, Nardi BW, Horn PA. HLA-G as a tolerogenic molecule in transplantation and pregnancy. *J Immunol Res.* 2014;1-16: doi:<https://doi.org/10.1155/2014/297073>

## SUPPORTING INFORMATION

Additional supporting information may be found online in the Supporting Information section.

**How to cite this article:** Madduru D, Dirsipam K, Goli M, Ramana Devi V, Jahan P. Association of reduced maternal sHLA-G5 isoform levels and elevated TNF- $\alpha$ /IL-4 cytokine ratio with Recurrent Pregnancy Loss: A study on South Indian women. *Scand J Immunol.* 2021;94:e13095. <https://doi.org/10.1111/sji.13095>

# Association of FOXP3 rs3761548 polymorphism and its reduced expression with unexplained recurrent spontaneous abortions: A South Indian study

Kethora Dirsipam<sup>1</sup> | Deepika Ponnala<sup>1</sup> | Dhatri Madduru<sup>2</sup> | Rajeswari Bonu<sup>3</sup> | Parveen Jahan<sup>4</sup>

<sup>1</sup>Institute of Genetics and Hospital for Genetic Diseases, Osmania University, Hyderabad, India

<sup>2</sup>Department of Biochemistry, Osmania University, Hyderabad, India

<sup>3</sup>Department of Obstetrics & Gynaecology, Niloufer Hospital, Hyderabad, India

<sup>4</sup>School of Sciences, Maulana Azad National Urdu University, Hyderabad, India

## Correspondence

Parveen Jahan, School of Sciences, Maulana Azad National Urdu University, Gachibowli, Hyderabad-32, India.  
Email: drparveenjahan2020@gmail.com

## Funding information

Indian Council for Medical Research, Grant/Award Number: ID 2019-1022

## Abstract

**Problem:** Fork Head Box Protein 3 (FOXP3) is an X-linked gene, codes for a master transcription regulatory protein that controls the development and function of immunosuppressive T regulatory (Treg) cells. They are crucial mediators of maternal foetal tolerance and successful pregnancy outcome. The aim of the study is to evaluate the association of FOXP3 rs3761548 functional polymorphism and to assess the serum concentrations of full-length FOXP3 protein in Unexplained Recurrent Spontaneous Abortions (URSA) patients of Southern India.

**Method of study:** The study included blood samples from 150 URSA patients and 150 healthy, pregnant parous women. Polymerase Chain Reaction-Restriction Fragment Length Polymorphism was done for rs3761548 FOXP3 genotyping. Serum concentrations of full-length FOXP3 protein were estimated by enzyme-linked immunosorbent assay.

**Results:** The frequencies of mutant A allele, CA and AA genotypes of rs3761548 functional polymorphism were significantly elevated in patients compared to healthy, pregnant parous women and exhibited a two, three and twofold increased risk respectively towards URSA. Serum concentrations of full-length FOXP3 protein were high in controls compared to patients ( $10.14 \pm .30$  vs.  $8.84 \pm 1.73$  ng/ml;  $p < .05$ ).

**Conclusion:** Our results advocate an association of FOXP3 rs3761548 polymorphism and reduced expression of full-length FOXP3 protein with URSA.

## KEYWORDS

FOXP3, polymorphism, regulatory T cells

## 1 | INTRODUCTION

Recurrent Pregnancy Loss (RPL) is a serious growing reproductive problem among the young couples, defined as three or more consecutive miscarriages before 20 weeks of gestational age,<sup>1</sup> while the

American Society for Reproductive Medicine (ASRM) defines recurrent miscarriage as two previous losses.<sup>2</sup> Despite various clinical and experimental tests, yet there is not an accurate and efficient diagnostic method during the early stages of pregnancy in more than half of RPL patients.<sup>3</sup> The risk factors linked to its pathogenesis are

Kethora Dirsipam and Deepika Ponnala contributed equally do this work.

© 2021 John Wiley & Sons A/S. Published by John Wiley & Sons Ltd

genetic disorders such as foetal chromosomal abnormalities, maternal factors including anatomical deformities, placental anomalies, thrombophilia, endocrine disorders, immune dysfunction, infection, smoking, psychological trauma, stress and environmental factors.<sup>4,5</sup> Among these factors, immune function appears to play a significant role in protecting the pregnancy by preventing response to the semi allograft.<sup>6</sup> Functional variations in the genes coding for the expression and regulation of immune response may predispose the mother to recurrent abortions.<sup>7-11</sup>

The Fork Head Box Protein 3 (FOXP3) gene, a member of transcription factor winged helix family, located on chromosome Xp11.23, regulates the development and function of CD4+CD25+ regulatory T (Treg) cells.<sup>12,13</sup> In unexplained recurrent spontaneous abortions (URSA), it is found that Tregs (CD4+CD25+) are reduced in peripheral blood as well as in decidua of pregnant women.<sup>14</sup> In addition, in peripheral blood and decidua, decreased expression of FOXP3 gene, a marker of Treg cell, indicating that alteration in the Treg cell-dependent maintenance of feto-maternal tolerance contributes to pregnancy loss.<sup>15,16</sup>

Increased FOXP3 promoter methylation downregulates the expression of the FOXP3 protein associated with URSA.<sup>17</sup> Further, different single-nucleotide variants (SNVs) in the promoter region of FOXP3, which affect the expression of FOXP3 and impair the Treg differentiation and function, have been allied with occurrence of URSA in various populations.<sup>7-11</sup> The rs3761548 FOXP3 (-3279) C>A variant is located in the core of 'TGCAGGCCTC' sequence of the putative binding site for the transcription factor specificity protein 1 (Sp1), and the A allele is correlated with the reduction in FOXP3 expression,<sup>18</sup> which was extensively studied in several human diseases. Previously, we reported an association of this polymorphism with the patients of preeclampsia, vitiligo and breast cancer in South Indian patients.<sup>19-21</sup>

The aim of the current study is not only to evaluate the association of FOXP3 rs3761548 (-3279) C>A functional polymorphism with URSA, but also to assess the full-length FOXP3 serum protein levels in URSA patients of Southern India.

## 2 | MATERIALS AND METHODS

The study population consists a total of 300 subjects that include 150 URSA patients, who had a history of at least two successive miscarriages with unexplained aetiology before 12 weeks of gestation, and 150 age-matched healthy, pregnant parous women as controls with at least two live births and with no history of spontaneous abortions or any other known diseases (age: 18–40 years) were recruited based

upon the information available from case sheets of patients, where (clinical pregnancies documented by ultrasound or histopathology) test reports of diabetes, thyroid, polycystic ovary syndrome, progesterone, oestrogen, cervical incompetence, chromosomal abnormality etc. were screened, diagnosed and investigated by the Department of Obstetrics & Gynaecology of Gandhi Medical and Niloufer Hospital, Hyderabad. Women with history of only one spontaneous abortion, with history of induced abortions and abortions with known reasons such as anatomical problems, hormonal imbalances etc. were excluded from the study. Clinical and demographical information such as age, Body Mass Index (BMI), Haemoglobin (Hb), age at menarche, age at first conception, number of abortions, consanguinity was collected from both patients and controls. Informed consent was obtained from all patients and controls. The study was approved by the institutional ethics committees, (Institute of Genetics and Hospital for Genetic Diseases, Osmania Medical College) Hyderabad. This manuscript refers URSA and RPL/RSA interchangeably.

### 2.1 | Selection of SNP—rs3761548 (-3279) C>A in FOXP3 gene region

For the present study, SNP databases, Ensembl (<http://www.ensembl.org/index.html>) and the International HapMap database (<http://hapmap.ncbi.nlm.nih.gov/index.html.en>) were used to select rs3761548 (-3279) C>A polymorphism in the FOXP3 gene region from chromosome X at nucleotide position 49,261,409 to 49,261,972. Further, published data show scientific evidence to illustrate potential role of rs3761548 in RPL<sup>7-11</sup> and auto-immune diseases.<sup>22</sup>

### 2.2 | Blood collection and DNA extraction

Blood samples (5 ml) from both URSA patients and healthy controls were collected in EDTA-coated and clot activator collection vials. Genomic DNA was extracted from whole blood using QIAamp DNA Blood Mini Kit (CAT No. /ID: 51104) according to the manufacturer's protocol.

### 2.3 | Genotyping of rs3761548 (-3279) C>A polymorphism

Genotypes of rs3761548 polymorphism were determined using the Polymerase Chain Reaction (PCR) and Restriction Fragment Length Polymorphism (RFLP), presented in Table 1. In short, PCR for amplification of 564 bp region in the FOXP3 promoter was performed in

TABLE 1 Primers used in the genotyping of -3279 C>A polymorphism by PCR-RFLP

Marker/method	Primer type	Primer sequence (5'-3')	Annealing temperature	Product size	Restriction enzyme
(-3279)C/A PCR-RFLP	Forward	GACTTAACCAGACAGCGTAG	51°C	564 bp	Pst1
	Reverse	CTGGTGTGCCTTTGGTCT			

a volume of 25  $\mu$ l, containing 2  $\mu$ g/ml of genomic DNA, 10 pmol of each primer, 2.0 mM of dNTPs, 1.5 mM of MgCl<sub>2</sub>, 10 $\times$  PCR buffer and 0.5 U Taq DNA polymerase (G Biosciences). The PCR conditions for amplification of rs3761548(-3279) C>A location were initial denaturation step at 95°C for 5 min, followed by 28 cycles of 94°C for 35 s, annealing temperature of 51°C for 40 s, extension at 72°C for 40 s, final extension at 72°C for 5 min and holds at 4°C. The amplified PCR product of 564 bp was digested with 0.5  $\mu$ l of Pst1 (CAT No: R01405) restriction enzyme at 37°C for an hour and then separated on a 2% agarose gel stained with ethidium bromide at 100 V for 20 min. and visualized under ultraviolet light with a 100-bp DNA ladder. Genotypes of rs3761548 C>A were identified by the presence of three different bands: C/C (374 bp, 190 bp), C/A (564 bp, 374 bp and 190 bp) and A/A (564 bp) in the ethidium bromide stained gel.

## 2.4 | Estimation of FOXP3 serum protein levels

The concentrations of full-length FOXP3 protein were measured before 12th week of pregnancy for all the patients and controls using enzyme-linked immunosorbent assay (ELISA) kit (KINESISDx, CAT No. K12-0693), as per the manufacturer's instructions.

**TABLE 2** Clinical and demographic characteristics of the study group

Category	Controls (150) X $\pm$ SD	Patients (150) X $\pm$ SD	p-Value
Age (years)	24.64 $\pm$ 3.13	24.91 $\pm$ 4.16	.53
BMI (kg/m <sup>2</sup> )	21.38 $\pm$ 4.38	21.91 $\pm$ 4.00	.27
Hb (g/dl)	10.23 $\pm$ 1.66	9.98 $\pm$ 1.31	.15
Age at menarche (years)	12.5 $\pm$ 1.35	12.84 $\pm$ 1.46	.03 <sup>*</sup>
Age at first conception (years)	19.18 $\pm$ 2.80	20.24 $\pm$ 3.64	.005 <sup>*</sup>
No. of abortions	NA	2.68 $\pm$ 1.01	NA
Mean gestational age (months)	4.36 $\pm$ 1.14	5.04 $\pm$ 1.32	<.0001 <sup>*</sup>

Note: Values are represented as mean  $\pm$  SEM.

\* $p$  < .05.

## 2.5 | Statistical analysis

Hardy-Weinberg equilibrium was tested for FOXP3 (-3279) C>A variant in URSA patients and healthy controls. Further deviation in the allele and genotype frequencies between patients and controls was tested for statistical significance by Fisher's exact test and the odds ratio at 95% Confidence Interval (C.I.) using Open EPI6 online statistical software (Open EPI v 2.3.1, Emory University). All the  $p$  values were two-sided, and the level of significance was considered at  $p$  < .05.  $t$ -test (Independent sample test) was used to test the difference between two sample means. ANOVA was done to test the significant difference among the groups using IBM SPSS statistics. Relationship between the risk factors for URSA with respect to genotypes was assessed through Multiple Logistic Regression (MLR).

## 3 | RESULTS

The clinical and demographic characteristics of the study group ( $N$  = 300) were presented in Table 2. A significant variation was observed between patients and controls with respect to mean age at menarche ( $p$  = .03) and mean age at first conception ( $p$  < .01).

Further, 7% of the patients showed irregular menstrual cycles in comparison with only 3% in controls. Eleven per cent of the patients experienced more than 3 pregnancy losses whereas 89% had  $\leq$ 3 pregnancy losses. The percentage of consanguinity was 25% in patients and 20% in control group ( $p$  = .3).

### 3.1 | Genotype and Allele distribution among controls and patients

The genotype distribution of rs3761548 (-3279) C>A of FOXP3 gene in URSA patients and healthy controls is presented in Table 3. Individuals with CC genotype predominated in controls compared to URSA patients (OR 0.10, 95% C.I.: 0.05–0.19,  $p$  = < .0001), while women with CA and AA genotypes were in higher frequency among the patients and exhibited an odds ratio of 3.18 and 2.23 (CA vs.

**TABLE 3** Genotype and allele frequency distribution of FOXP3 (-3279) C>A polymorphism among the study group

SNP	Genotype	Controls (150) n (%)	Patients (150) n (%)	$\chi^2$ value	OR (95% CI)	p Value
rs3761548 C/A	CC	72 (48)	13 (9)	55.22	0.10 (0.05–0.19)	<.0001 <sup>*</sup>
	CA	60 (40)	102 (68)	22.56	3.18 (1.98–5.11)	<.0001 <sup>*</sup>
	AA	18 (12)	35 (23)	5.86	2.23 (1.19–4.15)	<.01 <sup>*</sup>
	C	204 (68)	128 (43)	Reference		
	A	96 (32)	172 (57)	37.93	2.85 (2.04–3.98)	<.0001 <sup>*</sup>
	HWE	Controls			0.98 (0.32)	
	X <sup>2</sup> (p-value)	Patients		22.8 (0.000002)		

Abbreviation: 95% C.I., Confidence Interval.

\* $p$  < .05.

## Odds ratio for Genotypes and Alleles of FOXP3 (-3279) C&gt;A polymorphism

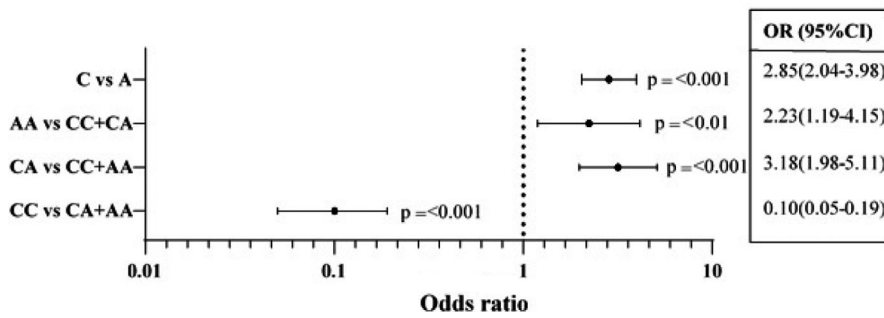


FIGURE 1 Forest plot representing the odds ratio for genotypes and alleles of FOXP3 (-3279) C>A polymorphism in URSA patients and controls

## MEAN FULL-LENGTH FOXP3 PROTEIN LEVELS(ng/ml) IN PATIENTS AND CONTROLS

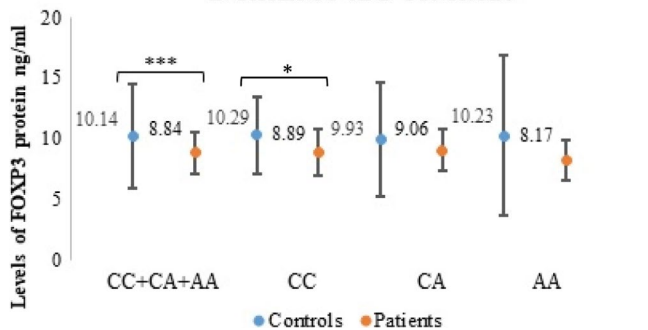


FIGURE 2 Full-length FOXP3 protein concentrations in patients and controls based on FOXP3 rs3761548 genotypes

CC+AA, OR 3.18, 95% C.I.: 1.98–5.11,  $p < .0001$ ; AA vs. CC+CA, OR 2.23, 95% C.I.: 1.19–4.15,  $p < .01$ , respectively. Further, variant allele A was significantly elevated in case of patients compared with healthy counterparts (A vs. C, OR: 2.85, 95% C.I.: 2.04–3.98,  $p < .0001$ ) shown in Figure 1.

### 3.2 | Circulating levels of full-length FOXP3 protein among the study group

Circulating levels of full-length FOXP3 protein were significantly higher in controls compared to patients ( $10.14 \pm 4.30$  vs.  $8.84 \pm 1.73$  ng/ml) shown in Figure 2. Further, genotype-dependent variation with respect to the protein concentrations was noted within the patients but not in controls. However, in correspondence to CC genotype, there was a significant variation between patients and controls, presented in Table 4.

### 3.3 | Multiple logistic regression analysis in the URSA group

The multiple logistic regression analysis was performed to identify the independent risk factors for recurrent abortions among URSA patients, but none of the clinical and demographic characters showed the association (Data not shown).

TABLE 4 Serum levels of full-length FOXP3 protein with respect to rs3761548 genotypes in URSA patients and healthy controls

Protein (ng/ml) Genotypes	Controls X $\pm$ SD (n)	Patients X $\pm$ SD (n)	p Value
CC+CA+AA	10.14 $\pm$ 4.30 (150)	8.84 $\pm$ 1.73 (150)	.001 <sup>***</sup>
CC	10.29 $\pm$ 3.20 (72)	8.89 $\pm$ 1.88 (13)	.03 <sup>*</sup>
CA	9.93 $\pm$ 4.68 (60)	9.06 $\pm$ 1.69 (102)	.17
AA	10.23 $\pm$ 6.59 (18)	8.17 $\pm$ 1.67 (35)	.2
(CC,CA & AA) p value	0.88	0.03 <sup>*</sup>	-

Note: Student t-test & ANOVA.

\*p-Value .05.; \*\*\*p-Value < 0.01.

## 4 | DISCUSSION

Normal pregnancy progression is the result of timely regulated local shifts between pro- and anti-inflammatory immune responses allowing implantation and placentation in a pro-inflammatory environment, foetal growth in an anti-inflammatory environment and finally the induction of labour and delivery again under pro-inflammatory conditions.<sup>23</sup> RPL is the complex and challenging scenario in reproductive medicine, needs coordination in evaluation and management of patients include gynaecologists, geneticists, immunologists and reproductive specialist. During pregnancy, human chorionic gonadotropin actively recruit peripheral Treg cells into the foetal-maternal interface,<sup>24</sup> mediate local expansion of decidual Treg cells<sup>25</sup> and convert conventional T cells into Treg cells.<sup>26,27</sup> This suggests that Tregs have a pivotal role in the induction and maintenance of foetal-maternal immunologic tolerance. Growth and development of Treg cells require expression of FOXP3 protein,<sup>28</sup> a Treg cell-specific marker; its attenuated expression due to epigenetics/FOXP3 gene variants may result in reduced production of regulatory T cells.<sup>29,30</sup>

Based upon the importance of FOXP3 protein for Treg cell function in pregnancy, firstly, we evaluated the link between functional variant of FOXP3 rs3761548 C>A, a recognized polymorphism



associated with decreased expression of full-length FOXP3 protein and, secondly, to measure the serum concentrations of full-length FOXP3 protein in RPL patients from Southern India.

The findings of the present study exhibited protective role of high producing CC genotype against RPL; a threefold and twofold increased risk for women carrying CA and AA genotypes correspondingly towards RPL. Moreover, A allele was shown to be significantly associated with RPL susceptibility. There is an inconsistency in the literature regarding the association of this polymorphism with RPL in different populations. Individually, a marked difference of FOXP3 rs3761548 genotype frequencies among URSA patients and healthy controls in Han Chinese and North Indian population was reported.<sup>7,9</sup> Allele A and AA genotype were also reported to be higher in RPL women in Gaza strip representing that this polymorphism is a risk factor for RPL, whereas a significant 2.5-fold increased risk of AA genotype towards RPL in Palestine population<sup>8,10</sup> and a significant association of CA and AA genotypes and A allele of FOXP3 rs3761548 polymorphism with URSA in Egyptian population was identified.<sup>11</sup> In contrast, there was no association seen in Iranian and North Indian URSA women.<sup>31-33</sup>

The functional aspect of FOXP3 rs3761548 polymorphism was first reported, showing that substitution of C>A leads to loss of binding to the c-Myb and E47 transcription factors, with subsequent defect in the FOXP3 gene transcription, as this region has a binding site for the transcription factor Sp1 where the A allele affects the interaction of sp-1 protein with FOXP3 gene promoter region.<sup>18</sup> Therefore, patients with the AA genotype may have weaker suppressive function and are difficult to accommodate foetal tolerance.

Having observed the CA and AA as risk and CC as protective genotypes, we sought to assess the genotype-dependent variation with respect to full-length FOXP3 protein among patients and controls. Overall, there was a prominent increase in the concentration of full-length FOXP3 protein in controls compared to patients. Further, genotype-dependent variation was observed within patients but not in the control group; a significant difference in protein levels between patients and controls of women with homozygous wild type (CC) was noted, which is considered to be a high producing genotype.

There are several studies that support our observation of low levels of FOXP3 protein in RPL patients than in controls. A study from China reported that the expressing quantity of FOXP3 protein in the decidua of URSA patients is lower than that in normal pregnant women.<sup>14</sup> In the decidua, significantly reduced proportions of (CD4+CD25+) Treg cells and FOXP3 expression were found in URSA patients with early miscarriages compared with normal early pregnant women.<sup>15</sup> FOXP3 protein quantity in the decidua of the URSA group was lower than that in Recurrent Spontaneous Abortion (RSA) patients with an abnormal embryo and in normal pregnant women.<sup>17</sup> Decreased concentration of FOXP3 was reported in RPL patients than in healthy controls among Egyptian women.<sup>34</sup> The FOXP3 expression in trophoblasts in the term placenta was significantly decreased compared with that in the normal early pregnancy.

Moreover, reduced expression of FOXP3 mRNA and protein was observed in women with RPL.<sup>35</sup> Our results are in agreement with above discussed reports, showing that circulating levels of full-length FOXP3 protein were significantly elevated in controls compared to patients.

In the light of existing literature and our observations, it may be surmised that high levels of FOXP3 in women during early pregnancy are crucial in regulating the immunological events through Treg cells at feto-maternal interphase; low levels may prove to be a risk in handling the dynamic events required in the continuation of the pregnancy, leading to adverse pregnancy outcome. This opinion needs to be substantiated by systematic cell-based studies.

Lack of genotype-dependent variation with respect to full-length FOXP3 protein levels within controls to certain extent can be contributed to other genetic factors like X-chromosomal inactivation<sup>36,37</sup> or FOXP3 isoform profile, as alternative splicing of FOXP3 appears to add another layer of complexity to Treg cell biology.<sup>38</sup>

## 5 | CONCLUSION

We conclude that A allele and AA/AC genotype of rs3761548 functional polymorphism of FOXP3 is associated with pregnancy loss in our ethnicity. Reduced concentrations of full-length FOXP3 protein linked with pregnancy loss appear to impact the Treg population at maternal-foetal interphase. Determination of genetic variants contributing to early miscarriages can be used for a better understanding of RPL's pathophysiology to improve molecular diagnosis. Large systematic studies in relation to genetic polymorphisms of FOXP3, its expression at various stages of gestation and Treg cells are warranted. Consequently, the information generated may open up novel Protein or cell-based medical interventions in the field of Unexplained Recurrent Pregnancy Loss which is crucial for species survival.

## ACKNOWLEDGEMENTS

We acknowledge the cooperation extended by the blood donors. This study is funded by Indian Council for Medical Research (ID 2019-1022), Government of India. We thank Dr. Arif Ahmed, MANUU, for his valuable inputs in the preparation of the manuscript.

## CONFLICT OF INTEREST

The authors have no conflict of interest.

## DATA AVAILABILITY STATEMENT

The data that support the findings of this study are available from the corresponding author upon reasonable request.

## REFERENCES

1. Regan L, Backos M, Rai R. The investigation and treatment of couples with recurrent first-trimester and second-trimester miscarriage. RCOG. Green-top Guideline17: 2011.

2. Practice Committee of American Society for Reproductive Medicine. Definitions of infertility and recurrent pregnancy loss: a committee opinion. *Fertil Steril*. 2013;99(1):63.
3. Moghbeli Meysam. Genetics of recurrent pregnancy loss among Iranian population. *Molecular Genetics & Genomic Medicine*. 2019;7 (9).
4. Park Han Sung, Ko Ki Han, Kim Jung Oh, An Hui Jeong, Kim Young Ran, Kim Ji Hyang, Lee Woo Sik, Kim Nam Keun. Association Study between the Polymorphisms of Matrix Metalloproteinase (MMP) Genes and Idiopathic Recurrent Pregnancy Loss. *Genes*. 2019;10 (5):347.
5. Ryu Chang Soo, Sakong Jung Hyun, Ahn Eun Hee, Kim Jung Oh, Ko Daeun, Kim Ji Hyang, Lee Woo Sik, Kim Nam Keun. Association study of the three functional polymorphisms (TAS2R46G>A, OR4C16G>A, and OR4X1A>T) with recurrent pregnancy loss. *Genes & Genomics*. 2019;41(1):61–70.
6. Mor G, Cardenas I. The immune system in pregnancy: a unique complexity. *Am J Reprod Immunol*. 2010;63(6):425–433.
7. Wu Z, You Z, Zhang C, et al. Association between functional polymorphisms of Foxp3 gene and the occurrence of unexplained recurrent spontaneous abortion in a Chinese Han population. *Clin Dev Immunol*. 2012;2012:1–7.
8. Jaber Mohammed, Sharif Fadel. Association between functional polymorphisms of Foxp3 and Interleukin-21 genes with the occurrence of recurrent pregnancy loss in Gaza strip-Palestine. *International Journal of Research in Medical Sciences*. 2014;2 (4):1687–1693.
9. Saxena D, Misra MK, Parveen F., Phadke SR, Agrawal S.. The transcription factor Forkhead Box P3 gene variants affect idiopathic recurrent pregnancy loss. *Placenta*. 2015;36 (2):226–231.
10. Fadel AS, Mohammed JS, Naim TB, Shadi FA&A. Polymorphism in Regulatory T-cell (Treg)-Related Genes Is Associated with Unexplained Recurrent Pregnancy Loss. *American Journal of Clinical and Experimental Medicine*. 2016;4(3):63–67. <http://dx.doi.org/10.11648/j.ajcem.20160403.15>
11. Farhan HM, Katta MH. Forkhead box p 3 (Foxp 3) gene polymorphisms and risk of unexplained recurrent spontaneous abortion among Egyptian women. *Gene Therapy & Molecular Biology*. 2018;18:34–42.
12. Pereira LMS, Gomes STM, Ishak R, Vallinoto ACR. Regulatory T cell and forkhead box protein 3 as modulators of immune homeostasis. *Front Immunol*. 2017;8:605.
13. Fontenot JD, Gavin MA, Rudensky AY. Foxp3 programs the development and function of CD4+CD25+ regulatory T cells. *Nat Immunol*. 2003;4(4):330–336.
14. Yang H, Qiu L, Chen G, Ye Z, Lü C, Lin Q. Proportional change of CD4+CD25+ regulatory T cells in decidua and peripheral blood in unexplained recurrent spontaneous abortion patients. *Fertil Steril*. 2008;89(3):656–661.
15. Mei S, Tan J, Chen H, Chen Y, Zhang J. Changes of CD4+CD25high regulatory T cells and FOXP3 expression in unexplained recurrent spontaneous abortion patients. *Fertil Steril*. 2010;94(6): 2244–2247.
16. Sayaka T, Akitoshi N, Tomoko S, Shigeru S. New paradigm in the role of regulatory t cells during pregnancy. *Front Immunol*. 2019;10:573.
17. Hou W, Li Z, Li Y, Fang L, Li J, Huang J, Li X, You Z. Correlation between protein expression of FOXP3 and level of FOXP3 promoter methylation in recurrent spontaneous abortion. *Journal of Obstetrics and Gynaecology Research*. 2016;42 (11):1439–1444.
18. Shen Z, Chen L, Hao F, Wang G, Fan P, Liu Y. Intron-1 rs3761548 is related to the defective transcription of Foxp3 in psoriasis through abrogating E47/c-Myb binding. *Journal of Cellular and Molecular Medicine*. 2010;14(1-2):226–241.
19. Jahan P, Sreenivasagari R, Goudi D, Komaravalli PL, Ishaq M. Role of Foxp3 Gene in Maternal Susceptibility to Pre-eclampsia - A Study From South India. *Scandinavian Journal of Immunology*. 2013;77 (2):104–108.
20. Jahan P, Cheruvu R, Tippisetty S, Komaravalli PL, Valluri V, Ishaq M. Association of FOXP3 (rs3761548) promoter polymorphism with nondermatomal vitiligo: A study from India. *Journal of the American Academy of Dermatology*. 2013;69(2):262–266.
21. Jahan P, Ramachander VRV, Maruthi G, Nalini S, Latha KP, Murthy TSR. Foxp3 promoter polymorphism (rs3761548) in breast cancer progression: a study from India. *Tumor Biology*. 2014;35 (4): 3785–3791.
22. Song P, Wang X-W, Li H-X, Li K, Liu L, Wei C, Jian Z, Yi X-L, Li Q, Wang G, Li C-Y, Gao T-W. Association betweenFOXP3polymorphisms and vitiligo in a Han Chinese population. *British Journal of Dermatology*. 2013;169(3):571–578.
23. Mor G, Aldo P, Alvero A. The unique immunological and microbial aspects of pregnancy. *Nat Rev Immunol*. 2017;17:469–482.
24. Schumacher A, Brachwitz N, Sohr S, et al. Human chorionic gonadotropin attracts regulatory T cells into the fetal-maternal interface during early human pregnancy. *J Immunol*. 2009;182(9):5488–5497.
25. Furcron AE, Romero R, Mial TN, et al. Human chorionic gonadotropin has anti-inflammatory effects at the maternal-fetal interface and prevents endotoxin-induced preterm birth, but causes dystocia and fetal compromise in mice. *Biol Reprod*. 2016;94(6):136.
26. Poloski E, Oettel A, Ehrentraut S, et al. JEG-3 Trophoblast cells producing human chorionic gonadotropin promote conversion of human CD4+FOXP3- T cells into CD4+FOXP3+ regulatory T cells and foster T cell suppressive activity. *Biol Reprod*. 2016;94(5):106.
27. Diao LH, Li GG, Zhu YC, Tu WW, Huang CY, Lian RC, Chen X, Li YY, Zhang T, Huang Y, Zeng Y. Human chorionic gonadotropin potentially affects pregnancy outcome in women with recurrent implantation failure by regulating the homing preference of regulatory T cells. *American Journal of Reproductive Immunology*. 2017;77(3).
28. Williams LM, Rudensky AY. Maintenance of the Foxp3-dependent developmental program in mature regulatory T cells requires continued expression of Foxp3. *Nat Immunol*. 2007;8(3):277–284.
29. Ziegler SF. FOXP3: of mice and men. *Annu Rev Immunol*. 2006;24:209–226.
30. Wan YY, Flavell RA. Regulatory T-cell functions are subverted and converted owing to attenuated Foxp3 expression. *Nature*. 2007;445(7129):766–770.
31. Hadinedoushan H, Abbasirad N, Aflatoonian A, Eslami G. The serum level of transforming growth factor beta1 and its association with Foxp3 gene polymorphism in Iranian women with recurrent spontaneous abortion. *Hum Fertil (Camb)*. 2015;18(1):54–59.
32. Naderi-Mahabadi F, Zarei S, Fatemi R, Kamali K, Pahlavanzadeh Z, Jeddi-Tehrani M, Kazemi T, Idali F. Association study of forkhead box P3 gene polymorphisms with unexplained recurrent spontaneous abortion. *Journal of Reproductive Immunology*. 2015;110: 48–53.
33. Mishra S, Srivastava A, Mandal K, Phadke SR. Study of the association of forkhead box P3 (FOXP3) gene polymorphisms with unexplained recurrent spontaneous abortions in Indian population. *J Genet*. 2018;97(2):405–410.
34. Zidan HE, Abdul-Maksoud RS, Mowafy HE, Elsayed WSH. The association of IL-33 and Foxp3 gene polymorphisms with recurrent pregnancy loss in Egyptian women. *Cytokine*. 2018;108:115–119.
35. Hu X, Wang Y, Mor G, Liao A. Forkhead box P3 is selectively expressed in human trophoblasts and decreased in recurrent pregnancy loss. *Placenta*. 2019;81:1–8.

36. Sui Y, Chen Q, Sun X. Association of skewed X chromosome inactivation and idiopathic recurrent spontaneous abortion: a systematic review and meta-analysis. *Reproductive BioMedicine Online*. 2015;31(2):140–148.
37. Wang J, Syretta CM, Kramerb MC, Basua A, Atchisona ML, Angueraa MC. Unusual maintenance of X chromosome inactivation predisposes female lymphocytes for increased expression from the inactive X. *PNAS*. 2016;113(14):E2029–E2038.
38. Mailer RKW. Alternative splicing of FOXP3—virtue and vice. *Front Immunol*. 2018;9:530.

**How to cite this article:** Dirsipam K, Ponnala D, Madduru D, Bonu R, Jahan P. Association of FOXP3 rs3761548 polymorphism and its reduced expression with unexplained recurrent spontaneous abortions: A South Indian study. *Am J Reprod Immunol*. 2021;00:e13431. <https://doi.org/10.1111/aji.13431>

# Miniaturized PMMA Electrochemical Platform With Carbon Fiber for Multiplexed and Noninterfering Biosensing of Real Samples

Jaligam Murali Mohan<sup>1</sup>, Khairunnisa Amreen<sup>1</sup>, Arshad Javed, Satish Kumar Dubey<sup>1</sup>,  
and Sanket Goel<sup>1</sup>, *Senior Member, IEEE*

**Abstract**—Several commonly known physiological analytes, such as ascorbic acid (AA), dopamine (D), uric acid (UA), and xanthine (X), are known to have significant impact on human metabolism. Therefore, it is quite imperative to develop a miniaturized, multiplexed, noninterfering, and inexpensive sensing platform to monitor these compounds. Reminiscing this, herein, a miniaturized electrochemical sensing platform over a poly methyl methacrylate substrate has been depicted for specific and selective sensing of AA, D, UA, and X. First, to create three electrode zones for electrochemical sensing, three microchannels were engraved on a PMMA sheet by CO<sub>2</sub> laser ablation process. Subsequently, these microchannels were filled with suitable electrode materials leading to a miniaturized electrochemical sensing platform. In the present article, the Toray carbon gas diffusion layer was the working electrode (WE), while screen-printed conductive carbon paste and silver chloride (Ag/AgCl) ink served as the counter electrode and the reference electrode, respectively. The electrocatalytic oxidation of these analytes exhibits an excellent electro-catalytic oxidation behavior. The effect of variable concentrations and interference from the coexisting analytes was also examined. The linear concentration ranges for these compounds (AA, D, UA, and X) under the optimized parameters were 100–1000, 40–1000, 20–1000, and 10–100  $\mu\text{M}$ , respectively, while the detection limits were 89.65, 38.94, 18.71, and 9.01  $\mu\text{M}$  correspondingly. The platform was also tested with real human serum samples. Such a multiplexed and miniaturized electrochemical sensing platform can be used in point-of-care devices for simultaneous sensing of multiple analytes.

**Index Terms**—Carbon dioxide lasers, carbon gas diffusion layer, electrochemical analysis, electrochemical electrodes, miniaturized devices, multisensor systems, physiological analytes, PMMA.

Manuscript received September 23, 2020; accepted November 26, 2020. Date of publication December 21, 2020; date of current version January 22, 2021. The work of Khairunnisa Amreen was supported in part by the Science and Engineering Research Board – National Post Doctoral Fellow (SERB-NPDF) Scheme (PDF/2018/003658). The review of this article was arranged by Editor W. Kim. (*Corresponding author: Sanket Goel.*)

Jaligam Murali Mohan, Arshad Javed, and Satish Kumar Dubey are with the Department of Mechanical Engineering, Birla Institute of Technology and Science (BITS) Pilani, Hyderabad 500078, India, and also with MEMS, Microfluidics and Nanoelectronics (MMNE) Lab, Birla Institute of Technology and Science (BITS) Pilani, Hyderabad 500078, India.

Khairunnisa Amreen and Sanket Goel are with the Department of Electrical and Electronics Engineering, Birla Institute of Technology and Science (BITS) Pilani, Hyderabad 500078, India, and also with MEMS, Microfluidics and Nanoelectronics (MMNE) Lab, Birla Institute of Technology and Science (BITS) Pilani, Hyderabad 500078, India (e-mail: sgoel@hyderabad.bits-pilani.ac.in).

Color versions of one or more figures in this article are available at <https://doi.org/10.1109/TED.2020.3043217>.

Digital Object Identifier 10.1109/TED.2020.3043217

0018-9383 © 2020 IEEE. Personal use is permitted, but republication/redistribution requires IEEE permission.  
See <https://www.ieee.org/publications/rights/index.html> for more information.

## I. INTRODUCTION

MINIATURIZED detection devices play a vital role in the healthcare sector as they offer features like affordability, easy handling, the requirement of less sample volume, and the possibility to get instant results. Owing to these benefits, miniaturized device-based diagnostic tools can be used to monitor and detect biomarkers for contagious diseases under nonlaboratory settings where expert technicians and advanced laboratories are not easily accessible. For miniaturized device fabrication, different substrates like paper, glass, polydimethylsiloxane (PDMS), and PMMA are generally used. Among these substrates, PMMA is being widely used in the microfabrication process [1]. In comparison to other well-known substrates, PMMA has salient advantages due to its unique features like electrochemical inertness, electric and mechanical properties, good transparency, and cost-effectiveness [2]. Literature reports substantial works wherein PMMA is used as a substrate for electrochemical detection. For instance, a PMMA microfluidic device, using thick photoresist film with screen-printed electrodes and a microchip for the detection of ascorbic acid (AA) and uric acid (UA). A portable electrochemical platform was fabricated on the PMMA substrate and the electrodes were integrated using the lift-off process. The platform was then validated for chromium detection [3]. In another work, the graphite electrode was integrated on a PMMA sheet and the setup was tested for dopamine and the detection limit was found to be 50 nM [4]. Three integrated microelectrodes were fabricated by the photolithography process on PMMA and the performance of the device was evaluated by testing dopamine and ruthenium chloride [5]. Another CO<sub>2</sub> laser ablation process was carried out on a glass substrate, and catechol, UA, and dopamine were analyzed for proof of application [6]. The CO<sub>2</sub> laser was used to create microchannels on a 1-mm PMMA sheet and the working electrodes (WEs) were fixed using the conventional photolithography method to sense carcinoembryonic antigen through the electrochemical method [7].

Furthermore, harnessing carbon nanomaterial deposited electrodes has seen tremendous growth in recent times. For instance, various electrodes, with different carbon nanotubes, were integrated on the PMMA substrate platform. Subsequently, they were used for the detection and separation of some purines and phenolic-based compounds using a capillary electrophoresis process. The literature reports a substantial amount of work wherein such carbon-based materials have been utilized in bulk systems for sensing applications.

For instance, the electroactivity of UA was studied with a single-walled carbon nanotube modified gold (Au) electrode [8]. The anodic peak was observed at 0.45 V, and a further limit of detection (LOD) was found to be  $0.005 \mu\text{M}$ . Even multiwalled carbon nanotubes modified on the standard glassy carbon electrode (GCE) electrode for the electrooxidation of caffeine and AA have been reported [9]. In another work, UA and dopamine were detected with improved selectivity and sensitivity by using a combination of glassy carbon and graphite pyrolytic electrode [10]. The mesoporous carbon, drop-coated on the graphite pyrolytic electrode [11], and GCE were also utilized for the successful detection of AA, UA, and dopamine. To validate the work, serum sample analysis was also performed. Helical carbon nanotubes were functionalized with polymers and pretreated with chemicals to increase its adhesion with the substrates and dispersibility. This was used for the sensing of dopamine, AA, and UA with a large linear range and a low level of detection limits [12]. Graphene has drawn tremendous interest from scientific societies in recent years as a new carbon substitute. Graphene oxide [13], graphene oxide/poly(L-lysine) [14], graphene-modified with gold and multiwalled carbon nanotubes [15], Gr/SnO<sub>2</sub>/Fe<sub>3</sub>O<sub>4</sub> [16], eriochrome T black and gold (Au) on graphene [17] have also been reported for electrochemical sensing.

In recent times, other carbon-based materials, carbon nanofibers, and its surface modified electrodes have proven to produce an excellent electrocatalytic effect. Owing to the high surface area, good electron transfer, and biocompatibility toward biological compounds, they have been utilized broadly for electrochemical sensing applications [18]. Furthermore, even though PMMA has been widely used as a substrate for fabricating microfluidic platforms, very scant reports about the integration of carbon fiber (Toray) onto it as an electrochemical sensing platform are available.

UA, AA, dopamine, and xanthine are present in biological fluids like urine and human serum. Dopamine acts as a neurotransmitter, influences hormonal activity, and plays a major role in the human body. Its abnormality can result in neurodegenerative disorders like Parkinson's disease. UA and Xanthine are purine metabolism degradation products. In humans, the concentration of UA ranges from 120–450  $\mu\text{M}$  per liter and in urine ranges from 1.4–4.4 mM per liter [19]. Abnormal levels of UA can cause several diseases including Lesch-Nyhan syndrome, Leukemia, and hyperuricemia. The clinical levels of xanthine are 10–20 mg per milliliter [20] in the blood, and the abnormal levels of xanthine can lead to diseases like xanthinuria, toxemia, and renal failure. AA is a major antioxidant and its deficiency can result in many disorders. It plays a significant role in many biological processes including improvement of immunity and cancer prevention.

Significant reports, wherein the analysis of individual analytes or multiple analytes is accomplished in a conventional bulk volume system encompassed with a modified GCE, have been reported. For example, Teymourian *et al.* [21] reported Fe<sub>3</sub>O<sub>4</sub> magnetic nanoparticle-based reduced graphene oxide nanosheet decorated GCE for multiple analyte detection like AA, D, UA, nicotinamide adenine dinucleotide (NAD) + hydrogen (H) (NADH), lactate, and H<sub>2</sub>O<sub>2</sub>, however, it involves a complex electrode preparation procedure. Similarly, Troiani *et al.* [22] reported pretreated

poly(1-aminoanthraquinone)-modified electrode for simultaneous determination of AA, dopamine, and UA in the bulk system. Han *et al.* [23] utilized GCE/chitosan-graphene-modified electrode for multiple detections of AA, D, and UA while Dursum and Gelmez [24] reported GCE modified with Pt nanoparticle and multiwalled carbon nanotubes for analysis of AA, UA, and D. Likewise, Thiagarajan and Chen [25] demonstrated the use of a hybrid of gold-platinum film for AA, UA, and D.

In a recent study, Atta *et al.* [26] explored crown ether-modified poly hydroquinone and carbon nanotube-based electrode for simultaneous determination of levodopa, UA, tyrosine, and AA in biological fluids. An interesting strategy for the detection of dopamine using electrostatic repulsion along with mitigated interference from AA and UA has also been reported. Similarly, various studies with the utilization of metal nanoparticles, such as Au, ZnO, FeO<sub>2</sub>, Ni nanocluster, carbon nanotubes, Tin-graphitic carbon, Carbon dots /Fe<sub>3</sub>O<sub>4</sub>, and Zeolite, have been reported recently. All these current studies either utilize lengthy electrode preparations, such as modifications with expensive nanoparticles or are performed in bulk volume, thereby making them handy in lab-based detections. Table I summarizes some of the recent reports in the literature with information on the technique used and the LODs obtained for various analytes. Most of the papers reported in the literature with low detection limits of AA, D, UA, and X, use a redox mediator as a catalyst for detection [27]–[29]. However, in the present case, the bare Toray paper is employed as the WE. It is plausible that the unique fibrous structure of this article enhanced the shuttling of electrons. The literature portrays that such types of studies involving carbon fiber as WE have been accomplished in bulk systems wherein, more electrolyte-sample volume is required. Very scant reports are available for miniaturized/microfluidic electrochemical sensing platforms. In fact, to the best of our knowledge, this report is the first of its kind.

In the current article, a simple and affordable electrode has been utilized as WE without any chemical modifications and purification. The uniqueness of this platform is conferred by the usage of bare Toray as a multiplexed sensing electrode. No extra tedious electrode fabrication procedures are involved. A droplet-based sensing platform has been fabricated, wherein the volume of sample required is minimal (10  $\mu\text{L}$ ). Herein, the combination of carbon fiber electrode (Toray) integrated with the PMMA substrate for AA, D, UA, and X detection has been utilized. Toray paper, conductive carbon ink, and Ag/AgCl paste have been harnessed as a WE, the counter electrode (CE) and the reference electrode (RE), respectively. All three electrodes were integrated into a single platform, therefore, making it portable for point-of-care analysis. Using a CO<sub>2</sub> laser, microchannels were created on PMMA. Counter and REs were screen-printed in the microchannels while the WE was integrated using adhesive. It was found that the fabricated platform gave remarkable electrochemical oxidation of the aforementioned bio-analytes. To validate the device, biological compounds in human blood serum samples were tested and remarkable recovery values were achieved. This fabricated device is an archetype for developing, multiple bio-analyte testing miniaturized platforms for point of care analysis in real-time.

TABLE I  
PREVIOUSLY REPORTED WORK DONE IN A BULK SYSTEM FOR THE  
DETERMINATION OF BIO COMPOUNDS

Technique	Working Electrode	Limit of Detection ( $\mu\text{M}$ )				Ref
		AA	D	UA	X	
Amperometric	Nanoporous Gold	2	--	--	--	[36]
EIS, CV, DPV, Amp	AuNP/Go/PY/CFP	2.4	0.1	1.6	--	[27]
CV, EIS, SWV, Amp	Poly/ZIF-67/CC	0.01	--	--	--	[37]
CV	Gold Nbp/MWCNT	--	0.01	--	--	[28]
CV, EIS, DPV	GCE/ $\beta$ -Naf $\text{eO}_2$	0.1	0.002	--	0.1	[29]
CV, DPV, EIS	GCE/PFSG	--	0.0008	--	--	[38]
CV, DPV	Polyhydroquinone/Carbon nanotubes	0.003	--	0.0007	--	[26]
DPV, CV	Zno/ZrO $_2$	--	--	0.29	--	[39]
EIS, CV, DPV	GCE/Au-PEDOT/Mwent	--	--	199.3	24.1	[40]
LSV, DPV, CV	CSO-gCN/GCE	--	29	--	--	[41]
Amp, CV	Ni-NCS	0.1	--	--	--	[42]
CV, SQW	Carbon fiber Paper	18.7	9.0	89.6	38.4	This Work

## II. CHEMICALS, APPARATUS, AND FABRICATION

### A. Materials and Apparatus

Sodium phosphate dibasic dihydrate, sodium phosphate monobasic anhydrous, AA (AA), Dopamine (D), UA, Xanthine (X) and were procured from Sigma Aldrich. The deionized (DI) water system procured from Milli-Q (18.2) M $\Omega$ .cm which is used throughout all the experiments to prepare a pH buffer solution. The screen-printed conductive carbon ink was purchased from Engineered Materials Systems, Inc. (Ohio, USA). The Ag/AgCl paste was obtained from ALS Corporation Pvt Ltd (Tokyo, Japan). Toray paper was procured from Fuel Cell Store (Texas, USA). The Potentiostat (SP-150) was purchased from Biologic (Seyssinet-Pariset, France) while the CO $_2$  Laser (VLS 3.60) was procured from Universal Laser Systems (AZ, USA).

### B. Toray Platform Fabrication

The electrochemical platform was fabricated using 2-mm poly (methyl methacrylate) PMMA as a substrate owing to its unique properties like transparency and resistance to fouling, and so on. In the first step, "dxf" file was designed using AutoCAD-2018 and transferred to the CO $_2$  engraver system via laser printer software. In this, a classic univariate approach was followed to engrave [30] the 2-mm acrylic sheet. Based on the initial trials, the optimized parameters like speed, power, and parts per inch (PPI) were optimized as: speed = 8 m/min, power = 10 W, parts per inch (PPI) = 1000. A plain PMMA

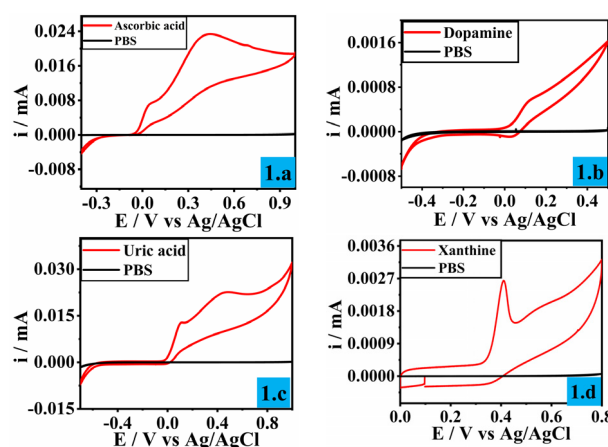


Fig. 1. Cyclic voltammetry response with 1-mM concentration of (a) AA, (b) dopamine, (c) UA, and (d) xanthine in pH 7 PBS at 10 mVs $^{-1}$ .

sheet (length = 35 mm, width = 20 mm, and thickness = 1 mm) as shown in the Scheme 1(a). Using a CO $_2$  laser, to hold the electrodes, three microchannels [Scheme 1(b)] were engraved on the PMMA substrate with dimensions 30 mm  $\times$  2 mm for the reference and CEs, and 30 mm  $\times$  3 mm for the WE. After engraving, the conductive carbon ink was filled in the CE microchannel and silver paste was filled in the RE microchannel using the screen printing process [as shown in Scheme 1(c) and (d)]. The platform was dried in the oven at about 70  $^{\circ}\text{C}$  for 20 min. The Toray carbon paper was integrated into the central microchannel using double-sided tape [Scheme 1(e)]. 10  $\mu\text{L}$  volume of working sample was used throughout the experiments.

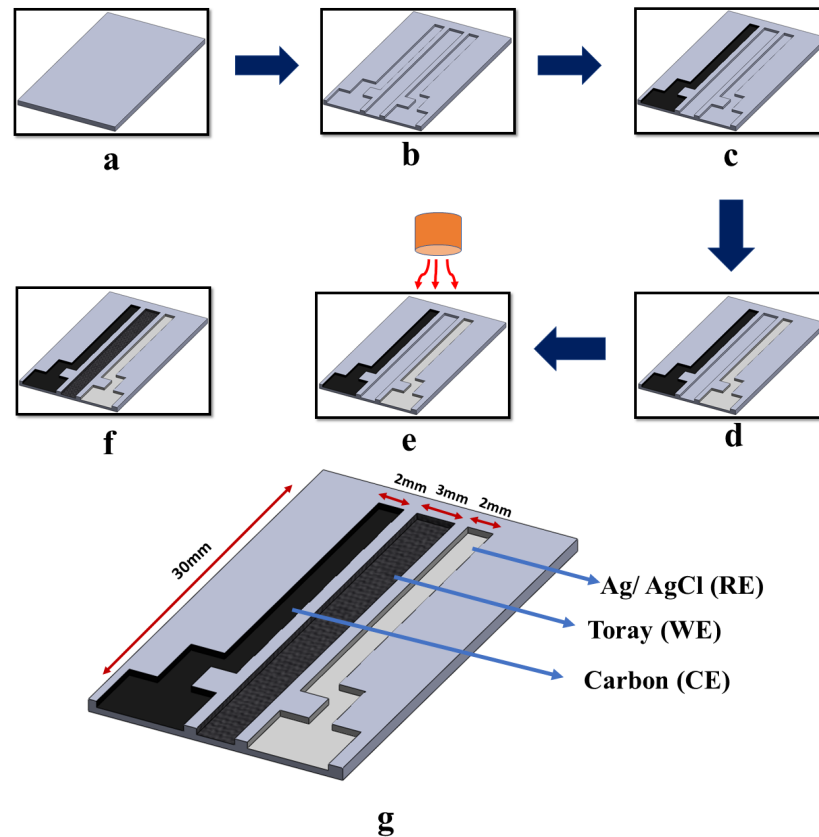
## III. RESULT AND DISCUSSIONS

### A. Electro-Catalytic Oxidation Studies

The aforementioned bio-compounds were tested on the fabricated platform for electrocatalytic oxidation using cyclic voltammetry in pH 7 PBS 1 mM of AA, D, UA, and X each were used as test samples. The optimized potential windows were  $-0.4$ – $1$ ,  $-0.5$ – $0.5$ ,  $-0.7$ – $1$ , and  $0$ – $0.8$  V, respectively. As can be seen in Fig. 1(a)–(d), distinctive oxidation peaks for AA, D, UA, and X were observed at a ( $E'$ ) potential of 0.19 V [31], 0.05 V [32], 0.22 V [33], and 0.40 V [34] respectively. It is suggestive that the Toray paper WE, in the designed platform, gave sensitive oxidation of the tested bio-analytes. The control experiments, wherein the WE was subjected to pH 7 PBS alone, failed to give any such response thereby, authenticating that the peaks obtained correspond to the electro-catalytic oxidation of AA, D, UA, and X only.

### B. Effect of Potential Scan Rate

The effect of varying potential scan rates on the electrocatalytic activity was analyzed to understand the electron transfer mechanism. Fig. 2(a)–(d) depicts the CV response of various scan rates for 1 mM of each of the analytes. The linear scan rate ranges were 10–200, 10–240, 10–120, and 10–200 mVs $^{-1}$  for AA, D, UA, and X, respectively. It is observed that, with the increase in the scan rate, there was a systematic linear growth in the anodic current for all the bio-compounds [Fig. 2(a)–(d)]. As shown in the inset of Fig. 2(a)–(d), the corresponding baseline-corrected calibration



**Scheme 1.** (a) Plane PMMA substrate. (b) CO<sub>2</sub> Laser engraved microchannels to place the electrodes. (c) CE by filling carbon paste in one of the microchannels using screen-printing process. (d) Reference electrode by filling Ag/AgCl paste in another microchannel. (e) PMMA platform was kept in an oven for drying. (f) WE by placing the Toray paper in the final microchannel. (g) Integrated three electrode PMMA electrochemical sensing platform.

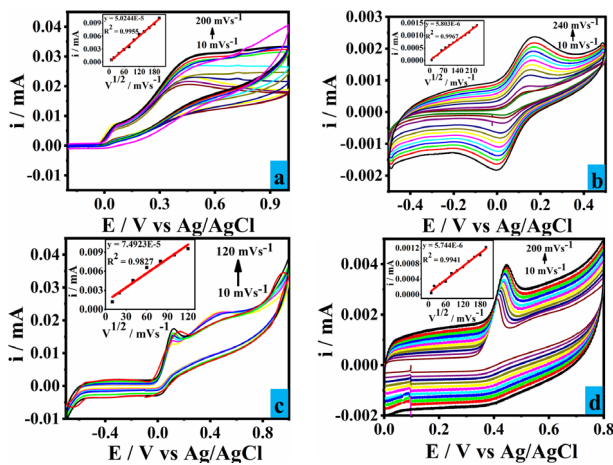


**Fig. 2.** Scan rate effect of (a) AA, (b) dopamine (c) UA, and (d) xanthine with an increase in scan rates. Inset baseline calibrated plots for the same.

plots showed linearity, depicting that the electrocatalytic oxidation of AA, D, UA, and X, mediated by Toray paper, obeys a surface-confined electron transfer and follows the Randles Sevcik equation [35]

$$I_p = (2.69 \times 10^5) n^{3/2} A D^{1/2} v^{1/2} C \quad (1)$$

wherein  $C$  = concentration of bio compounds,  $A$  = electrode surface area 2 mm<sup>2</sup>,  $v$  = scan rate,  $n$  = number of electrons involved in rate-determining step,  $D$  = charge transfer coefficient.

### C. Effect of Concentration

Square wave voltammetry (SWV) was performed to explore the effect of the variable concentrations of these biological compounds. The optimized parameters for SWV were pulsewidth = 50.0 ms, pulse height = 25.0 mV, step height = 10.0 mV, final potential ( $E_0 = 1, 0.5, 0.8$  and  $0.5$ ), and initial potential ( $E_i = -0.4, -0.5, -0.7$  and  $0$ ). It can be observed from Fig. 3(a)–(d) that with the increase in the concentration, a well ordered, increase in the oxidation peak is observed. The linear concentration ranges for these compounds (AA, D, UA, X) under the optimized parameters were 100–1000, 40–1000, 20–1000, and 10–100  $\mu\text{M}$ , respectively. Baseline corrected, respective calibration plots [inset of Fig. 3(a)–(d)], and between various concentrations and peak currents gave linearity passing from the origin. The calculated detection limits LODs were 89.65, 38.94, 18.71, and 9.01  $\mu\text{M}$ , respectively.

### D. Interference Study

The electrocatalytic oxidation potential for these biological compounds (AA, D, UA, and X) are observed to be quite close. Since these compounds co-exist in the physiological system, it is imperative to test them simultaneously for monitoring their interference. The appearance of a clear distinct peak for each analyte authenticated the interference mitigated analysis. As observed in Fig. 4(a), all the bio-chemicals (AA, D, UA, and X) gave distinct peaks without any overlap. Therefore, no interference with each other was observed.

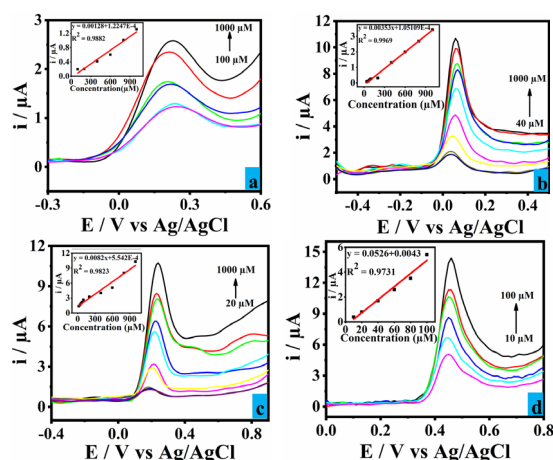


Fig. 3. SWV response of increasing concentration of (a) AA, (b) D, (c) UA and (d) X in 0.1 M of PBS. Inset are the baseline-corrected calibration plots for the same.

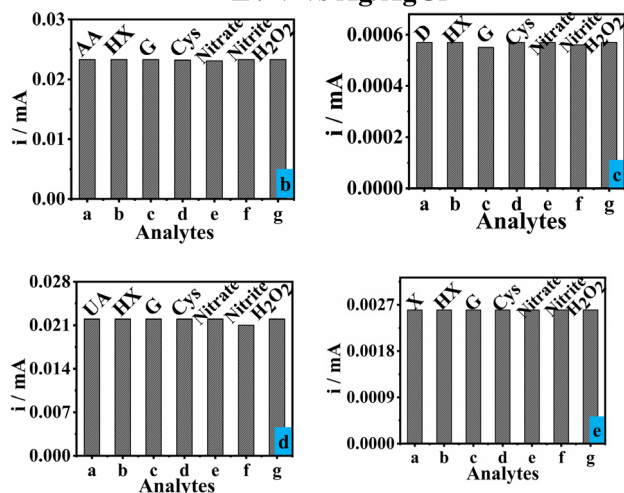
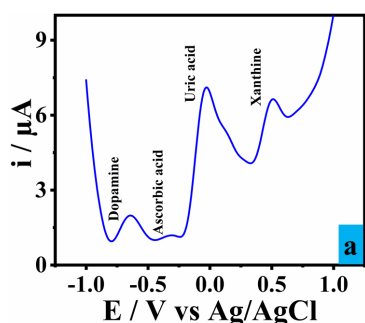


Fig. 4. (a) Squarewave voltammetry (SQW) response of effect of interference in 0.1-M PBS pH 7. (b)–(e) Interference with other biochemical.

Furthermore, various other bio-chemicals like hydrogen peroxide, nitrate, nitrite, cysteine, glucose, and hypoxanthine were also explored. As observed in Fig. 4(b)–(e), no significant interference is found as the peak current is unaltered post the addition of various biochemicals.

### E. Real Sample Analysis

To explore the amenability of the presented miniaturized platform for the real sample analysis, human blood serum samples were used. The samples were obtained from BITS-Pilani, Hyderabad Campus, Medical Center from healthy volunteers. The blood was centrifuged at around 3500 rpm for 15 min and the serum was then collected. A standard

TABLE II  
REAL BLOOD SERUM SAMPLE STUDY ON PMMA PLATFORM

Analyte	Added ( $\mu\text{M}$ )	Found ( $\mu\text{M}$ )	Recovery (%)
Ascorbic acid	100	100.13	99.8
	200	198.99	99.4
	400	399.64	99.9
Dopamine	40	40.15	100.3
	60	60.04	100.0
	80	80.07	100.0
Uric acid	20	20.18	100.9
	40	40.01	100.0
	60	59.79	99.6
Xanthine	10	9.89	98.9
	20	20.06	100.3
	40	39.99	99.9

addition approach was adopted. Standard solutions of AA with concentrations 100, 200, 400  $\mu\text{M}$ ; D with 40, 60, 80  $\mu\text{M}$ ; UA with 20, 40, 60  $\mu\text{M}$  and X with 10, 20, 40  $\mu\text{M}$  were spiked based on their linear standard concentration ranges as observed in Fig. 3(a)–(d). Finally, the SWV for each spike was taken and the recovery values were calculated. Table II reflects the real sample analysis wherein, excellent recovery values were obtained.

### IV. CONCLUSION

In the present article, a Toray paper-based miniaturized electrochemical sensing platform, using PMMA sheet for selective and specific sensing of AA, D, UA, and X has been realized.  $\text{CO}_2$  laser ablation technology was used to create microchannels on the PMMA to place the electrodes using different methods. In the developed platform, screen-printed carbon paste served as the CE, Ag/AgCl ink as RE and bare Toray paper as a WE. Toray paper exhibited remarkable oxidation of AA, D, UA, and X using cyclic voltammetry. The scan rate effect revealed that it is a surface-confined reaction mechanism. Further, concentration-effect was also carried out and linear concentration ranges for these compounds (AA, D, UA, and X) under the optimized parameters were 100–1000, 40–1000, 20–1000, and 10–100  $\mu\text{M}$ , respectively. The calculated detection limits (LOD) were 89.65, 38.94, 18.71, and 9.01  $\mu\text{M}$  respectively with an  $S/N$  ratio of 1.5. The miniaturized PMMA platform was also successfully applied to real sample analysis in human blood serum, which gave excellent recovery percentages thereby proving the practical applicability of the designed platform.

### ACKNOWLEDGMENT

The authors express their gratitude for MEMS, Miniaturized and Nanoelectronics Laboratory, BITS Pilani, Campus Hyderabad.

### REFERENCES

- [1] Y. Cui, "Electronic materials, devices, and signals in electrochemical sensors," *IEEE Trans. Electron Devices*, vol. 64, no. 6, pp. 2467–2477, Jun. 2017.
- [2] P. Rewatkar and S. Goel, "Next-generation 3D printed microfluidic membraneless enzymatic biofuel cell: Cost-effective and rapid approach," *IEEE Trans. Electron Devices*, vol. 66, no. 8, pp. 3628–3635, Aug. 2019.



- [3] D. Li, J. Li, X. Jia, Y. Xia, X. Zhang, and E. Wang, "A novel Au-Ag-Pt three-electrode microchip sensing platform for chromium(VI) determination," *Anal. Chim. Acta*, vol. 804, pp. 98–103, Dec. 2013.
- [4] A. Regel and S. Lunte, "Integration of a graphite/poly(methylmethacrylate) composite electrode into a poly(methylmethacrylate) substrate for electrochemical detection in microchips," *Electrophoresis*, vol. 34, no. 14, pp. 2101–2106, Jul. 2013.
- [5] J. Liu *et al.*, "Monolithic integration of three-material microelectrodes for electrochemical detection on PMMA substrates," *Electrochem. Commun.*, vol. 31, pp. 20–23, Jun. 2013.
- [6] E. T. da Costa, M. F. S. Santos, H. Jiao, C. L. do Lago, I. G. R. Gutz, and C. D. Garcia, "Fast production of microfluidic devices by CO<sub>2</sub> laser engraving of wax-coated glass slides," *Electrophoresis*, vol. 37, no. 12, pp. 1691–1695, Jul. 2016.
- [7] N. Van Anh *et al.*, "Development of a PMMA electrochemical microfluidic device for carcinoembryonic antigen detection," *J. Electron. Mater.*, vol. 45, no. 5, pp. 2455–2462, May 2016.
- [8] S. Wei, F. Zhao, and B. Zeng, "Electrochemical behavior and determination of uric acid at single-walled carbon nanotube modified gold electrodes," *Microchimica Acta*, vol. 150, nos. 3–4, pp. 219–224, Jul. 2005.
- [9] V. K. Gupta, A. K. Jain, and S. K. Shoor, "Multiwall carbon nanotube modified glassy carbon electrode as voltammetric sensor for the simultaneous determination of ascorbic acid and caffeine," *Electrochim. Acta*, vol. 93, pp. 248–253, Mar. 2013.
- [10] S. Hason, V. Vetterl, F. Jelen, and M. Fojta, "Improved sensitivity and selectivity of uric acid voltammetric sensing with mechanically grinded carbon/graphite electrodes," *Electrochim. Acta*, vol. 54, no. 6, pp. 1864–1873, Feb. 2009.
- [11] Y. Yue, G. Hu, M. Zheng, Y. Guo, J. Cao, and S. Shao, "A mesoporous carbon nanofiber-modified pyrolytic graphite electrode used for the simultaneous determination of dopamine, uric acid, and ascorbic acid," *Carbon*, vol. 50, no. 1, pp. 107–114, Jan. 2012.
- [12] B. Zhang *et al.*, "Simultaneous electrochemical determination of ascorbic acid, dopamine and uric acid with helical carbon nanotubes," *Electrochim. Acta*, vol. 91, pp. 261–266, Feb. 2013.
- [13] L. Yang, D. Liu, J. Huang, and T. You, "Simultaneous determination of dopamine, ascorbic acid and uric acid at electrochemically reduced graphene oxide modified electrode," *Sens. Actuators B, Chem.*, vol. 193, pp. 166–172, Mar. 2014.
- [14] Y. Zhang, W. Lei, Y. Xu, X. Xia, and Q. Hao, "Simultaneous detection of dopamine and uric acid using a poly(L-lysine)/graphene oxide modified electrode," *Nanomaterials*, vol. 6, no. 10, p. 178, Sep. 2016.
- [15] A. A. Abdelwahab and Y.-B. Shim, "Simultaneous determination of ascorbic acid, dopamine, uric acid and folic acid based on activated graphene/MWCNT nanocomposite loaded au nanoclusters," *Sens. Actuators B, Chem.*, vol. 221, pp. 659–665, Dec. 2015.
- [16] H. Bagheri, N. Pajooheshpour, B. Jamali, S. Amidi, A. Hajian, and H. Khoshafar, "A novel electrochemical platform for sensitive and simultaneous determination of dopamine, uric acid and ascorbic acid based on Fe<sub>3</sub>O<sub>4</sub>SnO<sub>2</sub>Gr ternary nanocomposite," *Microchemical J.*, vol. 131, pp. 120–129, Mar. 2017.
- [17] N. M. M. A. Edris, J. Abdullah, S. Kamaruzaman, M. I. Saiman, and Y. Sulaiman, "Electrochemical reduced graphene oxide-poly(eriochrome black T)/gold nanoparticles modified glassy carbon electrode for simultaneous determination of ascorbic acid, dopamine and uric acid," *Ara-bian J. Chem.*, vol. 11, no. 8, pp. 1301–1312, Dec. 2018.
- [18] K. Bala, D. Sharma, and N. Gupta, "Carbon-nanotube-based materials for electrochemical sensing of the neurotransmitter dopamine," *Chem-ElectroChem*, vol. 6, no. 2, pp. 274–288, Jan. 2019.
- [19] S. Behera and C. R. Raj, "Mercaptoethylpyrazine promoted electrochemistry of redox protein and amperometric biosensing of uric acid," *Biosensors Bioelectron.*, vol. 23, no. 4, pp. 556–561, Nov. 2007.
- [20] M. A. Raj and S. A. John, "Simultaneous determination of uric acid, xanthine, hypoxanthine and caffeine in human blood serum and urine samples using electrochemically reduced graphene oxide modified electrode," *Anal. Chim. Acta*, vol. 771, pp. 14–20, Apr. 2013.
- [21] H. Teymourian, A. Salimi, and S. Khezrian, "Fe<sub>3</sub>O<sub>4</sub> magnetic nanoparticles/reduced graphene oxide nanosheets as a novel electrochemical and bioelectrochemical sensing platform," *Biosens. Bioelectron.*, vol. 49, pp. 1–8, Nov. 2013.
- [22] E. D. P. Troiani and R. C. Faria, "Cathodically pretreated poly(1-aminoanthraquinone)-modified electrode for determination of ascorbic acid, dopamine, and uric acid," *J. Appl. Electrochem.*, vol. 43, no. 9, pp. 919–926, Sep. 2013.
- [23] D. Han, T. Han, C. Shan, A. Ivaska, and L. Niu, "Simultaneous determination of ascorbic acid, dopamine and uric acid with chitosan-graphene modified electrode," *Electroanalysis*, vol. 22, nos. 17–18, pp. 2001–2008, Sep. 2010.
- [24] Z. Dursun and B. Gelmez, "Simultaneous determination of ascorbic acid, dopamine and uric acid at Pt nanoparticles decorated multiwall carbon nanotubes modified GCE," *Electroanalysis*, vol. 22, no. 10, pp. 1106–1114, May 2010.
- [25] S. Thiagarajan and S. M. Chen, "Preparation and characterization of PtAu hybrid film modified electrodes and their use in simultaneous determination of dopamine, ascorbic acid and uric acid," *Talanta*, vol. 74, no. 2, pp. 212–222, 2007.
- [26] N. F. Atta, A. Galal, and A. R. El-Gohary, "Crown ether modified poly(hydroquinone)/carbon nanotubes based electrochemical sensor for simultaneous determination of levodopa, uric acid, tyrosine and ascorbic acid in biological fluids," *J. Electroanal. Chem.*, vol. 863, Apr. 2020, Art. no. 114032.
- [27] C. Tan, J. Zhao, P. Sun, W. Zheng, and G. Cui, "Gold nanoparticle decorated polypyrrole/graphene oxide nanosheets as a modified electrode for simultaneous determination of ascorbic acid, dopamine and uric acid," *New J. Chem.*, vol. 44, no. 12, pp. 4916–4926, 2020.
- [28] J. Cheng *et al.*, "A novel electrochemical sensing platform for detection of dopamine based on gold nanobipyramid/multi-walled carbon nanotube hybrids," *Anal. Bioanal. Chem.*, vol. 412, no. 11, pp. 2433–2441, Apr. 2020.
- [29] L. Durai and S. Badhulika, "Facile synthesis of large area pebble-like  $\beta$ -NaFeO<sub>2</sub> perovskite for simultaneous sensing of dopamine, uric acid, xanthine and hypoxanthine in human blood," *Mater. Sci. Eng., C*, vol. 109, Apr. 2020, Art. no. 110631.
- [30] E. F. M. Gabriel, W. K. T. Coltro, and C. D. Garcia, "Fast and versatile fabrication of PMMA microchip electrophoretic devices by laser engraving," *Electrophoresis*, vol. 35, no. 16, pp. 2325–2332, Aug. 2014.
- [31] M. Hadi and A. Rouhollahi, "Simultaneous electrochemical sensing of ascorbic acid, dopamine and uric acid at anodized nanocrystalline graphite-like pyrolytic carbon film electrode," *Anal. Chim. Acta*, vol. 721, pp. 55–60, Apr. 2012.
- [32] T. Selvaraju and R. Ramaraj, "Simultaneous determination of ascorbic acid, dopamine and serotonin at poly(phenosafranin) modified electrode," *Electrochem. Commun.*, vol. 5, no. 8, pp. 667–672, Aug. 2003.
- [33] L. Zhang and X. Lin, "Covalent modification of glassy carbon electrode with glutamic acid for simultaneous determination of uric acid and ascorbic acid," *Analyst*, vol. 126, no. 3, pp. 367–370, 2001.
- [34] R. Devi, S. Yadav, and C. S. Pundir, "Au-colloids-polypyrrole nanocomposite film based xanthine biosensor," *Colloids Surf. A, Physicochem. Eng. Aspects*, vol. 394, pp. 38–45, Jan. 2012.
- [35] K. L. Brown and S. Gray, "Cyclic voltammetric studies of electropolymerized films based on ruthenium(II/III) bis(1,10 phenanthroline) (4-methyl-4'-vinyl-2,2'-bipyridine)," *Int. J. Chem.*, vol. 2, no. 2, pp. 3–9, 2010.
- [36] A. Kumar *et al.*, "Amperometric microsensor based on nanoporous gold for ascorbic acid detection in highly acidic biological extracts," *Anal. Chim. Acta*, vol. 1095, pp. 61–70, Jan. 2020.
- [37] Y. Guo, L. Wang, L. Xu, C. Peng, and Y. Song, "A ascorbic acid-imprinted poly(o-phenylenediamine)/zeolite imidazole frameworks-67/carbon cloth for electrochemical sensing ascorbic acid," *J. Mater. Sci.*, vol. 55, no. 22, pp. 9425–9435, Aug. 2020.
- [38] L. Wang, R. Yang, L. Qu, and P. D. B. Harrington, "Electrostatic repulsion strategy for high-sensitive and selective determination of dopamine in the presence of uric acid and ascorbic acid," *Talanta*, vol. 210, Apr. 2020, Art. no. 120626.
- [39] Q. Wang, H. Si, L. Zhang, L. Li, X. Wang, and S. Wang, "A fast and facile electrochemical method for the simultaneous detection of epinephrine, uric acid and folic acid based on ZrO<sub>2</sub>/ZnO nanocomposites as sensing material," *Anal. Chim. Acta*, vol. 1104, pp. 69–77, Apr. 2020.
- [40] S. Sen and P. Sarkar, "A simple electrochemical approach to fabricate functionalized MWCNT-nanogold decorated PEDOT nanohybrid for simultaneous quantification of uric acid, xanthine and hypoxanthine," *Anal. Chim. Acta*, vol. 1114, pp. 15–28, Jun. 2020.
- [41] S. Vinoth, R. Ramaraj, and A. Pandikumar, "Facile synthesis of calcium stannate incorporated graphitic carbon nitride nanohybrid materials: A sensitive electrochemical sensor for determining dopamine," *Mater. Chem. Phys.*, vol. 245, Apr. 2020, Art. no. 122743.
- [42] Z. Zhuang and W. Chen, "One-step rapid synthesis of Ni<sub>6</sub>(C<sub>12</sub>H<sub>25</sub>S)<sub>12</sub> nanoclusters for electrochemical sensing of ascorbic acid," *Analyst*, vol. 145, no. 7, pp. 2621–2630, 2020.

## Design and Implementation of a portable Arduino based touchless thermometer with distance compensation

Dr.D.Sarala\*, Dr.Y. Seetha Mahalakshmi\*, W. Jaya Selva Vinita\*, V.SaiPrashanthi\*

*\*Department of Physics and Electronics, St. Ann's college for Women, Mehdiapatnam, Hyderabad, Telangana*

### **Abstract**

*Monitoring the human body temperature has become mandatory during the ongoing COVID-19 pandemic situation. With the constant rise in the case load, keeping the safety of the health care personnel and the elderly, contact-less devices rendering precise values are in great demand. Recent technological advancements have made infrared (IR) thermometers, the choice for touch less screening of multiple individuals. Even then the measurement accuracy of such thermometers is affected by many factors which may include the range of measurement from the individual's site, the location of the thermometer near forehead, wrist or ear and the presence of ambient temperature. Considering these factors, we describe the assembly of an Arduino-based digital IR thermometer with distance correction using the MLX90614 IR thermometer and HC-SR04 ultrasonic sensors and a 16 \*2 LCD display with both ambient and volunteers' temperature being displayed. Also, the distance compensation methods are incorporated in the program. This would ensure accurate readings and measurements for a final assembled digital IR thermometer.*

**Keywords:** Infrared, Ultrasonic sensor, Arduino nanoSKU 648418, touchless thermometer, HC-SR04, MLX90614, 16\*2 LCD.

### **Introduction**

Fever is one of the common symptoms [1] of COVID-19, but due to its contagious effect, its measurement methods become a challenging task to the medical community. Hence it is important to perform the temperature detection of patients fast and possibly without any physical contact, and without a human intervention. Besides, the epidemiological and laboratory researches have revealed that ambient temperature could possibly affect the existence and spread of Corona virus [2], so that a continuous monitoring of temperature, which includes both ambient and body temperature, is an essential parameter to be performed in the contrast of COVID-19.

The adoption of thermo graphic systems in the framework of pandemic situations, during the screening process for rapid temperature measurements of many individuals quickly and safely without allowing the thermometer to be a vector of pathogen transfer are crucial, thus making contact infeasible, ruling out the measurement sites.

Early methods of measuring body core temperature utilizing contact mercury thermometers are replaced by the safer and more convenient electronic thermometers at the sublingual, armpits, ear canals, and in some rare occasions, the rectum and auxiliary for

accuracy [3]. Many of these surface measurement sites, specifically the temporal and central forehead, reflect lower readings than internal sites such as the tympanic temperature readings, the current gold standard to represent the body core temperature [3], especially given the impracticality of rectal/anal temperature takings.

Infrared (IR) thermometers would fulfil this gap by measuring the surface temperature without direct contact, which is through detecting the amount of thermal or black-body radiation emitted by the object. Additionally, these thermometers are now commonly used in clinical practices [4], as well as routinely during the pandemic for self-monitoring and screening at the entrances of public places.

Thus the recent advancements made in infrared (IR) thermometers became a reliable choice for contactless screening of multiple individuals. Though the measurement accuracy of such thermometers is affected by many factors including the volunteers' forehead or hand or the ear and the distance range from the point of measurement. Considering these issues, an Arduino-based digital IR thermometer with range consideration using the MLX906149 [5] IR thermometer and HC-SR04[6] ultrasonic sensors with an LCD display is demonstrated in the present paper.

Coupled with some analysis of measurement sites, we also found ways to programme compensation methods for the final assembled digital IR thermometer to provide more accurate readings and measurements. Experiments were conducted to validate distance adjustments considered in the software, and also the effects of measurements on different measurement sites like fore head, right ear and wrist of the volunteers.

## 2. Materials and Methods

### 2.1. Components and Specifications

Arduino Nano (SKU 648418, Italy), ultrasonic sensor (HC-SR04) [6], infrared sensor (MLX90614) [5], and 16 \* 2 display were used. A factorycalibrated MLX90614 infrared sensor, suitable for a wide range of temperatures between- 40 °to 85 ° C for the ambient temperature and 70 to 1030 °C for the target object temperature, provided the average temperature of all objects within sweep angle of the sensor, as well as a standard accuracy of 0.5 °C around room temperature. The Ultrasonic Sensor HC-SR04 emits a 40 kHz ultrasound and computes the distance based on the time taken to detect the ultrasound wave reflected off an object. A 16\*2 mono colour character LED display is incorporated to observe the value.

### 2.2. Assembly of touch less Thermometer

The design and development of the thermometer in this sensor were imported and modified from online instructions [7] It consists of hardware design, mechanical assembly, the electronic circuit, the microcontroller programming using arduino nano.

#### 2.2.1. Physical Assembly

Figure 1a shows the physical mount of the touchless thermometer along with the components: IR sensor, ultrasound sensor, Arduino Nano and 16 \* 2 LCD display. It also

comprises of the battery holder and a reset button .The circuit design is implemented in ORCAD and the arduino nano is programmed in embedded C using the Arduino IDE 1.8.13

### **2.2.2. Circuitry Design and Implementation**

The Arduino Nano [8] microcontroller, in which the copper wires from the sensor pins of the ultrasonic sensor(Figure 2a), IR sensor(Figure 2b), LCD (Figure 2c) and reset button were soldered with a 9 V battery supplying 3.3 to 5 V to the circuit (**Figure 1a**).

### **2.3. Programming Arrangement**

The Arduino IDE 1.8.13 software is used to program the microcontroller. After every press of the reset button the sensor starts measurement within 2–4 cm from the site of measurement like forehead, ear or wrist. Ten readings from the ambient and surface body temperature are made and the average is shown. The ultrasonic sensor detects the distance from the target area and calculates the average of ten readings. With the inputs of distance and temperature to the algorithm, the compensated reading from the algorithm would be displayed on the mono colour 16 \* 2 LCD display

Compensation adjustment equation was derived from the regression analysis of the relationship between the oral temperature values and the measured values. Compensated values by the IR thermometer were used as the dependent value, while the measurement values by the IR thermometer and ambient temperature were each viewed as independent variables.

### **2.4 Sensor considerations**

#### **2.4.1. Infrared Sensor**

For precise measurement of the absolute temperature of the spot, the device temperature needs to be kept small with a stable ambient temperature. To compensate the proximity effects, a distance-to-site ratio (D/T ratio) is built in the algorithm. Specifically, the area measured increases as the distance increases. The IR temperature sensor MLX90614 used in this project has a sweep angle of 80 degrees as specified by the manufacturer. This translates to a D/T ratio of 1:1.60. Setting the average height of the position of the measuring unit to be at 59 mm as the condition [9]. For a maximum horizontal distance the IR temperature sensor can accurately measure the temperature of the spot approximately at 4 cm. Beyond this distance, flanking areas of the site of measurements would also be sensed so that the accuracy may get affected.

#### **2.4.2. Ultrasound Sensor**

The ultrasound sensor consists of a transmitter sending an ultrasound wave and a receiver detecting the reflected wave by the targeted physical object. The time taken between the transmission and detected wave is registered for the calculation of the distance from the speed of ultrasound waves at 330 m/s by the programmed Arduino Nano.

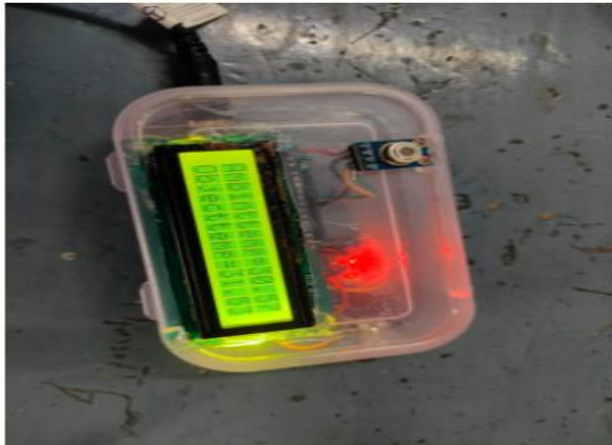


Figure 1a the physical picture of the touch less Thermometer

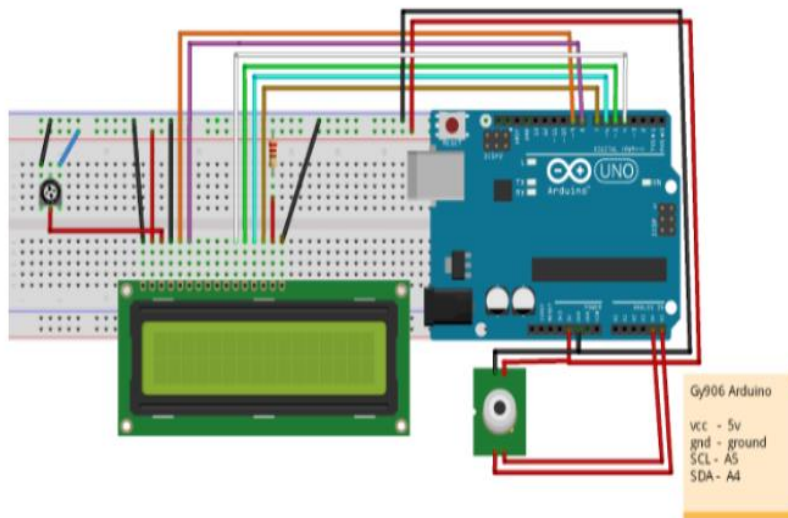


Figure 1b Schematic of the assembled digital IR thermometer consisting of: Ultrasonic sensor HC-SR04, reset button, Arduino Nano board, LCD display and IR temperature sensor MLX90614.

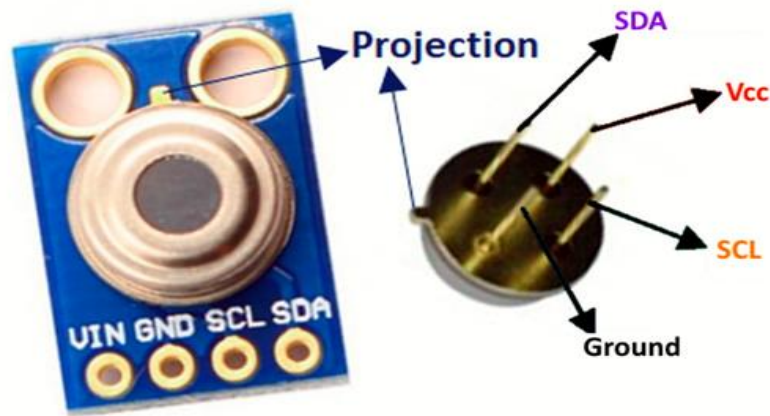


Figure 2a Ultrasonic sensor HC-SR04 component

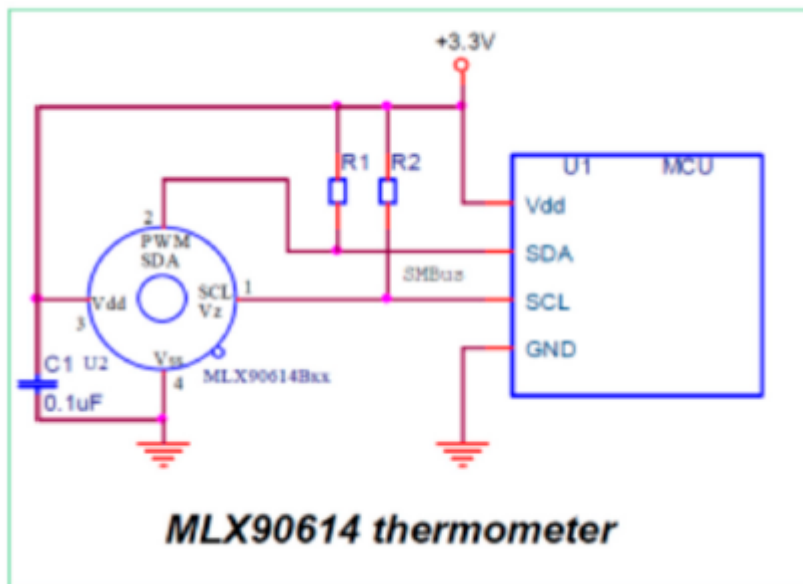


Figure 2b Infrared sensor MLX90614

### 3 Experimental section

The experiment is performed on 6 volunteers between the age limit of 20 to 40 years in order to study the accuracy of the unit. The observations were recorded in an air-conditioned environment of 20 to 24 °C for a relatively constant ambient temperature. Volunteers were allowed to relax for a time of 10 min before making their temperature measurements. A sterilized Omron digital thermometer MC-343F was used to measure the oral temperatures, which was also set as the target point for compensation adjustments.

In the first experiment, the IR thermometer was used to measure the volunteers' temperatures at three different body locations viz. forehead, wrist and the right ear and at varying distances from the forehead (2–4 cm, at 0.5 cm step measurements) as shown in

figure 3a and 3b . The range of 2–4 cm is based on the minimum and maximum allowable horizontal distance that the IR temperature sensor can accurately measure (2–4 cm) as per the manufacturer’s specifications. The IR and oral temperature readings from the first experiment set were used for compensation adjustments and stored. Then, the calibrated IR thermometer was used to measure the forehead temperatures of volunteers and test its performance and deviation from the oral temperature. Data from each experiment were plotted with the distance against the temperature as shown in figure 4a,4b and 4c.

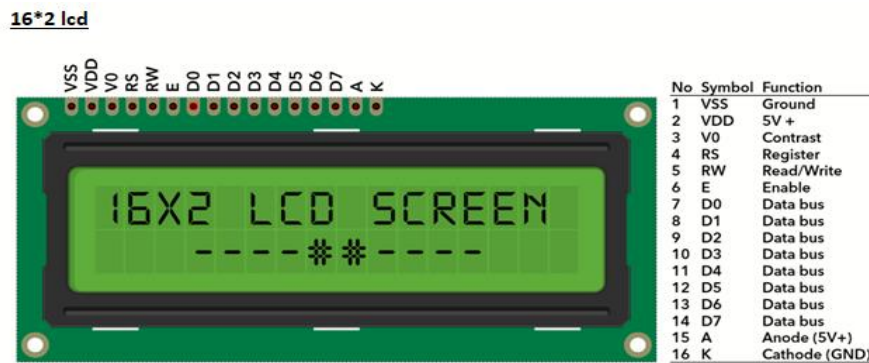


Figure 2c16 \*2 LCD display

### 3.1. Temperature measurement on the Forehead, wrist and right ear

Although not visible to the human eye, all objects emit infrared light rays and the concentration varies depending on temperature. By detecting the IR rays, we can perceive the temperature range. The MLX90614 thermometer sensor works using this principle.

MLX90614 is a powerful infrared sensing device with a very low noise amplifier and a 17-bit ADC. It enables high accuracy and resolution for the thermometer. The best part about the MLX90614 is it comes calibrated with a digital SMBus from the factory. This means that it will give an output with a high resolution of 0.02°C and can continuously transfer the measured temperature in the range of -20 to 120°C.

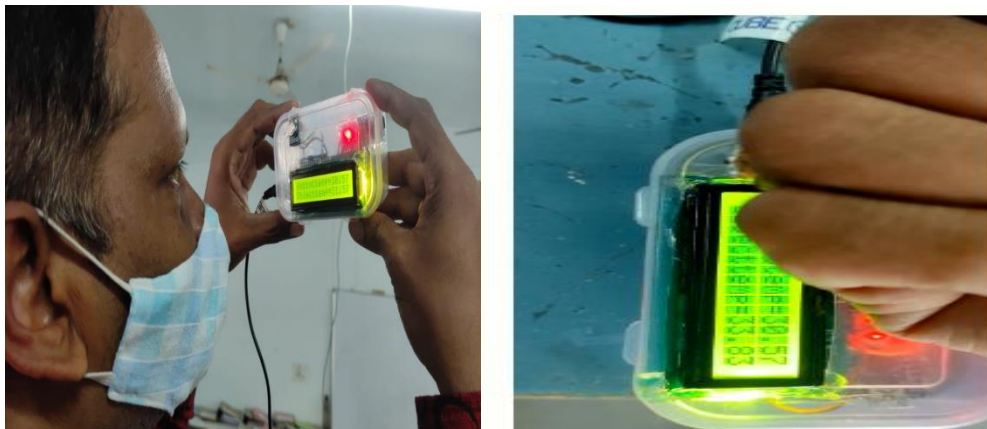


Figure 3a Volunteer measuring the forehead temperature Figure 1b Volunteer measuring the wrist temperature

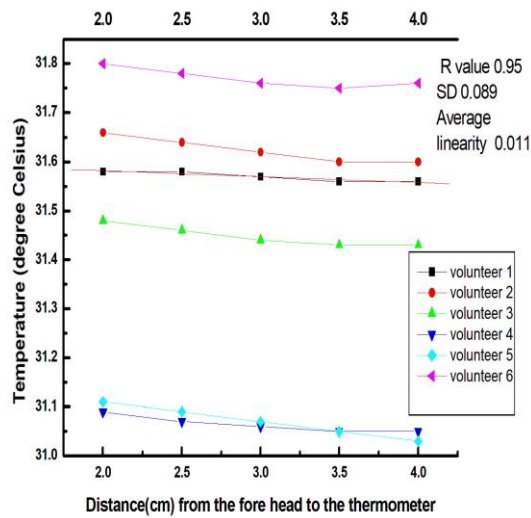


Figure 2a Graph plotted between distance vs. fore head temperature of six volunteers

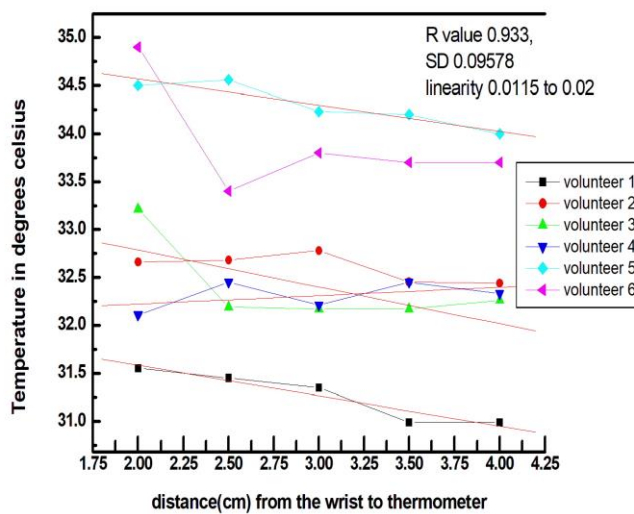


Figure 4b Graph plotted between distance vs wrist temperature of 6 volunteers



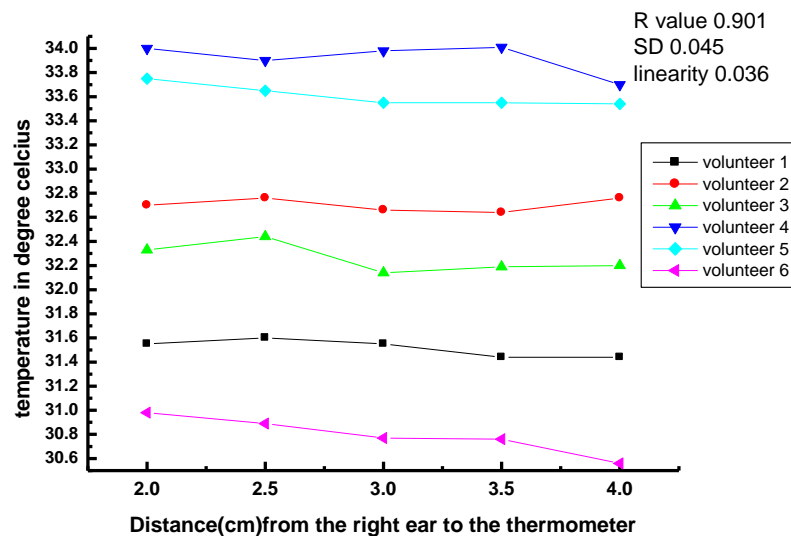


Figure 4c Graph plotted between distance vs. right ear temperature-of 6 volunteers

## Discussion

The touchless IR thermometer recorded an average temperature within  $0.3^{\circ}$  of the volunteers' oral temperature. As measurements for oral temperature are widely used to non-invasively measure the body temperature, measurements of the forehead, wrist and right ear temperature with varying distances showed a regression of about 0.95 to 0.901 with a linearity of 0.01 to 0.03 and hence can be used to establish a threshold in the screening for fever. The IR thermometer obtained a better precision compared to the alternative and more expensive non-contact IR devices and has improved distance compensation. In a separate study, tympanic and forehead temperatures taken by a BRAUN IRT-3020 had an error range of  $\pm 0.286^{\circ}$  and  $\pm 0.392^{\circ}$  C [10]. Another study showed tympanic and forehead temperature errors of  $\pm 0.37^{\circ}$  C and  $\pm 0.36^{\circ}$  C respectively [11]. However, other contact devices such as the rectal thermometer, with a small error range of  $0.05^{\circ}$  C [12] outperformed the current improved thermometer. Still, our improved device costs only a fraction of commercial IR thermometers and was sufficiently accurate to be considered as a low cost alternative ( $\sim$ USD 5) to the current entry level IR thermometers ( $>$ USD 80) in the market. This non-contact device is more convenient than the tympanic or rectal thermometers.

## Conclusions

Forehead temperature measurements using an IR thermometer play an important role of rapidly screening for fever to identify the infected individual. The performance and precision of an IR thermometer for forehead temperature screening were studied together with the design and implementation of an improved infrared temperature sensor-based system with distance sensing capabilities. It is observed that the measured temperatures were well within the  $0.3^{\circ}$  C variation of their oral temperature over the distance of 2–4 cm, resulting in a similar performance to commercial thermometers. While minimal, temperature differences between the actual temperature and the one

measured with the touch less thermometer at the forehead and the wrist or the right ear with a programmed software compensation in the distance of the site we conclude the validity of the human temperature measurements safely and effectively without a manual operator.

## References

1. Fulbrook, P. Core temperature measurement: A comparison of rectal, axillary and pulmonary artery blood temperature. *Intensive Crit. Care Nurs.* **1993**, 9, 217–225. [CrossRef]
2. Xie, J.; Zhu, Y. Association between ambient temperature and COVID-19 infection in 122 cities from China. *Sci. Total Environ.* **2020**, 724, 1–5. [CrossRef] [PubMed]
3. Mogensen, C.B.; Wittenhoff, L.; Fruerhøj, G.; Hansen, S. Forehead or ear temperature measurement cannot replace rectal measurements, except for screening purposes. *BMC Pediatrics* **2018**, 18, 15. [CrossRef]
4. Non-Contact Temperature Assessment Devices during the COVID-19 Pandemic. Available online: <https://www.fda.gov/medical-devices/coronavirus-covid-19-and-medical-devices/non-contacttemperature-assessment-devices-during-covid-19-pandemic> (accessed on 5 September 2020).
5. Melexis. Datasheet for MLX90614. Available online: [https://components101.com/sites/default/files/component\\_datasheet/MLX90614-Datasheet.pdf](https://components101.com/sites/default/files/component_datasheet/MLX90614-Datasheet.pdf) (accessed on 30 October 2020).
6. ElecFreaks. Ultrasonic Ranging Module HC—SR04. Available online: <https://cdn.sparkfun.com/datasheets/Sensors/Proximity/HCSR04.pdf> (accessed on 23 October 2020).
7. Raj, A. Make a Non-Contact Infrared Thermometer with MLX90614 IR Temperature Sensor. Available online: <https://circuitdigest.com/microcontroller-projects/ir-thermometer-using-arduino-and-ir-temperature-sensor> (accessed on 22 May 2021).
8. Arduino. Arduino Nano Datasheet. Available online: <http://www.farnell.com/datasheets/1682238.pdf> (accessed on 23 October 2020).
9. Sirinturk, S.; Govsa, F.; Pinar, Y.; Ozer, M.A. Study of frontal hairline patterns for natural design and restoration. *Surg. Radiol. Anat.* **2017**, 39, 679–684. [CrossRef]
10. Chen, H.-Y.; Chen, A.; Chen, C. Investigation of the Impact of Infrared Sensors on Core Body Temperature Monitoring by Comparing Measurement Sites. *Sensors* **2020**, 20, 2885. [CrossRef]
11. Liu, C.C.; Chang, R.E.; Chang, W.C. Limitations of forehead infrared body temperature detection for fever screening for severe acute respiratory syndrome. *Infect. Control. Hosp. Epidemiol.* **2004**, 25, 1109–1111. [CrossRef]

12. *Jensen, B.N.; Jensen, F.S.; Madsen, S.N.; Løssl, K. Accuracy of digital tympanic, oral, axillary, and rectal thermometers compared with standard rectal mercury thermometers. Eur. J. Surg. 2000, 166, 848–851. [CrossRef] [PubMed]*

# Implications of DTQW on quantum devices

**N Madhavi Reddy,**  
Assistant Professor

**B.Divya Bharathi,**  
Assistant Professor Department of Physics  
Kasturba Gandhi Degree and PG College for Women West Marredpally, Secunderabad,

**Dr Y.Seetha Mahalakshmi**  
Lecturer in Physics and Electronics, St.Anns College for Women, Mehdiapatnam, Hyderabad

## Abstract

The dynamics of DTQW can be accelerated by adjusting the evolution parameter over time (AQW). This paper shows how accelerated DTQW dynamics can be used to control and enhance system entanglement. Destruction of the coin characteristics in space and time can cause spatial and temporal disorder. Disordered DTQW can simulate Anderson localization, weak localization, and analyse localised dynamics. By accelerating the parameter in a disordered DTQW system, the disordered system can be de-localised.

## Introduction

DTQW has been realised on many quantum devices. On an NMR system, nuclear spins represent the coin and position state. Radio frequency is used to tune spin coupling between two neighbouring nuclei. Ion-trap simulates the coin state as being hyperfine, and position states as being quantized energy states caused by ion oscillation[1-3] wave-guides, q-plates, phase shifters, and beam splitters are used in photonic systems to implement quantum walk and evolution operations. In cavity QED, atoms' electronic levels are coin states, and photon numbers map to position states. The atomic level resonant interaction is linked to the coin operation and the change in photon numbers to the shift operation. Determining the practicality of DTQW algorithmic applications on quantum circuits is critical[4]. The first quantum circuit based DTQW implementation was on multi-qubit NMR. The number of steps is limited by the number of qubits and coherence time. One must map the position state to the multi-qubit state for DTQW on quantum circuits. Recently, one such mapping on  $N + 1$ -qubits superconducting system was reported to implement  $N$ -steps of DTQW.

Its postulates are to identify the “mathematical universe” for modelling quantum phenomena (as n-dimensional Hilbert spaces with n the maximum number of distinguishable states of the system); to establish a correspondence between a quantum system and its mathematical abstraction (a quantum state is a “ray” in n-dimensional Hilbert space); and to describe the spontaneous eigenstates of quantum systems. Atomic or sub-atomic particle states hold quantum information. A qubit is a quantum information unit. Today's qubit physical embodiments include:

Photon polarization encodes the information.

- An atom. The information is encoded in the electron spin.
- QDs. Little devices with a small number of free electrons.

Quantum dots can have a single electron or a cluster of thousands of electrons, depending on their size and form. Semiconductor materials; diameters range from nanometres to microns.

The information is encoded as electron presence/absence. • An optical cavity atom.

- An ion in a trap has two states.
- NMR liquid (Nuclear Magnetic Resonance).

Lattices NMR.

- macro-gas clouds
- Diamond nitrogen vacancies
- Josephson nexus

Quantum data has unique properties: We can't reliably distinguish non-orthogonal quantum states due to superposition. The randomization of a quantum computer's internal state owing to environmental interactions is known as decoherence[5-6].

Conceptually, decoherence can be avoided by using quantum fault-tolerant circuits, quantum error-correcting codes, and entanglement purification and distillation. Significant progress should be achieved in all of these areas before quantum computing is feasible. This tutorial introduces basic quantum computing and quantum information theory ideas and applications.

Then we give some experiments that reveal quantum effects. We review the fundamental quantum mechanics ideas required to comprehend quantum devices. Quantum gates and quantum circuits are used to change a quantum system's state and so process information. Each of these gates is a classical logic gate[7-8]. We can also mimic any  $n$ -qubit quantum circuit using one-qubit gates and CNOTs. These global quantum gates show: To perform any unitary transformation  $A$  on  $n$  qubits,  $U_k$  must act on two or fewer computational basis states. (ii) Each transformation  $U_k$  is a product of one-qubit gates and CNOTs. (iii) A one-qubit gate's transformation can be approximated well by the three gates in the set (H, S, T).

Mathematical calculations, internet searches, economic modelling, weather forecasting, and other tasks tax even the most powerful computers. Computers are fundamentally inefficient, not because microprocessors are slow. Modern (classical) computers work by dividing a task into elementary operations, which are then executed serially, one by one. Parallel computing has been attempted for some time, but progress has been slow and patchy[9]. The reason is because microprocessor logic is essentially serial (typical computers appear to be executing multiple tasks at once, such running a word processor and a spreadsheet software, but in reality the central processor is merely cycling fast between jobs). A parallel computer's nature would imply simultaneity. It would be able to search quickly through a huge list of options to find the one that solves the problem. These machines exist. QCs (Quantum Computers Quantum parallelism is the more fascinating aspect of quantum computing. A quantum system is in a "quantum state" which is a superposition of multiple classical or classical-like states. This is the linear superposition concept used to build quantum states. In order to avoid undesired entanglement with the environment (decoherence), a quantum computer must be shielded from unwanted entanglement. Quantum parallelism on a serial machine[10].

To compute all values of a function  $f(x)$  of a binary vector  $x$  of length  $n$ , we require either one copy of the circuit and  $2^n$  time steps (assuming one time step to compute one input) or one time step and  $2^n$  copies of the circuit. In one time step, a quantum circuit can compute all  $2^n$  values of the function. The circuit's output is a superposition of all possible  $f$  values ( $x$ ). We illustrate quantum parallelism with a "oracle" that can determine whether a binary function is balanced (the Deutsch problem). A practical example of a test to verify if a function is balanced is a voting

machine. Suggestion: use two input buttons one for each candidate and an output display. We analyse the results as we press each button[11].

If the findings are same, the machine is broken. If the two results differ, the machine may or may not work. A quantum circuit for Deutsch's dilemma and show how to calculate a quantum circuit's output: It is necessary to split the circuit into stages, compute the transfer matrix of each stage as tensor product of the transfer matrices of each gate changing each qubit, and calculate the state of the circuit at the input as tensor product of ket vectors (in Dirac's notation). This technique is repeated for each stage until we have the output state. While discussing quantum information theory, we briefly touch on dense coding and quantum teleportation. Quantum computers and quantum information theory have incredible promise.[12] Reversible quantum computers avoid conceptually irreversible processes and can dissipate energy arbitrarily efficiently. Solid state devices from 2000 require 31018 Joules/switching operation. Ralph Merkle of Xerox PARC calculated in 1992 that a 1 GHz computer with 1018 gates in a volume of around  $1 \text{ cm}^3$  would dissipate 3 MW of power. Solid state device power consumption grows with clock rate cube.

In the single-particle DTQW dynamics, any parameter can be disordered. The Anderson localization (strong localization) and weak localization (disordered DTQW) have been widely studied. Using the quantum coin operator and a phase operator, we may add acceleration and disorder to the quantum walk dynamics. This allowed us to investigate the impact of localization in strengthening and preserving entanglement between two initially separated particles across a large number of quantum steps. Particle Anderson localization has been experimentally simulated [12]. The two particles are initially separated but after a few steps of walking they entangle and how disorder in such a movement affects localisation. The interaction between the particles and their limitation to one spatial dimension due to bosonic/fermionic nature is also introduced. Along with the well-established link of quantum walks with enormous Dirac equation [13-15], these inter-winding connections can be used to examine the connection of acceleration, mass, and entanglement in relativistic quantum mechanics and quantum field theory. Based on these findings, we will be able to model the dynamics of accelerated quantum particles using quantum walks. An analytical investigation is followed by a dynamic analysis of

the dispersion relations, with numerical data supplementing the analysis. single- and two-particle AQW dispersion relation and transfer matrix This shows how the probability amplitude changes from one point to another for a particular time-step and how it depends on the evolution operator's parameter. Then, to explore weak and strong (Anderson) localization in the accelerated DTQW, temporal and spatial disorder is introduced in one of the evolution operator's parameters (coin operator).

With increasing acceleration, AQW probability amplitude extends over more space. In one dimension, two-particle DTQW entanglement is similar to single-particle AQW. We also show that in the case of two particles, even if the initial state is separable, the particles entangle after a few steps of quantum walk, but the entanglement decays with time. [16-17] The decay time decreases with acceleration. A similar trend holds for disordered two-particle AQW.

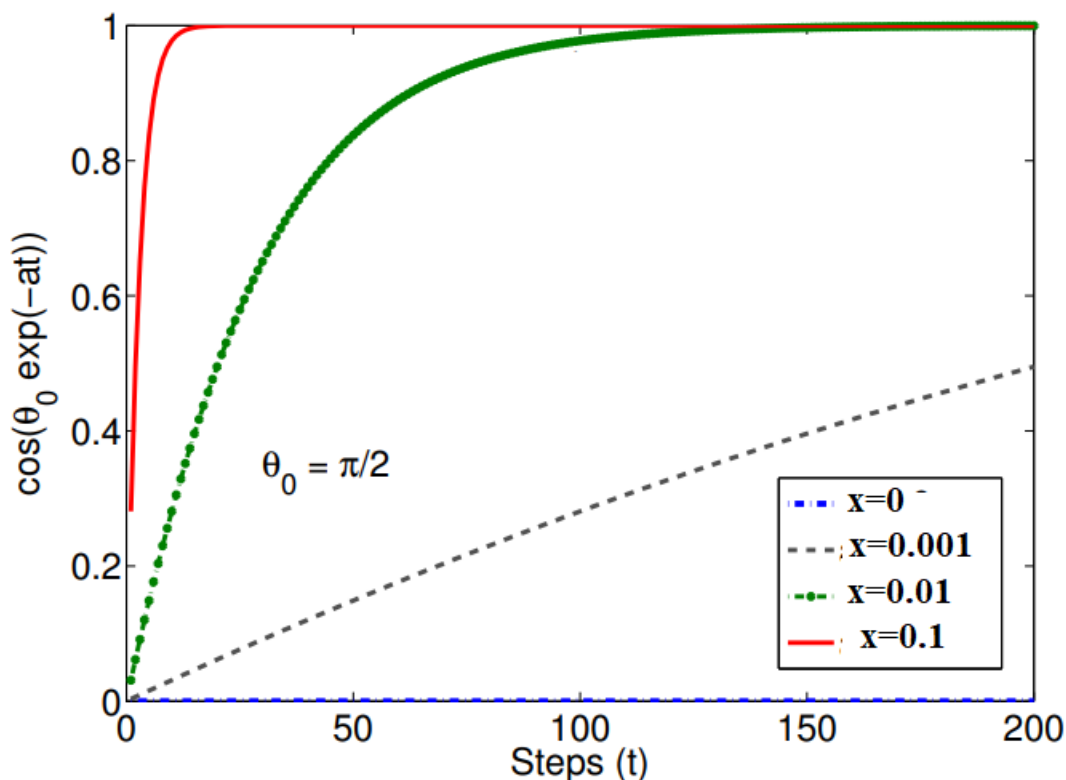


Fig Effect of accelerating parameter  $a$  on quantum component



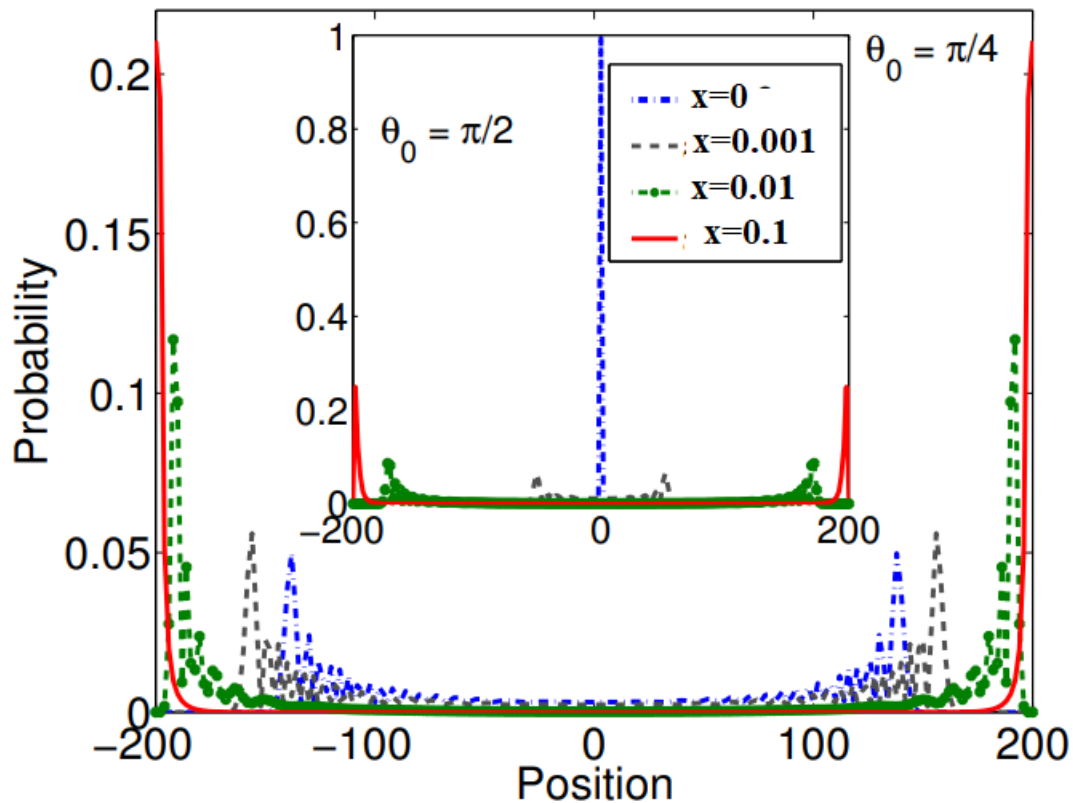


Fig. 2 Probability distribution

### Conclusion

Enhancement of entanglement between the particle and the space in which it moves Single-particle DTQW's entanglement between its particle and its position space reaches its maximum value faster for faster acceleration and then reaches its maximum value and then stops. There have been earlier results that show that entanglement between particles and space increases because of temporal disorder. This fits in well with that. A lot of the time, entanglement gets better because of how quantum coins work, but this is just one example of how randomness in time can make it even better.

### References

1. N. Gershenfeld, *The physics of information technology*. Cambridge University Press, 2000.
2. C. E. Shannon, "A mathematical theory of communication," *The Bell system technical journal*, vol. 27, no. 3, pp. 379–423, 1948.
3. R. Landauer, "Proceedings of the workshop on physics and computation: Physcomp'92," 1993.
4. A. Pathak, *Elements of quantum computation and quantum communication*. Taylor & Francis, 2013.
5. A. Ekert, N. Gisin, B. Huttner, H. Inamori, and H. Weinfurter, "Quantum cryptography," in *The physics of quantum information*, pp. 15–48, Springer, 2000.
6. S. J. Phoenix and P. D. Townsend, "Quantum cryptography: how to beat the code breakers using quantum mechanics," *Contemporary physics*, vol. 36, no. 3, pp. 165–195, 1995.
7. A. M. Childs, R. Cleve, E. Deotto, E. Farhi, S. Gutmann, and D. A. Spielman, "Exponential algorithmic speedup by a quantum walk," in *Proceedings of the thirtyfifth annual ACM symposium on Theory of computing*, pp. 59–68, 2003.
8. M. Szegedy, "Quantum speed-up of markov chain based algorithms," in *45th Annual IEEE symposium on foundations of computer science*, pp. 32–41, IEEE, 2004. 145
9. D. Bouwmeester, J.-W. Pan, K. Mattle, M. Eibl, H. Weinfurter, and A. Zeilinger, "Experimental quantum teleportation," *Nature*, vol. 390, no. 6660, pp. 575–579, 1997.
10. A. Furusawa, J. L. Sørensen, S. L. Braunstein, C. A. Fuchs, H. J. Kimble, and E. S. Polzik, "Unconditional quantum teleportation," *science*, vol. 282, no. 5389, pp. 706–709, 1998.
11. V. Bužek and M. Hillery, "Universal optimal cloning of arbitrary quantum states: from qubits to quantum registers," *Physical review letters*, vol. 81, no. 22, p. 5003, 1998.
12. J. H. Reina, L. Quiroga, and N. F. Johnson, "Decoherence of quantum registers," *Physical Review A*, vol. 65, no. 3, p. 032326, 2002.
13. R. P. Feynman, "Simulating physics with computers," in *Feynman and computation*, pp. 133–153, CRC Press, 2018.
14. J. W. Britton, B. C. Sawyer, A. C. Keith, C.-C. J. Wang, J. K. Freericks, H. Uys, M. J. Biercuk, and J. J. Bollinger, "Engineered two-dimensional ising interactions in a trapped-

- ion quantum simulator with hundreds of spins,” *Nature*, vol. 484, no. 7395, pp. 489–492, 2012.
15. J. T. Barreiro, M. Müller, P. Schindler, D. Nigg, T. Monz, M. Chwalla, M. Hennrich, C. F. Roos, P. Zoller, and R. Blatt, “An open-system quantum simulator with trapped ions,” *Nature*, vol. 470, no. 7335, pp. 486–491, 2011.
  16. D. Deutsch, “Quantum theory, the church–turing principle and the universal quantum computer,” *Proceedings of the Royal Society of London. A. Mathematical and Physical Sciences*, vol. 400, no. 1818, pp. 97–117, 1985. 146
  17. P. W. Shor, “Algorithms for quantum computation: discrete logarithms and factoring,” in *Proceedings 35th annual symposium on foundations of computer science*, pp. 124–134, Ieee, 1994

CONTEMPORARY GENDER STEREOTYPES AND THEIR  
IMPACT ON CHARACTERIZATIONS ABOUT  
OTHERS AND SELF – A THEORETICAL STUDY

G. Srilatha\*  
D. Sujatha\*\*

ABSTRACT

Gender orientation generalizations were additionally apparent in self-portrayals, with female raters rating themselves as less agentic than male raters and male raters rating themselves as less public than female raters, in spite of the fact that there were special cases (no distinctions in instrumental ability, freedom, and amiability self-evaluations for people). Examinations of self-appraisals and evaluations of people overall demonstrated that ladies would in general describe themselves in more stereotypic terms – as less emphatic and less equipped in authority – than they portrayed others in their sexual orientation gathering. Men, interestingly, portrayed themselves in less stereotypic terms – as more mutual. Generally speaking, our outcomes show that an emphasis on features of office and mutuality can give further bits of knowledge about generalization content than an attention on by and large office and collection.

**Keywords :** Gender Stereotypes, male raters, female raters, sexual orientation,

**Introduction :**

There is no doubt that a lot of progress has been made toward sex equity, and this advancement is especially obvious in the working environment. There additionally is no doubt that the objective of full sex balance has not yet been accomplished – not in pay (AAUW, 2016) or position level (Catalyst, 2016). In a new meeting concentrate with female supervisors, most of boundaries for ladies' headway that were distinguished were ramifications of sexual orientation generalizations (Peus et al., 2015). There is a long history of exploration in brain research that supports this finding (for audits, see Eagly and Sczesny, 2009; Heilman, 2012). These examinations uphold the possibility that sex generalizations can be obstacles to ladies' professional success, advancing both sex predisposition in work choices and ladies' self-restricting conduct (Heilman, 1983).

This examination is intended to research the present status of sexual orientation generalizations about people utilizing a multi-dimensional structure. A large

part of the first examination on the substance of sexual orientation generalizations was directed a very long while back (e.g., Rosenkrantz et al., 1968), and later exploration discoveries are conflicting, some recommending that there has been a change in customary sex generalizations (e.g., Duehr and Bono, 2006) and others proposing there has not (e.g., Haines et al., 2016). Proportions of generalizing in these investigations will in general contrast, all operationalizing the develops of office and mutuality, the two characterizing highlights of sex generalizations (Abele et al., 2008), however in an unexpected way. We recommend that the contention in discoveries may get partially from the attention on various features of these builds in various investigations. In this way, we try to acquire a total image of the particular substance of the present sex generalizations by regarding office and collection as multi-dimensioned develops.

**Sex Stereotypes :**

Sexual orientation generalizations will be speculations about which people are indistinguishable,

\*Lecturer - St. Ann's College for Women, Mehdiapatnam, Hyderabad

\*\*Lecturer (PhD) - St. Ann's College for Women, Mehdiapatnam, Hyderabad



**సి.ఎస్.ఎస్.ఆర్ & ఎస్.ఆర్.ఆర్.ఎం.డిగ్రీ & పి.జి కళాశాల**

Accredited by NAAC B++ Grade

Recognized under section 2(f) & 2(b) of the UGC Act, 1956

కమలాపురం - 516 289, కడప జిల్లా, ఆంధ్రప్రదేశ్.

**భావోపనిషత్ ప్రత్యేక సంచిక**

Journal of Literary, Culture & Language Studies



Vol. 18 - Issue. 10 - Spl. Edition - October 2021 - ISSN No. : 2456-4702



**తెలుగు శాఖ**

**అంతర్జాతీయ సదస్సు**

తేదీలు-4, & 5 అక్టోబర్ 2021

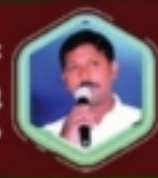
**ఆధునిక తెలుగు కవిత్వం -  
సమకాలీన సమస్యలు**

నేడే ఆకాశం తెలుగు రెళ్ళ



నిర్వహణ :  
**శ్రీ సి.వి. రాజగోపాలరెడ్డి**  
ప్రధానాచార్యులు

సదస్సు సంచాలకులు :  
**డా॥ పల్లా కృష్ణ**  
తెలుగు విభాగాధిపతి



# ఆధునిక తెలుగు కవిత్వం - సమకాలీన సమస్యలు

## అంతర్జాల అంతర్జాతీయ సదస్సు

భాషాపీఠ ప్రత్యేక సంచిక

ISSN No. : 2456-4702

RNI No. APTEL/2003/12253

UGC CARE - Journal - Arts & Humanities

ప్రథమ ముద్రణ : 5 అక్టోబర్ 2021

ప్రతులు : 500

కాపీలకు : సి.ఎస్.ఎస్.ఆర్ & ఎస్.ఆర్.ఆర్.ఎం. డిగ్రీ & పి.జి కళాశాల

గమనిక : ఈ సంచికలోని వ్యాసకర్తల అభిప్రాయములతో సంపాదక వర్గమునకు సంబంధం లేదు - సంపాదకవర్గం.

ఎడిటోరియల్ చిరునామా : చోళి చౌసె అపార్ట్‌మెంట్స్, పోస్టల్ కాలనీ, 4వ లైను,  
గుంటూరు - 522 002.

డి.టి.పి & ప్రింటింగ్ : తెనాలి ప్రైవేట్, జి.యల్.ఎస్. గ్రాఫిక్స్, లేమలై,  
అమరావతి మండలం, గుంటూరు జిల్లా. ఫోన్ : 9494 660 509.

26. సిరికి స్వామినాయుడు కవిత్వం - సమాజం	- డా॥ దార్లపూడి శివరామకృష్ణ	119
27. ప్రతిజ్ఞ గేయం - శ్రీశ్రీ దేవ్యం	- రఘుకు సణ్ణుఖరావు	121
28. వాన వెలిశాక కవిత్వం - సమకాలీన సమస్యల చిత్రణ	- డా॥ సత్యగాయత్రి జనమంచి	126
29. గురజాడ - రాయప్రోలు వారి సమకాలీన అంశాలు	- టి.మారెప్ప	131
30. ఆధునిక సాహిత్యంలో - గురజాడ వారి కన్యక	- పెరుమాంధ్ర శివకళ్యాణి	134
31. మైనారిటీ కవిత్వం - సమకాలీన మస్యలు	- డా॥ యల్. నాగలక్ష్మిదేవి	136
32. కాళోజి కవిత్వం - వ్యక్తిత్వ విశాసం	- డా॥ పుట్ట శ్రీనివాసులు	139
33. తెలంగాణ ఉద్యమ కవిత్వం - ప్రజా చైతన్యం	- గద్దం నాగేందర్	142
34. ఆనిమేష దీర్ఘ కవిత - పలన జిపుల సమస్యలు	- డా॥ వి. పవన్ కుమార్ రెడ్డి	148
35. ఆధునిక కవిత్వం - రూపురేఖలు - పరిశీలన	- చిరంజీవి వోనె	151
36. గురజాడ కవిత్వం సామాజిక సమస్యలు	- నందూరి అనంతలక్ష్మి	155
37. రాయప్రోలు సుబ్బారావు గారి స్పృహలత - సామాజిక సందేశం	- చెరుకుపెల్లి సునంద	158
38. శ్రీశ్రీ కవిత్వంలో సమకాలీనత విశ్లేషణ	- మొలలి సిద్ధయ్య	161
39. గురుజాడవారి కాసులు కవిత - ఒక పరిశీలన	- యామవరం రాజేష్ కుమార్	164
40. ఆధునిక తెలుగు కవిత్వం - శ్రీశ్రీ గారు	- కె. రంగనాయకులు	168
41. సూతలపాటి గంగాధరం రచనలు - సామాజిక దృష్టి	- డా॥ ఉదాలి విష్ణుప్రియ	172
42. స్త్రీవాద కవిత్వంలో దళిత స్త్రీవాద స్వరం	- టి. వెంకట నారాయణ	177
43. తిలక్ - తపాలా బంట్లోతు - మానవతా వాదం	- పట్నాన దర్శారావు	181
44. వచన కవిత్వం - బాలల సమస్యల చిత్రణ	- టి. అమ్ములు & - సి. త్రివేణి	185
45. గురజాడ కవిత్వం - సాంఘిక సమస్యల చిత్రణ	- యస్. కులదీపక్ & - టి. సుబ్బారాయుడు	187
46. ఆధునిక తెలుగు కవిత్వం - ప్రపంచీకరణ	- సి. వరలక్ష్మి & - టి. రజిత	189
47. ఆధునిక తెలుగు సాహిత్యం సమకాలీన సమస్యలు	- కె. వెంకట స్వామి	191

## నూతలపాటి గంగాధరం రచనలు - సామాజిక దృష్టి

- డా. శుశాల బట్టప్రయ్య, తెలుగుభాషాధ్యక్షులు, పెండ్ల అన్న మహిళా కళాశాల, మెహదీపట్నం, హైదరాబాదు, తెలంగాణ.

వ్యక్తి జీవితం, సామాజిక జీవితం రెండూ వేర్వేరుగా పుట్ట గనుక సాహిత్యం సమకాలీన ప్రతిబింబమై ఉండాలంటారు నూతలపాటి గంగాధరం గారు. కందుకూరి, శ్రీశ్రీల అగమనంలో ఆధునిక సాహిత్య ప్రక్రియలను సమాజ శ్రేయస్సును కేంద్రబిందువుగా చేసుకుని రూపొందుతూ వచ్చాయని అంటారు. సామాజికాంశాలను ఇతివృత్తంగా స్వీకరించి, మానవతావిలువలను ప్రబోధించే విచారణమైన కవితాంశాలతో రచన చేసారీయన

“నా కలం బలంతో చుక్కల్ని పెండి  
చిక్కటి కాంతి వది మందికి వంది పెడతాను  
నాకుంచె ప్రతిదానో  
నా జాతి స్వపాల్ని చిత్రించి  
నిఖల జగతికి నిండు బ్రతుకును ప్రసాదిస్తాను”

అంటున్న కవి వెనుక ఈ లోకం నిర్భయంగా నడుస్తోనంటుంది. చీకటి చిక్కదారుల్ని చీల్చి చిక్కటి కాంతి దారల్ని దారిపాడుతూ ప్రవహింపజేస్తోనని ప్రతిన బూను తున్న కవి నిశ్చయంగా ఒక మానవతావాది, ఒక ఆదర్శమూర్తి! అతడు మోడువారిని బ్రతుకుల్లో ఆశల చిగుళ్ళు తొంగిచూడడం కోసం వనంలాన్ని గొంతెత్తి పిలుస్తాడు. ఎండమావి జీవితాలను ఎగిసే కెరటాలుగా దర్శించడం కోసం మేఘాలను సంప్రదిస్తాడు. అత్యహత్యకు పాల్పడుతున్న ఆధాగ్యుడ్డి దగ్గరకు పిలిచి అతడి ఆరచేతిలో తన గుండెను పరచి మరొక్కసారి జీవించి చూడమంటాడు. అతడు వెలుగుకు అంగరక్షకుడు! తెలుగు సాహితీ శైలీలో అక్షరాల్ని విత్తులుగా వెదజల్లి నిలువెత్తు కిఖంలా ఎదిగిన ఆ కవనవనమే శ్రీ నూతల పాటి గంగాధరంగారు.

నూతలపాటి గంగాధరంగారు నవంబరు 15న 1939, చిత్తూరు జిల్లా, సత్యవేదు మండలం, రామగిరి గ్రామంలో

జన్మించాడు. ఇతని తల్లి కుచ్చమ్మ, తండ్రి మునస్వామి నాయుడు. ప్రాథమిక విద్య రామగిరిలో, ఉన్నత విద్యాభ్యాసం చిత్తూరులో పూర్తి చేశారు. తిరుపతి ప్రాచ్య కళాశాలలో విద్యానకోర్సు అనంతరం సత్యవేదులోనే తెలుగు పండితుడిగా ఉద్యోగం ప్రారంభించాడు. వీరు ఎన్నో కథలు, నవలలు, కవితాసంకలనాలు, విమర్శనాత్మక వ్యాసాలు, సాహిత్య వ్యాసాలు రాసారు. 1965లో ‘భారతి’ లో ప్రచురితమైన గురజాడకు మార్గదర్శి వేమన అనే వ్యాసం ఇతనికి మంచి పేరు తెచ్చింది. “సాహిత్య గంగాలహరి” అనే వ్యాసంకలనం విమర్శకుడిగా మంచి గుర్తింపు తెచ్చింది. తనాచీ కల, కొత్తచీర, పంచెం అనేవి వీరి ప్రముఖమైన కథలు. వీరు రాసిన ‘కాగితంపులి’ నవల ప్రముఖమైన నవల. ‘చీకటి నుంచి’ మరియు ‘వెలుగు లోనికి’ అనే కవితాసంకలనం వెలువడింది. నలభై కవితా ఖండికలున్న కవితాసంకలనం ఇది. ‘వెలుగులోనికి’ అనే కవితాసంపుటి 1974లో ప్రచురితమైనది. ఇవి కాకుండా పలువురు కవుల కవితలతో కూడిన ‘మానవ గీత’ అనే సంపుటంలో గంగాధరం కూడా రెండు కవితలు రచించారు. ఈ రెండు కవితల్లో ఒకదానిని తన ‘పేరుకోను, మరో కవితను ‘పాత్ర’ అనే కలం పేరుతోను ప్రకటించారు. ఈ రెండు కవితలలో పాటు కలిచర్లలో పశువుల వర్ణనందర్పంగా ఆ ఉత్సాహాలను పురస్కరించుకుని జరిగిన ఒక కవినమ్మోళనంలో ‘రక్తి’ అనే ఒక కవితను వీరు చదివారు. ఈయన 29-03-1975 శేదిన పాముకాటులో హఠాన్మరణం చెందారు. ముప్పయ్యేళ్ళకే నూరేళ్ళు నిండిన నూతలపాటి గంగాధరం పేరిట ప్రతియేడు ఒక సాహితీవేత్తకు పురస్కారాన్ని అందించి సత్కరించాలనే సదాశయంతో ఏర్పడింది గంగాధరం సాహితీ కుటుంబం. ప్రతి యేడు సాహిత్యంలో ప్రముఖమైన ముగ్గురు వ్యాయనిర్దేశాలు ఉత్తమ రచనను ఎంపిక చేసి ఈ సత్కారానికి



ఎంపిక చేయడం జరుగుతుంది. ప్రతి సంవత్సరం గంగాధరం వర్ణాంతరాలైన మే29వ తేదీన ఏర్పాటు చేసే సభలో అర్చనలైన వారికి ఈ సత్కారాన్ని అందజేస్తున్నారు.

సమాజానికి వెలుగుదివ్యలు నూతలపాటి గంగాధరం గారి కవితలు. చీకటి నుంచి బయలుదేరుతున్న మనిషికి వెలుగు కనిపిస్తుందనే ఆశ ఉంటేనే గానీ అడుగు ముందుకు సడదు. అందుకే కవి 'నా ప్రశ్న' అనే కవితలో

"అడిగేదే అంయితే నా ప్రశ్న  
అందరూ చెప్పేవాళ్ళే నా జవాబు  
కదలాడే నీళ్ళ మిది నీడ  
ఒడుగుతుందా కెమెరా యంత్రానికి !

అని ప్రశ్నిస్తారు". వీరు రాసిన "నిండని కుండ" కవితా ఖండికలో దరిద్రుడి జీవితాన్ని 'నిండని కుండ'లో పోలుస్తారు. జీవితాన్ని వర్ణించిన విస్తరిగా అనుభవిస్తున్న వాళ్ళంతా నిండిన కుండలే అవి తొణకపు, బెణకపు. నిండని కుండకే నిలువెత్తు కష్టాలు.

గోవు సాదుజంతువే  
కాదని ఎవరన్నారు !  
పాలు పితుకబోలే  
కుండ పగులదంతుంది ఒకప్పుడు !  
ఎప్పుడు  
తిండి పెట్టకుండా కడుపుకాల్చినప్పుడు !

'సేవకుడైతే మాత్రం ఎలా సహించగలడు అని ప్రశ్నిస్తారు కవి. కడుపు నిండుకుంటే మనిపైనా, మృగమైనా పోరాటం సాగిస్తూనే ఉంటాడంటారు కవి. జీవితంపై అనురక్తి, ఆశలేని వాళ్ళని పోరాట దృష్టి లేనివారిని కవి ఓటి కుండలో పోల్చిచెబుతాడు.

"ఓటి కుండ నిండుకుండా నిండుకుండా ఏనాటికైనా?  
నీళ్ళు లేని కుండ - నిర్జీవం !  
అది ఎలా తొణక గలదు ! అని అంటారీయన

క్రామిక వర్ణం ఎప్పుడు ఎదురుతిరుగుతుందని కవి ఇలా చెప్పాడు. తమ రెక్కల కష్టాన్ని నమ్ముకుని

న్యాయమైన మార్గంలో బ్రతుకుతున్న క్రామికవర్ణం ఏనాటికీ అన్యాయాలను సహించదు.

"దిక్క దిక్కలూ తిరిగి  
తెచ్చి పెట్టుకున్న తేనెపట్టుని  
తింటుంటాయి - తమ కష్టం  
తిన్నగా .... తేనెటీగలు !  
ఎప్పుడు ?

ఎవరు కదపస్తారు ! అని కవి తమ జోలికి రానంత వరకూ ఏ హాని చెయ్యని తేనెటీగలు సైన్యంలా ఒక్క సారిగా దండెత్తి తమ సత్తా ఏమిటో రుచి చూపిస్తాయి.

'నిండని కుండ' కవిత్వ సాదుజంతువులాంటి మనిషిని ఉక్కుపాదాల కింద తొక్కివట్టి సాదించాలని చూసే తిరగబడే చరిత్రను తిరగరాస్తాడని ఉద్బోధిస్తారు గంగాధరం గారు.

"కవి చేతి కలానికి  
పాలంలోని హలానికి  
సరిహద్దుల్లోని సైనికబలానికి  
ఈ ఉదయం  
తప్పక ఉదయిస్తుందనే ఆశ లేకుంటే  
ఆ అడుగు అక్కడే దిగబడి పోదా?

"ఆశే" తనను అడుగు ముందుకు నేయిస్తాడని, ఆ ఆశే లేకుంటే కిశరం వసంతం వరకూ నడవలేదన్న వాస్తవాన్ని ఆయన నమ్మాలంటారు. 'ఈ ఉదయం తప్పక ఉదయిస్తుంది' అనే కవిత్వలోనిదే సై సంక్షులు. కలానికి, హలానికి, సైనిక బలానికి ఆశే ప్రధానమైన ఊపిరిగా కవి అభివర్ణిస్తారు.

కాలాన్ని జయించడం అంత తేలికైన పని కాదని కవి ఇలా అంటాడు.

"నింగిలో నీలం ఉన్నట్లు  
కాలంలో జాలం ఉంది  
కాలానికి జాలే కాదు,  
జాలి కూడా లేదు,

సీతి నియమం మాత్రం ఉన్నాయంటారు.  
"కొన్ని గాయాలను నయం చేస్తూ  
కొన్ని గాయాలను మనం చేస్తూ  
ప్రయాణిస్తుంది కాలం ! అన్న పాదాల్లో జీవితంలోని  
చేదు అనుభవాలు కాలక్రమేణా మరిచిపోతే, మరికొన్ని  
ఎంత కాలమైనా గాయాలై నలుపుతుండడానికి కాలమే  
కారణంగా కవి పేర్కొంటారు. గంగాధరం గారు 'చేదు  
మాటలు' అనే కవితా ఖండికలో మహానీయుల ఆలోచనా  
మృత్యాలు ఎలా ఉంటాయో ఇలా అన్నారు.

"నడకలోనే తెలియనే  
నరుని గొప్పతనాలన్ని  
నాకమనగ ఏది ? ఏమల యశస్సు కాదె" !

అంటూ నశించని కీర్తిని సంపాదించడమే అసలైన  
స్వర్గమనీ, మనిషి గొప్పతనం అతని ప్రవర్తనలోనే  
తెలుస్తుందనీ అంటారు. మంచి పనులు చెయ్యడానికి  
కులమత భేదాలు మహానీయులకు అడ్డరాపని చెబు  
తారు. ఈ ప్రపంచంలో ఎక్కడున్న మాతృభాషాన్ని తలుచు  
కొంచె కొంత ఫలితం దక్కతుందనీ అంటారు.

'అశే' మానవునికి జీవితానికి ప్రేరణ కలిగిస్తుంది.  
'అకాపాళం' అనే కవితాఖండికలో అశే బ్రతుకును  
ముందుకు నడిపిస్తుందని నూతలపాటిగారు చెబుతారు.

"బ్రతుకు బొంగరాన్ని అకాపాళంతో తిప్ప!  
ఆ పాళం పాడవైనా గొడవే !  
పొట్టిదయినా బెడదే !

అంటూ అత్యాళ దుష్పరితాలనిస్తే, నిరాళ మొదటికే  
మోసమని చెబుతారు.

"ఏ సాధనం లేకుండా  
అకాళానికెగరాలనేది - దురాళ  
ఎట్టి ప్రయత్నాలైకుండా  
మట్టి మిద నిలబడాలనేది - నిరాళ  
సాధనాల సహాయంతో  
అకాళానికే ప్రయత్నమే - అశే" అంటూ అశను చిన్న

కోణంలో విశ్లేషిస్తారీయన అశ లేనిదే అశయం సిద్ధించ  
దని, బ్రతుకుపాటకు అశే కెరటం లాంటిది 'అశ' అని  
పేర్కొంటారు.

"ఈ తూరు  
నింగి రాతిలో చేసింది  
నేల ఉక్కుతో నిర్మించింది  
ఓక్క యక్క వర్షం పడదు  
ఓక్క గింజ ధాన్యం పండదు" అంటూ తన తూరి  
దీనస్థితిని నూతలపాటిగారు పై కవిత్యంలో ఇలా  
వర్ణించారు. సమాజానికి అవసరమైనవి ఏంటో తాను పుట్టి  
పెరిగిన తూరి గురించి పై కవిత్యంలో చెప్పిన తీరే మనకు  
అర్థమవుతుంది. అందరూ తాను పుట్టిపెరిగిన తూరిని  
గురించి గొప్పగా చెప్పుకుంటారు. కానీ తూరిని మాత్రం  
బాధ, జాలి కలుగుతాయి. తమ తూరిలో అప్పుచ్చేవాడు  
గానీ, చైర్యుడుగానీ, బ్రహ్మణ్యుడుగానీ ఎడతెగక  
ప్రవహించే ఏరు గానీ ఉండవంటారు.

"అ తూరిలో తెల్లవారిందని చెప్పడానికి కూడా  
ఓక్క కోడి లేదు  
ప్రకృతికీ, మా తూరికీ ఎప్పుడు పడదు" అని  
ఈ కవితలో నిట్టూరుస్తారాయన.  
"దేశపటంలో నల్లయక్కవైనా  
నోచుకొనిది మా తూరు"

ఈ తూరు మా తూరు అంటూ చిత్తూరుజిల్లాలోని తమ  
కుగ్రామమైన అనాటి రామగిరి స్థితిగతులను ఈ  
కవితాఖండికలో వెల్లడించారు కవి.

గంగాధరం గారు నేటి సమాజంలో మానవుని మను  
గడను గురించి, వాగరికత పేరున సాగుతున్న వింత  
పోకడల గురించి వ్యంగ్యంగా "కొన్ని వాస్తవాలు" అనే  
కవితాఖండికలో స్త్రోత్రపాఠంలా వర్ణిస్తున్నారు. మారుతున్న  
కాలానికి అనుగుణంగా మారలేకపోతున్న సనాతనుల్ని,  
ఇక్కడే అగిపోతాయనుకున్న వారి ఆలోచనల్ని కాలం  
ఈడ్చుకు పోతుందంటారాయన.

“నేటి విద్యార్థుల్ని సెలబస్ బస్ ఎక్కించలేక  
బడివంతులు నేటి ఐక్యరాజ్య సమితిలా దిమ్మెర  
పోతున్నాడు”.

అంటూ సంక్షిప్తమైన పోయిన విద్యావిదానాన్ని  
మాటుగా విమర్శిస్తారు.

“నాగరికతా ప్రపంచంలో మానవుని సహజ స్వభావం  
మూకుడు క్రింది దీవంలా ఊపిరి వీల్చడం  
మానుకుంది”.

అంటూ లేనిపోని ఔపాఖ్యాతాల్లో చిక్కినగటు మనిషి తన  
స్వాభావిక గుణాలకు దూరమవుతున్నాడని విచారిస్తారు.

ఇంతవరకు “చీకటిలోకి” కవితాఖండికలోని పలు  
కవితల సౌందర్యాక్షరాలను చదివి ఆస్వాదించాము.

నూతలపాటి గంగాధరం గారి ‘వెలుగులోనికి’ అనే  
కవితాసంపుటిలో “ఒంటరిగా ప్రేమించలేను”లో  
ఏమన్నారో చూడండి.

“నా దేశం కదలి అని

అన్ని బాపా వాహనుల కూడలి అని గర్విస్తున్నాను”

అన్న మాటల్లో కవి హృదయ వైకల్యం వ్యక్తమవు  
తుంది.

“పైదరాబాదు మంచి ఉరుదూ సాకి బెదురు కనులూ,  
అనంతపూరు నుంచి కన్నడ ప్రౌఢగడుసు చనులూ,  
దిక్కూరు నుంచి అరవ జవరాళి ధరకనాట్యం నడుమా”

అని ఆంధ్రదేశాన్నినా ఒంటరిగా పరించాలనుకున్నా  
కవని, పరిచరులను కూడా తనలో కలుపుకోక తప్పలేదు  
అన్నారు.

“వెలిగే దీవం వెయ్యి దీపాల్ని

వెలిగించగలదు

వెలగనివి కోటికి ఒక్కదైనా

ఒక్క వెలుగు చుక్క దక్కదు ! అని ఒక వ్యక్తి నడిచిన  
మార్గం తన ఒక్కడి కోసమే కాదని, తర్వాతితరం కూడా  
అదే బాటను అనుసరిస్తుందని కవి ఈ కవిత్యంలో  
పేర్కొన్నారు.

“నాముఖం కామందుల ఉమ్ములకు పాకీ  
నా వీపు కలవారి పరువులకు జాకీ  
నా భుజాలు నిప్పుల కార్యాల లంపట్లు”

అని అనడంలో కవి అథమ వర్గాల దుస్థితిని తనవిగ  
లావించి తెలియజేస్తున్నారు. బలవంతుడిచే రాజ్యమనీ,  
వారి సంతాలకు, బలవంతాలకూ బలైపోయిన ఈ మోడు  
బ్రతుకులు చిగురించినవి వాపోతున్నారు తన “కవి  
సమ్మేళనం” అనే కవితాఖండికలో.

వీరి ‘జాతి మనస్తత్వం’ కవిత్యంలో అభివృద్ధి  
మునుగులో ఆధోగతి పొలవుతున్న సమాజాన్ని పర  
మర్యాదలకు దాసోహమంటూ భావ దాస్యానికి పాల్పడు  
తున్న సంస్కృతిని నిరసస్తూ..

“నాకూ నా తరానికి కావలసిందిప్పుడు

నల్లటి చీకటికాదు.

తెల్లని కిరణాలు ప్రసరించే ఎర్రటికాంతే  
అంటున్నారు”.

నేటి సమాజం విశ్వంఖలంగా రాజ్యమేలుతున్న  
అవినీతి పాలనను లేలిత్తి చూపుతున్నారు. “చినుకు  
చెఱకలు” అనే కవితలో ఇలా..

“దశరథ తనయుడిది వట్టి అదృష్టం !

నాటి దౌర్జన్యానికి దశముఖాలు !

గాంచి నందనుడిది ఏమి అదృష్టం ?

మట్టి పుట్టే ఏమైనా మార్పును సంతరించుకుంటుంది  
అలాంటిది మానవుడు కూడా మంచి మార్పు దిశలో  
నడవాలని కవి ఆకాంక్షించాడు.

“మనిషి ప్రమిద చేసి మంచిని వెలిగించి

నాడు వెలుగు జేయువాడె నరుడు

అశలేకయున్న అశయమే లేదు

అశయమ్ము లేక అవని లేదు’ మానవుడికి దిశా  
నిర్దేశకాలు నూతలపాటి గారి సామాజిక దృష్టి నాటి  
సమాజంలో ప్రతి అనువు పైన ప్రసరించేయాలి.

“మానవ గీత” అనే కవితాసంపుటిలో వీరు రెండు కవితలు రాసారు. “లవ్ అండ్ లెట్ లివ్” అనే ఈ కవితా ఖండికకు ఆంగ్లశీర్షికను పెట్టాడు కవి. ఏకాంకంలో వ్యక్తి తన తప్పింపులను విశ్లేషించుకోనేటందుకు అవకాశం ఉంటుందని ఏకాంకం వివేచనను కలిగిస్తుందని కవి ఈ ఖండికలో పేర్కొంటారు. ఏకాంకమంటే అర్థం మనిషి ఒంటరిగా ఉండడం కాదంటూ .. “యౌవనంలో జంట... ఒంటరితనమే అచ్చమైన ఏకాంకం! అని కొత్త అర్థాన్ని పరిచయం చేశారు.

“అనుభవించగల నేర్పే ఉంటే

సంకలో ఏకాంకం ఉంది! అంటూ ఏకాంక భావన

మనసుకు సంబంధించిన అనుభూతిగా పేర్కొన్నారు నూతలపాటిగారు. ఈ కవిత్యాన్ని ‘పాత్ర’ అనే కలం పేరుతో రాసారు.

“సంప్రదాయపు పునాదుల మీదుగా వినూత్న కవితా సాధాన్ని విర్మించిన ఆధునిక అక్షరశిల్పి నూతలపాటి వీరి ‘చీకటినుంచి’ కవితా సంపుటిపై ‘ఉషారేఖలు’ వ్రస రింపచేస్తూ భావనా బలము కలిగి, మెదడుకు అపారాన్ని ఇవ్వగల చక్కని కవిత గంగాధరం గారిది”. అని దాశరథి గారు వ్రశంపిస్తూ అన్న మాటలు నూతలపాటి వ్రతల వాతావరణం అవిష్కరిస్తాయి. వీరి కవితలను పరామర్శించి నవుడు గొప్ప మానవతావాదిగా దర్శన మిస్తారు. మానవుడే వీరి కావ్య వస్తువు. మానవతవాదమే దాని

ఉపయుక్త గ్రంథ సూచిక :

1. “చీకటి నుంచి”(కవితాసంకలనం) - నూతలపాటి గంగాధరం, కళాసాహితీ, మద్రాసు.
2. “వెలుగులోనికి”(కవితాసంకలనం) - నూతలపాటి గంగాధరం, ఎస్వీపబ్లికేషన్స్, మద్రాసు.
3. “మానవగీత”(కవితాసంకలనం) - నూతలపాటి గంగాధరం, దీక్షవ్రచయరణలు, చిత్తూరు 1970.



గుణం. చీకటి నుంచి వెలుగులోనికి వ్రస్తానమైన కవి చూపు వెనుకకు మరలదు.

“మౌనిగా కూర్చున్న జ్ఞాని కన్నా  
మనిషిగా తిరుగుతున్న అజ్ఞానే నయం”

(చినుకులు - చెఱకులు)

అన్న పంక్తులు సమాజానికి వెలుగు చీపాలు.

మనసు వ్రమించే చేపి మంచిని వెలిగించి నాడు వెలుగు జెయు నాడె నరుడు” అన్న పాదాల్లో దేశాన్ని వెలుగు లోనికి తీసుకెళ్ళే అర్థంలో దేశానికి బదులుగా “నాడు” అనే మాటను వ్రయోగించారు.

“వ్యక్తి మనసు ఎప్పుడు మంచి నీళ్ళలాంటిది.

పరిసరాలు ఆ నీళ్ళలో ఏ రంగును కలిపితే అది ఆ రంగుతో మారిపోతుందని” కవి అంటున్నారు.

సంఘంలోని ఆసమానతలను, మానవ సంబంధాలను నిశితంగా పరిశీలించి ఉచితానుచితాలను గుర్తించి సమాజాన్ని, మానవుడి మంచిమార్గంలో పెట్టడానికి వ్రయత్నిస్తుంటారు. కాబట్టి వారి సాహిత్య జీవితం ప్రాముఖ్యాన్ని సంతరించుకొంటుంది. జీవిత పరమార్థాన్ని వ్రసాదించగలుగుతుంది. స్వల్పకాలంలో తన జీవిత ర్షేయాన్ని సాదించి, ఒక ఉత్తమ సాహితీనేత్రగా ఆధునిక సాహిత్య చరిత్రలో అమరులై తన అస్తిత్వాన్ని నిల బెట్టుకున్న సాహిత్యమూర్తి నూతలపాటి గంగాధరం.

# Phytochemical and antimicrobial paneling of ethnobotanical plant *Hyptis suaveolens* (L) Poit.

Sadaf Kalam and \* A.M. Sylaja

Lecturers, \* Head of the Department of Biochemistry,

St. Ann's College for Women, Mehdiapatnam, Hyderabad, Telangana, India.

## ABSTRACT

Plants are vast and diverse sources of bioactive compounds, among which secondary metabolites are the most dominant class of organic compounds. Researchers are keenly interested in natural products because of the complexity of their chemical structures and biosynthetic pathways. *Hyptis suaveolens* is an ethnobotanically important medicinal plant belonging to the lamiaceae family. Plant extracts of this medicinal plant are widely used in traditional system of medicines as anti-inflammatory, antispasmodic, antirheumatic, antiseptic etc. Present work highlights the phytochemical analysis of bioactive components in different *Hyptis* leaf extracts and antimicrobial activities of leaf extracts (LE) and leaf+inflorescence extract (LIE). The presence of phytochemicals like- glycosides, proteins, steroids, phenols and tannins was observed in all the leaf extracts. The antimicrobial activity of *Hyptis* leaf extracts against human pathogenic bacteria and fungi was also assessed in the form of zones of inhibitions. The microorganisms under study exhibited spectral differences in their susceptibility towards *Hyptis* leaf extracts and leaf+inflorescence extract (LIE). Out of the four leaf extracts (Steam distilled, methanolic, ethanolic and chloroform), steam distilled extracts exhibited broad spectrum antibiotic and antifungal activity against the tested microorganisms. Highest antibacterial and antifungal activity was observed against *Staphylococcus aureus* and *Fusarium oxysporum*. Further detailed characterizations of the phytochemicals may lead to discovery of new family of antimicrobial compounds.

**Keywords** - *Hyptis suaveolens*, leaf extract, inflorescence extract, antibacterial, antifungal, synergistic effect

## I. INTRODUCTION

Since times immemorial, plants have been treasured sources of natural products for maintaining human health. Indians and Chinese have been using plants as medicines for pain management, inflammation, weight reduction etc., in traditional system of medicines. Due to their medicinal importance, plant extracts have been extensively used in Ayurveda to treat major ailments in naturopathies. Plants contain an arsenal of compounds called as phytochemicals which are exploited by pharmaceutical companies for the development of novel drugs. There has been a burgeoning interest in isolating and characterizing novel non-nutritive plant chemicals and exploring their medicinal properties. Organic chemists have developed several isolation, separation, spectroscopic and structure elucidation methodologies constituting the foundation of contemporary phytochemistry. Phytochemicals which are products of secondary metabolism in plants, are known to possess antimicrobial activity and thus could be explored for therapeutic treatments (Edeoga et al., 2005; Savithamma et al., 2011). The antimicrobial properties of plants have been investigated by several researchers all over the world (Dorman and Stanley, 2000; Bhalodia and Shukla, 2011). *Hyptis suaveolens* L. Poit., commonly known as wilayat tulsi or bushmint belongs to the family Lamiaceae. It is a potential medicinal herb which is reported to have high medicinal value and is widely seen in Telangana, India. The extracts and oils of this aromatic herb have been reported to have antimicrobial activities. This plant possess antispasmodic, anti-inflammatory, antiseptic, anticancer, antirheumatic and antifertility activity (Mandal et al., 2007). Due to increased resistance of pathogenic microbial strains towards existing antimicrobials, natural products have proved to be an effective alternative for the discovery of novel drugs. In order to discover new antimicrobial compounds, several research groups have been screening plant extracts to detect secondary metabolites with potential biological activities. These observations provided us a platform to determine the antimicrobial activity of leaf and leaf+inflorescence extracts of *Hyptis suaveolens*. We are reporting for the first time the antimicrobial activity of leaf+inflorescence, combined extracts of *Hyptis suaveolens* which synergistically are more efficient than leaf extracts alone. Results indicate antimicrobial potential of both the extracts strengthening the concept of employing these in pharma industry in the development of new antimicrobials.

## II. Materials and Methods

### 2.1 Sample collection and Authentication

The fresh plant parts (leaves and inflorescence) of *H. suaveolens* were collected from *Hyptis* naturally populated area near shamshabad region of Hyderabad, Telangana in the month of September, 2018. The authentication of plant was done by Botanist, Dr. Mir Zahur Gul, Osmania University. The collected plants were initially washed thrice with tap water and finally once with distilled water. Excess water was drained by damping the plants on filter paper.

### 2.2 Preparation of extracts

Fresh samples (10g) each of *Hyptis* leaves and inflorescence were extracted with 100ml of the solvents such as methanol, ethanol and chloroform. The solutions were later filtered through Whatmann No.1 filter paper and the filtrate were collected (crude extracts) and were evaporated (at 40°C) with the help of heating mantle (Kumar and Thampi, 2015). While steam distillation of plant leaves and inflorescence was carried out according to the method of Moreira et al., (2010). The residues so obtained were weighed and reconstituted with respective solvents to a final concentration of 500µg/ml.

### 2.3 Phytochemical Paneling

Paneling of the plant extracts for various phytochemical constituents- carbohydrates, alkaloids, cardiac glycosides, coumarin, saponins, flavonoids, phytosterols, fats and oils, phenols, tannins and proteins present was carried out using standard methods (Mozhiyarsi and Anuradha, 2016).

### 2.4 Test bacterial and fungal cultures

The bacterial cultures were obtained from IMTECH Chandigarh-*Bacillus subtilis* (MTCC-441), *Staphylococcus aureus* (MTCC-737), and *Pseudomonas aeruginosa* (MTCC-424) whereas, the fungi- *Aspergillus niger*, *Aspergillus flavus* and *Fusarium oxysporum* were obtained from Fungal Germplasm Culture Collection (FGCC), Rani Durgavati University, Jabalpur. The bacterial cultures and fungal cultures were maintained on nutrient agar and sabouraud agar (SDA) slants respectively and stored at 4°C

### 2.5 Preparation of inoculum

Preparation of test bacteria inoculum was done by inoculating loopful of target bacteria (24 hour old culture) in 5 ml nutrient broth and incubated at 37±2°C for 6-8 hours till a moderate turbidity was developed. The turbidity was adjusted to 0.5 McFarland standard by adding distilled water which correspond to the cell density 1.5x10<sup>8</sup> (CFU/ml) (Mandal et al., 2007; Balouiri et al., 2016). Fungal cultures were grown for 5-7 days of respective fungi at 37±2 °C. The sample of solvent extracts residue were dissolved in respective solvents and used as test extracts. Steam distilled plant extracts were dissolved in DMSO, 5% (Dimethyl sulphoxide) solvent. Parallel controls of neat solvents served as negative controls.

### 2.6 Disc Diffusion test for determining antibacterial activity (Zaidan et al., 2005)

Nutrient agar and Sabouraud agar plates were employed for disc diffusion test. 1 ml inoculum suspension was spread uniformly over the agar medium to form a lawn of test bacteria using sterile spreader. The readily prepared sterile discs were loaded. Sterile filter paper discs (6mm diameter) each impregnated with different solvent extracted leaf and inflorescence extracts were placed at equidistance on upper surface of the seeded agar medium. The paper diffuse discs were placed on the medium suitably apart and the plate were incubated at 37±2 °C for 24-48 hours. The antimicrobial activity was recorded by measuring the width of the clear inhibition zone around the disc using zone reader (mm). Antibiotic disc Gentamycin sulfate (40mg/ml) was used as a positive control, while discs soaked in respective solvent were used as a blank control.

### 2.7 Poisoned food technique for determining antifungal activity (Das et al., 2010)

For determination of antifungal activity, 20ml of sterilized and cooled growth media (SDA) with 10mg streptomycin was poured into pre sterilized Petri plates. Requisite amount of plant extracts i.e. 1000 µg/ml were pipetted into the plates and were uniformly spread plated using spreader. The control plates contained the medium supplemented with different solvents instead of plant extract. After the solidification of the agar medium, inoculums of the test fungi (disc of 6 mm diameter cut from periphery from 7 days old culture with the help of sterile cork borer) were placed aseptically in each Petri plates of treated and control sets. The assay plates were than incubated at 30 ± 2°C for 5-7 days. Nystatin (20mg/ml) was taken as a positive control. After the desire period of incubation diameter of the fungal colony of treated as well as control sets were measured. The percentage of mycelial growth inhibition was calculated by mean value of colony diameter by the following formula and the experiment was conducted in triplicates.

$$\text{Percentage of mycelial inhibition} = \frac{dc - dt}{dc} \times 100$$

Where, dc – average diameter of fungal colony in control sets

dt - average diameter of fungal colony in treated sets.

## 2.8 Effect of mixture of *Hyptis* leaf and inflorescence extracts on microbial growth

The antimicrobial activity of a combination of essential plant extract (leaf+ inflorescence) was measured by using filter paper disc diffusion method (Vincent and Vincent, 1944) for determining their possible synergistic activity. The essential plant extracts-leaf and inflorescence were blended with each other in 1:1 ratio. Thereafter, the methodology mentioned under preparation of spore suspension and test sample heading was followed. Aliquots of 20 ml seeded medium were poured in each sterile nutrient agar plates. Sterile filter paper discs (6 mm diameter) each impregnated with 10 µl of different solvent extracts (1:1) was placed at equidistance on upper surface of the seeded agar medium. The plates were then left undisturbed for 30 minutes to allow diffusion of the sample into the agar at room temperature the diameter of inhibition zone formed by different combination of plant extract was recorded after 24-48 hrs of incubation at 37±2 °C. Whereas, fungitoxic nature of the plant mixture was determined by applying poisoned food technique as described earlier.

## III. RESULTS AND DISCUSSION

### 3.1 Phytochemical paneling

Plants produce a wide variety of bioactive metabolites including tannins, terpenoids, alkaloids, and flavonoids which possess potential antimicrobial properties. In our present research work, *Hyptis suaveolens*, different leaf extracts showed the presence of carbohydrates, alkaloids, cardiac glycosides, coumarin, saponins, flavonoids, phytosterols, fats and oils, phenols, tannins and proteins was confirmed by performing various phytochemical tests as depicted in Table 2. Similarly, phytochemical investigations of various extracts of leaf extracts of *Hyptis suaveolens* indicated the presence of carbohydrates, alkaloids, glycosides, steroids, flavonoids, phenols, terpenoids and proteins (Mozhiyarasi and Anuradha, 2016). Ethanolic extract contained alkaloids, glycosides, carbohydrates, proteins, steroids, flavonoids, phenols, terpenoids and quinones. Methanolic extract contained alkaloids, glycosides, carbohydrates, proteins, steroids, flavonoids and phenols. Chloroform extract exhibited positive results indicating the presence of alkaloids, glycosides, carbohydrates, proteins, steroids, flavonoids and phenols. Similar studies on phytochemical screening of *Hyptis* leaf extracts has been also undertaken by several researchers (Mandal et al., 2007; Kumar and Thampi, 2015; Mozhiyarasi and Anuradha, 2016).

### 3.2 Antibacterial paneling

In the present study, the antibacterial activity of *Hyptis* leaf extracts in different solvents was determined by measuring the width (mm) of the inhibitory zones by following disc diffusion method. The antibacterial activity was determined against two Gram positive bacteria i.e. *Bacillus subtilis* and *Staphylococcus aureus*; and one Gram negative bacteria- *Pseudomonas aureus*. The results obtained have been summarized in Table 2. Among all the extracts, steam distilled extract (essential oil) showed maximum antibacterial activity and significant inhibitory action against all the test bacteria. Maximum zone of inhibition was observed against Gram positive bacteria-*Bacillus subtilis* followed by Gram negative bacteria-*Pseudomonas aeruginosa*. In case of ethanolic extract, the inhibitory zone followed the same pattern as exhibited by steam distilled extract. On the other hand, chloroform extract showed significant and equal inhibitory action against *Bacillus subtilis* and *Staphylococcus aureus*. While methanolic extract exhibited least inhibitory action on nearly all the test bacteria as evidenced from the diameter of zones of inhibition. Reference antibiotic used was Gentamycin sulfate at 40mg/ml concentration and Table 2 also contains the zones of inhibition against different test bacteria.

### 3.3 Antifungal paneling

The fungitoxic spectrum of the plant leaf extract as measured by poisoned food technique is represented in Table 2. The antifungal activity of *Hyptis* leaf extracts in different solvents shows a distinctive pattern. As in the case of fungi, among all the extracts, steam distilled extract (essential oil) exhibited maximum antifungal activity against all the test fungi. Steam distilled extract (essential oil) was found to be the most effective antifungal against all the test fungi- *Aspergillus niger*, *Aspergillus flavus* and *Fusarium oxysporum* as evidenced by % mycelial growth inhibition, followed by chloroform, methanol and ethanol extracts. On the whole, comparing the antimicrobial effects, antibacterial effect was observed to be more effective than antifungal effect. Reference antifungal used was Nystatin at 20mg/ml concentration and Table 2 represents % mycelial growth inhibition or antifungal activity against the test fungi.

### 3.4 Antimicrobial paneling of a combination of *Hyptis* leaf and inflorescence extracts

The combination of *Hyptis* leaf and inflorescence extracts was also assessed for its antimicrobial activity as shown in Table 3. Results indicate a significant increase in overall antimicrobial activity. The combination of extracts was able to enhance the antibacterial activity towards all the test bacteria, while the fungitoxicity spectrum results too indicated an overall increase in antifungal activity. There was a simultaneous increase in both the antibacterial activity (Gram positive and negative) and antifungal activity by all the plant extracts indicating some synergistic action of the leaf and inflorescence extracts. Steam distilled leaf and inflorescence extracts synergistically enhanced antibacterial activity against *Bacillus subtilis*, followed by *Pseudomonas aeruginosa*. While maximum % growth inhibition was achieved against *Aspergillus niger* by a combination of steam distilled extracts, followed by antifungal effect on *Fusarium oxysporum* and *Aspergillus flavus*.

**3.5 Antimicrobial paneling-** Over the past few decades, there has been a whopping upsurge in the investigation of natural products as sources of novel antibacterial agents. Plants have been used to treat or prevent ailments since times immemorial and phytochemicals present in them possess a plethora of medicinal properties (Lewis and Ausubel, 2006; Sathish et al., 2010; Savithamma et al., 2011). Several plant extracts have been extracted in various solvents and have been evaluated for their antimicrobial activities. Steam distillation, petroleum ether, and ethanol extracts from *Hyptis suaveolens* leaves were evaluated for their antimicrobial activity *in vitro* (Mandal et al., 2007). They observed that among the various extracts, steam distillation extract exhibited broad-spectrum antibacterial and antifungal activity against the tested organisms. Highest antifungal and antibacterial activity was reported against *Aspergillus niger* and *Micrococcus luteus*, respectively. Steam distilled extracts (SDE) contain essential oils as their major constituents which are known to possess antimicrobial properties. Monoterpene constituents in SDE exert membrane-damaging effects on microbial strains and also stimulate leakage of cellular potassium ions which is lethal to microorganisms (Asekun et al., 1999).

In another research work, screening phyto-constituents and determining antimicrobial ability of various extracts of *Hyptis suaveolens* was done (Mozhiyaras and Anuradha, 2016). They employed disc diffusion method to evaluate antimicrobial activities of aqueous, ethanol, methanol, chloroform extract of *Hyptis*. Their studies indicated chloroform extract to exhibit inhibitory activity against *Escherichia coli* and *Staphylococcus aureus*; while ethanolic extract showed highest inhibitory activity against *Pseudomonas aeruginosa* and antifungal activity was recorded maximum against *Aspergillus Niger*. Thus, an arsenal of antimicrobial activities was recorded with various solvent extracts. In another interesting study, significant biological activity of *Hyptis carpinifolia* steam distilled leaf extracts was reported against Gram positive and negative bacteria at varied concentrations (Camargo et al., 2017).

Past and present investigations clearly indicate the antagonistic potential of *Hyptis* leaf extracts against an array of human pathogenic bacteria and fungi. But the hallmark of our study was that we report for the very first time the antimicrobial effects of leaf and inflorescence together synergistically.

## CONCLUSION

Present study thus highlights the antimicrobial activity of *Hyptis* leaf extracts and leaf+inflorescence extracts as effective antimicrobials. The steam distilled leaf extracts and leaf+inflorescence extracts proved to be active antibacterials against two Gram positive and one Gram negative test bacteria. Results of Antifungal activity indicated steam distilled extracts of *Hyptis* also to be good antifungal agents. Leaf and inflorescence extracts together elicited better antimicrobial properties. This synergistic property could be exploited towards the use of plants as therapeutic agents. Synergistic effects of ethnomedicinal plant *Hyptis suaveolens* leaf and inflorescence extracts on microorganisms was investigated successfully, thus providing new insights into core phytochemical research towards the discovery of novel and lucrative antimicrobials.

## ACKNOWLEDGEMENTS

The authors wish to thank Principal Sister Amrutha, St. Ann's College for Women, Mehdipatnam, Hyderabad, for providing the necessary laboratory facilities and also for the financial assistance.

**Table 1: Phytochemical analysis of *Hyptis suaveolens* leaf extracts**

Phytochemical tests	Steam distilled	Ethanol	Methanol	Chloroform
Carbohydrates	-	+	-	+
Alkaloids	-	+	-	-
Cardiac glycosides	-	-	+	+
Coumarin	-	+	+	-
Saponins	-	+	+	+
Flavonoids	-	+	+	+
Phytosterols	-	+	-	+
Fats and oils	+	-	-	+
Phenols	-	+	+	+
Tannins	-	+	+	+
Proteins	-	+	+	+



(+ ) Indicates Presence, (-) Indicates Absence

Table 2: Antibacterial activity of *Hyptis suaveolens* leaf extracts (500 µg/ml)

S.No	Plant extracts	Test organisms					
		Test bacteria Zones of Inhibition (mm)			% Growth Inhibition of Test fungi		
		B.s	S.a	P.a	A. n	A. f	F.o
1	Steam distilled	20±0.21	16±0.22	18±0.06	65±0.13	60±0.26	61±0.22
2	Ethanol	18±0.12	11±0.06	16±0.14	44±0.09	40±0.17	50±0.16
3	Methanol	12±0.08	12±0.16	14±0.08	52±0.15	53±0.09	46±0.09
4	Chloroform	16±0.11	14±0.12	13±0.16	60±0.30	58±0.14	53±0.11
5	Antibiotic/ Antifungal	33±0.09	42±0.08	36±0.14	100±0.18	100±0.11	100±0.25

Test Bacteria-B.s- *Bacillus subtilis*; S.a- *Staphylococcus aureus*; P.a- *Pseudomonas aeruginosa*Test Fungi- A.n- *Aspergillus niger*; A.f-*Aspergillus flavus*; F.o-*Fusarium oxysporum*

Values are the mean of triplicates (Mean ± SE)

Including the diameter of disc (6 mm)

Antibiotic- Gentamycin sulphate (40 mg/ml); Antifungal-Nystatin (20mg/ml)

Table 3: Antibacterial activity of *Hyptis suaveolens* LS (leaf+inflorescence) extracts (1000 µg/ml)

S.No	Plant extracts	Test organisms					
		Test bacteria Zones of Inhibition (mm)			% Growth Inhibition of Test fungi		
		B.s	S.a	P.a	A. n	A. f	F.o
1	Steam distilled	24±0.21	18±0.22	22±0.06	68±0.13	63±0.26	65±0.22
2	Ethanol	21±0.12	14±0.06	19±0.14	48±0.09	45±0.17	43±0.16
3	Methanol	15±0.08	15±0.16	16±0.08	55±0.15	58±0.09	51±0.09
4	Chloroform	19±0.11	16±0.12	15±0.16	62±0.30	60±0.14	56±0.11
5	Antibiotic/ Antifungal	33±0.09	42±0.08	36±0.14	100±0.18	100±0.11	100±0.25

Test Bacteria-B.s- *Bacillus subtilis*; S.a- *Staphylococcus aureus*; P.a- *Pseudomonas aeruginosa*Test Fungi- A.n- *Aspergillus niger*; A.f-*Aspergillus flavus*; F.o-*Fusarium oxysporum*

Values are the mean of triplicates (Mean ± SE)

Including the diameter of disc (6 mm)

Antibiotic- Gentamycin sulphate (40 mg/ml); Antifungal-Nystatin (20mg/ml)

## REFERENCES

1. Asekun, O. T., Ekundayo, O., and Adeniyi, B. A. (1999). Antimicrobial activity of the essential oil of *Hyptis suaveolens* leaves. *Fitoterapia*, 70(4), 440-442.
2. Balouiri, M., Sadiki, M., and Ibsouda, S. K. (2016). Methods for *in vitro* evaluating antimicrobial activity: A review. *Journal of pharmaceutical analysis*, 6(2), 71-79.
3. Bhalodia, N. R., and Shukla, V. J. (2011). Antibacterial and antifungal activities from leaf extracts of *Cassia fistula* l.: An ethnomedicinal plant. *Journal of advanced pharmaceutical technology and research*, 2(2), 104.
4. Camargo, K.C., Batista, L.R., de Souza, P.E., Teixeira, M.L., Sales, T.A., Ferreira, V.R.F., e Nogueira, J.O., Magalhães, M.L., Caetano, A.R.S., Nelson, D.L. and das Graças Cardoso, M., 2017. Antimicrobial Activity of the Essential Oil from *Hyptis carpinifolia* Benth. *American Journal of Plant Sciences*, 8(11):2871.
5. Das, K., Tiwari, R. K. S., and Shrivastava, D. K. (2010). Techniques for evaluation of medicinal plant products as antimicrobial agents: current methods and future trends. *Journal of medicinal plants research*, 4(2), 104-111.
6. Dorman, H. J. D., and Stanley G. Deans. "Antimicrobial agents from plants: antibacterial activity of plant volatile oils." *Journal of applied microbiology* 88, no. 2 (2000): 308-316.
7. Edeoga, H. O., Okwu, D. E., and Mbaebie, B. O. (2005). Phytochemical constituents of some Nigerian medicinal plants. *African journal of biotechnology*, 4(7), 685-688.
8. Kumar, S. N., and Thampi, N. (2015). Phytochemical screening and characterization of the bioactive compounds from the leaves of *Hyptis suaveolens* and *Spathodea campanulata*. *J. Chem. Pharm. Res.*, 7, 840-850.

9. Lewis, K., and Ausubel, F. M. (2006). Prospects for plant-derived antibacterials. *Nature biotechnology*, 24(12), 1504.
10. Mandal, K. C., Dey, S., and Pati, B. R. (2007). Antimicrobial activity of the leaf extracts of *Hyptis suaveolens* (L.) poit. *Indian Journal of Pharmaceutical Sciences*, 69(4), 568.
11. Moreira, A. C. P., Lima, E. D. O., Wanderley, P. A., Carmo, E. S., and Souza, E. L. D. (2010). Chemical composition and antifungal activity of *Hyptis suaveolens* (L.) poit leaves essential oil against *Aspergillus* species. *Brazilian Journal of Microbiology*, 41(1), 28-33.
12. Mozhiyarasi, P., and Anuradha, R. (2016). A study on phytochemical analysis and antimicrobial activity of *Hyptis suaveolens* (L.) Poit. *Journal of Chemical and Pharmaceutical Research*, 8(6), 438-442.
13. Sathish V, Ravichandran VD, Usha Gavani and Paarakh MP. Antimicrobial studies on the extracts of *Cocculus hirsutus* Linn and *Hyptis Suaveolens* Poit. *Ind J Nat Products and Resources* 2010; 1: 49-52.
14. Savithramma, N., Rao, M. L., and Suhrulatha, D. (2011). Screening of medicinal plants for secondary metabolites. *Middle-East Journal of Scientific Research*, 8(3), 579-584.
15. Vincent, J. G., Vincent, H. W., and Morton, J. (1944). Filter Paper Disc Modification of the Oxford Cup Penicillin Determination. *Proceedings of the Society for Experimental Biology and Medicine*, 55(3), 162-164.
16. Zaidan, M. R., Noor Rain, A., Badrul, A. R., Adlin, A., Norazah, A., and Zakiah, I. (2005). *In vitro* screening of five local medicinal plants for antibacterial activity using disc diffusion method. *Tropical Biomedicine*, 22(2), 165-170.

**Video guided and automatic medicine reminding Robot.****Dr.D.Sarala,Head, Department of Physics & Electronics****St.Ann's college for women, Mehdiapatnam, Hyderabad-500028.****Abstract:**

The Corona virus in India, undergoing many **mutations**, has been changing the perspectives of life ,challenging the health care workers, front line warriors and doctors. The scenario of human life has taken a **roller coaster ride** ever since the Covid-19 was diagnosed in our country. Keeping in view the strict **Covid protocols** of **Social distancing**, wearing masks and use of Sanitisers, the present work demonstrates a machine which can store the medicines for a week,would be supplied to the patient at the time set by doctor.This will ensure distancing from patients and nurses won't have to risk their lives to go and give medicine to the infected patient. Once the medicine is on the given rack from where the patient can take it, he/she is alerted via a speaker on the system to take the medicine.

**Keywords: mutations, roller coaster ride, Covid protocols, social distancing.****Objective:**

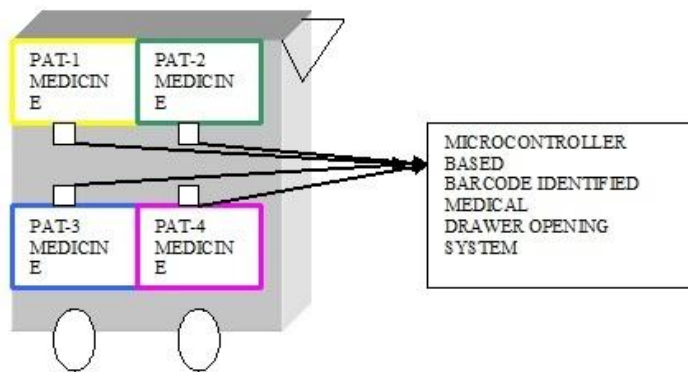
Most often, after the doctor's prescription, the case sheet is prepared by the medical and nursing staff, accordingly the medicines are administered to the in - patients. It is commonly observed that during the period of hospitalisation, the drugs are missed out by the patients at the prescribed time either they are attending the nature calls or fall asleep. This present model gives an indication to the nursing station if the medicine is not dispensed and the robot would re visit the patient. The errors accidental wrong medication were minimised, as the case sheet of the patient would be barcoded and scanned by the robot which would be monitored by the nurses using the ip camera.

**Working principle :**

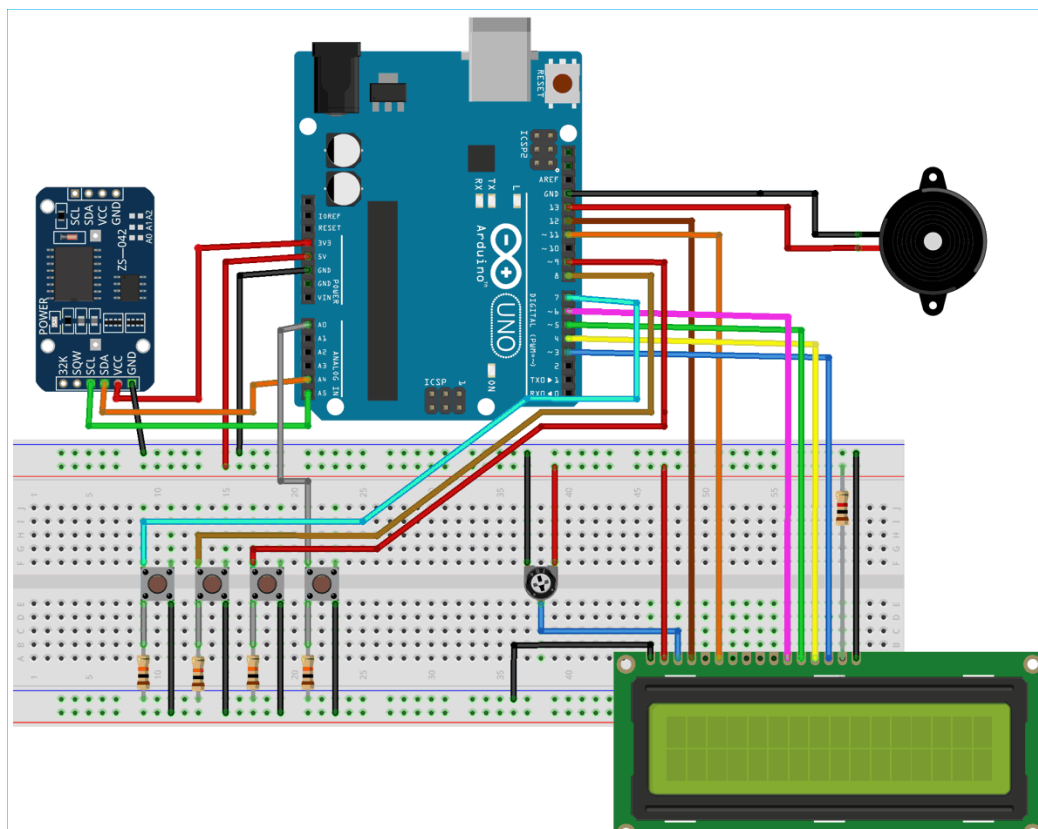
When the machine is first booted, the user is asked to set the dose times for all the doses of each day. If two racks are used, up to 28 Doses can be stored in a single refill. Each day, 4 doses can be delivered according to the time set. The LCD displays upcoming doses. The rotary encoder is used to set the time for each dose. Servo motors are used to deliver the medicine to the rack and clear the rack if the patient misses the dose. The IR sensor is used to detect the time at which the dose is dropped and taken by the patient and the data is stored in SD card in.csv format. Once the dose is delivered, the speaker plays a tone (a custom audio clip which is used to reminding to take the dose, followed by a ringtone) to alert the patient to take the dose.

The data which contains when the patient has taken the dose (or missed) is stored inside an SD card, thus doctors can review it at a later stage to see how a certain medicine dose affected the patient's symptoms. It can be exported as an excel sheet, The first column is of data, second is the day, the next column is of the dose time set by the nurse, and next to is the column which contains the time at which the patient takes the dose. If he/she misses the dose, it is also stored in an SD card.

Also in a ward ,if 20 to 30 patients with various ailments are admitted, it becomes difficult for the ward incharges to guide the nurses and attend the patients. It is very important to give the right medicine to the right patient at the rught time. Different specialists will be prescribing different medicines as and when they visit the patient. Since the amount of dosage varies with patient to patient, there are many incidences reported on the wrong medicines administered or over dose given. This problem was addressed by implementing a bar coded permanent label attached to each bed. As Soon as the trolley reaches the Patient's bed,that Particular drawer lock is opened with the total history and doses Instruction file. Proposed model:



**Schematic:**



Below are the **pin connections** of Arduino with different peripherals

Arduino Pins	Peripheral Pins
● 2	-----> D7 of 16x2 LCD Display
● 3	-----> D6 of 16x2 LCD Display
● 4	-----> D5 of 16x2 LCD Display
● 5	-----> D4 of 16x2 LCD Display
● 7	-----> 3rd push button
● 8	-----> 2nd push button
● 9	-----> 1st push button
● 11	-----> EN pin of 16x2 LCD Display
● 12	-----> RS pin of 16x2 LCD Display
● 13	-----> +Ve Pin of Buzzer and Led
● A0	-----> Stop Push Button
● A4	-----> SDA of DS3231
● A5	-----> SCL of DS3231
● 3.3V	-----> Vcc of DS3231
● Gnd	-----> Gnd

In the present model, the patients are reminded to take the medicine 3 times a day, the interval can be increased , depending on the case.

There is an increased demand for robos to be used in India in the healthcare system due to shortage of personnel, equipment.



### References:

1. <https://pubmed.ncbi.nlm.nih.gov/30136339/>
2. <https://www.livemint.com/news/india/adoption-of-robots-in-india-hospitals-to-grow-during-and-post-covid-11588139029183.html>

3. <https://circuitdigest.com/microcontroller-projects/diy-hand-gesture-controlled-robotic-arm-using-arduino-nano>
4. [https://create.arduino.cc/projecthub/ottoplus/otto-diy-arduino-bluetooth-robot-easy-to-3d-print-33406c?ref=tag&ref\\_id=robotics&offset=35](https://create.arduino.cc/projecthub/ottoplus/otto-diy-arduino-bluetooth-robot-easy-to-3d-print-33406c?ref=tag&ref_id=robotics&offset=35)
5. [https://create.arduino.cc/projecthub/jjj/stair-climbing-robot-ad2203?ref=tag&ref\\_id=robotics&offset=113](https://create.arduino.cc/projecthub/jjj/stair-climbing-robot-ad2203?ref=tag&ref_id=robotics&offset=113)
6. [https://create.arduino.cc/projecthub/msana/a-sudoku-solver-s-robot-fe9e88?ref=tag&ref\\_id=robotics&offset=171](https://create.arduino.cc/projecthub/msana/a-sudoku-solver-s-robot-fe9e88?ref=tag&ref_id=robotics&offset=171)
7. [https://create.arduino.cc/projecthub/mihir-khara/medicine-reminder-and-vending-machine-18f063?ref=tag&ref\\_id=robotics&offset=175](https://create.arduino.cc/projecthub/mihir-khara/medicine-reminder-and-vending-machine-18f063?ref=tag&ref_id=robotics&offset=175)
8. [https://create.arduino.cc/projecthub/ashwini-kumar-sinha/humanoid-a-i-talking-robot-with-arduino-433972?ref=search&ref\\_id=humanoid%20robotics&offset=2](https://create.arduino.cc/projecthub/ashwini-kumar-sinha/humanoid-a-i-talking-robot-with-arduino-433972?ref=search&ref_id=humanoid%20robotics&offset=2)

# Design and Implementation of a portable Arduino based touchless thermometer with distance compensation

**Dr.D.Sarala\*, Dr.Y. Seetha Mahalakshmi\*, W. Jaya Selva Vinita\*, V.SaiPrashanthi\***

*\*Department of Physics and Electronics, St. Ann's college for Women, Mehdiapatnam, Hyderabad, Telangana*

## **Abstract**

*Monitoring the human body temperature has become mandatory during the ongoing COVID-19 pandemic situation. With the constant rise in the case load, keeping the safety of the health care personnel and the elderly, contact-less devices rendering precise values are in great demand. Recent technological advancements have made infrared (IR) thermometers, the choice for touch less screening of multiple individuals. Even then the measurement accuracy of such thermometers is affected by many factors which may include the range of measurement from the individual's site, the location of the thermometer near forehead, wrist or ear and the presence of ambient temperature. Considering these factors, we describe the assembly of an Arduino-based digital IR thermometer with distance correction using the MLX90614 IR thermometer and HC-SR04 ultrasonic sensors and a 16 \*2 LCD display with both ambient and volunteers' temperature being displayed. Also, the distance compensation methods are incorporated in the program. This would ensure accurate readings and measurements for a final assembled digital IR thermometer.*

**Keywords:** Infrared, Ultrasonic sensor, Arduino nanoSKU 648418, touchless thermometer, HC-SR04, MLX90614, 16\*2 LCD.

## **Introduction**

Fever is one of the common symptoms [1] of COVID-19, but due to its contagious effect, its measurement methods become a challenging task to the medical community. Hence it is important to perform the temperature detection of patients fast and possibly without any physical contact, and without a human intervention. Besides, the epidemiological and laboratory researches have revealed that ambient temperature could possibly affect the existence and spread of Corona virus [2], so that a continuous monitoring of temperature, which includes both ambient and body temperature, is an essential parameter to be performed in the contrast of COVID-19.

The adoption of thermo graphic systems in the framework of pandemic situations, during the screening process for rapid temperature measurements of many individuals quickly and safely without allowing the thermometer to be a vector of pathogen transfer are crucial, thus making contact infeasible, ruling out the measurement sites.

Early methods of measuring body core temperature utilizing contact mercury thermometers are replaced by the safer and more convenient electronic thermometers at the sublingual, armpits, ear canals, and in some rare occasions, the rectum and auxiliary for



accuracy [3]. Many of these surface measurement sites, specifically the temporal and central forehead, reflect lower readings than internal sites such as the tympanic temperature readings, the current gold standard to represent the body core temperature [3], especially given the impracticality of rectal/anal temperature takings.

Infrared (IR) thermometers would fulfil this gap by measuring the surface temperature without direct contact, which is through detecting the amount of thermal or black-body radiation emitted by the object. Additionally, these thermometers are now commonly used in clinical practices [4], as well as routinely during the pandemic for self-monitoring and screening at the entrances of public places.

Thus the recent advancements made in infrared (IR) thermometers became a reliable choice for contactless screening of multiple individuals. Though the measurement accuracy of such thermometers is affected by many factors including the volunteers' forehead or hand or the ear and the distance range from the point of measurement. Considering these issues, an Arduino-based digital IR thermometer with range consideration using the MLX906149 [5] IR thermometer and HC-SR04[6] ultrasonic sensors with an LCD display is demonstrated in the present paper.

Coupled with some analysis of measurement sites, we also found ways to programme compensation methods for the final assembled digital IR thermometer to provide more accurate readings and measurements. Experiments were conducted to validate distance adjustments considered in the software, and also the effects of measurements on different measurement sites like fore head, right ear and wrist of the volunteers.

## 2. Materials and Methods

### 2.1. Components and Specifications

Arduino Nano (SKU 648418, Italy), ultrasonic sensor (HC-SR04) [6], infrared sensor (MLX90614) [5], and 16 \* 2 display were used. A factorycalibrated MLX90614 infrared sensor, suitable for a wide range of temperatures between- 40 °to 85 ° C for the ambient temperature and 70 to 1030 °C for the target object temperature, provided the average temperature of all objects within sweep angle of the sensor, as well as a standard accuracy of 0.5 °C around room temperature. The Ultrasonic Sensor HC-SR04 emits a 40 kHz ultrasound and computes the distance based on the time taken to detect the ultrasound wave reflected off an object. A 16\*2 mono colour character LED display is incorporated to observe the value.

### 2.2. Assembly of touch less Thermometer

The design and development of the thermometer in this sensor were imported and modified from online instructions [7] It consists of hardware design, mechanical assembly, the electronic circuit, the microcontroller programming using arduino nano.

#### 2.2.1. Physical Assembly

Figure 1a shows the physical mount of the touchless thermometer along with the components: IR sensor, ultrasound sensor, Arduino Nano and 16 \* 2 LCD display. It also

comprises of the battery holder and a reset button .The circuit design is implemented in ORCAD and the arduino nano is programmed in embedded C using the Arduino IDE 1.8.13

### **2.2.2. Circuitry Design and Implementation**

The Arduino Nano [8] microcontroller, in which the copper wires from the sensor pins of the ultrasonic sensor(Figure 2a), IR sensor(Figure 2b), LCD (Figure 2c) and reset button were soldered with a 9 V battery supplying 3.3 to 5 V to the circuit (**Figure 1a**).

### **2.3. Programming Arrangement**

The Arduino IDE 1.8.13 software is used to program the microcontroller. After every press of the reset button the sensor starts measurement within 2–4 cm from the site of measurement like forehead, ear or wrist. Ten readings from the ambient and surface body temperature are made and the average is shown. The ultrasonic sensor detects the distance from the target area and calculates the average of ten readings. With the inputs of distance and temperature to the algorithm, the compensated reading from the algorithm would be displayed on the mono colour 16 \* 2 LCD display

Compensation adjustment equation was derived from the regression analysis of the relationship between the oral temperature values and the measured values. Compensated values by the IR thermometer were used as the dependent value, while the measurement values by the IR thermometer and ambient temperature were each viewed as independent variables.

### **2.4 Sensor considerations**

#### **2.4.1. Infrared Sensor**

For precise measurement of the absolute temperature of the spot, the device temperature needs to be kept small with a stable ambient temperature. To compensate the proximity effects, a distance-to-site ratio (D/T ratio) is built in the algorithm. Specifically, the area measured increases as the distance increases. The IR temperature sensor MLX90614 used in this project has a sweep angle of 80 degrees as specified by the manufacturer. This translates to a D/T ratio of 1:1.60. Setting the average height of the position of the measuring unit to be at 59 mm as the condition [9]. For a maximum horizontal distance the IR temperature sensor can accurately measure the temperature of the spot approximately at 4 cm. Beyond this distance, flanking areas of the site of measurements would also be sensed so that the accuracy may get affected.

#### **2.4.2. Ultrasound Sensor**

The ultrasound sensor consists of a transmitter sending an ultrasound wave and a receiver detecting the reflected wave by the targeted physical object. The time taken between the transmission and detected wave is registered for the calculation of the distance from the speed of ultrasound waves at 330 m/s by the programmed Arduino Nano.

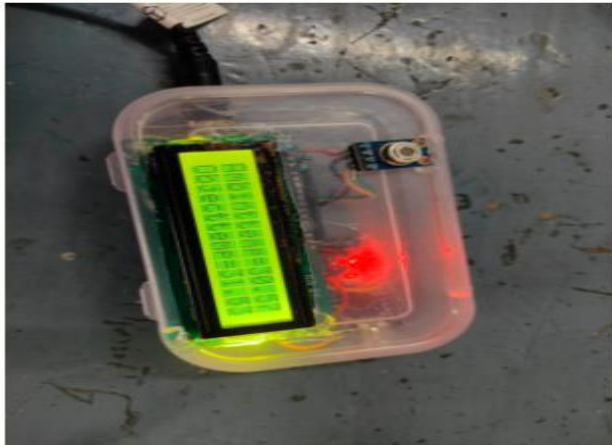


Figure 1a the physical picture of the touch less Thermometer

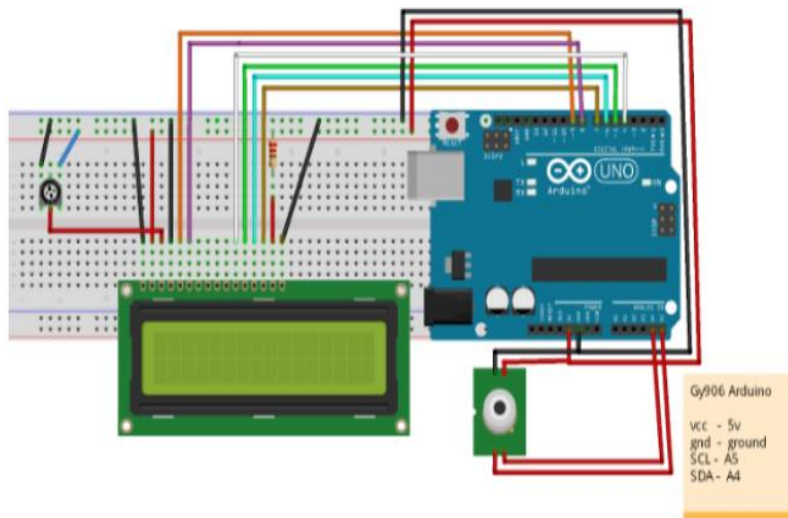


Figure 1b Schematic of the assembled digital IR thermometer consisting of: Ultrasonic sensor HC-SR04, reset button, Arduino Nano board, LCD display and IR temperature sensor MLX90614.

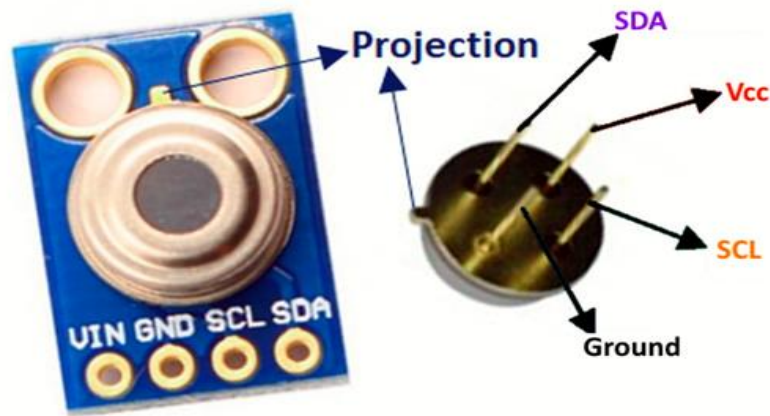


Figure 2a Ultrasonic sensor HC-SR04 component

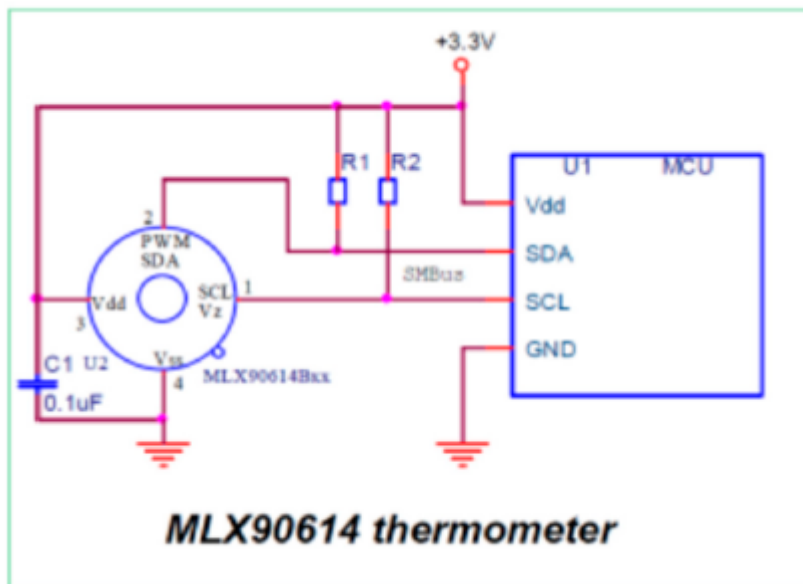


Figure 2b Infrared sensor MLX90614

### 3 Experimental section

The experiment is performed on 6 volunteers between the age limit of 20 to 40 years in order to study the accuracy of the unit. The observations were recorded in an air-conditioned environment of 20 to 24 °C for a relatively constant ambient temperature. Volunteers were allowed to relax for a time of 10 min before making their temperature measurements. A sterilized Omron digital thermometer MC-343F was used to measure the oral temperatures, which was also set as the target point for compensation adjustments.

In the first experiment, the IR thermometer was used to measure the volunteers' temperatures at three different body locations viz. forehead, wrist and the right ear and at varying distances from the forehead (2–4 cm, at 0.5 cm step measurements) as shown in

figure 3a and 3b . The range of 2–4 cm is based on the minimum and maximum allowable horizontal distance that the IR temperature sensor can accurately measure (2–4 cm) as per the manufacturer’s specifications. The IR and oral temperature readings from the first experiment set were used for compensation adjustments and stored. Then, the calibrated IR thermometer was used to measure the forehead temperatures of volunteers and test its performance and deviation from the oral temperature. Data from each experiment were plotted with the distance against the temperature as shown in figure 4a,4b and 4c.

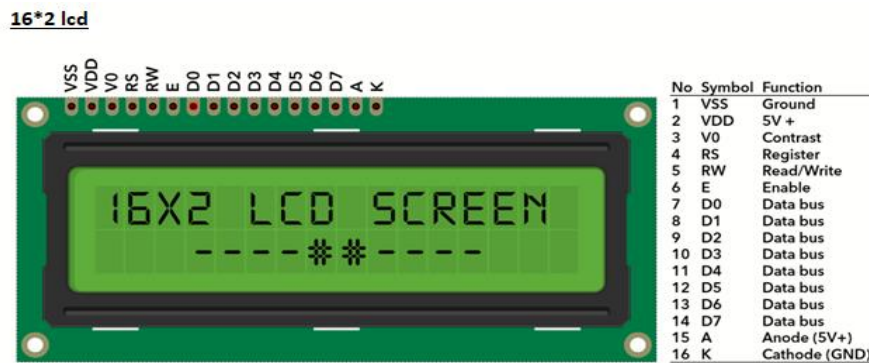


Figure 2c16 \*2 LCD display

### 3.1. Temperature measurement on the Forehead, wrist and right ear

Although not visible to the human eye, all objects emit infrared light rays and the concentration varies depending on temperature. By detecting the IR rays, we can perceive the temperature range. The MLX90614 thermometer sensor works using this principle.

MLX90614 is a powerful infrared sensing device with a very low noise amplifier and a 17-bit ADC. It enables high accuracy and resolution for the thermometer. The best part about the MLX90614 is it comes calibrated with a digital SMBus from the factory. This means that it will give an output with a high resolution of 0.02°C and can continuously transfer the measured temperature in the range of -20 to 120°C.

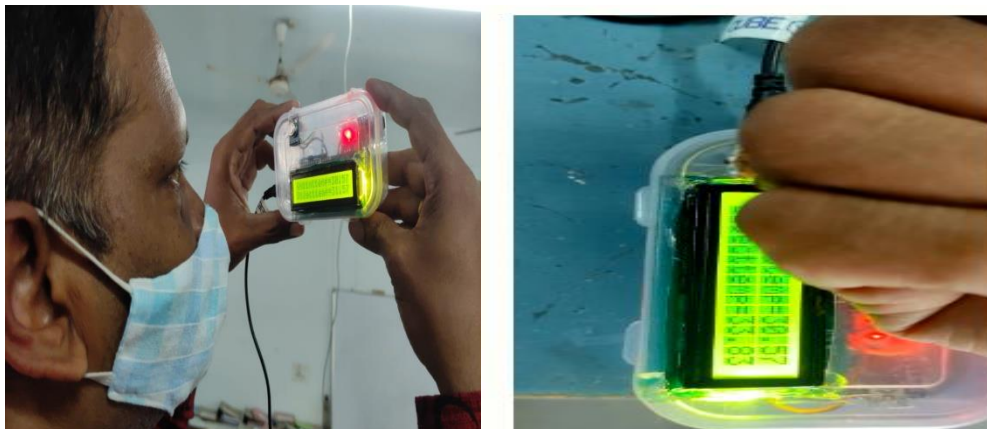


Figure 3a Volunteer measuring the forehead temperature Figure 1b Volunteer measuring the wrist temperature

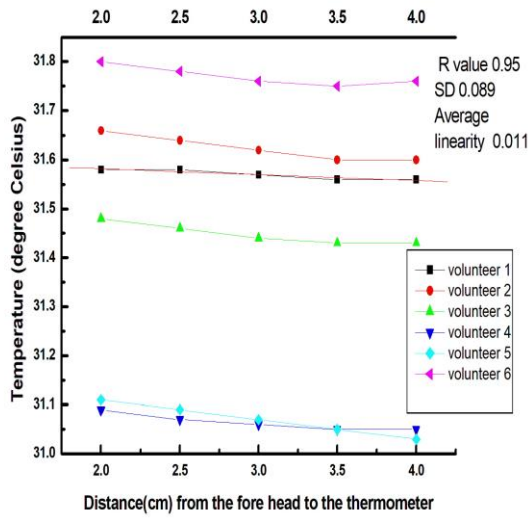


Figure 2a Graph plotted between distance vs. fore head temperature of six volunteers

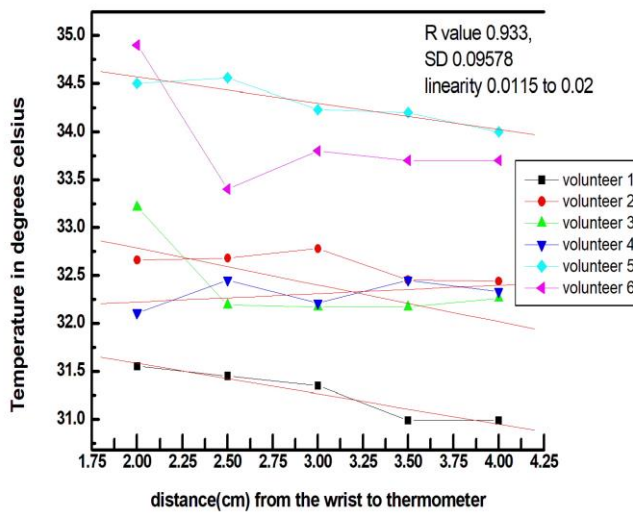


Figure 4b Graph plotted between distance vs wrist temperature of 6 volunteers

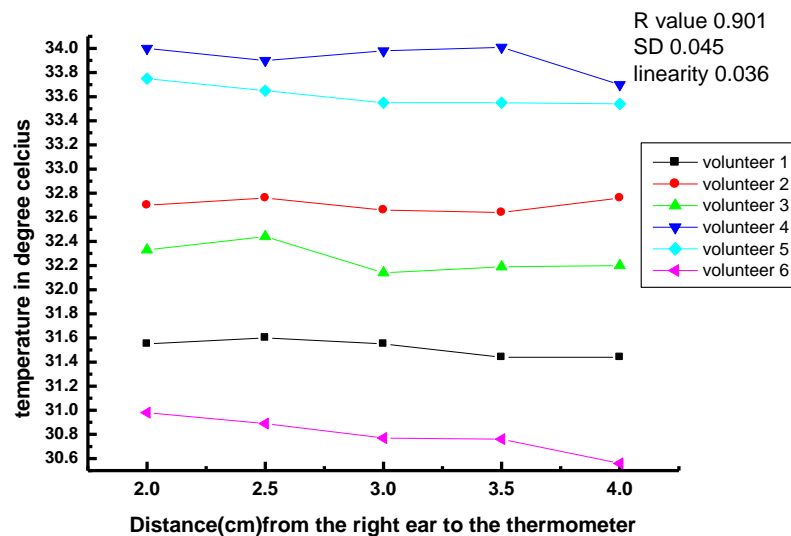


Figure 4c Graph plotted between distance vs. right ear temperature-of 6 volunteers

## Discussion

The touchless IR thermometer recorded an average temperature within  $0.3^{\circ}$  of the volunteers' oral temperature. As measurements for oral temperature are widely used to non-invasively measure the body temperature, measurements of the forehead, wrist and right ear temperature with varying distances showed a regression of about 0.95 to 0.901 with a linearity of 0.01 to 0.03 and hence can be used to establish a threshold in the screening for fever. The IR thermometer obtained a better precision compared to the alternative and more expensive non-contact IR devices and has improved distance compensation. In a separate study, tympanic and forehead temperatures taken by a BRAUN IRT-3020 had an error range of  $\pm 0.286^{\circ}$  and  $\pm 0.392^{\circ}$  C [10]. Another study showed tympanic and forehead temperature errors of  $\pm 0.37^{\circ}$  C and  $\pm 0.36^{\circ}$  C respectively [11]. However, other contact devices such as the rectal thermometer, with a small error range of  $0.05^{\circ}$  C [12] outperformed the current improved thermometer. Still, our improved device costs only a fraction of commercial IR thermometers and was sufficiently accurate to be considered as a low cost alternative (~USD 5) to the current entry level IR thermometers (>USD 80) in the market. This non-contact device is more convenient than the tympanic or rectal thermometers.

## Conclusions

Forehead temperature measurements using an IR thermometer play an important role of rapidly screening for fever to identify the infected individual. The performance and precision of an IR thermometer for forehead temperature screening were studied together with the design and implementation of an improved infrared temperature sensor-based system with distance sensing capabilities. It is observed that the measured temperatures were well within the  $0.3^{\circ}$  C variation of their oral temperature over the distance of 2–4 cm, resulting in a similar performance to commercial thermometers. While minimal, temperature differences between the actual temperature and the one

measured with the touch less thermometer at the forehead and the wrist or the right ear with a programmed software compensation in the distance of the site we conclude the validity of the human temperature measurements safely and effectively without a manual operator.

## References

1. Fulbrook, P. Core temperature measurement: A comparison of rectal, axillary and pulmonary artery blood temperature. *Intensive Crit. Care Nurs.* **1993**, 9, 217–225. [CrossRef]
2. Xie, J.; Zhu, Y. Association between ambient temperature and COVID-19 infection in 122 cities from China. *Sci. Total Environ.* **2020**, 724, 1–5. [CrossRef] [PubMed]
3. Mogensen, C.B.; Wittenhoff, L.; Fruerhøj, G.; Hansen, S. Forehead or ear temperature measurement cannot replace rectal measurements, except for screening purposes. *BMC Pediatrics* **2018**, 18, 15. [CrossRef]
4. Non-Contact Temperature Assessment Devices during the COVID-19 Pandemic. Available online: <https://www.fda.gov/medical-devices/coronavirus-covid-19-and-medical-devices/non-contacttemperature-assessment-devices-during-covid-19-pandemic> (accessed on 5 September 2020).
5. Melexis. Datasheet for MLX90614. Available online: [https://components101.com/sites/default/files/component\\_datasheet/MLX90614-Datasheet.pdf](https://components101.com/sites/default/files/component_datasheet/MLX90614-Datasheet.pdf) (accessed on 30 October 2020).
6. ElecFreaks. Ultrasonic Ranging Module HC—SR04. Available online: <https://cdn.sparkfun.com/datasheets/Sensors/Proximity/HCSR04.pdf> (accessed on 23 October 2020).
7. Raj, A. Make a Non-Contact Infrared Thermometer with MLX90614 IR Temperature Sensor. Available online: <https://circuitdigest.com/microcontroller-projects/ir-thermometer-using-arduino-and-ir-temperature-sensor> (accessed on 22 May 2021).
8. Arduino. Arduino Nano Datasheet. Available online: <http://www.farnell.com/datasheets/1682238.pdf> (accessed on 23 October 2020).
9. Sirinturk, S.; Govsa, F.; Pinar, Y.; Ozer, M.A. Study of frontal hairline patterns for natural design and restoration. *Surg. Radiol. Anat.* **2017**, 39, 679–684. [CrossRef]
10. Chen, H.-Y.; Chen, A.; Chen, C. Investigation of the Impact of Infrared Sensors on Core Body Temperature Monitoring by Comparing Measurement Sites. *Sensors* **2020**, 20, 2885. [CrossRef]
11. Liu, C.C.; Chang, R.E.; Chang, W.C. Limitations of forehead infrared body temperature detection for fever screening for severe acute respiratory syndrome. *Infect. Control. Hosp. Epidemiol.* **2004**, 25, 1109–1111. [CrossRef]



12. *Jensen, B.N.; Jensen, F.S.; Madsen, S.N.; Løssl, K. Accuracy of digital tympanic, oral, axillary, and rectal thermometers compared with standard rectal mercury thermometers. Eur. J. Surg. 2000, 166, 848–851. [CrossRef] [PubMed]*



# INTERNATIONAL JOURNAL OF CREATIVE RESEARCH THOUGHTS (IJCRT)

An International Open Access, Peer-reviewed, Refereed Journal

## Smart Learning- Role of IoT in Modern Education Systems

K.Rajeswari <sup>1</sup>, G. Nirmala Joycee <sup>2</sup>,

<sup>1</sup>Lecturer, Department of Computer Science (UG)

<sup>2</sup> Assistant Professor, Department of Computer Science (PG)

<sup>1,2</sup> St. Ann's College for Women, Mehdipatnam, Hyderabad.

### Abstract

In today's generation internet plays a vital role both in learning and teaching. IoT is the new era of computing Technology. It is an ecosystem of connected physical objects that are able to accessible through internet. IoT can change the educational system into a better understanding way. IoT is used in institutions to enhance learning outcomes by providing more affluent learning experiences, , and gaining real-time experience to improved operational efficiency actionable insight into student performance. By IoT in higher education its potentially increases benefits and reducing the risks involved in it. Without human assist the IoT can facilitates the devices/objects to identify and understand the situation. These devices/objects can represent themselves digitally and these devices can be to control from anywhere and anytime. The new wave of changes has started from IoT. It gives massive volume of connectivity. The Internet of things expected to give strong impact on various areas of life including healthcare, Entertainment, education, Business, Smart Home, Smart Campus and Smart City etc. IoT not only expected to give great impact but also expected to give new opportunities and possibilities for the improvement on the various area. The collaboration between the people and Technology are very power full. This paper provides the future of IoT in the higher education during the next few decades, which can be offered by a number of research organizations and enterprises. On the other hand, IoT brings tremendous challenges in higher education. Hence, this paper presents the importance and challenges of IoT in higher education.

**Keywords:** Internet of Things, enhanced learning, tremendous challenges, affluent

## 1. Introduction

The Internet and its associated services and applications have strongly developed and influenced communication, it gathers information and marketing across the world via websites, blogs, e-mail and social networks. The changes in education has been registered major, especially since 2000, towards a new orientation of teenagers' in education, reflected through online documentation, and implementation of projects in virtual teams, and in online tutorials and much more. In 1999, there emerged a new term in the field, Internet of Things (IoT). The interaction between objects, people, internet and environment is called as "IoT". We live in 21st century where the Information and communication Technology (ICT) cannot detach from human. The ICT plays a vital role in current education system. With the support of IoT education system can enhance the learning process. With the help of IoT can bring the live classroom, where student can observe, understand and interact easily. The impact of ICT has changed the traditional education system towards significantly improved modern and quality education systems at various levels of learning. IOT has become the most essential thing in every human's life. The main concept of connected devices or things has given a new version to Internet, that it anything, anywhere can get connected with the Internet and becomes 'Smart.' Connected devices can communicate with each other and share information which can then further be processed to take some decisions. According to Mark Weiser, "The most profound technologies are those that disappear. They weave themselves into the fabric of everyday life until they are indistinguishable from it" [1]. Kevin Ashton was the first to use the term Internet of Things in 1999. Early the beginning of Internet of Things (IoT) many researchers have tried to define IoT in various ways like Internet of Everything, Internet of Anything, Internet of People, Internet of Signs, Internet of Services, Internet of Data or Internet of Processes [2]. According to [3], IoT represents 'anything at all, depending on requirements.' Cisco defines IoT as a network of connected physical objects. Cisco also uses the term Internet of Everything for both physical and virtual objects. Cisco states that "IoE brings together people, process, data, and things to make networked connections more relevant and valuable than ever before—turning information into actions that create new capabilities, richer experiences, and unprecedented economic opportunities for businesses, individuals, and countries."

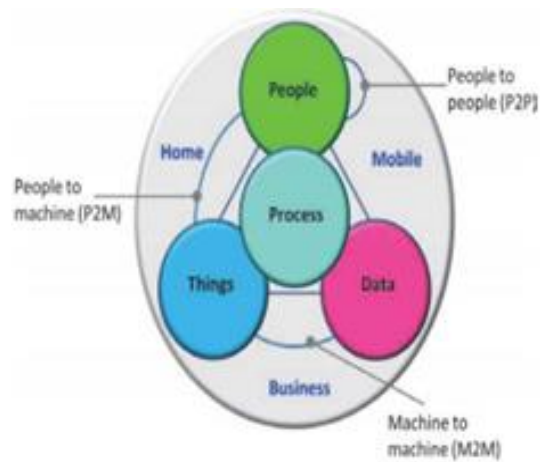


Fig:1 Internet of everything

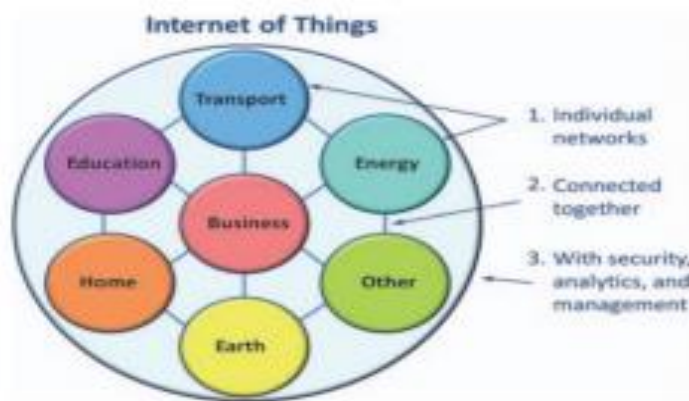


Fig:2 Using internet in all different sectors

According to Gartner's forecast, 20.8 billion new things will be connected by 2020. According to Machine Research, the growth of IoT connections is : from 6 billion in 2015 to 27 billion in 2025. The number of cellular IoT connections will be 2.2 billion, and 45% of these will be in connected cars. The revenue forecast of IoT in 2025 is 3 trillion US\$. IoT will also generate over two zettabytes of data, generally from consumer electronic devices.



Fig: 3 Five predictions of IOT till 2025

## Previous Studies

**2.1 The Traditional Education:** Traditional classroom education has been around for decades and almost all members of society, and for many centuries using it. Class room education continues to be an important way of learning, and there are many benefits that accompany this method of education. In a traditional education, students are able to interact with their teachers and personally.

### Online Education:

The results of this study indicated that the participants were aware of the facilities of using e-books and they were content with the facilities of usage. The main resource of multiplying education is the teachers therefore; the teachers should build a relationship with technology and should use it in a sufficient level in their current and future classes. Moreover, each teacher should follow technology and apply it in their course. Therefore, the design of the digital electronic book is prepared to be adaptive for this generation of students because in general, they are digital readers.

## 2. Objective of the study

The objective of this study is derived as below,

- To study the need of IoT in Education.
- To know the Technology enhanced learning
- To understand the Internet of Things

- Advantages of IoT in Modern Education

### 3. Research Methodology

This research was carried out based on the secondary data and the data. The data used for this research is descriptive and qualitative from secondary sources. This data has been filtered and analyzed in a structured analytical format. Since the topic is evolutionary and is subject to fast changes, only the qualitative data updated from time to time is used. The main source of data collection is wiki, websites, blogs, YouTube, books, articles and journals.

#### 2.1 To study the need of IoT in Education.

##### Individualization

The Student can more and inside based on the interest with personalized learning pattern and this will lead much more opportunity to learn with complete understanding the subject.

- **Smart Campus using IoT**

In general now a day's all universities, colleges and schools are connected with internet of things. The concept of smart campus involves with the intellectual environment equipped with fully sophisticated and installed with advanced technology smart things and aids. The smart classroom occupied with the set of smart things such as LCD Projector, Microphone, Speaker, cameras, smart board / Interactive board, Visualizer, Virtual classroom, Google Classroom which can be used for the ICT based enabled learning. A smart campus is a collection of smart multiple things [5]. The smart campus may include the following things.

- IoT based Classroom
- IoT based Laboratories
- Possibilities of E-Learning
- Smart Library
- Smart Attendance system for faculty and Student
- Smart canteen
- Smart office

In addition to smart parking, smart tracking of student, wi-fi enabled campus. The purpose of the smart campus is making the environment user friendly.

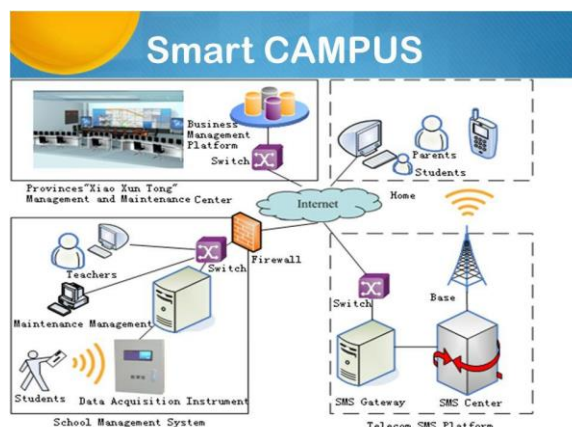


Fig :4 IOT in Smart campus

## 2.2 To know the Technology enhanced learning

- **IoT based Smart Classroom:**

The use of IoT devices for teaching and learning purposes is a top trend among institutions across the world which provides a new and innovative approach to education and classroom management [5]. Through smart classroom faculty can explain the subject in a more reality based and make the student to understand easily.

In the era of Digital technology, the rapid evaluation of Information and communication technology has created a new paradigm of internet known as Internet of Things. The Internet of Things changed the way to communicate with people and object in different manner. This has created the new form of communication between the teacher and student to allow them to improve the teaching and learning process. ICT have a great power to improve the quality outcomes of teaching learning.

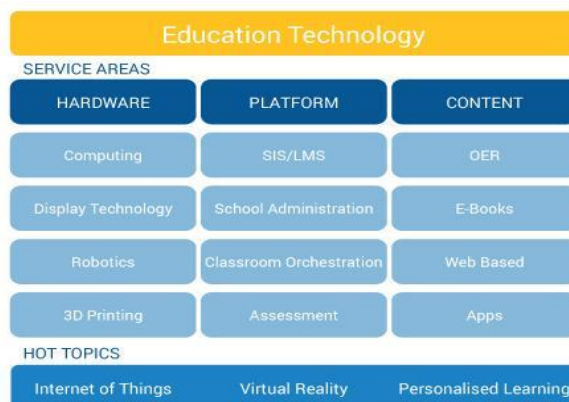


Fig:5 Educational Technology Market Research[8].

- **Advantage of Smart Classroom:**

Smart classroom plays a significant role in the student life. Smart classroom helps to transform the traditional education into modern education, with the help of smart education student can learn from anywhere, anytime anything and everything. The level of connectivity offered by the internet is beyond belief. It helps students to enrich the learning process all over the world. This offers to improve the quality of education and academic achievements. IoT enables to break the barrier of learning in the classroom. IoT give the platform to access globally. Some of the common tools are used in the classroom are.

- Smart board / Interactive white board
- LCD Projectors
- Lap tops and Tablet Pc
- E-Library
- ID Cards for Student and Faculty
- CC Cameras for security
- Attendance tracking systems
- Printer and Scanners
- Speakers and Mikes
- Media Center
- Environment friendly
- Advanced teaching and learning experience
- Easy maintenance



Fig:6 IOT in smart class rooms



Smart things are helps the teacher to explain the class in more interactive and more realistic way. The student can able to understand the concept very easily and put more attention with the help of the above mentioned smart devices in the Smart classroom. The flow of connected technology means professors and teachers could make grades faster. Their checking/grading also would be eased, less prejudiced and more efficient. When educators have devices connected to the cloud, they would be in better connect. Thus, tutor/ teachers could see which student requires more concern and focus. Other processes, with smart technology helps us in making lesson plans, adjusting schedules and many more. While the task is to connect over smart devices, teachers are able to focus more on their teaching and research.

- **IoT based Research:**

Research is a one of the emergent technology in the education system. Research gives the real opportunity to upgrade knowledge. Research will give the opportunity to know the concept very well. Internet of Things will give the more opportunity and it helps everyone to understand the concept and we come to know the opinion of others in the world. IoT will give the benefit of the wider research area and it will lead a valuable innovation to the world.



Fig :7 IOT in research

- **Smart Attendance System – Biometric Systems:**

Regularly taking attendance is a big task in the classroom. To overcome that we have introduced a new technology with the help of iot that is radio frequency identification (RFI) which will substantially help, biometric fingerprint sensor and password based technologies are integrated to develop a cost effective, reliable attendance management system [6]. Smart attendance system and biometric system are the most secured things, also it is very difficult to manipulate the data and complete integrity proof on the data and information.

The internet enabled radio frequency identification will enable to notify the assigned concerns on defined interval or customized periods.

The recorded data from the biometric can be stored and retrieved any time and each educational establishment wants it to be secure and endangered from any unsolicited visitors. However the specialists that are involved in security guard, they cannot monitor every corner of the facility. That is why IoT can help administration control. Facial recognition systems helps us to identify faces by scanning them and to be saved in data base. That is how the Internet of Things works and how it may be beneficial.



Fig:8 IOT used for security

- **IoT based Feedback Form:**

Google Form is a one of the platform to access the student with the help of the technology .It is a one of the easy way to take the feedback using the internet of things. Google Form is a open source available for everyone. Using this form student can answer the query from everywhere and any time.24/7 available in the internet.

- **IoT based Google Classroom:**

Google classroom is free. Google classroom can be accessed from any computer or mobile device via Google chrome. It is a blended platform with lot of benefits available for both faculty and students. Google classroom is a one of the online learning system, using this we can send, announce or pass any kind of information to the everyone. It has lot of benefits such as accessibility, Time saving, Communication, paperless transaction, collaboration, Data Analysis and feedback [7] etc. We don't need any papers to do assignments, as we can save our data through google classroom. The Internet of Things impacts education in a lot of ways. It is this asset

intellect, which enable institutions to make more informed decisions, in an attempt to improve operational efficiency, learning experience and campus security

### **2.3 To understand the Internet of Things**

As per the above discussion we can able to understand the value of Internet of Things in the society especially in the education system. IoT promotes a heightened level of awareness about our world [13]. IoT enables numerous applications ranging from the micro to macro and from the insignificant to the serious [13]. IoT plays a significant role in the field of education. IoT plays a major role everywhere in the society. The era of the technology our dream becomes true. IoT support the way to build the flexibility of the system and cost effective way. With the help of IOT we can transfer several areas in everyday life .Although it seem to be good in education.

Software development education is widely offered by most colleges and universities, offering fully online degree programs as well as the traditional on campus programs, which is helping the rural people who is far away from the university access get benefited.

### **2.4 Advantages of IoT in Modern Education**

Today's more and more tutors and educators are using the internet for the betterment of the education systems. The students are the main chain links of the education process. Internet of thing is a new system introduced to provide wide connectivity between the people and the technology where we cannot imagined before. The scope of learning is enormous with the help of the IOT based devices like Tablet, Laptops, Mobile Phones, Desktops, etc.It helps the students as follows.

#### **Individual learning**

Interactive based learning

- Increase the curiosity of learning
- Learn everywhere
- To learn and understand the things in easy and better way.
- To validate the information by interpret the data from various sources.

- Improve the learning Process
- No more loss of information
- Create the curiosity towards the subject
- The growth of engagement
- To improve the results
- Smart way to monitor the students

**Conclusion:**

The future of IoT is massively unlimited and will be improve a quality of education system because of advances in technology, though the IoT contain plenty of information ,however the user can get the relevant data and information by data interpreting, The Wi-Fi as made it possible to connect people and machines. IoT can change our whole world within few years.Strongly believed that the use of technology especially the era of IoT transform the educational environment towards the modern education [9].With the help of IoT we can collect the lot of data, that data we can convert to Information . These kinds of Information are going to help in the society for everybody everywhere.the students who is not able to attend the regular physical classes ,can be highly benefited on the learning progress ,because of the wider education by IoT the quality of human will be improved and the poverty of the nation subsequently improved .

**Reference:**

1. <http://ijsetr.org/wp-content/uploads/2016/02/IJSETR-VOL-5-ISSUE-2-472-476.pdf>
2. <https://www.happiestminds.com/Insights/internet-of-things/>
3. [https://en.wikipedia.org/wiki/Internet\\_of\\_things](https://en.wikipedia.org/wiki/Internet_of_things)
4. <http://journals.sfu.ca/onlinejour/index.php/i-jep/article/viewFile/7187/4604>
5. <https://www.forbes.com/sites/jacobmorgan/2014/05/13/simple-explanation-internet-things-that-anyone-can-understand/#406c48d51d09>
6. [https://www.researchgate.net/publication/323425616\\_IOT\\_CONCEPT\\_APPLICATION\\_IN\\_EDUCATIONAL\\_SECTOR\\_USING\\_COLLABORATION](https://www.researchgate.net/publication/323425616_IOT_CONCEPT_APPLICATION_IN_EDUCATIONAL_SECTOR_USING_COLLABORATION)
7. [http://paper.ijcsns.org/07\\_book/201705/20170520.pdf](http://paper.ijcsns.org/07_book/201705/20170520.pdf)
8. <https://ieeexplore.ieee.org/document/8249106/>
9. <https://www.thetechadvocate.org/10-benefits-of-google-classroom-integration/>
10. <http://journals.sfu.ca/onlinejour/index.php/i-jep/article/viewFile/7187/4604>
11. <https://medium.com/@TeksunGroup/importance-of-internet-of-things-iot-in-our-liveb71e53d50a44>
12. <https://www.ariasystems.com/blog/internet-things-important/>
13. <https://www.cleveroad.com/blog/iot-in-education-main-solutions-iot-brings-to-educational-sector>

# Enchaining Oral Competence Of Undergraduate Students: English Language Skills For Industry 4.0

Thummaloor Sreevani<sup>1</sup>, Dr.Mutyala Suresh<sup>2</sup>

<sup>1</sup>Research scholar in ELT, Dept. of English, KoneruLakshmaih Education Foundation  
(Deemed to be University), Vaddeswaram, Guntur District, A.P., India &

Lecturer, Dept. of English, St.Ann'sCollege For Women, Hyderabad, TS, India.

<sup>2</sup>Asso. Professor, Dept of English, KoneruLakshmaih Education Foundation(Deemed to be  
University), Vaddeswaram, Guntur District, A.P., India.

Email:<sup>1</sup>sreevani.vips@gmail.com, <sup>2</sup>msphd@kluniversity.in

## Abstract

English language competencies are essential for career readiness and advancement. English, being one of the popular world languages, is used for global communication and is commonly considered as an official language in many countries. In India, undergraduate students need English language competence to set a career in the global job market. At present, the fourth Industrial Revolution introduced innovative technological advancement in the industry. Thus, there is a great demand for professionals with new technologies and language competencies in this Industry 4.0. To possess these new career opportunities, undergraduate students need to upgrade their technical skills as well as English language competencies. Educators and Industry need to build the bridge for the students by providing Industry4.0 career readiness training programs. Here is a tremendous need for analyzing and mapping technical skills as well as the English language competencies of Undergraduate students. The present study is to analyse the need for oral Communicative Competence in the English Language of 120 final year undergraduate students in Hyderabad for Industry 4.0 Career Readiness. The researcher designed a specific need-based intensive course and the randomly selected group underwent training for 2 weeks. As a result, students developed commutative competency in the English language for Industry 4.0 career readiness.

**Keywords:** Oral Communicative Competence in English, Undergraduates, Industry4.0, Career Readiness, experimental study.

## 1. INTRODUCTION

English as an International language has a significant role in this world of globalization. Warschauer (2000) mentioned that globalization and English as an International language gained prominence together in the history of the world. The English language is used widely to establish international commerce, cultures, and communication in the process of globalization. Neeley (2014) quoted that English became a global language for business and was mandated as a common corporate language in many multinational companies around the world. English is commonly considered as an official language in many countries.

### *Evolution of English language and Industrial Revolutions*

Five hundred years ago, the English language was spoken mostly in the British Isles. Annika Lindok (2015) stated that In the early 18th century, the first industrial revolution brought the evolution of the English language. In fact, the English language is used to show to the world what was made of industrialized societies. History has proven that innovation in Technology and industry always influenced the English language. Revolution in the industry impacted the use of English and communication among people worldwide. The invention of the internet made English a global language (Crystal, 2012). English language learners are increasing due to the ongoing demand for this language in the competitive job market in the industry. According to the British council report at present 1.75 billion people are learning the English language across the globe and the number will increase up to 2 billions very soon.

### *Industry 4.0*

The initiation of the Fourth Industrial Revolution with modern technologies like Data Science, Artificial Intelligence (AI), Machine Learning(ML), Cyber Security, Internet of Things (IoT) Augment Reality (AR) and Virtual Reality (VR) spread all over the countries. The invention of the water and steam engine and Mechanical production in the year 1784 brought the first Industrial Revolution. Electrical energy and mass production existed in the Second Industrial Revolution in the year 1923. In the year 1969, the third Industrial Revolution was introduced by electronics and IT for higher automated production. From the year 2014, innovations of manufacturing logistics and revolutionizing traditional manufacturing processes inducted to the Fourth Industrial Revolution is addressed as Industry 4.0. Firstly, It started in Germany as a brainchild. Next, adopted by the USA, France, and Japan. Consequently, it influenced BRICS (Brazil, Russia, India, China, and South Africa) Nations as well as the whole world. According to Gilchrist, A (2016) "From a financial perspective, one market research report forecasts growth of \$ 151.01 billion U.S. by 2020, at a CAGR (Compound annual growth rate) of 8.03% between 2015 and 2020" (p.02).

According to new research Benefits of Industry 4.0 are 'Cost Optimization, New Opportunities, Greater Operational Efficiency, and External Factors'(Irudayaraj, 2017). Therefore, Business leaders, governments, academics, and technology vendors have realized this huge potential and are working together to tap these benefits to their nations. The cyber-world and the physical world are two kinds of potential in industry 4.0 solutions. For example, self-learning robots, centralized machinery planning, autonomous vehicles, logistic automation, etc.

PWC (2016) article stated that "Industry 4.0 is no longer a 'future trend' – for many companies, it is now at the heart of their strategic and research agenda" (Retrieved from <https://www.pwc.com>). This biggest change gave birth to smart factories, Smart process, smart products, smart cities, smart homes, etc. As a result, more new significant skilled jobs existed than losing of low skilled jobs. In addition to the current skills, the industry demands an additional skill set.

Accordinging to World Economic Forum report, Chapter 1: "The Future of Jobs and Skills (2016) stated that Core work-related skills can be classified into 3 categories and 9 sub-categories" (Retrieved from <http://reports.weforum.org>). The core work-related skills are known as Abilities, Basic Skills, and cross-function skills and the nine sub-categories are cognitive abilities, physical abilities, content skills, process skills, social skills, system skills, complex problem-solving skills, resources management skills, and technical skills.

### *The role of the English language in Education4.0 for Industry4.0*

History has proven that innovation in Technology and industry always influenced the English language. Revolution in an industry impacted the use of English and communication among people worldwide. The invention of the internet made English a global language (Crystal, 2012). The demand for learning the English language to sustain in the job market and industry increased tremendously around the globe. Industry 4.0 conditioned employees to learn English with different core skills by creating new job opportunities. Some of the new jobs are driverless car engineers, robot coordinator, industrial data scientist, industrial engineers, stimulation experts, demand-supply chain coordinators, digital assisted field-service engineers, salesforce, a specialist in data modeling and interpretations, 3-D computer-aided designer, 3-D modeling designing engineers and researchers in all-new fields. Next-generation students needed a high-level of competency skills and English language proficiency in this new job market world.

English language learners are mainly divided into two groups. They are English as a foreign language (EFL) learners and English as a second language (ESL) learners. English In India is learned as a second language. According to British Council in the article English Skills for Employability Think Tank,(2015), English and IT skills are the two key enabling skills that enable the delivery to a higher level of quality in achieving its ambitions. Although the new Education policy in India talked about multilingualism and the power of language, it agrees to focus on the English language due to its status of being an international common language in concurrence with the practice in all technologically advanced countries (National Education Policy, 2019). The government of India recognized the English language as a core skill which is a necessary component of the development of competency in the new job industry. Therefore, there is a need to conduct future research on the role of the English language in acquiring competency, which equips students to the real scenario of Education4.0 for Industry 4.0.

## **2. AIM OF THE RESEARCH**

The present research aims to find out innovative techniques in the English language teaching and learning process, to equip Undergraduate students with oral competence for Industry4.0 career readiness.

### *Statement of the problem*

New technological innovations in the industry demand workforce with the best competency. Teaching only to transfer the subject knowledge in the classroom doesn't support students to sustain in Industry4.0. The education system has taken a paradigm shift to meet the need of the Industry. The English language has a significant role in this shift to equip students with oral competence for Industry4.0 career readiness. The teaching-learning process in undergraduate colleges of Hyderabad is not given the scope to try out innovative techniques to tap the potential of the students. If the students' competencies are recognized on the campus, they can become efficient in the workplace.

### *Hypotheses*

- The teaching-learning process at the undergraduate level is by and large traditional.
- oral competence in English of the students for the Industry4.0 career readiness is ignored.

### *Objective of research*



- To find out innovative ways to tap oral competence in English of the students for the Industry4.0 career readiness.
- To design a module to equip oral competence in English of the students for the Industry4.0 career readiness

#### *Research Design*

The present study is to examine oral Communicative Competence in English of final year undergraduate students for Industry 4.0 Career Readiness. Effective Communicative Competencies in English improves job opportunities globally and provides elite social life in the future (MeenuPandey&Prabhat Pandey, 2014). Undergraduate students need to improve Communicative Competencies in the English Language to set a career in the global job market and also for career advancement. With this view, this study not only analyses the needs of students in language competencies for Industry 4.0 Career Readiness but also identifies and innovates training model to equip the student with effective Communicative Competencies in the English language for Industry 4.0 Career Readiness.

For this purpose, a research survey was conducted in various undergraduate colleges in and around Hyderabad. It was found that most of the learning was centered on the subjects of the mainstream not much focus was given to oral competence. After a few brainstorming sessions, stressing the importance of language and oral competence, the researcher selected 200 students randomly and administered a structured questionnaire to collect data. The needs of students were analyzed, tabulated, and interpreted. For each question, 5- point Likert scale, 0- lowest and 5- highest.

#### *Responses for the questionnaire:*

The questions were asked to make the learners understand the importance of oral competence to work in an organization. The researcher asked students to respond to every question in the column by marking tick.

- Oral competence in English is necessary for Industry 4.0 Career Readiness.
- Ability to face to face interviews
- Expressing confidently about your self during the interview process
- Communicating effectively in a group discussion round
- Effectively managing and negotiating
- Communication with colleagues using appropriate language for career readiness.

### **3. METHODOLOGY**

The data were analysed and calculated according to the 5- point Likert scale. The score for the questionnaire on Oral Communicative Competence is 3.8.

In the process of research, 120 randomly selected students were taken a pre-test on 'Oral Communicative Competence'. Based on the scores of the sample learners, an intensive training programme was designed to enhance the Oral Communicative Competence of the students for Industry 4.0 Career Readiness. the sample group was divided into two groups, the experimental group, and the control group and each group is consist of 60 students.

The researcher designed a 2weeks intensive training program for the experimental group to improve oral Communicative competence, by including student-centric language activities in their routine classes. On the other hand, the control group wasn't given any training.

### **4. TRAINING**

In the current 21st-century, the teaching-learning system in language classrooms needs to be shifted from a content-based model to a competency-based model and traditional teaching methodology to competency-based language teaching. This method enables a learner to learn the language in experiential learning through a real-life situation. This method of teaching must guarantee the achievement of required communicative competencies. The researcher used the following activities as part of the training, which enhances the students in their oral competence for Industry 4.0 Career Readiness.

#### *Activity 1*

##### *Building familiarity with career prospects*

This activity was planned by the researcher to enhance the awareness of various career opportunities and profile requirements available in the job market. The researcher introduced job portals, such as LinkedIn, Indeed, Monster, Glassdoor, Felxjob, The Ladder, AngelList, linkup, and Scouted to explore options according to their own suitable interest. Students researched to identify the following questionnaire :

- Availability of jobs based on their qualifications.
- Knowledge of skills and competencies demanded by the employers.
- Identify the job role.
- Access the work environment.
- Identify the skills required for the given job role.
- To analyze and develop the necessary competencies.

Upon a detailed study of the above, students have submitted an oral presentation on their research findings to the class. This activity aided to enhance their oral language and thinking skills. Besides, building collaborative learning and identifying career competencies.

#### *Activity 2*

##### *Self-Assessment and Proven Credibility*

Having learned the industry requirements and importance of self-knowledge, educational and occupational achievements, work and learning, competence and skills to perform tasks, occupational role, career planning, etc. from the previous activity, students were now driven to a practical presentation of their strengths and competencies to meet the scope of work of their dream job.

The purpose of this activity was to stimulate their presentation and communication skills needed to enact their given role. Despite their reluctant response, being challenged by Researchers' motivational approach, they came forward with their presentations stating this activity has enhanced their self-confidence towards, self-introduction, public communication and demonstration of their convincing capabilities all through the interview process.

#### *Activity 3*

##### *Enacting the responsibilities of the designated profile*

This activity was designed to ensure students' understanding and knowledge of the Company profile, scope of work, products and services, work culture, and ethics. Their classroom presentations involved the introduction of the Company, Team management, a delegation of tasks and roles relevant to their skills, competency, knowledge, and experience. This activity led to a phenomenal exposure of comparisons amongst various job roles against their skills and experiences, leading to integral thought-provoking conversations, broadening their horizons, and interview preparations.

#### *Post-test*

After successful completion of 2 weeks of training, a post-test was conducted for experimental groups to measure the application and impact of the students in oral competence for Industry 4.0 career readiness. A significant increase in scores can be observed and the

improvement was mainly observed along oral competence and presentation skills dimensions. The sample learners also felt they developed an instinct for learning the language.

## 5. CONCLUSION

Research findings validate the training program centered on innovative practice in teaching the English language to enhance the oral communicative competence of undergraduate students is remarkably effective. Students had better oral competence upon practicing activities and strategies, used to correlate the training content. Most of the undergraduate students identified that the English language plays a crucial role in job procurement and mandatory practicing principles of oral competence. Students evolved to be dynamic, confident, self-sufficient, as a result, the chances of acquiring a job or standing out in the industry 4.0 increases.

## 6. BIBLIOGRAPHY

- [1]. Warschauer, M. (2000). The Changing Global Economy and the Future of English Teaching. *TESOL Quarterly*, 34(3), 511-535. doi:10.2307/3587741
- [2]. Crystal, D. (2012). *English as a Global Language - Second Edition*. Stuttgart: Klett.
- [3]. Gilchrist, A., & John Wiley & Sons, Inc. (n.d.) (2016). *Industry 4.0: The Industrial Internet of Things*. Retrieved from <https://b-ok.org/book/5256626/334915>.
- [4]. Irudayaraj, J. (2017). *Industry-4\_A-Talent-Perspective\_Ranalytics-Advisors.pdf*. <http://www.ranalytics.com/>. [http://www.ranalytics.com/pdf/Industry-4\\_A-Talent-Perspective\\_Ranalytics-Advisors.pdf?cv=1](http://www.ranalytics.com/pdf/Industry-4_A-Talent-Perspective_Ranalytics-Advisors.pdf?cv=1)
- [5]. *Industry 4.0: Building the digital enterprise - PwC*. (n.d.). Retrieved from <https://www.pwc.com/gx/en/industries/industries-4.0/landing-page/industry-4.0-building-your-digital-enterprise-april-2016.pdf>.
- [6]. Chapter 1: *The Future of Jobs and Skills*. (n.d.). Retrieved from <http://reports.weforum.org/future-of-jobs-2016/chapter-1-the-future-of-jobs-and-skills/>.
- [7]. *English Skills for Employability Think Tank | British Council*. (2015). Retrieved from <https://www.britishcouncil.in/english-skills-employability-think-tank>
- [8]. *National Education Policy (2019)*. Retrieved from <https://innovate.mygov.in/wp-content/uploads/2019/06/mygov15596510111.pdf>.
- [9]. Lindok, A. (2015). *Impact of Industrial Revolution on English Literature*. [www.academia.edu](http://www.academia.edu). [https://www.academia.edu/12870801/Impact\\_of\\_Industrial\\_Revolution\\_on\\_English\\_Literature](https://www.academia.edu/12870801/Impact_of_Industrial_Revolution_on_English_Literature)
- [10]. Neeley, T. (2014). *What's Your Language Strategy?: It Should Bind Your Company's Global Talent Management and Vision*. <https://www.hbs.edu>. <https://www.hbs.edu/faculty/Pages/item.aspx?num=47753>
- [11]. Pandey, M., & Pandey, P. K. (2014). *Better English for Better Employment Opportunities*. [www.researchgate.net](http://www.researchgate.net). [https://www.researchgate.net/publication/264788119\\_Better\\_English\\_for\\_Better\\_Employment\\_Opportunities](https://www.researchgate.net/publication/264788119_Better_English_for_Better_Employment_Opportunities)



# INTERNATIONAL JOURNAL OF CREATIVE RESEARCH THOUGHTS (IJCRT)

An International Open Access, Peer-reviewed, Refereed Journal

## Smart Learning- Role of IoT in Modern Education Systems

K.Rajeswari <sup>1</sup>, G. Nirmala Joycee <sup>2</sup>,

<sup>1</sup>Lecturer, Department of Computer Science (UG)

<sup>2</sup> Assistant Professor, Department of Computer Science (PG)

<sup>1,2</sup> St. Ann's College for Women, Mehdipatnam, Hyderabad.

### Abstract

In today's generation internet plays a vital role both in learning and teaching. IoT is the new era of computing Technology. It is an ecosystem of connected physical objects that are able to accessible through internet. IoT can change the educational system into a better understanding way. IoT is used in institutions to enhance learning outcomes by providing more affluent learning experiences, , and gaining real-time experience to improved operational efficiency actionable insight into student performance. By IoT in higher education its potentially increases benefits and reducing the risks involved in it. Without human assist the IoT can facilitates the devices/objects to identify and understand the situation. These devices/objects can represent themselves digitally and these devices can be to control from anywhere and anytime. The new wave of changes has started from IoT. It gives massive volume of connectivity. The Internet of things expected to give strong impact on various areas of life including healthcare, Entertainment, education, Business, Smart Home, Smart Campus and Smart City etc. IoT not only expected to give great impact but also expected to give new opportunities and possibilities for the improvement on the various area. The collaboration between the people and Technology are very power full. This paper provides the future of IoT in the higher education during the next few decades, which can be offered by a number of research organizations and enterprises. On the other hand, IoT brings tremendous challenges in higher education. Hence, this paper presents the importance and challenges of IoT in higher education.

**Keywords:** Internet of Things, enhanced learning, tremendous challenges, affluent

## 1. Introduction

The Internet and its associated services and applications have strongly developed and influenced communication, it gathers information and marketing across the world via websites, blogs, e-mail and social networks. The changes in education has been registered major, especially since 2000, towards a new orientation of teenagers' in education, reflected through online documentation, and implementation of projects in virtual teams, and in online tutorials and much more. In 1999, there emerged a new term in the field, Internet of Things (IoT). The interaction between objects, people, internet and environment is called as "IoT". We live in 21st century where the Information and communication Technology (ICT) cannot detach from human. The ICT plays a vital role in current education system. With the support of IoT education system can enhance the learning process. With the help of IoT can bring the live classroom, where student can observe, understand and interact easily. The impact of ICT has changed the traditional education system towards significantly improved modern and quality education systems at various levels of learning. IOT has become the most essential thing in every human's life. The main concept of connected devices or things has given a new version to Internet, that it anything, anywhere can get connected with the Internet and becomes 'Smart.' Connected devices can communicate with each other and share information which can then further be processed to take some decisions. According to Mark Weiser, "The most profound technologies are those that disappear. They weave themselves into the fabric of everyday life until they are indistinguishable from it" [1]. Kevin Ashton was the first to use the term Internet of Things in 1999. Early the beginning of Internet of Things (IoT) many researchers have tried to define IoT in various ways like Internet of Everything, Internet of Anything, Internet of People, Internet of Signs, Internet of Services, Internet of Data or Internet of Processes [2]. According to [3], IoT represents 'anything at all, depending on requirements.' Cisco defines IoT as a network of connected physical objects. Cisco also uses the term Internet of Everything for both physical and virtual objects. Cisco states that "IoE brings together people, process, data, and things to make networked connections more relevant and valuable than ever before—turning information into actions that create new capabilities, richer experiences, and unprecedented economic opportunities for businesses, individuals, and countries."

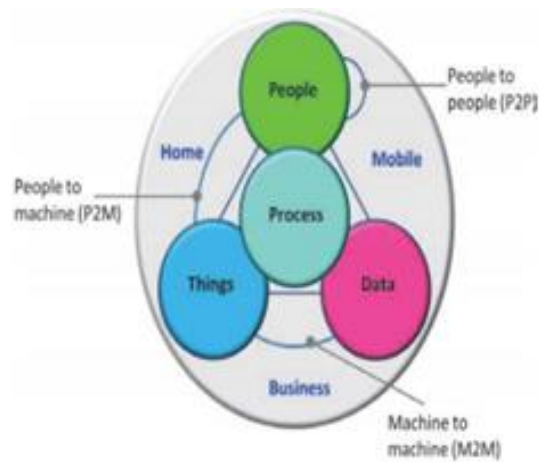


Fig:1 Internet of everything

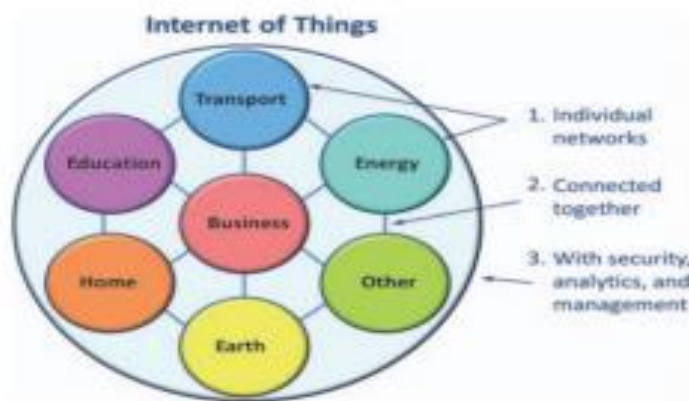


Fig:2 Using internet in all different sectors

According to Gartner's forecast, 20.8 billion new things will be connected by 2020. According to Machine Research, the growth of IoT connections is : from 6 billion in 2015 to 27 billion in 2025. The number of cellular IoT connections will be 2.2 billion, and 45% of these will be in connected cars. The revenue forecast of IoT in 2025 is 3 trillion US\$. IoT will also generate over two zettabytes of data, generally from consumer electronic devices.



Fig: 3 Five predictions of IOT till 2025

## Previous Studies

**2.1 The Traditional Education:** Traditional classroom education has been around for decades and almost all members of society, and for many centuries using it. Class room education continues to be an important way of learning, and there are many benefits that accompany this method of education. In a traditional education, students are able to interact with their teachers and personally.

### Online Education:

The results of this study indicated that the participants were aware of the facilities of using e-books and they were content with the facilities of usage. The main resource of multiplying education is the teachers therefore; the teachers should build a relationship with technology and should use it in a sufficient level in their current and future classes. Moreover, each teacher should follow technology and apply it in their course. Therefore, the design of the digital electronic book is prepared to be adaptive for this generation of students because in general, they are digital readers.

## 2. Objective of the study

The objective of this study is derived as below,

- To study the need of IoT in Education.
- To know the Technology enhanced learning
- To understand the Internet of Things

- Advantages of IoT in Modern Education

### **3. Research Methodology**

This research was carried out based on the secondary data and the data. The data used for this research is descriptive and qualitative from secondary sources. This data has been filtered and analyzed in a structured analytical format. Since the topic is evolutionary and is subject to fast changes, only the qualitative data updated from time to time is used. The main source of data collection is wiki, websites, blogs, YouTube, books, articles and journals.

#### **2.1 To study the need of IoT in Education.**

##### **Individualization**

The Student can more and inside based on the interest with personalized learning pattern and this will lead much more opportunity to learn with complete understanding the subject.

- **Smart Campus using IoT**

In general now a day's all universities, colleges and schools are connected with internet of things. The concept of smart campus involves with the intellectual environment equipped with fully sophisticated and installed with advanced technology smart things and aids. The smart classroom occupied with the set of smart things such as LCD Projector, Microphone, Speaker, cameras, smart board / Interactive board, Visualizer, Virtual classroom, Google Classroom which can be used for the ICT based enabled learning. A smart campus is a collection of smart multiple things [5]. The smart campus may include the following things.

- IoT based Classroom
- IoT based Laboratories
- Possibilities of E-Learning
- Smart Library
- Smart Attendance system for faculty and Student
- Smart canteen
- Smart office



In addition to smart parking, smart tracking of student, wi-fi enabled campus. The purpose of the smart campus is making the environment user friendly.

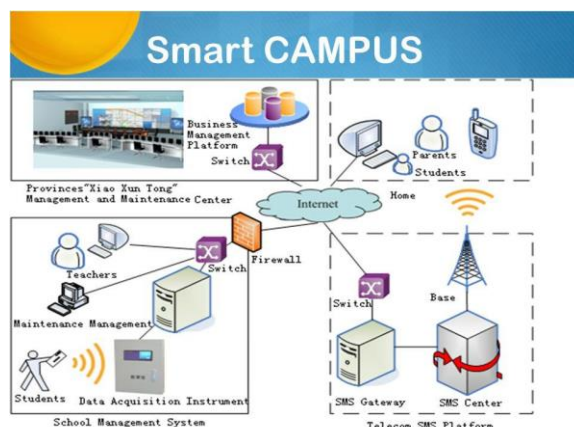


Fig :4 IOT in Smart campus

## 2.2 To know the Technology enhanced learning

- **IoT based Smart Classroom:**

The use of IoT devices for teaching and learning purposes is a top trend among institutions across the world which provides a new and innovative approach to education and classroom management [5]. Through smart classroom faculty can explain the subject in a more reality based and make the student to understand easily.

In the era of Digital technology, the rapid evaluation of Information and communication technology has created a new paradigm of internet known as Internet of Things. The Internet of Things changed the way to communicate with people and object in different manner. This has created the new form of communication between the teacher and student to allow them to improve the teaching and learning process. ICT have a great power to improve the quality outcomes of teaching learning.

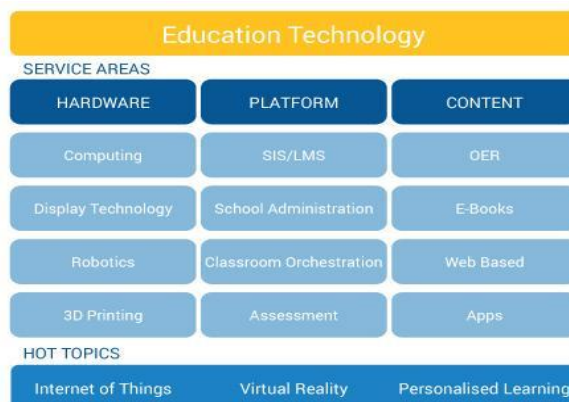


Fig:5 Educational Technology Market Research[8].

- **Advantage of Smart Classroom:**

Smart classroom plays a significant role in the student life. Smart classroom helps to transform the traditional education into modern education, with the help of smart education student can learn from anywhere, anytime anything and everything. The level of connectivity offered by the internet is beyond belief. It helps students to enrich the learning process all over the world. This offers to improve the quality of education and academic achievements. IoT enables to break the barrier of learning in the classroom. IoT give the platform to access globally. Some of the common tools are used in the classroom are.

- Smart board / Interactive white board
- LCD Projectors
- Lap tops and Tablet Pc
- E-Library
- ID Cards for Student and Faculty
- CC Cameras for security
- Attendance tracking systems
- Printer and Scanners
- Speakers and Mikes
- Media Center
- Environment friendly
- Advanced teaching and learning experience
- Easy maintenance



Fig:6 IOT in smart class rooms

Smart things are helps the teacher to explain the class in more interactive and more realistic way. The student can able to understand the concept very easily and put more attention with the help of the above mentioned smart devices in the Smart classroom. The flow of connected technology means professors and teachers could make grades faster. Their checking/grading also would be eased, less prejudiced and more efficient. When educators have devices connected to the cloud, they would be in better connect. Thus, tutor/ teachers could see which student requires more concern and focus. Other processes, with smart technology helps us in making lesson plans, adjusting schedules and many more. While the task is to connect over smart devices, teachers are able to focus more on their teaching and research.

- **IoT based Research:**

Research is a one of the emergent technology in the education system. Research gives the real opportunity to upgrade knowledge. Research will give the opportunity to know the concept very well. Internet of Things will give the more opportunity and it helps everyone to understand the concept and we come to know the opinion of others in the world. IoT will give the benefit of the wider research area and it will lead a valuable innovation to the world.



Fig :7 IOT in research

- **Smart Attendance System – Biometric Systems:**

Regularly taking attendance is a big task in the classroom. To overcome that we have introduced a new technology with the help of iot that is radio frequency identification (RFI) which will substantially help, biometric fingerprint sensor and password based technologies are integrated to develop a cost effective, reliable attendance management system [6]. Smart attendance system and biometric system are the most secured things, also it is very difficult to manipulate the data and complete integrity proof on the data and information.

The internet enabled radio frequency identification will enable to notify the assigned concerns on defined interval or customized periods.

The recorded data from the biometric can be stored and retrieved any time and each educational establishment wants it to be secure and endangered from any unsolicited visitors. However the specialists that are involved in security guard, they cannot monitor every corner of the facility. That is why IoT can help administration control. Facial recognition systems helps us to identify faces by scanning them and to be saved in data base. That is how the Internet of Things works and how it may be beneficial.



Fig:8 IOT used for security

- **IoT based Feedback Form:**

Google Form is a one of the platform to access the student with the help of the technology .It is a one of the easy way to take the feedback using the internet of things. Google Form is a open source available for everyone. Using this form student can answer the query from everywhere and any time.24/7 available in the internet.

- **IoT based Google Classroom:**

Google classroom is free. Google classroom can be accessed from any computer or mobile device via Google chrome. It is a blended platform with lot of benefits available for both faculty and students. Google classroom is a one of the online learning system, using this we can send, announce or pass any kind of information to the everyone. It has lot of benefits such as accessibility, Time saving, Communication, paperless transaction, collaboration, Data Analysis and feedback [7] etc. We don't need any papers to do assignments, as we can save our data through google classroom. The Internet of Things impacts education in a lot of ways. It is this asset

intellect, which enable institutions to make more informed decisions, in an attempt to improve operational efficiency, learning experience and campus security

### **2.3 To understand the Internet of Things**

As per the above discussion we can able to understand the value of Internet of Things in the society especially in the education system. IoT promotes a heightened level of awareness about our world [13]. IoT enables numerous applications ranging from the micro to macro and from the insignificant to the serious [13]. IoT plays a significant role in the field of education. IoT plays a major role everywhere in the society. The era of the technology our dream becomes true. IoT support the way to build the flexibility of the system and cost effective way. With the help of IOT we can transfer several areas in everyday life .Although it seem to be good in education.

Software development education is widely offered by most colleges and universities, offering fully online degree programs as well as the traditional on campus programs, which is helping the rural people who is far away from the university access get benefited.

### **2.4 Advantages of IoT in Modern Education**

Today's more and more tutors and educators are using the internet for the betterment of the education systems. The students are the main chain links of the education process. Internet of thing is a new system introduced to provide wide connectivity between the people and the technology where we cannot imagined before. The scope of learning is enormous with the help of the IOT based devices like Tablet, Laptops, Mobile Phones, Desktops, etc.It helps the students as follows.

#### **Individual learning**

Interactive based learning

- Increase the curiosity of learning
- Learn everywhere
- To learn and understand the things in easy and better way.
- To validate the information by interpret the data from various sources.

- Improve the learning Process
- No more loss of information
- Create the curiosity towards the subject
- The growth of engagement
- To improve the results
- Smart way to monitor the students

**Conclusion:**

The future of IoT is massively unlimited and will be improve a quality of education system because of advances in technology, though the IoT contain plenty of information ,however the user can get the relevant data and information by data interpreting, The Wi-Fi as made it possible to connect people and machines. IoT can change our whole world within few years.Strongly believed that the use of technology especially the era of IoT transform the educational environment towards the modern education [9].With the help of IoT we can collect the lot of data, that data we can convert to Information . These kinds of Information are going to help in the society for everybody everywhere.the students who is not able to attend the regular physical classes ,can be highly benefited on the learning progress ,because of the wider education by IoT the quality of human will be improved and the poverty of the nation subsequently improved .

**Reference:**

1. <http://ijsetr.org/wp-content/uploads/2016/02/IJSETR-VOL-5-ISSUE-2-472-476.pdf>
2. <https://www.happiestminds.com/Insights/internet-of-things/>
3. [https://en.wikipedia.org/wiki/Internet\\_of\\_things](https://en.wikipedia.org/wiki/Internet_of_things)
4. <http://journals.sfu.ca/onlinejour/index.php/i-jep/article/viewFile/7187/4604>
5. <https://www.forbes.com/sites/jacobmorgan/2014/05/13/simple-explanation-internet-things-that-anyone-can-understand/#406c48d51d09>
6. [https://www.researchgate.net/publication/323425616\\_IOT\\_CONCEPT\\_APPLICATION\\_IN\\_EDUCATIONAL\\_SECTOR\\_USING\\_COLLABORATION](https://www.researchgate.net/publication/323425616_IOT_CONCEPT_APPLICATION_IN_EDUCATIONAL_SECTOR_USING_COLLABORATION)
7. [http://paper.ijcsns.org/07\\_book/201705/20170520.pdf](http://paper.ijcsns.org/07_book/201705/20170520.pdf)
8. <https://ieeexplore.ieee.org/document/8249106/>
9. <https://www.thetechadvocate.org/10-benefits-of-google-classroom-integration/>
10. <http://journals.sfu.ca/onlinejour/index.php/i-jep/article/viewFile/7187/4604>
11. <https://medium.com/@TeksunGroup/importance-of-internet-of-things-iot-in-our-liveb71e53d50a44>
12. <https://www.ariasystems.com/blog/internet-things-important/>
13. <https://www.cleveroad.com/blog/iot-in-education-main-solutions-iot-brings-to-educational-sector>

# Enchaining Oral Competence Of Undergraduate Students: English Language Skills For Industry 4.0

Thummaloor Sreevani<sup>1</sup>, Dr.Mutyala Suresh<sup>2</sup>

<sup>1</sup>*Research scholar in ELT, Dept. of English, KoneruLakshmaih Education Foundation  
(Deemed to be University), Vaddeswaram, Guntur District, A.P., India &  
Lecturer, Dept. of English, St.Ann'sCollege For Women, Hyderabad, TS, India.*

<sup>2</sup>*Asso. Professor, Dept of English, KoneruLakshmaih Education Foundation(Deemed to be  
University), Vaddeswaram, Guntur District, A.P., India.*

*Email:*<sup>1</sup>*sreevani.vips@gmail.com,* <sup>2</sup>*msphd@kluniversity.in*

## Abstract

English language competencies are essential for career readiness and advancement. English, being one of the popular world languages, is used for global communication and is commonly considered as an official language in many countries. In India, undergraduate students need English language competence to set a career in the global job market. At present, the fourth Industrial Revolution introduced innovative technological advancement in the industry. Thus, there is a great demand for professionals with new technologies and language competencies in this Industry 4.0. To possess these new career opportunities, undergraduate students need to upgrade their technical skills as well as English language competencies. Educators and Industry need to build the bridge for the students by providing Industry4.0 career readiness training programs. Here is a tremendous need for analyzing and mapping technical skills as well as the English language competencies of Undergraduate students. The present study is to analyse the need for oral Communicative Competence in the English Language of 120 final year undergraduate students in Hyderabad for Industry 4.0 Career Readiness. The researcher designed a specific need-based intensive course and the randomly selected group underwent training for 2 weeks. As a result, students developed commutative competency in the English language for Industry 4.0 career readiness.

**Keywords:** Oral Communicative Competence in English, Undergraduates, Industry4.0, Career Readiness, experimental study.

## 1. INTRODUCTION

English as an International language has a significant role in this world of globalization. Warschauer (2000) mentioned that globalization and English as an International language gained prominence together in the history of the world. The English language is used widely to establish international commerce, cultures, and communication in the process of globalization. Neeley (2014) quoted that English became a global language for business and was mandated as a common corporate language in many multinational companies around the world. English is commonly considered as an official language in many countries.



### *Evolution of English language and Industrial Revolutions*

Five hundred years ago, the English language was spoken mostly in the British Isles. Annika Lindok (2015) stated that In the early 18th century, the first industrial revolution brought the evolution of the English language. In fact, the English language is used to show to the world what was made of industrialized societies. History has proven that innovation in Technology and industry always influenced the English language. Revolution in the industry impacted the use of English and communication among people worldwide. The invention of the internet made English a global language (Crystal, 2012). English language learners are increasing due to the ongoing demand for this language in the competitive job market in the industry. According to the British council report at present 1.75 billion people are learning the English language across the globe and the number will increase up to 2 billions very soon.

### *Industry 4.0*

The initiation of the Fourth Industrial Revolution with modern technologies like Data Science, Artificial Intelligence (AI), Machine Learning(ML), Cyber Security, Internet of Things (IoT) Augment Reality (AR) and Virtual Reality (VR) spread all over the countries. The invention of the water and steam engine and Mechanical production in the year 1784 brought the first Industrial Revolution. Electrical energy and mass production existed in the Second Industrial Revolution in the year 1923. In the year 1969, the third Industrial Revolution was introduced by electronics and IT for higher automated production. From the year 2014, innovations of manufacturing logistics and revolutionizing traditional manufacturing processes inducted to the Fourth Industrial Revolution is addressed as Industry 4.0. Firstly, It started in Germany as a brainchild. Next, adopted by the USA, France, and Japan. Consequently, it influenced BRICS (Brazil, Russia, India, China, and South Africa) Nations as well as the whole world. According to Gilchrist, A (2016) "From a financial perspective, one market research report forecasts growth of \$ 151.01 billion U.S. by 2020, at a CAGR (Compound annual growth rate) of 8.03% between 2015 and 2020" (p.02).

According to new research Benefits of Industry 4.0 are 'Cost Optimization, New Opportunities, Greater Operational Efficiency, and External Factors'(Irudayaraj, 2017). Therefore, Business leaders, governments, academics, and technology vendors have realized this huge potential and are working together to tap these benefits to their nations. The cyber-world and the physical world are two kinds of potential in industry 4.0 solutions. For example, self-learning robots, centralized machinery planning, autonomous vehicles, logistic automation, etc.

PWC (2016) article stated that "Industry 4.0 is no longer a 'future trend' – for many companies, it is now at the heart of their strategic and research agenda" (Retrieved from <https://www.pwc.com>). This biggest change gave birth to smart factories, Smart process, smart products, smart cities, smart homes, etc. As a result, more new significant skilled jobs existed than losing of low skilled jobs. In addition to the current skills, the industry demands an additional skill set.

Accordinging to World Economic Forum report, Chapter 1: "The Future of Jobs and Skills (2016) stated that Core work-related skills can be classified into 3 categories and 9 sub-categories" (Retrieved from <http://reports.weforum.org>). The core work-related skills are known as Abilities, Basic Skills, and cross-function skills and the nine sub-categories are cognitive abilities, physical abilities, content skills, process skills, social skills, system skills, complex problem-solving skills, resources management skills, and technical skills.

### *The role of the English language in Education4.0 for Industry4.0*

History has proven that innovation in Technology and industry always influenced the English language. Revolution in an industry impacted the use of English and communication among people worldwide. The invention of the internet made English a global language (Crystal, 2012). The demand for learning the English language to sustain in the job market and industry increased tremendously around the globe. Industry 4.0 conditioned employees to learn English with different core skills by creating new job opportunities. Some of the new jobs are driverless car engineers, robot coordinator, industrial data scientist, industrial engineers, stimulation experts, demand-supply chain coordinators, digital assisted field-service engineers, salesforce, a specialist in data modeling and interpretations, 3-D computer-aided designer, 3-D modeling designing engineers and researchers in all-new fields. Next-generation students needed a high-level of competency skills and English language proficiency in this new job market world.

English language learners are mainly divided into two groups. They are English as a foreign language (EFL) learners and English as a second language (ESL) learners. English In India is learned as a second language. According to British Council in the article English Skills for Employability Think Tank,(2015), English and IT skills are the two key enabling skills that enable the delivery to a higher level of quality in achieving its ambitions. Although the new Education policy in India talked about multilingualism and the power of language, it agrees to focus on the English language due to its status of being an international common language in concurrence with the practice in all technologically advanced countries (National Education Policy, 2019). The government of India recognized the English language as a core skill which is a necessary component of the development of competency in the new job industry. Therefore, there is a need to conduct future research on the role of the English language in acquiring competency, which equips students to the real scenario of Education4.0 for Industry 4.0.

## **2. AIM OF THE RESEARCH**

The present research aims to find out innovative techniques in the English language teaching and learning process, to equip Undergraduate students with oral competence for Industry4.0 career readiness.

### *Statement of the problem*

New technological innovations in the industry demand workforce with the best competency. Teaching only to transfer the subject knowledge in the classroom doesn't support students to sustain in Industry4.0. The education system has taken a paradigm shift to meet the need of the Industry. The English language has a significant role in this shift to equip students with oral competence for Industry4.0 career readiness. The teaching-learning process in undergraduate colleges of Hyderabad is not given the scope to try out innovative techniques to tap the potential of the students. If the students' competencies are recognized on the campus, they can become efficient in the workplace.

### *Hypotheses*

- The teaching-learning process at the undergraduate level is by and large traditional.
- oral competence in English of the students for the Industry4.0 career readiness is ignored.

### *Objective of research*

- To find out innovative ways to tap oral competence in English of the students for the Industry4.0 career readiness.
- To design a module to equip oral competence in English of the students for the Industry4.0 career readiness

#### *Research Design*

The present study is to examine oral Communicative Competence in English of final year undergraduate students for Industry 4.0 Career Readiness. Effective Communicative Competencies in English improves job opportunities globally and provides elite social life in the future (MeenuPandey&Prabhat Pandey, 2014). Undergraduate students need to improve Communicative Competencies in the English Language to set a career in the global job market and also for career advancement. With this view, this study not only analyses the needs of students in language competencies for Industry 4.0 Career Readiness but also identifies and innovates training model to equip the student with effective Communicative Competencies in the English language for Industry 4.0 Career Readiness.

For this purpose, a research survey was conducted in various undergraduate colleges in and around Hyderabad. It was found that most of the learning was centered on the subjects of the mainstream not much focus was given to oral competence. After a few brainstorming sessions, stressing the importance of language and oral competence, the researcher selected 200 students randomly and administered a structured questionnaire to collect data. The needs of students were analyzed, tabulated, and interpreted. For each question, 5- point Likert scale, 0- lowest and 5- highest.

#### *Responses for the questionnaire:*

The questions were asked to make the learners understand the importance of oral competence to work in an organization. The researcher asked students to respond to every question in the column by marking tick.

- Oral competence in English is necessary for Industry 4.0 Career Readiness.
- Ability to face to face interviews
- Expressing confidently about your self during the interview process
- Communicating effectively in a group discussion round
- Effectively managing and negotiating
- Communication with colleagues using appropriate language for career readiness.

### **3. METHODOLOGY**

The data were analysed and calculated according to the 5- point Likert scale. The score for the questionnaire on Oral Communicative Competence is 3.8.

In the process of research, 120 randomly selected students were taken a pre-test on 'Oral Communicative Competence'. Based on the scores of the sample learners, an intensive training programme was designed to enhance the Oral Communicative Competence of the students for Industry 4.0 Career Readiness. the sample group was divided into two groups, the experimental group, and the control group and each group is consist of 60 students.

The researcher designed a 2weeks intensive training program for the experimental group to improve oral Communicative competence, by including student-centric language activities in their routine classes. On the other hand, the control group wasn't given any training.

### **4. TRAINING**

In the current 21st-century, the teaching-learning system in language classrooms needs to be shifted from a content-based model to a competency-based model and traditional teaching methodology to competency-based language teaching. This method enables a learner to learn the language in experiential learning through a real-life situation. This method of teaching must guarantee the achievement of required communicative competencies. The researcher used the following activities as part of the training, which enhances the students in their oral competence for Industry 4.0 Career Readiness.

#### *Activity 1*

##### *Building familiarity with career prospects*

This activity was planned by the researcher to enhance the awareness of various career opportunities and profile requirements available in the job market. The researcher introduced job portals, such as LinkedIn, Indeed, Monster, Glassdoor, Felxjob, The Ladder, AngelList, linkup, and Scouted to explore options according to their own suitable interest. Students researched to identify the following questionnaire :

- Availability of jobs based on their qualifications.
- Knowledge of skills and competencies demanded by the employers.
- Identify the job role.
- Access the work environment.
- Identify the skills required for the given job role.
- To analyze and develop the necessary competencies.

Upon a detailed study of the above, students have submitted an oral presentation on their research findings to the class. This activity aided to enhance their oral language and thinking skills. Besides, building collaborative learning and identifying career competencies.

#### *Activity 2*

##### *Self-Assessment and Proven Credibility*

Having learned the industry requirements and importance of self-knowledge, educational and occupational achievements, work and learning, competence and skills to perform tasks, occupational role, career planning, etc. from the previous activity, students were now driven to a practical presentation of their strengths and competencies to meet the scope of work of their dream job.

The purpose of this activity was to stimulate their presentation and communication skills needed to enact their given role. Despite their reluctant response, being challenged by Researchers' motivational approach, they came forward with their presentations stating this activity has enhanced their self-confidence towards, self-introduction, public communication and demonstration of their convincing capabilities all through the interview process.

#### *Activity 3*

##### *Enacting the responsibilities of the designated profile*

This activity was designed to ensure students' understanding and knowledge of the Company profile, scope of work, products and services, work culture, and ethics. Their classroom presentations involved the introduction of the Company, Team management, a delegation of tasks and roles relevant to their skills, competency, knowledge, and experience. This activity led to a phenomenal exposure of comparisons amongst various job roles against their skills and experiences, leading to integral thought-provoking conversations, broadening their horizons, and interview preparations.

#### *Post-test*

After successful completion of 2 weeks of training, a post-test was conducted for experimental groups to measure the application and impact of the students in oral competence for Industry 4.0 career readiness. A significant increase in scores can be observed and the

improvement was mainly observed along oral competence and presentation skills dimensions. The sample learners also felt they developed an instinct for learning the language.

## 5. CONCLUSION

Research findings validate the training program centered on innovative practice in teaching the English language to enhance the oral communicative competence of undergraduate students is remarkably effective. Students had better oral competence upon practicing activities and strategies, used to correlate the training content. Most of the undergraduate students identified that the English language plays a crucial role in job procurement and mandatory practicing principles of oral competence. Students evolved to be dynamic, confident, self-sufficient, as a result, the chances of acquiring a job or standing out in the industry 4.0 increases.

## 6. BIBLIOGRAPHY

- [1]. Warschauer, M. (2000). The Changing Global Economy and the Future of English Teaching. *TESOL Quarterly*, 34(3), 511-535. doi:10.2307/3587741
- [2]. Crystal, D. (2012). *English as a Global Language - Second Edition*. Stuttgart: Klett.
- [3]. Gilchrist, A., & John Wiley & Sons, Inc. (n.d.) (2016). *Industry 4.0: The Industrial Internet of Things*. Retrieved from <https://b-ok.org/book/5256626/334915>.
- [4]. Irudayaraj, J. (2017). *Industry-4\_A-Talent-Perspective\_Ranalytics-Advisors.pdf*. <http://www.ranalytics.com/>. [http://www.ranalytics.com/pdf/Industry-4\\_A-Talent-Perspective\\_Ranalytics-Advisors.pdf?cv=1](http://www.ranalytics.com/pdf/Industry-4_A-Talent-Perspective_Ranalytics-Advisors.pdf?cv=1)
- [5]. *Industry 4.0: Building the digital enterprise - PwC*. (n.d.). Retrieved from <https://www.pwc.com/gx/en/industries/industries-4.0/landing-page/industry-4.0-building-your-digital-enterprise-april-2016.pdf>.
- [6]. Chapter 1: *The Future of Jobs and Skills*. (n.d.). Retrieved from <http://reports.weforum.org/future-of-jobs-2016/chapter-1-the-future-of-jobs-and-skills/>.
- [7]. *English Skills for Employability Think Tank | British Council*. (2015). Retrieved from <https://www.britishcouncil.in/english-skills-employability-think-tank>
- [8]. *National Education Policy (2019)*. Retrieved from <https://innovate.mygov.in/wp-content/uploads/2019/06/mygov15596510111.pdf>.
- [9]. Lindok, A. (2015). *Impact of Industrial Revolution on English Literature*. [www.academia.edu](http://www.academia.edu). [https://www.academia.edu/12870801/Impact\\_of\\_Industrial\\_Revolution\\_on\\_English\\_Literature](https://www.academia.edu/12870801/Impact_of_Industrial_Revolution_on_English_Literature)
- [10]. Neeley, T. (2014). *What's Your Language Strategy?: It Should Bind Your Company's Global Talent Management and Vision*. <https://www.hbs.edu>. <https://www.hbs.edu/faculty/Pages/item.aspx?num=47753>
- [11]. Pandey, M., & Pandey, P. K. (2014). *Better English for Better Employment Opportunities*. [www.researchgate.net](http://www.researchgate.net). [https://www.researchgate.net/publication/264788119\\_Better\\_English\\_for\\_Better\\_Employment\\_Opportunities](https://www.researchgate.net/publication/264788119_Better_English_for_Better_Employment_Opportunities)



# INTERNATIONAL JOURNAL OF CREATIVE RESEARCH THOUGHTS (IJCRT)

An International Open Access, Peer-reviewed, Refereed Journal

## Smart Learning- Role of IoT in Modern Education Systems

K.Rajeswari <sup>1</sup>, G. Nirmala Joycee <sup>2</sup>,

<sup>1</sup>Lecturer, Department of Computer Science (UG)

<sup>2</sup> Assistant Professor, Department of Computer Science (PG)

<sup>1,2</sup> St. Ann's College for Women, Mehdipatnam, Hyderabad.

### Abstract

In today's generation internet plays a vital role both in learning and teaching. IoT is the new era of computing Technology. It is an ecosystem of connected physical objects that are able to accessible through internet.IoT can change the educational system into a better understanding way.IoT is used in institutions to enhance learning outcomes by providing more affluent learning experiences, , and gaining real-time experience to improved operational efficiency actionable insight into student performance. By IoT in higher education its potentially increases benefits and reducing the risks involved in it. Without human assist the IoT can facilitates the devices/objects to identify and understand the situation. These devices/objects can represent themselves digitally and these devices can be to control from anywhere and anytime. The new wave of changes has started from IoT.It gives massive volume of connectivity. The Internet of things expected to give strong impact on various areas of life including healthcare, Entertainment, education, Business, Smart Home, Smart Campus and Smart City etc.IoT not only expected to give great impact but also expected to give new opportunities and possibilities for the improvement on the various area. The collaboration between the people and Technology are very power full. This paper provides the future of IoT in the higher education during the next few decades, which can be offered by a number of research organizations and enterprises. On the other hand, IoT brings tremendous challenges in higher education. Hence, this paper presents the importance and challenges of IoT in higher education.

**Keywords:** Internet of Things, enhanced learning, tremendous challenges, affluent

## 1. Introduction

The Internet and its associated services and applications have strongly developed and influenced communication, it gathers information and marketing across the world via websites, blogs, e-mail and social networks. The changes in education has been registered major, especially since 2000, towards a new orientation of teenagers' in education, reflected through online documentation, and implementation of projects in virtual teams, and in online tutorials and much more. In 1999, there emerged a new term in the field, Internet of Things (IoT). The interaction between objects, people, internet and environment is called as "IoT". We live in 21st century where the Information and communication Technology (ICT) cannot detach from human. The ICT plays a vital role in current education system. With the support of IoT education system can enhance the learning process. With the help of IoT can bring the live classroom, where student can observe, understand and interact easily. The impact of ICT has changed the traditional education system towards significantly improved modern and quality education systems at various levels of learning. IOT has become the most essential thing in every human's life. The main concept of connected devices or things has given a new version to Internet, that it anything, anywhere can get connected with the Internet and becomes 'Smart.' Connected devices can communicate with each other and share information which can then further be processed to take some decisions. According to Mark Weiser, "The most profound technologies are those that disappear. They weave themselves into the fabric of everyday life until they are indistinguishable from it" [1]. Kevin Ashton was the first to use the term Internet of Things in 1999. Early the beginning of Internet of Things (IoT) many researchers have tried to define IoT in various ways like Internet of Everything, Internet of Anything, Internet of People, Internet of Signs, Internet of Services, Internet of Data or Internet of Processes [2]. According to [3], IoT represents 'anything at all, depending on requirements.' Cisco defines IoT as a network of connected physical objects. Cisco also uses the term Internet of Everything for both physical and virtual objects. Cisco states that "IoE brings together people, process, data, and things to make networked connections more relevant and valuable than ever before—turning information into actions that create new capabilities, richer experiences, and unprecedented economic opportunities for businesses, individuals, and countries."

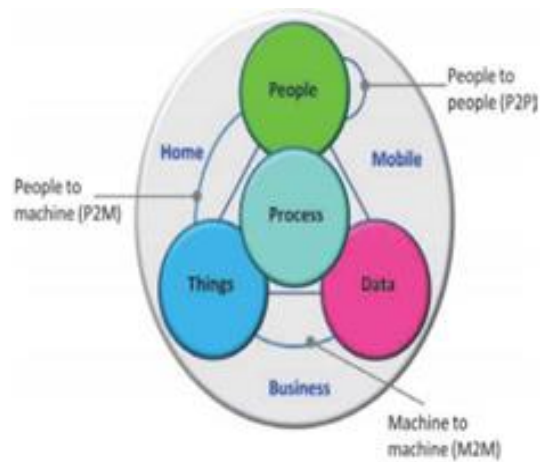


Fig:1 Internet of everything

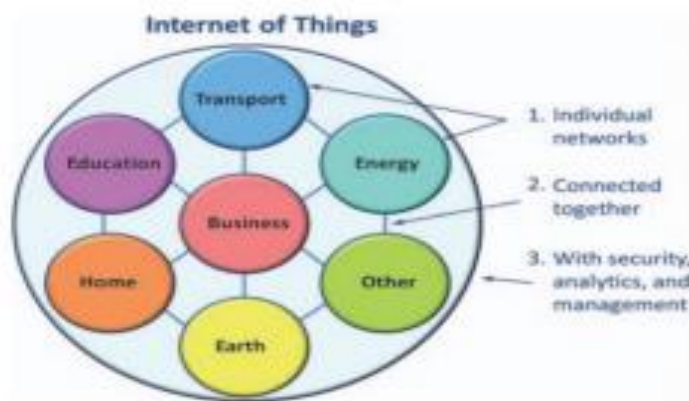


Fig:2 Using internet in all different sectors

According to Gartner's forecast, 20.8 billion new things will be connected by 2020. According to Machine Research, the growth of IoT connections is : from 6 billion in 2015 to 27 billion in 2025. The number of cellular IoT connections will be 2.2 billion, and 45% of these will be in connected cars. The revenue forecast of IoT in 2025 is 3 trillion US\$. IoT will also generate over two zettabytes of data, generally from consumer electronic devices.





Fig: 3 Five predictions of IOT till 2025

## Previous Studies

**2.1 The Traditional Education:** Traditional classroom education has been around for decades and almost all members of society, and for many centuries using it. Class room education continues to be an important way of learning, and there are many benefits that accompany this method of education. In a traditional education, students are able to interact with their teachers and personally.

### Online Education:

The results of this study indicated that the participants were aware of the facilities of using e-books and they were content with the facilities of usage. The main resource of multiplying education is the teachers therefore; the teachers should build a relationship with technology and should use it in a sufficient level in their current and future classes. Moreover, each teacher should follow technology and apply it in their course. Therefore, the design of the digital electronic book is prepared to be adaptive for this generation of students because in general, they are digital readers.

## 2. Objective of the study

The objective of this study is derived as below,

- To study the need of IoT in Education.
- To know the Technology enhanced learning
- To understand the Internet of Things

- Advantages of IoT in Modern Education

### **3. Research Methodology**

This research was carried out based on the secondary data and the data. The data used for this research is descriptive and qualitative from secondary sources. This data has been filtered and analyzed in a structured analytical format. Since the topic is evolutionary and is subject to fast changes, only the qualitative data updated from time to time is used. The main source of data collection is wiki, websites, blogs, YouTube, books, articles and journals.

#### **2.1 To study the need of IoT in Education.**

##### **Individualization**

The Student can more and inside based on the interest with personalized learning pattern and this will lead much more opportunity to learn with complete understanding the subject.

- **Smart Campus using IoT**

In general now a day's all universities, colleges and schools are connected with internet of things. The concept of smart campus involves with the intellectual environment equipped with fully sophisticated and installed with advanced technology smart things and aids. The smart classroom occupied with the set of smart things such as LCD Projector, Microphone, Speaker, cameras, smart board / Interactive board, Visualizer, Virtual classroom, Google Classroom which can be used for the ICT based enabled learning. A smart campus is a collection of smart multiple things [5]. The smart campus may include the following things.

- IoT based Classroom
- IoT based Laboratories
- Possibilities of E-Learning
- Smart Library
- Smart Attendance system for faculty and Student
- Smart canteen
- Smart office

In addition to smart parking, smart tracking of student, wi-fi enabled campus. The purpose of the smart campus is making the environment user friendly.

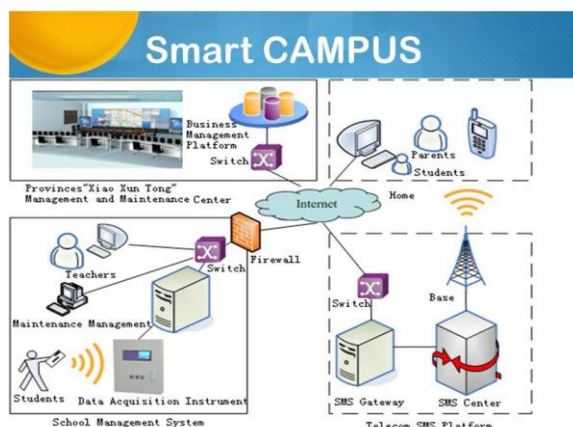


Fig :4 IOT in Smart campus

## 2.2 To know the Technology enhanced learning

- **IoT based Smart Classroom:**

The use of IoT devices for teaching and learning purposes is a top trend among institutions across the world which provides a new and innovative approach to education and classroom management [5]. Through smart classroom faculty can explain the subject in a more reality based and make the student to understand easily.

In the era of Digital technology, the rapid evaluation of Information and communication technology has created a new paradigm of internet known as Internet of Things. The Internet of Things changed the way to communicate with people and object in different manner. This has created the new form of communication between the teacher and student to allow them to improve the teaching and learning process. ICT have a great power to improve the quality outcomes of teaching learning.

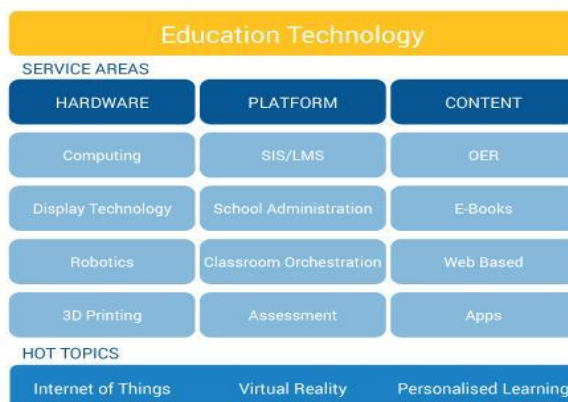


Fig:5 Educational Technology Market Research[8].

- **Advantage of Smart Classroom:**

Smart classroom plays a significant role in the student life. Smart classroom helps to transform the traditional education into modern education, with the help of smart education student can learn from anywhere, anytime anything and everything. The level of connectivity offered by the internet is beyond belief. It helps students to enrich the learning process all over the world. This offers to improve the quality of education and academic achievements. IoT enables to break the barrier of learning in the classroom. IoT give the platform to access globally. Some of the common tools are used in the classroom are.

- Smart board / Interactive white board
- LCD Projectors
- Lap tops and Tablet Pc
- E-Library
- ID Cards for Student and Faculty
- CC Cameras for security
- Attendance tracking systems
- Printer and Scanners
- Speakers and Mikes
- Media Center
- Environment friendly
- Advanced teaching and learning experience
- Easy maintenance



Fig:6 IOT in smart class rooms

Smart things are helps the teacher to explain the class in more interactive and more realistic way. The student can able to understand the concept very easily and put more attention with the help of the above mentioned smart devices in the Smart classroom. The flow of connected technology means professors and teachers could make grades faster. Their checking/grading also would be eased, less prejudiced and more efficient. When educators have devices connected to the cloud, they would be in better connect. Thus, tutor/ teachers could see which student requires more concern and focus. Other processes, with smart technology helps us in making lesson plans, adjusting schedules and many more. While the task is to connect over smart devices, teachers are able to focus more on their teaching and research.

- **IoT based Research:**

Research is a one of the emergent technology in the education system. Research gives the real opportunity to upgrade knowledge. Research will give the opportunity to know the concept very well. Internet of Things will give the more opportunity and it helps everyone to understand the concept and we come to know the opinion of others in the world. IoT will give the benefit of the wider research area and it will lead a valuable innovation to the world.



Fig :7 IOT in research

- **Smart Attendance System – Biometric Systems:**

Regularly taking attendance is a big task in the classroom. To overcome that we have introduced a new technology with the help of iot that is radio frequency identification (RFI) which will substantially help, biometric fingerprint sensor and password based technologies are integrated to develop a cost effective, reliable attendance management system [6]. Smart attendance system and biometric system are the most secured things, also it is very difficult to manipulate the data and complete integrity proof on the data and information.

The internet enabled radio frequency identification will enable to notify the assigned concerns on defined interval or customized periods.

The recorded data from the biometric can be stored and retrieved any time and each educational establishment wants it to be secure and endangered from any unsolicited visitors. However the specialists that are involved in security guard, they cannot monitor every corner of the facility. That is why IoT can help administration control. Facial recognition systems helps us to identify faces by scanning them and to be saved in data base. That is how the Internet of Things works and how it may be beneficial.



Fig:8 IOT used for security

- **IoT based Feedback Form:**

Google Form is a one of the platform to access the student with the help of the technology .It is a one of the easy way to take the feedback using the internet of things. Google Form is a open source available for everyone. Using this form student can answer the query from everywhere and any time.24/7 available in the internet.

- **IoT based Google Classroom:**

Google classroom is free. Google classroom can be accessed from any computer or mobile device via Google chrome. It is a blended platform with lot of benefits available for both faculty and students. Google classroom is a one of the online learning system, using this we can send, announce or pass any kind of information to the everyone. It has lot of benefits such as accessibility, Time saving, Communication, paperless transaction, collaboration, Data Analysis and feedback [7] etc. We don't need any papers to do assignments, as we can save our data through google classroom. The Internet of Things impacts education in a lot of ways. It is this asset

intellect, which enable institutions to make more informed decisions, in an attempt to improve operational efficiency, learning experience and campus security

### **2.3 To understand the Internet of Things**

As per the above discussion we can able to understand the value of Internet of Things in the society especially in the education system. IoT promotes a heightened level of awareness about our world [13]. IoT enables numerous applications ranging from the micro to macro and from the insignificant to the serious [13]. IoT plays a significant role in the field of education. IoT plays a major role everywhere in the society. The era of the technology our dream becomes true. IoT support the way to build the flexibility of the system and cost effective way. With the help of IOT we can transfer several areas in everyday life .Although it seem to be good in education.

Software development education is widely offered by most colleges and universities, offering fully online degree programs as well as the traditional on campus programs, which is helping the rural people who is far away from the university access get benefited.

### **2.4 Advantages of IoT in Modern Education**

Today's more and more tutors and educators are using the internet for the betterment of the education systems. The students are the main chain links of the education process. Internet of thing is a new system introduced to provide wide connectivity between the people and the technology where we cannot imagined before. The scope of learning is enormous with the help of the IOT based devices like Tablet, Laptops, Mobile Phones, Desktops, etc.It helps the students as follows.

#### **Individual learning**

Interactive based learning

- Increase the curiosity of learning
- Learn everywhere
- To learn and understand the things in easy and better way.
- To validate the information by interpret the data from various sources.

- Improve the learning Process
- No more loss of information
- Create the curiosity towards the subject
- The growth of engagement
- To improve the results
- Smart way to monitor the students

**Conclusion:**

The future of IoT is massively unlimited and will be improve a quality of education system because of advances in technology, though the IoT contain plenty of information ,however the user can get the relevant data and information by data interpreting, The Wi-Fi as made it possible to connect people and machines. IoT can change our whole world within few years.Strongly believed that the use of technology especially the era of IoT transform the educational environment towards the modern education [9].With the help of IoT we can collect the lot of data, that data we can convert to Information . These kinds of Information are going to help in the society for everybody everywhere.the students who is not able to attend the regular physical classes ,can be highly benefited on the learning progress ,because of the wider education by IoT the quality of human will be improved and the poverty of the nation subsequently improved .



**Reference:**

1. <http://ijsetr.org/wp-content/uploads/2016/02/IJSETR-VOL-5-ISSUE-2-472-476.pdf>
2. <https://www.happiestminds.com/Insights/internet-of-things/>
3. [https://en.wikipedia.org/wiki/Internet\\_of\\_things](https://en.wikipedia.org/wiki/Internet_of_things)
4. <http://journals.sfu.ca/onlinejour/index.php/i-jep/article/viewFile/7187/4604>
5. <https://www.forbes.com/sites/jacobmorgan/2014/05/13/simple-explanation-internet-things-that-anyone-can-understand/#406c48d51d09>
6. [https://www.researchgate.net/publication/323425616\\_IOT\\_CONCEPT\\_APPLICATION\\_IN\\_EDUCATIONAL\\_SECTOR\\_USING\\_COLLABORATION](https://www.researchgate.net/publication/323425616_IOT_CONCEPT_APPLICATION_IN_EDUCATIONAL_SECTOR_USING_COLLABORATION)
7. [http://paper.ijcsns.org/07\\_book/201705/20170520.pdf](http://paper.ijcsns.org/07_book/201705/20170520.pdf)
8. <https://ieeexplore.ieee.org/document/8249106/>
9. <https://www.thetechadvocate.org/10-benefits-of-google-classroom-integration/>
10. <http://journals.sfu.ca/onlinejour/index.php/i-jep/article/viewFile/7187/4604>
11. <https://medium.com/@TeksunGroup/importance-of-internet-of-things-iot-in-our-liveb71e53d50a44>
12. <https://www.ariasystems.com/blog/internet-things-important/>
13. <https://www.cleveroad.com/blog/iot-in-education-main-solutions-iot-brings-to-educational-sector>



# A Review on enhanced Multilabel Classification Techniques using Artificial Neural Networks

G.NIRMALA JOYCEE<sup>1</sup>, P.PRASHANTHI<sup>2</sup>

<sup>1,2</sup> Assistant Professor ,  
Department of Computer Science,  
St. Ann's College for Women (A),Mehdipatnam,  
Osmania University Hyderabad, India

**Abstract:** This paper considers the multilabel classification problem, which is a generalization of traditional two-class or multi-class classification problem. In multilabel classification a set of labels (categories) is given and each training instance is associated with a subset of this label-set. The task is to output the appropriate subset of labels (generally of unknown size) for a given, unknown testing instance. Some improvements to the existing neural network multilabel classification algorithm, named BP-MLL, are proposed here. The modifications concern the form of the global error function used in BP-MLL. The modified classification system is tested in the domain of functional genomics, on the yeast genome data set. Experimental results show that proposed modifications visibly improve the performance of the neural network based multilabel classifier. The results are statistically significant.

**Keywords:** Classifications, Artificial Neural Networks, Machine Learning.

## 1. Introduction

Classification in machine learning is the problem of identifying the function  $f(x)$  that maps each attribute vector  $x_i$  to its associated target label  $y_i$ ,  $i = 1, 2, \dots, n$ , where  $n$  is the total number of training samples [1]. Traditional classification problems in machine learning involve associating each of the sample instances with a single target label. i.e. unique target association. This type of classification is called single label classification. On the contrary, several real world classification problems involve data samples which correspond to a subset of target labels [6]. This results in the emergence of a new category of machine learning classification called the multi-label classification. The multi-label classification problems are gaining much importance and attention in the recent years due to the rapidly increasing real world application areas. Some of the real world application domains that require multi-label classification are medical diagnosis, text categorization [4-8], genomics, bioinformatics, multimedia, emotion, music categorization, scene and video categorization, map labeling, marketing etc. Due to the omnipresence of multi-label problems in a wide range of real world scenarios, multi-label classification is an emerging field in machine learning classification [15].

Classification errors occur when the classes overlap in the selected feature space. Various classification methods have been developed to provide [9] different operating characteristics, including linear discriminate functions, artificial neural networks (ANN), k-nearest-neighbor (k-NN), radial basis functions (RBF) and support vector machines (SVM).

## 2. Background

The sparse literature on multi-label classification is primarily geared to text classification or bioinformatics. For text classification, Schapire and Singer [21] proposed BoosTexter, extending AdaBoost to handle multi-label text categorization. However, they note that controlling complexity due to overfitting [7] in their model is an open issue. McCallum [14] proposed a mixture model trained by EM, selecting the most probable set of labels from the power set of possible classes and using heuristics to overcome the associated computational complexity [12]. However, his generative model is based on learning text frequencies in documents, and is thus specific to text applications. Bosubabu Sambana' approach is most similar to ours in that he uses a set of binary SVM classifiers [14]. He finds that SVM classifiers achieve higher accuracy than others. However, he does not discuss multi-label training models or specific testing criteria. In bioinformatics, Bosubabu Sambana [11][15] extended the definition of analysis to include multi-label data, but they use a conclusionhierarchy as their baseline algorithm approaches [6]. As they stated, they chose a decision tree because of the sparseness of the data and because they needed to learn accurate rules, not a complete classification. However we desire to use Support Vector Machines for their high accuracy in classification [8].

A related approach to image classification consists of segmenting and classifying image regions (e.g., sky, grass). A seemingly natural approach to multi-label scene classification is to model such scenes using combinations of these labels. For example, if a mountain scene is defined as one containing rocks and sky and a field scene as one containing grass and sky, then an image with grass, rocks, and sky would be considered both a field scene and a mountain scene [6].

However, in some classification tasks, it is likely that some data belongs to multiple classes, causing the actual classes to overlap by definition. In text or music categorization, documents may belong to multiple genres, such as government and health, or rock and blues [4-6] [18][19][20]. Architecture may belong to multiple genres as well. In medical diagnosis, a disease may belong to multiple categories, and genes may have multiple functions, yielding multiple labels [15]. A problem domain receiving renewed attention is semantic scene classification categorizing images into semantic classes such as beaches, sunsets or parties. Semantic scene classification finds application in many areas, including content-based indexing and organization and content-sensitive image enhancement. Many current digital library systems allow a user to specify a query image and search for images "similar" to it, where similarity is often defined only by color or texture properties [7].

This so-called query by example process has often proved to be inadequate. Knowing the category of a scene helps narrow the search space dramatically, reducing the search space, and simultaneously increasing the hit rate and reducing the false alarm rate. Knowledge about the scene category can find also application in context-sensitive image enhancement. While an algorithm might enhance the quality of some classes of pictures [6], it can degrade others. Rather than applying a generic algorithm to all images, we could customize it to the scene type [8]. In the scene classification domain, many images may belong to multiple semantic classes. The Figure -2 shows an image that had been classified by a human as a beach scene. However, it is clearly both a beach scene and an urban scene. It is not a fuzzy member of each (due to ambiguity), but is fully a member of each class (due to multiplicity) issimilar [14].

Automatic data classifiers, where a tested object is assigned to one of pre-defined classes, are broadly used worldwide and they are very useful in many applications. However, some data do not fit into this classification scheme [10]. For instance, when listening to a piece of music from an audio database, one can feel various emotions, and when such data are classified with respect to these emotional states, multi-label classification is much more useful [11].

In this case, each piece of music can be labeled with various emotions associated to this music. Therefore, the authors decided to investigate multi-label classification of data, how one can produce a classifier, and how the classification quality can be tested in multi-label case [7].

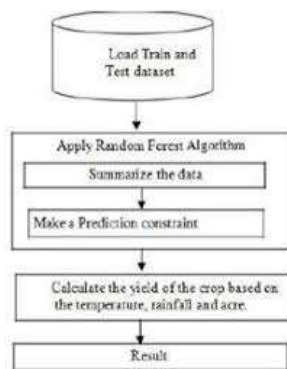


Figure.1: Working Mechanism

The traditional single label classification problems maps each of the input samples to a unique target label from the pool of available target labels. The single label classification problems can be categorized into binary and multi-class classification [8]. When the number of available target labels is two, it is called binary classification. Binary classification is the most fundamental classification problem in which the input sample belongs to either of the two target class labels [5]. Examples of binary classification problems include biometric security, medical diagnosis, etc.

When the number of available target labels is greater than two, the classification problem is called multi-class classification. Biometric identification, character recognition and other similar classification problems are examples of multi-class classification. Binary classification is a special case of multi-class classification in which the number of target labels is two [11]. There are several real world applications in which the target labels are not mutually exclusive and require the need for multi-label classification.

Multi-label classification involves associating each of the input samples with a set of target labels. Therefore, multi-label classification forms the superset of binary and multi-class classification problems [13]. When compared to single label classification, multi-label classification is more difficult and more complex due to the increased generality of the multi-label problems [16]. Several machine learning techniques is available in the literature for multi-label classification problems. The existing multi-label classifiers available in the literature are based on Support Vector Machines (SVM), Decision Trees (DT), and Extreme Learning Machines (ELM) etc.

The machine learning techniques available can be broadly categorized into two categories: Batch learning and online learning. Batch learning techniques involve collection of all the data samples in prior and estimating the system parameters by processing all the data concurrently [14]. Batch learning techniques require all the training data beforehand and cannot learn from streaming data [15].

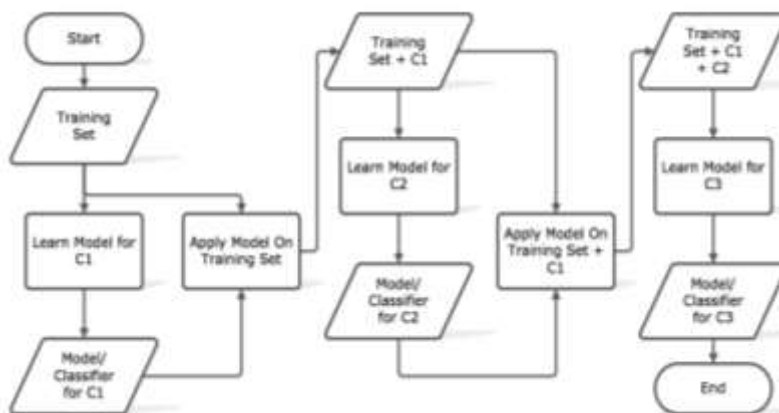


Figure.2: Block diagram of internal Mechanism

## Online Learning Methods

There is limited number of techniques available in the literature on multi-label classification for data streams. A simpler approach is to use batch learning classifiers that trains on new batches of data streams by replacing the classifiers of previous batches. This type of learning is called batch incremental learning. The first work on multi-label classifier for data streams is based on ensemble of classifiers which are trained on successive data chunks [11]. The paper by proposes multi-label stream classification by extending the heoffding tree by using batch multi-label classifier in each node.

Spyromitros-Xioufis proposes binary relevance and kNN based multi-label classifier for data streams. Microsoft developed an Active Learning framework for multi-label classification as the result of the increase in demand for the need of multi-label classification in real world multimedia datasets. A Passive-Aggressive method is proposed by Crammer et. al for multi-label classification [12]. The Passive Aggressive and the Bayesian Online Multi-label Classification techniques are application specific and are implemented only for text categorization datasets [22].

## Extreme Learning Machines

ELM is a single-hidden layer feed forward neural network based learning technique. The special feature of ELM is that the initial weights and the hidden layer bias can be selected at random [8]. This results in high speed training and small number of tunable parameters thus enabling ELM to have fast learning speed and generalization of performance [11]. The universal approximation capability and generalization ability are the key distinguishing factors of ELM. Several variants of ELM have been developed [13].

## Multi-label Classification Methods

Multi-label classification has already been performed in numerous applications in text mining and scene classification domains, where documents or images can be labeled with several labels describing their contents [1-3]. Such a classification requires considering additional issues, including the selection of the training model, as well as set-up of testing and evaluation of results on their classification [14][18].

We can group the existing methods for multi-label classification into two main categories: a) problem transformation methods, and b) algorithm adaptation methods. We call problem transformation methods, those methods that transform the multi-label classification problem either into one or more single-label classification or regression problems, for both of which there exists a huge bibliography of learning algorithm [6]s. We call algorithm adaptation methods, those methods that extend specific learning algorithms in order to handle multi-label data directly [16].

The second improvement of is SVM-specific and concerns the margin ofSVMs in multi-label classification problems [6]. They improve the margin by a) removing very similarnegative training instances which are within a threshold distance from the learnt hyper plane, and b)removing negative training instances of a complete class if it is very similar to the positive class,based on a confusion matrix that is estimated using any fast and moderately accurate classifier on a held out validation set. Note here that the second approach for margin improvement is actually SVMindependent. Therefore, it could also be used as an extension to PT4.

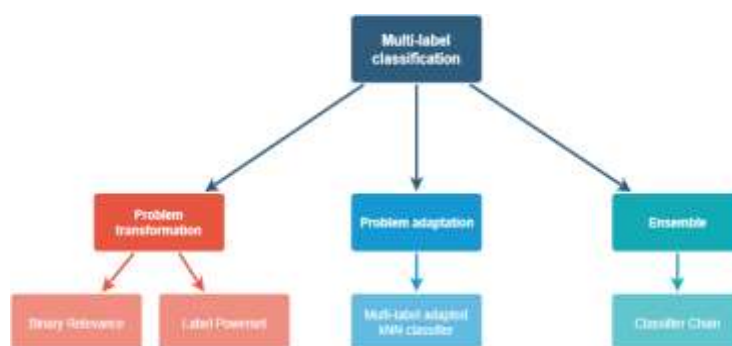


Figure.3: Multi-Label Text Classification

A probabilistic generative model according to which, each label generates different words. Based on this model a multi-label document is produced by a mixture of the word distributions of its labels [6][11]. The parameters of the model are learned by maximum a posteriori estimation from labeled training documents, using Expectation Maximization to calculate which labels were both the mixture weights and the word distributions for each label. Given a new document the label set that is most likely is selected with Bayes rule. This approach for the classification of a new document actually follows the paradigm of PT3, where each different set of labels is considered independently as a new class [17].

Elisseff and Weston present a ranking algorithm for multi-label classification. Their algorithm follows the philosophy of SVMs: it is a linear model that tries to minimize a cost function while maintaining a large margin [11]. The cost function they use is ranking loss, which is defined as the average fraction of pairs of labels that are ordered incorrectly. However, as stated earlier, the disadvantage of a ranking algorithm is that it does not output a set of labels [19].

### Application to Classification

Bosubabu Sambana proposed a new work Multilevel classification problem generalizes traditional two-class or multi-class classification [15] since each instance in the training/testing set is associated with several (usually more than one) classes (labels). The problem is not easy to solve also because the size of the label-set associate with particular unseen instance is generally unknown [18]. Various approaches to tackle this problem were presented in the literature, but – up to our knowledge and there has been only one attempt to apply a neural network for solving this task [2][6]. In this paper a few modifications of the global error function proposed in are presented and experimentally evaluated. Generally, all of them improve performance of the multilevel neural classifier [12].

The improvements in case of the two most elaborate functions, and are noticeable and statistically significant [7]. Overall, including the threshold values into the error function and considering differences between the rank values and the thresholds proved to be a promising direction for improvement of the multilevel classifier performance [9]. Currently, we are focused on performing more tests (especially with other sizes of hidden layer) and on other data sets in order to further verify the efficacy of proposed modifications [10].

### 3. Proposed Approach Classification Analysis

This paper exploits the inherent high speed nature of the ELM and OS-ELM to develop an online sequential multi-label classifier for real-time streaming data applications. The key novelty of the proposed approach is that, there are no online techniques available thus far in literature to perform real-time multi-label classification [6]. In single label classification problems such as binary and multi-class classification, each input sample corresponds to a single target label.

A task that also belongs to the general family of supervised learning and is very relevant to multi-label Classification is that of ranking. In ranking the task is to order a set of labels  $L$ , so that the topmost labels are more related with the new instance [16]. There exist a number of multi-label classifications methods that learn a ranking function from multi-label data. However, a ranking of labels requires Post-processing in order to give a set of labels, which is the proper output of a multi-label classifier [8].

In certain classification problems the labels belong to a hierarchical structure. A web page may be labeled using one or more of those classes, which can belong to different levels of the hierarchy[19]. The top level of the MIPS (Munich Information Centre for Protein Sequences) hierarchy consists of classes such as: Metabolism, Energy, Transcription and Protein Synthesis. Each of these classes is then subdivided into more specific classes, and these are in turn subdivided, and then again subdivided, so the hierarchy is up to 4 levels deep[20]. When the labels in a data set belong to a hierarchical structure then we call the task hierarchical classification. If each example is labeled with more than one node of the hierarchical structure, then the task is called hierarchical multi-label classification. In this paper we focus on flat (non-hierarchical) multi-label classification methods [6].

Therefore the classifier is required to identify the single target label corresponding to the input sample. On the contrary, in multi-label classification[21][8], each of the input samples belongs to a subset of target labels. Therefore, the multi-

label classifier is required to identify both the number of labels and the identity of the labels in order to perform multi-label classification. This results in the increased complexity of the multi-label classification problems. Another key challenge in implementing a generic multi-label classifier is that, not all datasets are equally multi-labeled [15]. The degree of multi-liableness varies for every dataset [18]. The increased complexity and the varying degree of multi-liableness are the two major challenges in developing a multi-label classifier [12].

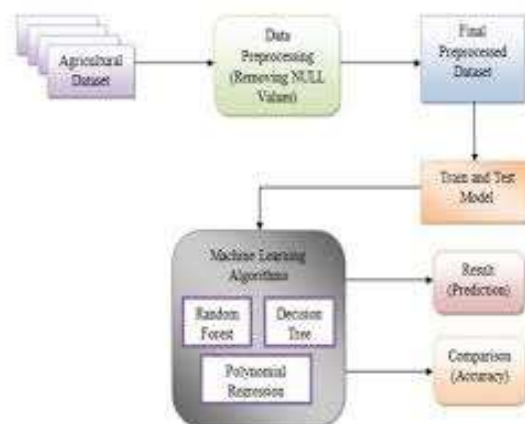


Figure.4: Multi-level preprocessing operations

Pre-processing and post-processing of data are of prime importance in extending the ELM based technique for multilevel classification.

**Initialization:** The fundamental parameters of the ELM network such as the number of hidden layer neurons and the activation function are initialized [15]. The number of hidden layer neurons is selected for each dataset so as to avoid the over fitting problem. The input weights and the bias value of the network are randomly initialized [8].

**Pre-processing:** In single label classification, each of the input samples corresponds to only one target class. Therefore, the dimension of the target output label is always fixed at 1. On the contrary, in multi-label classification, each input is associated with an M-tuple output label with each element of the set as 0 or 1 representing the belongingness of the input corresponding to the target labels. Therefore the dimension of the target output label is 'M'. The label set denoting the belongingness for each of the labels is converted from unipolar representation to bipolar representation [13].

**ELM Training:** The processed input is then supplied sequentially to the online sequential variant of the ELM technique.

**Multi-label Identification:** The multi-label identification step is the key step in extending the ELM based technique for multi-label classification. As foreshadowed, multi-label classifiers are required to predict both the number of target labels and the identity of the target labels corresponding to 5 each of the input samples [6]. Since the number of labels corresponding to each input is completely unknown and dynamic, a thresholding based technique is used.

The threshold value is selected during the training phase such that it maximizes the separation between the family of labels the input belongs to and the family of labels the input does not belong to. Setting up of the threshold value is of prime importance as it directly [15] affects the performance of the classifier. The raw output values Y obtained from the previous step is then compared to the threshold value [8]. The number of raw output values that are greater than the threshold determines the number of target labels corresponding the input sample and the index of the corresponding values determines the identity of the target labels. The overview of the proposed algorithm is summarized [6][21].

## 4. Conclusion

The proposed multi level classification technique is a real-time online multi-label classifier for streaming data applications. The performance of the proposed method is experimented on five datasets of different domains with a wide range of LC and LD. From the analysis of evident that the modified method is consistent and outperforms the existing state-of-the-art techniques in terms of speed and remains one of the top methods in terms of performance.

This paper introduces a step-by-step and end-to-end methodology of how to design and train a scalable multilabel classifier. This methodology also shows how to expand the capability of a single labeled deep learning model into a multilabel classifier by leveraging on transfer learning with low cost of labeling and achieving impressive accuracy. Using our methodology, a single model can achieve multiple classifications on an image without an increased cost. This method is quite useful for exploiting a single image for various classifications.

## References

- [1] “ Multi-Label Classification: An Overview “, Grigorios Tsoumakas, Ioannis Katakis
- [2] R. Grodzicki, J. Mańdziuk, and L. Wang , “ Improved Multilabel Classification with Neural Networks “
- [3] Y. Jia, E. Shelhamer, J. Donahue, S. Karayev, J. Long, R. Girshick, S. Guadarrama, and T. Darrell, “Caffe: Convolutional architecture for fast feature embedding,” in Proceedings of the 22nd ACM international conference on Multimedia. ACM, 2014, pp. 675–678.
- [4] Boutell, M., Shen, X., Luo, J., Brown, C.: Multi-label Semantic Scene Classification. Technical Report, Dept. of Computer Science, U. Rochester (2003)
- [5] L. Zhang, Y. Jin, X. Yang, X. Li, X. Duan, Y. Sun, and H. Liu, “Convolutional neural network-based multi-label classification of pcb defects,” *The Journal of Engineering*, vol. 2018, no. 16, pp. 1612–1616, 2018.
- [6] Bosubabu Sambana,” Block chain approach to cyber security vulnerabilities attacks and potential Countermeasures”, *International Journal of Security and Its Applications*, ISSN: 2207-9629 IJSIA, Vol. 14, No. 1 (2020), pp.1-14, <http://dx.doi.org/10.33832/ijisia.2020.14.1.01>
- [7] Bosubabu Sambana, “Internet of Things: Applications and Future Trends”, *International Journal of Innovative Research in Computer and Communication Engineering*, Vol. 5, Issue 3, March 2017, ISSN (Online): 2320-9801,
- [8] Bosubabu Sambana, “Identifying Datasets by Pattern Recognition Techniques using Neural Networks” *Asian Journal of Computer Science and Technology* ISSN: 2249-0701 Vol. 6 No. 1, 2017, pp.34-39.
- [9] Bosubabu Sambana, “Signal Processing and Display of Linear Frequency Modulated Continuous Wave Radar on a Chip” Published in *International Journal of Trend in Research and Development (IJTRD)*, ISSN: 2394-9333, Special Issue, NCETC-17, April 2017.
- [10] Bosubabu Sambana , “An Artificial Intelligence Approach to Social Networks Agent Task Scheduling Analysis in Map Reduce for Sentiment Opinion Analysis” , 2020 IEEE International Symposium on Sustainable Energy, Signal Processing and Cyber Security (IEEE-iSSSC 2020)
- [11] Bosubabu Sambana et al. “Implementation of Securely Sharing Critical Information in Cloud Environment Using Mediated Certificate less Encryption System”, *International Journal & Magazine of Engineering, Technology, Management and Research*, ISSN No: 2348-4845, Volume No: 2 (2015), Issue No: 11(November).
- [12] Bosubabu Sambana, “An artificial intelligence approach to fake currency detection system”, *International Journal of Signal Processing, Image Processing and Pattern Recognition*, ISSN: 2207-970X, IJSIP, Vol. 12, No. 3 (2019), pp.1-16 . <http://dx.doi.org/10.33832/ijcip.2019.12.3.01>.
- [13] Shoulder Surfing Experiments: A Systematic Literature Review. Available from: [https://www.researchgate.net/publication/343978396\\_Shoulder\\_Surfing\\_Experiments\\_A\\_Systematic\\_Literature\\_Review](https://www.researchgate.net/publication/343978396_Shoulder_Surfing_Experiments_A_Systematic_Literature_Review).
- [14] Bosubabu Sambana, "Integrative Spectrum Sensing in Cognitive Radio using Wireless Network”, *Springer Nature Conference - International conference on Remote Sensing for Disaster Management (ICRSDM-2017)* during 11-13 October 2017 at Andhra University-Visakhapatnam. First Online: 24 June 2018, Publisher Name: Springer, Cham. Print ISBN: 978-3-319-77275-2, Online ISBN: 978-3-319-77276-9
- [15] Bosubabu Sambana, " Air Pollution Monitoring and Prediction System using the Internet of Things " , *International Journal of Research and Development in Engineering Sciences* , ISSN:2582-4201 , Volume: 2, Issue: 3 , Year: 2020
- [16] Bosubabu Sambana, “ Smart Agricultural activities Monitoring and Control system using an Internet of Things” , *Journal of Xidian University*, ISSN No:1001-2400 , Volume-14 Issue-7, July 2020,Page No: 1645 – 1654



- [17] Bosubabu Sambana, “ Artificial Intelligent Structure User-Friendly Multi-flexible Bed Cum Wheelchair Using Internet of Things ”, Springer Nature - Lecture Notes in Networks and Systems book series (LNNS, volume 105), Springer Nature Singapore Pte Ltd. 2020
- [18] Bosubabu Sambana, “ Vehicle Tracking and Accident Detection System using Internet of Things ”, International Conference on Smart Technologies in Data Science and Communication (Smart DSC-2018) , Advanced Science and Technology Letters Vol.147 (SMART DSC-2017), pp.463-467.
- [19] Bosubabu Sambana, “Implementation of Securely Sharing Critical Information in Cloud Environment Using Mediated Certificate less Encryption System”, International Journal & Magazine of Engineering, Technology, Management and Research, ISSN No: 2348-4845, Volume No: 2 (2015), Issue No: 11(November).
- [20] Bosubabu Sambana, “Identifying Datasets by Pattern Recognition Techniques using Neural Networks” , Asian Journal of Computer Science and Technology ISSN: 2249-0701 Vol. 6 No. 1, 2017, pp.34-39.
- [21] Bosubabu Sambana, “ Privacy-preserving Authentication Protocol using Trusted Third Party Secure Data Sharing in Cloud Computing ”, International Journal & Magazine of Engineering, Technology, Management and Research , ISSN No: 2348-4845, Volume No: 3 (2016), Issue No: 3 (March)
- [22] Bosubabu Sambana, “World Wide Web: Web Page Segmentation”, International Journal & Magazine of Engineering, Technology, Management and Research, ISSN No: 2348-4845, Volume No: 3 (2016), Issue No: 3 (March).
- [23] Rajasekar Venkatesan<sup>1\*</sup>, Shiqian Wu , Mahardhika Pratama, “ A Novel Online Real-time Classifier for Multi-label Data Streams”.





*Anal. Bioanal. Chem. Res., Vol. 8, No. 3, 209-217, July 2021.*

## Nanomaterial Assisted Electrochemical Detection of Isolated Piperine: a Phytochemical From Long Pepper

Khairunnisa Amreen\* and M. Sujatha

*Department of Chemistry-PG, St. Anns' College for Women-Mehdipatnam, Hyderabad-500078, India*

*(Received 22 October 2020 Accepted 16 February 2021)*

Herein, piperine, a phytochemical present in long pepper was quantitatively analyzed *via* an electrochemical technique using a chemically modified electrode. Mesoporous nanomaterial was utilized as a base matrix to carry out the experiments. The piperine was isolated from crude long pepper through a standard procedure. Glassy carbon electrode was chemically modified with mesoporous carbon matrix and isolated piperine designated as GCE/GMC@piperine. The cyclic voltammetry response gave a perfect redox response of piperine at  $E' = +0.2$  V vs. Ag/AgCl at  $50 \text{ mV s}^{-1}$  in pH 7 PBS. Effects of scan rate and solution pH were studied. Further, it was observed that a change in concentration of piperine is directly proportional to the redox peak current obtained. Therefore, this study could act as a key for quantitative analysis of piperine, a naturally occurring phytochemical in natural products such as pepper, long pepper, white pepper, etc. This is a prototype study and can be further extended to disposable screen printed electrodes for portable analysis.

**Keywords:** Piperine, Mesoporous carbon, Quantitative, Long pepper, Isolation

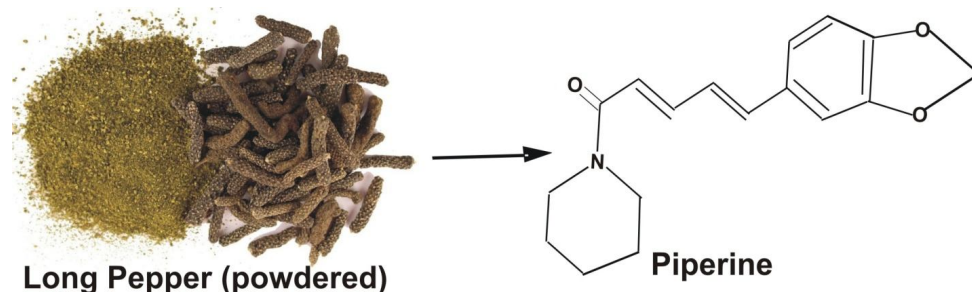
### INTRODUCTION

Nanotechnology has emerged as a cutting edge tool in various broad way applications such as medicinal, environmental, pharmaceutical, industrial, health management, information technology, electronics, engineering, etc. [1]. Employing nanotechnology, the researchers are successful to develop structured materials with target specified uses, for instance, nano material assisted drug delivery [2]. In addition, several other aspects including designing of energy storage devices [3], energy harvesting devices [4], anti-corrosive coatings [5] electrochemical/biosensors [6-9], greatly depend upon the usage of fabricated nano structures. They have also shown promising results as diagnostic tools, imaging and therapeutic substances for various diseases and their biomarkers [10]. Recent advanced application of nanomaterial is in phytochemistry. Herein, numerous well known

nanomaterials such as carbon nanotubes [11], metal-based nanoparticles [12], graphene oxide [13], mesoporous carbons [14], etc. are being utilized for detection of phytochemicals and phytotoxins [15].

Phytotoxins are the chemicals produced internally by the plants that can be hazardous to human. For example, chemicals such as cyanides, terpenes, metabolites, alkaloids, etc. which are essential for plant growth can be toxic to humans especially if consumed in high dose. Similarly, there are several bio-active phytochemicals provided by plants that are highly beneficial to human health [16]. These are generally referred as secondary metabolites produced *via* different mechanisms happening in chemical reactions of plant metabolism. The studies conducted showed that a massive group of phytochemicals can play a key role in functioning of human cells [17]. Many studies have proven that phytochemical rich foods help in improving health [18]. Furthermore, many phytochemicals are reported to be useful as the therapeutic agents [19]. Drugs developed from significant phytochemical are prevailing the pharmaceutical market in recent times. Some of the well known

\*Corresponding author. E-mail: khairunnisa.amreen90@gmail.com



*Scheme 1.* The image of crude long pepper and the chemical structure of piperine

phytochemicals with known therapeutic value are curcumin [20] from turmeric, eugenol [21] from cloves, zingerone [22] from ginger, carotene [23] from carrot, capsaicin [24] from capsicum, and allicin [25] from garlic. One of the simple phytochemicals present in every house hold kitchen is piperine [26]. It is a significant bio-active phytochemical present in black pepper, long pepper, white pepper.

Piperine is an alkaloid in pepper. Hans Christian Orsted, in 1819, was the first person to isolate and extract piperine. It is a yellow crystal compound. The IUPAC name of piperine is 1-(5-[1,3-benzodioxol5-yl]-1-oxo-2,4-pentadienyl) piperidine [27]. Scheme I shows a typical structure of piperine. It is basically a weak base which decomposes to piperic acid upon acid/basic hydrolysis [28]. Some of the therapeutic uses of piperine include antioxidant property, anti-inflammatory, anti-bacterial, anti-fungal, anti-ulcer, anti-diabetic, anti-septic, anti-asthmatic, anti-cancer effects, cold, flu, fever, diuretic, and gastrointestinal disorders [29]. Although, piperine's therapeutic, culinary, and biological activities are well known, very few reports are available exploring the piperine electrochemical activity. The present work focuses on isolation of piperine from long pepper through traditional method and studying its electro-active nature *via* nanomaterial-based electrodes. Long pepper, also known as "Pipli" or "Pipal" is a well known therapeutic agent in Ayurveda [30]. Scheme 1 gives a typical image of long pepper. The major constituent of long pepper is alkaloids which impart pepper like pungency. The maximum amount of piperine is present in the underground part of the stem and roots of long pepper. The piperine is slightly more in amount in long pepper in comparison to black pepper [28]. A conventional Soxhlet

apparatus is employed here for a selective isolation of piperine from long pepper. The isolated piperine is further explored for electro-chemical redox behavior through graphitized mesoporous carbon (GMC) nano material matrix. GMC is a porous carbon encompassing shallow graphitic networks. The pore size is (2-50 nm) amid the range of microporous (which is < 2 nm) and macroporous (which is > 50 nm) materials [31]. The usage of electrochemical techniques [32,33] for quantification of phytochemicals is very effective in comparison to other conventional methods. It offers features like high selectivity, reduced analysis time and reproducibility. Wang *et al.* reported electrochemical quantification of piperine extracted from black pepper corns utilizing a bare GCE. However, they avoided usage of nanomaterial, because of which they got an irreversible peak of piperine [34]. Nevertheless, the incorporation of the nanomaterial in the present work, assisted the piperine to undergo stable redox reaction, resulting in a perfect redox response of piperine. To the best of our knowledge, it is the first study utilizing piperine from long pepper. This study is a prototype, wherein, various phytochemicals, having potential to undergo oxidation/reduction reaction can be explored. In future, this approach can be a potential tool for quantification of phytochemicals in natural products with respect to their electro-active redox behavior.

## EXPERIMENTAL

### Chemicals Required

Long pepper was purchased from a local super market in Hyderabad. 95% ethanol was procured from Jolly

industries, Hyderabad, India. Potassium hydroxide (KOH), graphitized mesoporous carbon (GMC), multiwalled carbon nano tube (MWCNT), single walled carbon nanotube, double walled carbon nano tube (DWCNT), carbon nano fiber (CNF), graphite nano powder (GNP), and piperine were obtained from Sigma Aldrich. Phosphate buffer solution of pH 7 was prepared by monobasic/di-basic sodium hydrogen phosphate. All the other chemicals used were of analytical grade and used as received.

### Apparatus and Glassware

The apparatus and glassware used include Soxhlet from Borosil, CHI 660 instrument from Sinsil, magnetic stirrer, Whatman filter paper, glassy carbon electrode, platinum wire, Ag/AgCl electrode, electrochemical cell, water bath, beakers, round bottom (RB) flask, and funnel.

### Procedure

**Isolation of piperine.** The isolation of piperine was done by a reported standard procedure with slight modifications [35]. 50 gram of long pepper was weighed and crushed into fine powder and packed. It was inserted into the Soxhlet apparatus which was fixed to a RB flask. The RB flask was filled with approximately 250-300 ml of 95% ethanol. The entire set-up was kept on reflux for 3 h. Then, the ethanol was distilled and 50 ml of warm ethanolic-KOH solution (2%) was added. The mixture was stirred using a magnetic stirrer, and the insoluble part was dissolved in 4-5 min. After which, the mixture was filtered using a Whatman filter paper to eliminate the undissolved particles. The filtrate was warmed on the hot water bath for 15 min and 20 ml of distilled water was added. At this point, turbidity appeared and the yellow needle like particles of piperine formed were isolated. It was left over night to evaporate and then filtered again to obtain needle like crystals of piperine [35].

**Electrochemical studies.** The electrochemical studies were carried out using cyclic voltammetry (CV) in a standard conventional three electrode system comprising of a working electrode (WE); *i.e.*, glassy carbon (GCE) modified-carbon nano material, reference electrode (RE); *i.e.*, Ag/AgCl, counter electrode (CE), and platinum wire in 10 ml working volume of pH 7 phosphate buffer solution

(PBS). The set potential window was -0.5 to +0.8 V *vs.* Ag/AgCl at a scan rate of 50 mV s<sup>-1</sup>. Scheme 2a gives a representation of the electrochemical set up.

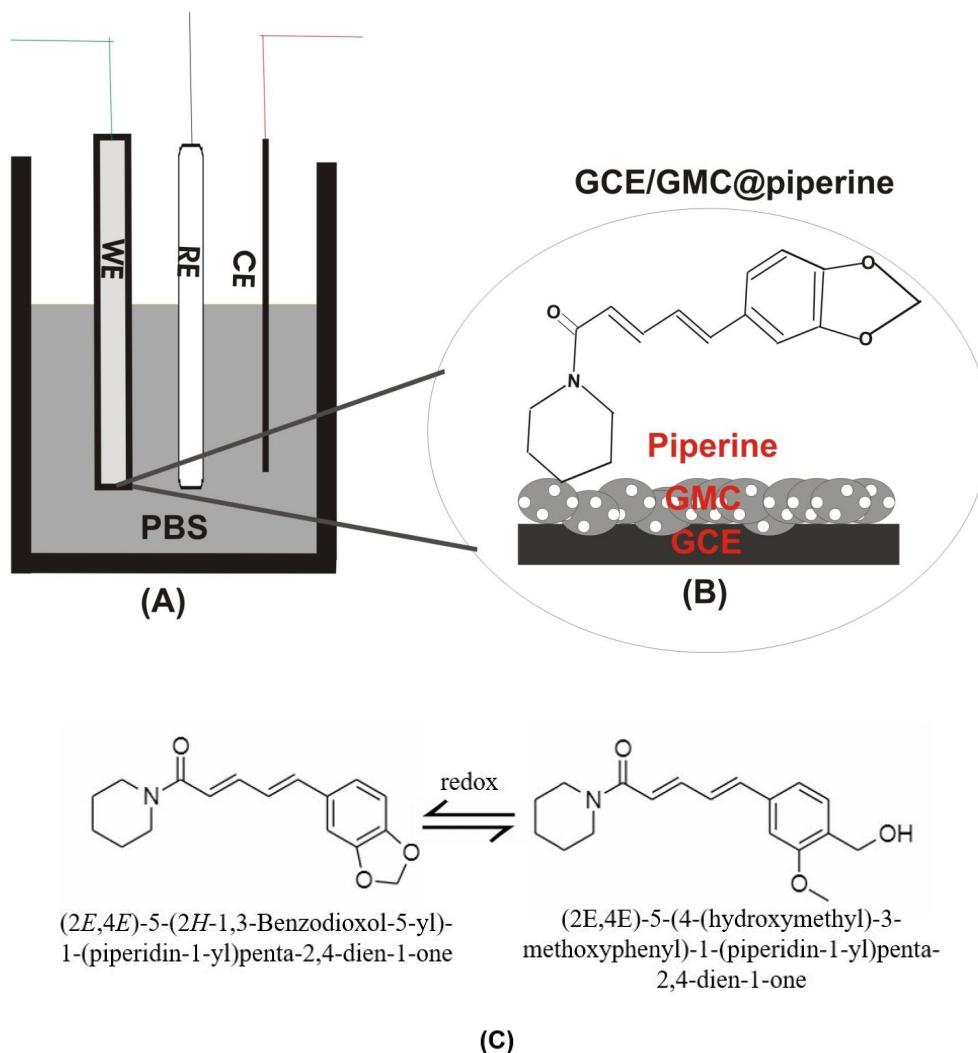
**Preparation of GCE/carbon-nanomaterial electrode.** GCE@carbon-nanomaterial electrode was prepared by drop casting 5  $\mu$ l dispersion of 2 mg of specified carbon nano material dispersed in 500  $\mu$ l of ethanol and sonicated for 15 min in an ultrasonicator bath. The electrode was left for air drying for about 5 min at room temperature.

**Preparation of GCE/carbon-nanomaterial@piperine electrode.** 2 mg of the obtained piperine through Soxhlet was dissolved in 1 ml of acetone. 5  $\mu$ l of this solution was top coated on the GCE/carbon-nanomaterial electrode. It was air dried for 5 min. Scheme 2b gives pictorial representation of the modified electrode.

## RESULTS AND DISCUSSION

### Screening of Various Carbon Nanomaterials

The phytochemicals are usually the concoction of polyhydrocarbons which are expected to be electroactive in nature and give electron transfer when a specified potential is applied. However, not all the phytochemicals have a feasibility to undergo electron transfer mechanism. Therefore, in such scenarios, nanomaterial matrix enhances the ability of phytochemicals to undergo oxidation and reduction. Piperine was expected to undergo electrochemical redox reaction when CV is performed. When CV was performed in the specified aforementioned parameters (50 mV s<sup>-1</sup>, for 10 cycles at -0.5 to 0.8 V *vs.* Ag/AgCl), piperine alone (GCE@piperine) failed to give any redox reaction as can be seen in Fig. 1a, wherein, glassy carbon electrode (GCE) was drop casted with 5  $\mu$ l of piperine, air dried and CV was performed. No current signal or peak is observed authenticating that, GCE alone could not support the electro activity of piperine. Nevertheless, when various carbon nanomaterial matrixes-based GCE were modified with piperine, a feeble response was observed. As observed in Figs. 1b-f, various nano materials such as DWCNT, SWCNT, MWCNT, GNP and CNF were tested. These nanomaterials assisted a little bit of electron transfer of piperine but could not give a perfect redox response.



*Scheme 2.* (A) Cartoon for the experimental set up. (B) Schematic representation of GCE/GMC@piperine. (C) Plausible mechanism of the redox reaction of piperine

### Optimized Carbon Nanomaterial Matrix

Figure 2a shows the optimal carbon nano material suitable to derive electro-activity of piperine. Graphitized mesoporous carbon (GMC) was the only carbon nanomaterial amongst all the tested materials that gave a perfect redox response of piperine. Probably, owing to the mesoporous nature,  $\pi$ - $\pi$  interactions [22] between the pores of carbon nanomaterial and piperine lead to the electron transfer behavior giving a perfect redox peak. CV response (Fig. 2a) showed a well-established, stable redox peak at

$E' = +0.2$  V vs. Ag/AgCl at  $50 \text{ mV s}^{-1}$  in 10 ml of pH 7 PBS with a surface excess  $\Gamma_{\text{pip}}$  value as  $19.8 \times 10^{-9} \text{ mol}^{-1} \text{ cm}^2$ . In order to get the confirmation that the obtained response was due to isolated piperine alone and not due to any other impurity, a control experiment was performed wherein commercially available piperine was subjected to CV in the same manner as that with the isolated one. It was found that the experimentally isolated piperine from long pepper and commercially purified bought piperine both give the redox peaks at the same peak potential coinciding with each other

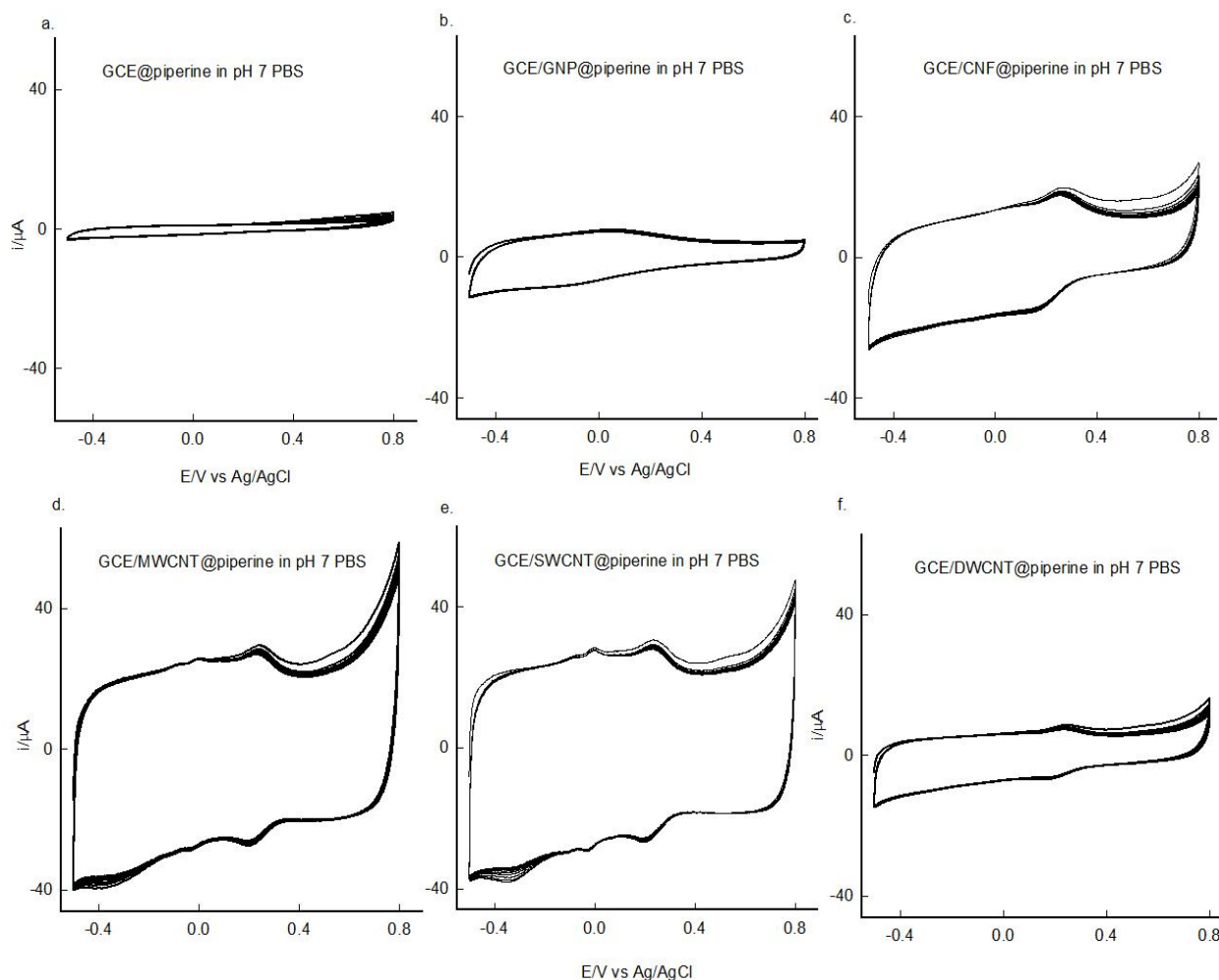


**Fig. 1.** A typical CV response of (a) GCE alone, (b) GNP, (c) CNF, (d) MWCNT, (e) SWCNT and (f) DWCNT@piperine in pH 7 PBS at  $50 \text{ mV s}^{-1}$ .

(Fig. 2b). Hence, it was confirmed that the electro active redox behavior recorded was of isolated piperine alone and not due to any other contaminant or constituent of long pepper. Scheme 2C is the plausible mechanism that piperine molecule undergoes. While applying the forward potential, the oxypiene moiety possibly undergoes oxidation giving an oxidation peak and the same undergoes reduction upon reversing the CV potential. Thus, a redox response with a stable peak is obtained. The chemical in-vitro oxidation mechanism gets mimicked over the electrode surface electrochemical redox mechanism [36].

### Microscopic Characterization

Figure 3 shows the microscopic characterization of the modified electrode with piperine. Herein, TEM images were taken at different magnifications including 50 nm, 100 nm and 200 nm. The mark A shows the areas with porous nature of GMC, B area is dark masked spots wherein piperine got adsorbed. The porous structures were masked by dark spots indicating the interaction of pores of GMC and isolated piperine.

### Effect of Potential Scan Rate

Effect of variable potential scan rate on the CV response

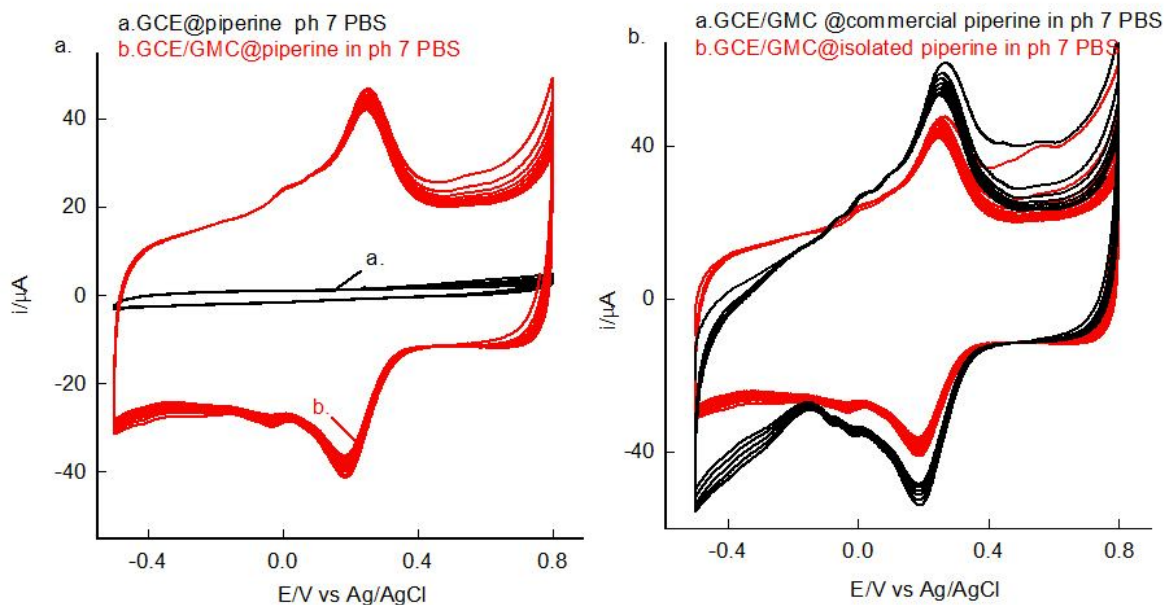


**Fig. 2.** (a) A comparative CV response of (a) GCE@piperine, and (b) GCE/GMC@piperine in pH 7 PBS at  $50 \text{ mV s}^{-1}$ ,  $n = 10$ . (b) A comparative CV response of GCE/GMC@commercial piperine and GCE/GMC@isolated piperine in pH 7 PBS at  $50 \text{ mV s}^{-1}$ ,  $n = 10$ .

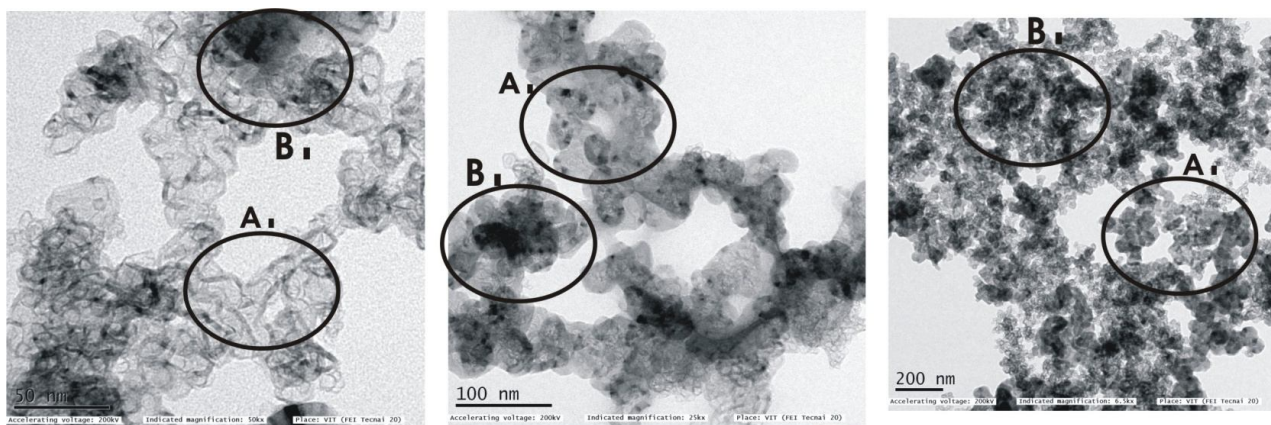


**Fig. 3.** TEM image of GCE/GMC@piperine at different magnifications. (a) The unmasked porous structure, and (b) the dark spots due to the piperine immobilization.

of GCE/GMC@piperine was also analyzed. Figure 4a demonstrates a comparative CV of various scan rates ranging from  $10$ – $500 \text{ mV s}^{-1}$ . A well-defined, stable, ordered increment in both the anodic and cathodic peak current value was obtained (Fig. 4a). A base-line corrected

calibration plot of peak current vs. different scan rates  $v$  ( $\text{mV s}^{-1}$ ) showed a linearity starting from the origin representing a surface-confined electron-transfer mechanism of the modified electrode (Inset Fig. 4a). This behavior also demonstrates an exceptional immobilization,

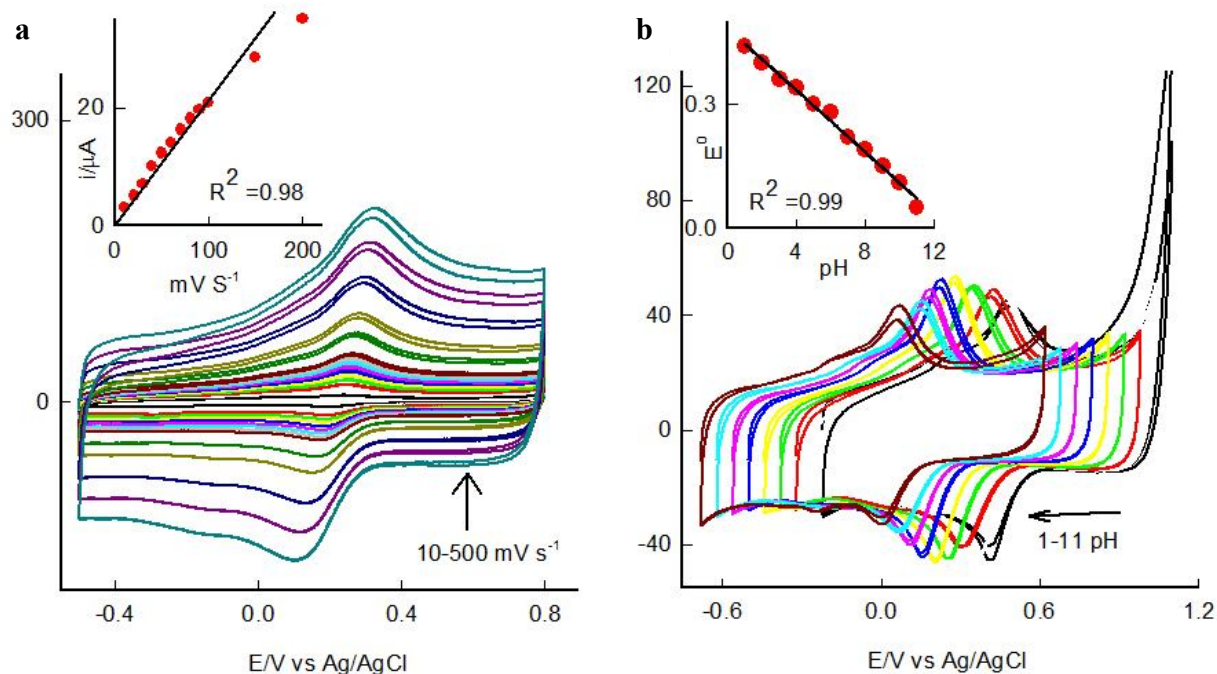


**Fig. 4.** (a) CV response of effect of various scan rates ( $10\text{-}500\text{ mV s}^{-1}$ ) of GCE/GMC@piperine in pH 7 PBS. Inset, base-line corrected calibration plot. (b) CV response of GCE/GMC@piperine in various pHs of PBS (1-11). Inset, base-line corrected calibration plot.

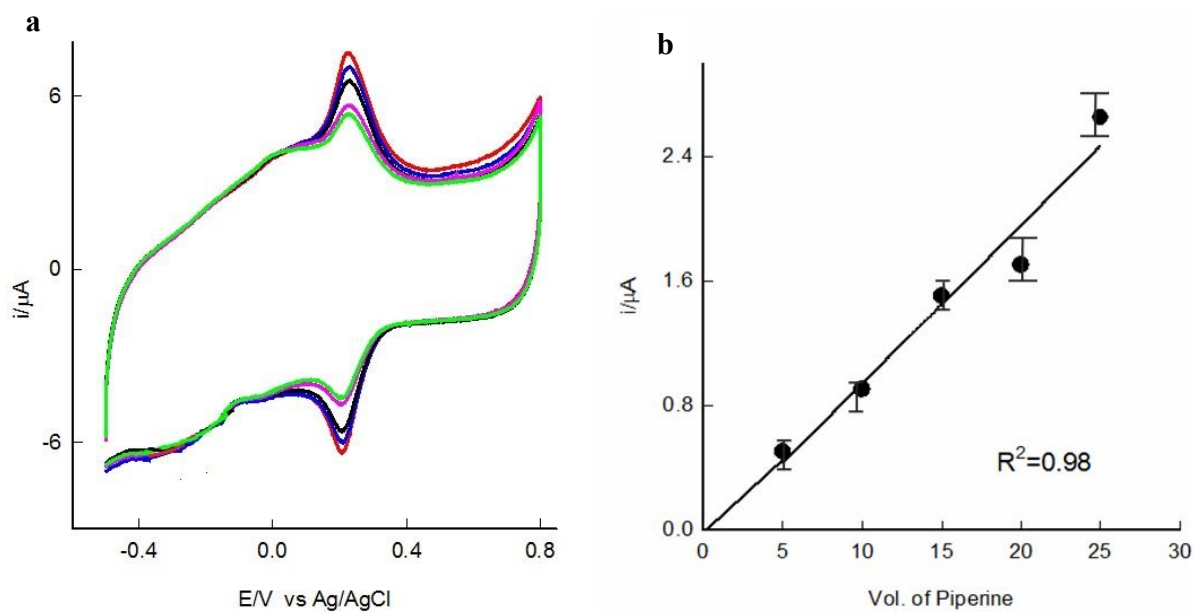


**Fig. 5.** (a) CV response of various volumes of piperine-modified GCE/GMC taken in pH PBS at  $5\text{ mV s}^{-1}$  (slow scan rate) for  $n = 4$ . (b) Corresponding base-line corrected calibration plot with triplicated experiment and error bars.



and an active electron-transfer mechanism of the isolated piperine in accordance with GMC. The results observed are accordance to the following equation which is followed by a reversible electrochemical reaction [37].

$$I_{pa} \text{ or } i_{pc} = n^2 F^2 A \Gamma_{pip} \nu / 4RT \quad (1)$$

Herein,  $n$  is the number of electrons involved,  $F$  = faraday constant (96500),  $A$  = geometrical surface area of the electrode,  $\Gamma_{pip}$  is the calculated surface excess value,  $\nu$  is the scan rate.

### Variable Solution pH Effect

The effect of varying pH of the PBS on the redox activity of GCE/GMC@Piperine was examined by taking CV in various pHs of PBS (1-11 pH). Figure 4b depicts a CV response from 1-9 pHs of PBS solutions which demonstrated a negative Nernstian shift of the redox potential peak with respect to pH [38]. A base-line corrected calibration plot of  $E^0$  vs. pH (inset Fig. 4b) shows linearity with a slope value of  $-49.75 \pm 1$  mV  $\text{pH}^{-1}$ . This clearly portrays a characteristic Nernstian behavior wherein equal number of protons and electrons are participating in the electron transfer reaction [38].

### Effect of Changing Piperine Concentration

Figure 5 shows a typically comparative CV response wherein different volumes of piperine were top coated on the GCE/GMC. CV was recorded at a slow scan rate of  $5 \text{ mV s}^{-1}$  in pH 7 of PBS. Quantitative analysis is preferred in slow scan rate. The volumes of piperine solution drop coated were  $5 \mu\text{l}$ - $25 \mu\text{l}$ . As the volume increased, the concentration of piperine was also increased. Subsequently, the peak current of the redox peak also increased linearly (Fig. 5a). However, due to slow scan rate, the peak current is low and slight disturbance is observed which is in an acceptable limit. The base-line corrected calibration plot (Fig. 5b), volume of piperine vs. redox peak current gave linearity with a regression square of 0.98. This observation, evidently authenticated that the change in concentration of piperine is directly proportional to the redox peak current obtained. Hence, this technique could be utilized for quantitative phytochemical analysis; *i.e.*, piperine in long pepper.

## CONCLUSIONS

A highly stable and reproducible electrochemical sensor for an isolated piperine phytochemical from long pepper was fabricated here. Graphitized mesoporous carbon assisted chemically modified electrode decorated with isolated piperine, designated as GCE/GMC@piperine, was used as the electrode. A conventional three-electrode-based system containing GCE/GMC@piperine as a working electrode, platinum as a counter electrode and Ag/AgCl as a reference electrode, in 10 ml working volume of pH 7 PBS was used at  $50 \text{ mV s}^{-1}$ ,  $n = 10$ . The fabricated GCE/GMC@piperine gave a highly stable, reversible redox peak at  $E' = +0.2 \text{ V vs. Ag/AgCl}$  at  $50 \text{ mV s}^{-1}$  in 10 ml of pH 7 PBS with a surface excess  $\Gamma_{pip}$  value of  $19.8 \times 10^{-9} \text{ mol}^{-1} \text{ cm}^2$ . The microscopic characterization by TEM revealed the interaction of piperine with GMC. Parameters such as the effects of potential scan rate, and solution pH were also examined. Further, quantitative analysis of various piperine concentrations was performed with respect to the redox peak current. This work is a prototype of electrochemical quantitative detection of phytochemicals in natural products.

## ACKNOWLEDGEMENTS

The authors acknowledge St. Anns' college for women-Mehdipatnam, Hyderabad for the support to carry out the research work.

### Conflict of Interest

No conflicts to declare.





## REFERENCES

- [1] P.S. Ved, S. Utkarsh, C. Mahadev, V.N. Shukla, 5 (2018) 6376.
- [2] R. Hindumathi, M. Jagannatham, P. Haridoss, C. P. Sharma, Nano Structures and Nano Objects 13 (2018) 30.
- [3] S.S. Magendran, F.S.A. Khan, N.M. Mubarak, M. Vaka, R. Walvekar, M. Khalid, E.C. Abdullah, S. Nizamuddin, R.R. Karri, Nano Structures and Nano Objects 20 (2019) 100399.

- [4] H. K. Ja, S. Jungmok, L. Taeyoon, *Thin Solid Films* 5 (2012) 1.
- [5] A. Mathiazhagan, J. Rani, *Int. J. Chem. Eng.* 2 (2011) 225.
- [6] A. Amania, M. Salehib, M. Jamshidi, *Anal. Bioanal. Chem. Res.* 7 (2020) 541.
- [7] C. Aicheng, C. Sanghamitra, *Chem. Soc. Rev.* 42 (2013) 5425.
- [8] M.M. Ardakani, M. Yavari, A. Khoshroo, *Anal. Bioanal. Chem. Res.* 6 (2019) 183.
- [9] J.V. Peter, R.W. Krista, *Environ. Sci. Technol.* 44 (2010) 3656.
- [10] F.R. James, S. Gregory, P. Fotios, *Bioelectrochemistry* 76 (2009) 189.
- [11] Z. Dehghania, S. Dadfarniaa, A.M.H. Shabania, M.H. Ehrampoush, *Anal. Bioanal. Chem. Res.* 7 (2020) 509.
- [12] R.K. Janardhan, K.K. Suresh, R.B. Jigna, K. Ki-Hyun, D. Tanushree, V. Kowsalya, *Adv. Colloid Interface Sci.* 256 (2018) 326.
- [13] C. Hwei-Jay, L. Chi-Young, T. Nyan-Hwa, *Carbon* 80 (2014) 725.
- [14] K. Amreen, V.K. Shukla, S. Shukla, D. Rajagopalan, A.S. Kumar, *Nano Structures and Nano Objects* 11 (2017) 56.
- [15] E. Antonio, A. Anna, V. Maurizio, C.Z. Maria, *Phytochem. Anal.* 12 (2001) 383.
- [16] K. Duduku, S. Rosalam, B. Awang, *Biotechnol. Mol. Biol. Rev.* 1 (2007) 97.
- [17] L. Claus, *Forsch Komplementmed* 23 (2016) 69.
- [18] C. Anoma, J.K. Thamilini, *Int. J. Food Sci.* (2016).
- [19] K.M. Pulok, K.N. Neelesh, M. Niladri, K.S. Birendra, *Fitoterapia* 84 (2013) 227.
- [20] H.R. Arshad, A.A. Mohammed, M.A. Salah, A.K. Masood, H.A. Yousef, *Adv. Biomed. Res.* 7 (2018) 38.
- [21] C.L. Gopu, A. Suyog, M. Hiral, A.R. Paradkar, K.R. Mahadik, *Phytochem. Anal.* 19 (2008) 116.
- [22] M. Sunita, D. Sukriti, H. Saikat, L. Mohan, *J. Essent. Oil Bear. Pl.* 21 (2018) 994.
- [23] P.G. Van, *Eur. J. Clin. Nutr.* 50 (1996) 57.
- [24] K.S. Surinder, S.V. Amarji, S. Mohit, *Eur. J. Pharmacol.* 720 (2013) 55.
- [25] M. Peyman, M. Surush, M. Milad, A. Shahin, S. Shadi, *Iran. J. Basic Med. Sci.* 16 (2013) 1031.
- [26] Q.P. Yin, *Epilepsia* 24 (1983) 177.
- [27] G. Leila, M. Maedeh, D.N. Ghasem, N. Maryam, *Compr. Rev. Food Sci. Food Saf.* 16 (2017) 124.
- [28] K.N. Babu, M. Divakaran, P.N. Ravindran, K.V. Peter, *Hand Book of Herbs and Spices.*
- [29] M. Murlidhar, T.K. Goswami, *Phytother. Res.* 27 (2013) 1121.
- [30] P. Subramani, S.T. Gan, A.D. Sokkalingam, *Pharmacogn. Rev.* 8 (2014) 73.
- [31] T. Rajendiran, A.S. Kumar, *Anal. Methods* 4 (2012) 2162.
- [32] Y. Xiaofeng, G. Miaomiao, H. Haidong, Z. Huajie, *Phytochem. Anal.* 22 (2011) 291.
- [33] C.T. Gerardo, D.C. Antonio, F. Bruno, P. Erwan, F. Alain, *Phytochem. Anal.* 28 (2017) 171.
- [34] W. Yuanzhe, C. Lifu, C. Korbua, G.C. Richard, *Food Chem.* 309 (2020) 125606.
- [35] P.N. Shingate, P.N. Dongre, D.M. Kannur, *Int. J. Pharm. Sci. Res.* 4 (2013) 3165.
- [36] C.R. Quijia, M. Chorilli, *Acta Pharm.* 71 (2021).
- [37] A.S. Kumar, R. Shanmugam, N. Vishnu, K.C. Pillai, S. Kamaraj, *J. Electroanal. Chem.* 782 (2016) 215.
- [38] P. Barathi, A.S. Kumar, *Electrochim. Acta* 135 (2014) 1.

Review

# Plant Growth Promoting Rhizobacteria (PGPR) as Green Bioinoculants: Recent Developments, Constraints, and Prospects

Anirban Basu <sup>1</sup>, Priyanka Prasad <sup>2</sup>, Subha Narayan Das <sup>2</sup>, Sadaf Kalam <sup>3,\*</sup>, R. Z. Sayyed <sup>4,\*</sup>, M. S. Reddy <sup>5</sup> and Hesham El Enshasy <sup>6,7</sup>

<sup>1</sup> Department of Plant Sciences, School of Life Sciences, University of Hyderabad, Telangana 500046, India; anirbanbasu99@gmail.com

<sup>2</sup> Department of Botany, Indira Gandhi National Tribal University, Amarkantak 484887, India; prasadjpriyanka696@gmail.com (P.P.); subha.bunu@igntu.ac.in (S.N.D.)

<sup>3</sup> Department of Biochemistry, St. Ann's College for Women, Hyderabad 500028, India

<sup>4</sup> Department of Microbiology, PSGVP Mandal's Arts, Science and Commerce College, Shahada 425409, India

<sup>5</sup> Asian PGPR Society for Sustainable Agriculture & Auburn Ventures, Department of Plant Pathology and Entomology, Auburn University, Auburn, AL 36849, USA; prof.m.s.reddy@gmail.com

<sup>6</sup> Institute of Bioproduct Development (IBD), Universiti Teknologi Malaysia (UTM), Skudai, Johor Bahru 81310, Malaysia; henshasy@ibd.utm.my

<sup>7</sup> City of Scientific Research and Technology Applications, Alexandria 21934, Egypt

\* Correspondence: sadaf2577@gmail.com (S.K.); sayyedrz@gmail.com (R.Z.S.)

**Abstract:** The quest for enhancing agricultural yields due to increased pressure on food production has inevitably led to the indiscriminate use of chemical fertilizers and other agrochemicals. Biofertilizers are emerging as a suitable alternative to counteract the adverse environmental impacts exerted by synthetic agrochemicals. Biofertilizers facilitate the overall growth and yield of crops in an eco-friendly manner. They contain living or dormant microbes, which are applied to the soil or used for treating crop seeds. One of the foremost candidates in this respect is rhizobacteria. Plant growth promoting rhizobacteria (PGPR) are an important cluster of beneficial, root-colonizing bacteria thriving in the plant rhizosphere and bulk soil. They exhibit synergistic and antagonistic interactions with the soil microbiota and engage in an array of activities of ecological significance. They promote plant growth by facilitating biotic and abiotic stress tolerance and support the nutrition of host plants. Due to their active growth endorsing activities, PGPRs are considered an eco-friendly alternative to hazardous chemical fertilizers. The use of PGPRs as biofertilizers is a biological approach toward the sustainable intensification of agriculture. However, their application for increasing agricultural yields has several pros and cons. Application of potential biofertilizers that perform well in the laboratory and greenhouse conditions often fails to deliver the expected effects on plant development in field settings. Here we review the different types of PGPR-based biofertilizers, discuss the challenges faced in the widespread adoption of biofertilizers, and deliberate the prospects of using biofertilizers to promote sustainable agriculture.

**Keywords:** biofertilizer; bioinoculant; PGPR; rhizosphere; sustainable agriculture



**Citation:** Basu, A.; Prasad, P.; Das, S.N.; Kalam, S.; Sayyed, R.Z.; Reddy, M.S.; El Enshasy, H. Plant Growth Promoting Rhizobacteria (PGPR) as Green Bioinoculants: Recent Developments, Constraints, and Prospects. *Sustainability* **2021**, *13*, 1140. <https://doi.org/10.3390/su13031140>

Received: 24 December 2020

Accepted: 18 January 2021

Published: 22 January 2021

**Publisher's Note:** MDPI stays neutral with regard to jurisdictional claims in published maps and institutional affiliations.



**Copyright:** © 2021 by the authors. Licensee MDPI, Basel, Switzerland. This article is an open access article distributed under the terms and conditions of the Creative Commons Attribution (CC BY) license (<https://creativecommons.org/licenses/by/4.0/>).

## 1. Introduction

The advent of the Green Revolution in the latter part of the twentieth century triggered a worldwide boom in the agriculture sector. By introducing new high-yielding seed varieties and increasing the use of synthetic fertilizers, pesticides, and other agrochemicals, the Green Revolution contributed significantly to enhanced plant productivity and crop yields [1]. The global agricultural landscape has drastically changed since then. Rampant overuse of synthetic agrochemicals for enhancing crop productivity has deteriorated the biological and physicochemical health of the arable soil, leading to a declining trend

in agricultural productivity across the globe over the past few decades [2–4]. In the present scenario, there is a shrinkage of land resources and the depletion of biological wealth. In order to fulfill the escalating demand for sustainable agriculture, the yield and productivity of agricultural crops need to be concurrently increased with the production of agriculture-related commodities. There is no single or straightforward solution to the above-mentioned intricate, ecological, socio-economic, and technical glitches existing in promoting sustainable agriculture [1].

Promoting sustainable agriculture with a gradual decrease in the use of synthetic agrochemicals and more prominent utilization of the biowaste-derived substances [5,6] as well as the biological and genetic potential of crop plants and microorganisms is an effective strategy to combat the rapid environmental deterioration while ensuring high agricultural productivity and better soil health [7]. In addition to the genetic manipulation of the crop physiology and metabolism for yield enhancement, certain members of the soil microbial community, particularly those residing in the plant rhizosphere, might assist plants in preventing or partially overcoming the environmental stresses [8,9]. Search for eco-friendly alternatives to mitigate the harmful effects of toxic agrochemicals led to the discovery and subsequent use of biofertilizers and other microbial-based products, including organic extracts and vermicompost teas [10–12]. These microbial products are non-toxic, environment-friendly, and act as potential tools for plant growth promotion and disease control. Thus, the biological potential and fertility of soil could be increased, whereas the hazardous effects of agrochemicals could be decreased by employing microbial formulations to fertilize agricultural crops [13–15]. The use of efficient plant growth promoting rhizobacteria (PGPR) as biofertilizers and biological control agents is deliberated as a suitable substitute for minimizing the use of synthetic agrochemicals in crop production [16–19]. This review concisely and holistically provides deeper insights into the various aspects of PGPR-based biofertilizers, their prospects and constraints, and finally the roadmap to their commercialization.

## 2. Biofertilizers

During the past two decades, the term biofertilizer or bioinoculant has been derived in various ways due to the commendable progress achieved in the studies of the association between microorganisms and plants. A biofertilizer is most commonly defined as “a substance which contains living microorganisms which, when applied to seed, plant surfaces, or soil, colonizes the rhizosphere or the interior of the plant and promotes growth by increasing the supply or availability of primary nutrients to the host plant” [16]. Dinesh Kumar et al. [20] later proposed a modified definition of biofertilizers as “products (carrier or liquid based) containing living or dormant microbes (bacteria, actinomycetes, fungi, algae) alone or in combination, which help in fixing atmospheric nitrogen or solubilizers soil nutrients in addition to the secretion of growth promoting substances for enhancing crop growth and yield”.

The microorganisms present in the biofertilizers employ several mechanisms to provide benefits to the crop plants. They can either be efficient in nitrogen fixation, phosphate solubilization, and plant growth promotion or can possess a combination of all such traits [21–24]. Biofertilizers can fix atmospheric N<sub>2</sub> through the biological nitrogen fixation (BNF) process, solubilize nutrients required by the plants, such as phosphate, zinc, and potassium, and also secrete plant growth promoting substances, including various hormones [25,26]. Further, when applied as seed or soil inoculants, biofertilizers can multiply, participate in nutrient cycling, and help in crop production for sustainable farming [27–29].

The microbial inoculants possess several advantages over their chemical counterparts [30–32]. They are eco-friendly, sound sources of renewable nutrients required for maintaining soil health and biology [13,23,29]. Furthermore, they exhibit antagonistic activity against several agricultural pathogens and combat abiotic stresses [8,33–36]. Various microbial taxa have been commercially used as efficient biofertilizers, based on their

ability to obtain nutrients from the soil, fix atmospheric N<sub>2</sub>, stimulate the solubilization of nutrients, and act as biocontrol agents [37].

### 3. Plant Growth Promoting Rhizobacteria (PGPR)—The Phyto-Friendly Soil Microbes

Plant rhizosphere, the narrow zone of soil surrounding the root system of growing plants, represents a hotspot for microbial activity in the soil [38]. The rhizosphere is colonized by a wide range of microbial taxa, including both prokaryotes (archaea, bacteria, and viruses) and eukaryotes (fungi, oomycetes, nematodes, protozoa, algae, and arthropods), out of which bacteria and fungi comprise the most abundant groups [39,40] exhibiting fundamental ecological functions. Free-living soil bacteria that thrive in the rhizosphere, aggressively colonize plant roots, and facilitate plant growth are designated as plant growth promoting rhizobacteria (PGPR), a term introduced by Kloepper and Schroth in 1978 [41].

This heterogeneous group of bacteria, representing a vital component of the soil microbiome, is known to produce and secrete various regulatory chemicals in the plant roots' vicinity that aid in plant growth promotion [42,43]. PGPRs influence plants' overall health by contributing to enhanced nutrient acquisition by host plants, protecting against phytopathogenic microbes, and promoting resistance to various abiotic stresses [30,44]. Different PGPR strains are capable of increasing crop yields, exhibit biocontrol, enhance resistance to foliar pathogens, promote nodulation in legumes, and enhance the emergence of seedlings [45–50]. Reported PGPRs include members of the genera *Acinetobacter*, *Aeromonas*, *Agrobacterium*, *Allorhizobium*, *Arthrobacter*, *Azoarcus*, *Azorhizobium*, *Azospirillum*, *Azotobacter*, *Bacillus*, *Bradyrhizobium*, *Burkholderia*, *Caulobacter*, *Chromobacterium*, *Delftia*, *Enterobacter*, *Flavobacterium*, *Frankia*, *Gluconacetobacter*, *Klebsiella*, *Mesorhizobium*, *Micrococcus*, *Paenibacillus*, *Pantoea*, *Pseudomonas*, *Rhizobium*, *Serratia*, *Streptomyces*, *Thiobacillus*, and others [16,43,44,46,51–53]. An overview of the diverse phytobeneficial effects of PGPRs is represented in Table 1.

#### 3.1. Characteristics of an Ideal PGPR

A rhizobacterial strain is considered to be a putative PGPR if it possesses specific plant growth promoting traits and can enhance plant growth upon inoculation. An ideal PGPR strain should fulfill the following criteria [45]:

- (1) It should be highly rhizosphere-competent and eco-friendly.
- (2) It should colonize the plant roots in significant numbers upon inoculation.
- (3) It should be able to promote plant growth.
- (4) It should exhibit a broad spectrum of action.
- (5) It should be compatible with other bacteria in the rhizosphere.
- (6) It should be tolerant of physicochemical factors like heat, desiccation, radiations, and oxidants.
- (7) It should demonstrate better competitive skills over the existing rhizobacterial communities.

**Table 1.** An overview of the benefits of plant growth promoting rhizobacteria (PGPR) inoculation to plants.

Benefits of PGPR Inoculation to Plants	PGPR Strain(s)	Tested Plant(s)	Reference(s)
Tolerance to drought stress	<i>Pseudomonas fluorescens</i> DR11, <i>Enterobacter hormaechei</i> DR16, <i>Pseudomonas migulae</i> DR35, <i>Bacillus subtilis</i> , <i>Achromobacter piechaudii</i> ARV8, <i>Phyllobacterium brassicacearum</i> , <i>Paenibacillus polymyxa</i> , <i>Rhizobium tropici</i> , <i>Azospirillum brasilense</i>	Foxtail millet ( <i>Setaria italica</i> L.), Maize ( <i>Zea mays</i> L.), Bean ( <i>Phaseolus vulgaris</i> L.), <i>Arabidopsis thaliana</i> , Tomato ( <i>Lycopersicon esculentum</i> Mill cv. F144), Pepper ( <i>Capsicum annuum</i> L. cv. Maor), Wheat ( <i>Triticum aestivum</i> L.)	[36,54–59]
Tolerance to salinity stress	<i>Bacillus pumilus</i> , <i>Exiguobacterium oxidotolerans</i> , <i>Bacillus megaterium</i> , <i>Azospirillum</i> sp., <i>Achromobacter piechaudii</i> , <i>Enterobacter</i> sp. PR14	Brahmi ( <i>Bacopa monnieri</i> L.), Maize ( <i>Zea mays</i> L.), Lettuce ( <i>Lactuca sativa</i> L.), Tomato ( <i>Lycopersicon esculentum</i> Mill.), Rice ( <i>Oryza sativa</i> cv. Sahbhagi), Sorghum ( <i>Sorghum bicolor</i> ), Finger Millets ( <i>Eleusine coracana</i> )	[60–64]
Tolerance to biotic stress (biocontrol)	<i>Paenibacillus xylanexedens</i> , <i>Bacillus amyloliquefaciens</i> , <i>Streptomyces</i> sp., <i>Ochrobactrum intermedium</i> , <i>Paenibacillus lentimorbus</i> , <i>Pseudomonas</i> spp.	Wheat ( <i>Triticum aestivum</i> L.), Rice ( <i>Oryza sativa</i> ), Pine ( <i>Pinus taeda</i> L.), Tomato ( <i>Lycopersicon esculentum</i> Mill.)	[65–70]
Increased nutrient absorption	<i>Pantoea</i> sp. S32, <i>Paenibacillus polymyxa</i>	Rice ( <i>Oryza sativa</i> L.), Habanero pepper ( <i>Capsicum chinense</i> )	[71–73]
Seed germination enhancement	<i>Serratia marcescens</i> , <i>Pseudomonas fluorescens</i> , <i>Azospirillum lipoferum</i> , <i>Pseudomonas putida</i> , <i>Bacillus subtilis</i> , <i>Providencia</i> sp., <i>Brevundimonas diminuta</i>	Maize ( <i>Zea mays</i> L.), Wheat ( <i>Triticum aestivum</i> L.)	[74–76]
Biostimulation by phytohormone(s) production	<i>Azospirillum lipoferum</i> , <i>Bacillus subtilis</i> , <i>Arthrobacter protophormiae</i> , <i>Dietzia natronolimnaea</i> , <i>Bacillus</i> sp.	Rice ( <i>Oryza sativa</i> L.), Tomato ( <i>Solanum lycopersicum</i> L.), Wheat ( <i>Triticum aestivum</i> L.)	[46,77–79]
Soil fertility enhancement	<i>Bacillus subtilis</i> , <i>Bacillus cereus</i> , <i>Rhizobium</i> spp.	Poplar ( <i>Populus</i> sp.), Mung bean ( <i>Vigna radiata</i> L.)	[80–82]
Bioremediation of heavy metals and pollutants	<i>Ochrobactrum</i> sp., <i>Bacillus</i> spp., <i>Pseudomonas</i> spp., <i>Pseudomonas fluorescens</i> , <i>Bacillus cereus</i> , <i>Alcaligenes faecalis</i> RZS2, <i>Pseudomonas aeruginosa</i> RZS3, <i>Enterobacter</i> sp. RZS5	Rice ( <i>Oryza sativa</i> L.), Groundnut ( <i>Arachis hypogaea</i> ), Maize ( <i>Zea mays</i> L.), Ashwagandha ( <i>Withania somnifera</i> )	[83–88]
Modulation of plant secondary metabolites	<i>Bacillus subtilis</i> , <i>Azotobacter chroococcum</i> , <i>Pseudomonas putida</i> , <i>Bacillus pumilus</i> , <i>Exiguobacterium oxidotolerans</i>	Basil ( <i>Ocimum basilicum</i> ), Brahmi ( <i>Bacopa monnieri</i> L.)	[89,90]

### 3.2. Mechanisms of PGPR Action

Being the dominant rhizosphere microbial community, PGPRs are actively or passively involved in plant growth promotion. They can act as biofertilizers that promote plants' growth and development by facilitating biotic and abiotic stress tolerance and supporting host plants' nutrition [64,86,91,92]. These beneficial groups of bacteria, through their multifaceted modes of action, including root colonization, positive effects on plant physiology and growth, biofertilization, induced systemic resistance, biocontrol of phytopathogens, etc., offer protection to plants and facilitate plant growth promotion. The detailed mechanisms of PGPR action and their specific contribution to plant growth promotion have been reviewed comprehensively [30,41–44,47–49,51,52,93–102]. The modes of action by which PGPRs promote plant growth have been traditionally classified into direct and indirect mechanisms occurring inside and outside the plant, respectively [51,99] (Figure 1).

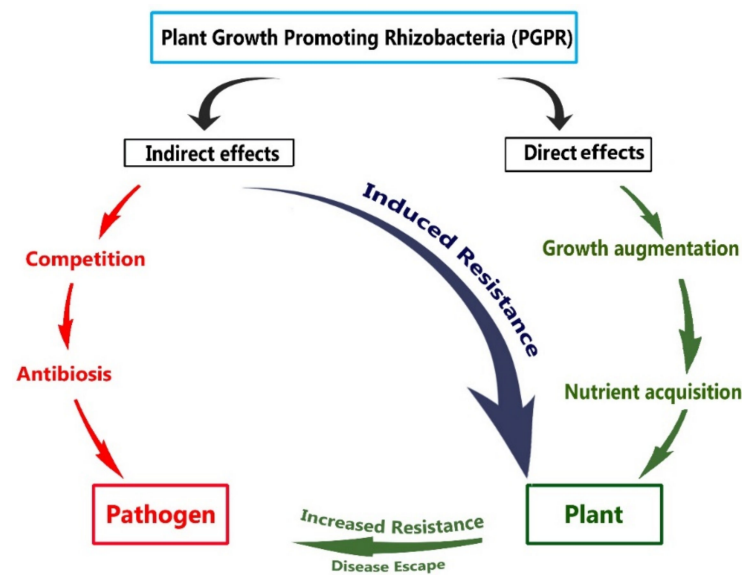


**Figure 1.** Main overview of interactions between plant growth promoting rhizobacteria (PGPR), plants, and pathogens. PGPRs directly promote plant growth by improving nutrient acquisition by the plant and growth augmentation via regulating phytohormone levels. The indirect effects of PGPRs include suppression of phytopathogens and inducing systemic resistance in plants against a wide range of pathogenic microbes.

Direct modes of PGPR action include improving plant nutrition by providing phytonutrients like fixed nitrogen or solubilized minerals from the soil (like P, K, Zn, Fe, and other essential mineral nutrients) and/or stimulating plant growth and development by regulating phytohormone levels (like auxins, cytokinins, gibberellins, abscisic acid, and ethylene) [44,46,95]. The indirect effects of PGPRs include influencing the plant health by suppressing phytopathogens and other deleterious microorganisms through parasitism, competing for nutrients and niche within the rhizosphere, producing antagonistic substances (like hydrogen cyanide, siderophores, antibiotics, and antimicrobial metabolites) and lytic enzymes (like chitinases, glucanases, and proteases), and inducing systemic resistance in plants against a broad spectrum of root and foliar pathogens [32,81,103,104]. Due to these direct and indirect effects elicited by PGPRs on host plants, they prove to be ideal candidates to be formulated and commercialized as bioinoculants and phytoprotective microbial products. However, the mode and mechanism of PGPR action vary with the host plant type [105]. In addition to this, certain other factors also influence PGPR action, viz. biotic factors like plant genotype, developmental stages, plant defense mechanisms, and presence of other members of the microbial community and abiotic factors like soil type, composition, soil management history, and prevalent environmental conditions [95,106].

#### 4. Global Biofertilizer Market

During the past few decades, the biofertilizer market has seen a global boom in its production and utilization. Due to the unavailability of cultivable land and to cater to the need of the exploding population for agricultural products, the global biofertilizers market has gathered enough momentum. The global biofertilizer market represents a tiny fraction of the synthetic agrochemicals market [107]. The nitrogen-fixing biofertilizers dominate the market with the lion's share of about 80%, followed by the phosphate-solubilizing biofertilizers with a meager 14% share (Figure 2) [107,108]. *Rhizobium* spp., *Azotobacter* spp., and *Azospirillum* spp. are the major nitrogen-fixing biofertilizers available in the market. Although these nitrogen-fixing biofertilizers are primarily used for growing pulses and other leguminous crops, they are also applied to grow selected cereals and cash crops as well [107,109].

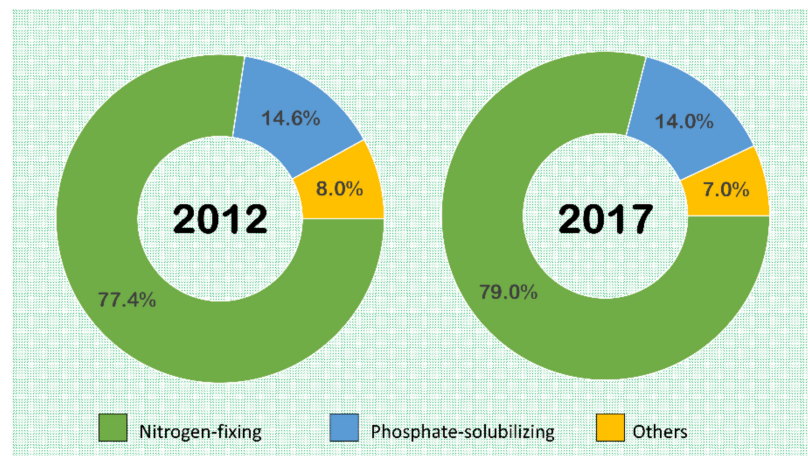


**Figure 2.** Global biofertilizer market share by product typology (nitrogen-fixing and phosphate-solubilizing microbe-based biofertilizers and others). Market data of 2012 (left panel) and 2017 (right panel) respectively compiled from Timmusk et al. [107] and Soumare et al. [108].

Geographically, the global biofertilizer market canopies several regions of the world, such as North America, Europe, Asia-Pacific, Latin America, Middle East, and Africa (Figure 3). In terms of revenues generated from biofertilizer production, North America (USA, Canada, and Mexico) dominates the global biofertilizer market, followed by Europe (Germany, UK, Spain, Italy, Hungary, and France) and the Asia-Pacific region (China, Japan, India, Australia, New Zealand, and the rest of Asia). As of 2017, the biofertilizer markets were valued at USD 495 million in North America, USD 450 million in Europe, USD 284 million in Asia-Pacific, USD 240 million in South America, and USD 44 million in Africa [108]. It is estimated that the global biofertilizer market would reach USD 3.5 billion by 2025. Some of the commonly used PGPR-based biofertilizer products commercially available across the globe are represented in Table 2.

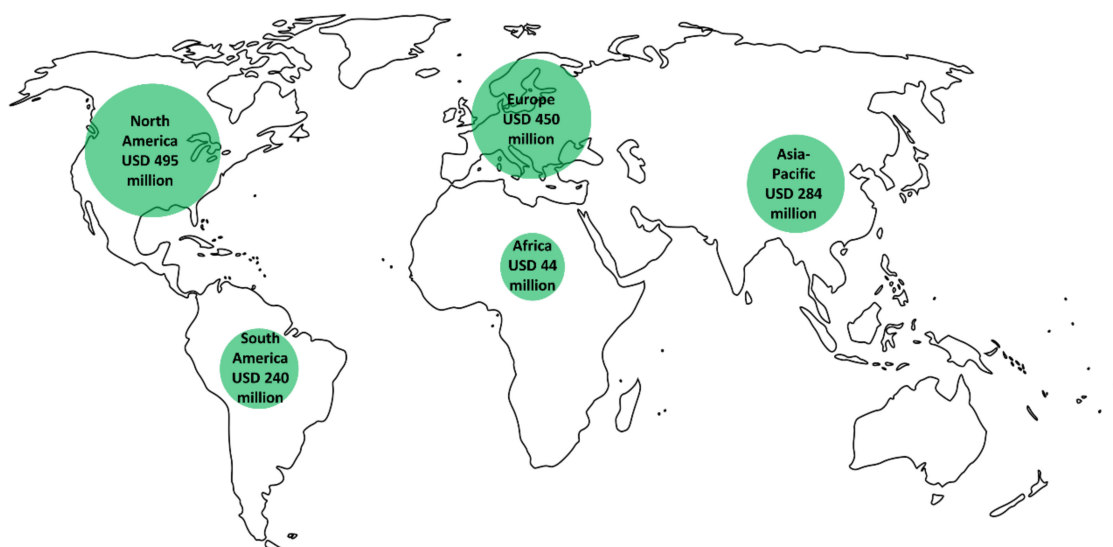


**Figure 3.** Size and distribution of the global biofertilizer market in USD million per region. The area of each circle is proportional to the size of the biofertilizer market (in USD million) in the specific region. Data compiled from Soumare et al. [108].



**Table 2.** An overview of globally available PGPR-based biofertilizer products.

Type of Biofertilizer	Name of Biofertilizer	PGPR Strain(s)	Manufacturer's Country	Market Region	Reference(s)
Nitrogen fixer	Nitragin Gold®	Rhizobia	USA	North America	[110]
	Cell-Tech®	Rhizobia	USA	North America	[110]
	TagTeam®	Rhizobia, <i>Penicillium bilaii</i>	USA	North America	[110]
	Custom N2	<i>Paenibacillus polymyxa</i>	USA	North America	[110]
	Nodulator®	<i>Bradyrhizobium japonicum</i>	Canada	North America	[110]
	Nodulator® PRO	<i>Bacillus subtilis</i> , <i>Bradyrhizobium japonicum</i>	Canada	North America	[110]
	Bioboost®	<i>Delftia acidovorans</i> , <i>Bradyrhizobium</i> sp.	Canada	North America	[105,110]
	Azofer®	<i>Azospirillum brasilense</i>	Mexico	North America	[110]
	Rhizofer®	<i>Rhizobium etli</i>	Mexico	North America	[110]
	Nitrofix®	<i>Azospirillum</i> sp.	Cuba	North America	[105,110]
	Rhizosum N®	<i>Azotobacter vinelandii</i> , <i>Rhizophagus irregularis</i>	Spain	Europe	[110,111]
	Rhizosum Aqua	<i>Azospirillum</i> sp.	Spain	Europe	[105,110]
	Legume Fix	<i>Rhizobium</i> sp., <i>Bradyrhizobium japonicum</i>	UK	Europe	[112,113]
	BactoFil® A10	<i>Azospirillum brasilense</i> , <i>Azotobacter vinelandii</i> , <i>Bacillus megaterium</i>	Hungary	Europe	[112]
	BactoFil® Soya	<i>Bradyrhizobium japonicum</i>	Hungary	Europe	[114]
	Phylazonit M	<i>Azotobacter chroococcum</i> , <i>Bacillus megaterium</i>	Hungary	Europe	[115]
	Azotobacterin®	<i>Azospirillum brasilense</i> B-4485	Russia	Europe	[105,110]
	Azoter	<i>Azotobacter chroococcum</i> , <i>Azospirillum brasilense</i> , <i>Bacillus megaterium</i>	Slovakia	Europe	[116]
	TwinN®	<i>Azorhizobium</i> sp., <i>Azoarcus</i> sp., <i>Azospirillum</i> sp.	Australia	Asia-Pacific	[113]
	TripleN®	<i>Azorhizobium</i> spp., <i>Azoarcus</i> spp., <i>Azospirillum</i> spp.	Australia	Asia-Pacific	[111]

Table 2. Cont.

Type of Biofertilizer	Name of Biofertilizer	PGPR Strain(s)	Manufacturer's Country	Market Region	Reference(s)
Nitrogen fixer	Bio-N	<i>Azospirillum</i> spp.	Philippines, Australia	Asia-Pacific	[112,117]
	BioGro®	<i>Pseudomonas fluorescens / putida</i> , <i>Klebsiella pneumoniae</i> , <i>Citrobacter freundii</i>	Vietnam	Asia-Pacific	[117]
	Mamezo®	Rhizobia	Japan	Asia-Pacific	[105,110]
	Agrilife Nitrofix	<i>Azotobacter chroococcum</i> , <i>A. vinelandii</i> , <i>Acetobacter diazotrophicus</i> , <i>Azospirillum lipoferum</i> , <i>Rhizobium japonicum</i>	India	Asia-Pacific	[118]
	Ajay Azospirillum	<i>Azospirillum</i> sp.	India	Asia-Pacific	[112]
	Symbion N	<i>Azospirillum</i> sp., <i>Rhizobium</i> sp., <i>Acetobacter</i> sp., <i>Azotobacter</i> sp.	India	Asia-Pacific	[115]
	Zadspirillum	<i>Azospirillum brasilense</i>	Argentina	South America	[112]
	Rizo-Liq	<i>Bradyrhizobium</i> sp., <i>Mesorhizobium ciceri</i> , <i>Rhizobium</i> spp.	Argentina	South America	[112,113]
	Nodulest 10	<i>Bradyrhizobium japonicum</i>	Argentina	South America	[118]
	Rizo-Liq Top	<i>Bradyrhizobium japonicum</i>	Argentina	South America	[113]
	BiAgro 10®	<i>Bradyrhizobium japonicum</i>	Argentina, Brazil, Bolivia	South America	[117]
	Dimargon®	<i>Azotobacter chroococcum</i>	Colombia	South America	[117]
	Nitrasesc	<i>Rhizobium</i> sp.	Uruguay	South America	[112]
	Biofix	Rhizobia	Kenya	Africa	[112,113]
	Nodumax	<i>Bradyrhizobium</i> spp.	Nigeria	Africa	[112,113]
	Azo-N	<i>Azospirillum brasilense</i> , <i>A. lipoferum</i>	South Africa	Africa	[113]
Azo-N Plus	<i>Azospirillum brasilense</i> , <i>A. lipoferum</i> , <i>Azotobacter chroococcum</i>	South Africa	Africa	[113]	

Table 2. Cont.

Type of Biofertilizer	Name of Biofertilizer	PGPR Strain(s)	Manufacturer's Country	Market Region	Reference(s)
Phosphate solubilizer	Fosforina <sup>®</sup>	<i>Pseudomonas fluorescens</i>	Cuba	North America	[117]
	Rhizosum PK <sup>®</sup>	<i>Bacillus megaterium</i> , <i>Frateuria aurantia</i> , <i>Rhizophagus irregularis</i>	Spain	Europe	[110,111]
	Phosphobacterin	<i>Bacillus megaterium</i> var. <i>phosphaticum</i>	Russia	Europe	[31]
	CataPult	<i>Bacillus</i> spp., <i>Glomus intraradices</i>	Australia	Asia-Pacific	[118]
	Symbion van Plus	<i>Bacillus megaterium</i>	India	Asia-Pacific	[112]
	P Sol B	<i>Pseudomonas striata</i> , <i>Bacillus polymyxa</i> , <i>B. megaterium</i>	India	Asia-Pacific	[115,118]
	CBF	<i>Bacillus mucilaginosus</i> , <i>B. subtilis</i>	China	Asia-Pacific	[117]
Potassium solubilizer	Bio Phos <sup>®</sup>	<i>Bacillus megaterium</i>	Sri Lanka	Asia-Pacific	[115,118]
	Rhizosum K	<i>Frateuria aurantia</i>	Spain	Europe	[105,110]
Zinc solubilizer	K Sol B	<i>Frateuria aurantia</i>	India	Asia-Pacific	[118]
	Biozink <sup>®</sup>	PGPR consortia	India	Asia-Pacific	[110]
Phytostimulator	Zn Sol B	<i>Thiobacillus thiooxidans</i>	India	Asia-Pacific	[118]
	EVL Coating <sup>®</sup>	PGPR consortia	Canada	North America	[105]
	Amase <sup>®</sup>	<i>Pseudomonas azotoformans</i>	Sweden	Europe	[114,118]
	Bio Gold	<i>Azotobacter chroococcum</i> , <i>Pseudomonas fluorescens</i>	Sri Lanka	Asia-Pacific	[115,118]
Biocontrol	Bioativo	PGPR consortia	Brazil	South America	[112]
	Cedomon <sup>®</sup>	<i>Pseudomonas chlororaphis</i>	Sweden	Europe	[114]
	Cedress <sup>®</sup>	<i>Pseudomonas chlororaphis</i>	Sweden	Europe	[114]
	Cerall <sup>®</sup>	<i>Pseudomonas chlororaphis</i>	Sweden	Europe	[114]
	Biotilis	<i>Bacillus subtilis</i>	India	Asia-Pacific	[118]
	Soilfix	<i>Brevibacillus laterosporus</i> , <i>Paenibacillus chitinolyticus</i>	South Africa	Africa	[112]

## 5. Challenges and Constraints with PGPR-Based Biofertilizers

Presently, there is an escalating interest in the use of microbial-based products as bioinoculants. Still, their use is associated with several challenges moving from the lab to the field. The preliminary use of these bioinoculants has been made on crop plants such as

legumes and cereals [119]. For developing a new PGPR strain as an effective bioinoculant, an initial laboratory screening is required, which depends on specific direct and indirect mechanisms of plant growth promotion by PGPRs. Mere primary screening of axenic culture isolates for PGPR traits does not guarantee efficacious plant growth promotion under field conditions. Parallely, those pure culture isolates that exhibit less in vitro growth promoting activities might possess different plant growth promotion strategies. Because these mechanisms are not fully understood, such isolates exhibit difficulty in screening under standard conditions. Henceforth, sometimes such useful strains exhibiting these mechanisms get discarded due to their poor in vitro performance [120]. The large-scale utilization and application of PGPRs necessitate addressing several important issues and overcoming quite a few challenges and constraints (Figure 4).

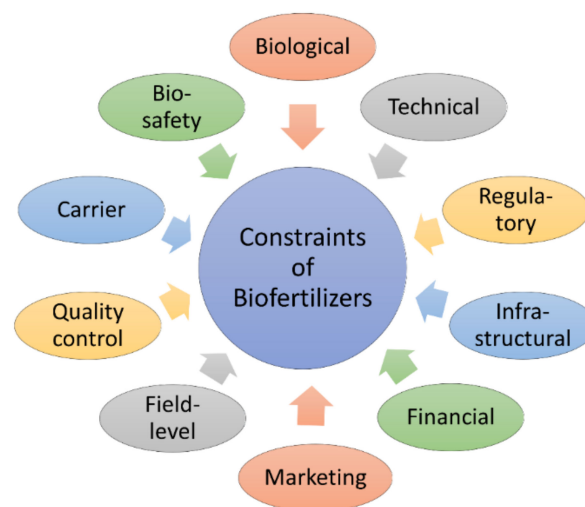


**Figure 4.** Constraints in the utilization, production, and commercialization of PGPR-based biofertilizers.

### 5.1. Biological Constraints

Selection of specific PGPR strain(s) for biofertilizer development is a challenge in itself. The strain(s) should not be selective or highly targeted (to specific crops) in nature, and it should exhibit a broad host range. One of the main limiting issues is their selectivity. Conventional agrochemicals tend to impact the entire resident microbiota, whereas PGPRs remain highly targeted and specific. Nevertheless, the quality and efficacy of these PGPRs under field conditions invariably changes due to the presence of several other microorganisms. Potential isolates should be selected based on their performance under field conditions with a wide range of crops across diverse soil types and environmental conditions [32]. The strains must be effective in replacing the native inefficient strains and should not antagonize with other beneficial microbes in the rhizosphere [31].

As biofertilizers, PGPRs should be able to sufficiently colonize host plant roots, create a proper rhizosphere for plant growth, and increase the bioavailability of N, P, K, and antagonistic properties [16,45]. PGPRs should possess specific characteristics for their utilization as an efficient and successful bioinoculant. It should be able to survive in soil, compatible with the crop on which it is inoculated, and interact with indigenous microflora in soil and abiotic factors. Necessary measures should be taken to avoid any non-target effect of the bioinoculant and stabilize them in soil systems. These measures will guarantee the durability of the plant growth effect and the good performance of introduced PGPRs as bioinoculants.

An important factor in PGPR colonization is PGPR dynamics, which mainly changes with the host crop, the midterm and long-term effects, the crop-rotation impact, and site variation. Another challenge using PGPRs is their diverse mode of action, as all the rhizobacteria do not possess the same mechanisms of action for plant growth promotion [121]. Several Gram-negative rhizobacteria are known to exhibit biocontrol potential. The con-

straint arises in their formulation, as they are difficult to formulate because of their inability to produce spores. In addition to this, their formulations lack a longer shelf life, and the bacteria are prone to get killed upon desiccation [51,122,123].

### 5.2. Technical Constraints

One of the significant challenges encountered during the development of a biofertilizer and the commercialization of an effective PGPR strain is its shelf life [22,124]. Biofertilizers with a short shelf life carry the risk of recycling if they are not used or sold before expiry resulting in a net monetary loss to the marketing agency. Since biofertilizers contain live microbial cells, their storage and transportation require extra care and precaution. The technical constraints involve the risk of deterioration of the product due to shorter shelf life or spontaneous mutations arising during fermentation or storage [31]. The mutations result in a net reduction in bioinoculant effectiveness and lead to a severe problem that raises the cost of production and quality of the bioinoculant. Inadequate availability of soil-specific strains region-wise considerably limits the widespread use of bioinoculants.

### 5.3. Regulatory Constraints

Regulatory constraints include the challenges in product registration and patent filing. The rules often vary between different regions and nations and are not consistent. In addition, the regulatory processes are quite complex, and the fees, though variable, are mostly on the higher side [32,107]. The documentation procedures for product registration are equally extensive and complicated. The absence of a standardized legal and regulatory definition for “plant biostimulants” is the primary reason behind the lack of a globally coordinated uniform regulatory policy [30,125].

The process of registering the biocontrol agent within a country is normally in two phases and is quite lengthy and complicated [32,107]. Generally, in any country, the active ingredient present within a biofertilizer must get an authorization certificate from the Directorate-General for Health and Consumer Affairs, and after that, the formulated product has to be nationally approved. The Food Safety Authority and the National Commission of any country will critically analyze and give relevant comments followed by several rounds of review by experts, sometimes taking an additional two to three years. Thus, the entire process starting from registration to commercializing a potential biofertilizer is lengthy and might stretch to several years. The countries have their own guidelines and norms to respond in their specific language, and the registering agency can also require even additional data.

### 5.4. Infrastructural Constraints

Manufacturing and quality control of biofertilizers involve sophisticated technology and qualified and trained human resources. Lack of sophisticated technology, necessary technical support and proper equipment, trained workforce, and skilled technical personnel are the major infrastructural constraints [31].

### 5.5. Financial Constraints

Lack of sufficient financial resources in the large-scale production of biofertilizers is a significant drawback [124]. Once the biofertilizer is manufactured, small producers do not have enough funds to distribute on their own. Because of this delay in distribution, lowering of the quality of the product occurs, deteriorating its biocontrol potential [31].

### 5.6. Marketing Constraints

One of the major limitations for developing the product in the market is the unavailability of proper transportation services along with storage facilities. Farmers possess little or inadequate knowledge regarding the advantages of biofertilizers over hazardous agrochemicals for sustainable agriculture. Thus, the demand for such eco-friendly products

is reduced. The establishment of extension centers does not help in creating awareness among farmers due to the lack of well-qualified technical staff [31].

The biofertilizer developers face a significant problem because the agricultural crops are grown under various physicochemical and environmental conditions, including diverse ranges of temperature, rainfall, soil type, and crop variety. These conditions tend to change from farm to farm or even within a single field. Therefore, such variations cause a discrepancy in the efficacy of PGPR-based biofertilizers [122,126].

There is a general strategy followed in any state within a country before any microbial products attain the stage of commercialization. The ministry/department of agriculture gives a green signal for placing orders mostly from their own production units. From here, biofertilizer packets are transported to several districts. A chain of extension workers gets involved in the next step before these packets reach the field. During this course, the microorganisms present as bioinoculants get exposed to high temperatures (above 40 °C), which might lead to either their inactivation or death, thus rendering them low- or poor-quality biofertilizers. Henceforth, these low-quality packets will be disadvantageous for the farmers, as well as for the entire crop yield.

### 5.7. Field-Level Constraints

The response of crops toward the applied biofertilizers is very slow and sometimes futile since the inoculum will take time to build its concentration and root colonization. This results in a low level of acceptance of biofertilizers by the farmers. The purity of inoculants, along with inoculation techniques, play a vital role in field application. The effectiveness of biofertilizers gets reduced because of the harmful residual effects of synthetic chemicals and existing unfavorable abiotic conditions [31,127]. Environmental stresses such as salt and drought in certain areas play another important role in reducing biological activity. The inoculants are under biotic and abiotic stresses [124]. In addition to these factors, several other factors that holistically result in poor performance of the bioinoculants include acidity and alkalinity of the soil and application of pesticides and high concentrations of nitrate in the soil, limiting the N-fixing ability of the bioinoculants. Many soils possess toxic concentrations of heavy metals like Cd, Hg, Cr, etc., and a deficiency of other important nutrients like P, Cu, Mo, and Co that reduce the biological potential of the PGPR-based fertilizers [23,128].

PGPRs function through a series of mechanisms. The foremost step in plant growth promotion is the colonization of plant roots by the microbe, which is an intricate process requiring the ability of bacteria to compete in the rhizosphere soil for a suitable niche to bring about a positive plant-microbe interaction [129]. In addition to this, the abiotic factors, viz. soil type, temperature, pH, radiation, oxygen concentration, nutrient availability, and the degree of interaction with the native soil microbiota, too drastically affect the plant-microbe interaction, affecting their existence and survivability within the host plant. Thus, the success of the field application of PGPRs depends upon the climatic factors required for a particular variety of cultivated crops [21]. Identification of region-specific microbial strains is highly recommended to exhibit maximum effectiveness by the employed PGPR strain. Quite often, PGPRs are directly used as an inoculum for host plants without mixing them with an appropriate carrier. In addition to this, their quantities are insufficient to allow efficient rhizosphere colonization existing in a field because of the competition with the already existing soil micro- and macro-biota [130].

Broad-spectrum biocidal fumigants are generally used to fumigate soils associated with high-value crops. These fumigants result in altering the microbial community of such soils. As a consequence of long-term fumigation, soil microbial community, and their beneficial interactions that help host plants obtain nutrients and mobilization, get largely affected [131]. This leads to decreased rhizosphere colonization by the PGPR inoculant.

### 5.8. Quality Control Constraints

The most important parameter which the farmers look for in any biofertilizer is quality control. Being natural products, living microorganisms possess a very short shelf life [32]. The failure of any microbial-based product in fields can be due to the supply of low- or spurious-quality products. Presently, there is the unavailability of any quality check for biofertilizers. Henceforth, in order to prove the plant growth promoting efficacy in the fields, setting up quality control standards for biofertilizers is quite essential [31].

### 5.9. Biofertilizer Carrier

A suitable carrier is required for field application of biofertilizer because of the short shelf life of the bioinoculant agent. Thus, the unavailability of an appropriate carrier proves to be one of the major constraints for its large-scale use in fields. Ideal carriers used in biofertilizer production are peat, charcoal, lignite, etc. These carriers again pose technical constraints because most of them are unavailable in developing countries like India. There is a lack of sufficient quantities and a desirable quality of these carriers. Only charcoal is readily available in the Indian market, and therefore it can be used as a formulating agent [31]. Peat is recognized as the most suitable carrier among the available carriers, but the challenge is its shorter shelf life, which is less than six months. Due to its ability to improve soil and plant health, biochar can be used as a suitable carrier for biofertilizers [14,30]. In order to prove itself as an efficient and potential carrier, the bioinoculant should possess several other characteristics. It should be of low cost, the organic matter content and water-holding capacity should be high, and the organism-retention capacity should be longer. It should be nearly sterile, with zero moisture content, and it should be non-polluting, non-toxic, and with nearly neutral pH so that the biofertilizer is of good quality [132].

### 5.10. Biosafety of PGPRs

PGPRs are considered to be practical candidates for sustainable agriculture. An essential characteristic of PGPRs and other biofertilizer agents is that these microbes should not elicit any harmful effects on the environment or humans. According to the guidelines on biosafety in microbiological and biomedical laboratories, published by the U.S. Department of Health and Human Services in 1999 and World Health Organization guidelines on the usage of microorganisms, biosafety levels (BSLs) were made to categorize the usable microorganisms in a range of biosafety classes, based on the different categories of risk posed by them [32]. The communicable agents were classified into four risk groups (BSL-1–4) based on their pathogenicity to human health, mode of transmission, and available treatments. These levels have to be strictly followed in handling these microorganisms. The microbial strains selected for biofertilizer development should preferably belong to the low-risk group of non-pathogenic BSL-1 microorganisms.

## 6. Guidelines and Precautions for Using PGPRs as Biofertilizers

The major safety measures and guidelines [31] essential for using PGPRs as biofertilizers are:

- (1) It is essential that the supplied biofertilizer to be used in fields is of good quality, contains  $10^7$  viable cells per gram as an inoculum, and is purchased from a reputed manufacturer only.
- (2) Since the biofertilizer exhibits specificity, it should only be used for the crop(s) specified on the commercially available product packet.
- (3) The culture bag should have a tag of the name of the crop for which it has to be used.
- (4) While inoculating, excess culture should be inoculated, or any remnants/residual culture should be immediately put in grooves of the field so that inoculum microorganisms start interacting with other microbiota in the rhizosphere and begin colonizing the rhizosphere.

- (5) Since the biofertilizers are microbial products, for achieving better shelf life, before their application in fields, they should be stored in cool and shady places, preferably at room temperature (25–28 °C).
- (6) During storage or application, direct contact of the biofertilizers with agrochemicals (herbicides/weedicides/pesticides) should be strictly avoided.
- (7) Generally speaking, 200g biofertilizer can be effectively used to treat 10 kg of seeds.
- (8) In the case of unfavorable soil conditions, especially where the soil is strongly acidic, soil amendments such as lime or rock phosphate, are usually preferred.

## 7. Roadmap to the Commercialization of PGPR-Based Biofertilizers

Using PGPRs as biofertilizers for promoting plant growth and crop yield, improving soil fertility, and biocontrol of phytopathogens promotes sustainable agriculture by offering eco-friendly alternatives to synthetic agrochemicals like chemical fertilizers and pesticides. The development and commercialization of PGPR-based biofertilizers generally follow the following roadmap (Figure 5) [30,108].

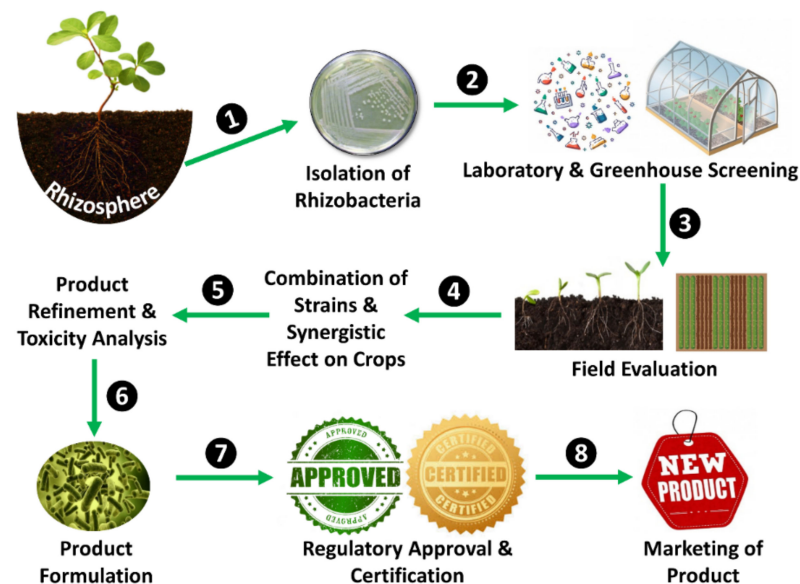


Figure 5. A roadmap for commercializing PGPR-based biofertilizers.

## 8. Conclusions and Future Perspectives

Among various industries present within a nation, the agriculture industry not only plays a pivotal role in survival but also facilitates meeting the demands of the growing population and economic exports. Post Green Revolution, the agroindustry has witnessed several scientific advances that resulted in better crop productivity but with environmental complications. Chemical fertilizers prove detrimental to soil and environmental health, while biofertilizers are natural products and do not pose threats to the ecosystem. Thus, to manage long-term soil fertility and sustain crop productivity, natural-products-based fertilizers prove to be an integral and vital component of sustainable agriculture. The last decade has inevitably seen a revolution because of the increased use of biological inoculants instead of agrochemicals for sustainable agriculture globally. The triad of interactions existing between the bioinoculant microorganism(s), resident soil microbiota, and host plant(s) is vital not only for the overall growth and higher productivity of the crop plants but also for maintaining the integrity of our planet's health and proper biogeochemical cycling.

A growing apprehension concerning food safety and the rising need for controlling food production quality to cater to the changing consumer demand is expected to shift farmers' attention toward organic farming and adopt sustainable agricultural practices. Thus, while seeking eco-friendly alternatives to toxic chemicals, there is a need to consider



the three crucial “Ps”, which include the people, prosperity, and the planet. Before its complete implementation, however, this microbial product-based technology needs to be researched profoundly and improved to elicit desired results and gain the trust of the farmers, the real stakeholders of agriculture. The thrust areas that need to be further focused on for research include quantifying commercial production, strain improvement, and authentication. Governments and federal agencies should promote the use of biofertilizers as eco-friendly alternatives for crop improvement. Entrepreneurs should invest more in the biofertilizer industry and provide financial assistance for start-ups. In addition to this, mass public awareness is required to educate the farmers and consumers alike on the advantages of using microbe-based biofertilizers for ensuring a greener tomorrow.

**Author Contributions:** Conceptualization, A.B. and S.K.; writing—original draft preparation, A.B., P.P., S.N.D., and S.K.; writing—review and editing, S.K., R.Z.S., M.S.R., and H.E.E. All authors have read and agreed to the published version of the manuscript.

**Funding:** H.E.E. would like to thank Universiti Teknologi Malaysia (UTM) for financial support through project No. QJ130000.3609.02M43 and All Cosmos Industries Sdn. Bhd. for financial support with project No. R.J130000.7344.4B200.

**Institutional Review Board Statement:** Not applicable.

**Informed Consent Statement:** Not applicable.

**Data Availability Statement:** Not applicable.

**Acknowledgments:** A.B. and P.P. acknowledge University Grants Commission (UGC), New Delhi, India, for research fellowships. A.B. acknowledges his mentor, Prof. Appa Rao Podile, Vice-Chancellor, University of Hyderabad, for his constant support and encouragement. S.N.D. acknowledges the UGC start-up research grant for financial support. S.K. acknowledges Principal Sister Amrutha, St. Ann’s College for Women, Hyderabad, Telangana, India, for her incessant support and Department of Biotechnology (DBT), New Delhi, India, for infrastructural support to the department under the DBT-STAR College Scheme.

**Conflicts of Interest:** The authors declare no conflict of interest.

## References

1. Kesavan, P.C.; Swaminathan, M.S. Modern technologies for sustainable food and nutrition security. *Curr. Sci.* **2018**, *115*, 1876–1883. [[CrossRef](#)]
2. Pingali, P.L. Green revolution: Impacts, limits, and the path ahead. *Proc. Natl. Acad. Sci. USA* **2012**, *109*, 12302–12308. [[CrossRef](#)] [[PubMed](#)]
3. Yang, X.; Fang, S. Practices, perceptions, and implications of fertilizer use in East-Central China. *Ambio* **2015**, *44*, 647–652. [[CrossRef](#)] [[PubMed](#)]
4. Bishnoi, U. Agriculture and the dark side of chemical fertilizers. *Environ. Anal. Ecol. Stud.* **2018**, *3*, EAES.000552.2018. [[CrossRef](#)]
5. Fascella, G.; Montoneri, E.; Ginepro, M.; Francavilla, M. Effect of urban biowaste derived soluble substances on growth, photosynthesis and ornamental value of *Euphorbia × lomi*. *Sci. Hort.* **2015**, *197*, 90–98. [[CrossRef](#)]
6. Fascella, G.; Montoneri, E.; Francavilla, M. Biowaste versus fossil sourced auxiliaries for plant cultivation: The Lantana case study. *J. Clean. Prod.* **2018**, *185*, 322–330. [[CrossRef](#)]
7. Liu, J.; Ma, K.; Ciais, P.; Polasky, S. Reducing human nitrogen use for food production. *Sci. Rep.* **2016**, *6*, 30104. [[CrossRef](#)]
8. Ilangumaran, G.; Smith, D.L. Plant growth promoting rhizobacteria in amelioration of salinity stress: A systems biology perspective. *Front. Plant Sci.* **2017**, *8*, 1768. [[CrossRef](#)]
9. De Souza, R.; Ambrosini, A.; Passaglia, L.M.P. Plant growth-promoting bacteria as inoculants in agricultural soils. *Genet. Mol. Biol.* **2015**, *38*, 401–419. [[CrossRef](#)]
10. Mishra, S.; Wang, K.-H.; Sipes, B.S.; Tian, M. Suppression of root-knot nematode by vermicompost tea prepared from different curing ages of vermicompost. *Plant Dis.* **2017**, *101*, 734–737. [[CrossRef](#)]
11. Arancon, N.Q.; Owens, J.D.; Converse, C. The effects of vermicompost tea on the growth and yield of lettuce and tomato in a non-circulating hydroponics system. *J. Plant Nutr.* **2019**, *42*, 2447–2458. [[CrossRef](#)]
12. Akinnuoye-Adelabu, D.B.; Steenhuisen, S.; Bredenhand, E. Improving pea quality with vermicompost tea and aqueous biochar: Prospects for sustainable farming in Southern Africa. *S. Afr. J. Bot.* **2019**, *123*, 278–285. [[CrossRef](#)]
13. Raklami, A.; Bechtaoui, N.; Tahiri, A.; Anli, M.; Meddich, A.; Oufdou, K. Use of rhizobacteria and mycorrhizae consortium in the open field as a strategy for improving crop nutrition, productivity and soil fertility. *Front. Microbiol.* **2019**, *10*, 1106. [[CrossRef](#)] [[PubMed](#)]

14. Jabborova, D.; Wirth, S.; Kannepalli, A.; Narimanov, A.; Desouky, S.; Davranov, K.; Sayyed, R.Z.; El Enshasy, H.; Malek, R.A.; Syed, A.; et al. Co-Inoculation of rhizobacteria and biochar application improves growth and nutrients in soybean and enriches soil nutrients and enzymes. *Agronomy* **2020**, *10*, 1142. [[CrossRef](#)]
15. Sharma, S.B.; Sayyed, R.Z.; Trivedi, M.H.; Gobi, T.A. Phosphate solubilizing microbes: Sustainable approach for managing phosphorus deficiency in agricultural soils. *Springerplus* **2013**, *2*, 587. [[CrossRef](#)]
16. Vessey, J.K. Plant growth promoting rhizobacteria as biofertilizers. *Plant Soil* **2003**, *255*, 571–586. [[CrossRef](#)]
17. Anli, M.; Baslam, M.; Tahiri, A.; Raklami, A.; Symanczik, S.; Boutasknit, A.; Ait-El-Mokhtar, M.; Ben-Laouane, R.; Toubali, S.; Ait Rahou, Y.; et al. Biofertilizers as strategies to improve photosynthetic apparatus, growth, and drought stress tolerance in the date palm. *Front. Plant Sci.* **2020**, *11*, 516818. [[CrossRef](#)]
18. Dong, L.; Li, Y.; Xu, J.; Yang, J.; Wei, G.; Shen, L.; Ding, W.; Chen, S. Biofertilizers regulate the soil microbial community and enhance *Panax ginseng* yields. *Chin. Med.* **2019**, *14*, 20. [[CrossRef](#)]
19. Atieno, M.; Herrmann, L.; Nguyen, H.T.; Phan, H.T.; Nguyen, N.K.; Srean, P.; Than, M.M.; Zhiyong, R.; Tittabutr, P.; Shut-srirung, A.; et al. Assessment of biofertilizer use for sustainable agriculture in the Great Mekong Region. *J. Environ. Manag.* **2020**, *275*, 111300. [[CrossRef](#)]
20. Dineshkumar, R.; Kumaravel, R.; Gopalsamy, J.; Sikder, M.N.A.; Sampathkumar, P. Microalgae as bio-fertilizers for rice growth and seed yield productivity. *Waste Biomass Valorization* **2018**, *9*, 793–800. [[CrossRef](#)]
21. Mahanty, T.; Bhattacharjee, S.; Goswami, M.; Bhattacharyya, P.; Das, B.; Ghosh, A.; Tribedi, P. Biofertilizers: A potential approach for sustainable agriculture development. *Environ. Sci. Pollut. Res.* **2017**, *24*, 3315–3335. [[CrossRef](#)] [[PubMed](#)]
22. Zandi, P.; Basu, S.K. Role of plant growth-promoting rhizobacteria (PGPR) as biofertilizers in stabilizing agricultural ecosystems. In *Organic Farming for Sustainable Agriculture*; Nandwani, D., Ed.; Springer: Cham, Switzerland, 2016; pp. 71–87. [[CrossRef](#)]
23. Bhardwaj, D.; Ansari, M.W.; Sahoo, R.K.; Tuteja, N. Biofertilizers function as key player in sustainable agriculture by improving soil fertility, plant tolerance and crop productivity. *Microb. Cell Fact.* **2014**, *13*, 1–10. [[CrossRef](#)]
24. Ritika, B.; Utpal, D. Biofertilizer, a way towards organic agriculture: A review. *Afr. J. Microbiol. Res.* **2014**, *8*, 2332–2343. [[CrossRef](#)]
25. Borkar, S.G. *Microbes as Bio-Fertilizers and Their Production Technology*, 1st ed.; WPI Publishing: New York, NY, USA, 2015.
26. Kumar, S.M.; Reddy, C.G.; Phogat, M.; Korav, S. Role of bio-fertilizers towards sustainable agricultural development: A review. *J. Pharm. Phytochem.* **2018**, *7*, 1915–1921.
27. Itelima, J.; Bang, W.J.; Onyimba, I.A.; Sila, M.D.; Egbere, O.J. Bio-fertilizers as key player in enhancing soil fertility and crop productivity: A review. *J. Microbiol. Biotechnol. Rep.* **2018**, *2*, 22–28.
28. Singh, J.S.; Pandey, V.C.; Singh, D.P. Efficient soil microorganisms: A new dimension for sustainable agriculture and environmental development. *Agric. Ecosyst. Environ.* **2011**, *140*, 339–353. [[CrossRef](#)]
29. Sun, B.; Bai, Z.; Bao, L.; Xue, L.; Zhang, S.; Wei, Y.; Zhang, Z.; Zhuang, G.; Zhuang, X. *Bacillus subtilis* biofertilizer mitigating agricultural ammonia emission and shifting soil nitrogen cycling microbiomes. *Environ. Int.* **2020**, *144*, 105989. [[CrossRef](#)]
30. Backer, R.; Rokem, J.S.; Ilangumaran, G.; Lamont, J.; Praslickova, D.; Ricci, E.; Subramanian, S.; Smith, D.L. Plant growth-promoting rhizobacteria: Context, mechanisms of action, and roadmap to commercialization of biostimulants for sustainable agriculture. *Front. Plant Sci.* **2018**, *9*, 1473. [[CrossRef](#)]
31. Mahajan, A.; Gupta, R.D. Bio-fertilizers: Their kinds and requirement in India. In *Integrated Nutrient Management (INM) in a Sustainable Rice—Wheat Cropping System*; Mahajan, A., Gupta, R.D., Eds.; Springer: Dordrecht, The Netherlands, 2009; pp. 75–100.
32. Meena, M.; Swapnil, P.; Divyanshu, K.; Kumar, S.; Tripathi, Y.N.; Zehra, A.; Marwal, A.; Upadhyay, R.S. PGPR-mediated induction of systemic resistance and physiochemical alterations in plants against the pathogens: Current perspectives. *J. Basic Microbiol.* **2020**, *60*, 828–861. [[CrossRef](#)]
33. Timmusk, S.; Kim, S.-B.; Nevo, E.; Abd El Daim, I.; Ek, B.; Bergquist, J.; Behers, L. Sfp-type PPTase inactivation promotes bacterial biofilm formation and ability to enhance wheat drought tolerance. *Front. Microbiol.* **2015**, *6*, 387. [[CrossRef](#)]
34. Bharti, N.; Pandey, S.S.; Barnawal, D.; Patel, V.K.; Kalra, A. Plant growth promoting rhizobacteria *Dietzia natronolimnaea* modulates the expression of stress responsive genes providing protection of wheat from salinity stress. *Sci. Rep.* **2016**, *6*, 34768. [[CrossRef](#)] [[PubMed](#)]
35. Sharma, S.; Kulkarni, J.; Jha, B. Halotolerant rhizobacteria promote growth and enhance salinity tolerance in peanut. *Front. Microbiol.* **2016**, *7*, 1600. [[CrossRef](#)] [[PubMed](#)]
36. Timmusk, S.; Abd El-Daim, I.A.; Copolovici, L.; Tanilas, T.; Kännaste, A.; Behers, L.; Nevo, E.; Seisenbaeva, G.; Stenström, E.; Niinemets, Ü. Drought-tolerance of wheat improved by rhizosphere bacteria from harsh environments: Enhanced biomass production and reduced emissions of stress volatiles. *PLoS ONE* **2014**, *9*, e96086. [[CrossRef](#)] [[PubMed](#)]
37. Schütz, L.; Gattinger, A.; Meier, M.; Müller, A.; Boller, T.; Mäder, P.; Mathimaran, N. Improving crop yield and nutrient use efficiency via biofertilization—A global meta-analysis. *Front. Plant Sci.* **2018**, *8*, 2204. [[CrossRef](#)] [[PubMed](#)]
38. De la Fuente Cantó, C.; Simonin, M.; King, E.; Moulin, L.; Bennett, M.J.; Castrillo, G.; Laplaze, L. An extended root phenotype: The rhizosphere, its formation and impacts on plant fitness. *Plant J.* **2020**, *103*, 951–964. [[CrossRef](#)] [[PubMed](#)]
39. Kalam, S.; Das, S.N.; Basu, A.; Podile, A.R. Population densities of indigenous Acidobacteria change in the presence of plant growth promoting rhizobacteria (PGPR) in rhizosphere. *J. Basic Microbiol.* **2017**, *57*, 376–385. [[CrossRef](#)]
40. Buée, M.; de Boer, W.; Martin, F.; van Overbeek, L.; Jurkevitch, E. The rhizosphere zoo: An overview of plant-associated communities of microorganisms, including phages, bacteria, archaea, and fungi, and of some of their structuring factors. *Plant Soil* **2009**, *321*, 189–212. [[CrossRef](#)]

41. Dutta, S.; Podile, A.R. Plant Growth Promoting Rhizobacteria (PGPR): The bugs to debug the root zone. *Crit. Rev. Microbiol.* **2010**, *36*, 232–244. [[CrossRef](#)]
42. Khoshru, B.; Mitra, D.; Khoshmanzar, E.; Myo, E.M.; Uniyal, N.; Mahakur, B.; Mohapatra, P.K.; Panneerselvam, P.; Boutaj, H.; Alizadeh, M.; et al. Current scenario and future prospects of plant growth-promoting rhizobacteria: An economic valuable resource for the agriculture revival under stressful conditions. *J. Plant Nutr.* **2020**, *43*, 3062–3092. [[CrossRef](#)]
43. Ahemad, M.; Kibret, M. Mechanisms and applications of plant growth promoting rhizobacteria: Current perspective. *J. King Saud Univ. Sci.* **2014**, *26*, 1–20. [[CrossRef](#)]
44. Parray, J.A.; Jan, S.; Kamili, A.N.; Qadri, R.A.; Egamberdieva, D.; Ahmad, P. Current perspectives on plant growth-promoting rhizobacteria. *J. Plant Growth Regul.* **2016**, *35*, 877–902. [[CrossRef](#)]
45. Vejan, P.; Abdullah, R.; Khadiran, T.; Ismail, S.; Nasrulhaq Boyce, A. Role of plant growth promoting rhizobacteria in agricultural sustainability - A review. *Molecules* **2016**, *21*, 573. [[CrossRef](#)] [[PubMed](#)]
46. Kalam, S.; Basu, A.; Podile, A.R. Functional and molecular characterization of plant growth promoting *Bacillus* isolates from tomato rhizosphere. *Heliyon* **2020**, *6*, e04734. [[CrossRef](#)] [[PubMed](#)]
47. Swarnalakshmi, K.; Yadav, V.; Tyagi, D.; Dhar, D.W.; Kannepalli, A.; Kumar, S. Significance of plant growth promoting rhizobacteria in grain legumes: Growth promotion and crop production. *Plants* **2020**, *9*, 1596. [[CrossRef](#)] [[PubMed](#)]
48. Gopalakrishnan, S.; Sathya, A.; Vijayabharathi, R.; Varshney, R.K.; Gowda, C.L.L.; Krishnamurthy, L. Plant growth promoting rhizobia: Challenges and opportunities. *3 Biotech* **2015**, *5*, 355–377. [[CrossRef](#)]
49. Bhattacharyya, P.N.; Jha, D.K. Plant growth-promoting rhizobacteria (PGPR): Emergence in agriculture. *World J. Microbiol. Biotechnol.* **2012**, *28*, 1327–1350. [[CrossRef](#)]
50. Vaikuntapu, P.R.; Dutta, S.; Samudrala, R.B.; Rao, V.R.V.N.; Kalam, S.; Podile, A.R. Preferential promotion of *Lycopersicon esculentum* (tomato) growth by plant growth promoting bacteria associated with tomato. *Indian J. Microbiol.* **2014**, *54*, 403–412. [[CrossRef](#)]
51. Goswami, D.; Thakker, J.N.; Dhandhukia, P.C. Portraying mechanics of plant growth promoting rhizobacteria (PGPR): A review. *Cogent Food Agric.* **2016**, *2*, 1127500. [[CrossRef](#)]
52. Ankati, S.; Podile, A.R. Understanding plant-beneficial microbe interactions for sustainable agriculture. *J. Spices Aromat. Crop.* **2018**, *27*, 93–105. [[CrossRef](#)]
53. Ahmad, F.; Ahmad, I.; Khan, M.S. Screening of free-living rhizospheric bacteria for their multiple plant growth promoting activities. *Microbiol. Res.* **2008**, *163*, 173–181. [[CrossRef](#)]
54. Niu, X.; Song, L.; Xiao, Y.; Ge, W. Drought-tolerant plant growth-promoting rhizobacteria associated with foxtail millet in a semi-arid agroecosystem and their potential in alleviating drought stress. *Front. Microbiol.* **2018**, *8*, 2580. [[CrossRef](#)] [[PubMed](#)]
55. De Lima, B.C.; Moro, A.L.; Santos, A.C.P.; Bonifacio, A.; Araujo, A.S.F.; de Araujo, F.F. *Bacillus subtilis* ameliorates water stress tolerance in maize and common bean. *J. Plant Interact.* **2019**, *14*, 432–439. [[CrossRef](#)]
56. Bresson, J.; Varoquaux, F.; Bontpart, T.; Touraine, B.; Vile, D. The PGPR strain *Phyllobacterium brassicacearum* STM196 induces a reproductive delay and physiological changes that result in improved drought tolerance in *Arabidopsis*. *New Phytol.* **2013**, *200*, 558–569. [[CrossRef](#)] [[PubMed](#)]
57. Figueiredo, M.V.B.; Burity, H.A.; Martínez, C.R.; Chanway, C.P. Alleviation of drought stress in the common bean (*Phaseolus vulgaris* L.) by co-inoculation with *Paenibacillus polymyxa* and *Rhizobium tropici*. *Appl. Soil Ecol.* **2008**, *40*, 182–188. [[CrossRef](#)]
58. Yang, J.; Kloepper, J.W.; Ryu, C.M. Rhizosphere bacteria help plants tolerate abiotic stress. *Trends Plant Sci.* **2009**, *14*, 1–4. [[CrossRef](#)]
59. Ilyas, N.; Mumtaz, K.; Akhtar, N.; Yasmin, H.; Sayyed, R.Z.; Khan, W.; El Enshasy, H.A.; Dailin, D.J.; Elsayed, E.A.; Ali, Z. Exopolysaccharides producing bacteria for the amelioration of drought stress in wheat. *Sustainability* **2020**, *12*, 8876. [[CrossRef](#)]
60. Mayak, S.; Tirosch, T.; Glick, B.R. Plant growth-promoting bacteria confer resistance in tomato plants to salt stress. *Plant Physiol. Biochem.* **2004**, *42*, 565–572. [[CrossRef](#)]
61. Bharti, N.; Yadav, D.; Barnawal, D.; Maji, D.; Kalra, A. Exiguobacterium oxidotolerans, a halotolerant plant growth promoting rhizobacteria, improves yield and content of secondary metabolites in *Bacopa monnieri* (L.) Pennell under primary and secondary salt stress. *World J. Microbiol. Biotechnol.* **2013**, *29*, 379–387. [[CrossRef](#)]
62. Marulanda, A.; Azcón, R.; Chaumont, F.; Ruiz-Lozano, J.M.; Aroca, R. Regulation of plasma membrane aquaporins by inoculation with a *Bacillus megaterium* strain in maize (*Zea mays* L.) plants under unstressed and salt-stressed conditions. *Planta* **2010**, *232*, 533–543. [[CrossRef](#)]
63. Fasciglione, G.; Casanovas, E.M.; Quillehauquy, V.; Yommi, A.K.; Gō Ni, M.G.; Roura, S.I.; Barassi, C.A. *Azospirillum* inoculation effects on growth, product quality and storage life of lettuce plants grown under salt stress. *Sci. Hortic.* **2015**, *195*, 154–162. [[CrossRef](#)]
64. Sagar, A.; Sayyed, R.Z.; Ramteke, P.W.; Sharma, S.; Marraiki, N.; Elgorban, A.M.; Syed, A. ACC deaminase and antioxidant enzymes producing halophilic *Enterobacter* sp. PR14 promotes the growth of rice and millets under salinity stress. *Physiol. Mol. Biol. Plants* **2020**, *26*, 1847–1854. [[CrossRef](#)] [[PubMed](#)]
65. Verma, P.; Yadav, A.N.; Khannam, K.S.; Kumar, S.; Saxena, A.K.; Suman, A. Molecular diversity and multifarious plant growth promoting attributes of Bacilli associated with wheat (*Triticum aestivum* L.) rhizosphere from six diverse agro-ecological zones of India. *J. Basic Microbiol.* **2016**, *56*, 44–58. [[CrossRef](#)] [[PubMed](#)]

66. Srivastava, S.; Bist, V.; Srivastava, S.; Singh, P.C.; Trivedi, P.K.; Asif, M.H.; Chauhan, P.S.; Nautiyal, C.S. Unraveling aspects of *Bacillus amyloliquefaciens* mediated enhanced production of rice under biotic stress of *Rhizoctonia solani*. *Front. Plant Sci.* **2016**, *7*, 587. [[CrossRef](#)]
67. De Vasconcellos, R.L.F.; Cardoso, E.J.B.N. Rhizospheric streptomycetes as potential biocontrol agents of *Fusarium* and *Armillaria* pine rot and as PGPR for *Pinus taeda*. *Biocontrol* **2009**, *54*, 807–816. [[CrossRef](#)]
68. Gowtham, H.G.; Hariprasad, P.; Nayak, S.C.; Niranjana, S.R. Application of rhizobacteria antagonistic to *Fusarium oxysporum* f. sp. *lycopersici* for the management of *Fusarium* wilt in tomato. *Rhizosphere* **2016**, *2*, 72–74. [[CrossRef](#)]
69. Khan, N.; Mishra, A.; Nautiyal, C.S. *Paenibacillus lentimorbus* B-30488 r controls early blight disease in tomato by inducing host resistance associated gene expression and inhibiting *Alternaria solani*. *Biol. Control* **2012**, *62*, 65–74. [[CrossRef](#)]
70. Reshma, P.; Naik, M.K.; Aiyaz, M.; Niranjana, S.K.; Chennappa, G.; Shaikh, S.S.; Sayyed, R.Z. Induced systemic resistance by 2,4-diacetylphloroglucinol positive fluorescent *Pseudomonas* strains against rice sheath blight. *Indian J. Exp. Biol.* **2018**, *56*, 207–212.
71. Chen, Q.; Liu, S. Identification and characterization of the phosphate-solubilizing bacterium *Pantoea* sp. S32 in reclamation soil in Shanxi, China. *Front. Microbiol.* **2019**, *10*, 2171. [[CrossRef](#)]
72. Pii, Y.; Mimmo, T.; Tomasi, N.; Terzano, R.; Cesco, S.; Crecchio, C. Microbial interactions in the rhizosphere: Beneficial influences of plant growth-promoting rhizobacteria on nutrient acquisition process. A review. *Biol. Fertil. Soils* **2015**, *51*, 403–415. [[CrossRef](#)]
73. Castillo-Aguilar, C.; Garruña, R.; Zúñiga-Aguilar, J.J.; Guzmán-Antonio, A.A. PGPR inoculation improves growth, nutrient uptake and physiological parameters of *Capsicum chinense* plants. *Phyton Int. J. Exp. Bot.* **2017**, *86*, 199–204. [[CrossRef](#)]
74. Almaghrabi, O.A.; Abdelmoneim, T.S.; Albishri, H.M.; Moussa, T.A. Enhancement of maize growth using some plant growth promoting rhizobacteria (PGPR) under laboratory conditions. *Life Sci. J.* **2014**, *11*, 764–772.
75. Nezarat, S.; Gholami, A. Screening plant growth promoting rhizobacteria for improving seed germination, seedling growth and yield of maize. *Pak. J. Biol. Sci.* **2009**, *12*, 26–32. [[CrossRef](#)] [[PubMed](#)]
76. Rana, A.; Saharan, B.; Joshi, M.; Prasanna, R.; Kumar, K.; Nain, L. Identification of multi-trait PGPR isolates and evaluating their potential as inoculants for wheat. *Ann. Microbiol.* **2011**, *61*, 893–900. [[CrossRef](#)]
77. Cassán, F.D.; Lucangeli, C.D.; Bottini, R.; Piccoli, P.N. *Azospirillum* spp. metabolize [17,17-2H<sub>2</sub>] gibberellin A20 to [17,17-2H<sub>2</sub>] gibberellin A1 in vivo in dy rice mutant seedlings. *Plant Cell Physiol.* **2001**, *42*, 763–767. [[CrossRef](#)]
78. Tahir, H.A.S.; Gu, Q.; Wu, H.; Raza, W.; Hanif, A.; Wu, L.; Colman, M.V.; Gao, X. Plant growth promotion by volatile organic compounds produced by *Bacillus subtilis* SYST2. *Front. Microbiol.* **2017**, *8*, 171. [[CrossRef](#)]
79. Barnawal, D.; Bharti, N.; Pandey, S.S.; Pandey, A.; Chanotiya, C.S.; Kalra, A. Plant growth-promoting rhizobacteria enhance wheat salt and drought stress tolerance by altering endogenous phytohormone levels and *TaCTR1/TaDREB2* expression. *Physiol. Plant.* **2017**, *161*, 502–514. [[CrossRef](#)]
80. Jang, J.H.; Woo, S.Y.; Kim, S.H.; Khaine, I.; Kwak, M.J.; Lee, H.K.; Lee, T.Y.; Lee, W.Y. Effects of increased soil fertility and plant growth-promoting rhizobacteria inoculation on biomass yield, energy value, and physiological response of poplar in short-rotation coppices in a reclaimed tideland: A case study in the Saemangeum area of Korea. *Biomass Bioenergy* **2017**, *107*, 29–38. [[CrossRef](#)]
81. Islam, S.; Akanda, A.M.; Prova, A.; Islam, M.T.; Hossain, M.M. Isolation and identification of plant growth promoting rhizobacteria from cucumber rhizosphere and their effect on plant growth promotion and disease suppression. *Front. Microbiol.* **2016**, *6*, 1360. [[CrossRef](#)]
82. Ahmad, M.; Zahir, Z.A.; Asghar, H.N.; Asghar, M. Inducing salt tolerance in mung bean through coinoculation with rhizobia and plant-growth promoting rhizobacteria containing 1-aminocyclopropane-1-carboxylate deaminase. *Can. J. Microbiol.* **2011**, *57*, 578–589. [[CrossRef](#)]
83. Pandey, S.; Ghosh, P.K.; Ghosh, S.; De, T.K.; Maiti, T.K. Role of heavy metal resistant *Ochrobactrum* sp. and *Bacillus* spp. strains in bioremediation of a rice cultivar and their PGPR like activities. *J. Microbiol.* **2013**, *51*, 11–17. [[CrossRef](#)]
84. Khan, N.; Bano, A. Role of plant growth promoting rhizobacteria and Ag-nano particle in the bioremediation of heavy metals and maize growth under municipal wastewater irrigation. *Int. J. Phytoremediat.* **2016**, *18*, 211–221. [[CrossRef](#)] [[PubMed](#)]
85. Das, A.J.; Kumar, R. Bioremediation of petroleum contaminated soil to combat toxicity on *Withania somnifera* through seed priming with biosurfactant producing plant growth promoting rhizobacteria. *J. Environ. Manag.* **2016**, *174*, 79–86. [[CrossRef](#)] [[PubMed](#)]
86. Kalam, S.; Basu, A.; Ankati, S. Plant root-associated biofilms in bioremediation. In *Biofilms in Plant and Soil Health*; Ahmad, I., Husain, F.M., Eds.; John Wiley & Sons, Ltd.: Chichester, UK, 2017; pp. 337–355.
87. Patel, P.; Shaikh, S.; Sayyed, R. Dynamism of PGPR in bioremediation and plant growth promotion in heavy metal contaminated soil. *Indian J. Exp. Biol.* **2016**, *54*, 286–290. [[PubMed](#)]
88. Sayyed, R.Z.; Patel, P.R.; Shaikh, S.S. Plant growth promotion and root colonization by EPS producing *Enterobacter* sp. RZS5 under heavy metal contaminated soil. *Indian J. Exp. Biol.* **2015**, *53*, 116–123. [[PubMed](#)]
89. Banchio, E.; Xie, X.; Zhang, H.; Paré, P.W. Soil bacteria elevate essential oil accumulation and emissions in sweet basil. *J. Agric. Food Chem.* **2009**, *57*, 653–657. [[CrossRef](#)]
90. Ordookhani, K.; Sharafzadeh, S.; Zare, M. Influence of PGPR on growth, essential oil and nutrients uptake of sweet basil. *Adv. Environ. Biol.* **2011**, *5*, 672–677.
91. Etesami, H.; Maheshwari, D.K. Use of plant growth promoting rhizobacteria (PGPRs) with multiple plant growth promoting traits in stress agriculture: Action mechanisms and future prospects. *Ecotoxicol. Environ. Saf.* **2018**, *156*, 225–246. [[CrossRef](#)]

92. Mahdi, I.; Fahsi, N.; Hafidi, M.; Allaoui, A.; Biskri, L. Plant growth enhancement using rhizospheric halotolerant phosphate solubilizing bacterium *Bacillus licheniformis* QA1 and *Enterobacter asburiae* QF11 isolated from *Chenopodium quinoa* willd. *Microorganisms* **2020**, *8*, 948. [[CrossRef](#)]
93. Etesami, H.; Alikhani, H.A.; Mirseyed Hosseini, H. Indole-3-acetic acid and 1-aminocyclopropane-1-carboxylate deaminase: Bacterial traits required in rhizosphere, rhizoplane and/or endophytic competence by beneficial bacteria. In *Bacterial Metabolites in Sustainable Agroecosystem*; Maheshwari, D.K., Ed.; Springer: Cham, Switzerland, 2015; pp. 183–258.
94. Umsha, S.; Singh, P.K.; Singh, R.P. Microbial biotechnology and sustainable agriculture. In *Biotechnology for Sustainable Agriculture: Emerging Approaches and Strategies*; Singh, R.L., Mondal, S., Eds.; Woodhead Publishing: Cambridge, UK, 2018; pp. 185–205.
95. Gouda, S.; Kerry, R.G.; Das, G.; Paramithiotis, S.; Shin, H.-S.; Patra, J.K. Revitalization of plant growth promoting rhizobacteria for sustainable development in agriculture. *Microbiol. Res.* **2018**, *206*, 131–140. [[CrossRef](#)]
96. Khatoun, Z.; Huang, S.; Rafique, M.; Fakhar, A.; Kamran, M.A.; Santoyo, G. Unlocking the potential of plant growth-promoting rhizobacteria on soil health and the sustainability of agricultural systems. *J. Environ. Manag.* **2020**, *273*, 111118. [[CrossRef](#)]
97. Oleńska, E.; Małek, W.; Wójcik, M.; Swiecicka, I.; Thijs, S.; Vangronsveld, J. Beneficial features of plant growth-promoting rhizobacteria for improving plant growth and health in challenging conditions: A methodical review. *Sci. Total Environ.* **2020**, *743*, 140682. [[CrossRef](#)] [[PubMed](#)]
98. Beneduzi, A.; Ambrosini, A.; Passaglia, L.M.P. Plant growth-promoting rhizobacteria (PGPR): Their potential as antagonists and biocontrol agents. *Genet. Mol. Biol.* **2012**, *35*, 1044–1051. [[CrossRef](#)] [[PubMed](#)]
99. Glick, B.R. Plant growth-promoting bacteria: Mechanisms and applications. *Scientifica* **2012**, *2012*, 963401. [[CrossRef](#)] [[PubMed](#)]
100. Glick, B.R. Bacteria with ACC deaminase can promote plant growth and help to feed the world. *Microbiol. Res.* **2014**, *169*, 30–39. [[CrossRef](#)] [[PubMed](#)]
101. Singh, I. Plant growth promoting rhizobacteria (PGPR) and their various mechanisms for plant growth enhancement in stressful conditions: A review. *Eur. J. Biol. Res.* **2018**, *8*, 191–213. [[CrossRef](#)]
102. Kumar, A.; Bahadur, I.; Maurya, B.R.; Raghuwanshi, R.; Meena, V.S.; Singh, D.K.; Dixit, J. Does a plant growth promoting rhizobacteria enhance agricultural sustainability? *J. Pure Appl. Microbiol.* **2015**, *9*, 715–724.
103. Berg, G.; Köberl, M.; Rybakova, D.; Müller, H.; Grosch, R.; Smalla, K. Plant microbial diversity is suggested as the key to future biocontrol and health trends. *Fems Microbiol. Ecol.* **2017**, *93*, 50. [[CrossRef](#)]
104. Sayyed, R.Z.; Seifi, S.; Patel, P.R.; Shaikh, S.S.; Jadhav, H.P.; El Enshasy, H. Siderophore production in groundnut rhizosphere isolate, *Achromobacter* sp. RZS2 influenced by physicochemical factors and metal ions. *Environ. Sustain.* **2019**, *2*, 117–124. [[CrossRef](#)]
105. García-Fraile, P.; Menéndez, E.; Rivas, R. Role of bacterial biofertilizers in agriculture and forestry. *Aims Bioeng.* **2015**, *2*, 183–205. [[CrossRef](#)]
106. Vacheron, J.; Desbrosses, G.; Bouffaud, M.L.; Touraine, B.; Moëgne-Loccoz, Y.; Muller, D.; Legendre, L.; Wisniewski-Dyé, F.; Prigent-Combaret, C. Plant growth-promoting rhizobacteria and root system functioning. *Front. Plant Sci.* **2013**, *4*, 356. [[CrossRef](#)]
107. Timmusk, S.; Behers, L.; Muthoni, J.; Muraya, A.; Aronsson, A.C. Perspectives and challenges of microbial application for crop improvement. *Front. Plant Sci.* **2017**, *8*, 49. [[CrossRef](#)] [[PubMed](#)]
108. Soumare, A.; Diedhiou, A.G.; Thuita, M.; Hafidi, M.; Ouhdouch, Y.; Gopalakrishnan, S.; Kouisni, L. Exploiting biological nitrogen fixation: A route towards a sustainable agriculture. *Plants* **2020**, *9*, 1011. [[CrossRef](#)] [[PubMed](#)]
109. Ferguson, B.J.; Mens, C.; Hastwell, A.H.; Zhang, M.; Su, H.; Jones, C.H.; Chu, X.; Gresshoff, P.M. Legume nodulation: The host controls the party. *Plant. Cell Environ.* **2019**, *42*, 41–51. [[CrossRef](#)] [[PubMed](#)]
110. García-Fraile, P.; Menéndez, E.; Celador-Lera, L.; Díez-Méndez, A.; Jiménez-Gómez, A.; Marcos-García, M.; Cruz-González, X.A.; Martínez-Hidalgo, P.; Mateos, P.F.; Rivas, R. Bacterial probiotics: A truly green revolution. In *Probiotics and Plant Health*; Kumar, V., Kumar, M., Sharma, S., Prasad, R., Eds.; Springer: Singapore, 2017; pp. 131–162.
111. Dal Cortivo, C.; Ferrari, M.; Visioli, G.; Lauro, M.; Fornasier, F.; Barion, G.; Panozzo, A.; Vameralli, T. Effects of seed-applied biofertilizers on rhizosphere biodiversity and growth of common wheat (*Triticum aestivum* L.) in the field. *Front. Plant Sci.* **2020**, *11*, 72. [[CrossRef](#)] [[PubMed](#)]
112. Aloo, B.N.; Makumba, B.A.; Mbega, E.R. Plant growth promoting rhizobacterial biofertilizers for sustainable crop production: The past, present, and future. *Preprints* **2020**, 2020090650. [[CrossRef](#)]
113. Adeleke, R.A.; Raimi, A.R.; Roopnarain, A.; Mokubedi, S.M. Status and prospects of bacterial inoculants for sustainable management of agroecosystems. In *Biofertilizers for Sustainable Agriculture and Environment*; Giri, B., Prasad, R., Wu, Q.-S., Varma, A., Eds.; Springer: Cham, Switzerland, 2019; pp. 137–172.
114. Mustafa, S.; Kabir, S.; Shabbir, U.; Batool, R. Plant growth promoting rhizobacteria in sustainable agriculture: From theoretical to pragmatic approach. *Symbiosis* **2019**, *78*, 115–123. [[CrossRef](#)]
115. Maçik, M.; Gryta, A.; Fraç, M. Biofertilizers in agriculture: An overview on concepts, strategies and effects on soil microorganisms. In *Advances in Agronomy*; Sparks, D.L., Ed.; Academic Press Inc.: Cambridge, MA, USA, 2020; Volume 162, pp. 31–87.
116. Artyszak, A.; Gozdowski, D. The effect of growth activators and plant growth-promoting rhizobacteria (PGPR) on the soil properties, root yield, and technological quality of sugar beet. *Agronomy* **2020**, *10*, 1262. [[CrossRef](#)]
117. Uribe, D.; Sánchez-Nieves, J.; Vanegas, J. Role of microbial biofertilizers in the development of a sustainable agriculture in the Tropics. In *Soil Biology and Agriculture in the Tropics*; Dion, P., Ed.; Springer: Berlin/Heidelberg, Germany, 2010; pp. 235–250.

118. Mehnaz, S. An overview of globally available bioformulations. In *Bioformulations: For Sustainable Agriculture*; Arora, N., Mehnaz, S., Balestrini, R., Eds.; Springer: New Delhi, India, 2016; pp. 268–281.
119. Sessitsch, A.; Mitter, B. 21st century agriculture: Integration of plant microbiomes for improved crop production and food security. *Microb. Biotechnol.* **2015**, *8*, 32–33. [[CrossRef](#)]
120. Cardinale, M.; Ratering, S.; Suarez, C.; Zapata Montoya, A.M.; Geissler-Plaum, R.; Schnell, S. Paradox of plant growth promotion potential of rhizobacteria and their actual promotion effect on growth of barley (*Hordeum vulgare* L.) under salt stress. *Microbiol. Res.* **2015**, *181*, 22–32. [[CrossRef](#)]
121. Amara, U.; Khalid, R.; Hayat, R. Soil bacteria and phytohormones for sustainable crop production. In *Bacterial Metabolites in Sustainable Agroecosystem*; Maheshwari, D.K., Ed.; Springer: Cham, Switzerland, 2015; pp. 87–103. [[CrossRef](#)]
122. Kamilova, F.; Okon, Y.; Deweerdt, S.; Horal, K. Commercialization of microbes: Manufacturing, inoculation, best practice for objective field testing, and registration. In *Principles of Plant-Microbe Interactions: Microbes for Sustainable Agriculture*; Lugtenberg, B., Ed.; Springer: Cham, Switzerland, 2015; pp. 319–327. [[CrossRef](#)]
123. Thomas, L.; Singh, I. Microbial biofertilizers: Types and applications. In *Biofertilizers for Sustainable Agriculture and Environment*; Giri, B., Prasad, R., Wu, Q.S., Varma, A., Eds.; Springer: Cham, Switzerland, 2019; pp. 1–19.
124. Arora, N.K.; Khare, E.; Maheshwari, D.K. Plant growth promoting rhizobacteria: Constraints in bioformulation, commercialization, and future strategies. In *Plant Growth and Health Promoting Bacteria*; Maheshwari, D., Ed.; Springer: Berlin/Heidelberg, Germany, 2010; pp. 97–116.
125. Du Jardin, P. Plant biostimulants: Definition, concept, main categories and regulation. *Sci. Hortic.* **2015**, *196*, 3–14. [[CrossRef](#)]
126. Barea, J.M. Future challenges and perspectives for applying microbial biotechnology in sustainable agriculture based on a better understanding of plant-microbiome interactions. *J. Soil Sci. Plant Nutr.* **2015**, *15*, 261–282. [[CrossRef](#)]
127. Parnell, J.J.; Berka, R.; Young, H.A.; Sturino, J.M.; Kang, Y.; Barnhart, D.M.; Dileo, M.V. From the lab to the farm: An industrial perspective of plant beneficial microorganisms. *Front. Plant Sci.* **2016**, *7*, 1110. [[CrossRef](#)] [[PubMed](#)]
128. Ndeddy Aka, R.J.; Babalola, O.O. Effect of bacterial inoculation of strains of *Pseudomonas aeruginosa*, *Alcaligenes faecalis* and *Bacillus subtilis* on germination, growth and heavy metal (Cd, Cr, and Ni) uptake of *Brassica juncea*. *Int. J. Phytoremediat.* **2016**, *18*, 200–209. [[CrossRef](#)]
129. Kumar, A.; Verma, H.; Singh, V.K.; Singh, P.P.; Singh, S.K.; Ansari, W.A.; Yadav, A.; Singh, P.K.; Pandey, K.D. Role of *Pseudomonas* sp. in sustainable agriculture and disease management. In *Agriculturally Important Microbes for Sustainable Agriculture*; Meena, V.S., Mishra, P.K., Bisht, J.K., Pattanayak, A., Eds.; Springer: Singapore, 2017; Volume 2, pp. 195–215.
130. Malusà, E.; Pinzari, F.; Canfora, L. Efficacy of biofertilizers: Challenges to improve crop production. In *Microbial Inoculants in Sustainable Agricultural Productivity*; Singh, D.P., Singh, H.B., Prabha, R., Eds.; Springer: New Delhi, India, 2016; pp. 17–40.
131. Dangi, S.R.; Tirado-Corbalá, R.; Gerik, J.; Hanson, B.D. Effect of long-term continuous fumigation on soil microbial communities. *Agronomy* **2017**, *7*, 37. [[CrossRef](#)]
132. Bashan, Y.; de-Bashan, L.E.; Prabhu, S.R.; Hernandez, J.P. Advances in plant growth-promoting bacterial inoculant technology: Formulations and practical perspectives (1998–2013). *Plant Soil* **2014**, *378*, 1–33. [[CrossRef](#)]